

Electroweak Radiative Corrections for Collider Physics

Ansgar Denner^a, Stefan Dittmaier^{b,*}

^aUniversität Würzburg, Institut für Theoretische Physik und Astrophysik, Emil-Hilb-Weg 22, 97074 Würzburg, Germany

^bAlbert-Ludwigs-Universität Freiburg, Physikalisches Institut, Hermann-Herder-Str. 3, 79104 Freiburg, Germany

Abstract

Current particle phenomenology is characterized by the spectacular agreement of the predictions of the Standard Model of particle physics (SM) with all results from collider experiments and by the absence of significant signals of non-standard physics, despite the fact that we know that the SM cannot be the ultimate theory of nature. In this situation, confronting theory and experiment with high precision is a promising direction to look for potential traces of physics beyond the SM. On the theory side, the calculation of radiative corrections of the strong and electroweak interactions is at the heart of this task, a field that has seen tremendous conceptual and technical progress in the last decades. This review aims at a coherent introduction to the field of *electroweak corrections* and tries to fill gaps in the literature between standard textbook knowledge and the current state of the art. The SM and the machinery for its perturbative evaluation are reviewed in detail, putting particular emphasis on renormalization, on one-loop techniques, on modern amplitude methods and tools, on the separation of infrared singularities in real-emission corrections, on electroweak issues connected with hadronic initial or final states in collisions, and on the issue of unstable particles in quantum field theory together with corresponding practical solutions.

Keywords: Electroweak theory, electroweak corrections, NLO calculations, Standard Model, renormalization, unstable particles

PACS: 12.15.-y, 12.15.Lk, 12.38.Bx, 13.40.Ks

Contents

1	Introduction	4
2	The Standard Model of particle physics	7
2.1	Lagrangian of the Standard Model	7
2.1.1	Lagrangian of the Electroweak Standard Model in the symmetric basis	7
2.1.2	Lagrangian of the Electroweak Standard Model in the physical basis	9
2.1.3	Quantization	12
2.1.4	Inclusion of QCD	13
2.1.5	θ -terms and strong CP violation	13
2.2	Slavnov–Taylor and Ward identities	14
2.3	Background-field quantization	16
2.3.1	Quantized Lagrangian in the background-field method	16
2.3.2	Background-field Ward identities	18
2.4	Standard-Model effective theory	19
2.4.1	Conventions and definition of the effective operator basis	20

*We dedicate the review to the late Manfred Böhm who introduced us to the field of electroweak radiative corrections.

^{*}Corresponding author

Email addresses: Ansgar.Denner@physik.uni-wuerzburg.de (Ansgar Denner), Stefan.Dittmaier@physik.uni-freiburg.de (Stefan Dittmaier)

2.4.2	Translation to the physical basis	22
2.4.3	Applications	24
3	Electroweak radiative corrections—virtual effects	25
3.1	Renormalization of the Electroweak Standard Model in the on-shell scheme	25
3.1.1	Historical development and variants	25
3.1.2	Renormalization transformation in the on-shell scheme	26
3.1.3	Renormalization conditions	27
3.1.4	Charge renormalization	29
3.1.5	Renormalization of the quark-mixing matrix	29
3.1.6	Tadpole renormalization	30
3.1.7	Explicit form of the renormalization constants for parameters and fields in the physical basis	34
3.1.8	Renormalization of the unphysical sector	36
3.2	Renormalization within the background-field method	37
3.3	Renormalization of QCD	39
3.4	Techniques for electroweak one-loop calculations	40
3.4.1	Dimensional versus mass regularization	40
3.4.2	The γ_5 problem	41
3.4.3	Tensor-integral reduction	43
3.4.4	Reduction of tensor integrals at the integrand level	48
3.4.5	The OPP method	50
3.4.6	Scalar one-loop integrals	53
3.4.7	Purely numerical methods	54
3.5	Automation and tools	54
3.5.1	Conventional approach	57
3.5.2	RECOLA	59
3.5.3	OPENLOOPS	61
3.5.4	MADGRAPH	62
4	Electroweak radiative corrections—real emission effects	65
4.1	Infrared divergences in real electroweak corrections	65
4.1.1	Soft singularities	65
4.1.2	Collinear singularities	66
4.2	Techniques for calculating real electroweak corrections	69
4.2.1	Two-cutoff slicing	70
4.2.2	Dipole subtraction	74
4.3	Electromagnetic corrections to parton distribution functions	82
4.3.1	Factorization of photonic initial-state singularities	82
4.3.2	QED-corrected PDFs and photon distribution function	85
4.3.3	Photon-induced processes	86
4.4	Photon-jet systems	87
4.4.1	Photon-jet separation	87
4.4.2	Photon-to-jet conversion	89
4.5	Radiation effects in lepton-photon systems	90
4.5.1	Prominent features of radiation effects	90
4.5.2	QED structure functions to higher orders	93
4.5.3	QED structure functions versus parton showers	96

5 Electroweak radiative corrections—general features	96
5.1 Input-parameter schemes	96
5.1.1 The $\alpha(0)$, $\alpha(M_Z^2)$, and G_μ schemes	97
5.1.2 $\overline{\text{MS}}$ scheme and running couplings	99
5.2 The structure of NLO electroweak corrections	102
5.2.1 EW and QCD corrections for general processes	102
5.2.2 Disentangling weak and electromagnetic corrections	103
5.3 Goldstone-boson equivalence theorem	104
5.4 Electroweak corrections at high energies	106
5.4.1 General results for one-loop electroweak logarithmic corrections	107
5.4.2 Resummation of EW double-logarithmic corrections	114
5.4.3 EW logarithmic corrections from Soft-Collinear Effective Theory	118
5.4.4 EW logarithmic corrections for practical calculations	120
6 Issues with unstable particles	122
6.1 Unstable particles and resonances	122
6.2 Narrow-width approximation and naive width schemes	124
6.3 The issue of gauge invariance	126
6.4 Mass and width of unstable particles	126
6.5 Pole scheme and pole approximation	127
6.5.1 Pole scheme—general idea and subtleties	127
6.5.2 Weak corrections to Drell–Yan-like Z-boson production in the pole scheme	129
6.5.3 Pole approximation	131
6.5.4 NLO EW corrections to Drell–Yan-like Z-boson production in the pole approximation	134
6.5.5 Multiple resonances in pole approximation and gauge-boson pair production in double-pole approximation	135
6.6 Complex-mass scheme	139
6.6.1 LO procedure and general properties	139
6.6.2 Complex renormalization	139
6.6.3 Simplified version of the complex renormalization	142
6.6.4 Input parameters to the complex-mass scheme	145
6.6.5 Complex renormalization—background-field method	145
6.7 Further schemes for unstable particles	146
7 Conclusions	148
Appendix A Feynman rules	149
Appendix B Green functions and their generating functionals	165
Appendix C Ward identity for the on-shell $A\bar{f}f$ vertex	167
Acknowledgements	172
References	172

1. Introduction

The Standard Model of particle physics

The *Standard Model (SM) of particle physics* provides a successful theory for three out of the four known interactions of fundamental particles: The strong interaction is described by *Quantum Chromodynamics (QCD)* [1–4], and the description of the electromagnetic and weak interactions is unified in the *Glashow–Salam–Weinberg (GSW) model* of the electroweak (EW) interaction, also called the *Electroweak Standard Model (EWSM)*. In this article we review the salient features of the EWSM and the basic concepts that are required to prepare precise predictions for EW phenomena that can be tested at particle colliders. Since perturbation theory is the method of choice in such precision calculations, *electroweak radiative corrections* are at the heart of this task and represent the main theme of this review. Effects of the strong interaction only play a minor role, and gravitational effects no role in the following.

The modern era of the theory of EW interaction began in the 1960s when the previously suggested phenomenological model of intermediate massive vector bosons was turned into a Yang–Mills gauge theory by Glashow [5], Weinberg [6] and Salam [7]. The obstacle that pure Yang–Mills gauge fields predict massless gauge bosons, but experimental facts require the force carriers of the weak interaction to be massive, was overcome by spontaneously breaking the EW $SU(2)_w \times U(1)_Y$ gauge symmetry down to electromagnetic $U(1)_{\text{em}}$ invariance. This spontaneous symmetry breaking is driven by the gauge interaction with an elementary scalar field that develops a non-vanishing vacuum expectation value (vev)—a mechanism nowadays known as *Brout–Englert–Higgs* or simply *Higgs mechanism* that was actually developed in a series of papers by several groups [8–12]. Specifically, the GSW model employs a complex scalar doublet to break EW symmetry, so that three out of the four scalar degrees of freedom deliver the longitudinal polarizations of the massive weak gauge bosons W^\pm and Z , while the photon remains massless. The fourth scalar degree of freedom corresponds to a neutral, massive boson, the SM *Higgs boson*.

The dynamical generation of masses for the elementary particles¹ by interaction with the Higgs field also offers a solution to another theoretical problem in the fermionic sector of the theory. Owing to observation of parity (P) violation, fermions are *chiral*, i.e. left- and right-handed fermions interact differently with the weak gauge bosons, a fact that forbids the introduction of plain fermion mass terms in the underlying Lagrangian due to the gauge-invariance requirement. The so-called *Yukawa couplings* between left- and right-handed fermions and the Higgs doublet introduce both fermion masses and Higgs-boson–fermion interactions in a consistent manner. For leptons, this structure was already part of the original GSW model, where neutrinos were taken as massless.² The description of hadronic degrees of freedom in EW interactions was suggested by Glashow, Iliopoulos and Maiani [16] in the early 1970s. Up to currently achievable energies (TeV range), both leptons and quarks appear in three generations. In particular, from the experiments at LEP1 we know that there are exactly three with light neutrinos [17, 18]. While leptons of different generations do not mix as long as neutrinos are mass degenerate (e.g. if taken massless), mixing of the three quark generations occurs and is extremely well described by the *Cabibbo–Kobayashi–Maskawa (CKM) matrix* [19, 20], which contains the only source of CP violation in the SM. Note that the introduction of fermion masses via Yukawa couplings to the single Higgs doublet field leads to a distinctive phenomenological imprint in the coupling structure, i.e. all fermionic couplings to the Higgs boson are proportional to the mass of the corresponding fermion.

The breakthrough of the SM came in the early 1970s with the proof of the renormalizability of gauge theories with and without spontaneous symmetry breaking given by 't Hooft and Veltman [21–24] and Lee and Zinn-Justin [25–28]. Moreover, the fermionic matter content of the SM renders the model anomaly free. In summary, the SM is a mathematically consistent quantum field theory, a fact that serves as our basis to work out predictions for collider experiments at a level of precision that is essentially only limited by our technical capabilities to evaluate higher orders in perturbation theory and by the level to which we can extract necessary non-perturbative information (parton distribution functions, hadronic vacuum polarization, etc.) from experiment.

Electroweak precision tests and theoretical concepts

After their discovery at the UA1 and UA2 experiments in 1983 [29–32], the precise experimental investigation of the

¹In this context *elementary* means *point-like*, in contrast to composite particles like nucleons. For the latter, the binding energy even delivers the major part of the mass.

²The observation of neutrino oscillations [13–15] requires the introduction of neutrino masses, which are usually not considered part of the EWSM. These are, however, irrelevant for physics at high-energy colliders and not considered in this review.

EW gauge bosons started at the CERN Large Electron–Positron Collider (LEP) and at the Stanford Linear Collider (SLC) at SLAC in the late 1980s. In the first LEP phase (LEP1, 1989–1995) and at the SLC, millions of Z bosons were produced as s -channel resonances, i.e. in the reaction $e^+e^- \rightarrow Z/\gamma^* \rightarrow f\bar{f}$, providing extremely precise measurements of the Z-boson mass, decay widths, cross sections, and asymmetries. From these observables, pseudo-observables such as effective couplings of the Z boson to various fermions were deduced, in particular the *effective weak mixing angle* which determines the EW coupling strength at the Z-boson resonance. On the theory side, the concepts for perturbative precision calculations had to be worked out, a process that started in the late 1970s with technical articles from 't Hooft and Veltman [33] and Passarino and Veltman [34], and that produced the concept of renormalization in the EWSM in different formulations [35–40] in the work-up and early phase of LEP1 and the SLC. Moreover, a concept was worked out to describe the Z-boson resonance and its (pseudo-)observables to high precision (see, for instance, the reviews [41–44] and references therein).

The second phase of LEP (LEP2, 1996–2000), provided first direct experimental access to the non-abelian gauge-boson interactions between photons, Z, and W bosons as well as precision measurements of the W-boson mass via the reaction $e^+e^- \rightarrow W^+W^- \rightarrow 4f$ above the W-boson pair production threshold. On the theory side, this implied more challenges, too. Precision calculations for four (and more) particles in the final state triggered great advances in the development of Monte Carlo integrators and generators (see, e.g., Refs. [45, 46]). In particular, the technique of adaptive *multi-channel Monte Carlo integration* [47–50] was developed, the method that has served as basis for almost all major Monte Carlo generators for collider experiments in the previous two decades. Moreover, the inclusion of real-emission effects in the description of multi-particle processes lead to more involved patterns in the structure of infrared (IR) singularities caused by phase-space regions of soft and/or collinear photon (or QCD parton) emission. To resolve this issue, techniques to isolate IR singularities via *phase-space slicing* [51, 52] or *subtraction* [53–55] were further developed and formulated in an algorithmic way that allows for automated evaluation. Finally, a more general concept for describing resonances in combination with radiative corrections but without violating basic principles like gauge invariance was required. Systematic expansions of matrix elements about the resonance poles [56, 57] and approximations based on the leading terms provided a successful framework for describing W-pair production at LEP2 (see, e.g., Ref. [46]), but also triggered further developments towards a *theory of unstable particles*. The most flexible method that emerged from this learning process, in our view, is the *complex-mass scheme* [58, 59], which provides a gauge-invariant, uniform description of cross sections in resonant and non-resonant regions at next-to-leading order (NLO) in perturbation theory.

After the millennium, the $p\bar{p}$ collider Tevatron at Fermilab continued and further tightened the EW precision tests, in particular, by providing precision measurements of the W-boson and top-quark masses. The SM passed all those tests with very little tension between observations and predictions (see, e.g., Refs. [60, 61]). It should be emphasized that this agreement between experiment and theory was (and still is) only seen if higher-order radiative corrections of QCD and EW origin are properly taken into account in predictions, i.e. the SM is truly tested as quantum field theory. The major outcome of the SM fit to all precision data was a prediction of a preferred range for the mass of the Higgs boson well before its discovery in 2012 by the ATLAS [62] and CMS [63] collaborations at the CERN Large Hadron Collider (LHC).

Electroweak phenomenology and theory challenges in the LHC era

Among the global search for new phenomena and the detailed confrontation of all observations with SM predictions, one of the central questions of present-day particle physics is whether or to which extent the discovered Higgs boson represents the SM Higgs boson. Or more generally, is EW symmetry breaking realized in nature as described by the Higgs mechanism; if so, is the Higgs sector realized in the minimal form as in the SM, or are there more Higgs bosons; if not, what is the right formulation of EW symmetry breaking, and what is the role of the discovered Higgs boson in it; is the observed Higgs boson a composite state, etc.? Since practically all SM extensions modify the sector of EW symmetry breaking of the SM, Higgs-boson physics is certainly the right place to look for potential deviations from the SM. Up to now, no significant discrepancies between observed properties of the Higgs boson (production cross sections, decay branching ratios, Higgs couplings) and SM predictions have been found, showing that any potential differences are small and subtle. Given the fact that no spectacular signals of physics beyond the SM are in sight, the ultimate answer to this question can only be given via *precision* in theory and experiment [64–67].

Again, switching from EW physics at LEP, the SLC, and Tevatron to the LHC, brought further theoretical challenges. While only a few processes at Tevatron, such as the Drell–Yan-like production of Z or W bosons, required the

inclusion of EW radiative corrections in predictions, the higher luminosity and the deeper energy reach of the LHC render EW corrections to all major processes important or at least relevant in the upcoming high-luminosity phase. For a proper account of EW corrections, their consistent inclusion in the perturbative evaluation of cross sections in the QCD-improved parton model for hadronic collisions is necessary. In particular, the photon appears as additional parton in the colliding protons with an own photon distribution function. Moreover, multi-particle final states play a much more important role at the LHC. On the one hand, the higher scattering energy at the LHC globally leads to higher jet multiplicities in association with any signature of colour-neutral particles, and the number of partonic channels grows enormously. On the other hand, new interesting classes of EW processes with multi-particle final states become accessible, including EW vector-boson scattering, $pp \rightarrow 4l + 2 \text{ jets} + X$, or triple-EW-gauge-boson production such as $pp \rightarrow WWW \rightarrow 3l/3\nu + X$. To make one-loop calculations of such multi-particle amplitudes possible and numerically efficient, it was necessary to develop techniques and automated amplitude generators that are not based on individual Feynman diagrams anymore, but proceed recursively on the basis of appropriate substructures of amplitudes such as off-shell currents or subamplitudes based on generalized unitarity. For the automated calculation of NLO EW corrections, the programs **MADLoop** [68], **OPENLOOPS** [69–71], and **RECOLA** [72, 73] are the most powerful amplitude generators, which can deal with up to $\sim 8\text{--}9$ external particles in one-loop amplitudes.

Structure of the review

The above statements have illustrated how the conceptual and technical progress towards EW precision for present-day collider physics step by step came along with new collider experiments with increasing precision and energy reach. We are not aware of any comprehensive document or textbook that collects the corresponding theoretical progress of the previous 30 years in the field of EW radiative corrections in a coherent form. This situation renders it particularly difficult for newcomers to grow into the field; typically they have to read series of papers with some redundancy or with gradual improvements or generalizations from paper to paper. It is the aim of this review to improve on this situation by presenting the major concepts for the calculation of EW corrections in a unified manner. Of course, some disclaimer is in order at this point. No review can be fully comprehensive, and the selection of topics and their emphasis is necessarily subjective to some extent. We have tried to be as complete as possible, and if we did not spell out all techniques, methods, or concepts in detail, we at least intend to give the most important references for alternatives. Generally, we put more emphasis on topics, both theoretical and phenomenological, where we see the more urgent need in the literature. For further links to the current research frontier in higher-order calculations and phenomenological applications, we recommend to consult dedicated working-group reports like those of the Les Houches workshops on TeV colliders [74–76], of the LHC Higgs Cross Section Working Group [64–67], or reviews and books on phenomenological applications like Refs. [77–81].

In detail, the structure of the review is as follows:

- In Section 2 we introduce the SM, defining all sectors in detail. Its quantization is performed with the standard Faddeev–Popov method and, alternatively, employing background-field quantization, which is beneficial for some subsequent sections where gauge-invariance properties play a role. Moreover, some Slavnov–Taylor identities are recalled that are used in the renormalization and in the formulation of the Goldstone-boson equivalence theorem. Finally, Section 2 concludes with a brief introduction to the *Standard Model Effective Theory* which is used in current analyses of LHC data to look for potential deviations from SM predictions in a widely model-independent way.
- Section 3 provides an introduction to various concepts and techniques for the calculation of virtual one-loop EW corrections. We provide a detailed description of one-loop renormalization of the EWSM in the on-shell scheme both in the conventional and in the background-field formalism and discuss techniques for calculating one-loop integrals. Moreover, methods for evaluating one-loop amplitudes and different one-loop amplitude generators are briefly introduced.
- Section 4 turns to real-emission corrections, starting from a general discussion of the IR (soft and collinear) limits of one-particle emission amplitudes relevant for NLO EW calculations and followed by a brief introduction into the techniques of *two-cutoff slicing* and *dipole subtraction* for the isolation of IR singularities in real EW corrections. Subsequently, we turn to specific issues connected with hadrons in the initial or final states of collisions: electromagnetic corrections to parton distribution functions and the separation of photons and jets in the final state. Finally, we end the section with a discussion of enhanced photonic corrections induced by collinear photon–lepton splittings and the evolution of their leading logarithmic behaviour beyond NLO.

- Section 5 is devoted to some general aspects of EW NLO corrections. We discuss the EW input-parameter schemes and the possibilities to classify EW corrections into gauge-independent subcontributions. We sketch the Goldstone-boson equivalence theorem including the correction factors appearing in higher orders. Section 5 closes with a discussion of the structure of EW corrections at high scattering energies, which is particularly important for new-particle searches at the LHC.
- Section 6 picks up the issue of unstable particles in quantum field theory and methods to describe resonances in perturbative calculations. The discussion starts with a description of the general problem, the naive *narrow-width approximation* and possible improvements, the issue of gauge invariance, and the precise definition of mass and width of a resonance in perturbation theory. The rest of the section is devoted to the most frequently applied schemes to treat resonances in EW higher-order calculations: the *pole scheme* and *pole approximation*, the *complex-mass scheme*, and brief comments on further schemes.
- In Section 7 we give our conclusions and a brief outlook.
- The appendices provide further useful details, such as a complete set of Feynman rules for the SM, our conventions for Green functions, as well as a derivation of the Ward identity used to simplify the renormalization of the electric charge.

2. The Standard Model of particle physics

2.1. Lagrangian of the Standard Model

We formulate the classical Lagrangian of the EWSM in a form in which the gauge symmetry is manifest and then pass to the representation in terms of fields corresponding to charge and mass eigenstates and experimentally accessible parameters so that its particle content and the physical meaning of its free parameters become visible. In the following we refer to this form as “physical basis” of fields and parameters.

2.1.1. Lagrangian of the Electroweak Standard Model in the symmetric basis

As the gauge group is not simple but rather a product of $SU(2)_w$ and $U(1)_Y$, EW interactions are described by two *gauge coupling constants*: g_2 for the *weak isospin* group $SU(2)_w$ and g_1 for the *weak hypercharge* group $U(1)_Y$. We denote the three generators of weak isospin by I_w^a ($a = 1, 2, 3$) and the generator of weak hypercharge by Y_w . The generator Q of the electric charge is defined via the Gell-Mann–Nishijima relation

$$Q = I_w^3 + \frac{Y_w}{2}. \quad (1)$$

According to the dimension of the gauge group $SU(2)_w \times U(1)_Y$ there are four EW gauge fields, which transform according to the adjoint representation. The gauge fields belonging to the weak-isospin group $SU(2)_w$ are denoted $W_\mu^a(x)$ and the one belonging to the weak-hypercharge group $U(1)_Y$ is called $B_\mu(x)$. The corresponding field strengths read

$$B_{\mu\nu} = \partial_\mu B_\nu - \partial_\nu B_\mu, \quad W_{\mu\nu}^a = \partial_\mu W_\nu^a - \partial_\nu W_\mu^a + g_2 \epsilon^{abc} W_\mu^b W_\nu^c, \quad (2)$$

where ϵ^{abc} are the totally antisymmetric structure constants of $SU(2)$. The gauge interaction of the matter fields is determined by the covariant derivative³

$$D_\mu = \partial_\mu - ig_2 I_w^a W_\mu^a + ig_1 \frac{Y_w}{2} B_\mu. \quad (3)$$

In order to generate mass terms for the weak gauge bosons, the Higgs mechanism is employed to break the $SU(2)_w \times U(1)_Y$ symmetry in such a way that the electromagnetic symmetry $U(1)_{\text{em}}$ remains exact. To this end, a

³ We adopt the conventions of Refs. [38, 40, 82, 83]. Different sign conventions are used in the literature. Often the form $D_\mu = \partial_\mu + ig_2 I_w^a W_\mu^a + ig_1 \frac{Y_w}{2} B_\mu$ is used [84, 85], which differs in the sign of the $SU(2)_w$ gauge fields W_μ^a . In the field basis corresponding to charge and mass eigenstates this corresponds to a sign change in the W^\pm and Z fields. Peskin and Schroeder [86] and Schwartz [87], on the other hand, use the convention $D_\mu = \partial_\mu - ig_2 I_w^a W_\mu^a - ig_1 \frac{Y_w}{2} B_\mu$, which is related to our convention by a sign change in the $U(1)_Y$ gauge field B_μ and the photon field A_μ . Parameter relations are not affected by these transformations. However, the signs of Feynman rules and Green functions change.

weak-isospin doublet $\Phi(x)$ of two complex scalar fields, the Higgs doublet, is introduced which couples in a gauge-invariant way to the vector bosons ($I_w^a = \tau^a/2$ with Pauli matrices τ^a , $a = 1, 2, 3$). To allow for an electrically neutral component with non-vanishing *vacuum expectation value* (vev), its hypercharge must be $Y_{w,\Phi} = \pm 1$. Using the convention $Y_{w,\Phi} = +1$, we can write the Higgs doublet as $\Phi(x) = (\phi^+(x), \phi^0(x))^T$, where the upper indices indicate the electric charges of the components fixed by the Gell-Mann–Nishijima relation (1). The choice of a weak-isospin doublet with hypercharge $Y_{w,\Phi} = \pm 1$ also allows for *Yukawa couplings*, i.e. gauge-invariant couplings between scalar and fermion fields, which are necessary for the generation of fermion masses via spontaneous symmetry breaking.

The left-handed fermions of each lepton (L) and quark (Q) generation are grouped into $SU(2)_w$ doublets (we suppress the colour index of the quark fields)

$$L'_j^L = \omega_- L'_j = \begin{pmatrix} v'_j^L \\ l'_j^L \end{pmatrix}, \quad Q'_j^L = \omega_- Q'_j = \begin{pmatrix} u'_j^L \\ d'_j^L \end{pmatrix} \quad (4)$$

with representation matrices $I_w^a = \tau^a/2$, and the right-handed fermions into singlets ($I_w^a = 0$)

$$l'_j^R = \omega_+ l'_j, \quad u'_j^R = \omega_+ u'_j, \quad d'_j^R = \omega_+ d'_j, \quad (5)$$

where

$$\omega_{\pm} = \frac{1}{2}(1 \pm \gamma_5) \quad (6)$$

is the projector on right- and left-handed fields, respectively, $j = 1, 2, 3$ is the generation index, and v , l , u , and d stand for neutrinos, charged leptons, up-type quarks, and down-type quarks, respectively. The weak hypercharges of the right- and left-handed multiplets are chosen in such a way that the known electric charges of the fermions are reproduced by the Gell-Mann–Nishijima relation (1), leading to

$$\begin{aligned} Y_{w,L,i} + 1 &= 2Q_{v,i} = 0, & Y_{w,l,i} &= Y_{w,L,i} - 1 = 2Q_{l,i} = -2, \\ Y_{w,u,i} + 1 &= 2Q_{u,i} = \frac{4}{3}, & Y_{w,d,i} &= Y_{w,Q,i} - 1 = 2Q_{d,i} = -\frac{2}{3}. \end{aligned} \quad (7)$$

We do not include right-handed neutrinos, since these are irrelevant for collider physics.⁴ The primes at the fermion fields indicate eigenstates of the EW interaction, i.e. the covariant derivatives are diagonal with respect to the generation indices in this basis. These states are not necessarily mass eigenstates. Because left- and right-handed fields transform according to different representations of the symmetry group $SU(2)_w \times U(1)_Y$, the theory is chiral, and explicit mass terms for the fermions are forbidden.

The classical Lagrangian $\mathcal{L}_{\text{class}}$ of the GSW theory consists of all renormalizable terms that respect the $SU(2)_w \times U(1)_Y$ symmetry:

$$\begin{aligned} \mathcal{L}_{\text{class}} = & -\frac{1}{4}B_{\mu\nu}B^{\mu\nu} - \frac{1}{4}W_{\mu\nu}^aW^{a,\mu\nu} \\ & + (D_\mu\Phi)^\dagger(D^\mu\Phi) + \mu^2(\Phi^\dagger\Phi) - \frac{\lambda}{4}(\Phi^\dagger\Phi)^2 \\ & + \sum_i (\bar{L}'_i^L i\cancel{D} L'_i^L + \bar{Q}'_i^L i\cancel{D} Q'_i^L) + \sum_i (\bar{l}'_i^R i\cancel{D} l'_i^R + \bar{u}'_i^R i\cancel{D} u'_i^R + \bar{d}'_i^R i\cancel{D} d'_i^R) \\ & - \sum_{i,j} (\bar{L}'_i^L G_{ij}^l l'_j^R \Phi + \bar{Q}'_i^L G_{ij}^u u'_j^R \Phi^c + \bar{Q}'_i^L G_{ij}^d d'_j^R \Phi + \text{h.c.}), \end{aligned} \quad (8)$$

where h.c. means hermitean conjugate. The first line of Eq. (8) represents the pure gauge-field Lagrangian. The second line describes the kinetic terms of the scalar doublet, its interaction with the gauge fields, and the *Higgs potential*, involving the quartic coupling λ , which is positive as required by vacuum stability, and the mass parameter μ^2 . The third line summarizes the kinetic terms of the fermions and their gauge interaction. Finally, the last line represents

⁴Right-handed Dirac neutrinos can be easily included in the SM without affecting its basic structure. This is in fact necessary in order to allow for the description of the experimental results on neutrino oscillations. However, if the right-handed neutrinos are Majorana particles, additional Majorana mass terms appear (see, for instance, Refs. [88–90]).

the Yukawa interactions of the scalar doublet with the fermions, where G^f denote Yukawa coupling matrices. Since the two-dimensional representation of $SU(2)$ is equivalent to its complex conjugate representation, the scalar doublet allows for Yukawa couplings to down-type right-handed fermion fields via Φ and to up-type right-handed fermion fields via the charge-conjugate field

$$\Phi^c(x) = i\tau^2 \Phi^* = (\phi^{0*}(x), -\phi^-(x))^T. \quad (9)$$

For $\mu^2 > 0$, the Higgs field acquires a non-vanishing vev that leads to mass terms for the gauge bosons and—arising from the Yukawa couplings—also for the fermions.

The Lagrangian (8) is invariant under the infinitesimal *gauge transformations*,

$$\begin{aligned} W_\mu^a(x) &\rightarrow W_\mu^a(x) + \partial_\mu \delta\theta^a(x) + \epsilon^{abc} g_2 W_\mu^b \delta\theta^c(x), \\ B_\mu(x) &\rightarrow B_\mu(x) + \partial_\mu \delta\theta^Y(x), \\ \Phi(x) &\rightarrow \left[1 - i\frac{1}{2}g_1 \delta\theta^Y(x) + i\frac{\tau^a}{2} g_2 \delta\theta^a(x) \right] \Phi(x), \\ F'_i^L(x) &\rightarrow \left[1 - i\frac{Y_{w,F,i}}{2} g_1 \delta\theta^Y(x) + i\frac{\tau^a}{2} g_2 \delta\theta^a(x) \right] F'_i^L(x), \quad F = L, Q, \\ f'_i^R(x) &\rightarrow \left[1 - i\frac{Y_{w,f,i}}{2} g_1 \delta\theta^Y(x) \right] f'_i^R(x), \quad f = l, u, d, \end{aligned} \quad (10)$$

where $\delta\theta^a$ and $\delta\theta^Y$ are the parameters of the gauge transformations corresponding to the groups $SU(2)_w$ and $U(1)_Y$, respectively.⁵

The Lagrangian $\mathcal{L}_{\text{class}}$ depends on the two gauge couplings g_1 and g_2 , the Yukawa couplings G_{ij}^f , and the parameters μ^2 and λ of the scalar potential.

2.1.2. Lagrangian of the Electroweak Standard Model in the physical basis

The scalar-field self-interaction is chosen in such a way that the classical ground state appears for non-vanishing scalar field, i.e. the scalar potential has a minimum for

$$|\langle \Phi \rangle|^2 = \frac{2\mu^2}{\lambda} = \frac{v^2}{2} \neq 0. \quad (11)$$

We choose a ground state Φ_0 that is annihilated by the electric charge operator Q ,

$$Q\Phi_0 = \left(\frac{\tau^3}{2} + \frac{1}{2} Y_{w,\Phi} \right) \Phi_0 = \begin{pmatrix} 1 & 0 \\ 0 & 0 \end{pmatrix} \Phi_0 = 0, \quad (12)$$

so that the remaining (unbroken) symmetry is the one of electromagnetic gauge transformations $U(1)_{\text{em}}$. Using the solution of Eqs. (11) and (12),

$$\Phi_0 = \begin{pmatrix} 0 \\ \frac{v}{\sqrt{2}} \end{pmatrix}, \quad (13)$$

which is unique up to a phase, we can parametrize the scalar doublet as

$$\Phi(x) = \begin{pmatrix} \phi^+(x) \\ \frac{1}{\sqrt{2}}[v + H(x) + i\chi(x)] \end{pmatrix}, \quad \phi^-(x) = [\phi^+(x)]^\dagger, \quad (14)$$

where $v > 0$ and $H(x), \chi(x)$, and $\phi^\pm(x)$ have vanishing vev. The fields $\phi^+(x), \phi^-(x)$, and $\chi(x)$, the *would-be Goldstone fields*, turn out to be unphysical degrees of freedom and can be eliminated by a transition to the *unitary gauge*, where $\phi^\pm = \chi = 0$ and the physical content of the EWSM can be extracted most easily.

⁵The signs of the parameters $\delta\theta$ are linked to the corresponding fields and should be adapted to different conventions analogously as specified in footnote 3.

The physical degrees of freedom can be classified as eigenstates of electric charge and mass. Inserting Eq. (14) into the Lagrangian Eq. (8) and diagonalizing the resulting mass matrices one obtains the following fields corresponding to mass eigenstates

$$W_\mu^\pm = \frac{1}{\sqrt{2}} (W_\mu^1 \mp i W_\mu^2), \quad \begin{pmatrix} Z_\mu \\ A_\mu \end{pmatrix} = \begin{pmatrix} c_w & s_w \\ -s_w & c_w \end{pmatrix} \begin{pmatrix} W_\mu^3 \\ B_\mu \end{pmatrix},$$

$$f_i^L = \sum_k U_{ik}^{f,L} f_k^L, \quad f_i^R = \sum_k U_{ik}^{f,R} f_k^R, \quad (15)$$

where

$$c_w = \cos \theta_w = \frac{g_2}{\sqrt{g_2^2 + g_1^2}}, \quad s_w = \sin \theta_w, \quad (16)$$

with the *weak mixing angle* θ_w , and f stands for ν , l , u , or d . The resulting masses read

$$M_W = \frac{1}{2} g_2 v, \quad M_Z = \frac{1}{2} \sqrt{g_1^2 + g_2^2} v, \quad m_\gamma = 0,$$

$$M_H = \sqrt{2\mu^2} = \sqrt{\frac{\lambda}{2}} v, \quad m_{f,i} = \frac{v}{\sqrt{2}} \sum_{k,m} U_{ik}^{f,L} G_{km}^f U_{mi}^{f,R\dagger}, \quad (17)$$

where M_H is the mass of the *Higgs boson*. The mass terms for the fermions result from the Yukawa interactions and can be diagonalized by a bi-unitary transformation with $U_{ik}^{f,L}$ and $U_{ik}^{f,R}$ for left-handed and right-handed fermion fields, respectively [see Eq. (15)]. The neutrinos stay massless in accordance with the absence of right-handed neutrinos. With Eqs. (16) and (17) we find

$$c_w = \frac{M_W}{M_Z} \quad (18)$$

for the weak mixing angle. The photon remains massless as a consequence of the unbroken electromagnetic gauge invariance.

After diagonalization of the fermion mass matrices, the interaction of the Higgs field $H(x)$ with fermions is diagonal in flavour space, and the associated couplings $m_{f,i}/v$ are proportional to the fermion masses.

The W-boson fields transform according to the adjoint representation of $SU(2)_w$ (i.e. $I_w = 1$, $Y_w = 0$), and the fields defined in Eq. (15) correspond to eigenstates of the electric charge operator, since

$$QW_\mu^\pm(x) = I_w^3 W_\mu^\pm(x) = \pm W_\mu^\pm(x), \quad QZ_\mu(x) = QA_\mu(x) = 0. \quad (19)$$

Thus, we have one positively charged gauge boson, W^+ , one negatively charged one, W^- , and two neutral ones, Z and γ .

Identifying the coupling of the photon field A_μ to the fermions with their electrical charge $Q_f e$ we can relate the coupling constants g_1 and g_2 to the elementary charge e ,

$$\sqrt{4\pi\alpha} = e = \frac{g_1 g_2}{\sqrt{g_1^2 + g_2^2}} = g_2 s_w = g_1 c_w, \quad (20)$$

with $\alpha = \alpha(0) = 1/137.0 \dots$ denoting the fine-structure constant.

Owing to their unitarity, the matrices $U_{ik}^{f,L}$ and $U_{ik}^{f,R}$ drop out in the interaction terms of fermions and neutral gauge bosons, i.e. there are no flavour-changing neutral currents at tree level. In the quark–W-boson interaction a non-trivial matrix remains, the unitary *quark-mixing matrix* or *Cabibbo–Kobayashi–Maskawa matrix* [20]

$$V = U^{u,L} U^{d,L\dagger}. \quad (21)$$

Since we do not include right-handed neutrinos, all neutrinos remain massless and thus mass degenerate, and we can choose $U^{\nu,L} = U^{l,L}$ to eliminate the mixing matrix in the lepton–W-boson interaction rendering their charged-current interaction flavour diagonal.⁶

⁶If one includes right-handed neutrinos, a mixing matrix in the lepton sector appears, the *Pontecorvo–Maki–Nakagawa–Sakata (PMNS) matrix* [91, 92].

Replacing the original set of parameters and fields by the “physical parameters” e , M_W , M_Z , M_H , $m_{f,i}$, and V_{ij} and by the fields corresponding to charge and mass eigenstates, A_μ , Z_μ , W_μ^\pm , H , l , v , u , d , and the would-be Goldstone fields ϕ^\pm and χ , we can write the complete classical Lagrangian $\mathcal{L}_{\text{class}}$ of the EWSM as follows:

$$\begin{aligned}
\mathcal{L}_{\text{class}} = & \sum_{f=l,v,u,d} \sum_i \left(\bar{f}_i (\mathbf{i}\not{\partial} - m_{f,i}) f_i - e Q_f \bar{f}_i \gamma^\mu f_i A_\mu \right) + \sum_{f=l,v,u,d} \sum_i \frac{e}{s_w c_w} \left(I_{w,f}^3 \bar{f}_i^L \gamma^\mu f_i^L - s_w^2 Q_f \bar{f}_i \gamma^\mu f_i \right) Z_\mu \\
& + \sum_{i,j} \frac{e}{\sqrt{2} s_w} \left(\bar{u}_i^L \gamma^\mu V_{ij} d_j^L W_\mu^+ + \bar{d}_i^L \gamma^\mu V_{ij}^\dagger u_j^L W_\mu^- \right) + \sum_i \frac{e}{\sqrt{2} s_w} \left(\bar{v}_i^L \gamma^\mu l_i^L W_\mu^+ + \bar{l}_i^L \gamma^\mu v_i^L W_\mu^- \right) \\
& - \frac{1}{4} \left(\partial_\mu A_\nu - \partial_\nu A_\mu - ie (W_\mu^- W_\nu^+ - W_\nu^- W_\mu^+) \right)^2 - \frac{1}{4} \left(\partial_\mu Z_\nu - \partial_\nu Z_\mu + ie \frac{c_w}{s_w} (W_\mu^- W_\nu^+ - W_\nu^- W_\mu^+) \right)^2 \\
& - \frac{1}{2} \left| \partial_\mu W_\nu^+ - \partial_\nu W_\mu^+ - ie (W_\mu^+ A_\nu - W_\nu^+ A_\mu) + ie \frac{c_w}{s_w} (W_\mu^+ Z_\nu - W_\nu^+ Z_\mu) \right|^2 \\
& + \frac{1}{2} \left| \partial_\mu (H + i\chi) - i \frac{e}{s_w} W_\mu^- \phi^+ + i M_Z Z_\mu + i \frac{e}{2 c_w s_w} Z_\mu (H + i\chi) \right|^2 \\
& + \left| \partial_\mu \phi^+ + ie A_\mu \phi^+ - ie \frac{c_w^2 - s_w^2}{2 c_w s_w} Z_\mu \phi^+ - i M_W W_\mu^+ - i \frac{e}{2 s_w} W_\mu^+ (H + i\chi) \right|^2 \\
& - \frac{1}{2} M_H^2 H^2 - e \frac{M_H^2}{2 s_w M_W} H \left(\phi^- \phi^+ + \frac{1}{2} |H + i\chi|^2 \right) - e^2 \frac{M_H^2}{8 s_w^2 M_W^2} \left(\phi^- \phi^+ + \frac{1}{2} |H + i\chi|^2 \right)^2 \\
& - \sum_{f=l,u,d} \sum_i \frac{m_{f,i}}{2 s_w M_W} \left(\bar{f}_i f_i H - 2 I_{w,f}^3 \bar{f}_i \gamma_5 f_i \chi \right) \\
& + \sum_{i,j} \frac{e}{\sqrt{2} s_w M_W} \left[m_{u,i} \bar{u}_i^R V_{ij} d_j^L \phi^+ + m_{u,j} \bar{d}_i^L V_{ij}^\dagger u_j^R \phi^- - m_{d,j} \bar{u}_i^L V_{ij} d_j^R \phi^+ - m_{d,i} \bar{d}_i^R V_{ij}^\dagger u_j^L \phi^- \right] \\
& - \sum_i \frac{e}{\sqrt{2} s_w M_W} m_{l,i} \left(\bar{v}_i^L l_i^R \phi^+ + \bar{l}_i^R v_i^L \phi^- \right), \tag{22}
\end{aligned}$$

where we have omitted an irrelevant constant term. Here $I_{w,f}^3$ and Q_f are the third component of the weak isospin and the relative charge of the fermion f , respectively.

The Lagrangian (22) is invariant under gauge transformations that follow from Eq. (10) by inserting the fields and parameters of the physical basis,

$$\begin{aligned}
\delta A_\mu &= \partial_\mu \delta \theta^A + ie (W_\mu^+ \delta \theta^- - W_\mu^- \delta \theta^+), \\
\delta Z_\mu &= \partial_\mu \delta \theta^Z - ie \frac{c_w}{s_w} (W_\mu^+ \delta \theta^- - W_\mu^- \delta \theta^+), \\
\delta W_\mu^\pm &= \partial_\mu \delta \theta^\pm \mp i \frac{e}{s_w} \left[W_\mu^\pm \left(s_w \delta \theta^A - c_w \delta \theta^Z \right) - (s_w A_\mu - c_w Z_\mu) \delta \theta^\pm \right], \\
\delta H &= \frac{e}{2 s_w c_w} \chi \delta \theta^Z + \frac{ie}{2 s_w} (\phi^+ \delta \theta^- - \phi^- \delta \theta^+), \\
\delta \chi &= -\frac{e}{2 s_w c_w} (v + H) \delta \theta^Z + \frac{e}{2 s_w} (\phi^+ \delta \theta^- + \phi^- \delta \theta^+), \\
\delta \phi^\pm &= \mp ie \phi^\pm \left(\delta \theta^A - \frac{c_w^2 - s_w^2}{2 c_w s_w} \delta \theta^Z \right) \pm \frac{ie}{2 s_w} (v + H \pm i\chi) \delta \theta^\pm, \\
\delta F_{\pm,i}^L &= -ie \left[Q_\pm \delta \theta^A + \frac{s_w}{c_w} \left(Q_\pm \mp \frac{1}{2 s_w^2} \right) \delta \theta^Z \right] F_{\pm,i}^L + i \frac{e}{\sqrt{2} s_w} \delta \theta^\pm \sum_j v_{ij}^\pm F_{\mp,j}^L, \\
\delta f_i^R &= -ie Q_f \left(\delta \theta^A + \frac{s_w}{c_w} \delta \theta^Z \right) f_i^R, \tag{23}
\end{aligned}$$

with the parameters

$$\delta\theta^\pm = \frac{1}{\sqrt{2}} (\delta\theta^1 \mp i\delta\theta^2), \quad \delta\theta^A = c_w\delta\theta^Y - s_w\delta\theta^3, \quad \delta\theta^Z = c_w\delta\theta^3 + s_w\delta\theta^Y \quad (24)$$

of the gauge transformation, the generic fermion fields

$$(F_{+,i}, F_{-,i}) = (u_i, d_i) \quad \text{or} \quad (\nu_i, l_i), \quad (25)$$

and

$$v_{ij}^+ = V_{ij}, \quad v_{ij}^- = V_{ij}^\dagger \quad \text{for quarks,} \quad v_{ij}^\pm = \delta_{ij} \quad \text{for leptons.} \quad (26)$$

2.1.3. Quantization

Quantization of $\mathcal{L}_{\text{class}}$ requires the specification of a gauge. A general linear renormalizable gauge is given by the gauge-fixing functionals

$$C^\pm = \partial^\mu W_\mu^\pm \mp iM_W \xi'_W \phi^\pm, \quad C^Z = \partial^\mu Z_\mu - M_Z \xi'_Z \chi, \quad C^A = \partial^\mu A_\mu \quad (27)$$

and the gauge-fixing Lagrangian

$$\mathcal{L}_{\text{fix}} = -\frac{1}{2\xi_A} (C^A)^2 - \frac{1}{2\xi_Z} (C^Z)^2 - \frac{1}{\xi_W} C^+ C^-. \quad (28)$$

In the '*t Hooft gauge*', where $\xi'_W = \xi_W$ and $\xi'_Z = \xi_Z$ and which is used in the following, the terms involving the would-be Goldstone-boson fields in the gauge-fixing functions are chosen in such a way that they cancel the mixing terms $V_\mu \partial^\mu \phi$ in the classical Lagrangian (22) up to irrelevant total derivatives. On the other hand, these gauge-fixing terms give rise to masses for the would-be Goldstone-boson fields,

$$M_\phi = \sqrt{\xi_W} M_W, \quad M_\chi = \sqrt{\xi_Z} M_Z, \quad (29)$$

and equivalent masses for the scalar components [polarization vector $\varepsilon(k) \propto k$] of the vector-boson fields.

The corresponding Faddeev–Popov ghost Lagrangian is obtained as

$$\mathcal{L}_{\text{FP}} = - \int d^4y \bar{u}^a(x) \frac{\delta C^a(x)}{\delta \theta^b(y)} u^b(y), \quad (30)$$

where $\delta C^a(x)/\delta \theta^b(y)$ is the variation of the gauge-fixing function C^a under infinitesimal gauge transformations characterized by $\theta^b(y)$, and $u^a(x)$, $\bar{u}^a(x)$, $a = A, Z, \pm$, are Faddeev–Popov ghost fields. The masses for the Faddeev–Popov fields coincide with those of the corresponding would-be Goldstone-boson fields.

The '*t Hooft gauge*' leads to propagators that behave as $1/k^2$ for large momenta and thus to a renormalizable Lagrangian for finite values of the gauge parameters ξ_a . For $\xi_a \rightarrow \infty$ the masses of the unphysical degrees of freedom (except for u^A) tend to infinity, the unphysical degrees of freedom decouple, and we are left with the theory in the unitary gauge, where renormalizability is not obvious.

For $\xi_a = 1$, $a = A, Z, W$, the '*t Hooft–Feynman gauge*', pole positions and residues of the longitudinal parts of the gauge-boson propagators coincide with those of the transverse parts, so that $k_\mu k_\nu$ parts of the gauge-boson propagators are absent. Moreover, the masses of the unphysical Faddeev–Popov ghost and would-be Goldstone-boson fields equal those of the corresponding gauge fields in the physical basis. Therefore, the '*t Hooft–Feynman gauge*' is most convenient for practical higher-order calculations.

Adding up all terms of Eqs. (22), (28), and (30), we obtain the complete *quantized Lagrangian* of the EWSM suitable for higher-order calculations,

$$\mathcal{L}_{\text{EW}} = \mathcal{L}_{\text{class}} + \mathcal{L}_{\text{fix}} + \mathcal{L}_{\text{FP}}. \quad (31)$$

The corresponding Feynman rules are given in Appendix A.

2.1.4. Inclusion of QCD

The strong interaction described by the colour gauge group $SU(3)_c$ can be easily incorporated in the SM. We denote the generators of $SU(3)_c$ by T^A , $A = 1, \dots, 8$, and the corresponding gauge fields, the *gluon fields*, by G^A . The gluon gauge field strength reads

$$G_{\mu\nu}^A = \partial_\mu G_\nu^A - \partial_\nu G_\mu^A + g_s f^{ABC} G_\mu^B G_\nu^C, \quad (32)$$

where g_s is the strong gauge coupling and f^{ABC} are the structure constants of $SU(3)$. The covariant derivative (3) is extended to

$$D_\mu = \partial_\mu - ig_s T^A G_\mu^A - ig_2 I_w^a W_\mu^a + ig_1 \frac{Y_w}{2} B_\mu. \quad (33)$$

Quarks transform according to the fundamental representation of $SU(3)_c$ with the generators $T^A = \lambda^A/2$, where λ^A are the Gell-Mann matrices. The leptons, the Higgs-doublet, and the EW gauge fields are singlets with respect to $SU(3)_c$ ($T^A = 0$). Conversely, the gluons do not carry weak isospin and hypercharge.

Apart from the extension of the covariant derivative, the Lagrangian (8) gets an additional kinetic term for the $SU(3)_c$ gauge fields,

$$\mathcal{L}_{\text{class}} \rightarrow \mathcal{L}_{\text{class}} - \frac{1}{4} G_{\mu\nu}^A G^{A,\mu\nu}. \quad (34)$$

Corresponding changes apply to the Lagrangian (22) in the physical basis.

Quantization of the $SU(3)_c$ part requires to include the usual gauge-fixing and Faddeev–Popov ghost terms [83, 86, 87, 93].

2.1.5. θ -terms and strong CP violation

The requirements of $SU(3)_c \times SU(2)_w \times U(1)_Y$ gauge invariance and renormalizability admit the presence of the following terms in the SM Lagrangian (see, e.g., Ref. [87], which is compatible with our conventions in this subsection),

$$\mathcal{L}_\theta = -\theta_{\text{QCD}} \frac{g_s^2}{16\pi^2} \tilde{G}_{\mu\nu}^a G^{a,\mu\nu} - \theta_2 \frac{g_2^2}{16\pi^2} \tilde{W}_{\mu\nu}^a W^{a,\mu\nu} - \theta_1 \frac{g_1^2}{16\pi^2} \tilde{B}_{\mu\nu} B^{\mu\nu} \quad (35)$$

with the dual field-strength tensors

$$\tilde{X}_{\mu\nu} = -\frac{1}{2} \epsilon_{\mu\nu\rho\sigma} X^{\rho\sigma}, \quad X = G^A, W^a, B, \quad (36)$$

which we define with $\epsilon^{0123} = +1$. Since \mathcal{L}_θ can be written as total derivative $\partial^\mu \Theta_\mu(x)$ of some quantity $\Theta_\mu(x)$ (known as *Chern–Simons current*), effects of \mathcal{L}_θ can never show up in perturbative calculations. For non-abelian gauge fields, however, topologically non-trivial, non-perturbative field configurations (*instantons*) can potentially lead to observable effects caused by \mathcal{L}_θ , while abelian gauge fields do not admit such configurations (see Refs. [94, 95] and references therein). While the parameter θ_1 could, thus, be set to 0, we nevertheless keep it in the following and show that it is unphysical, as it can be eliminated via field redefinitions. To answer the question of observability for the θ parameters in Eq. (35) it is necessary to inspect the behaviour of the complete Lagrangian under phase transformations of the fermion fields, because the functional integral of the fermion fields shows a non-trivial behaviour under chiral phase transformations. In detail, the global phase transformations

$$f_R(x) \rightarrow e^{i\theta_R} f_R(x), \quad f_L(x) \rightarrow e^{i\theta_L} f_L(x) \quad (37)$$

effectively modify the Lagrangian of the SM by the term [96]

$$\mathcal{L}_{\text{phase}} = - \sum_q \frac{1}{2} (\theta_{q_R} - \theta_{q_L}) \frac{g_s^2}{16\pi^2} \tilde{G}_{\mu\nu}^a G^{a,\mu\nu} + \sum_f \frac{1}{2} \theta_{f_L} \frac{g_2^2}{16\pi^2} \tilde{W}_{\mu\nu}^a W^{a,\mu\nu} - \sum_f \frac{1}{4} (Y_{w,f_R}^2 \theta_{f_R} - Y_{w,f_L}^2 \theta_{f_L}) \frac{g_1^2}{16\pi^2} \tilde{B}_{\mu\nu}^a B^{a,\mu\nu}, \quad (38)$$

where the sum over q runs over all six quark flavours and the one over f over all fermion flavours of the SM. Note that the phases $\theta_{f_{R/L}}$ are not all independent. We should rather ensure that the SM Lagrangian $\mathcal{L}_{\text{class}}$ (8) is left unchanged by the phase transformations (37). The transformations in the quark and lepton sectors can be considered independently.

Focusing on the quark sector with three generations, we have 12 independent phase transformations. To keep the CKM matrix unchanged in the hadronic charged-current interaction, only one global phase change by some angle θ_{Q_L} is still allowed, i.e. 5 out of the 6 phases of the q_L fields are fixed relative to the phase of one of those. These constraints can be formulated as

$$\theta_{u_{i,L}} = \theta_{d_{i,L}} \equiv \theta_{Q_L}, \quad (39)$$

where $i = 1, 2, 3$ is the generation index. This is exactly the reduction in the number 9 of real degrees of freedom of a general unitary matrix to the number 4 of physically relevant ones in the CKM matrix. To keep the hadronic Yukawa couplings in $\mathcal{L}_{\text{class}}$ invariant as well, and allowing for a phase transformation of the Higgs doublet by an angle θ_Φ , we get the further constraints

$$0 = -\theta_{Q_L} + \theta_{d_{i,R}} + \theta_\Phi, \quad 0 = -\theta_{Q_L} + \theta_{u_{i,R}} - \theta_\Phi, \quad (40)$$

which fix all the phases of the right-handed quark fields q_R in terms of θ_{Q_L} and θ_Φ . Respecting the constraints (39) and (40), the parameters θ_{QCD} and θ_2 change as follows,

$$\theta_{\text{QCD}} \rightarrow \theta_{\text{QCD}} + \sum_q \frac{1}{2} (\theta_{q_R} - \theta_{q_L}) = \theta_{\text{QCD}} + \sum_{i=1}^3 \frac{1}{2} (\theta_{u_{i,R}} - \theta_{u_{i,L}} + \theta_{d_{i,R}} - \theta_{d_{i,L}}) = \theta_{\text{QCD}}, \quad (41)$$

$$\theta_2 \rightarrow \theta_2 - \sum_q \frac{1}{2} \theta_{q_L} = \theta_2 - 3\theta_{Q_L}, \quad (42)$$

$$\theta_1 \rightarrow \theta_1 + \sum_q \frac{1}{4} (Y_{w,q_R}^2 \theta_{q_R} - Y_{w,q_L}^2 \theta_{q_L}) = \theta_1 + \sum_i \frac{1}{9} (4\theta_{u_{i,R}} + \theta_{d_{i,R}}) - \frac{1}{6} \theta_{Q_L}. \quad (43)$$

Thus, θ_{QCD} is uniquely fixed by the phase choice of the CKM matrix and the fermion masses, which are taken real and non-negative, while θ_2 can be transformed to zero by a phase transformation that leaves the SM Lagrangian invariant. In other words, θ_{QCD} is a physically measurable parameter, whereas θ_2 is not. If at least one of the quarks, say q , was massless, the phase of q_R would not be constrained, so that θ_{QCD} could be transformed to zero as well; this possibility is, however, ruled out by experiment. Since the leptons do not contribute to the θ_{QCD} term in \mathcal{L}_θ , taking into account phase transformations of lepton fields does not change the above conclusions on θ_{QCD} , and θ_2 can still be transformed to zero by adjusting θ_{Q_L} . Since phase changes of the right-handed lepton fields neither influence θ_{QCD} nor θ_2 , the phase of those can be adjusted to render θ_1 zero.⁷

The Lagrangian \mathcal{L}_θ is particularly interesting, since it violates CP symmetry (*strong CP violation*). Experimentally the upper bound on $|\theta_{\text{QCD}}|$ is of the order 10^{-10} [97], which is deduced from experimentally constraining the neutron electric dipole moment [98, 99]. Within the SM, there is no explanation of this fine-tuning of θ_{QCD} , which asks for a solution by physics beyond the SM, as, e.g., suggested by axion models (see, e.g., Refs. [87, 94] and references therein). Since \mathcal{L}_θ does not play any role in collider physics, we will not consider it any further in this review.

2.2. Slavnov–Taylor and Ward identities

The quantized Lagrangian (31) of the EWSM, \mathcal{L}_{EW} , is invariant under *Becchi–Rouet–Stora (BRS) transformations* [100], defined as

$$\delta_{\text{BRS}} \Psi_I = \delta \lambda s \Psi_I, \quad (44)$$

where $\delta \lambda$ is an infinitesimal anticommuting constant and Ψ_I represents any of the fields V_μ^a , u^a , \bar{u}^a ($a = A, Z, \pm$), ϕ^\pm , χ , H , $F_{\pm,i}^L$, or f_i^R . The BRS transformations $s\Psi_I$ in the physical basis read

$$\begin{aligned} sA_\mu &= \partial_\mu u^A + ie(W_\mu^+ u^- - W_\mu^- u^+), \\ sZ_\mu &= \partial_\mu u^Z - ie \frac{c_w}{s_w} (W_\mu^+ u^- - W_\mu^- u^+), \end{aligned}$$

⁷For massless neutrinos, where no generation mixing exists in the lepton sector, the only constraints on the phase changes for leptons are $\theta_{l_{i,L}} = \theta_{\nu_{i,L}} \equiv \theta_{L_{i,L}}$ and $0 = -\theta_{L_{i,L}} + \theta_{l_{i,R}} + \theta_\Phi$, so that the phases $\theta_{l_{i,R}}$ can be adjusted to transform θ_1 to zero. For massive neutrinos with mixing, we have to include right-handed neutrino fields which bring in new phases $\theta_{\nu_{i,R}}$, but also new constraints: $\theta_{l_{i,L}} = \theta_{\nu_{i,L}} \equiv \theta_{L_L}$, $0 = -\theta_{L_L} + \theta_{l_{i,R}} + \theta_\Phi$, and $0 = -\theta_{L_L} + \theta_{\nu_{i,R}} - \theta_\Phi$. Here the freedom in choosing $\theta_{\nu_{i,R}}$ is sufficient to transform θ_1 to zero.

$$\begin{aligned}
sW_\mu^\pm &= \partial_\mu u^\pm \mp ie \left[W_\mu^\pm \left(u^A - \frac{c_w}{s_w} u^Z \right) - \left(A_\mu - \frac{c_w}{s_w} Z_\mu \right) u^\pm \right], \\
sH &= \frac{e}{2s_w c_w} \chi u^Z + \frac{ie}{2s_w} (\phi^+ u^- - \phi^- u^+), \\
s\chi &= -\frac{e}{2s_w c_w} (v + H) u^Z + \frac{e}{2s_w} (\phi^+ u^- + \phi^- u^+), \\
s\phi^\pm &= \mp ie \phi^\pm \left(u^A - \frac{c_w^2 - s_w^2}{2c_w s_w} u^Z \right) \pm \frac{ie}{2s_w} (v + H \pm i\chi) u^\pm, \\
sF_{\pm,i}^L &= -ie \left[Q_\pm u^A + \frac{s_w}{c_w} \left(Q_\pm \mp \frac{1}{2s_w^2} \right) u^Z \right] F_{\pm,i}^L + i \frac{e}{\sqrt{2}s_w} u^\pm \sum_j v_{ij}^\pm F_{\mp,j}^L, \\
sf_i^R &= -ie Q_f \left(u^A + \frac{s_w}{c_w} u^Z \right) f_i^R, \\
su^\pm &= \pm i \frac{e}{s_w} u^\pm (s_w u^A - c_w u^Z), \quad su^Z = -ie \frac{c_w}{s_w} u^- u^+, \quad su^A = ie u^- u^+, \\
s\bar{u}^\pm &= -\frac{1}{\xi_w} C^\mp, \quad s\bar{u}^Z = -\frac{1}{\xi_z} C^Z, \quad s\bar{u}^A = -\frac{1}{\xi_A} C^A,
\end{aligned} \tag{45}$$

with $F_{\pm,i}$ defined in Eq. (25) and v_{ij}^\pm in Eq. (26).

The BRS symmetry gives rise to relations between different Green functions, called *Slavnov–Taylor identities*. The identities for the full (reducible) Green functions $G_c^{\Psi_{I_1} \dots} = \langle T \prod_l \Psi_{I_l} \rangle$ (symbolically written as vevs of time-ordered fields) are obtained from the invariance of Green functions under BRS transformations (see, for instance, Refs. [83, 101]):

$$0 = \frac{\delta_{\text{BRS}}}{\delta \lambda} \langle T \prod_l \Psi_{I_l} \rangle. \tag{46}$$

Applying this to Green functions involving an antighost field \bar{u}^a and arbitrary physical, on-shell (OS) fields $\Psi_{I_l}^{\text{phys}}$, one obtains

$$0 = \langle T C^a \prod_l \Psi_{I_l}^{\text{phys}} \rangle, \tag{47}$$

up to terms that vanish after truncation, since BRS variations of the physical components of asymptotic OS fields vanish. Using the equations of motion of the antighost fields, this can be generalized to Green functions with more gauge-fixing terms:

$$\langle T C^a(x) \left(\prod_m C^{a_m}(x_m) \right) \prod_l \Psi_{I_l}^{\text{phys}} \rangle = -i\xi_a \sum_k \delta^{aa_k} \delta^{(4)}(x - x_k) \langle T \left(\prod_{m \neq k} C^{a_m}(x_m) \right) \prod_l \Psi_{I_l}^{\text{phys}} \rangle. \tag{48}$$

An important special case of this relation reads

$$\langle T C^a(x) C^b(y) \rangle = -i\xi_a \delta^{ab} \delta^{(4)}(x - y), \tag{49}$$

which is known as *Slavnov identity* in the case of unbroken gauge symmetries. Using the gauge-fixing functions (27) in the 't Hooft gauge ($\xi'_a = \xi_a$) and transforming to momentum space, we find the following relations for the propagators of the gauge bosons,

$$\begin{aligned}
-i\xi_w &= k^\mu k^\nu G_{\mu\nu}^{W^+ W^-}(k, -k) - \xi_w M_w k^\mu G_\mu^{W^+ \phi^-}(k, -k) - \xi_w M_w k^\mu G_\mu^{\phi^+ W^-}(k, -k) + \xi_w^2 M_w^2 G^{\phi^+ \phi^-}(k, -k), \\
-i\xi_z &= k^\mu k^\nu G_{\mu\nu}^{ZZ}(k, -k) - 2i\xi_z M_z k^\mu G_\mu^{Z\chi}(k, -k) + \xi_z^2 M_z^2 G^{\chi\chi}(k, -k), \\
0 &= k^\mu k^\nu G_{\mu\nu}^{AZ}(k, -k) - i\xi_z M_z k^\mu G_\mu^{A\chi}(k, -k), \\
-i\xi_A &= k^\mu k^\nu G_{\mu\nu}^{AA}(k, -k).
\end{aligned} \tag{50}$$

According to our conventions (see Appendix B) the field labels in non-truncated Green functions indicate the outgoing fields, but those in truncated Green functions or vertex functions the incoming fields. The momentum arguments

denote incoming momenta corresponding to the fields in the superscripts. The relations (50) between the longitudinal parts of the gauge-boson propagators, the gauge-field–would-be Goldstone-field mixing propagators, and the propagators of the would-be Goldstone bosons are exact. They show, in particular, that the poles of the unphysical parts of the propagators coincide. The relation for the photon propagator ensures that its longitudinal part gets no higher-order corrections.

2.3. Background-field quantization

Gauge-invariance relations between Green functions can be greatly simplified within the background-field method (BFM), which is a modified version of the conventional formalism for the quantization of gauge fields (see, e.g., Refs. [83, 87, 94]). The BFM was introduced originally for quantum gravity in Ref. [102] and subsequently generalized to QCD in Refs. [103–106]. Its application to the EWSM was formulated in Ref. [107]. As in the latter reference, we neglect quark mixing in this section.⁸

2.3.1. Quantized Lagrangian in the background-field method

In the conventional formalism the fields appearing in the classical Lagrangian are quantized. Instead, in the BFM, the fields of the classical Lagrangian are additively split into classical background fields (denoted with a caret), $\hat{\Psi}$, and quantum fields, Ψ ,

$$\mathcal{L}_{\text{class}}(\Psi) \rightarrow \mathcal{L}_{\text{class}}(\hat{\Psi} + \Psi). \quad (51)$$

While the quantum fields are the variables of integration in the functional integral, i.e. quantized, the classical fields serve as external sources. Invariance of the classical Lagrangian with respect to the transformations (10) then implies its invariance under two kinds of transformations: *quantum gauge transformations*

$$\begin{aligned} \delta W_\mu^a &= \partial_\mu \delta \theta^a + g_2 \epsilon^{abc} (W_\mu^b + \hat{W}_\mu^b) \delta \theta^c, & \delta B_\mu &= \partial_\mu \delta \theta^Y, & \delta \Phi &= \left(-\frac{i}{2} g_1 \delta \theta^Y + i \frac{\tau^a}{2} g_2 \delta \theta^a \right) (\Phi + \hat{\Phi}), \\ \delta \hat{W}_\mu^a &= 0, & \delta \hat{B}_\mu &= 0, & \delta \hat{\Phi} &= 0, \end{aligned} \quad (52)$$

and *background gauge transformations*

$$\begin{aligned} \delta \hat{W}_\mu^a &= \partial_\mu \delta \hat{\theta}^a + g_2 \epsilon^{abc} \hat{W}_\mu^b \delta \hat{\theta}^c, & \delta \hat{B}_\mu &= \partial_\mu \delta \hat{\theta}^Y, & \delta \hat{\Phi} &= \left(-\frac{i}{2} g_1 \delta \hat{\theta}^Y + i \frac{\tau^a}{2} g_2 \delta \hat{\theta}^a \right) \hat{\Phi}, \\ \delta W_\mu^a &= g_2 \epsilon^{abc} W_\mu^b \delta \hat{\theta}^c, & \delta B_\mu &= 0, & \delta \Phi &= \left(-\frac{i}{2} g_1 \delta \hat{\theta}^Y + i \frac{\tau^a}{2} g_2 \delta \hat{\theta}^a \right) \Phi, \end{aligned} \quad (53)$$

where we mark the gauge-transformation parameters of the latter by a caret. Since we do not split the fermion fields, they transform under both types of transformations as in Eq. (10).⁹ The splitting of the Higgs-doublet field is done in such a way that the background Higgs field $\hat{\Phi}$ has the usual non-vanishing vev v , while the one of the quantum Higgs field Φ is zero,

$$\hat{\Phi}(x) = \begin{pmatrix} \hat{\phi}^+(x) \\ \frac{1}{\sqrt{2}}[v + \hat{H}(x) + i\hat{\chi}(x)] \end{pmatrix}, \quad \Phi(x) = \begin{pmatrix} \phi^+(x) \\ \frac{1}{\sqrt{2}}[H(x) + i\chi(x)] \end{pmatrix}. \quad (54)$$

A gauge-fixing term is added that breaks the invariance under quantum gauge transformations, but retains the invariance with respect to background gauge transformations:

$$\begin{aligned} \mathcal{L}_{\text{fix,BFM}} &= -\frac{1}{2\xi_W} \left[\left(\delta^{ac} \partial_\mu + g_2 \epsilon^{abc} \hat{W}_\mu^b \right) W^{c\mu} - i g_2 \xi'_W \frac{1}{2} \left(\hat{\Phi}^\dagger \tau^a \Phi - \Phi^\dagger \tau^a \hat{\Phi} \right) \right]^2 \\ &\quad - \frac{1}{2\xi_B} \left[\partial_\mu B^\mu + i g_1 \xi'_B \frac{1}{2} \left(\hat{\Phi}^\dagger \Phi - \Phi^\dagger \hat{\Phi} \right) \right]^2. \end{aligned} \quad (55)$$

⁸As shown in Ref. [108], the vertex functions of the BFM in the Feynman gauge coincide with the results of the *pinch technique* [109–111] sometimes used in the literature.

⁹For fields that do not enter the gauge-fixing term, quantization in the BFM is equivalent to the conventional formalism, and the Feynman rules for background and quantum fields are identical.

Invariance under background gauge transformations requires that the background gauge fields appear only within a covariant derivative in the gauge-fixing term, so that the terms in square brackets transform according to the adjoint representation of the gauge group. Only four independent gauge parameters are allowed, ξ_W and ξ'_W for $SU(2)_W$ and ξ_B and ξ'_B for $U(1)_Y$. Mixing between gauge bosons and the corresponding would-be Goldstone bosons is eliminated by choosing $\xi'_W = \xi_W$ and $\xi'_B = \xi_B$, resulting in the '*t Hooft gauge*' for the background-field formalism. In order to avoid tree-level mixing between the quantum photon and Z-boson fields, we set $\xi = \xi_W = \xi_B$. Note that Eq. (55) translates to the conventional gauge-fixing term (28) for $\xi_W = \xi_Z = \xi_A$ upon replacing the background Higgs field by its vev and omitting the background $SU(2)_W$ triplet field \hat{W}_μ^a .

Expressing the gauge-fixing Lagrangian in terms of fields in the physical basis yields

$$\mathcal{L}_{\text{fix,BFM}} = -\frac{1}{2\xi} \left[(C^A)^2 + (C^Z)^2 + 2C^+C^- \right], \quad (56)$$

where

$$\begin{aligned} C^A &= \partial^\mu A_\mu + ie(\hat{W}_\mu^+ W^{-\mu} - W_\mu^+ \hat{W}^{-\mu}) + ie\xi(\hat{\phi}^- \phi^+ - \hat{\phi}^+ \phi^-), \\ C^Z &= \partial^\mu Z_\mu - ie\frac{c_w}{s_w}(\hat{W}_\mu^+ W^{-\mu} - W_\mu^+ \hat{W}^{-\mu}) - ie\xi\frac{c_w^2 - s_w^2}{2c_w s_w}(\hat{\phi}^- \phi^+ - \hat{\phi}^+ \phi^-) - \xi M_Z \chi + e\xi\frac{1}{2c_w s_w}(\hat{\chi} H - \hat{H}\chi), \\ C^\pm &= \partial^\mu W_\mu^\pm \pm ie\left(\hat{A}^\mu - \frac{c_w}{s_w}\hat{Z}^\mu\right)W_\mu^\pm \mp ie\left(A^\mu - \frac{c_w}{s_w}Z^\mu\right)\hat{W}_\mu^\pm \mp ie\xi M_W \phi^\pm \mp ie\xi\frac{1}{2s_w}[(\hat{H} \mp i\hat{\chi})\phi^\pm - (H \mp i\chi)\hat{\phi}^\pm]. \end{aligned} \quad (57)$$

The Faddeev–Popov Lagrangian $\mathcal{L}_{\text{FP,BFM}}$ can be derived from Eq. (30) using the variation of the gauge-fixing functions C^a (57) under the infinitesimal quantum gauge transformations (52) [107].

Starting from the Lagrangian

$$\mathcal{L}_{\text{BFM}}(\Psi, \hat{\Psi}) = \mathcal{L}_{\text{class}}(\Psi + \hat{\Psi}) + \mathcal{L}_{\text{fix,BFM}}(\Psi, \hat{\Psi}) + \mathcal{L}_{\text{FP,BFM}}(\Psi, \hat{\Psi}, u, \bar{u}), \quad (58)$$

the generating functionals for Green functions and connected Green functions can be defined as usual with background fields as additional external sources. A Legendre transformation with respect to the sources of the quantum fields leads to an effective action depending on quantum fields and background fields. From this the background-field effective action $\hat{\Gamma}[\hat{\Psi}] = \Gamma[\hat{\Psi} = 0, \hat{\Psi}]$ is obtained upon setting the Legendre transforms $\hat{\Psi}$ of the sources of the quantum fields to zero (apart from those for the fermion fields). Note that $\hat{\Gamma}[\hat{\Psi}]$ is invariant with respect to background gauge transformations (53). This procedure is described in Refs. [83, 106, 112], where it is also shown that the gauge-invariant effective action is equivalent to a conventional effective action in a particular gauge.

Upon differentiating the gauge-invariant effective action $\hat{\Gamma}[\hat{\Psi}]$ with respect to its arguments, the background-field vertex functions are generated. These can be calculated from Feynman rules that distinguish between quantum and background fields. While the quantum fields appear only inside loops, the background fields are associated with the external lines of vertex functions. Apart from doubling the gauge and Higgs fields, the BFM Feynman rules differ from the conventional ones only owing to the gauge-fixing and ghost terms, which affect only vertices involving both background and quantum fields. Since the gauge-fixing functions are non-linear in the fields, the gauge parameters enter also the gauge-boson vertices. As the gauge-fixing Lagrangian is quadratic in the quantum fields, only vertices that involve exactly two quantum fields or Faddeev–Popov fields are different from the conventional ones. The fermions, which are not split into background and quantum fields, appear both inside loops and on external lines, and the Feynman rules involving fermion fields are the same as in the conventional formalism.

The S matrix is constructed in the usual way by forming trees with vertices from $\hat{\Gamma}[\hat{\Psi}]$ which are connected by lowest-order background-field propagators. The definition of the background-field propagators requires the introduction of a gauge fixing for the background fields, which is independent of the gauge fixing for the quantum fields. It has been shown that the resulting S matrix is identical to the one of the conventional formalism [113, 114]. After introducing the gauge fixing for the background fields a generating functional \hat{T}_c of connected background-field Green functions can be obtained via a Legendre transformation [115].

The BFM can be used to simplify calculations in the EWSM. This is partly due to the fact that the gauge fixing of the background fields is totally unrelated to the gauge fixing of the quantum fields, which allows to choose a particularly suitable background gauge, e.g. the unitary gauge. Moreover, in the '*t Hooft–Feynman gauge*' ($\xi = 1$) for the quantum fields, many vertices simplify with respect to the conventional formalism [107, 108].

2.3.2. Background-field Ward identities

An important property of the background-field formalism is the invariance of the background-field effective action under background-field gauge transformations with associated group parameters $\hat{\theta}^a$,

$$\frac{\delta \hat{\Gamma}[\hat{\Psi}]}{\delta \hat{\theta}^a} = 0, \quad a = A, Z, \pm. \quad (59)$$

This invariance implies ghost-free identities for the vertex functions that are precisely the *Ward identities* related to the classical Lagrangian. For the EWSM, these identities were derived originally for one-particle irreducible (1PI) vertex functions $\hat{\Gamma}_{\text{1PI}}^{\dots}$ [107], which are obtained by taking functional derivatives of $\hat{\Gamma}[\hat{\Psi}]$ w.r.t. background fields and setting all background fields to zero afterwards. In this formulation the Ward identities for the bosonic 2-point functions read

$$k^\mu \hat{\Gamma}_{\text{1PI},\mu\nu}^{\hat{A}\hat{A}}(k, -k) = 0, \quad k^\mu \hat{\Gamma}_{\text{1PI},\mu\nu}^{\hat{A}\hat{Z}}(k, -k) = 0, \quad k^\mu \hat{\Gamma}_{\text{1PI},\mu}^{\hat{A}\hat{X}}(k, -k) = 0, \quad k^\mu \hat{\Gamma}_{\text{1PI},\mu}^{\hat{A}\hat{H}}(k, -k) = 0, \quad (60)$$

$$k^\mu \hat{\Gamma}_{\text{1PI},\mu\nu}^{\hat{Z}\hat{Z}}(k, -k) - iM_Z \hat{\Gamma}_{\text{1PI},\nu}^{\hat{X}\hat{Z}}(k, -k) = 0, \quad k^\mu \hat{\Gamma}_{\text{1PI},\mu}^{\hat{Z}\hat{X}}(k, -k) - iM_Z \hat{\Gamma}_{\text{1PI}}^{\hat{X}\hat{X}}(k, -k) + \frac{ie}{2s_w c_w} T^{\hat{H}} = 0, \quad (61)$$

$$k^\mu \hat{\Gamma}_{\text{1PI},\mu\nu}^{\hat{W}^\pm \hat{W}^\mp}(k, -k) \mp M_W \hat{\Gamma}_{\text{1PI},\nu}^{\hat{\phi}^\pm \hat{W}^\mp}(k, -k) = 0, \quad k^\mu \hat{\Gamma}_{\text{1PI},\mu}^{\hat{W}^\pm \hat{W}^\mp}(k, -k) \mp M_W \hat{\Gamma}_{\text{1PI}}^{\hat{\phi}^\pm \hat{W}^\mp}(k, -k) \pm \frac{e}{2s_w} T^{\hat{H}} = 0, \quad (62)$$

where fields and momenta are defined as incoming and $T^{\hat{H}} = \hat{\Gamma}_{\text{1PI}}^{\hat{H}}(0)$ (see Section 3.1.6).

Note that the vertex functions derived from the background-field effective action $\hat{\Gamma}[\hat{\Psi}]$ do not involve contributions of gauge-fixing terms for the background fields. For “full” vertex functions $\hat{\Gamma}^{\dots}$ (involving also tadpole loop diagrams) some of the corresponding identities change; in one-loop approximation those are given by

$$\begin{aligned} k^\mu \hat{\Gamma}_{\mu\nu}^{\hat{Z}\hat{Z}}(k, -k) - iM_Z r_{\hat{H}} \hat{\Gamma}_\nu^{\hat{X}\hat{Z}}(k, -k) &= 0, & k^\mu \hat{\Gamma}_\mu^{\hat{Z}\hat{X}}(k, -k) - iM_Z r_{\hat{H}} \hat{\Gamma}^{\hat{X}\hat{X}}(k, -k) &= 0, \\ k^\mu \hat{\Gamma}_{\mu\nu}^{\hat{W}^\pm \hat{W}^\mp}(k, -k) \mp M_W r_{\hat{H}} \hat{\Gamma}_\nu^{\hat{\phi}^\pm \hat{W}^\mp}(k, -k) &= 0, & k^\mu \hat{\Gamma}_\mu^{\hat{W}^\pm \hat{W}^\mp}(k, -k) \mp M_W r_{\hat{H}} \hat{\Gamma}^{\hat{\phi}^\pm \hat{W}^\mp}(k, -k) &= 0, \end{aligned} \quad (63)$$

where the background Higgs field $\hat{\Phi}$ is set to its vev (including higher-order corrections) after taking functional derivatives. We give our precise definition of the vertex functions in Appendix B and refer to Appendix E of Ref. [116] and to Section 3.1.6 for a discussion of the different tadpole schemes. The extra factors

$$r_{\hat{H}} = 1 + \frac{T^{\hat{H}}}{M_H^2 v} \quad (64)$$

can be interpreted as describing the shift from the bare vev to the correct vev.¹⁰

For the photon–fermion and the photon–W-boson vertices, QED-like Ward identities are found,

$$k^\mu \hat{\Gamma}_\mu^{\hat{A}\hat{f}f}(k, \bar{p}, p) = -e Q_f \left[\hat{\Gamma}^{\hat{f}\hat{f}}(\bar{p}, -\bar{p}) - \hat{\Gamma}^{\hat{f}\hat{f}}(-p, p) \right], \quad (65)$$

$$k^\mu \hat{\Gamma}_{\mu\rho\sigma}^{\hat{A}\hat{W}^\pm \hat{W}^\mp}(k, k_+, k_-) = e \left[\hat{\Gamma}_{\rho\sigma}^{\hat{W}^\pm \hat{W}^\mp}(k_+, -k_+) - \hat{\Gamma}_{\rho\sigma}^{\hat{W}^\pm \hat{W}^\mp}(-k_-, k_-) \right], \quad (66)$$

$$k_+^\rho \hat{\Gamma}_{\mu\rho\sigma}^{\hat{A}\hat{W}^\pm \hat{W}^\mp}(k, k_+, k_-) - M_W r_{\hat{H}} \hat{\Gamma}_{\mu\sigma}^{\hat{A}\hat{\phi}^\pm \hat{W}^\mp}(k, k_+, k_-) = e \left[\hat{\Gamma}_{\mu\sigma}^{\hat{W}^\pm \hat{W}^\mp}(-k_-, k_-) - \hat{\Gamma}_{\mu\sigma}^{\hat{A}\hat{A}}(k, -k) + \frac{c_w}{s_w} \hat{\Gamma}_{\mu\sigma}^{\hat{A}\hat{Z}}(k, -k) \right], \quad (67)$$

which hold for full ($\hat{\Gamma}^{\dots}$) and as well for 1PI vertex functions ($\hat{\Gamma}_{\text{1PI}}^{\dots}$) after setting $r_{\hat{H}} = 1$. From Eq. (65) the universality of the electric charge in the EWSM can be derived in the same way as for *Quantum Electrodynamics (QED)* [83, 117].

The Ward identities (59) for the effective action $\hat{\Gamma}[\hat{\Psi}]$ translate into identities for the generating functional \hat{T}_c of connected Green functions, which were explicitly derived in Ref. [115]. The connected 2-point functions involving neutral gauge bosons, for instance, obey

$$k^\mu G_{c,\mu\nu}^{\hat{A}\hat{A}}(k, -k) = \frac{-i\hat{\xi}_A k_\nu}{k^2}, \quad k^\mu G_{c,\mu\nu}^{\hat{A}\hat{Z}}(k, -k) = 0,$$

¹⁰When we take into account tadpole renormalization constants in vertex functions in Section 3.1.6, Eqs. (63) and the subsequent equations of this section remain valid with Eq. (64) in the FJTS variant described there. In the PRTS variant described in Section 3.1.6, those identities hold with $r_{\hat{H}} = 1$.

$$\begin{aligned}
k^\mu G_{c,\mu\nu}^{\hat{Z}\hat{Z}}(k, -k) + i\hat{\xi}_Z M_Z G_{c,\nu}^{\hat{X}\hat{Z}}(k, -k) &= \frac{-i\hat{\xi}_Z k_\nu}{k^2 - \hat{\xi}_Z M_Z^2 r_{\hat{H}}}, \\
k^\mu G_{c,\mu}^{\hat{Z}\hat{X}}(k, -k) + i\hat{\xi}_Z M_Z G_c^{\hat{X}\hat{X}}(k, -k) &= \frac{-\hat{\xi}_Z M_Z r_{\hat{H}}}{k^2 - \hat{\xi}_Z M_Z^2 r_{\hat{H}}}, \\
k^\mu G_{c,\mu\nu}^{\hat{W}^\pm \hat{W}^\mp}(k, -k) \pm \hat{\xi}_W M_W G_{c,\nu}^{\hat{\phi}^\pm \hat{W}^\mp}(k, -k) &= \frac{-i\hat{\xi}_W k_\nu}{k^2 - \hat{\xi}_W M_W^2 r_{\hat{H}}}, \\
k^\mu G_{c,\mu}^{\hat{W}^\pm \hat{\phi}^\mp}(k, -k) \pm \hat{\xi}_W M_W G_c^{\hat{\phi}^\pm \hat{\phi}^\mp}(k, -k) &= \frac{\pm i\hat{\xi}_W M_W r_{\hat{H}}}{k^2 - \hat{\xi}_W M_W^2 r_{\hat{H}}}, \tag{68}
\end{aligned}$$

where $\hat{\xi}_a$ are the gauge parameters of the background-field 't Hooft gauge-fixing terms, which are assumed to have the form of Eqs. (27) and (28) for background fields. The identities in Eq. (68) can be combined to derive Eq. (50), where all explicit tadpole contributions drop out. The photon–fermion vertex fulfils the same Ward identity as in QED,

$$-\frac{i}{\hat{\xi}_A} k^2 k^\mu G_{c,\mu}^{\hat{A}f\bar{f}}(k, \bar{p}, p) = -e Q_f \left[G_c^{f\bar{f}}(-p, p) - G_c^{f\bar{f}}(\bar{p}, -\bar{p}) \right]. \tag{69}$$

For truncated OS Green functions (defined in Appendix B) the Ward identities simplify, for instance, to [115]

$$k^\nu G_{\text{trunc},\nu}^{\hat{A}\dots} = 0, \quad k^\nu G_{\text{trunc},\nu}^{\hat{Z}\dots} = i M_Z r_{\hat{H}} G_{\text{trunc}}^{\hat{X}\dots}, \quad k^\nu G_{\text{trunc},\nu}^{\hat{W}^\pm \dots} = \pm M_W r_{\hat{H}} G_{\text{trunc}}^{\hat{\phi}^\pm \dots}, \tag{70}$$

where the ellipses stand for any OS fields, i.e. the corresponding legs are truncated, put on shell, and contracted with wave functions.¹¹ While the first of these identities expresses electromagnetic current conservation, the others imply the Goldstone-boson equivalence theorem, as spelled out in Section 5.3.

We finally mention that the validity of the background-field Ward identities for connected Green functions can even be sustained in finite orders of perturbation theory if the resummed propagators are used to connect the vertex functions and the inverse propagators are calculated in the same order of perturbation theory as all the other vertex functions [115]. The necessary prerequisite for this property is the linearity of the background-field Ward identities for vertex functions, as featured by the identities (60)–(62) for the 1PI vertex functions and by the identities (63) for the vertex functions including reducible tadpole contributions.¹² As a consequence, these Ward identities and all identities derived therefrom hold exactly in finite orders of perturbation theory. In contrast, Slavnov–Taylor identities of the conventional Faddeev–Popov quantization in general hold for connected Green functions in a given order of perturbation theory only if all contributions, including the propagators, are expanded up to this order.

2.4. Standard-Model effective theory

Presently, there is no significant evidence for physics beyond the SM in the TeV region, so that new-physics effects at the LHC are expected to be small. In this situation, deviations from the SM Lagrangian can conveniently and consistently be described within an effective Lagrangian framework. The effective Lagrangian results from the Lagrangian of a more comprehensive theory by integrating out the heavy degrees of freedom, so that the different terms in the effective Lagrangian are obtained from a systematic expansion in inverse powers of the heavy scale Λ of new physics. In this way, the effective Lagrangian provides a parametrization of possible deviations from SM predictions. It should be noted, however, that such an approach assumes that no light degrees of freedom beyond those of the SM are present.

The description of BSM physics based on an effective Lagrangian in terms of the SM fields was pioneered by Buchmüller and Wyler [118], who provided a list of operators of dimensions 5 and 6 in the linear parametrization of the Higgs sector with a Higgs doublet. In the sequel various authors have considered subsets of this operator

¹¹Recall that the field indices denote outgoing fields for the connected Green functions G_c^{\dots} , but incoming fields for the truncated Green functions G_{trunc}^{\dots} .

¹²Note that the identities (63) are only linear in the BFM vertex functions if the constant $r_{\hat{H}}$ is interpreted as part of the parameters and not as vertex function.

basis or introduced different sets of operators adapted to specific goals. A complete minimal basis of dimension-6 operators was presented in Ref. [85], where *minimal* means that equations of motion are used as far as possible to reduce the number of operators. Note that operators that can be expressed in terms of others via equations of motion do not additionally affect physical S -matrix elements. Other bases were proposed, and different authors prefer to use different sets of operator bases, motivated by different expectations for the form of new physics [66, 67, 119–125]. In this review, we restrict ourselves to the *Warsaw basis* of Ref. [85] which is based on a linear representation of the Higgs sector involving a single Higgs doublet, like the usual formulation of the SM. For a more comprehensive discussion of the SM effective field theory (SMEFT) we refer to Ref. [126].

We define an effective Lagrangian based on a linear representation of the EW gauge symmetry with a Higgs-doublet field Φ following closely the framework introduced in Ref. [118] and further developed in Ref. [85].¹³ The effective Lagrangian has the general form

$$\mathcal{L}_{\text{eff}} = \mathcal{L}_{\text{SM}}^{(4)} + \frac{1}{\Lambda} \sum_k C_k^{(5)} \mathcal{O}_k^{(5)} + \frac{1}{\Lambda^2} \sum_k C_k^{(6)} \mathcal{O}_k^{(6)} + \mathcal{O}\left(\frac{1}{\Lambda^3}\right), \quad (71)$$

where $\mathcal{L}_{\text{SM}}^{(4)}$ is the symmetric SM Lagrangian (8), including also QCD as described in Section 2.1.4, $\mathcal{O}_k^{(5)}$ denotes dimension-5 operators and $C_k^{(5)}$ the corresponding Wilson coefficients, and $\mathcal{O}_k^{(6)}$ denotes dimension-6 operators with corresponding Wilson coefficients $C_k^{(6)}$. The operators $\mathcal{O}_k^{(D)}$ are invariant under $\text{SU}(3)_c \times \text{SU}(2)_w \times \text{U}(1)_Y$ transformations. Since the effective Lagrangian must be hermitean, in Eq. (71) for each non-hermitean operator \mathcal{O}_k the hermitean-conjugate operator \mathcal{O}_k^\dagger appears with the complex-conjugate Wilson coefficient C_k^* .

2.4.1. Conventions and definition of the effective operator basis

We employ the conventions for the SM used above as far as possible. Colour and weak-isospin indices in the fundamental representations are denoted as $\alpha = 1, 2, 3$ and $\sigma = 1, 2$, respectively, those in the adjoint representations as $A = 1, \dots, 8$ and $a = 1, 2, 3$, while the generation indices are written as $i = 1, 2, 3$. The matter fields of the SM comprise the left-handed lepton doublets $L_{\sigma,i}$, the right-handed charged leptons l_i , the left-handed quark doublets $Q_{\alpha,\sigma,i}$, the right-handed quarks $u_{\alpha,i}$, $d_{\alpha,i}$, and the Higgs doublet Φ_σ with hypercharges $Y_w = -1, -2, 1/3, 4/3, -2/3, 1$, respectively. Right-handed neutrinos are not included. The fermion fields appearing in this section are the interaction eigenstates and should therefore be primed, but we suppress the primes in this section. The charge-conjugate Higgs field Φ^c is given in Eq. (9). The field-strength tensors and the covariant derivative are defined in Eqs. (2), (32), and (33).

Using the dual field-strength tensors defined in Eq. (36), we introduce hermitean derivatives

$$\Phi^\dagger i \overleftrightarrow{D}_\mu \Phi = i \left[\Phi^\dagger D_\mu \Phi - (D_\mu \Phi)^\dagger \Phi \right], \quad \Phi^\dagger i \overleftrightarrow{D}_\mu^a \Phi = i \left[\Phi^\dagger \tau^a D_\mu \Phi - (D_\mu \Phi)^\dagger \tau^a \Phi \right], \quad (72)$$

and $\sigma^{\mu\nu} = i(\gamma^\mu \gamma^\nu - \gamma^\nu \gamma^\mu)/2$. Finally, $\epsilon_{\sigma\tau}$ is totally antisymmetric with $\epsilon_{12} = +1$.

The SM gauge symmetry allows for only one dimension-5 operator up to hermitean conjugation and flavour assignments [127],

$$\mathcal{O}_{vv} = (\Phi^{c,\dagger} L_i)^T C (\Phi^{c,\dagger} L_j), \quad (73)$$

where C is the charge-conjugation matrix in Dirac space. Here and in the following, generation indices i, j , etc. are suppressed in the operator names. The operator \mathcal{O}_{vv} violates lepton number and generates neutrino masses and mixing after EW symmetry breaking.

The independent dimension-6 operators allowed by the SM gauge symmetries are listed in Tables 1 and 2. They are obtained by transforming the results of Ref. [85] to our conventions. The generation indices are suppressed on the left-hand sides of the equations. Dirac indices are contracted within the parentheses and suppressed. This is also done for colour and isospin indices as far as possible. In addition to the operators in Tables 1 and 2, for each non-hermitean operator its hermitean conjugate must be included. The Wilson coefficients of these operators are in general complex, while those of the hermitean operators are real.

¹³We slightly adapt the conventions in order to conform with our conventions for the SM Lagrangian (8). To this end, we have to change the signs of the $\text{SU}(2)_w$ W^a fields and of the $\text{SU}(3)_c$ fields G^A . Moreover, we use the convention $\epsilon^{0123} = -\epsilon_{0123} = +1$, while Ref. [85] uses $\epsilon_{0123} = +1$.

Φ^6 and $\Phi^4 D^2$	$\psi^2 \Phi^3$	X^3
$O_\Phi = (\Phi^\dagger \Phi)^3$	$O_{l\Phi} = (\Phi^\dagger \Phi)(\bar{L}_i l_j \Phi)$	$O_G = -f^{ABC} G_\mu^{Av} G_v^{B\rho} G_\rho^{C\mu}$
$O_{\Phi\square} = (\Phi^\dagger \Phi) \square (\Phi^\dagger \Phi)$	$O_{u\Phi} = (\Phi^\dagger \Phi)(\bar{Q}_i u_j \Phi^c)$	$O_{\bar{G}} = -f^{ABC} \bar{G}_\mu^{Av} G_v^{B\rho} G_\rho^{C\mu}$
$O_{\Phi D} = (\Phi^\dagger D^\mu \Phi)^* (\Phi^\dagger D_\mu \Phi)$	$O_{d\Phi} = (\Phi^\dagger \Phi)(\bar{Q}_i d_j \Phi)$	$O_W = -\epsilon^{abc} W_\mu^{av} W_v^{b\rho} W_\rho^{c\mu}$
		$O_{\bar{W}} = -\epsilon^{abc} \bar{W}_\mu^{av} W_v^{b\rho} W_\rho^{c\mu}$
$X^2 \Phi^2$	$\psi^2 X \Phi$	$\psi^2 \Phi^2 D$
$O_{\Phi G} = (\Phi^\dagger \Phi) G_{\mu\nu}^A G^{A\mu\nu}$	$O_{uG} = -(\bar{Q}_i \sigma^{\mu\nu} \frac{\lambda^A}{2} u_j) \Phi^c G_{\mu\nu}^A$	$O_{\Phi L}^{(1)} = (\Phi^\dagger i \overset{\leftrightarrow}{D}_\mu \Phi)(\bar{L}_i \gamma^\mu L_j)$
$O_{\Phi \bar{G}} = (\Phi^\dagger \Phi) \bar{G}_{\mu\nu}^A G^{A\mu\nu}$	$O_{dG} = -(\bar{Q}_i \sigma^{\mu\nu} \frac{\lambda^A}{2} d_j) \Phi G_{\mu\nu}^A$	$O_{\Phi L}^{(3)} = (\Phi^\dagger i \overset{\leftrightarrow}{D}_\mu \Phi)(\bar{L}_i \gamma^\mu \tau^a L_j)$
$O_{\Phi W} = (\Phi^\dagger \Phi) W_{\mu\nu}^a W^{a\mu\nu}$	$O_{lW} = -(\bar{L}_i \sigma^{\mu\nu} l_j) \tau^a \Phi W_{\mu\nu}^a$	$O_{\Phi l} = (\Phi^\dagger i \overset{\leftrightarrow}{D}_\mu \Phi)(\bar{l}_i \gamma^\mu l_j)$
$O_{\Phi \bar{W}} = (\Phi^\dagger \Phi) \bar{W}_{\mu\nu}^a W^{a\mu\nu}$	$O_{uW} = -(\bar{Q}_i \sigma^{\mu\nu} u_j) \tau^a \Phi^c W_{\mu\nu}^a$	$O_{\Phi Q}^{(1)} = (\Phi^\dagger i \overset{\leftrightarrow}{D}_\mu \Phi)(\bar{Q}_i \gamma^\mu Q_j)$
$O_{\Phi B} = (\Phi^\dagger \Phi) B_{\mu\nu} B^{\mu\nu}$	$O_{dW} = -(\bar{Q}_i \sigma^{\mu\nu} d_j) \tau^a \Phi W_{\mu\nu}^a$	$O_{\Phi Q}^{(3)} = (\Phi^\dagger i \overset{\leftrightarrow}{D}_\mu \Phi)(\bar{Q}_i \gamma^\mu \tau^a Q_j)$
$O_{\Phi \bar{B}} = (\Phi^\dagger \Phi) \bar{B}_{\mu\nu} B^{\mu\nu}$	$O_{lB} = (\bar{L}_i \sigma^{\mu\nu} l_j) \Phi B_{\mu\nu}$	$O_{\Phi u} = (\Phi^\dagger i \overset{\leftrightarrow}{D}_\mu \Phi)(\bar{u}_i \gamma^\mu u_j)$
$O_{\Phi WB} = -(\Phi^\dagger \tau^a \Phi) W_{\mu\nu}^a B^{\mu\nu}$	$O_{uB} = (\bar{Q}_i \sigma^{\mu\nu} u_j \Phi^c) B_{\mu\nu}$	$O_{\Phi d} = (\Phi^\dagger i \overset{\leftrightarrow}{D}_\mu \Phi)(\bar{d}_i \gamma^\mu d_j)$
$O_{\Phi \bar{W}B} = -(\Phi^\dagger \tau^a \Phi) \bar{W}_{\mu\nu}^a B^{\mu\nu}$	$O_{dB} = (\bar{Q}_i \sigma^{\mu\nu} d_j) \Phi B_{\mu\nu}$	$O_{\Phi ud} = (\Phi^{c\dagger} i D_\mu \Phi)(\bar{u}_i \gamma^\mu d_j)$

Table 1: Dimension-6 operators involving the Higgs-doublet field or gauge-boson fields. For all $\psi^2 \Phi^3$, $\psi^2 X \Phi$ operators and for $O_{\Phi ud}$ the hermitean conjugates must be included as well (taken from Ref. [85]).

$(\bar{L}L)(\bar{L}L)$	$(\bar{R}R)(\bar{R}R)$	$(\bar{L}L)(\bar{R}R)$
$O_{LL} = (\bar{L}_i \gamma_\mu L_j)(\bar{L}_k \gamma^\mu L_l)$	$O_{ll} = (\bar{l}_i \gamma_\mu l_j)(\bar{l}_k \gamma^\mu l_l)$	$O_{LI} = (\bar{L}_i \gamma_\mu L_j)(\bar{l}_k \gamma^\mu l_l)$
$O_{QQ}^{(1)} = (\bar{Q}_i \gamma_\mu Q_j)(\bar{Q}_k \gamma^\mu Q_l)$	$O_{uu} = (\bar{u}_i \gamma_\mu u_j)(\bar{u}_k \gamma^\mu u_l)$	$O_{Lu} = (\bar{L}_i \gamma_\mu L_j)(\bar{u}_k \gamma^\mu u_l)$
$O_{QQ}^{(3)} = (\bar{Q}_i \gamma_\mu \tau^a Q_j)(\bar{Q}_k \gamma^\mu \tau^a Q_l)$	$O_{dd} = (\bar{d}_i \gamma_\mu d_j)(\bar{d}_k \gamma^\mu d_l)$	$O_{Ld} = (\bar{L}_i \gamma_\mu L_j)(\bar{d}_k \gamma^\mu d_l)$
$O_{LQ}^{(1)} = (\bar{L}_i \gamma_\mu L_j)(\bar{Q}_k \gamma^\mu Q_l)$	$O_{lu} = (\bar{l}_i \gamma_\mu l_j)(\bar{u}_k \gamma^\mu u_l)$	$O_{Ql} = (\bar{Q}_i \gamma_\mu Q_j)(\bar{l}_k \gamma^\mu l_l)$
$O_{LQ}^{(3)} = (\bar{L}_i \gamma_\mu \tau^a L_j)(\bar{Q}_k \gamma^\mu \tau^a Q_l)$	$O_{ld} = (\bar{l}_i \gamma_\mu l_j)(\bar{d}_k \gamma^\mu d_l)$	$O_{Qu}^{(1)} = (\bar{Q}_i \gamma_\mu Q_j)(\bar{u}_k \gamma^\mu u_l)$
	$O_{ud}^{(1)} = (\bar{u}_i \gamma_\mu u_j)(\bar{d}_k \gamma^\mu d_l)$	$O_{Qu}^{(8)} = (\bar{Q}_i \gamma_\mu \frac{\lambda^A}{2} Q_j)(\bar{u}_k \gamma^\mu \frac{\lambda^A}{2} u_l)$
	$O_{ud}^{(8)} = (\bar{u}_i \gamma_\mu \frac{\lambda^A}{2} u_j)(\bar{d}_k \gamma^\mu \frac{\lambda^A}{2} d_l)$	$O_{Qd}^{(1)} = (\bar{Q}_i \gamma_\mu Q_j)(\bar{d}_k \gamma^\mu d_l)$
		$O_{Qd}^{(8)} = (\bar{Q}_i \gamma_\mu \frac{\lambda^A}{2} Q_j)(\bar{d}_k \gamma^\mu \frac{\lambda^A}{2} d_l)$
$(\bar{L}R)(\bar{R}L)$ and $(\bar{L}R)(\bar{L}R)$	B-violating	
$O_{LldQ} = (\bar{L}_i^\sigma l_j)(\bar{d}_k Q_l^\sigma)$	$O_{duQ} = \epsilon^{\alpha\beta\gamma} \epsilon_{\sigma\tau} \left[(d_i^\alpha)^T C u_j^\beta \right] \left[(Q_k^\gamma)^T C L_l^\tau \right]$	
$O_{QuQd}^{(1)} = (\bar{Q}_i^\sigma u_j) \epsilon_{\sigma\tau} (\bar{Q}_k^\tau d_l)$	$O_{QQu} = \epsilon^{\alpha\beta\gamma} \epsilon_{\sigma\tau} \left[(Q_i^\alpha)^T C Q_j^\beta \right] \left[(u_k^\gamma)^T C l_l \right]$	
$O_{QuQd}^{(8)} = (\bar{Q}_i^\sigma \frac{\lambda^A}{2} u_j) \epsilon_{\sigma\tau} (\bar{Q}_k^\tau \frac{\lambda^A}{2} d_l)$	$O_{QQQ} = \epsilon^{\alpha\beta\gamma} \epsilon_{\sigma\tau} \epsilon_{\sigma'\tau'} \left[(Q_i^\alpha)^T C Q_j^\beta \right] \left[(Q_k^{\gamma\sigma'})^T C L_l^{\tau'} \right]$	
$O_{LlQu}^{(1)} = (\bar{L}_i^\sigma l_j) \epsilon_{\sigma\tau} (\bar{Q}_k^\tau u_l)$	$O_{duu} = \epsilon^{\alpha\beta\gamma} \left[(d_i^\alpha)^T C u_j^\beta \right] \left[(u_k^\gamma)^T C l_l \right]$	
$O_{LlQu}^{(3)} = (\bar{L}_i^\sigma \sigma_{\mu\nu} l_j) \epsilon_{\sigma\tau} (\bar{Q}_k^\tau \sigma^{\mu\nu} u_l)$		

Table 2: Dimension-6 operators involving four fermion fields (taken from Ref. [85]).

Counting the number of dimension-6 operators in Tables 1 and 2 that conserve baryon and lepton number, we find 15 bosonic operators, 19 operators with a single fermionic current, and 25 B-conserving four-fermion operators. For three generations, the dimension-6 Lagrangian involves 1350 CP-even and 1149 CP-odd B- and L-conserving operators.

2.4.2. Translation to the physical basis

The higher-dimensional operators do not only introduce new coupling structures, they also contribute to the linear, to the bilinear, and to the interaction terms of the Lagrangian. This leads to modifications of the relations between properly normalized fields and parameters of the physical basis and their counterparts of the symmetric Lagrangian with respect to the original SM relations. We outline these modifications in the following, but restrict ourselves to the B-conserving dimension-6 operators and to terms linear in the Wilson coefficients. The discussion is largely taken from Refs. [128, 129], but translated to our conventions.

The operator \mathcal{O}_Φ changes the scalar potential at order v^2/Λ^2 to

$$V(\Phi) = -\mu^2(\Phi^\dagger\Phi) + \frac{1}{4}\lambda(\Phi^\dagger\Phi)^2 - \frac{C_\Phi}{\Lambda^2}(\Phi^\dagger\Phi)^3, \quad (74)$$

leading to the new minimum

$$|\langle\Phi\rangle|^2 = \frac{2\mu^2}{\lambda} \left(1 + \frac{12C_\Phi\mu^2}{\Lambda^2\lambda^2}\right) = \frac{v^2}{2} \quad (75)$$

by expanding the exact solution to first order in C_Φ .

The Higgs-doublet kinetic terms are modified by the operators $\mathcal{O}_{\Phi\square}$ and $\mathcal{O}_{\Phi D}$. By parametrizing the scalar doublet field as

$$\Phi(x) = \begin{pmatrix} \phi^+(x) \\ \frac{1}{\sqrt{2}}[v + (1 + c_{H,\text{kin}})H(x) + i(1 + c_{\chi,\text{kin}})\chi(x)] \end{pmatrix}, \quad (76)$$

with the coefficients

$$c_{H,\text{kin}} = \left(C_{\Phi\square} - \frac{1}{4}C_{\Phi D}\right)\frac{v^2}{\Lambda^2}, \quad c_{\chi,\text{kin}} = -\frac{1}{4}C_{\Phi D}\frac{v^2}{\Lambda^2}, \quad (77)$$

the scalar kinetic terms are properly normalized when dimension-6 terms are included. The Higgs-boson mass is obtained as

$$M_H^2 = \frac{1}{2}\lambda v^2 \left(1 - \frac{6C_\Phi}{\lambda}\frac{v^2}{\Lambda^2} + 2c_{H,\text{kin}}\right). \quad (78)$$

The operators $\mathcal{O}_{\Phi G}$, $\mathcal{O}_{\Phi W}$, $\mathcal{O}_{\Phi B}$, and $\mathcal{O}_{\Phi WB}$ affect the kinetic terms of the gauge fields, resulting in the broken theory in the following contribution to the Lagrangian

$$\begin{aligned} & -\frac{1}{2}W_{\mu\nu}^+W^{-\mu\nu} - \frac{1}{4}W_{\mu\nu}^3W^{3,\mu\nu} - \frac{1}{4}B_{\mu\nu}B^{\mu\nu} - \frac{1}{4}G_{\mu\nu}^A G^{A,\mu\nu} \\ & + \frac{1}{2}\frac{v^2}{\Lambda^2} \left(C_{\Phi W}W_{\mu\nu}^a W^{a,\mu\nu} + C_{\Phi B}B_{\mu\nu}B^{\mu\nu} + C_{\Phi WB}W_{\mu\nu}^3 B^{\mu\nu} + C_{\Phi G}G_{\mu\nu}^A G^{A,\mu\nu}\right), \end{aligned} \quad (79)$$

i.e. the gauge fields are not canonically normalized. The gauge-boson mass terms are obtained as

$$\frac{1}{4}g_2^2v^2W_\mu^+W^{-\mu} + \frac{1}{8}v^2 \left(1 + \frac{1}{2}\frac{v^2}{\Lambda^2}C_{\Phi D}\right)(g_2W_\mu^3 + g_1B_\mu)^2. \quad (80)$$

Properly normalized kinetic terms are obtained upon redefining the gauge fields as

$$G_\mu^A = \mathcal{G}_\mu^A \left(1 + \frac{C_{\Phi G}}{\Lambda^2}v^2\right), \quad W_\mu^a = \mathcal{W}_\mu^a \left(1 + \frac{C_{\Phi W}}{\Lambda^2}v^2\right), \quad B_\mu = \mathcal{B}_\mu \left(1 + \frac{C_{\Phi B}}{\Lambda^2}v^2\right). \quad (81)$$

It is customary to introduce the modified coupling constants

$$\bar{g}_s = g_s \left(1 + \frac{C_{\Phi G}}{\Lambda^2}v^2\right), \quad \bar{g}_2 = g_2 \left(1 + \frac{C_{\Phi W}}{\Lambda^2}v^2\right), \quad \bar{g}_1 = g_1 \left(1 + \frac{C_{\Phi B}}{\Lambda^2}v^2\right), \quad (82)$$

so that the products $g_s G_\mu^A = \bar{g}_s \mathcal{G}_\mu^A$, etc. are unchanged and the form of the covariant derivative is not modified.

The transformation from the $\mathcal{W}^3, \mathcal{B}$ fields to the Z, A fields can be written as

$$\begin{pmatrix} \mathcal{W}_\mu^3 \\ \mathcal{B}_\mu \end{pmatrix} = \begin{pmatrix} 1 & \frac{1}{2} \frac{v^2}{\Lambda^2} C_{\Phi WB} \\ \frac{1}{2} \frac{v^2}{\Lambda^2} C_{\Phi WB} & 1 \end{pmatrix} \begin{pmatrix} \bar{c}_w & -\bar{s}_w \\ \bar{s}_w & \bar{c}_w \end{pmatrix} \begin{pmatrix} \mathcal{Z}_\mu \\ \mathcal{A}_\mu \end{pmatrix}, \quad (83)$$

with the rotation angle $\bar{\theta}_w$ determined from

$$\bar{c}_w = \cos \bar{\theta}_w = \frac{\bar{g}_2}{\sqrt{\bar{g}_2^2 + \bar{g}_1^2}} \left(1 - \frac{1}{2} \frac{v^2}{\Lambda^2} \frac{\bar{g}_1}{\bar{g}_2} \frac{\bar{g}_2^2 - \bar{g}_1^2}{\bar{g}_2^2 + \bar{g}_1^2} C_{\Phi WB} \right), \quad \bar{s}_w = \sin \bar{\theta}_w. \quad (84)$$

The masses of the W and Z bosons result in

$$M_W^2 = \frac{1}{4} \bar{g}_2^2 v^2, \quad M_Z^2 = \frac{1}{4} (\bar{g}_1^2 + \bar{g}_2^2) v^2 + \frac{1}{8} (\bar{g}_1^2 + \bar{g}_2^2) \frac{v^4}{\Lambda^2} C_{\Phi D} + \frac{1}{2} \bar{g}_1 \bar{g}_2 \frac{v^4}{\Lambda^2} C_{\Phi WB}. \quad (85)$$

The EW part of the covariant derivative becomes

$$D_\mu = \partial_\mu - i \frac{\bar{g}_2}{\sqrt{2}} (I_w^+ \mathcal{W}_\mu^+ + I_w^- \mathcal{W}_\mu^-) - i \bar{g}_Z (I_w^3 - \bar{s}_w^2 Q) \mathcal{Z}_\mu + i \bar{e} Q \mathcal{A}_\mu, \quad (86)$$

with the effective couplings

$$\bar{e} = \frac{\bar{g}_1 \bar{g}_2}{\sqrt{\bar{g}_1^2 + \bar{g}_2^2}} \left(1 - \frac{\bar{g}_1 \bar{g}_2}{\bar{g}_1^2 + \bar{g}_2^2} \frac{v^2}{\Lambda^2} C_{\Phi WB} \right), \quad \bar{g}_Z = \frac{\bar{e}}{\bar{s}_w \bar{c}_w} \left(1 + \frac{\bar{g}_1^2 + \bar{g}_2^2}{2 \bar{g}_1 \bar{g}_2} \frac{v^2}{\Lambda^2} C_{\Phi WB} \right), \quad (87)$$

and $I_w^\pm = I_w^1 \pm i I_w^2$. The ρ parameter, defined as the ratio of charged and neutral currents at low energies [130], results in

$$\rho = \frac{\bar{g}_2^2 M_Z^2}{\bar{g}_Z^2 M_W^2} = 1 + \frac{1}{2} \frac{v^2}{\Lambda^2} C_{\Phi D}. \quad (88)$$

The Yukawa coupling matrices and the fermion mass matrices are modified by the presence of $\psi^2 \Phi^3$ operators. The fermion mass matrices are obtained as

$$M_{ij}^f = \frac{1}{\sqrt{2}} v \left(G_{ij}^f - \frac{1}{2} \frac{v^2}{\Lambda^2} C_{ij}^{f\Phi} \right), \quad f = u, d, l \quad (89)$$

after EW symmetry breaking. The coupling matrices of the Higgs boson to the fermions appearing in $-H \bar{f} \tilde{G}^f f / \sqrt{2}$, on the other hand, read

$$\tilde{G}_{ij}^f = G_{ij}^f (1 + c_{H,\text{kin}}) - \frac{3}{2} \frac{v^2}{\Lambda^2} C_{ij}^{f\Phi} = \frac{\sqrt{2}}{v} M_{ij}^f (1 + c_{H,\text{kin}}) - \frac{v^2}{\Lambda^2} C_{ij}^{f\Phi}. \quad (90)$$

The Higgs–fermion couplings are thus not necessarily proportional to the fermion mass matrices as in the SM and will in general not be simultaneously diagonalizable. Consequently, the Yukawa couplings do not necessarily have to be suppressed by the corresponding fermion masses.

Expressing the Lagrangian in terms of the redefined physical basis of fields and parameters, the quadratic part of the Lagrangian looks exactly as in the SM. After adding the usual 't Hooft–Feynman gauge-fixing term (note that A stands for the photon field and D for the colour index of the gluon field)

$$\mathcal{L}_{\text{fix}} = -C^+ C^- - \frac{1}{2} (C^Z)^2 - \frac{1}{2} (C^A)^2 - \frac{1}{2} C^{G,D} C^{G,D} \quad (91)$$

with

$$C^{G,D} = \partial_\mu G^{D\mu}, \quad C^A = \partial_\mu A^\mu, \quad C^Z = \partial_\mu Z^\mu - M_Z \chi, \quad C^\pm = \partial_\mu W^{\pm\mu} \mp i M_W \phi^\pm \quad (92)$$

in terms of the fields and parameters of the new physical basis, we obtain the quadratic part of the Lagrangian

$$\begin{aligned} \mathcal{L}_{\text{SM},0}^{(4)} = & -\frac{1}{2}(\partial_\mu \mathcal{G}_v^D)(\partial^\mu \mathcal{G}^{Dv}) - (\partial_\mu \mathcal{W}_v^+)(\partial^\mu \mathcal{W}^{-v}) - \frac{1}{2}(\partial_\mu \mathcal{Z}_v)(\partial^\mu \mathcal{Z}^v) - \frac{1}{2}(\partial_\mu \mathcal{A}_v)(\partial^\mu \mathcal{A}^v) \\ & + M_W^2 \mathcal{W}_\mu^+ \mathcal{W}^{-\mu} + \frac{1}{2} M_Z^2 \mathcal{Z}_\mu \mathcal{Z}^\mu + \frac{1}{2}(\partial_\mu H)(\partial^\mu H) - \frac{1}{2} M_H^2 H^2 \\ & + (\partial_\mu \phi^+)(\partial^\mu \phi^-) - M_W^2 \phi^+ \phi^- + \frac{1}{2}(\partial_\mu \chi)(\partial^\mu \chi) - \frac{1}{2} M_Z^2 \chi^2 \\ & + \sum_{f=l,u,d} \sum_i \bar{f}_i (i\cancel{\partial} - m_{f,i}) f_i + \sum_i \bar{\nu}_i i\cancel{\partial} \nu_i. \end{aligned} \quad (93)$$

The value of the vev can be obtained in the SM from the measurement of the Fermi coupling in μ decay. In SMEFT (neglecting lepton masses) this relation is modified to

$$\frac{4G_\mu}{\sqrt{2}} = \frac{2}{v^2} - \frac{1}{\Lambda^2} (C_{LL,\mu ee\mu} + C_{LL,e\mu\mu e} - 2C_{\Phi L,ee}^{(3)} - 2C_{\Phi L,\mu\mu}^{(3)}). \quad (94)$$

Similarly the determination of the modified gauge coupling $\bar{g}_{1,2}$ from M_Z and M_W or from M_Z and $\alpha(0)$ is affected by contributions of dimension-6 operators.

After applying the field transformations to canonically normalized fields, defined in Eqs. (76) and (81), to the full Lagrangian, the Feynman rules can be derived as usual, and observables can be calculated. At this point, we emphasize that SMEFT predictions for observables should be parametrized by a minimal set of input parameters like, e.g., $\alpha = \bar{e}^2/(4\pi)$, $\alpha_s = \bar{g}_s^2/(4\pi)$, M_W , M_Z , M_H , $m_{f,i}$, V_{ij} , and all SMEFT Wilson coefficients $C_{...}/\Lambda^n$ and consistently linearized in the latter. Otherwise the appearance of quadratic or higher terms in $C_{...}/\Lambda^n$ could spoil the consistency of the predictions.

As an example for couplings modified by dimension-6 operators, we consider the CP-even couplings of the Higgs boson to the weak gauge bosons, which receive contributions from the Lagrangian terms

$$(D_\mu \Phi)^\dagger (D^\mu \Phi) + \frac{C_{\Phi W}}{\Lambda^2} \mathcal{O}_{\Phi W} + \frac{C_{\Phi B}}{\Lambda^2} \mathcal{O}_{\Phi B} + \frac{C_{\Phi WB}}{\Lambda^2} \mathcal{O}_{\Phi WB} + \frac{C_{\Phi D}}{\Lambda^2} \mathcal{O}_{\Phi D}. \quad (95)$$

After translation to the physical basis these lead to the interactions

$$\begin{aligned} \mathcal{L}_{HVV,\text{CP}} = & \frac{1}{2} \bar{g}_2^2 v H \mathcal{W}_\mu^+ \mathcal{W}^{-\mu} (1 + c_{H,\text{kin}}) + \frac{1}{4} (\bar{g}_2^2 + \bar{g}_1^2) v \left(1 + c_{H,\text{kin}} + \frac{v^2}{\Lambda^2} C_{\Phi D} + \frac{2\bar{g}_1\bar{g}_2}{\bar{g}_2^2 + \bar{g}_1^2} \frac{v^2}{\Lambda^2} C_{\Phi WB} \right) H \mathcal{Z}^\mu \mathcal{Z}_\mu \\ & + 2 \frac{C_{\Phi W}}{\Lambda^2} v H \mathcal{W}_{\mu\nu}^+ \mathcal{W}^{-\mu\nu} + \frac{\alpha_{ZZ}}{\Lambda^2} v H \mathcal{Z}^{\mu\nu} \mathcal{Z}_{\mu\nu} - \frac{\alpha_{AZ}}{\Lambda^2} v H \mathcal{A}^{\mu\nu} \mathcal{Z}_{\mu\nu} + \frac{\alpha_{AA}}{\Lambda^2} v H \mathcal{A}^{\mu\nu} \mathcal{A}_{\mu\nu}, \end{aligned} \quad (96)$$

with the coefficients

$$\begin{aligned} \alpha_{ZZ} &= \bar{c}_w^2 C_{\Phi W} + \bar{s}_w^2 C_{\Phi B} + \bar{c}_w \bar{s}_w C_{\Phi WB}, \\ \alpha_{AZ} &= 2\bar{c}_w \bar{s}_w (C_{\Phi W} - C_{\Phi B}) - (\bar{c}_w^2 - \bar{s}_w^2) C_{\Phi WB}, \\ \alpha_{AA} &= \bar{s}_w^2 C_{\Phi W} + \bar{c}_w^2 C_{\Phi B} - \bar{c}_w \bar{s}_w C_{\Phi WB}. \end{aligned} \quad (97)$$

While the operators $\mathcal{O}_{\Phi \square}$ and $\mathcal{O}_{\Phi D}$ change only the normalization of the couplings, the operators $\mathcal{O}_{\Phi W}$, $\mathcal{O}_{\Phi B}$, and $\mathcal{O}_{\Phi WB}$ yield extra momentum-dependent contributions. The former drop out in the ratio of the Higgs-boson couplings to W and Z bosons, but the latter do not.

The dimension-6 operators contribute to practically all interaction terms. Their contributions to anomalous triple gauge couplings are, for instance, given in Ref. [129].

2.4.3. Applications

The theoretical preparation of phenomenological predictions towards a full fit of all SMEFT Wilson coefficients to experimental data from the LHC and previous colliders is a very active line of research. In this context, the evaluation of SMEFT predictions with NLO QCD and EW corrections is quite a challenge.

The renormalization-group evolution of the complete set of SM dimension-6 operators was presented in Refs. [128, 131, 132]. Results for operator renormalization in the Warsaw basis were elaborated in Refs. [123, 133].

The calculation of NLO corrections in SMEFT was discussed in Refs. [67, 129]. The first pioneering calculations in this framework were for the processes $\mu \rightarrow e\gamma$ [134], $H \rightarrow \gamma\gamma$ [133, 135, 136], and $H \rightarrow \gamma Z, ZZ, WW$ [133]. More recently, NLO QCD corrections were calculated in SMEFT for instance for W-pair production at the LHC [137] (see also references therein) and the Higgs decay in bottom quarks [138]. NLO EW corrections to Z-boson decays were investigated in Refs. [139, 140], while those to Higgs-boson decays were calculated in Ref. [141] and references therein. EW and QCD corrections to Z and W pole observables within SMEFT were computed in Ref. [142]. NLO EW corrections to $t\bar{t}$ Production at the LHC were recently published [143]. An overview of SMEFT calculations and tools can be found in Ref. [144].

3. Electroweak radiative corrections—virtual effects

3.1. Renormalization of the Electroweak Standard Model in the on-shell scheme

3.1.1. Historical development and variants

As a non-abelian gauge theory with spontaneous symmetry breaking the SM of particle physics including the EWSM and QCD is renormalizable [21–28, 100]. All ultraviolet (UV) singularities can be absorbed into renormalization constants that are generated by a renormalization of the independent input parameters and the fields and/or the external wave functions.

In order to define a *renormalization scheme* one has to choose a set of independent parameters. One possibility is to start from the Lagrangian in its symmetric form (8). To absorb all UV singularities of the effective action, one needs to introduce renormalization constants for all parameters of the theory in the symmetric basis, a renormalization of the vacuum expectation value (vev) of the Higgs field, and a rescaling of the field multiplets [28]. In this framework, the calculation of S -matrix elements requires the inclusion of finite wave-function renormalization constants for the external states.¹⁴

For practical calculations it is more convenient to fix the renormalization constants by renormalization conditions imposed directly on the parameters in the physical basis. It has become customary to require the renormalized masses of the gauge bosons, of the Higgs boson, and of the fermions to equal the physical masses, “physical” in the sense of being derived from the locations of the poles of the propagators. Moreover, the renormalized electric charge can be fixed in such a way that it coincides with the one measured in the *Thomson limit*, i.e. in the limit of low-energy Compton scattering of on-shell (OS) particles. This is the so-called *on-shell renormalization scheme* which was originally proposed by Ross and Taylor [35] and later worked out and used by many authors [36–38, 40, 82, 117, 145–150]. The OS scheme is distinguished by the fact that all renormalized parameters have a direct physical meaning and can be measured most directly in suitable experiments. For most of the particle masses this is evident.¹⁵ It is also true for the definition of the electric charge, because in the Thomson limit of Compton scattering all higher-order corrections vanish, and the lowest-order QED cross section known as *Thomson cross section* becomes exact in all orders of perturbation theory [151, 152]. The renormalization of the parameters together with the renormalization of the external wave functions, which is dictated by the correct normalization of S -matrix elements, is sufficient to obtain UV-finite predictions without any additional field renormalization. This fact has been exploited for instance by Passarino and Veltman [34] and Sirlin [36].

In order to obtain finite Green functions, field renormalization is required in addition. When renormalizing the Lagrangian in its symmetric form, it is sufficient to introduce only one field renormalization constant for each multiplet. This minimal field renormalization [38] of the EW sector of the SM requires one renormalization constant for the triplet of $SU(2)_W$ gauge fields, one for the $U(1)_Y$ gauge field, one for the complex Higgs-doublet field, one for each left-handed fermion doublet, and one for each right-handed fermion singlet. In this scheme, additional UV-finite wave-function renormalizations have to be applied when calculating S -matrix elements.

¹⁴By wave-function renormalization constants we denote the renormalization factors of the external states, which are also known as *LSZ factors*. The wave-function renormalization has to be applied to obtain correctly normalized S -matrix elements. It is not needed, if the field renormalization is performed appropriately.

¹⁵This does not hold for the masses of the light quarks owing to the presence of the strong interaction and confinement. However, their contributions can often be absorbed into directly measurable and thus more appropriate input quantities.

Another possibility is to renormalize the fields in the physical basis [37, 40]. Since fields that carry identical conserved quantum numbers in general mix, the field renormalization constants (and possibly the wave-function renormalization constants) take the form of matrices. This allows us to fix the field renormalization in such a way that the renormalized fields do not mix on shell and that no wave-function renormalization is required. Alternatively, one can combine non-diagonal mass renormalization constants and field-renormalization matrices involving fewer non-zero, non-diagonal entries, as has been done for the renormalization of the photon–Z-boson system in Refs. [39, 150].

In this review, we restrict our account of renormalization to the one-loop level. Two-loop renormalization of the EWSM is, for instance, discussed in Refs. [153, 154], and a complete renormalization framework for the EWSM at the two-loop level is laid out in Refs. [155–157]. In this section, we put our emphasis on OS renormalization in the EW sector, which is the most frequent choice in the calculation of EW corrections; we briefly sketch EW $\overline{\text{MS}}$ renormalization in Section 5.1.2.

In this section we sometimes assume CP conservation. This is correct when neglecting the CP-violating phase of the quark-mixing matrix, an approximation that is justified for the majority of processes accessible at high-energy colliders. In this respect, we note that at least four quark-mixing-matrix elements in an appropriate combination are required to construct CP-violating observables [158, 159].

3.1.2. Renormalization transformation in the on-shell scheme

We perform the renormalization directly for the parameters and fields of the physical basis introduced in Section 2.1.2. The *bare* parameters are split into *renormalized parameters* and *counterterms* as follows (bare quantities are denoted by a subscript 0):

$$\begin{aligned} M_{0,W}^2 &= M_W^2 + \delta M_W^2, & M_{0,Z}^2 &= M_Z^2 + \delta M_Z^2, & M_{0,H}^2 &= M_H^2 + \delta M_H^2, \\ m_{0,f,i} &= m_{f,i} + \delta m_{f,i}, & V_{0,ij} &= V_{ij} + \delta V_{ij}, \\ e_0 &= Z_e e = (1 + \delta Z_e) e = e + \delta e. \end{aligned} \quad (98)$$

Here M_W , M_Z , M_H , and $m_{f,i}$ are the renormalized masses of the corresponding particles. In OS renormalization schemes these correspond to the physical masses defined by the locations of the poles of the propagators (*OS* or *pole masses*).¹⁶ The renormalization of tadpoles is discussed in Section 3.1.6.

We introduce field renormalization for fields with equal quantum numbers via renormalization matrices. We assume that the physical Higgs field does not mix with other fields, which is valid in the one-loop approximation. More generally, this holds if CP conservation is required, since then the physical Higgs field has CP parity + while the other neutral bosons have CP parity –. The bare fields in the physical basis are split according to

$$\begin{aligned} W_0^\pm &= Z_W^{1/2} W^\pm = \left(1 + \frac{1}{2} \delta Z_W\right) W^\pm, \\ \begin{pmatrix} Z_0 \\ A_0 \end{pmatrix} &= \begin{pmatrix} Z_{ZZ}^{1/2} & Z_{ZA}^{1/2} \\ Z_{AZ}^{1/2} & Z_{AA}^{1/2} \end{pmatrix} \begin{pmatrix} Z \\ A \end{pmatrix} = \begin{pmatrix} 1 + \frac{1}{2} \delta Z_{ZZ} & \frac{1}{2} \delta Z_{ZA} \\ \frac{1}{2} \delta Z_{AZ} & 1 + \frac{1}{2} \delta Z_{AA} \end{pmatrix} \begin{pmatrix} Z \\ A \end{pmatrix}, \\ H_0 &= Z_H^{1/2} H = \left(1 + \frac{1}{2} \delta Z_H\right) H, \\ f_{0,i}^L &= \sum_j (Z_{ij}^{f,L})^{1/2} f_j^L = \sum_j \left(\delta_{ij} + \frac{1}{2} \delta Z_{ij}^{f,L} \right) f_j^L, & f_{0,i}^R &= \sum_j (Z_{ij}^{f,R})^{1/2} f_j^R = \sum_j \left(\delta_{ij} + \frac{1}{2} \delta Z_{ij}^{f,R} \right) f_j^R, \end{aligned} \quad (99)$$

where the last expressions in each line are valid in first-order approximation. This general transformation allows us to define the fields in such a way that their quanta are mass eigenstates also in the presence of higher-order corrections.

The renormalization constants introduced so far are sufficient to render S -matrix elements and Green functions involving only physical external states UV finite. A complete renormalization of the EWSM in addition requires the renormalization of the unphysical sector. This amounts to the field renormalization of the would-be Goldstone fields,

$$\chi_0 = Z_\chi^{1/2} \chi = \left(1 + \frac{1}{2} \delta Z_\chi\right) \chi, \quad \phi_0^\pm = Z_\phi^{1/2} \phi^\pm = \left(1 + \frac{1}{2} \delta Z_\phi\right) \phi^\pm, \quad (100)$$

¹⁶The subtle difference between OS and pole masses will be discussed in the context of unstable-particle effects in Section 6.4.

of the Faddeev–Popov ghost fields,

$$u_0^\pm = \tilde{Z}_\pm u^\pm = (1 + \delta\tilde{Z}_\pm) u^\pm,$$

$$\begin{pmatrix} u_0^Z \\ u_0^A \end{pmatrix} = \begin{pmatrix} \tilde{Z}_{ZZ} & \tilde{Z}_{ZA} \\ \tilde{Z}_{AZ} & \tilde{Z}_{AA} \end{pmatrix} \begin{pmatrix} u^Z \\ u^A \end{pmatrix} = \begin{pmatrix} 1 + \delta\tilde{Z}_{ZZ} & \delta\tilde{Z}_{ZA} \\ \delta\tilde{Z}_{AZ} & 1 + \delta\tilde{Z}_{AA} \end{pmatrix} \begin{pmatrix} u^Z \\ u^A \end{pmatrix}, \quad (101)$$

and of the renormalization of the gauge parameters,

$$\xi_{0,W}^{(\prime)} = Z_{\xi_W^{(\prime)}} \xi_W^{(\prime)}, \quad \xi_{0,Z}^{(\prime)} = Z_{\xi_Z^{(\prime)}} \xi_Z^{(\prime)}, \quad \xi_{0,A} = Z_{\xi_A} \xi_A. \quad (102)$$

We use the convention not to renormalize the Faddeev–Popov antighost fields \bar{u} . This is possible, since the antighost fields always appear together with the ghost fields, so that all related UV divergences can be absorbed via a renormalization of the Faddeev–Popov ghost fields u .

By choosing $\xi'_W = \xi_W$ and $\xi'_Z = \xi_Z$, the would-be Goldstone bosons decouple from the scalar gauge bosons, and the poles of their propagators are located at $p^2 = \xi_W M_W^2$ and $\xi_Z M_Z^2$ in lowest order, respectively. In order to conserve these features at higher orders, one has to renormalize ξ'_a and ξ_a independently. The renormalization of ξ'_a and ξ_a can be performed in such a way that the gauge-fixing functionals remain unchanged, so that they do not generate counterterms at all.

Upon inserting the renormalization transformations into the bare Lagrangian (31) and writing $Z = 1 + \delta Z$ for the multiplicative renormalization constants (matrices) we can split the bare Lagrangian as

$$\mathcal{L}(\Psi_0, p_0) = \mathcal{L}(\Psi, p) + \mathcal{L}_{\text{ct}}(\Psi, p, \delta Z), \quad (103)$$

where Ψ_0 and p_0 represent the bare fields and parameters and Ψ and p their renormalized counterparts. The renormalized Lagrangian $\mathcal{L}(\Psi, p)$ has the same functional form as $\mathcal{L}(\Psi_0, p_0)$, but with unrenormalized parameters and fields replaced by renormalized ones. The *counterterm Lagrangian* $\mathcal{L}_{\text{ct}}(\Psi, p, \delta Z)$ gives rise to the counterterms containing the renormalization constants δZ . If not stated otherwise, we restrict ourselves to one-loop corrections and consistently neglect terms of order $(\delta Z)^2$ in the following.

3.1.3. Renormalization conditions

The renormalization constants are fixed by imposing *renormalization conditions*. These consist of three sets: the conditions that define the renormalized physical parameters, those that define the renormalized fields corresponding to physical particle states, and those that fix the renormalization in the unphysical sector. While only the first set is relevant for the calculation of observables (S -matrix elements), a clever choice of the second set allows us not only to eliminate the explicit wave-function renormalization of the external particles, but also to simplify the explicit form of the renormalization conditions for the physical parameters. The choice of the third set determines the form of the renormalized Slavnov–Taylor identities.

The renormalized mass parameters of the particles are fixed by the requirement that they are equal to the physical masses, which are defined via the locations of the poles of the corresponding propagators. These poles are equivalent to the zeros of the inverse connected 2-point functions projected onto physical states, i.e. on polarization vectors $\epsilon^\mu(k)$ for gauge bosons and on spinors $u(p)$ and $v(p)$ for fermions.¹⁷ In case of mass matrices these conditions have to be fulfilled by the corresponding eigenvalues, in general resulting in complicated expressions. These can be considerably simplified by requiring the OS conditions for the field renormalization matrices in addition [37, 40]. The latter conditions require that close to its pole each propagator is given by its lowest-order expression with the bare mass replaced by the renormalized mass. As a consequence, an OS particle does not mix with others, and its propagator has residue one, i.e. the quanta of the renormalized fields are canonically normalized mass eigenstates. Thus, we arrive at the following renormalization conditions for the renormalized 2-point functions Γ_R for OS fields for physical external states:

$$\left[\widetilde{\text{Re}} \Gamma_{R,\mu\nu}^{V'V}(-k, k) \right] \epsilon^\nu(k) \Big|_{k^2 = M_V^2} = 0, \quad V, V' = W, Z, A,$$

¹⁷For issues concerning the renormalization in the presence of unstable particles we refer to Section 6.

$$\begin{aligned}
\lim_{k^2 \rightarrow M_V^2} \frac{1}{k^2 - M_V^2} \left[\widetilde{\text{Re}} \Gamma_{\text{R},\mu\nu}^{V^\dagger V}(-k, k) \right] \varepsilon^\nu(k) &= -\varepsilon_\mu(k), \quad V = W, Z, A, \\
\widetilde{\text{Re}} \Gamma_{\text{R}}^{HH}(-k, k) \Big|_{k^2=M_{\text{H}}^2} &= 0, \\
\lim_{k^2 \rightarrow M_{\text{H}}^2} \frac{1}{k^2 - M_{\text{H}}^2} \widetilde{\text{Re}} \Gamma_{\text{R}}^{HH}(-k, k) &= 1, \\
\left[\widetilde{\text{Re}} \Gamma_{\text{R},ij}^{\bar{f}f}(-p, p) \right] u_j(p) \Big|_{p^2=m_{f,j}^2} &= 0, \\
\lim_{p^2 \rightarrow m_{f,i}^2} \frac{\not{p} + m_{f,i}}{p^2 - m_{f,i}^2} \left[\widetilde{\text{Re}} \Gamma_{\text{R},ii}^{\bar{f}f}(-p, p) \right] u_i(p) &= u_i(p). \tag{104}
\end{aligned}$$

The polarization vectors and spinors of the external fields are denoted by $\varepsilon^\mu(k)$ and $u_i(p)$, respectively. The definition of $\widetilde{\text{Re}}$ depends on the scheme. In the traditional OS scheme, it takes the real part of the vertex functions. In the presence of genuinely complex couplings, e.g. resulting from a phase in the quark-mixing matrix, it takes the real part of the loop integrals, i.e. it eliminates the absorptive parts, but does not affect the complex couplings. Thus in the CP-conserving SM, $\widetilde{\text{Re}}$ can be replaced by Re everywhere. Finally, in the complex-mass scheme discussed in Section 6 the real part is not taken at all.

The renormalization conditions (104) can be simplified upon inserting the Lorentz decompositions of the 2-point functions,

$$\begin{aligned}
\Gamma_{\mu\nu}^{V^\dagger V}(-k, k) &= \left(g_{\mu\nu} - \frac{k_\mu k_\nu}{k^2} \right) \Gamma_{\text{T}}^{V^\dagger V}(k^2) + \frac{k_\mu k_\nu}{k^2} \Gamma_{\text{L}}^{V^\dagger V}(k^2), \\
\Gamma_{ij}^{\bar{f}f}(-p, p) &= \not{p} \frac{1 - \gamma_5}{2} \Gamma_{ij}^{f,\text{L}}(p^2) + \not{p} \frac{1 + \gamma_5}{2} \Gamma_{ij}^{f,\text{R}}(p^2) + \frac{1 - \gamma_5}{2} \Gamma_{ij}^{f,\text{L}}(p^2) + \frac{1 + \gamma_5}{2} \Gamma_{ij}^{f,\text{R}}(p^2), \tag{105}
\end{aligned}$$

which hold for renormalized vertex functions Γ_{R} analogously. If we neglect absorptive parts, which are irrelevant for the (one-loop) renormalization, the hermiticity of the Lagrangian implies the hermiticity of the effective action. Therefore, the fermionic 2-point functions must have the symmetry

$$\widetilde{\text{Re}} \Gamma_{ij}^{\bar{f}f}(-p, p) = \widetilde{\text{Re}} \gamma^0 \left(\Gamma_{ji}^{\bar{f}f}(-p, p) \right)^\dagger \gamma^0, \tag{106}$$

which implies

$$\widetilde{\text{Re}} \Gamma_{ij}^{f,\text{L}}(p^2) = \widetilde{\text{Re}} \left(\Gamma_{ji}^{f,\text{L}}(p^2) \right)^*, \quad \widetilde{\text{Re}} \Gamma_{ij}^{f,\text{R}}(p^2) = \widetilde{\text{Re}} \left(\Gamma_{ji}^{f,\text{R}}(p^2) \right)^*, \quad \widetilde{\text{Re}} \Gamma_{ij}^{f,\text{L}}(p^2) = \widetilde{\text{Re}} \left(\Gamma_{ji}^{f,\text{R}}(p^2) \right)^*, \tag{107}$$

where $\widetilde{\text{Re}}$ eliminates the absorptive parts in the loop integrals, but has no effect on complex couplings and Dirac matrices. CP symmetry, which holds in the SM for the one-loop 2-point functions or for real V_{ij} in general, implies

$$\Gamma_{ij}^{f,\text{L}}(p^2) = \Gamma_{ji}^{f,\text{L}}(p^2), \quad \Gamma_{ij}^{f,\text{R}}(p^2) = \Gamma_{ji}^{f,\text{R}}(p^2), \quad \Gamma_{ij}^{f,\text{L}}(p^2) = \Gamma_{ji}^{f,\text{R}}(p^2). \tag{108}$$

Moreover, at the one-loop level in the SM the scalar coefficients of the fermion self-energy take the form

$$\Gamma_{ij}^{f,\text{L}}(p^2) = m_{f,i} \Gamma_{ij}^{f,\text{S}}(p^2), \quad \Gamma_{ij}^{f,\text{R}}(p^2) = m_{f,j} \Gamma_{ij}^{f,\text{S}}(p^2), \tag{109}$$

i.e. $\Gamma_{ij}^{f,\text{L}}$ and $\Gamma_{ij}^{f,\text{R}}$ are proportional to the single function $\Gamma_{ij}^{f,\text{S}}$. This will be used in later sections. The relations Eqs. (107)–(109) can be maintained for the renormalized self-energies as well.

Inserting the Lorentz decompositions (105), we obtain¹⁸ from Eq. (104)

$$\widetilde{\text{Re}} \Gamma_{\text{R},\text{T}}^{V^\dagger V}(M_V^2) = 0, \quad \widetilde{\text{Re}} \frac{\partial \Gamma_{\text{R},\text{T}}^{V^\dagger V}(k^2)}{\partial k^2} \Big|_{k^2=M_V^2} = -1, \tag{110}$$

¹⁸The subscript R for renormalization should be confused with the superscript R for right handed fermions.

$$\widetilde{\text{Re}} \Gamma_R^{HH}(M_H^2) = 0, \quad \widetilde{\text{Re}} \left. \frac{\partial \Gamma_R^{HH}(k^2)}{\partial k^2} \right|_{k^2=M_H^2} = 1, \quad (111)$$

$$m_{f,j} \widetilde{\text{Re}} \Gamma_{R,ij}^{f,L}(m_{f,j}^2) + \widetilde{\text{Re}} \Gamma_{R,ij}^{f,R}(m_{f,j}^2) = 0, \quad m_{f,j} \widetilde{\text{Re}} \Gamma_{R,ij}^{f,R}(m_{f,j}^2) + \widetilde{\text{Re}} \Gamma_{R,ij}^{f,I}(m_{f,j}^2) = 0, \quad (112)$$

$$\widetilde{\text{Re}} \left\{ \Gamma_{R,ii}^{f,R}(m_{f,i}^2) + \Gamma_{R,ii}^{f,L}(m_{f,i}^2) + 2 \frac{\partial}{\partial p^2} \left[m_{f,i}^2 \left(\Gamma_{R,ii}^{f,R}(p^2) + \Gamma_{R,ii}^{f,L}(p^2) \right) + m_{f,i} \left(\Gamma_{R,ii}^{f,R}(p^2) + \Gamma_{R,ii}^{f,I}(p^2) \right) \right] \right\}_{p^2=m_{f,i}^2} = 2. \quad (113)$$

We mention that Eq. (112) together with the relations (107) or alternatively (108) for the renormalized self-energies implies

$$m_{f,i} \widetilde{\text{Re}} \Gamma_{R,ii}^{f,R}(m_{f,i}^2) = m_{f,i} \widetilde{\text{Re}} \Gamma_{R,ii}^{f,L}(m_{f,i}^2) = -\widetilde{\text{Re}} \Gamma_{R,ii}^{f,R}(m_{f,i}^2) = -\widetilde{\text{Re}} \Gamma_{R,ii}^{f,I}(m_{f,i}^2). \quad (114)$$

Finally, note that the condition $\Gamma_{R,T}^{AA}(0) = 0$ is automatically fulfilled as a consequence of the Slavnov–Taylor identities and the analyticity properties¹⁹ of the 2-point functions and does not imply a constraint on the counterterms.

3.1.4. Charge renormalization

The electric charge is defined as the full $ee\gamma$ coupling for OS electrons in the *Thomson limit*, i.e. for vanishing photon momentum. The full $ee\gamma$ coupling consists of the corresponding vertex function including possible wave-function renormalization constants. Owing to the photon–Z-boson mixing, also the eeZ coupling enters in general. In the complete OS renormalization scheme the field renormalization is chosen in such a way that the OS photon does not mix with the Z boson and that no wave-function renormalization is needed. Then, the *charge renormalization condition* takes the simple form

$$\bar{u}(p) \Gamma_{R,\mu}^{A\bar{e}e}(0, -p, p) u(p) \Big|_{p^2=m_e^2} = e \bar{u}(p) \gamma_\mu u(p) \quad (115)$$

for the (truncated) vertex function $\Gamma_{R,\mu}^{A\bar{e}e}(k, \bar{p}, p)$. Owing to *charge universality* we could impose the above renormalization condition on any charged particle to obtain the same renormalized charge e .

3.1.5. Renormalization of the quark-mixing matrix

For a non-trivial *quark-mixing matrix* V , also the corresponding parameters need to be renormalized. There is a vast literature on the renormalization of V_{ij} , and various prescriptions for its renormalization have been advocated [160–168]. For scattering processes at high-energy colliders, the renormalization of the quark-mixing matrix in the SM is practically irrelevant, since in higher-order corrections neglecting the quark mixing is a good approximation.

Therefore, we here sketch only the original, simple renormalization prescription [160] for V_{ij} . This prescription can be motivated as follows. The bare quark-mixing matrix V_0 is given by Eq. (21),

$$V_{0,ij} = \sum_k U_{0,ik}^{u,L} U_{0,kj}^{d,L\dagger}, \quad (116)$$

where the matrices $U_0^{f,L}$ transform the bare fields f'_0 corresponding to weak-interaction eigenstates to the fields f_0 of the bare mass eigenstates,

$$\sum_j U_{0,ij}^{f,L\dagger} f_{0,j}^L = f_{0,i}^L. \quad (117)$$

In the OS renormalization scheme, the fields of the fermion mass eigenstates are related in higher orders to their bare counterparts through the field renormalization constants of the fermions,

$$f_{0,i}^L = \sum_j Z_{ij}^{1/2,f,L} f_j^L. \quad (118)$$

¹⁹Since $\Gamma_{\mu\nu}^{AA}(k, -k)$ cannot develop a pole for $k^2 \rightarrow 0$, we have $\Gamma_{R,T}^{AA}(0) = \Gamma_{R,L}^{AA}(0)$. On the other hand, the last identity of Eq. (50) implies $\Gamma_{R,L}^{AA}(k^2) \equiv 0$ and thus $\Gamma_{R,T}^{AA}(0) = 0$.

The renormalized quark-mixing matrix is defined in analogy to the unrenormalized one through the rotation from the weak-interaction basis to the renormalized mass basis. Since both the bare and renormalized quark-mixing matrices have to be unitary, only the unitary part of the field renormalization matrices can enter.

In one-loop approximation the rotation contained in the fermion wave-function renormalization $\mathbb{1} + \frac{1}{2}\delta Z^L$ is simply given by its antihermitean part

$$\delta Z_{ij}^{f,L,AH} = \frac{1}{2} (\delta Z_{ij}^{f,L} - \delta Z_{ij}^{f,L\dagger}). \quad (119)$$

This leads us to define the renormalized quark-mixing matrix as

$$\begin{aligned} V_{ij} &= \sum_{k,n} \left(\delta_{ik} + \frac{1}{2} \delta Z_{ik}^{u,L,AH\dagger} \right) V_{0,kn} \left(\delta_{nj} + \frac{1}{2} \delta Z_{nj}^{d,L,AH} \right) \\ &= V_{0,ij} + \frac{1}{2} \sum_k \left(\delta Z_{ik}^{u,L,AH\dagger} V_{0,kj} + V_{0,ik} \delta Z_{kj}^{d,L,AH} \right) = V_{0,ij} - \delta V_{ij}. \end{aligned} \quad (120)$$

This condition absorbs all one-loop UV divergences, yields $V_{ij} = V_{0,ij}$ in the limit of degenerate up- or down-type quark masses [160], and treats all quarks on the same footing.

It has been criticised that the resulting renormalization constant depends on the gauge, if the fermion wave-function renormalization constants fixed by the OS conditions (110) are used to fix the renormalization constant of the quark-mixing matrix [161]. However, δV_{ij} can be fixed by definition in a specific gauge [164, 165]. If this value of δV_{ij} is kept in other gauges, the S -matrix elements in fact depend on renormalized input parameters in a gauge-independent way. In the light of this fact, the original renormalization condition for the quark-mixing matrix [160] emerges as a consistent and simple recipe [116].

3.1.6. Tadpole renormalization

When calculating higher-order corrections in spontaneously broken gauge theories like the SM, so-called tadpole diagrams arise, i.e. Feynman diagrams containing one or more subdiagrams of the form

$$T^H = \text{---} \overset{H}{\text{---}} \text{---} \circ . \quad (121)$$

The vertex functions, defined via a Legendre transformation from the connected Green functions, involve such tadpole contributions if the splitting $\bar{v} + H(x)$ of the physical Higgs field into a constant shift \bar{v} and a field excitation $H(x)$ does not provide an expansion of the effective Higgs potential about its true minimum (see for instance App. C of Ref. [116]). The location of the minimum is quantified by the vev v , which itself is not a free parameter, but determined by the free parameters of the theory. Minimizing the Higgs potential to define v in perturbation theory necessarily leads to tadpole-like contributions beyond tree level, just by the perturbative ordering and truncation of contributions. Technically, it is desirable to organize the perturbative bookkeeping by appropriate parameter and field definition and renormalization in such a way that the occurrence of tadpole contributions is widely suppressed.

At tree level, tadpole contributions can be easily eliminated upon demanding that the classical ground state $\langle \Phi \rangle$ of the Higgs field minimizes the tree-level potential of the Lagrangian (8). In the SM, this leads to the condition

$$|\langle \Phi \rangle|^2 = \frac{2\mu_0^2}{\lambda_0} = \frac{v_0^2}{2}, \quad v_0 = 2 \sqrt{\frac{\mu_0^2}{\lambda_0}}. \quad (122)$$

Keeping the definition of $\bar{v} = v_0$ at least to leading order, implies that the tadpole subdiagrams (121) involve at least one loop. The freedom of defining the shift \bar{v} can be exploited to generate a counterterm contribution $\delta t H$ in the counterterm Lagrangian $\delta \mathcal{L}$ in order to compensate all explicit loop subdiagrams of the form (121) which define the unrenormalized tadpole contribution T^H (in momentum space) to the Higgs-field 1-point vertex function Γ^H . Demanding that T^H is fully cancelled by the tadpole counterterm δt can, thus, be expressed by the following renormalization condition for the renormalized 1-point function Γ_R^H ,

$$\Gamma_R^H = \Gamma_{\text{1PI}}^H + \delta t = T^H + \delta t = 0 \quad \Rightarrow \quad \delta t = -T^H. \quad (123)$$

If this condition is fulfilled the corresponding \bar{v} is equal to the true minimum of the effective Higgs potential in the considered order, i.e. $\bar{v} = v$. As a consequence of the condition (123) no Feynman diagrams involving tadpoles as subdiagrams need to be considered in actual calculations. Instead, δt enters several counterterm structures of the theory, i.e. δt enters $\delta\mathcal{L}$ not just as the single term $\delta t H$. Effectively the introduction of δt just redistributes tadpole contributions. Since the definition of the higher-order contributions to \bar{v} is a matter of convention, the technical details of how \bar{v} is defined and how δt is introduced should not affect any predictions of observables.

In the following we describe several different *tadpole schemes* for the definition of \bar{v} and δt . All of them make use of Eq. (123) to calculate δt from the explicit diagrammatic tadpole contribution T^H , but the additional tadpole contributions to counterterms are different. Since T^H and, thus, also δt are gauge-dependent quantities, the discussion of gauge dependences in the various tadpole schemes is interesting.

(a) *Fleischer–Jegerlehner tadpole scheme (FJTS)*

In the FJTS [147, 169, 170], the bare vev v_0 from Eq. (122) is used to define the bare masses in terms of the original bare parameters of the Lagrangian,

$$\begin{aligned} M_{0,W} &= \frac{1}{2}g_{0,2}v_0, & M_{0,Z} &= \frac{1}{2}\sqrt{g_{0,1}^2 + g_{0,2}^2}v_0, \\ M_{0,H}^2 &= 2\mu_0^2 = \frac{\lambda_0}{2}v_0^2, & m_{0,f,i} &= \frac{v_0}{\sqrt{2}}\sum_{k,m}U_{0,ik}^{f,L}G_{0,km}^fU_{0,mi}^{f,R\dagger}. \end{aligned} \quad (124)$$

The tadpole counterterm is introduced by the field transformation

$$H_0 \rightarrow H_0 + \Delta v, \quad (125)$$

with a constant Δv . This transformation can be interpreted as a change of the integration variable H_0 in the functional integral (with unit Jacobian), which has no physical effect, so that Δv can be chosen arbitrarily. The field shift (125) introduces Δv terms in the Lagrangian wherever the field H_0 occurs. At one-loop order, only the terms linear in Δv are relevant, so that

$$\begin{aligned} \delta\mathcal{L}_{\Delta v} &= -\frac{1}{4}\Delta v\lambda_0\left[2H_0v_0^2 + v_0(2\phi_0^-\phi_0^+ + 3H_0^2 + \chi_0^2) + H_0(2\phi_0^-\phi_0^+ + H_0^2 + \chi_0^2)\right] \\ &\quad + \text{terms from kinetic and Yukawa parts of the Higgs Lagrangian}. \end{aligned} \quad (126)$$

Diagrammatically the Feynman rules for the Δv terms result from replacing external H lines by Δv in the original Feynman rules, so that in particular quartic couplings with Δv do not exist. On the other hand, tadpole contributions arise in all bosonic vertices with less than four fields and in all 2-point functions.

The term in Eq. (126) that is linear in H_0 can be directly identified with the desired $\delta t H$ counterterm for the explicit tadpole diagrams, so that

$$\delta t = (v_0 + \Delta v)\left(\mu_0^2 - \frac{1}{4}\lambda_0(v_0 + \Delta v)^2\right) = \Delta v\left(\mu_0^2 - \frac{3}{4}\lambda_0v_0^2\right) + \mathcal{O}(\Delta v^2) = -\frac{1}{2}\Delta v\lambda_0v_0^2 + \mathcal{O}(\Delta v^2). \quad (127)$$

For later convenience we did not yet make use of $v_0 = 2\sqrt{\mu_0^2/\lambda_0}$ and the linearization in Δv in the first equation. Solving this relation for Δv in one-loop approximation and using Eq. (124), fixes Δv to

$$\Delta v = -\frac{\delta t}{M_H^2}. \quad (128)$$

Using this and Eq. (124) to eliminate v_0 in favour of $M_{0,W}$ in Eq. (126), the tadpole contributions to the Lagrangian can be written as

$$\delta\mathcal{L}_{\delta t}^{\text{FJTS}} = \delta t H + \frac{1}{4}\frac{\delta t e}{M_W s_W}\left[2\phi^-\phi^+ + 3H^2 + \chi^2\right] + \frac{1}{8}\frac{\delta t e^2}{M_W^2 s_W^2}H\left[2\phi^-\phi^+ + H^2 + \chi^2\right]$$

$$+ \text{ terms from kinetic and Yukawa parts of the Higgs Lagrangian.} \quad (129)$$

Since δt is already a one-loop correction, all bare quantities in $\delta\mathcal{L}_{\delta t}$ can be replaced by their renormalized counterparts. In the FJTS, all parameter counterterms are gauge independent. To this end, it is crucial that we use self-energies that are defined from complete inverse connected 2-point Green functions including tadpole contributions to determine the counterterms.²⁰

As an alternative to the field shift (125), the Δv contributions to $\delta\mathcal{L}$ can be obtained via the parameter shift [170]

$$v_0 \rightarrow v_0 + \Delta v = v_0 - \frac{\delta t}{M_H^2} \quad (130)$$

before the vev v_0 is fixed by minimizing the scalar potential and thus related to λ_0 and μ_0^2 via Eq. (122).

Recall that without the field shift (125), there is no tadpole counterterm and all tadpole diagrams would have to be included explicitly. Thus, the FJTS is equivalent to the inclusion of all tadpole diagrams. Finally, we also mention that the FJTS scheme is equivalent to the β_t scheme of Ref. [155].

(b) Parameter-renormalized tadpole scheme (PRTS)

The tadpole scheme of Ref. [40] generates the tadpole counterterm as part of the parameter renormalization transformation without touching the fields. Following Ref. [116], we call this scheme *parameter renormalized tadpole scheme (PRTS)*. Introducing a shifted neutral scalar field $\bar{v} + H_0(x)$ into the bare Lagrangian (8) without any constraint on \bar{v} , leads to a linear term $t_0 H_0$ in the Lagrangian with

$$t_0 = \bar{v} \left(\mu_0^2 - \frac{1}{4} \lambda_0 \bar{v}^2 \right). \quad (131)$$

Instead of setting the bare tadpole parameter t_0 to zero, as done in the FJTS in Eq. (122), this parameter is directly taken as tadpole counterterm, i.e. $\delta t = t_0$, leading to the identification $\bar{v} = v$. This is equivalent to the statement of setting the renormalized tadpole t to zero after the tadpole renormalization transformation $t_0 = t + \delta t$, and

$$\delta t = v \left(\mu_0^2 - \frac{1}{4} \lambda_0 v^2 \right). \quad (132)$$

Isolating the terms in the Lagrangian that are quadratic in H_0 , the bare Higgs-boson mass can be related to the original input parameters,

$$M_{0,H}^2 = -\mu_0^2 + \frac{3}{4} \lambda_0 v^2. \quad (133)$$

Similarly, the bare masses of the other particles are defined as the coefficients of the terms in the Lagrangian quadratic in the fields, i.e.

$$M_{0,W} = \frac{1}{2} g_{0,2} v, \quad M_{0,Z} = \frac{1}{2} \sqrt{g_{0,1}^2 + g_{0,2}^2} v, \quad m_{0,f,i} = \frac{v}{\sqrt{2}} \sum_{k,m} U_{0,ik}^{f,L} G_{0,km}^f U_{0,mi}^{f,R\dagger}. \quad (134)$$

Using the relations (132), (133), and (134) together with Eqs. (20) and (21) for bare parameters, the bare Lagrangian (8) can be expressed in terms of the bare masses, the bare coupling e_0 , the quark-mixing matrix V_0 , and the tadpole counterterm δt . Then, renormalized parameters and fields are introduced using Eqs. (98) and (99).

An alternative way to generate the δt terms can be found by inspecting the two relations (132) and (133), which are linear in μ_0^2 and λ_0 and the only source for δt terms. Thus, the δt terms of the PRTS can be generated by making the substitutions [170],

$$\lambda_0 \rightarrow \lambda_0 + 2 \frac{\delta t}{v^3}, \quad \mu_0^2 \rightarrow \mu_0^2 + \frac{3}{2} \frac{\delta t}{v} \quad (135)$$

²⁰At variance with Refs. [40, 83, 107], where all self-energies Σ are 1PI, we use self-energies Σ based on complete inverse connected 2-point functions and denote their 1PI parts by $\Sigma_{1\text{PI}}$, see Eq. (141).

in the bare Lagrangian with all relations between bare and renormalized quantities in Section 3.1.2 without any tadpole contributions. This results in

$$\begin{aligned}\delta\mathcal{L}_{\delta t}^{\text{PRTS}} = & \delta t H + \frac{1}{4} \frac{\delta t e}{M_W s_W} [2\phi^- \phi^+ + \chi^2] - \frac{1}{8} \frac{\delta t e^2}{M_W^2 s_W^2} H [2\phi^- \phi^+ + H^2 + \chi^2] \\ & - \frac{1}{64} \frac{\delta t e^3}{M_W^3 s_W^3} [4(\phi^- \phi^+)^2 + 4\phi^- \phi^+ (H^2 + \chi^2) + (H^2 + \chi^2)^2].\end{aligned}\quad (136)$$

Note that tadpole contributions appear only in vertex functions with external scalar fields, and by definition no tadpole contribution appears in the 2-point function of the physical Higgs field.

Concerning the issue of gauge dependences, the PRTS shows the unpleasant feature that the mass counterterms of all particles become gauge dependent. This is due to the fact that Eq. (132) relates the parameter v not only to the gauge-independent bare parameters μ_0^2 and λ_0 , but also to the gauge-dependent term $t_0 = \delta t$, and this gauge dependence is transferred to all mass renormalization constants via v .

(c) β_h tadpole scheme

This tadpole scheme was introduced in Ref. [155]. The tadpole counterterm and the masses of the vector bosons and fermions are introduced as in the PRTS in Eqs. (132) and (134), however, the bare Higgs-boson mass is defined as

$$M_{0,H}^2 = \frac{1}{2} \lambda_0 v^2. \quad (137)$$

The bare Lagrangian (8) can be expressed in terms of the bare masses, the bare coupling e_0 , the bare quark-mixing matrix V_0 , and the tadpole counterterm δt in a similar way as for the PRTS, and renormalized quantities can be introduced thereafter via Eqs. (98) and (99). Alternatively, the tadpole contributions are obtained from the bare Lagrangian via the shift [170]

$$\mu_0^2 \rightarrow \mu_0^2 + \frac{\delta t}{v_0}. \quad (138)$$

The resulting tadpole contributions to the counterterm Lagrangian are given by

$$\delta\mathcal{L}_{\delta t}^{\beta_h} = \delta t H + \frac{1}{4} \frac{\delta t e}{M_W s_W} [2\phi^- \phi^+ + \chi^2 + H^2]. \quad (139)$$

In this scheme, tadpole counterterms appear only in 2-point functions involving scalar fields. Concerning gauge dependences, the same comments as for the PRTS apply, i.e. mass renormalization constants become gauge dependent.

(d) Tadpole scheme of Ref. [117]

Finally, we mention that Ref. [117] uses yet another tadpole scheme. It is constructed in a similar way as the PRTS and the β_h scheme, but introduces the bare Higgs-boson mass via

$$M_{0,H}^2 = 2\mu_0^2. \quad (140)$$

In the PRTS [40] and the β_h scheme of Ref. [155] all bare masses are gauge dependent, since the bare masses are related to the gauge-independent bare parameters of the Lagrangian via the gauge-dependent tadpole terms.²¹ This leads to a gauge-dependent parametrization of S -matrix elements in terms of bare input parameters. However, this gauge dependence cancels in physical quantities if all parameters of the theory are defined by OS renormalization conditions as is the case in the renormalization of the EWSM described above.²² The gauge dependence of the

²¹This holds also for the tadpole scheme of Ref. [117] with the exception of the bare Higgs-boson mass.

²²The renormalization conditions for the quark-mixing matrix do not involve tadpole contributions, so that the argument is not spoiled if the CKM matrix is not renormalized by OS conditions.

counterterms results from tadpole contributions that are momentum independent. Thus, these contributions cancel in OS or momentum-subtraction schemes, where the corresponding quantity is subtracted at some point in momentum space. On the other hand, when some parameters are renormalized in the $\overline{\text{MS}}$ scheme, the extra tadpole contributions do not cancel and lead to a possible gauge dependence in the S -matrix. This issue becomes relevant in extensions of the SM like the Two-Higgs-Doublet Model or the Higgs-Singlet Extension of the SM, where usually some parameters are renormalized within the $\overline{\text{MS}}$ scheme, as discussed in Ref. [116] (see also references therein).

3.1.7. Explicit form of the renormalization constants for parameters and fields in the physical basis

The renormalized vertex functions consist of unrenormalized loop contributions and counterterms. The renormalization conditions allow us to express the counterterms in terms of unrenormalized vertex functions at specific external momenta. While the charge renormalization constant is fixed from a condition on the photon–fermion–fermion vertex function, a Ward identity allows us to express it in terms of self-energies as well. Following the convention of Ref. [116], we define self-energies $\Sigma(k^2)$ to comprise 1PI contributions $\Sigma_{\text{1PI}}(k^2)$, 2-point tadpole counterterms $\Sigma_{\delta t,2}$, (reducible) tadpole loop contributions Σ_{tad} , and 1-point tadpole counterterms $\Sigma_{\delta t,1}$. As indicated, only the 1PI part depends on the virtuality k^2 of the transferred momentum k of the 2-point function. At the one-loop level, the various contributions are illustrated as follows,

$$\Sigma(k^2) = \Sigma_{\text{1PI}}(k^2) + \Sigma_{\delta t,2} + \Sigma_{\text{tad}} + \Sigma_{\delta t,1}, \quad (141)$$

where the “1” in the blobs stands for one loop. In the FJTS, the tadpole contributions $\Sigma_{\delta t,1}$ and $\Sigma_{\delta t,2}$ cancel exactly so that Eq. (141) is the usual definition of the self-energy. The introduction of these terms allows us to eliminate the explicit tadpole contributions Σ_{tad} in favour of the implicit tadpoles $\Sigma_{\delta t,2}$. In the PRTS, the terms $\Sigma_{\delta t,2}$ are absent by definition, with the exception of the self-energies of the would-be Goldstone bosons, while $\Sigma_{\delta t,1}$ cancels Σ_{tad} . As a consequence, all but the self-energies of the would-be Goldstone-boson fields only consist of 1PI parts.

The renormalized 2-point functions entering the renormalization conditions for the parameters and fields in the physical basis are decomposed into lowest-order contributions, unrenormalized self-energies, and counterterms (in addition to the implicitly contained δt terms) according to

$$\begin{aligned} \Gamma_{\text{R,T}}^{W^+W^-}(k^2) &= -(k^2 - M_W^2) - \Sigma_{\text{T}}^W(k^2) - (k^2 - M_W^2)\delta Z_W + \delta M_W^2, \\ \Gamma_{\text{R,T}}^{VV'}(k^2) &= -\delta_{VV'}(k^2 - M_V^2) - \Sigma_{\text{T}}^{VV'}(k^2) - \left[\frac{1}{2}(k^2 - M_V^2)\delta Z_{VV'} + \frac{1}{2}(k^2 - M_{V'}^2)\delta Z_{V'V} - \delta_{VV'}\delta M_V^2 \right], \quad V, V' = A, Z, \\ \Gamma_{\text{R}}^{HH}(k^2) &= k^2 - M_H^2 + \Sigma^H(k^2) + (k^2 - M_H^2)\delta Z_H - \delta M_H^2, \\ \Gamma_{\text{R},ij}^{f,\text{L}}(p^2) &= \delta_{ij} + \Sigma_{ij}^{f,\text{L}}(p^2) + \frac{1}{2}(\delta Z_{ij}^{f,\text{L}} + \delta Z_{ij}^{f,\text{L}\dagger}), \\ \Gamma_{\text{R},ij}^{f,\text{R}}(p^2) &= \delta_{ij} + \Sigma_{ij}^{f,\text{R}}(p^2) + \frac{1}{2}(\delta Z_{ij}^{f,\text{R}} + \delta Z_{ij}^{f,\text{R}\dagger}), \\ \Gamma_{\text{R},ij}^{f,\text{l}}(p^2) &= -m_{f,i}\delta_{ij} + \Sigma_{ij}^{f,\text{l}}(p^2) - \frac{1}{2}(m_{f,i}\delta Z_{ij}^{f,\text{L}} + m_{f,j}\delta Z_{ij}^{f,\text{R}\dagger}) - \delta_{ij}\delta m_{f,i}, \\ \Gamma_{\text{R},ij}^{f,\text{r}}(p^2) &= -m_{f,i}\delta_{ij} + \Sigma_{ij}^{f,\text{r}}(p^2) - \frac{1}{2}(m_{f,i}\delta Z_{ij}^{f,\text{R}} + m_{f,j}\delta Z_{ij}^{f,\text{L}\dagger}) - \delta_{ij}\delta m_{f,i}. \end{aligned} \quad (142)$$

The renormalization of the longitudinal parts of the gauge-boson self-energies belongs to the unphysical sector, discussed briefly in Section 3.1.8.

Inserting these equations into the renormalization conditions, we find for the mass renormalization constants

$$\begin{aligned} \delta M_W^2 &= \widetilde{\text{Re}} \Sigma_{\text{T}}^W(M_W^2), \quad \delta M_Z^2 = \widetilde{\text{Re}} \Sigma_{\text{T}}^{ZZ}(M_Z^2), \quad \delta M_H^2 = \widetilde{\text{Re}} \Sigma^H(M_H^2), \\ \delta m_{f,i} &= \frac{1}{2} \widetilde{\text{Re}} \left[m_{f,i} \left(\Sigma_{ii}^{f,\text{L}}(m_{f,i}^2) + \Sigma_{ii}^{f,\text{R}}(m_{f,i}^2) \right) + \Sigma_{ii}^{f,\text{l}}(m_{f,i}^2) + \Sigma_{ii}^{f,\text{r}}(m_{f,i}^2) \right]. \end{aligned} \quad (143)$$

The mass counterterms are real even for a complex quark mixing matrix, which is not affected by $\widetilde{\text{Re}}$. The field renormalization constants of the boson fields are obtained as

$$\begin{aligned}\delta Z_W &= -\widetilde{\text{Re}} \frac{\partial \Sigma_{\text{T}}^W(k^2)}{\partial k^2} \Big|_{k^2=M_W^2}, & \delta Z_{VV} &= -\widetilde{\text{Re}} \frac{\partial \Sigma_{\text{T}}^{VV}(k^2)}{\partial k^2} \Big|_{k^2=M_V^2}, & V &= A, Z, \\ \delta Z_{AZ} &= -2 \widetilde{\text{Re}} \frac{\Sigma_{\text{T}}^{AZ}(M_Z^2)}{M_Z^2}, & \delta Z_{ZA} &= 2 \frac{\Sigma_{\text{T}}^{AZ}(0)}{M_Z^2}, \\ \delta Z_H &= -\widetilde{\text{Re}} \frac{\partial \Sigma^H(k^2)}{\partial k^2} \Big|_{k^2=M_H^2},\end{aligned}\tag{144}$$

and those of the fermion fields read

$$\begin{aligned}\delta Z_{ii}^{f,\text{L}} &= -\widetilde{\text{Re}} \Sigma_{ii}^{f,\text{L}}(m_{f,i}^2) - m_{f,i} \frac{\partial}{\partial p^2} \widetilde{\text{Re}} \left[m_{f,i} \left(\Sigma_{ii}^{f,\text{L}}(p^2) + \Sigma_{ii}^{f,\text{R}}(p^2) \right) + \Sigma_{ii}^{f,\text{L}}(p^2) + \Sigma_{ii}^{f,\text{R}}(p^2) \right] \Big|_{p^2=m_{f,i}^2}, \\ \delta Z_{ii}^{f,\text{R}} &= -\widetilde{\text{Re}} \Sigma_{ii}^{f,\text{R}}(m_{f,i}^2) - m_{f,i} \frac{\partial}{\partial p^2} \widetilde{\text{Re}} \left[m_{f,i} \left(\Sigma_{ii}^{f,\text{L}}(p^2) + \Sigma_{ii}^{f,\text{R}}(p^2) \right) + \Sigma_{ii}^{f,\text{L}}(p^2) + \Sigma_{ii}^{f,\text{R}}(p^2) \right] \Big|_{p^2=m_{f,i}^2}, \\ \delta Z_{ij}^{f,\text{L}} &= \frac{2}{m_{f,i}^2 - m_{f,j}^2} \widetilde{\text{Re}} \left[m_{f,j}^2 \Sigma_{ij}^{f,\text{L}}(m_{f,j}^2) + m_{f,i} m_{f,j} \Sigma_{ij}^{f,\text{R}}(m_{f,j}^2) + m_{f,i} \Sigma_{ij}^{f,\text{L}}(m_{f,j}^2) + m_{f,i} \Sigma_{ij}^{f,\text{R}}(m_{f,j}^2) \right], & i &\neq j, \\ \delta Z_{ij}^{f,\text{R}} &= \frac{2}{m_{f,i}^2 - m_{f,j}^2} \widetilde{\text{Re}} \left[m_{f,j}^2 \Sigma_{ij}^{f,\text{R}}(m_{f,j}^2) + m_{f,i} m_{f,j} \Sigma_{ij}^{f,\text{L}}(m_{f,j}^2) + m_{f,j} \Sigma_{ij}^{f,\text{L}}(m_{f,j}^2) + m_{f,j} \Sigma_{ij}^{f,\text{R}}(m_{f,j}^2) \right], & i &\neq j.\end{aligned}\tag{145}$$

Owing to Eq. (107),

$$\delta Z_{ij}^{f,\sigma\dagger} = \delta Z_{ij}^{f,\sigma} \Big|_{m_i \leftrightarrow m_j, \Sigma_{ij}^{f,\sigma} \leftrightarrow \Sigma_{ij}^{f,\dagger}}, \quad \sigma = \text{L, R},\tag{146}$$

where the interchange $m_i \leftrightarrow m_j$ applies to all explicit masses in Eq. (145). For $i = j$ the renormalization conditions Eq. (110) fix only the hermitean part $\delta Z_{ii}^{f,\sigma} + \delta Z_{ii}^{f,\sigma\dagger}$ of the fermion field renormalization constant, while its antihermitean part corresponds to the free global phase of the fermion fields [117, 166]. It is customary to require that the antihermitean part vanishes, so that

$$\delta Z_{ii}^{f,\sigma\dagger} = \delta Z_{ii}^{f,\sigma}.\tag{147}$$

To be precise, defining this relation for $\sigma = \text{R}$, it is automatically fulfilled for $\sigma = \text{L}$, or vice versa.

Since there is no generation mixing in the lepton sector, all (one-loop) lepton self-energies are diagonal in generation space, and the off-diagonal lepton wave-function renormalization constants are zero. The same holds for the quark sector if one replaces the quark-mixing matrix V by the unit matrix, as often done in calculations of radiative corrections for high-energy processes.

The renormalization constant for the quark-mixing matrix V can be directly read off from Eq. (120),

$$\delta V_{ij} = \frac{1}{4} \left[(\delta Z_{ik}^{u,\text{L}} - \delta Z_{ik}^{u,\text{L}\dagger}) V_{kj} - V_{ik} (\delta Z_{kj}^{d,\text{L}} - \delta Z_{kj}^{d,\text{L}\dagger}) \right].\tag{148}$$

Inserting the fermion-field renormalization constants (145) yields

$$\begin{aligned}\delta V_{ij} &= \frac{1}{2} \widetilde{\text{Re}} \sum_k \left\{ \frac{1}{m_{u,i}^2 - m_{u,k}^2} \left[m_{u,i}^2 \Sigma_{ik}^{u,\text{L}}(m_{u,i}^2) + m_{u,k}^2 \Sigma_{ik}^{u,\text{L}}(m_{u,k}^2) + m_{u,i} m_{u,k} (\Sigma_{ik}^{u,\text{R}}(m_{u,i}^2) + \Sigma_{ik}^{u,\text{R}}(m_{u,k}^2)) \right. \right. \\ &\quad \left. \left. + m_{u,i} \Sigma_{ik}^{u,\text{L}}(m_{u,k}^2) + m_{u,i} \Sigma_{ik}^{u,\text{L}}(m_{u,i}^2) + m_{u,k} \Sigma_{ik}^{u,\text{R}}(m_{u,i}^2) + m_{u,k} \Sigma_{ik}^{u,\text{R}}(m_{u,k}^2) \right] V_{kj} \right. \\ &\quad \left. - V_{ik} \frac{1}{m_{d,k}^2 - m_{d,j}^2} \left[m_{d,k}^2 \Sigma_{kj}^{d,\text{L}}(m_{d,k}^2) + m_{d,j}^2 \Sigma_{kj}^{d,\text{L}}(m_{d,j}^2) + m_{d,k} m_{d,j} (\Sigma_{kj}^{d,\text{R}}(m_{d,k}^2) + \Sigma_{kj}^{d,\text{R}}(m_{d,j}^2)) \right. \right. \\ &\quad \left. \left. + m_{d,k} \Sigma_{kj}^{d,\text{L}}(m_{d,k}^2) + m_{d,k} \Sigma_{kj}^{d,\text{L}}(m_{d,j}^2) + m_{d,j} \Sigma_{kj}^{d,\text{R}}(m_{d,k}^2) + m_{d,j} \Sigma_{kj}^{d,\text{R}}(m_{d,j}^2) \right] \right\}.\end{aligned}\tag{149}$$

It remains to fix the charge renormalization constant δZ_e . The renormalized vertex function for the $\gamma\bar{f}f$ vertex reads

$$\Gamma_{R,ij,\mu}^{A\bar{f}f}(k, \bar{p}, p) = -eQ_f\gamma_\mu\delta_{ij} + e\Lambda_{R,ij,\mu}^{A\bar{f}f}(k, \bar{p}, p). \quad (150)$$

For equal ($i = j$) OS external fermions the higher-order contribution can be decomposed as ($k = -\bar{p} - p$)

$$\Lambda_{R,ii,\mu}^{A\bar{f}f}(k, \bar{p}, p) = \left(\gamma_\mu\Lambda_{R,V}^f(k^2) - \gamma_\mu\gamma_5\Lambda_{R,A}^f(k^2) + \frac{(p - \bar{p})_\mu}{2m_f}\Lambda_{R,S}^f(k^2) - \frac{(p + \bar{p})_\mu}{2m_f}\gamma_5\Lambda_{R,P}^f(k^2) \right). \quad (151)$$

Expressing the renormalized quantities in terms of the unrenormalized ones and the counterterms, using the renormalization condition (115) for arbitrary fermions, and making use of the Gordon identities and the Ward identity

$$\bar{u}(p)\Lambda_{ii,\mu}^{A\bar{f}f}(0, -p, p)u(p) = -Q_f\bar{u}(p)\left[\frac{\partial}{\partial p^\mu}\Sigma_{ii}^{\bar{f}f}(-p, p) \right]u(p) - a_f\bar{u}(p)\gamma_\mu(1 - \gamma_5)u(p)\frac{\Sigma_T^{AZ}(0)}{M_Z^2}, \quad (152)$$

where $\Sigma_{ii}^{\bar{f}f}(-p, p)$ is the higher-order contribution to $\Gamma_{ii}^{\bar{f}f}(-p, p)$, one finally finds [40, 83]

$$\delta Z_e = \frac{\delta e}{e} = -\frac{1}{2}\delta Z_{AA} - \frac{s_w}{c_w}\frac{1}{2}\delta Z_{ZA} = \frac{1}{2}\frac{\partial\Sigma_T^{AA}(k^2)}{\partial k^2}\bigg|_{k^2=0} - \frac{s_w}{c_w}\frac{\Sigma_T^{AZ}(0)}{M_Z^2}. \quad (153)$$

The result (153) is independent of the fermion species, reflecting electric charge universality. Consequently, the analogue of Eq. (115) holds for arbitrary fermions f .

The Ward identity (152) is known to hold in the EWSM at the one-loop level. In Refs. [38–40, 82], Eq. (153) was derived via explicit one-loop calculation of self-energy and vertex diagrams. In Appendix C we provide a derivation of Eq. (153) from Slavnov–Taylor and Lee identities valid at the one-loop level. While this derivation proceeds in an arbitrary ’t Hooft gauge, it can easily be generalized to other gauges. It holds as well for extensions of the SM that do not modify its gauge structure. Moreover, the derivation presented in Appendix C may serve as a basis for a generalization of the identity (153) to higher orders.

In the OS scheme the *weak mixing angle* is a derived quantity, i.e. merely an abbreviation. Following Sirlin [36], it is generally defined as

$$\sin^2\theta_w = s_w^2 = 1 - c_w^2 = 1 - \frac{M_w^2}{M_Z^2}, \quad (154)$$

in terms of the physical, renormalized gauge-boson masses. This definition is independent of a specific process and valid to all orders of perturbation theory. We note that the weak mixing angle is not a directly measurable quantity and (in higher orders) could be defined in different ways. In particular, this *OS weak mixing angle* differs from the *effective weak mixing angle* defined from the OS fermion–Z-boson couplings that is often used in the analysis of LEP1/SLC data.

Since the auxiliary parameters s_w^2 and c_w^2 frequently appear, it is useful to introduce the corresponding renormalization constants

$$c_{0,w}^2 = c_w^2 + \delta c_w^2, \quad s_{0,w}^2 = s_w^2 + \delta s_w^2. \quad (155)$$

Because of Eq. (154) these are directly related to the renormalization constants for the gauge-boson masses, i.e. to one-loop order

$$\frac{\delta c_w^2}{c_w^2} = \frac{\delta M_w^2}{M_w^2} - \frac{\delta M_Z^2}{M_Z^2} = \widetilde{\text{Re}}\left(\frac{\Sigma_T^W(M_w^2)}{M_w^2} - \frac{\Sigma_T^{ZZ}(M_Z^2)}{M_Z^2}\right), \quad \frac{\delta s_w^2}{s_w^2} = -\frac{c_w^2}{s_w^2}\frac{\delta c_w^2}{c_w^2}. \quad (156)$$

3.1.8. Renormalization of the unphysical sector

The renormalization of the unphysical fields and of the gauge parameters does not affect S -matrix elements. Therefore, the choice of the corresponding renormalization conditions is a pure matter of convenience.

An appropriate field renormalization of the would-be Goldstone-boson and the Faddeev–Popov fields allows us to render vertex and Green functions involving these fields finite. A simple way to achieve this is to require that the corresponding propagators have residue equal to one at the poles and that the mixing between the Faddeev–Popov ghosts corresponding to the photon and Z-boson fields vanishes for $k^2 = 0$ and $k^2 = \xi_Z M_Z^2$.

It can be shown that in linear gauges such as the 't Hooft–Feynman gauge, the gauge-fixing term need not be renormalized [24, 28]. We therefore require that the gauge-fixing Lagrangian has the form of Eq. (28) with Eq. (27) in terms of renormalized fields and parameters. This renormalized form of the gauge-fixing Lagrangian can be translated back into an expression in terms of unrenormalized quantities by inverting the renormalization transformation of the parameters and fields given in Section 3.1.2. Bare and renormalized gauge-fixing Lagrangians can even be brought into identical functional form by introducing bare and renormalized sets of gauge parameters and adjusting the transformation between the two sets accordingly. Finally, from the bare gauge-fixing functionals the Faddeev–Popov Lagrangian is derived as usual and expressed in terms of renormalized fields.

The renormalization of the unphysical sector can be arranged in such a way that the Slavnov–Taylor identities still hold in terms of renormalized fields and parameters. To this end, it is sufficient to renormalize the sources of the BRS-transformed fields in the generating functionals of renormalized Green functions appropriately. More details can be found in Refs. [37, 38, 83].

3.2. Renormalization within the background-field method

In the *background-field formalism* for the SM (see Section 2.3) the parameters and quantum fields are renormalized in the same way as in the conventional formalism, given in Eqs. (98)–(102). In fact, the renormalization of the quantum fields is irrelevant for S -matrix elements and background-field vertex functions, since field-renormalization counterterms related to internal lines in Feynman diagrams generally cancel. In one-loop calculations, renormalization constants for quantum fields do not even appear. On the other hand, the renormalization of the background fields is required for finiteness of the background-field vertex functions and the validity of the background-field Ward identities for renormalized vertex functions,

$$\begin{aligned} \hat{W}_0^\pm &= Z_{\hat{W}}^{1/2} \hat{W}^\pm = \left(1 + \frac{1}{2} \delta Z_{\hat{W}}\right) \hat{W}^\pm, \\ \begin{pmatrix} \hat{Z}_0 \\ \hat{A}_0 \end{pmatrix} &= \begin{pmatrix} Z_{\hat{Z}\hat{Z}}^{1/2} & Z_{\hat{Z}\hat{A}}^{1/2} \\ Z_{\hat{A}\hat{Z}}^{1/2} & Z_{\hat{A}\hat{A}}^{1/2} \end{pmatrix} \begin{pmatrix} \hat{Z} \\ \hat{A} \end{pmatrix} = \begin{pmatrix} 1 + \frac{1}{2} \delta Z_{\hat{Z}\hat{Z}} & \frac{1}{2} \delta Z_{\hat{Z}\hat{A}} \\ \frac{1}{2} \delta Z_{\hat{A}\hat{Z}} & 1 + \frac{1}{2} \delta Z_{\hat{A}\hat{A}} \end{pmatrix} \begin{pmatrix} \hat{Z} \\ \hat{A} \end{pmatrix}, \\ \hat{\phi}_0^\pm &= Z_{\hat{\phi}}^{1/2} \hat{\phi}^\pm = \left(1 + \frac{1}{2} \delta Z_{\hat{\phi}}\right) \hat{\phi}^\pm, \quad \hat{S}_0 = Z_{\hat{S}}^{1/2} \hat{S} = \left(1 + \frac{1}{2} \delta Z_{\hat{S}}\right) \hat{S}, \quad \hat{S} = \hat{H}, \hat{\chi}. \end{aligned} \quad (157)$$

The renormalization constants in Eq. (157) can be fixed in such a way that the renormalized effective action is invariant under background-field gauge transformations. This implies relations between the renormalization constants for the background fields and the parameter renormalization constants [107]. At the one-loop level, these read

$$\begin{aligned} \delta Z_{\hat{A}\hat{A}} &= -2\delta Z_e, \quad \delta Z_{\hat{Z}\hat{A}} = 0, \quad \delta Z_{\hat{A}\hat{Z}} = 2 \frac{c_w}{s_w} \frac{\delta c_w^2}{c_w^2}, \\ \delta Z_{\hat{Z}\hat{Z}} &= -2\delta Z_e - \frac{c_w^2 - s_w^2}{s_w^2} \frac{\delta c_w^2}{c_w^2}, \quad \delta Z_{\hat{W}} = -2\delta Z_e - \frac{c_w^2}{s_w^2} \frac{\delta c_w^2}{c_w^2}, \\ \delta Z_{\hat{H}} = \delta Z_{\hat{\chi}} = \delta Z_{\hat{\phi}} &= -2\delta Z_e - \frac{c_w^2}{s_w^2} \frac{\delta c_w^2}{c_w^2} + \frac{\delta M_W^2}{M_W^2} + 2 \frac{\Delta v}{v}, \end{aligned} \quad (158)$$

with δc_w^2 from Eq. (156). The explicit term

$$2 \frac{\Delta v}{v} = 2 \frac{T^{\hat{H}}}{M_H^2 v} = \frac{e T^{\hat{H}}}{s_w M_W M_H^2} \quad (159)$$

in $\delta Z_{\hat{H}}$ is only present in the FJTS, and the explicit tadpole $T^{\hat{H}}$ appearing there has been replaced by the shift of the vev upon using Eqs. (123) and (128).

Although the expressions of the scalar field renormalization constants $\delta Z_{\hat{H}} = \delta Z_{\hat{\chi}} = \delta Z_{\hat{\phi}}$ in terms of the parameter renormalization constants differ between the FJTS and the PRTS, $\delta Z_{\hat{H}}$ in the two tadpole schemes is the same; the Δv term results from tadpole contributions and is implicitly contained in δM_W^2 in the PRTS. The relations (158) express the

field renormalization constants of all gauge bosons and scalars completely in terms of the renormalization constants of the electric charge and the particle masses. Note, in particular, that we get the same relation as in QED between the charge and the background-photon-field renormalization constant,

$$Z_{\hat{A}\hat{A}} = (Z_e)^{-2}. \quad (160)$$

In the background-field formalism, this relation holds to all orders of perturbation theory. It has been employed to calculate the two-loop counterterm for the renormalization of the electric charge in the SM [171]. In addition, the field renormalization constants of the fermions obey

$$\delta Z^{F,\text{L}} = \delta Z^{F_+,\text{L}} = \delta Z^{F_-,\text{L}}, \quad (161)$$

i.e. the renormalization constants for the two left-handed fermions in a doublet $F = (F_+, F_-)^T$ must be equal (as in the minimal renormalization scheme of Ref. [38]).

As the field renormalization constants are fixed by Eq. (158), in general the propagators acquire residues different from one, and different fields can mix on shell. This is similar to the minimal OS scheme [38] of the conventional formalism. Therefore, when calculating S -matrix elements, one has to introduce (UV-finite) wave-function renormalization constants, which are explicitly given in Ref. [115] for the gauge fields. However, just as in QED, the OS definition of the electric charge together with gauge invariance automatically fixes the residue of the photon propagator to one. Moreover, the photon-Z-boson mixing vanishes for OS photons as a consequence of Eq. (60) and the analyticity of the 2-point functions.

The gauge-invariance relations among the renormalizations constants can also be derived by demanding that the form of the BFM Ward identities discussed in Section 2.3 remains the same after renormalization [107]. In this context, we emphasize that the self-energies in Ref. [107] contain only 1PI contributions, so that the form of Eqs. (29)–(32) of that reference is changed in the notation of this review by some tadpole contributions, while Eqs. (25)–(28) of Ref. [107] formally remain the same. To illustrate the derivation of some of the relations (158) among the BFM renormalization constants in our conventions, we introduce the BFM self-energies Σ in the gauge-boson–Goldstone-boson sector analogous to our definitions in the conventional formalism as follows,

$$\begin{aligned} \hat{\Gamma}_{\text{R,L}}^{\hat{W}^+ \hat{W}^-}(k^2) &= M_W^2 - \Sigma_{\text{R,L}}^{\hat{W}}(k^2) = M_W^2 - \Sigma_{\text{L}}^{\hat{W}}(k^2) + \left(\delta Z_{\hat{W}} + \frac{\delta M_W^2}{M_W^2} \right) M_W^2, \\ \hat{\Gamma}_{\text{R,L}}^{\hat{Z} \hat{Z}}(k^2) &= M_Z^2 - \Sigma_{\text{R,L}}^{\hat{Z} \hat{Z}}(k^2) = M_Z^2 - \Sigma_{\text{L}}^{\hat{Z} \hat{Z}}(k^2) + \left(\delta Z_{\hat{Z}} + \frac{\delta M_Z^2}{M_Z^2} \right) M_Z^2, \\ \hat{\Gamma}_{\text{R},\mu}^{\hat{W}^\pm \hat{\phi}^\mp}(k, -k) &= \pm k_\mu \left[M_W + \Sigma_{\text{R}}^{\hat{W} \hat{\phi}}(k^2) \right] = \pm k_\mu \left[M_W + \Sigma^{\hat{W} \hat{\phi}}(k^2) + \frac{1}{2} \left(\delta Z_{\hat{\phi}} + \delta Z_{\hat{W}} + \frac{\delta M_W^2}{M_W^2} \right) M_W \right], \\ \hat{\Gamma}_{\text{R},\mu}^{\hat{Z} \hat{\chi}}(k, -k) &= k_\mu \left[iM_Z + \Sigma_{\text{R}}^{\hat{Z} \hat{\chi}}(k^2) \right] = k_\mu \left[iM_Z + \Sigma^{\hat{Z} \hat{\chi}}(k^2) + \frac{1}{2} \left(\delta Z_{\hat{\chi}} + \delta Z_{\hat{Z}} + \frac{\delta M_Z^2}{M_Z^2} \right) iM_Z \right], \\ \hat{\Gamma}_{\text{R}}^{\hat{\phi}^+ \hat{\phi}^-}(k, -k) &= \hat{\Gamma}_{\text{R}}^{\hat{\phi}^+ \hat{\phi}^-}(k^2) = k^2 + \Sigma_{\text{R}}^{\hat{\phi}}(k^2) = k^2 + \Sigma^{\hat{\phi}}(k^2) + \delta Z_{\hat{\phi}} k^2, \\ \hat{\Gamma}_{\text{R}}^{\hat{\chi} \hat{\chi}}(k, -k) &= \hat{\Gamma}_{\text{R}}^{\hat{\chi} \hat{\chi}}(k^2) = k^2 + \Sigma_{\text{R}}^{\hat{\chi}}(k^2) = k^2 + \Sigma^{\hat{\chi}}(k^2) + \delta Z_{\hat{\chi}} k^2. \end{aligned} \quad (162)$$

Recall that the tree-level contributions to the vertex functions differ from the conventional ones, since the BFM vertex functions do not include gauge-fixing terms. As already pointed out in Section 2.3.2, the unrenormalized vertex functions including tadpole contributions, as encoded in the tree-level parts plus the Σ functions, obey Eq. (63) with $r_{\hat{H}}$ as in Eq. (64) or $r_{\hat{H}} = 1$ in the FJTS or PRTS, respectively. Expressed in terms of self-energies Σ , the identities are given by

$$\begin{aligned} \Sigma_{\text{L}}^{\hat{W}}(k^2) + M_W \Sigma^{\hat{W} \hat{\phi}}(k^2) + M_W^2 \frac{\Delta v}{v} &= 0, & k^2 \Sigma^{\hat{W} \hat{\phi}}(k^2) - M_W \Sigma^{\hat{\phi}}(k^2) - M_W k^2 \frac{\Delta v}{v} &= 0, \\ \Sigma_{\text{L}}^{\hat{Z} \hat{Z}}(k^2) - iM_Z \Sigma^{\hat{Z} \hat{\chi}}(k^2) + M_Z^2 \frac{\Delta v}{v} &= 0, & k^2 \Sigma^{\hat{Z} \hat{\chi}}(k^2) - iM_Z \Sigma^{\hat{\chi}}(k^2) - iM_Z k^2 \frac{\Delta v}{v} &= 0, \end{aligned} \quad (163)$$

with the Δv terms only contributing in the FJTS. Demanding that these relations carry over to renormalized quantities in the form

$$\begin{aligned}\Sigma_{R,L}^{\hat{W}}(k^2) + M_W \Sigma_R^{\hat{W}\hat{\phi}}(k^2) &= 0, & k^2 \Sigma_R^{\hat{W}\hat{\phi}}(k^2) - M_W \Sigma_R^{\hat{\phi}}(k^2) &= 0, \\ \Sigma_{R,L}^{\hat{Z}\hat{Z}}(k^2) - i M_Z \Sigma_R^{\hat{Z}\hat{X}}(k^2) &= 0, & k^2 \Sigma_R^{\hat{Z}\hat{X}}(k^2) - i M_Z \Sigma_R^{\hat{X}}(k^2) &= 0\end{aligned}\quad (164)$$

is a non-trivial requirement, which has the unique solution

$$\delta Z_{\hat{\phi}} = \delta Z_{\hat{W}} + \frac{\delta M_W^2}{M_W^2} + \frac{2\Delta v}{v}, \quad \delta Z_{\hat{X}} = \delta Z_{\hat{Z}\hat{Z}} + \frac{\delta M_Z^2}{M_Z^2} + \frac{2\Delta v}{v}. \quad (165)$$

The derivation of these relations, which are part of Eq. (158), is valid both in the FJTS and the PRTS. The relations (158) and (165) can be alternatively derived by requiring that the renormalization transformations applied to gauge-invariant terms of the bare Lagrangian result in equivalent terms expressed by renormalized parameters and fields up to global factors. Taking into account the expressions of Eq. (158) for $\delta Z_{\hat{W}}$ and $\delta Z_{\hat{Z}\hat{Z}}$, the relations (165) are compatible with the requirement $\delta Z_{\hat{H}} = \delta Z_{\hat{X}} = \delta Z_{\hat{\phi}}$, which expresses rigid invariance, and lead to the last relation of (158).

As a consequence of the relations between the renormalization constants, the counterterm vertices of the background fields have a much simpler structure than the ones in the conventional formalism. In fact, all vertices originating from a single gauge-invariant term in the Lagrangian acquire the same renormalization constants. The explicit form of the counterterm vertices at one-loop order can be found in Appendix A.

3.3. Renormalization of QCD

When QCD is included as described in Section 2.1.4, the renormalization has to be extended. Additional counter-terms for the strong coupling constant g_s and the gluon fields G are introduced according to

$$g_{0,s} = (1 + \delta Z_{g_s}) g_s, \quad G_0 = Z_G^{1/2} G = \left(1 + \frac{1}{2} \delta Z_G\right) G. \quad (166)$$

Moreover, the counterterms introduced in Eqs. (98) and (99), in particular those for the quark masses and quark fields receive additional contributions from the strong interaction. In order to render all Green functions finite, field renormalization constants for the Faddeev–Popov ghosts of the strong interaction and for the gauge parameter of QCD have to be introduced in analogy to the strategy outlined in Section 3.1.8.

Although the gluon field renormalization constant δZ_G is often defined in the $\overline{\text{MS}}$ scheme in the QCD literature, it can also be fixed conveniently by an OS renormalization condition in analogy to the second condition of Eq. (104),

$$\lim_{k^2 \rightarrow 0} \frac{1}{k^2} \Gamma_{R,\mu\nu}^{GG}(-k, k) \varepsilon^\nu(k) \Big|_{k^2=0} = -\varepsilon_\mu(k), \quad (167)$$

leading to

$$\delta Z_G = -\frac{\partial \Sigma_T^G(k^2)}{\partial k^2} \Big|_{k^2=0}. \quad (168)$$

Since 2-point functions at momentum transfer zero do not develop absorptive parts, it is not necessary to include the Re operation. The corresponding explicit result for δZ_G can, e.g., be found in Ref. [172].

The strong coupling g_s is usually fixed in the $\overline{\text{MS}}$ scheme, which is tied to dimensional regularization (DR) with $D = 4 - 2\epsilon$ dimensions. In this scheme, the renormalization constant contains only the UV divergence along with related finite constants in the form

$$\Delta = \frac{2}{4 - D} + \ln 4\pi - \gamma_E, \quad (169)$$

where $\gamma_E = 0.577\dots$ is the Euler–Mascheroni constant. In the $\overline{\text{MS}}$ scheme, the renormalization constant δZ_{g_s} can be determined from any vertex function that involves the strong coupling in leading order (LO), a convenient choice being the quark–antiquark–gluon coupling. A common definition is

$$\delta Z_{g_s} = -\frac{\alpha_s(\mu_R^2)}{4\pi} \left[\left(\frac{11}{2} - \frac{N_f}{3} \right) \left(\Delta + \ln \frac{\mu^2}{\mu_R^2} \right) - \frac{1}{3} \sum_F \left(\Delta + \ln \frac{\mu^2}{m_F^2} \right) \right] \quad (170)$$

in the N_f -flavour scheme. Here μ is the mass parameter of DR (see Section 3.4.1) and μ_R the renormalization scale for the strong coupling. Furthermore, N_f is the number of active (light) flavours, and F runs over the inactive (heavy) flavours. The contribution of active flavours (and gluons) is renormalized in the $\overline{\text{MS}}$ scheme, while the one from inactive flavours, i.e. heavy degrees of freedom like the top quark, is subtracted at zero momentum transfer. As a consequence, the contribution of heavy flavours disappears (decouples) from the renormalized gluon self-energy if the corresponding masses tend to infinity. Most of the higher-order calculations for high-energy scattering processes at the LHC are carried out in the 5-flavour scheme, where $N_f = 5$ and \sum_F comprises only the top-quark contribution.

In the BFM, background-field gauge invariance implies the relation

$$Z_G = (Z_{g_s})^{-2} \quad (171)$$

to all orders in perturbation theory. Consequently, δZ_{g_s} can be obtained from the gluon self-energy alone (without any vertex corrections) in the BFM [106].

3.4. Techniques for electroweak one-loop calculations

In this section we give an overview of the techniques used for calculating EW one-loop corrections. We first discuss the regularization of soft and collinear singularities based on DR and mass regularization (MR). Then we sketch the traditional tensor-integral reduction method that goes back to Brown and Feynman [173] and Passarino and Veltman [34] and the reduction at the integrand level introduced by Ossola, Pittau, and Papadopoulos [174]. Finally, we discuss codes for tensor and scalar one-loop integrals and make some remarks on purely numerical methods for the calculation of NLO corrections.

3.4.1. Dimensional versus mass regularization

Perturbative calculations in relativistic quantum field theories lead to divergent integrals. To allow for a proper treatment of perturbative quantities a *regularization* procedure is needed. This amounts to a modification of the theory so that possibly divergent expressions become well defined and that in a suitable limit the original (divergent) theory is recovered. Once renormalization has been performed and virtual and real corrections are properly combined, all singularities cancel, and the limit to the original theory is well defined. The final results are independent of the regularization procedure.

Quantum field theories involve both UV and infrared (IR) divergences. The former result from regions of the loop integrals where the integration momentum tends to infinity, the latter originate from regions in phase space where loop momenta or momenta of external particles become small or collinear to each other.

For the regularization of UV and IR singularities various regularization schemes exist. Naive regularization schemes based on momentum cutoffs violate Lorentz invariance and gauge invariance and are therefore not used in practical calculations. Lattice regularization in space-time is very useful for the numerical calculation of non-perturbative quantities but too complicated for perturbative calculations.

The method of choice for perturbative calculations in relativistic quantum field theories and gauge theories is *dimensional regularization*, because it is convenient and respects Lorentz and gauge invariance. It was introduced by Bollini and Giambiagi [175] and 't Hooft and Veltman [23]. For a precise definition and thorough discussion we refer to Section 4 of the book of Collins [101].

In DR, calculations are performed in D instead of four dimensions. Since the loop integrals converge in suitably chosen numbers of dimensions (small dimensions for UV singularities, large dimensions for IR singularities), the usual calculational rules for integrals, such as linearity, translational and rotational invariance, and scaling properties can be used. The structure of the loop integrals allows for a continuation to arbitrary complex values of D so that integrals involving UV and IR singularities can be regularized and the limit $D \rightarrow 4$ can be taken.²³ The divergences manifest themselves as poles at integer values of D . Changing the space-time dimension of an integral also changes its mass dimension. This effect gets compensated by multiplying each integral $\int d^D q$ over a 4-momentum q with a factor $(2\pi\mu)^{4-D}$, where μ has the dimension of a mass. In one-loop calculations the poles appear always in the combination Δ as defined in Eq. (169).

²³For integrals that are both UV and IR divergent, this analytic continuation is subtle, since no value of D exists for which those integrals are finite (for proper arguments, see, e.g., Ref. [176]).

DR is the de facto standard for regularizing UV singularities in gauge theories. It is the basis for the $\overline{\text{MS}}$ renormalization scheme (cf. Section 5.1.2), where the renormalization constants just consist of terms of the form (169) involving the UV divergence along with some universal finite terms. This renormalization scheme is widely used in QCD, where the masses of the light quarks are often neglected. DR regularizes also the soft and collinear singularities related to massless gluons and quarks. Since UV and IR singularities result from different parts of the integration region, they can be discriminated by introducing formally different regulator parameters Δ_{UV} and Δ_{IR} corresponding to different numbers of dimensions, D_{UV} and D_{IR} . In practice, this separation can be done in different ways. Since IR divergences are tied to specific kinematical configurations such as OS conditions or massless limits, the UV divergences can be extracted from a given integral upon first considering the integral with general off-shell external momenta, determining the divergent parts, which are all of UV origin, and finally specializing the result to the actual kinematic situation. Alternatively, the $1/\epsilon$ poles of UV origin can be obtained by regularizing all IR singularities by small mass parameters, so that no $1/\epsilon$ poles of IR origin exist.²⁴ At the one-loop level, no standard scalar integral is both IR and UV singular. Thus, when expressing amplitudes by the standard scalar integrals, the separation of IR and UV singularities becomes trivial.

DR can be used in the EW theory in the same way as in QCD. However, in QED and the EWSM, IR singularities have been traditionally regularized with infinitesimal photon masses and small fermion masses, i.e. in *mass regularization*. In contrast to the non-abelian theories, the photon mass does not ruin the renormalizability of a U(1) gauge theory (see, for instance, Ref. [178] or Ref. [101], Section 12.9) and can be used to regularize soft singularities without violating Ward identities. Furthermore, the small lepton masses are well-defined physical parameters, which offer a physical regularization of corresponding collinear singularities in QED and in the SM. DR of UV singularities can be combined with MR of IR singularities, providing a natural separation of the two kinds of singularities. The basic loop and phase-space integrals depend on the chosen regularization, but are available for one-loop calculations in both regularization schemes and are of similar complexity [177, 179]. More details on IR singularities, their regularization and evaluation can be found in Section 4.

Finally, the choice of the regularization scheme is a matter of convenience. For hadron-collider processes, the partonic cross sections have to be combined with parton distributions. Since the latter are usually defined in the $\overline{\text{MS}}$ scheme, their combination with perturbative matrix elements is more convenient in DR. If on the other hand final-state fermions and photons are not recombined in the collinear regions, as it may be relevant for muons, then EW corrections become sensitive to the masses of the fermions, so that MR of the corresponding singularities is appropriate. In any case, results can be translated between regularization schemes, and different regularization methods can be combined with the due care.

Further regularization schemes, including in particular 4-dimensional methods, are discussed in the review [180].

3.4.2. The γ_5 problem

While DR preserves Lorentz and gauge invariance, it does not preserve chiral invariance. This is due to the fact that the matrix

$$\gamma_5 = i\gamma^0\gamma^1\gamma^2\gamma^3 \quad (172)$$

appearing in chiral projectors $\omega_{\pm} = (1 \pm \gamma^5)/2$ is a genuinely 4-dimensional object. The definition (172) is consistent in D dimensions, but breaks D -dimensional Lorentz invariance, since the first four dimensions are distinguished. From the existence of the axial anomaly it is clear that no fully Lorentz-invariant generalization of the Dirac algebra exists. On an algebraic level, it is impossible to define a D -dimensional γ algebra with

$$\{\gamma^{\mu}, \gamma^{\nu}\} = \gamma^{\mu}\gamma^{\nu} + \gamma^{\nu}\gamma^{\mu} = 2g^{\mu\nu}, \quad \mu = 0, \dots, D-1 \quad (173)$$

that obeys both the anticommutation relation

$$\{\gamma^{\mu}, \gamma_5\} = \gamma^{\mu}\gamma_5 + \gamma_5\gamma^{\mu} = 0 \quad (174)$$

²⁴To this end, it is even enough to give all internal massless particles some infinitesimal regulator mass λ , even though this procedure does not correspond to a consistent IR regularization of gauge theories. More details on translating mass singularities between different regularization schemes can, e.g., be found in Ref. [177].

and the trace condition

$$\text{Tr}[\gamma^\mu \gamma^\nu \gamma^\rho \gamma^\sigma \gamma_5] = -4i \epsilon^{\mu\nu\rho\sigma}, \quad (175)$$

or a D -dimensional generalization thereof. In a theory with chiral fields, as the SM, a gauge-invariant DR can only be obtained by giving up either anticommutativity (174) or the trace condition (175) [181].

In the literature, different prescriptions for the treatment of γ_5 within DR have been proposed:

- In the '*t Hooft–Veltman* prescription' [23, 182–184] the 4-dimensional trace condition (175) is preserved. Dirac matrices are split into 4-dimensional ($\hat{\gamma}^\mu$) and $(D-4)$ -dimensional ($\check{\gamma}^\mu$) parts, $\gamma^\mu = \hat{\gamma}^\mu + \check{\gamma}^\mu$, obeying the (anti)commutation relations

$$\{\hat{\gamma}^\mu, \gamma_5\} = 0, \quad [\check{\gamma}^\mu, \gamma_5] = 0, \quad \{\check{\gamma}^\mu, \gamma_5\} \neq 0. \quad (176)$$

This prescription is algebraically consistent, but violates gauge invariance, i.e. modifies the Ward identities. These can be restored upon adding extra $(D-4)$ -dimensional counterterms. Results on those counterterms (even beyond one loop) as well as a technical variant to treat γ_5 in the '*t Hooft–Veltman* scheme that avoids the split of D -dimensional indices into $(D-4)$ -dimensional and 4-dimensional ones in practical calculations can be found in Ref. [185].

- In *naive dimensional regularization (NDR)* [186], which can be safely used at the one-loop level, the anticommutation relations (174) as well as the trace condition (175) are kept. The algebraic inconsistency of this scheme leads to ambiguities in the results for Feynman diagrams that are related to the Adler–Bell–Jackiw anomaly [187, 188]. All diagrams without closed fermion loops and contributions to closed fermion loops with an even number of γ_5 can be calculated consistently in D dimensions. Contributions to closed fermion loops exhibiting traces involving an odd number of γ_5 cannot be obtained uniquely by dimensional continuation. In theories with a chiral anomaly, the anomalous terms in the usual conventions are recovered upon requiring Bose symmetry and vector-current conservation [181, 187, 189].
- Kreimer, Körner and Schilcher (KKS) proposed a scheme [190–192] with anticommuting γ_5 by giving up the cyclicity of Dirac traces. Instead, traces in different diagrams have to be written down using the same *reading point*, defining the starting point of the γ -string in a Dirac trace. In addition, specific rules have to be used to calculate Dirac traces involving an odd number of γ_5 . As a consequence all ambiguities disappear, and the anomalies in the usual conventions are obtained. Beyond one loop, the detailed application is sometimes under debate. In practice, the consistency of the scheme can be checked by verifying the relevant Ward identities before loop integration.

In theories without chiral anomalies, such as the SM, traces with an odd number of γ_5 matrices can be calculated using NDR while ensuring that all potentially anomalous terms cancel. At the one-loop level the ambiguities concern fermion-loop diagrams with three or four external vector bosons. The ambiguous terms are UV-finite, polynomial (rational) terms involving $\epsilon^{\mu\nu\rho\sigma}$ and are linear in the external momenta for the 3-point functions and independent of the external momenta for the 4-point functions. In a consistent calculation these rational terms cancel when summing over complete fermion generations. To ensure the cancellation in practical calculations, the same analytical expressions have to be used for all diagrams involving (linearly UV-divergent) triangular fermion loops, and the diagrams with clockwise and counterclockwise fermion flow have to be related appropriately. It is crucial that Dirac traces with reversed order of Dirac matrices are calculated in the same way as the traces with the original order. This can be ensured by starting the traces at the same vertex and performing the same algebraic manipulations. It can also be guaranteed by requiring Bose symmetry or in case of charged vector bosons the symmetry under the interchange of their momenta, Lorentz indices, and couplings. The rules of the KKS scheme also ensure cancellation of the ambiguities. The NDR scheme has been used in the majority of one-loop calculations in the past, including Refs. [38, 40, 117, 147, 150, 193–196].

In modern recursive approaches (see Section 3.5), the numerators of the loop diagrams are calculated in four dimensions, and the extra rational terms are calculated with dedicated Feynman rules [197]. Only the latter depend on the treatment of γ_5 . Feynman rules for the rational parts of the EW one-loop amplitudes have been calculated in the KKS scheme [198, 199]. No rational terms proportional to ϵ tensors show up, confirming the absence of rational terms associated with anomalies in the SM and the equivalence of the NDR and KKS schemes at the one-loop level.

3.4.3. Tensor-integral reduction

A general one-loop amplitude $\delta\mathcal{M}$ can be written as a linear combination of one-loop tensor integrals $T_{(j)}^{N_j, \mu_1 \dots \mu_{r_j}}$ with tensor coefficients $c_{\mu_1 \dots \mu_{r_j}}^{(j, r_j, N_j)}$ and a contribution \mathcal{M}_{ct} from counterterms, i.e.

$$\delta\mathcal{M} = \sum_j c_{\mu_1 \dots \mu_{r_j}}^{(j, r_j, N_j)} T_{(j)}^{N_j, \mu_1 \dots \mu_{r_j}} + \mathcal{M}_{\text{ct}}, \quad (177)$$

where the Lorentz indices and tensors have to be understood as D -dimensional objects in DR. The indices j characterize the different tensor integrals, and N_j denotes the number of propagators of these integrals. In the 't Hooft–Feynman gauge the rank of the tensor integrals is bounded by $r_j \leq N_j$ in renormalizable theories. The counterterms cancel the UV singularities present in the tensor integrals which manifest themselves as poles in $\epsilon = (4 - D)/2$ [cf. Eq. (169)].

If the Lorentz indices are only allowed to take 4-dimensional values, as is the case if the amplitudes are calculated numerically in 4 dimensions, finite *rational terms of type R_2* [197] are missed in the amplitude calculation (see Section 3.4.5), since algebraic terms $f(D)$ depending on $D = 4 - 2\epsilon$ produce finite rational terms when they multiply $1/\epsilon$ poles, i.e. $f(D)/\epsilon = f(4)/\epsilon + \text{finite rational terms}$. If $f(D)$ appears as $f(4)$ from the beginning, the missing rational terms have to be supplemented by hand, and the matrix element (177) takes the form

$$\delta\mathcal{M} = \sum_j \hat{c}_{\mu_1 \dots \mu_{r_j}}^{(j, r_j, N_j)} T_{(j)}^{N_j, \mu_1 \dots \mu_{r_j}} + \mathcal{M}_{\text{ct}} + \mathcal{M}_{R_2}, \quad (178)$$

where the caret on the tensor coefficient $\hat{c}_{\mu_1 \dots \mu_{r_j}}^{(j, r_j, N_j)}$ indicates that it involves only 4-dimensional components.

In Refs. [200, 201] it was demonstrated that rational terms of type R_2 of IR origin cancel in unrenormalized scattering amplitudes and only result from wave-function renormalization constants. Thus, only the rational terms of type R_2 of UV origin have to be calculated. Since the UV-divergent terms of one-loop integrals are always polynomial in internal masses and external momenta (see, e.g., App. A in Ref. [202] for explicit results) and are not subject to specific kinematical configurations (in contrast to IR singularities), the calculation of rational terms of type R_2 is simple and easy to automate (see Section 3.4.5d).

Tensor integrals have the general form [202]

$$T^{N, \mu_1 \dots \mu_P}(p_1, \dots, p_{N-1}, m_0, \dots, m_{N-1}) = \frac{(2\pi\mu)^{4-D}}{i\pi^2} \int d^D q \frac{q^{\mu_1} \dots q^{\mu_P}}{D_0 D_1 \dots D_{N-1}} \quad (179)$$

with the denominator factors

$$D_k = (q + p_k)^2 - m_k^2 + i\epsilon, \quad k = 0, \dots, N-1, \quad p_0 = 0, \quad (180)$$

where $i\epsilon$ ($\epsilon > 0$) is an infinitesimally small imaginary part.²⁵ Here N denotes the number of propagators in the loop, and P the rank of the tensor integral. For $P = 0$, i.e. rank zero, Eq. (179) defines the scalar N -point integral T_0^N . Following the notation of Ref. [33], we set $T^1 = A$, $T^2 = B$, $T^3 = C$, $T^4 = D$, $T^5 = E$, $T^6 = F$.

We use the conventions of Refs. [40, 202, 203] to decompose the tensor integrals into Lorentz-covariant structures. For tensor integrals up to rank five the decompositions read

$$\begin{aligned} T^{N, \mu} &= \sum_{i_1=1}^{N-1} p_{i_1}^\mu T_{i_1}^N, & T^{N, \mu\nu} &= \sum_{i_1, i_2=1}^{N-1} p_{i_1}^\mu p_{i_2}^\nu T_{i_1 i_2}^N + g^{\mu\nu} T_{00}^N, \\ T^{N, \mu\nu\rho} &= \sum_{i_1, i_2, i_3=1}^{N-1} p_{i_1}^\mu p_{i_2}^\nu p_{i_3}^\rho T_{i_1 i_2 i_3}^N + \sum_{i_1=1}^{N-1} \{gp\}_{i_1}^{\mu\nu\rho} T_{00i_1}^N, \\ T^{N, \mu\nu\rho\sigma} &= \sum_{i_1, i_2, i_3, i_4=1}^{N-1} p_{i_1}^\mu p_{i_2}^\nu p_{i_3}^\rho p_{i_4}^\sigma T_{i_1 i_2 i_3 i_4}^N + \sum_{i_1, i_2=1}^{N-1} \{gpp\}_{i_1 i_2}^{\mu\nu\rho\sigma} T_{00i_1 i_2}^N + \{gg\}_{0000}^{\mu\nu\rho\sigma} T_{0000}^N, \end{aligned}$$

²⁵Note that the ϵ in the propagator denominators and the ϵ that parametrizes the deviation of the dimension from 4 are different, although we use the same symbol. The meaning should be clear from the context.

$$T^{N,\mu\nu\rho\sigma\tau} = \sum_{i_1,i_2,i_3,i_4,i_5=1}^{N-1} p_{i_1}^\mu p_{i_2}^\nu p_{i_3}^\rho p_{i_4}^\sigma p_{i_5}^\tau T_{i_1 i_2 i_3 i_4 i_5}^N + \sum_{i_1,i_2,i_3=1}^{N-1} \{gppp\}_{i_1 i_2 i_3}^{\mu\nu\rho\sigma\tau} T_{00 i_1 i_2 i_3}^N + \sum_{i_1=1}^{N-1} \{ggp\}_{i_1}^{\mu\nu\rho\sigma\tau} T_{0000 i_1}^N. \quad (181)$$

Because of the symmetry of the tensor $T_{\mu_1 \dots \mu_p}^N$ all coefficients $T_{i_1 \dots i_p}^N$ are symmetric under permutation of all indices. The symmetrized tensors in Eq. (181) read

$$\begin{aligned} \{gp\}_{i_1}^{\mu\nu\rho} &= g^{\mu\nu} p_{i_1}^\rho + g^{\nu\rho} p_{i_1}^\mu + g^{\rho\mu} p_{i_1}^\nu, \\ \{gpp\}_{i_1 i_2}^{\mu\nu\rho\sigma} &= g^{\mu\nu} p_{i_1}^\rho p_{i_2}^\sigma + g^{\mu\rho} p_{i_1}^\sigma p_{i_2}^\nu + g^{\mu\sigma} p_{i_1}^\nu p_{i_2}^\rho + g^{\nu\rho} p_{i_1}^\sigma p_{i_2}^\mu + g^{\rho\sigma} p_{i_1}^\nu p_{i_2}^\mu + g^{\sigma\nu} p_{i_1}^\rho p_{i_2}^\mu, \\ \{gg\}^{\mu\nu\rho\sigma} &= g^{\mu\nu} g^{\rho\sigma} + g^{\nu\rho} g^{\mu\sigma} + g^{\rho\mu} g^{\nu\sigma}, \end{aligned} \quad (182)$$

with obvious generalizations to other tensors like $\{gppp\}$, i.e. the curly brackets denote symmetrization so that all non-equivalent permutations of the Lorentz indices of metric tensors and a generic momentum are included. The decomposition of general tensor integrals can be found in Ref. [202]. The following presentation consistently sticks to the conventions introduced there.

Tensor-integral reduction allows us to reduce the tensor integrals to those with less denominators or lower rank. Thus, in the reduction of the tensor integral $T_{\mu_1 \dots \mu_p}^{N+1}$, tensor integrals appear that are obtained by omitting the k th denominator D_k ; such integrals are denoted $T_{\mu_1 \dots \mu_p}^N(k)$. In the Lorentz decomposition of $T_{\mu_1 \dots \mu_p}^N(k)$, $k = 1, \dots, N$, shifted indices appear which are denoted as

$$(i_r)_k = \begin{cases} i_r & \text{for } k > i_r, \\ i_r - 1 & \text{for } k < i_r. \end{cases} \quad (183)$$

When cancelling the first denominator D_0 the resulting tensor integrals are not in the standard form, but can be expressed in terms of standard integrals by shifting the integration momentum. Choosing the shift $q \rightarrow q - p_1$, the following N -point integrals appear:

$$\tilde{T}^{N,\mu_1 \dots \mu_p}(0) = \frac{(2\pi\mu)^{(4-D)}}{i\pi^2} \int d^D q \frac{q^{\mu_1} \dots q^{\mu_p}}{\tilde{D}_1 \dots \tilde{D}_N}, \quad \tilde{D}_k = (q + p_k - p_1)^2 - m_k^2 + i\epsilon, \quad k = 1, \dots, N. \quad (184)$$

The scalar integral $T_0^N = T^N$ and the tensor coefficients $T_{00}^N, T_{0000}^N, \dots$ are invariant under this shift. The other coefficients of $T_{\mu_1 \dots \mu_p}^N(k)$ can be recursively obtained as

$$\begin{aligned} \underbrace{T_{0 \dots 0}^N}_{2n} i_{2n+1 \dots i_p}(0) &= \underbrace{T_{0 \dots 0}^N}_{2n} i_{2n+1-1, \dots, i_p-1}(0), \quad i_{2n+1}, \dots, i_p > 1, \\ \underbrace{T_{0 \dots 0}^N}_{2n} i_{2n+2 \dots i_p}(0) &= - \underbrace{T_{0 \dots 0}^N}_{2n} i_{2n+2 \dots i_p}(0) - \sum_{r=2}^N \underbrace{T_{0 \dots 0}^N}_{2n} i_{2n+2 \dots i_p}(0), \quad i_{2n+2}, \dots, i_p > 0. \end{aligned} \quad (185)$$

We also use the notation $\bar{\delta}_{ij} = 1 - \delta_{ij}$, i.e. $\sum_i \bar{\delta}_{ij}(\dots) = \sum_{i \neq j}(\dots)$, and employ the caret “ $\hat{}$ ” to indicate indices that are omitted, i.e.

$$T_{i_1 \dots \hat{i}_r \dots i_p}^N = T_{i_1 \dots i_{r-1} i_{r+1} \dots i_p}^N. \quad (186)$$

(a) Reduction of tensor integrals up to $N \leq 4$ according to Passarino–Veltman

All one-loop tensor integrals can be algebraically reduced to one-loop standard scalar integrals. The standard procedure is known as *Passarino–Veltman reduction* [34], which proceeds via contracting the tensor integrals (179) with the external momenta p_k^μ and the metric tensor $g^{\mu\nu}$. Using

$$\begin{aligned} 2p_k q &= D_k - D_0 - f_k, \quad f_k = p_k^2 - m_k^2 + m_0^2, \\ q^2 &= D_0 + m_0^2, \end{aligned} \quad (187)$$

all scalar products with an integration momentum in the numerator can be cancelled against propagator denominators D_k , resulting in tensor integrals with lower rank and/or lower number of propagators. Inserting the Lorentz decompositions of the tensor integrals (181) results in systems of linear equations for the tensor-integral coefficients. These equations have the solutions [40]

$$T_{00i_3\dots i_p}^N = \frac{1}{2(3+P-N)} \left[-2(D-4)T_{00i_3\dots i_p}^N + T_{i_3\dots i_p}^{N-1}(0) + 2m_0^2 T_{i_3\dots i_p}^N + \sum_{n=1}^{N-1} f_n T_{ni_3\dots i_p}^N \right], \quad (188)$$

$$T_{i_1\dots i_p}^N = \sum_{n=1}^{N-1} (Z^{(N-1)})_{i_1n}^{-1} \left(T_{(i_2)\dots(i_p)_n}^{N-1}(n) \bar{\delta}_{ni_2} \dots \bar{\delta}_{ni_p} - T_{i_2\dots i_p}^{N-1}(0) - f_n T_{i_2\dots i_p}^N - 2 \sum_{r=2}^P \delta_{ni_r} T_{00i_2\dots i_r\dots i_p}^N \right), \quad i_1 \neq 0. \quad (189)$$

The matrix $(Z^{(N)})^{-1}$ is the inverse of the Gram matrix

$$Z^{(N)} = \begin{pmatrix} 2p_1p_1 & \dots & 2p_1p_N \\ \vdots & \ddots & \vdots \\ 2p_Np_1 & \dots & 2p_Np_N \end{pmatrix}. \quad (190)$$

The relations (188) and (189) determine $T_{i_1\dots i_p}^N$ in terms of $T_{i_1\dots i_{p-1}}^N$, $T_{i_1\dots i_{p-2}}^N$, $T_{i_1\dots i_{p-1}}^{N-1}$, and $T_{i_1\dots i_{p-2}}^{N-1}$. Using these relations recursively, all coefficients of N -point functions can be expressed in terms of $(N-1)$ -point functions and the scalar N -point function T_0^N . The finite polynomial quantities $(D-4)T_{00i_3\dots i_p}^N$, the *rational terms of type R_1* (defined in Section 3.4.5d), can easily be derived by exploiting Eqs. (188) and (189) for the UV-singular parts and using those for the scalar 1-point and 2-point functions as input; explicit results for tensors up to rank 7 are summarized in Ref. [202]. Rational terms of type R_1 do not result from IR divergences, since $T_{00i_3\dots i_p}^N$ do not involve IR singularities [202]. More explicit formulas for the Passarino–Veltman reduction for all tensor functions up to rank 5 are, e.g., given in Appendix B of Ref. [203].

Equation (189) becomes numerically unstable if the Gram matrix $Z^{(N-1)}$ is nearly singular, i.e. if its determinant, the Gram determinant $\Delta^{(N-1)} = \det(Z^{(N-1)})$, is close to zero. In this case different iterative solutions of the reduction equations that avoid those instabilities are possible, as described in detail in Ref. [202]. This reference contains also an alternative Passarino–Veltman reduction that is numerically more stable in specific phase-space regions.

Different variants of Passarino–Veltman reduction can be found in the literature. Van Oldenborgh and Vermaseren constructed a different tensor basis that concentrates some of the numerical instabilities into a number of determinants [204]. Ezawa et al. performed the reduction using an orthonormal tensor basis [205]. A reduction in Feynman-parameter space, which is equivalent to the Passarino–Veltman scheme, is used in the GRACE package [206].

Alternative tensor reduction schemes have been developed using different sets of master integrals. Davydychev could relate the coefficients of one-loop tensor integrals to scalar integrals in a different number of space–time dimensions [207], and Tarasov found recursion relations between those integrals [208]. These methods have been further elaborated by different groups [209–213]. In this approach all one-loop tensor integrals can be reduced to finite 4-point integrals in $(D+2)$ dimensions and divergent 3-point and 2-point integrals in D dimensions. These basic integrals are typically reduced to the usual scalar integrals or, in particular for small Gram determinants, calculated by numerical integration [214].

(b) Reduction of tensor integrals with $N \geq 5$

Owing to the 4-dimensionality of space–time further reduction formulas exist for scalar and tensor integrals with $N \geq 5$. It was realized already in the 1960s by Melrose [215] that scalar integrals with more than four lines in the loop, i.e. 5-point and higher-point scalar integrals, can be reduced to scalar integrals with fewer internal propagators in four dimensions. These methods were subsequently extended and improved by several authors [40, 202–204, 207, 209–211, 216–220] and generalized to DR in Refs. [172, 177, 209]. In Ref. [203], a method for the reduction of 5-point integrals that completely avoids inverse leading Gram determinants was worked out. Later, a similar reduction was found that reduces 5-point tensor integrals to 4-point integrals with rank reduced by one [202, 214].

We here present the results for the reduction of ($N \geq 5$)-point integrals using the conventions of Ref. [202]. These can be directly written in terms of tensor integrals without the need to introduce Lorentz decompositions. For $N \geq 6$ the reduction formulas read

$$T_{\mu\mu_1\dots\mu_{P-1}}^N = \sum_{n=1}^5 \sum_{\substack{m=1 \\ m \neq k}}^5 (M_{(k)}^{-1})_{nm} p_{m,\mu} [T_{\mu_1\dots\mu_{P-1}}^{N-1}(n) - T_{\mu_1\dots\mu_{P-1}}^{N-1}(0)] + T_{\alpha\mu_1\dots\mu_{P-1}}^N (g_\mu^\alpha - \hat{g}_\mu^\alpha), \quad N \geq 6, \quad (191)$$

which express the N -point tensor integral of rank P in terms of six ($N - 1$)-point tensor integrals of rank $(P - 1)$. The matrix $M_{(k)}^{-1}$ is the inverse of

$$M_{(k)} = \begin{pmatrix} 2p_1p_1 & \dots & 2p_1p_5 \\ \vdots & \ddots & \vdots \\ 2p_{k-1}p_1 & \dots & 2p_{k-1}p_5 \\ f_1 & \dots & f_5 \\ 2p_{k+1}p_1 & \dots & 2p_{k+1}p_5 \\ \vdots & \ddots & \vdots \\ 2p_5p_1 & \dots & 2p_5p_5 \end{pmatrix}. \quad (192)$$

The index k can be chosen arbitrarily, and for $N > 6$ any five momenta p_i can be selected out of the $(N - 1)$ available momenta of the N -point function. The last term in Eq. (191), which involves the 4-dimensional metric tensor \hat{g}_μ^α gives rise to rational terms and only contributes if $T_{\alpha\mu_1\dots\mu_{P-1}}^N$ is singular. For UV singularities this is the case if $P \geq 2N - 4$, which is not needed in renormalizable theories, where $P \leq N$. IR (soft and collinear) singularities of $T_{\alpha\mu_1\dots\mu_{P-1}}^N$ only appear in contributions that are proportional to some momentum $p_{i,\alpha}$ and thus drop out in the last term of Eq. (191). Therefore, the terms involving $(g - \hat{g})$ in Eq. (191) can be omitted for $P \leq 2N - 5$. Further variants of the reduction (191) can be found in Ref. [202].

Equation (191) is not applicable to the reduction of scalar functions. These can be reduced via

$$T_{\mu_1\dots\mu_P}^N = - \sum_{n=0}^5 \eta_n T_{\mu_1\dots\mu_P}^{N-1}(n), \quad \eta_n = \frac{\det(Y_n^{(5)})}{\det(Y^{(5)})}. \quad (193)$$

The modified Cayley matrix $Y^{(5)} = (Y_{ij}^{(5)})$, $i, j = 0, \dots, 5$ is defined by

$$Y_{ij}^{(5)} = m_i^2 + m_j^2 - (p_i - p_j)^2 \quad (194)$$

in terms of the momenta and masses of five different propagators of the N -point function, and the matrix $Y_n^{(5)}$ is obtained from $Y^{(5)}$ by replacing all entries in the n th column by 1. For the scalar integral T_0^N , this result is identical with the one of Ref. [215]. For $P > 0$, it provides an alternative, though less efficient reduction for the tensor integrals of rank $N \geq 6$ [40, 202].

The formulas for the reduction of 5-point functions are somewhat more complicated. The relation analogous to Eq. (191) reads [202]

$$\begin{aligned} T_{\mu\mu_1\dots\mu_{P-1}}^5 = & \sum_{n,m=1}^4 (X^{(4)})_{nm}^{-1} p_{m,\mu} [T_{\mu_1\dots\mu_{P-1}}^4(n) - T_{\mu_1\dots\mu_{P-1}}^4(0)] + \sum_{n=1}^4 (X^{(4)})_{0n}^{-1} [-p_{n,\mu} T_{\mu_1\dots\mu_{P-1}}^4(0) + \mathcal{T}_{\mu\mu_1\dots\mu_{P-1}}^4(n)] \\ & - \sum_{n=1}^4 \mathcal{T}_{\alpha\mu_1\dots\mu_{P-1}}^4(n) \sum_{m,l=1}^4 2p_m^\alpha p_{l,\mu} \left[(X^{(4)})_{0n}^{-1} (X^{(4)})_{ml}^{-1} - (X^{(4)})_{0l}^{-1} (X^{(4)})_{mn}^{-1} \right] + 2m_0^2 (X^{(4)})_{00}^{-1} (g_\mu^\alpha - \hat{g}_\mu^\alpha) T_{\alpha\mu_1\dots\mu_{P-1}}^5 \\ & + 2 \sum_{n=1}^4 (X^{(4)})_{0n}^{-1} [p_{n,\mu} (g^{\alpha\beta} - \hat{g}^{\alpha\beta}) - p_n^\beta (g_\mu^\alpha - \hat{g}_\mu^\alpha)] T_{\alpha\beta\mu_1\dots\mu_{P-1}}^5, \end{aligned} \quad (195)$$

which expresses the 5-point function of rank P in terms of five 4-point functions of rank $(P - 1)$ and contributions of the corresponding 4-point functions of rank P involving metric tensors in their covariant decomposition as well as rational terms. The matrix $X^{(4)}$ reads

$$X^{(4)} = \begin{pmatrix} 2m_0^2 & f_1 & \dots & f_4 \\ f_1 & 2p_1p_1 & \dots & 2p_1p_4 \\ \vdots & \vdots & \ddots & \vdots \\ f_4 & 2p_4p_1 & \dots & 2p_4p_4 \end{pmatrix}, \quad (196)$$

and

$$\mathcal{T}_{\alpha\mu_1\dots\mu_{P-1}}^4(i) = \left[T_{\alpha\mu_1\dots\mu_{P-1}}^4(i) - T_{\alpha\mu_1\dots\mu_{P-1}}^4(0) \right] \Big|_{\text{contributions with } g_{\alpha\mu_r}}, \quad i = 1, \dots, 4. \quad (197)$$

The rational terms proportional to $(g_\mu^\alpha - \hat{g}_\mu^\alpha)$ only contribute if $T_{\alpha\beta\mu_1\dots\mu_{P-1}}^5$ is UV divergent, i.e. for $P \geq 5$. The rational terms for $P = 5$ are given in Ref. [202], and the case $P > 5$ does not appear in renormalizable theories and renormalizable gauges.

The scalar 5-point function can be reduced to scalar 4-point functions with the relation

$$\begin{aligned} T_{\mu_1\dots\mu_p}^5 = & - \sum_{n=0}^4 \eta_n T_{\mu_1\dots\mu_p}^4(n) + \sum_{n,m=1}^4 \left[(X^{(4)})_{00}^{-1} (X^{(4)})_{nm}^{-1} - (X^{(4)})_{n0}^{-1} (X^{(4)})_{0m}^{-1} \right] 2p_m^\alpha \mathcal{T}_{\alpha\mu_1\dots\mu_p}^4(n) \\ & + 2T_{\alpha\beta\mu_1\dots\mu_p}^5 (X^{(4)})_{00}^{-1} (g^{\alpha\beta} - \hat{g}^{\alpha\beta}). \end{aligned} \quad (198)$$

The η_n are defined analogously to those in Eq. (193) from the 5-dimensional modified Cayley matrix $Y^{(4)} = (Y_{ij}^{(4)})$, $i, j = 0, \dots, 4$. For the scalar case, $P = 0$, the result is identical with the one of Ref. [215]. For $P > 0$, Eq. (198) provides an alternative, though less efficient, reduction for the tensor integrals. Explicit expressions for the rational terms for $P = 4$ can be found in Refs. [202, 203].

Reduction formulas for tensor integrals can be directly used in reduction algorithms for one-loop amplitudes, i.e. tensor components can be employed instead of tensor coefficients for a basis of covariants. This approach is, e.g., implemented in RECOLA [72, 73]. Avoiding the introduction of tensor coefficients allows for a speedup of the calculations. On the other hand, these reduction formulas can be transferred to those for the tensor coefficients upon inserting the Lorentz decompositions of the tensor integrals.

(c) Libraries for tensor-integral reduction

There are various software packages for tensor-integral reduction on the market:

- **LoopTools** [221] is a package for the evaluation of scalar and tensor one-loop integrals based on the FF package by van Oldenborgh [222]. It provides the actual numerical implementations of the functions appearing in FORMCALC output [223]. UV singularities are regularized dimensionally, IR singularities are regularized either dimensionally or in MR. Complex masses are supported using the implementation of Ref. [224].
- **GOLEM95C** [225–227] is a program for the numerical evaluation of scalar and tensor one-loop integrals which supports the use of complex masses. It performs an alternative reduction to a set of basis integrals involving 4-point functions in 6 dimensions, which are IR and UV finite, UV-divergent 4-point functions in $D + 4$ dimensions, and various 2-point and 3-point functions as defined in Refs. [210, 214].
- The Fortran package **COLLIER** [228, 229] provides a numerically stable reduction of tensor integrals to scalar integrals based on conventional methods and expansions in regions with small kinematical determinants [202] and simultaneously calculates the scalar integrals. It supports DR and MR of IR singularities and complex masses.
- The C++ package **PJFRY** [230] encodes a numerical reduction of one-loop tensor integrals in terms of scalar 1- to 4-point functions, which have to be supplied by an external library.
- **PACKAGE χ** is a Mathematica package for the analytic calculation and symbolic manipulation of one-loop Feynman integrals in relativistic quantum field theory [231, 232]. It generates analytic expressions for dimensionally regulated tensor integrals with up to four distinct propagators and arbitrarily high rank.

3.4.4. Reduction of tensor integrals at the integrand level

In Refs. [233, 234] an alternative method was proposed that allows for recursively reducing tensor integrals to tensor integrals of lower rank and integrals with fewer propagator denominators. Therewith, high-rank tensor integrals can be recursively expressed in terms of lower-rank ones at the integrand level. Here, we sketch a reformulation of this method as described in Ref. [235]. The idea of the algorithm is to express products of two integration momenta in the numerators of the tensor integrals by terms involving at most one integration momentum in combination with denominators of the tensor integrals. In four space-time dimensions, the basic identity reads

$$\hat{q}^\mu \hat{q}^\nu = \left[A_{-1}^{\mu\nu} + A_0^{\mu\nu} \hat{D}_0 \right] + \left[B_{-1,\lambda}^{\mu\nu} + \sum_{j=0}^3 B_{j,\lambda}^{\mu\nu} \hat{D}_j \right] \hat{q}^\lambda. \quad (199)$$

The rank-1 polynomial on the r.h.s. is a linear combination of four 4-dimensional loop denominators, $\hat{D}_0, \dots, \hat{D}_3$, and the corresponding tensor coefficients, $A_j^{\mu\nu}$ and $B_{j,\lambda}^{\mu\nu}$, depend only on the three external momenta p_1, p_2, p_3 corresponding to the loop-propagator denominators $\hat{D}_1, \hat{D}_2, \hat{D}_3$ as defined in Eq. (180) but for 4-dimensional loop momenta \hat{q} . The coefficients of the loop denominators $\hat{D}_0, \hat{D}_1, \hat{D}_2, \hat{D}_3$ are labelled with indices $j = 0, \dots, 3$, while $j = -1$ is used for the constant parts.

The identity (199) provides an exact representation of $\hat{q}^\mu \hat{q}^\nu$ in terms of 4-dimensional loop denominators, but can be easily generalized to D -dimensional denominators by substituting

$$\hat{D}_j = D_j - \check{q}^2, \quad j = 0, 1, 2, 3, \quad (200)$$

where quantities with a check denote $(D - 4)$ -dimensional objects, e.g. $q^2 = \hat{q}^2 + \check{q}^2$. The terms of the form $D_i - \hat{D}_i = \check{q}^2$ account for the mismatch between the D -dimensional and 4-dimensional parts of loop denominators. The corresponding tensor integrals with $(D - 4)$ -dimensional \check{q}^2 terms in the numerator give rise to finite terms [197, 233], so-called rational terms of type R_1 (see Section 3.4.5d).

The reduction identities of Ref. [233] are based on a decomposition of the 4-dimensional loop momentum,

$$\hat{q}^\mu = \sum_{i=1}^4 c_i l_i^\mu, \quad (201)$$

in a basis l_1, \dots, l_4 , formed by massless momenta l_i , which span two orthogonal planes,

$$l_i^2 = 0, \quad i = 1, 2, 3, 4, \quad l_j l_k = 0, \quad j = 1, 2, \quad k = 3, 4. \quad (202)$$

This reduction basis $\{l_i\}$ is constructed from two external momenta p_1, p_2 which appear in the propagators D_1, D_2 . The momenta l_1, l_2 lie in the plane spanned by p_1 and p_2 ,

$$l_1^\mu = p_1^\mu - \alpha_1 p_2^\mu, \quad l_2^\mu = p_2^\mu - \alpha_2 p_1^\mu. \quad (203)$$

The momenta l_3, l_4 are defined as

$$l_3^\mu = \bar{v}(l_1) \gamma^\mu \omega_{-u}(l_2), \quad l_4^\mu = \bar{v}(l_2) \gamma^\mu \omega_{-u}(l_1), \quad (204)$$

with the massless Dirac spinors u and \bar{v} , and thus lie in the plane orthogonal to p_1, p_2 . The basis is normalized according to

$$\kappa = 2(l_1 l_2) = -\frac{1}{2}(l_3 l_4), \quad (205)$$

and the coefficients $\alpha_{1,2}$ in Eq. (203) read

$$\alpha_i = \frac{p_i^2}{p_1 p_2 + \text{sgn}(p_1 p_2) \sqrt{\Delta}}, \quad (206)$$

where Δ is the negative of the rank-2 Gram determinant,

$$\Delta = (p_1 p_2)^2 - p_1^2 p_2^2 = -\det(p_1 p_2), \quad (207)$$

and the sign in front of the positive square root is chosen such that α_i behaves smoothly in the limits $p_i^2 \rightarrow 0$. The Gram determinant is related to the normalization factor κ via

$$\kappa = \frac{4\Delta}{p_1 p_2 + \text{sgn}(p_1 p_2) \sqrt{\Delta}}. \quad (208)$$

Rewriting Eq. (199) in the more generic form

$$\hat{q}^\mu \hat{q}^\nu = \sum_{j=-1}^3 (A_j^{\mu\nu} + B_{j,\lambda}^{\mu\nu} \hat{q}^\lambda) \hat{D}_j, \quad \hat{D}_{-1} = 1, \quad (209)$$

the reduction coefficients $A_j^{\mu\nu}$, $B_{j,\lambda}^{\mu\nu}$ are expressed in terms of the vectors l_i as follows,

$$\begin{aligned} A_{-1}^{\mu\nu} &= m_0^2 A_0^{\mu\nu}, & A_0^{\mu\nu} &= \frac{1}{4\kappa} \left(\alpha L_{33}^{\mu\nu} + \frac{1}{\alpha} L_{44}^{\mu\nu} - L_{34}^{\mu\nu} \right), & A_{1,2,3}^{\mu\nu} &= 0, \\ B_{-1,\lambda}^{\mu\nu} &= \sum_{i=1}^3 f_{i0} B_{i,\lambda}^{\mu\nu}, & B_{0,\lambda}^{\mu\nu} &= - \sum_{i=1}^3 B_{i,\lambda}^{\mu\nu}, \\ B_{1,\lambda}^{\mu\nu} &= \frac{1}{4\kappa^2} \left[\frac{2(p_3 r_2)}{p_3 l_3} \left(L_{33}^{\mu\nu} l_{4,\lambda} + \frac{1}{\alpha} L_{44}^{\mu\nu} l_{3,\lambda} \right) - (r_2^\mu L_{34,\lambda}^\nu + r_2^\nu L_{34,\lambda}^\mu) \right] + \frac{1}{\kappa} (r_2^\mu \delta_\lambda^\nu - A_0^{\mu\nu} r_{2,\lambda}), \\ B_{2,\lambda}^{\mu\nu} &= B_{1,\lambda}^{\mu\nu} \Big|_{r_1 \leftrightarrow r_2}, & B_{3,\lambda}^{\mu\nu} &= - \frac{1}{4\kappa(p_3 l_3)} \left(L_{33}^{\mu\nu} l_{4,\lambda} + \frac{1}{\alpha} L_{44}^{\mu\nu} l_{3,\lambda} \right), \end{aligned} \quad (210)$$

with

$$L_{33}^{\mu\nu} = l_3^\mu l_3^\nu, \quad L_{44}^{\mu\nu} = l_4^\mu l_4^\nu, \quad L_{34}^{\mu\nu} = l_3^\mu l_4^\nu + l_4^\mu l_3^\nu, \quad \alpha = \frac{p_3 l_4}{p_3 l_3}, \quad (211)$$

and

$$r_1^\mu = l_1^\mu - \alpha_1 l_2^\mu, \quad r_2^\mu = l_2^\mu - \alpha_2 l_1^\mu, \quad f_{i0} = m_i^2 - m_0^2 - p_i^2. \quad (212)$$

Equation (199) is applicable to any integrand with $N \geq 4$ loop propagators,

$$\int d^D q \frac{\hat{q}^\mu \hat{q}^\nu S(\hat{q})}{D_0 \cdots D_{N-1}} = \int d^D q \frac{(A_{-1}^{\mu\nu} + B_{-1,\lambda}^{\mu\nu} \hat{q}^\lambda) S(\hat{q})}{D_0 \cdots D_{N-1}} + \sum_{j=0}^3 \int d^D q \frac{(A_j^{\mu\nu} + B_{j,\lambda}^{\mu\nu} \hat{q}^\lambda) S(\hat{q})}{D_0 \cdots D_{j-1} D_{j+1} \cdots D_{N-1}} + \text{rational terms}, \quad (213)$$

where $S(\hat{q})$ is an arbitrary polynomial in the integration momentum. The relation (213) allows for reducing tensor integrals of arbitrary high rank to simpler tensor integrals. In the on-the-fly reduction approach of Refs. [71, 235], sketched at the end of Section 3.5.3, it is applied to incomplete loop integrals during the recursive construction and avoids the calculation of tensor integrals and the manipulation of tensors of rank higher than 2.

For 3-point integrals of rank $P \leq 3$ a similar relation can be derived [233, 235]:

$$\int d^D q \frac{\hat{q}^\mu \hat{q}^\nu S(\hat{q})}{D_0 \cdots D_2} = \int d^D q \frac{(A_{-1}^{\mu\nu} + B_{-1,\lambda}^{\mu\nu} \hat{q}^\lambda) S(\hat{q})}{D_0 \cdots D_2} + \sum_{j=0}^2 \int d^D q \frac{(A_j^{\mu\nu} + B_{j,\lambda}^{\mu\nu} \hat{q}^\lambda) S(\hat{q})}{D_0 \cdots D_{j-1} D_{j+1} \cdots D_2} + \text{rational terms}. \quad (214)$$

Here $S(\hat{q}) = S + S_\rho \hat{q}^\rho$ is an arbitrary rank-1 polynomial, the sum over j runs only from 0 to 2, and the tensors $A_j^{\mu\nu}$ and $B_{j,\lambda}^{\mu\nu}$ are obtained from Eq. (210) through the trivial replacements

$$L_{33}^{\mu\nu} \rightarrow 0, \quad L_{44}^{\mu\nu} \rightarrow 0. \quad (215)$$

The identity (214) allows for a reduction of 3-point tensor integrals of ranks 2 and 3 to rank-1 integrals.

While similar methods can be found for the reduction of 2-point functions, these do not provide advantages with respect to conventional reduction methods. Formulae for the reduction of rank-1 integrals at the integrand level can be found in Ref. [233].

The algorithm described above has also been used in Ref. [236]. As tensor-integral reduction, it suffers from the appearance of inverse Gram determinants. A systematic way of avoiding Gram-determinant instabilities in this reduction algorithm was presented in Refs. [71, 235].

3.4.5. The OPP method

The *reduction at the integrand level* or *OPP method* according to its authors Ossola, Papadopoulos, and Pithan [174] is based on the fact that any one-loop amplitude can be expressed in terms of scalar 1-, 2-, 3-, and 4-point functions and that, as shown in Ref. [233], already at the integrand level the dependence of numerators on loop-integration momenta can be expressed in terms of propagator denominators.

(a) Coefficients of scalar functions

The integrand of any N -point one-loop amplitude with loop momentum q has the form

$$A(q) = \frac{N(q)}{D_0 D_1 \cdots D_{N-1}}, \quad D_i = (q + p_i)^2 - m_i^2, \quad p_0 \neq 0, \quad (216)$$

and the choice $p_0 \neq 0$ allows for a completely symmetric treatment of all denominators D_i . The OPP method starts from the related quantity

$$\hat{A}(q) = \frac{\hat{N}(\hat{q})}{D_0 D_1 \cdots D_{N-1}}, \quad (217)$$

with the purely 4-dimensional numerator $\hat{N}(\hat{q})$. According to Ref. [174], this numerator can be cast into the form

$$\begin{aligned} \hat{N}(\hat{q}) = & \sum_{i_0 < i_1 < i_2 < i_3}^{N-1} [d(i_0 i_1 i_2 i_3) + \tilde{d}(\hat{q}; i_0 i_1 i_2 i_3)] \prod_{i \neq i_0, i_1, i_2, i_3}^{N-1} \hat{D}_i + \sum_{i_0 < i_1 < i_2}^{N-1} [c(i_0 i_1 i_2) + \tilde{c}(\hat{q}; i_0 i_1 i_2)] \prod_{i \neq i_0, i_1, i_2}^{N-1} \hat{D}_i \\ & + \sum_{i_0 < i_1}^{N-1} [b(i_0 i_1) + \tilde{b}(\hat{q}; i_0 i_1)] \prod_{i \neq i_0, i_1}^{N-1} \hat{D}_i + \sum_{i_0}^{N-1} [a(i_0) + \tilde{a}(\hat{q}; i_0)] \prod_{i \neq i_0}^{N-1} \hat{D}_i + \tilde{P}(\hat{q}) \prod_i^{N-1} \hat{D}_i. \end{aligned} \quad (218)$$

The quantity $d(i_0 i_1 i_2 i_3)$ is the coefficient of the scalar 4-point function with the denominator $D_{i_0} D_{i_1} D_{i_2} D_{i_3}$. Analogously, $c(i_0 i_1 i_2)$, $b(i_0 i_1)$, and $a(i_0)$ are the coefficients of all possible scalar 3-point, 2-point, and 1-point functions, respectively.

(b) Spurious terms

The *spurious terms* \tilde{d} , \tilde{c} , \tilde{b} , \tilde{a} , and \tilde{P} still depend on \hat{q} , but are required to vanish upon integration over $d^D q$. The complete set of spurious terms in renormalizable theories (and renormalizable gauges) was constructed in Ref. [174] in terms of the massless momenta l_i introduced in Section 3.4.4. The actual form of the spurious terms depends on the maximal rank of the tensors formed from loop momenta in the amplitude. The 4-point-like spurious terms involve only one coefficient,

$$\tilde{d}(\hat{q}; 0123) = \tilde{d}(0123) (\hat{q} + p_0) n, \quad (219)$$

where

$$n^\mu \propto \epsilon^{\mu\nu\rho\sigma} l_{1\nu} l_{2\rho} (p_3 - p_0)_\sigma, \quad (220)$$

is a four-vector orthogonal to all momenta $p_i - p_0$ ($i = 1, 2, 3$), and l_1, l_2 are constructed in the same way from $p_1 - p_0$ and $p_2 - p_0$ as described in the previous section for p_1 and p_2 . The 3-point-like spurious terms are of the form

$$\tilde{c}(\hat{q}; 012) = \sum_{j=1}^{j_{\max}} \left\{ \tilde{c}_{1j}(012) [(\hat{q} + p_0) l_3]^j + \tilde{c}_{2j}(012) [(\hat{q} + p_0) l_4]^j \right\} \quad (221)$$

with constants $\tilde{c}_{1j}(012)$, $\tilde{c}_{2j}(012)$, where $j_{\max} = 3$ in renormalizable theories. The number of constant coefficients of spurious terms is eight for the 2-point and four for the 1-point functions in renormalizable theories. The spurious term $\tilde{P}(q)$ vanishes in renormalizable theories.

(c) Determination of coefficients

All integration momenta \hat{q} in the numerator $\hat{N}(\hat{q})$ of Eq. (218) are 4-dimensional. Equation (218) is thus directly applicable to the purely 4-dimensional terms, which are usually the most difficult to compute. To this end, we can set $D_i \rightarrow \hat{D}_i$ and $q \rightarrow \hat{q}$ in Eq. (217).

Since the standard scalar 1-, 2-, 3-, 4-point functions are known, Eq. (218) reduces the problem of calculating $\hat{A}(q)$ to the algebraic problem of extracting all possible coefficients in Eq. (218) by computing $\hat{N}(\hat{q})$ a sufficient number of times, for different values of \hat{q} , and then inverting the system of equations. This procedure can be directly performed *at the amplitude level*, provided that the sum of all Feynman diagrams is known. Note, however, that using the tensor decomposition Eq. (178) is crucial in minimizing the evaluation time of the many evaluations of $N(q)$ that the OPP method requires.

The resulting system of algebraic equations is in general pretty large, and various strategies have been proposed to solve it efficiently. The original solution suggested in Ref. [174] consists in using particular choices of \hat{q} so that, systematically, 4, 3, 2, or 1 among all possible denominators \hat{D}_i vanish. Then, the system of equations becomes block-triangular, and one can solve first for the coefficients of all possible 4-point functions, then for those of all 3-point functions, and so on.

For the determination of the coefficients of the 4-point function with denominators $\hat{D}_0, \dots, \hat{D}_3$ one determines \hat{q} in such a way that

$$\hat{D}_0 = \hat{D}_1 = \hat{D}_2 = \hat{D}_3 = 0, \quad (222)$$

resulting in two complex solutions \hat{q}_0^\pm . Since $(\hat{q}_0^+ + p_0)n = -(\hat{q}_0^- + p_0)n$, one finds in terms of these solutions,

$$\begin{aligned} d(0123) &= \frac{1}{2} \left[\frac{N(\hat{q}_0^+)}{\prod_{i=4}^{N-1} D_i(\hat{q}_0^+)} + \frac{N(\hat{q}_0^-)}{\prod_{i=4}^{N-1} D_i(\hat{q}_0^-)} \right], \\ \tilde{d}(0123) &= \frac{1}{2(\hat{q}_0^+ + p_0)n} \left[\frac{N(\hat{q}_0^+)}{\prod_{i=4}^{N-1} D_i(\hat{q}_0^+)} - \frac{N(\hat{q}_0^-)}{\prod_{i=4}^{N-1} D_i(\hat{q}_0^-)} \right]. \end{aligned} \quad (223)$$

The coefficients of the 3-point functions are determined in a similar way after subtracting the known contributions of the 4-point functions from the integrand. When selecting \hat{q} in such a way that

$$\hat{D}_0 = \hat{D}_1 = \hat{D}_2 = 0, \quad \hat{D}_i \neq 0, \quad i \neq 0, 1, 2, \quad (224)$$

Eq. (218) becomes

$$\hat{N}(\hat{q}) - \sum_{i_3 > 2} [d(012i_3) + \tilde{d}(\hat{q}; 012i_3)] \prod_{i \neq 0, 1, 2, i_3} \hat{D}_i(\hat{q}) = R'(\hat{q}) \prod_{i \neq 0, 1, 2} \hat{D}_i(\hat{q}) = [c(012) + \tilde{c}(\hat{q}; 012)] \prod_{i \neq 0, 1, 2} \hat{D}_i(\hat{q}), \quad (225)$$

and one can extract $c(012)$ together with all the six coefficients $\tilde{c}_{ij}(012)$ of Eq. (221) by computing $R'(\hat{q})$ at seven different \hat{q} 's that fulfil Eq. (224). In fact, there is an infinite number of complex solutions of Eq. (224).

Once the coefficients of the 3-point contributions are known, those for the 2-point and subsequently for the 1-point functions can be determined in an analogous manner.

The determination of the coefficients was improved in Ref. [237] by making use of the polynomial structure of the integrand when evaluated at values of the loop momentum fulfilling multiple cut conditions. The coefficients can be efficiently extracted by means of a projection technique based on discrete Fourier transform. A further improvement was introduced in Ref. [238] exploiting the asymptotic behaviour of the integrand decomposition. It is based on the systematic application of a Laurent expansion to the integrand decomposition which is implemented through polynomial division.

(d) Rational terms

For the calculation of the rational terms one has to use Eq. (218) in D dimensions. The mismatch between the D -dimensional denominators and the 4-dimensional inverse propagators in Eq. (218) can be dealt with by using Eq. (200). The resulting terms depending on \check{q}^2 are the *rational terms of type R_1* defined as [197],

$$R_1 = \frac{1}{(2\pi)^D} \int d^D q \frac{f(\check{q}^2, \hat{q})}{D_0 D_1 \cdots D_{N-1}}, \quad (226)$$

where $f(\check{q}^2, \hat{q})$ is some polynomial in \check{q}^2 with $f(0, \hat{q}) = 0$. Rational terms of type R_1 arise from the $(D-4)$ -dimensional part of the denominators. They can be determined through a mass shift $m_i^2 \rightarrow m_i^2 - \check{q}^2$ (to be applied also for $m_i = 0$)

in all the coefficients of Eq. (218). This procedure is formally equivalent to the application of D -dimensional cuts in the generalized unitarity framework. In this way all coefficients of the OPP expansion start depending on \check{q}^2 . The coefficients of the various powers of \check{q}^2 , obtained through this mass shift, are the coefficients of the extra integrals introduced in Ref. [233]. In renormalizable theories the only possible contributions to those rational terms come from the extra scalar integrals

$$\begin{aligned} \int d^D q \frac{\check{q}^4}{D_i D_j D_k D_l} &= -\frac{i\pi^2}{6} + O(\epsilon), \\ \int d^D q \frac{\check{q}^2}{D_i D_j D_k} &= -\frac{i\pi^2}{2} + O(\epsilon), \\ \int d^D q \frac{\check{q}^2}{D_i D_j} &= -\frac{i\pi^2}{2} \left[m_i^2 + m_j^2 - \frac{(p_i - p_j)^2}{3} \right] + O(\epsilon). \end{aligned} \quad (227)$$

Despite the fact that these integrals involve powers of $(D - 4)$ -dimensional momenta in the numerator they give rise to finite contributions for $D \rightarrow 4$. The \check{q}^2 dependence of the 2- and 3-point coefficients can be written as

$$b(ij; \check{q}^2) = b(ij) + \check{q}^2 b^{(2)}(ij), \quad c(ijk; \check{q}^2) = c(ijk) + \check{q}^2 c^{(2)}(ijk). \quad (228)$$

The results for the contributions of the 4-point functions are slightly more complicated and involve $(\check{q}^2)^2$ terms [197, 239].

To determine the R_1 terms, i.e. the coefficients of the integrals (227), in practice in the OPP method, the fits of the coefficients are redone for different values of \check{q}^2 , once the 4-dimensional coefficients have been determined. An alternative approach to compute the R_1 terms [240] only requires the knowledge of the coefficients in Eq. (218) without the need to refit them at different values of \check{q}^2 . It is based on rewriting the denominators in Eq. (217) using

$$\frac{1}{D_i} = \frac{Z_i}{\hat{D}_i}, \quad Z_i = 1 - \frac{\check{q}^2}{D_i}. \quad (229)$$

While in this formulation more integrals than those in Eq. (227) contribute to the rational parts, these are all classified and calculated in Ref. [240]. When using tensor reduction techniques as described in Section 3.4.3, the rational terms of type R_1 are obtained directly by the D -dimensional tensor reduction without extra effort.

Rational terms of type R_1 arise only in the presence of $1/(D - 4)$ poles of UV origin and can be easily identified by means of simple power counting. The fact that rational terms of type R_1 of IR origin do not occur at the one-loop level follows from the observation that no such terms result from the Passarino–Veltman reduction of one-loop integrals [202].

The difference between Eq. (216) and Eq. (217) leads to the *rational terms of type R_2* . The D -dimensional numerator function $N(q)$ can be split into its 4-dimensional part $\hat{N}(\hat{q})$ plus a $(D - 4)$ -dimensional part

$$N(q) = \hat{N}(\hat{q}) + \check{N}(\check{q}^2, \hat{q}, \epsilon). \quad (230)$$

The R_2 terms induced by the $(D - 4)$ -dimensional part $\check{N}(\check{q}^2, \hat{q}, \epsilon)$ are given by [197]

$$R_2 = \frac{1}{(2\pi)^D} \int d^D q \frac{\check{N}(\check{q}^2, \hat{q}, \epsilon)}{D_0 D_1 \cdots D_{N-1}}. \quad (231)$$

As already pointed out in Section 3.4.3, only the rational terms of type R_2 of UV origin remain in unrenormalized scattering amplitudes, while R_2 terms of IR origin can only originate from wave-function renormalization constants [200, 201].

Based on this observation, it was shown in Ref. [197] that the rational terms of type R_2 can be obtained from a tree-level amplitude with a finite, universal set of theory-dependent Feynman rules, with at most quartic vertices in renormalizable theories. Besides these new Feynman rules, this approach does not introduce additional complications, and its computational complexity is negligible compared to the one for the 4-dimensional parts. Therefore, it is the most widely used method nowadays in integrand reduction and recursive loop calculation techniques. The Feynman

rules for the R_2 terms have been determined for QCD [241], for the EWSM [198, 199, 242], for a generic theory containing scalars, vectors, and fermions [243], as well as for specific BSM theories [244, 245].

While the calculation of rational terms via dedicated Feynman rules is widely employed, different methods for the calculation of the rational terms have been used in the QCD literature, in particular in the context of generalized unitarity methods. An early method [246] relies on OS recursion relations and a unitarity-factorization bootstrap [247]. An alternative is provided by D -dimensional unitarity methods [248–250]. Here the rational terms are determined in a similar manner as the 4-dimensional terms in the OPP formalism by evaluating the amplitude in different integer space–time dimensions such as $D = 6$ and $D = 8$. The calculations in additional dimensions can be avoided by using appropriate mass shifts and exchanging the D -dimensional cuts by 4-dimensional massive cuts [251].

(e) Libraries for OPP reduction

The OPP reduction algorithm has been implemented in different numerical codes. The original implementation by Ossola, Papadopoulos and Pittau is `CutTools` [239], which was subsequently improved by the libraries `SAMURAI` [252] and `NINJA` [253]. `SAMURAI` extends the OPP approach to accommodate an implementation of the generalized D -dimensional unitarity-cut technique and uses a polynomial interpolation exploiting the discrete Fourier transform [237]. `NINJA` implements an alternative reduction algorithm based on the systematic application of Laurent series expansion [238].

(f) Generalized unitarity methods

The OPP reduction technique is closely related to *generalized unitarity methods*. While unitarity can be verified by using ordinary cuts of Feynman diagrams, generalized unitarity is based on multiple cuts that do not necessarily correspond to physical intermediate particle states. These are defined by the requirement that a subset of loop denominators vanishes, i.e. that the corresponding momenta are on shell [for examples see Eqs. (222) and (224)]. In Ref. [254] it was shown that the coefficients of the master integrals in the OPP reduction can be expressed in terms of tree-level amplitudes with complex external momenta. The use of cut equations in D dimensions corresponds to the D -dimensional unitarity method [250]. While generalized unitarity methods have been applied in NLO calculations within QCD, they have not been generalized to the calculation of EW NLO corrections yet.

3.4.6. Scalar one-loop integrals

Apart from purely numerical approaches, all methods for the calculation of one-loop amplitudes eventually need results for the one-loop scalar integrals A_0 , B_0 , C_0 , and D_0 .

The classic paper with analytic expressions for general one-loop scalar 1-, 2-, 3-, and 4-point integrals is due to 't Hooft and Veltman [33]. For the regular 1-, 2-, 3-point integrals compact explicit expressions are given for arbitrary internal masses and arbitrary physical momenta. For the regular scalar 4-point function results in terms of 24 or 48 dilogarithms were presented for real internal masses. A compact expression with 16 dilogarithms for the general scalar 4-point function with real masses was provided in Ref. [255]. The general result for the regular box integral with real masses in D dimensions was calculated in Ref. [256].

In the EWSM and in particular in QCD, many particles are massless, so that soft and/or collinear singularities appear in the scalar integrals. Explicit results for soft-divergent scalar 3-point and 4-point integrals in MR were published in Ref. [257]. Results for scalar box integrals with vanishing internal masses were calculated in Refs. [258–260]. A compilation of mass-singular 3-point integrals in DR and MR can be found in the appendix of Ref. [177]. Finally, all scalar one-loop integrals required for calculations in QCD have been compiled in Ref. [261] (see also Ref. [179]).

For calculations with unstable particles loop integrals with complex masses are needed. For 1-, 2-, 3-point functions, the results of Ref. [33] can be directly used. This reference contains also a result for the regular 4-point function with complex masses in the physical region in terms of 108 dilogarithms. Based on this result, a code for the scalar 4-point function with complex masses was presented in Ref. [224]. More compact results for the 4-point function with complex masses, together with results for all IR-singular 4-point functions both in MR and in DR were worked out in Ref. [179].

A novel approach for the computation of one-loop scalar 3- and 4-point functions that proceeds in terms of quantities driving the algebraic reduction methods, like the Gram and Cayley determinants, was recently proposed in Refs. [262–264].

Various codes are available for the numerical evaluation of one-loop scalar integrals:

- **LoopTools** [221] is a package for the evaluation of scalar and tensor one-loop integrals based on the FF package by van Oldenborgh [222]. Like the FF package, LoopTools can handle one-loop integrals with complex masses up to 3-point functions. For the calculation of 4-point functions with complex masses the code of Ref. [224] has been integrated. UV singularities are regularized dimensionally, IR singularities are regularized either dimensionally or in MR.
- **GOLEM95C** [225–227] is a program for the numerical evaluation of scalar and tensor one-loop integrals which supports the use of complex masses.
- **ONELoop** [265] is a program to evaluate the one-loop scalar 1-point, 2-point, 3-point, and 4-point functions, for all kinematical configurations relevant for collider physics, and for complex internal squared masses based on the formulas of Ref. [224]. It deals with all UV and IR divergences within DR. Furthermore, it provides routines to evaluate these functions using straightforward numerical integration.
- **QCDLoop 2.0** [266], a C++ reimplementation and extension of the Fortran library QCDLoop [261], provides all finite and singular one-loop integrals in DR with at least one vanishing internal mass. It allows for complex masses based on a generalization of the results of Ref. [255] and offers the possibility to switch from double to quadruple precision on the fly.
- **COLLIER** [229] is a Fortran library for the numerical evaluation of one-loop scalar and tensor integrals appearing in perturbative relativistic quantum field theory. While UV singularities are treated in DR, soft and collinear singularities can be handled in both DR and MR. Complex masses are fully supported based on the results of Ref. [179] for the 4-point function and of Ref. [33] for lower-point functions.

3.4.7. Purely numerical methods

Besides the methods described above that rely on algebraic reduction (even if performed numerically) and numerical evaluation of scalar integrals there are alternative approaches that aim at calculating the loop integrals directly via numerical integration. While all these methods are presently of minor importance in actual one-loop calculations, they may turn out to be useful when generalized to higher orders. For an overview of the methods for the numerical evaluation of multi-loop integrals we refer to Ref. [267].

As far as the one-loop level is concerned, different numerical approaches exist. The method of Ref. [268] uses the Bernstein–Tkachov theorem [269, 270] together with a dedicated treatment of phase-space singularities to evaluate arbitrary one-loop Feynman-parameter integrals via numerical integration. This approach has been used to calculate the two-loop EW corrections to Higgs production in gluon fusion [271] and the Higgs decays to photons and gluons [272, 273].

Other numerical methods have so far only been used for QCD calculations so that we mention them only briefly. A general method using subtraction techniques for the numerical calculation of one-loop QCD matrix elements has been proposed in Ref. [274]. It consists in performing a simultaneous numerical integration over the phase space and the loop momentum of NLO amplitudes and has been further investigated by various groups. For details and references we refer to the contribution of Seth and Weinzierl in Ref. [76]. These methods have been proven to work for multi-jet production in e^+e^- annihilation [275–277]. A related approach is based on the *loop–tree duality* [278], which links loop graphs to tree graphs. The loop integrals are transformed into phase-space integrals and are evaluated numerically along with the phase-space integral over of the external partons of the process under consideration. Consequently, there is only one step of numerical integration involved in the computation of any particular integrated cross section or distribution. For more details and references we refer to Ref. [279] and the contribution of Chachamis et al. in Ref. [76].

3.5. Automation and tools

Compared to QCD, the Lagrangian of the EWSM involves many terms and gives rise to a large set of Feynman rules, rendering calculations of EW corrections more tedious. Therefore, already very early efforts towards the

automation of the calculation of EW corrections have been undertaken.²⁶ For the pioneering calculations of EW corrections to fermion-pair production [34, 280] and W-pair production [193] in e^+e^- annihilation and Higgs decays [147] the computer program SCHOONSCHIP [281] for the symbolic evaluation of algebraic expressions, originally developed by Veltman, was used. This code was later replaced by the still very popular symbolic manipulation system FORM by Vermaseren [282, 283].

(a) Traditional methods

The original strategy for the calculation of EW corrections has been to interfere the one-loop contributions to the matrix elements with the LO matrix element and to algebraically reduce the expressions to tensor integrals and coefficient functions or form factors (see Section 3.4.3). The tensor integrals are then numerically reduced with Passarino–Veltman reduction [34] to scalar integrals [33] which in turn are evaluated numerically based on explicit representations in form of logarithms and dilogarithms. For simple processes the reduction to scalar integrals can also be done algebraically. Computer algebra packages that have been developed along these lines are FEYNCALC [284, 285] and FORMCALC [221, 223]. Note, however, that these have been continuously improved over time to include state-of-the-art methods.

When considering processes with more external particles it has been realized that methods calculating the helicity amplitudes are more efficient than those calculating directly squared amplitudes, since the computational complexity scales only linearly with the number of Feynman diagrams instead of quadratically. While, on the one hand, methods for the analytic calculation of helicity amplitudes have been developed (cf. Refs. [47, 286] and references therein), on the other hand, tools for the direct numerical evaluation have become popular. One of these codes is HELAS [287], designed for the calculation of helicity amplitudes for arbitrary tree-level Feynman diagrams with sequences of calls of Fortran subroutines. HELAS can be used to recycle substructures of Feynman diagrams and is, thus, already much better than a naive diagram-by-diagram calculation. HELAS was combined with the MADGRAPH [288] Feynman-diagram generator to generate and calculate tree-level amplitudes in QCD, the EWSM, and beyond. Starting from MADGRAPH5 [68], the HELAS library was replaced by ALOHA [289], which automatically generates the HELAS library for any quantum field theory based on Feynman rules provided in the *Universal FeynRules Output (UFO)* format [290]. This procedure is, however, still based on Feynman diagrams so that the complexity increases factorially with increasing number of external particles.

(b) Feynman diagram generation

In the traditional methods, the calculation of matrix elements starts with the generation of Feynman diagrams. To this end, various programs are available, including:

- FEYNARTS 3 [291], an extension of FEYNARTS 1 [292], is a Mathematica package for the generation and visualization of Feynman diagrams and amplitudes. It generates diagrams at generic or specific levels for particle insertions, employs user-definable model files, supports supersymmetric models, and provides publication-quality Feynman diagrams in Postscript or LATEX.
- The Fortran program QGRAF [293] generates Feynman diagrams and represents them by symbolic expressions. A graphical representation can be obtained with the Feynman diagram analyzer DIANA [294], which also translates the output of QGRAF into a source code for analytical or numerical evaluations.

The Mathematica package FEYNRULES [295, 296] derives the Feynman rules for a particle physics model from a list of fields and parameters, and a corresponding Lagrangian. The output can be given in the *Universal FeynRules Output (UFO)* format [290], a generic form suitable for the translation to any Feynman diagram calculation program. Translation interfaces exist for CALCHEP/CompHEP [297], FEYNARTS [291], GoSAM [298, 299], MADGRAPH/MADEVENT [300], SHERPA [301], and WHIZARD [302–304]. A tool similar to FEYNRULES is the program LANHEP [305]. Starting from a Lagrangian it derives Feynman rules and writes them in terms of physical fields and independent parameters in the form of CompHEP [306] or CALCHEP [297] model files, or in the FEYNARTS [291] or UFO formats [290]. The program can also generate one-loop counterterms in the FEYNARTS format.

²⁶We do not restrict the term *automation* to the complete calculation of observables without user intervention, but use it also for generic tools that perform part of this task.

(c) Modern recursive methods

Berends and Giele [307] had shown that tree-level gluon amplitudes can be calculated via recursion relations with a computational complexity growing only exponentially. This recursive algorithm was generalized to calculate tree-level matrix elements in the complete SM in the codes ALPHA [308] and HELAC [309] based on Dyson–Schwinger equations [310–312].

The calculation of one-loop amplitudes, in particular in QCD, has been boosted with the advent of generalized unitarity techniques [254, 313–316] some ten years ago, which allow for expressing loop amplitudes in terms of (generalized) tree-level amplitudes. The related OPP method (cf. Section 3.4.5) has been more or less directly implemented in generic codes. In parallel, powerful automated tools have been developed based on improvements of traditional techniques. Van Hameren [317] proposed to generalize the recursive construction of tree-level amplitudes to the coefficient functions of tensor integrals in one-loop calculations.

Presently there is a variety of tools available for the automated calculation of NLO QCD corrections. For generic processes the following codes exist:

- In GoSAM [298, 299] the amplitudes are constructed from Feynman diagrams and evaluated using D -dimensional reduction at the integrand level, based on NINJA and SAMURAI, or alternatively with tensor reduction using the formalism described in Ref. [214], based on GOLEM95C.
- HELAC-1LOOP [318], which is part of the HELAC-NLO Monte Carlo framework [319], uses the OPP method [174, 197, 241] for the reduction of one-loop amplitudes at the integrand level, specifically the implementation CUTTOOLS [239].
- The OpenLoops generator [71] computes matrix elements by applying a numerical recursion analogous to the one of Ref. [317] to colour-stripped cut-opened loop diagrams. In OpenLoops1 [69] the reduction to scalar integrals is done at the integral or integrand level using external tools, while OpenLoops2 [71] implements the *on-the-fly reduction* technique of Ref. [235].
- The algorithm developed for OpenLoops1 is also adopted in the code MADGRAPH5_AMC@NLO [68].
- The matrix-element generator RECOLA [72, 73] generates arbitrary one-loop amplitudes based on an implementation of the recursive algorithm of Ref. [317] for amplitudes with colour structures.

Other codes are limited to specific process classes:

- The program BLACKHAT [320] implements the unitarity method and OS recursion to construct one-loop amplitudes in a numerical approach. As input, it uses compact analytic formulae for tree-level amplitudes for 4-dimensional helicity states. The program has been used to calculate NLO QCD corrections to vector-boson plus jets production with up to 5 jets [321, 322].
- NJET [323] is a library for multi-parton one-loop matrix elements in massless QCD. It is based on the generalized unitarity program NGLUON [324] and uses QCDDLoop [261] and FF [222] for evaluating scalar integrals. It was used to calculate the NLO QCD corrections to 5-jet production at the LHC [325].

(d) Automated tools for NLO EW corrections

The automation of the calculation of EW corrections is presently still ongoing. The methods are basically the same as for QCD corrections with some necessary modifications. The complexity increases due to the mixing of QCD and EW corrections, the increasing number of contributions, and the presence of more and very different mass scales. Additional complications arise from the chiral structure of the EW interactions and the instability of many SM particles. Since the SM particles decay via EW interactions, the instability can be counted as an NLO EW effect (cf. Section 6).

The following tools exist for the calculation of NLO EW corrections:

- FORMCALC [221, 223] is a Mathematica package for the calculation of tree-level and one-loop Feynman diagrams. It is based on the conventional approach and speeds up the calculation by the automatic isolation of subexpressions. FORMCALC has been used for a large number of applications within but notably also beyond the SM. The emphasis of FORMCALC is on flexibility and not so much on the calculation of high-multiplicity processes.
- GoSAM [298, 299] was extended to allow for the calculation of NLO EW corrections [326]. It is based on algebraic generation of D -dimensional integrals derived from Feynman diagrams generated with QGRAF [293] and FORM [283]. The amplitudes are evaluated using D -dimensional reduction at integrand level [174, 237, 316], which is available through two different reduction procedures and libraries, SAMURAI [252] and NINJA [253], and GOLEM95C

[225–227] is used as the default rescue system. GoSAM proceeds purely algebraically, grouping diagrams with identical loop topologies and performing colour projections at the symbolic level, and writing optimized numerical code with the help of FORM. While this purely analytical route for code generation is comparably slow, it offers great flexibility in the manipulation of the output. The scalar one-loop integrals can be evaluated using `OneLoop` [265], `Golem95C` [225, 226], or `QCDLoop` [261].

- `MADLoop` [68] has demonstrated that it can calculate the EW corrections to arbitrary $2 \rightarrow 2$ and $2 \rightarrow 3$ processes in the SM within the framework of `MADGRAPH5_AMC@NLO` [327, 328], but its technical capabilities are not restricted to those multiplicities. It is capable of calculating EW corrections also in models beyond the SM and is publicly available. More details on the `MADGRAPH5_AMC@NLO` implementation can be found in Section 3.5.4.
- `NLOX` [329] provides QCD and EW one-loop corrections to SM processes at the squared-amplitude level for all possible coupling-power combinations in the strong and EW couplings and for processes with up to six external particles. It is based on a Feynman-diagrammatic approach, utilizing `QGRAF`, `FORM`, and `PYTHON`, to algebraically generate C++ code for the Born and virtual contributions. The one-loop tensor coefficients are calculated recursively at run time through an integrated C++ library based on the tensor-reduction methods of Refs. [34, 202]. The scalar one-loop integrals are evaluated by either using `OneLoop` [265] or `QCDLoop` [261]. The code has been used to calculate one-loop corrections to selected processes such as QCD and EW corrections to $Z + b$ production [330].
- With `OPENLOOPS` [69], EW and QCD corrections have been calculated for vector-boson plus 1,2,3-jet production [70, 331], $pp \rightarrow e^+ \mu^- \nu_e \nu_{\bar{\mu}} / e^+ e^- \nu \bar{\nu} + X$ [332], and $pp \rightarrow \mu^+ \mu^- e^+ \nu_e jj + X$ [333]. Moreover, the NLO QCD and EW corrections to $pp \rightarrow Hll(j)/Hvl(j) + X$ [334] have been combined with QCD+QED parton shower via the `POWHEG BOX RES` framework [335], an extension of the `POWHEG BOX` [336], and the processes $pp \rightarrow tt + 0, 1$ jets have been studied with multi-jet merging at NLO QCD and EW [337]. `OPENLOOPS` process libraries for many processes are publicly available. More details on `OPENLOOPS` are given in Section 3.5.3.
- With the code `RECOLA` [72, 73] several cutting-edge calculations have been performed such as the EW corrections to the processes $pp \rightarrow e^+ \nu_e \mu^- \bar{\nu}_\mu b \bar{b} + X$ [338], $pp \rightarrow e^+ \nu_e \mu^- \bar{\nu}_\mu b \bar{b} H + X$ [339], $pp \rightarrow \mu^\pm \nu_\mu e^\pm \nu_e jj + X$ [340–342], $pp \rightarrow \mu^+ \mu^- e^+ \nu_e jj + X$ [333], and $pp \rightarrow l_1^- \bar{\nu}_{l_1} l_2^- \bar{\nu}_{l_2} l_3^+ \nu_{l_3} + X$ [343]. `RECOLA` is fully public and allows for the calculation of EW corrections also in models beyond the SM for which `RECOLA` model files are available [116, 170]. More details on `RECOLA` are provided in Section 3.5.2.

A performance comparison of the different one-loop providers was presented in Ref. [344].

After a sketch of the conventional approach for the calculation of one-loop matrix elements, in the following we give some more details on the implementation of the general one-loop matrix element providers `RECOLA`, `OPENLOOPS`, and `MADGRAPH5_AMC@NLO`, using widely the notation of the original literature. We note that many NLO EW calculations, such as the first (EW) NLO calculation for a $2 \rightarrow 4$ process, $e^+ e^- \rightarrow 4$ fermions [59, 196], have been carried out with non-public semi-automated tools.

3.5.1. Conventional approach

We begin by describing the conventional technique for the calculation of one-loop matrix elements. More details for processes without coloured particles can be found in Ref. [40]; for a more detailed discussion of the treatment of colour we refer to Refs. [345, 346]. Upon inserting the Lorentz decompositions (181) of the one-loop tensor integrals, an arbitrary one-loop matrix element with E external particles with momenta p_i and polarizations λ_i , $i = 1, \dots, E$, Eq. (177) can be written as

$$\delta \mathcal{M}_{\lambda_1 \dots \lambda_E}(\{p_k\}) = \sum_a C_a \delta \mathcal{A}_{a, \lambda_1 \dots \lambda_E}(\{p_k\}) = \sum_i \sum_a C_a \mathcal{A}_{i, \lambda_1 \dots \lambda_E}(\{p_k\}) F_{i,a}(\{p_k p_i\}), \quad (232)$$

where $\delta \mathcal{A}_a$ are colour-stripped amplitudes and the colour structures C_a form a basis in colour space for the process under consideration (colour indices are suppressed). The *standard matrix elements* \mathcal{A}_i carry the dependence on polarizations of the external particles. They are simple, purely kinematical, model-independent functions of the external momenta. The Lorentz-invariant form factors $F_{i,a}$, on the other hand, are independent of the polarizations and depend only on scalar products of external momenta. They are linear functions of the scalar coefficients of the tensor integrals T^N and the counterterms and contain all dynamical information. The tree-level amplitude $\mathcal{M}_{0, \lambda_1 \dots \lambda_E}(\{p_k\})$ has

the same structure as Eq. (232), however, with typically fewer non-vanishing and much simpler form factors without integrals,

$$\mathcal{M}_{0,\lambda_1 \dots \lambda_E}(\{p_k\}) = \sum_a C_a \mathcal{A}_{0,a,\lambda_1 \dots \lambda_E}(\{p_k\}) = \sum_i \sum_a C_a \mathcal{A}_{i,\lambda_1 \dots \lambda_E}(\{p_k\}) F_{0,i,a}(\{p_k p_l\}). \quad (233)$$

The LO scattering probability density \mathcal{W}_0 and the corresponding virtual one-loop correction $\delta\mathcal{W}$ are obtained after summing/averaging over polarizations and colours,

$$\begin{aligned} \mathcal{W}_0 &= \frac{1}{N_{s,c}} \sum_{\text{pol,col}} |\mathcal{M}_0^2| = \overline{\sum_{\text{pol,col}} |\mathcal{M}_0^2|} = \overline{\sum_{\text{pol}} \sum_{a,b} \mathcal{A}_{0,a}^* \mathcal{A}_{0,b} \sum_{\text{col}} C_a^* C_b}, \\ \delta\mathcal{W} &= \frac{1}{N_{s,c}} \sum_{\text{pol,col}} 2 \operatorname{Re} [\mathcal{M}_0^* \delta\mathcal{M}] = \overline{\sum_{\text{pol,col}} 2 \operatorname{Re} [\mathcal{M}_0^* \delta\mathcal{M}]} = \overline{\sum_{\text{pol}} \sum_{a,b} 2 \operatorname{Re} [\mathcal{A}_{0,a}^* \delta\mathcal{A}_b]} \overline{\sum_{\text{col}} C_a^* C_b}, \end{aligned} \quad (234)$$

where $N_{s,c}$ is the number of combinations of colour and spin degrees of freedom in the initial state. The corresponding average is denoted by a bar over the summation symbol. The sum over external colours can be carried out once and for all at the level of the colour basis,

$$\mathcal{K}_{ab} = \overline{\sum_{\text{col}} C_a^* C_b}. \quad (235)$$

The representation (232) allows us to write the one-loop correction to the scattering probability in the form

$$\delta\mathcal{W} = 2 \operatorname{Re} \sum_{i,b} \left(\overline{\sum_{\text{pol}} \sum_a \mathcal{K}_{ab} \mathcal{A}_{0,a}^* \mathcal{A}_i} \right) F_{i,b}, \quad (236)$$

i.e. the one-loop contribution is a linear function of the loop integrals. The colour–Born interference terms $\overline{\sum_{\text{pol}} \sum_a \mathcal{K}_{ab} \mathcal{A}_{0,a}^* \mathcal{A}_i}$ can be precomputed without knowledge of the one-loop contributions. For the calculation of the polarization sum only the basis of standard matrix elements has to be known. Thus, for the calculation of polarization-summed squared matrix elements the expensive evaluation of the form factors $F_{i,b}$ has to be performed only once per phase-space point, while the polarization and colour sums inside the brackets of Eq. (236) can be performed independently before the actual evaluation of the loop integrals.

Individual Feynman diagrams d that do not involve quartic gluon couplings consist of a single colour-stripped amplitude $\mathcal{A}_a^{(d)}$ multiplied by a single colour factor $C_a^{(d)}$, i.e. the colour structure factorizes. Diagrams with quartic gluon couplings can be decomposed in subamplitudes with factorizing colour part. Therefore, in a diagram-by-diagram approach [345, 346], also the sum over b in Eq. (236) is absent in the contributions of (sub)diagrams, rendering the colour treatment even more efficient. Writing the contribution of d to the form factor as $F_{i,b}^{(d)} = C_b^{(d)} f_i^{(d)}$ and likewise the contribution of some Born diagram d_0 to the LO form factor as $F_{0,i,b}^{(d_0)} = C_{0,b}^{(d_0)} f_{0,i}^{(d_0)}$, the contribution of d to the probability $\delta\mathcal{W}$ can be arranged as follows,

$$\delta\mathcal{W}^{(d)} = 2 \operatorname{Re} \sum_i f_i^{(d)} \sum_{d_0} \left(\sum_{a,b} (C_{0,a}^{(d_0)})^* \mathcal{K}_{ab} C_b^{(d)} \right) \left[\sum_j \overline{\sum_{\text{pol}} (f_{0,j}^{(d_0)})^* \mathcal{A}_j^* \mathcal{A}_i} \right]. \quad (237)$$

The colour sum within round brackets neither depends on phase space, nor on polarizations, nor on the basis of standard matrix elements (indices i, j), so that this sum can be precomputed even before generating phase-space points. The sum over j and polarizations neither depends on colour, nor on the specific (sub)diagram d and can, thus, be precomputed after phase-space generation before summing over the (sub)diagrams d . These optimizations speed up the numerical evaluation considerably, since only one set of CPU-expensive form factors $f_i^{(d)}$ has to be calculated for all colour and polarization structures, which are in this sense treated simultaneously.

The form factors $F_{i,b}$ or $f_i^{(d)}$ are reduced to scalar one-loop integrals either algebraically or numerically. In the traditional methods, $\delta\mathcal{M}$ is derived from Feynman diagrams, and the resulting expression is simplified algebraically. Finally, the so-obtained algebraic expressions are evaluated numerically.

For loop-induced processes, i.e. those with vanishing \mathcal{M}_0 , the scattering probability density is obtained as

$$\mathcal{W} = \frac{1}{N_{s,c}} \sum_{\text{pol,col}} |\delta\mathcal{M}|^2 = \overline{\sum_{\text{pol,col}} |\delta\mathcal{M}|^2}. \quad (238)$$

This quantity depends quadratically on the loop amplitude, implying that optimizations somewhat different from those of Eq. (237) may be required. Notably, tensor-integral reduction is superior to the OPP method in this case (see Section 3.5.4).

3.5.2. RECOLA

Modern methods for the evaluation of one-loop corrections use recursive techniques. These are consistently applied in RECOLA [72, 73]. In order to explain the underlying algorithm, we start with the recursive construction of tree-level amplitudes [72]. The basic building block is the *tree-level off-shell current*,

which is the sum of all Feynman diagrams with an external off-shell leg P and n external OS legs with corresponding wave functions. The dot indicates the off-shell part of the current, and the corresponding leg includes the propagator for the particle P for $n \geq 2$. For $n = 1$, the off-shell current coincides with the wave function (spinor or polarization vector) of the particle P . The multi-index β represents the Lorentz index for a vector and the spinor index for a spinor as well as possible colour indices.

In a theory with tri- and quadri-linear couplings only, like renormalizable quantum field theories, the off-shell currents can be constructed using the Dyson–Schwinger equations [310–312] recursively,

Each term in the sums on the r.h.s. is obtained by multiplication of the generating currents $w_\gamma(P_i, \{i\})$, $w_\delta(P_j, \{j\})$ [and $w_\alpha(P_k, \{k\})$] with the interaction vertex, indicated by the small box, and the propagator of P , marked by the thick line. The sums run over all partitions of the set of n external particles into subsets $\{i\}$, $\{j\}$ [and $\{k\}$] with $i + j (+ k) = n$. More explicitly, for the terms involving triple vertices this amounts to

$$w_\beta(P, \{n\}) \Big|_{\text{triple vertex}} = \sum_{\substack{\{i\}, \{j\} \\ i+j=n}} \sum_{P_i, P_j} w_\gamma(P_i, \{i\}) w_\delta(P_j, \{j\}) \mathcal{P}_{\beta\alpha}^P(p_P, m_P) \mathcal{V}_{PP_i P_j}^{\alpha\gamma\delta}(p_P, p_i, p_j), \quad (241)$$

where $\mathcal{V}_{P_i P_j}^{\alpha\gamma\delta}(p_P, p_i, p_j)$ describes the vertex connecting the lines P, P_i, P_j with momenta p_P, p_i, p_j , and $\mathcal{P}^P(p_P, m_P)$ is the propagator of the particle P . Since all quantities depend only on the momenta, colours, and helicities of the external particles, the recursion can be implemented as simple matrix multiplication on numerical matrices. Working with off-shell currents rather than Feynman diagrams allows one to avoid recomputing identical subgraphs contributing to different diagrams. The generalization to theories with elementary couplings of more than four fields is straightforward. The recursive evaluation of the currents begins with the external currents ($n = 1$), which, for colourless particles of a given polarization λ and momentum p , are given by the corresponding wave functions:

$$\lambda \xrightarrow[p]{\text{--}} \bullet = u_\lambda(p), \quad \lambda \xrightarrow[p]{\text{--}} \bullet = \bar{v}_\lambda(p), \quad \lambda \xrightarrow[p]{\text{--}} \bullet = \varepsilon_\lambda(p), \quad \xrightarrow[p]{\text{--}} \bullet = 1. \quad (242)$$

For coloured external particles the colour indices have to be added.

Finally, the S -matrix element with $n+1$ external particles is obtained by multiplying the off-shell current $w_\beta(P, \{n\})$ with the inverse propagator and the appropriate wave function of particle P ,

$$\mathcal{M} = n \begin{array}{c} \text{---} \\ \text{---} \\ \text{---} \end{array} \times \left(\begin{array}{c} \text{---} \\ \text{---} \\ \text{---} \end{array} \right)^{-1}_{\beta\gamma} \times \begin{array}{c} \text{---} \\ \text{---} \\ \text{---} \end{array} \times \begin{array}{c} \text{---} \\ \text{---} \\ \text{---} \end{array} \quad (243)$$

In the code, the truncation of the external line is performed by discarding the propagator of the $(n + 1)$ th external line, since the propagator for an external OS line does not exist. To construct S -matrix elements for physical processes, incoming and outgoing particles can be interchanged upon using crossing symmetry.

Following an idea of van Hameren [317] the recursive calculation of tree amplitudes can be generalized to the calculation of the coefficients $\hat{c}_{\mu_1 \dots \mu_{r_j}}^{(j, r_j, N_j)}$ of the tensor integrals in Eq. (178) at one loop. Since the numerical calculation proceeds in four dimensions, the rational terms of type R_2 [197] have to be supplemented. While the integration momenta in the numerator of the loop integrals are 4-dimensional, those in the propagator denominators are D -dimensional. As in Section 3.4.5 we indicate 4-dimensional loop momenta with carets. Upon cutting one of the *loop lines*, each loop diagram with E external lines can be mapped to a tree-level diagram with $E + 2$ external legs. The correspondence between loop and tree-level diagrams can be made unique via defining precisely which loop line has to be cut [72]. For the resulting tree-level amplitudes with two external loop lines a recursion relation similar to Eq. (240) can be formulated. One of the loop lines is identified with the off-shell line P , the second loop line is part of the OS lines n but marked as a loop line. The basic building blocks involving a loop line are called *loop off-shell currents*. In contrast to the tree-level off-shell currents they are not pure numerical spinors or vectors but depend on the integration momentum and on the momenta and masses of the propagators that enter their construction. In the 't Hooft–Feynman gauge the product of the vertex and the propagator in the generalization of Eq. (241) has the following dependence on the integration momentum q :

$$\mathcal{P}_{\beta\alpha}^P(q, \hat{q}, p_P, m_P) \mathcal{V}_{PP_iP_j}^{\alpha\gamma\delta}(\hat{q}, p_P, p_i, p_j) = \frac{a_{\beta\mu}^{\gamma\delta}(p_i, p_j)\hat{q}^\mu + b_{\beta}^{\gamma\delta}(p_i, p_j)}{(q + p_P)^2 - m_P^2}. \quad (244)$$

After l recursion steps, the loop off-shell current takes the form

$$w_{\beta}^{(l)}(P, \{n\}, q, \hat{q}, \{p_h\}, \{m_h\}) = \sum_{k=0}^l \frac{d_{\beta, \mu_1 \dots \mu_k}^{(k, l)}(P, \{n\}, \{p_h\}, \{m_h\})\hat{q}^{\mu_1} \dots \hat{q}^{\mu_k}}{\prod_{h=1}^l [(q + p_h)^2 - m_h^2]}. \quad (245)$$

A generalization of the algorithm to arbitrary gauges or non-renormalizable theories is straightforward and amounts to including terms with higher powers of integration momenta in Eqs. (244) and (245).

While the loop off-shell currents obey a recursion relation like Eq. (240), this cannot be used straightforwardly to compute them numerically since they depend on the loop momentum. However, the recursion relation can be turned into a recursion relation for the coefficients $d_{\beta, \mu_1 \dots \mu_k}^{(k, l)}$, which can be evaluated numerically. At the end of the recursion, the coefficients $d_{\beta, \mu_1 \dots \mu_k}^{(k, l)}$ determine the tensor coefficients $\hat{c}_{\mu_1 \dots \mu_{r_j}}^{(j, r_j, N_j)}$ in Eq. (178), where each set $\{p_h, m_h\}$ corresponds to an index j . The loops are closed by forming traces of the free spinor or Lorentz indices of the two corresponding loop lines.

In RECOLA, the colour matrices are included in the recursive numerical treatment, i.e. RECOLA directly calculates coloured amplitudes. In order to optimize the colour treatment, RECOLA uses the colour-flow representation [347–349], where the conventional 8 gluon fields G_μ^A are replaced by a traceless 3×3 matrix $(\mathcal{G}_\mu)_j^i = \frac{1}{\sqrt{2}} G_\mu^A (\lambda^A)_j^i$. Quarks and antiquarks carry the usual colour index $i = 1, 2, 3$, while gluons get a pair of indices $i, j = 1, 2, 3$. The Gell-Mann matrices λ^A and the structure constants in the Feynman rules are thus substituted by combinations of Kronecker deltas. Moreover, instead of colour-dressed amplitudes, RECOLA introduces *structure-dressed* amplitudes, where each current gets an explicit *colour structure* corresponding to a product of Kronecker deltas in colour indices (for more details see Ref. [72]). In the code, the colour structures are represented by integer numbers in a binary notation. Basing the reduction on these colour structures instead of using directly colour-dressed amplitudes reduces the number of currents and renders the recursive construction more efficient.

Rational terms and counterterms are included via additional tree-level Feynman rules [197, 199, 241, 242]. For the calculation of the tensor integrals RECOLA uses the *COLLIER* library [229]. No other external libraries are required.

RECOLA calculates loop-induced processes based on the same recursive algorithm for the one-loop matrix elements [73].

The enhanced version RECOLA2 [350] allows for the calculation of EW corrections in models beyond the SM for which RECOLA model files are available [116, 170]. Such model files, which include counterterms and rational terms, can be generated in a semi-automatic way using the tool *REPT1L* [351].

3.5.3. OPENLOOPS

In OPENLOOPS [69] one-loop amplitudes are generated via a numerical algorithm for the recursive construction of Feynman diagrams. Colour sums are performed by exploiting the factorization of individual (sub)diagrams d into colour factors and colour-stripped amplitudes discussed at the end of Section 3.5.1,

$$\mathcal{M}^{(d)} = C^{(d)} \mathcal{A}^{(d)}. \quad (246)$$

The algebraic reduction of the colour factors to a standard basis $\{C_a\}$ permits one to encode all colour sums in the matrix $\mathcal{K}_{ab} = \sum_{\text{col}} C_a^* C_b$, which needs to be computed only once per process. Tree amplitudes in OpenLoops are computed through a numerical recursion of Dyson–Schwinger type [see Eq. (241)] for individual colour-stripped tree diagrams. In contrast to RECOLA, instead of off-shell currents, individual topologies are constructed.

In OPENLOOPS the construction of one-loop diagrams proceeds as follows: A colour-stripped N -point one-loop diagram is an ordered set $\mathcal{I}_N = \{i_1, \dots, i_N\}$ of N subtrees i_n , called segments, connected by loop propagators:

$$\delta \mathcal{A}^{(d)} = \int d^D q \frac{\mathcal{N}(\mathcal{I}_N; \hat{q})}{D_0 D_1 \dots D_{N-1}} = \begin{array}{c} \text{Diagram: } \text{A central circle labeled } 0 \text{ with vertices labeled } 1, n-1, n, \text{ and } n-1. \text{ External circles labeled } i_1, i_2, \dots, i_n \text{ are connected to these vertices.} \\ \text{Equation: } \delta \mathcal{A}^{(d)} = \int d^D q \frac{\mathcal{N}(\mathcal{I}_N; \hat{q})}{D_0 D_1 \dots D_{N-1}} \end{array} \quad (247)$$

The ordered set $\{i_1, \dots, i_N\}$ defines the topology of this particular Feynman diagram. The denominators D_i are the ones of Eq. (180). All other contributions from loop propagators, vertices, and external subtrees are summarized in the numerator, which (in the 't Hooft–Feynman gauge) is a polynomial of degree $R \leq N$ in the 4-dimensional part \hat{q} of the loop momentum,

$$\mathcal{N}(\mathcal{I}_N; \hat{q}) = \sum_{r=0}^R \mathcal{N}_{\mu_1 \dots \mu_r}(\mathcal{I}_N) \hat{q}^{\mu_1} \dots \hat{q}^{\mu_r}. \quad (248)$$

Ambiguities related to possible shifts in the loop momentum are eliminated by setting $p_0 = 0$, singling out the D_0 propagator. Cutting the loop at this propagator and removing the denominators results in the *open loop*

$$\mathcal{N}_\alpha^\beta(\mathcal{I}_N; \hat{q}) = \sum_{r=0}^R \mathcal{N}_{\mu_1 \dots \mu_r; \alpha}^\beta(\mathcal{I}_N) \hat{q}^{\mu_1} \dots \hat{q}^{\mu_r}, \quad (249)$$

where the indices α, β belong to the ends of the cut line. The original polynomial (248) is obtained upon taking the trace with respect to α, β . Open loops are constructed with an algorithm similar to the numerical recursion of Ref. [317]. While the one-loop off-shell currents as used in RECOLA correspond to complete amplitudes, the open loops correspond to colour-stripped Feynman diagrams. The efficiency of the open-loop recursion is increased by using parts of pre-computed open loops for the construction of more involved open loops, whenever the same open loop occurs in more than one diagram. Finally, the contribution of a one-loop diagram to the unpolarized transition probability results in a linear combination

$$\delta \mathcal{W}^{(d)} = \text{Re} \left[\sum_{r=0}^R \delta \mathcal{W}_{\mu_1 \dots \mu_r}^{(d)} T^{N, \mu_1 \dots \mu_r} \right] \quad (250)$$

with the helicity and colour-summed coefficients

$$\delta \mathcal{W}_{\mu_1 \dots \mu_r}^{(d)} = 2 \sum_{\text{hel}} \left(\sum_{\text{col}} \mathcal{M}_0^* C^{(d)} \right) \mathcal{N}_{\mu_1 \dots \mu_r}(\mathcal{I}_N). \quad (251)$$

The open-loop algorithm can be interfaced to both OPP and tensor-integral reduction. For tensor-integral reduction the COLIER [229] library is used, while OPP reduction is performed with CUTTOOLS [239]. The R_2 rational terms are restored via process-independent counterterms [241].

More recently, **OPENLOOPS** 2 was introduced [71, 235]. It implements a new method, dubbed *on-the-fly reduction*, which unifies the construction of loop amplitudes and their reduction in a single recursive algorithm. This is achieved by factorizing the loop amplitude into segments and interleaving segment multiplications with reduction operations at the integrand level. The latter are based on the algorithm by del Aguila and Pittau [233] described in Section 3.4.4. Using this method, objects with tensor rank higher than two are avoided throughout the calculation. While the complexity due to the tensor rank is kept low, the creation of pinched topologies potentially leads to a huge proliferation of open loops to be processed. This problem is solved by on-the-fly merging of pinched open loops with open loops of the same topology and the same undressed segments. Here, a segment S_i consists of a subtree that involves a certain set of external particles connected to the i th loop vertex and the adjacent loop propagator D_i . An undressed segment refers to a segment that has not yet been used in the calculation of the numerator. The final rank-0 and rank-1 tensor integrals are reduced to scalar integrals with $N \leq 4$ using OPP reduction for $N \geq 5$, integrand-level identities for $N = 4$, and Passarino–Veltman reduction for $N \leq 3$ [233, 235].

Exploiting the factorized structure of open loops in a systematic way, besides tensor reduction also helicity summation and diagram merging are performed on the fly during open-loop recursion. This approach reduces the complexity of intermediate results and leads to improvements in CPU efficiency. Numerical instabilities can be avoided by isolating them in triangle topologies, expressing the tensor integrals in terms of scalar integrals and expanding the scalar integrals in the limit of small Gram determinants, similar to the expansions described in App. B of Ref. [202]. The algorithm is implemented in double and quadruple precision. Moreover, it is equipped with a hybrid precision system that avoids residual instabilities in a CPU-efficient way by restricting the usage of quadruple precision to specific reduction steps.

3.5.4. MADGRAPH

The construction of tree-level amplitudes in **MADGRAPH5_AMC@NLO** [68] is based on Feynman diagrams, helicity amplitudes, and colour decomposition. Employing colour decompositions [349], the colour matrix appearing in the squared amplitude is computed automatically once and for all and then stored in memory, similarly as in **OPENLOOPS**. **MADGRAPH5_AMC@NLO** has its own diagram-generation algorithm **MADGRAPH5** [300] that needs as an input the Feynman rules corresponding to the Lagrangian of a given theory. The information on the Feynman rules is typically provided by **FEYNRULES** [295] in the **UFO** format [290]. With the information from **UFO**, the dedicated routines that actually perform the computation of the elementary blocks that enter helicity amplitudes are built by a modified version of **ALOHA** [289].

Loop amplitudes are calculated with the module **MADLOOP5** [352]. It is based on an independent implementation of the recursive procedure used in **OPENLOOPS**. Like **OPENLOOPS**, **MADLOOP5** is based on subamplitudes $\mathcal{A}_{0,h,b}$ with definite helicities that possess a single colour factor C_b , so that the full tree-level amplitude $\mathcal{M}_{0,h}$ can be written as

$$\mathcal{M}_{0,h}(\{p_k\}) = \sum_b C_b \mathcal{A}_{0,h,b}, \quad (252)$$

where the index $h = \{\lambda_k\}$ indicates the dependence on helicities. The contributions to the subamplitudes $\mathcal{A}_{0,h,b}$ are in one-to-one correspondence with the amplitudes of the constituting Feynman diagrams, except for those involving vertices featuring multiple colour factors (such as 4-gluon vertices); in this case individual diagrams contribute to several $\mathcal{A}_{0,h,b}$. The one-loop amplitude is decomposed in the same way and can be written as

$$\delta \mathcal{M}_h = \sum_t \sum_{l \in t} C_l \int d^D q \frac{\mathcal{N}_{h,l}^{(t)}(\hat{q})}{D_0^{(t)} D_1^{(t)} \dots D_{N_t-1}^{(t)}}. \quad (253)$$

The expression is organized as a sum over sets of *topologies* t that are characterized by a specific product $D_0^{(t)} \dots D_{N_t-1}^{(t)}$ of propagator denominators.

The one-loop contribution to the unpolarized transition probability can be written as

$$\delta \mathcal{W} = \sum_t \int d^D q \frac{1}{D_0^{(t)} \dots D_{N_t-1}^{(t)}} \overline{\sum_h} \sum_{l \in t} \sum_b \sum_{\text{col}} (C_b^* C_l) \mathcal{A}_{0,h,b}^* \mathcal{N}_{h,l}^{(t)}(\hat{q}) \quad (254)$$

with

$$\mathcal{N}_{h,l}^{(t)}(\hat{q}) = \sum_{r=0}^{r_t} \hat{c}_{h,l;\mu_1 \dots \mu_r}^{(t,r,N_t)} \hat{q}^{\mu_1} \dots \hat{q}^{\mu_r}. \quad (255)$$

Equation (254) like Eq. (237) is optimized to reduce the number of evaluations of loop integrals. As in **OPENLOOPS**, the representation (254) can be used both for OPP reduction and for tensor-integral reduction. For OPP, after determination of the coefficients $\hat{c}_{h,l;\mu_1 \dots \mu_r}^{(t,r,N_t)}$ the calculation of the numerators can be performed upon using Eq. (255). When inserting Eq. (255) into Eq. (254) the tensor integrals emerge. In fact, **MADLOOP5** supports the possibility to switch between the OPP and tensor-integral reduction methods. To this end, it uses **NINJA** [253], **SAMURAI** [252], and **CUTTOOLS** [239] or the internal tensor-integral library **IREGI**, **PJFRY** [219], **GOLEM95C** [226], and **COLLIER** [228, 229], respectively. **MADLOOP5** dynamically switches between different integral reduction codes based on user-defined preferences and allows for dynamic switching between double and quadruple precision. This ensures a robust stability rescue mechanism as well as a reliable measure of the numerical uncertainty of the result.

As in **RECOLA** and **OPENLOOPS**, the counterterms and rational terms of type R_2 have to be added to the result of the loop-integration procedure. Both are cast into the form of a tree-level-like amplitude times the Born amplitude. The Feynman rules for the counterterms and rational terms of type R_2 have to be provided as a set of instructions in the **UFO** file. The implementation of such Feynman rules is automated in **FEYNRULES** via **NLOCT** [353] and similarly in **RECOLA2** [350] via **REPT1L** [351].

MADGRAPH5_AMC@NLO also offers an automated implementation of cross-section computation and event generation for loop-induced processes [354]. The unpolarized transition probability reads in this case

$$\mathcal{W} = \overline{\sum_h \sum_{l_1} \sum_{l_2} \left[\int d^D q \frac{1}{D_0^{(l_1)} \dots D_{N_{l_1}-1}^{(l_1)}} \mathcal{N}_{h,l_1}(\hat{q}) \right]^* \left[\int d^D q \frac{1}{D_0^{(l_2)} \dots D_{N_{l_2}-1}^{(l_2)}} \mathcal{N}_{h,l_2}(\hat{q}) \right] \sum_{\text{col}} (C_{l_1}^* C_{l_2})}. \quad (256)$$

The sums over l_1 and l_2 run over the subamplitudes corresponding to single colour factors each. The quadratic scaling with the number of diagrams is problematic for more complicated processes. To circumvent this problem, the colour factors C_i are projected into the colour-flow basis [349]. The corresponding number of basis vectors grows only power-like, reducing the computational cost considerably. This is similar to the approach in **OPENLOOPS** and the use of colour structures in **RECOLA**. The inability to perform integrand reduction at the squared-matrix-element level leads to a crucial difference between tensor-integral reduction and the OPP reduction methods. While the OPP reduction operates on the helicity-dependent numerators (255), the tensor integral reduction is based on helicity-independent tensor integrals. Consequently, the number of independent OPP reductions for a kinematic configuration is necessarily $L \times H \times C$, where L is the number of independent loop integrals, H the number of helicities, and C the number of independent colour configurations. On the other hand, the number of independent tensor-integral reductions per phase-space point is only L .

In Ref. [328] the EW corrections are quoted for the integrated cross sections with minimal selection cuts for many $2 \rightarrow 2$ and $2 \rightarrow 3$ processes at the 13 TeV LHC. The results, which are reproduced in Table 3, demonstrate, on the one hand, the power of the automated tools, on the other hand, they illustrate the spectrum of the size of the EW corrections (in the G_μ scheme) for inclusive cross sections at the LHC. The EW corrections tend to increase with the number of final-state particles and are larger for bosons in the final state than for fermions. Owing to the virtual contributions the EW corrections are mostly negative. While they are below 5% in size for the majority of processes, there are some notable exceptions. The positive corrections, for instance for $pp \rightarrow e^+ \nu_e \mu^- \bar{\nu}_\mu + X$ (see also Refs. [355–357]), $pp \rightarrow W^+ W^- W^+ + X$ (see also Refs. [343, 358–360]), or $pp \rightarrow H Z W^+ + X$ result from contributions of photon-quark-induced processes that are enhanced by the presence of the AW^+W^- coupling and by quasi-soft-collinear W -boson emission from photons. It should, however, be realized that photon-quark-induced contributions imply an additional jet in the final state, so that their impact is often shadowed by QCD corrections and drastically reduced if jet vetoes are applied. For some processes for charged-particle production via neutral initial states, such as WW production, even partonic $\gamma\gamma$ channels can produce significant positive contributions. Typically, they appear at high partonic scattering energies, but in some cases they can even lead to significant corrections to integrated cross sections, as observed for $pp \rightarrow W^+ W^- Z + X$ [361] (not included in Table 3). For a further discussion of possible patterns in EW corrections we refer to dedicated articles on specific processes and to Ref. [328]. Note that the size of

Final state F	$\sigma_{\text{LO}} [\text{pb}]$	$\sigma_{\text{NLO EW}} [\text{pb}]$	$\delta_{\text{EW}} [\%]$
$e^+ \nu_e$	$5.2498 \pm 0.0005 \cdot 10^3$	$5.2113 \pm 0.0006 \cdot 10^3$	-0.73 ± 0.01
$e^+ \nu_e j$	$9.1468 \pm 0.0012 \cdot 10^2$	$9.0449 \pm 0.0014 \cdot 10^2$	-1.11 ± 0.02
$e^+ \nu_e jj$	$3.1562 \pm 0.0003 \cdot 10^2$	$3.0985 \pm 0.0005 \cdot 10^2$	-1.83 ± 0.02
$e^+ e^-$	$7.5367 \pm 0.0008 \cdot 10^2$	$7.4997 \pm 0.0010 \cdot 10^2$	-0.49 ± 0.02
$e^+ e^- j$	$1.5059 \pm 0.0001 \cdot 10^2$	$1.4909 \pm 0.0002 \cdot 10^2$	-1.00 ± 0.02
$e^+ e^- jj$	$5.1424 \pm 0.0004 \cdot 10^1$	$5.0410 \pm 0.0007 \cdot 10^1$	-1.97 ± 0.02
$e^+ e^- \mu^+ \mu^-$	$1.2750 \pm 0.0000 \cdot 10^{-2}$	$1.2083 \pm 0.0001 \cdot 10^{-2}$	-5.23 ± 0.01
$e^+ \nu_e \mu^- \bar{\nu}_\mu$	$5.1144 \pm 0.0007 \cdot 10^{-1}$	$5.3019 \pm 0.0009 \cdot 10^{-1}$	$+3.67 \pm 0.02$
$\text{He}^+ \nu_e$	$6.7643 \pm 0.0001 \cdot 10^{-2}$	$6.4914 \pm 0.0012 \cdot 10^{-2}$	-4.03 ± 0.02
$\text{He}^+ e^-$	$1.4554 \pm 0.0001 \cdot 10^{-2}$	$1.3700 \pm 0.0002 \cdot 10^{-2}$	-5.87 ± 0.02
Hjj	$2.8268 \pm 0.0002 \cdot 10^0$	$2.7075 \pm 0.0003 \cdot 10^0$	-4.22 ± 0.01
$W^+ W^- W^+$	$8.2874 \pm 0.0004 \cdot 10^{-2}$	$8.8017 \pm 0.0012 \cdot 10^{-2}$	$+6.21 \pm 0.02$
ZZW^+	$1.9874 \pm 0.0001 \cdot 10^{-2}$	$2.0189 \pm 0.0003 \cdot 10^{-2}$	$+1.58 \pm 0.02$
ZZZ	$1.0761 \pm 0.0001 \cdot 10^{-2}$	$0.9741 \pm 0.0001 \cdot 10^{-2}$	-9.47 ± 0.02
HZZ	$2.1005 \pm 0.0003 \cdot 10^{-3}$	$1.9155 \pm 0.0003 \cdot 10^{-3}$	-8.81 ± 0.02
HZW^+	$2.4408 \pm 0.0000 \cdot 10^{-3}$	$2.4809 \pm 0.0005 \cdot 10^{-3}$	$+1.64 \pm 0.02$
HHW^+	$2.7827 \pm 0.0001 \cdot 10^{-4}$	$2.4259 \pm 0.0027 \cdot 10^{-4}$	-12.82 ± 0.10
HHZ	$2.6914 \pm 0.0003 \cdot 10^{-4}$	$2.3926 \pm 0.0003 \cdot 10^{-4}$	-11.10 ± 0.02
$t\bar{t}W^+$	$2.4119 \pm 0.0003 \cdot 10^{-1}$	$2.3025 \pm 0.0003 \cdot 10^{-1}$	-4.54 ± 0.02
$t\bar{t}Z$	$5.0456 \pm 0.0006 \cdot 10^{-1}$	$5.0033 \pm 0.0007 \cdot 10^{-1}$	-0.84 ± 0.02
$t\bar{t}H$	$3.4480 \pm 0.0004 \cdot 10^{-1}$	$3.5102 \pm 0.0005 \cdot 10^{-1}$	$+1.81 \pm 0.02$
$t\bar{t}j$	$3.0277 \pm 0.0003 \cdot 10^2$	$2.9683 \pm 0.0004 \cdot 10^2$	-1.96 ± 0.02
jjj	$7.9639 \pm 0.0010 \cdot 10^6$	$7.9472 \pm 0.0011 \cdot 10^6$	-0.21 ± 0.02
tj	$1.0613 \pm 0.0001 \cdot 10^2$	$1.0539 \pm 0.0001 \cdot 10^2$	-0.70 ± 0.02

Table 3: Cross sections at LO, σ_{LO} , and including NLO EW corrections, $\sigma_{\text{NLO EW}}$ ($= \sigma_{\text{NLO}_2}$ as defined in Section 5.2.1), as well as relative EW corrections, $\delta_{\text{EW}} = \sigma_{\text{NLO EW}}/\sigma_{\text{LO}} - 1$, for a variety of scattering processes $\text{pp} \rightarrow F + X$ at the LHC with $\sqrt{s} = 13 \text{ TeV}$ (taken from Ref. [328]).

	$\text{pp} \rightarrow t\bar{t} + X$	$\text{pp} \rightarrow t\bar{t}Z + X$	$\text{pp} \rightarrow t\bar{t}W^+ + X$
LO_1	$4.3803 \pm 0.0005 \cdot 10^2 \text{ pb}$	$5.0463 \pm 0.0003 \cdot 10^{-1} \text{ pb}$	$2.4116 \pm 0.0001 \cdot 10^{-1} \text{ pb}$
LO_2	$+0.405 \pm 0.001 \%$	$-0.691 \pm 0.001 \%$	$+0.000 \pm 0.000 \%$
LO_3	$+0.630 \pm 0.001 \%$	$+2.259 \pm 0.001 \%$	$+0.962 \pm 0.000 \%$
NLO_1	$+46.164 \pm 0.022 \%$	$+44.809 \pm 0.028 \%$	$+49.504 \pm 0.015 \%$
NLO_2	$-1.075 \pm 0.003 \%$	$-0.846 \pm 0.004 \%$	$-4.541 \pm 0.003 \%$
NLO_3	$+0.552 \pm 0.002 \%$	$+0.845 \pm 0.003 \%$	$+12.242 \pm 0.014 \%$
NLO_4	$+0.005 \pm 0.000 \%$	$-0.082 \pm 0.000 \%$	$+0.017 \pm 0.003 \%$

Table 4: Cross sections for $\text{pp} \rightarrow t\bar{t} + X$, $t\bar{t}Z + X$, and $t\bar{t}W^+ + X$. Besides the leading LO_1 contribution in pb, the subleading LO and NLO contributions are given as percentage fractions of LO_1 (taken from Ref. [328]).

EW corrections to integrated cross sections may depend strongly on the imposed cuts and the corrections are typically significantly larger in differential distributions, most notably in high-energy tails.

As discussed in Section 5.2.1, for general processes contributions of different orders in the strong and EW couplings appear at LO and at NLO. While one naively expects that the size of the contributions is set by the corresponding coupling powers, this is not always the case. In Table 4, we reproduce some results from **MADGRAPH5_AMC@NLO** on $t\bar{t}$ production processes at the LHC [328] using the notation introduced in Refs. [327, 328, 362] and Section 5.2.1. For inclusive rates all contributions apart from the LO_1 and NLO_1 ones are small, with the exception of the NLO_3 term and, to a smaller extent, of the NLO_2 one in $t\bar{t}W^+$ production. The $+12\%$ correction to the LO_1 cross section owing to the NLO_3 contribution results from the opening of a tW scattering channel, as noted in Refs. [363, 364].

Another example, where the hierarchy of the NLO corrections differs from the naive expectation is vector-boson scattering. While the NLO QCD corrections are comparably small for these processes, the NLO EW corrections dominate the NLO corrections. More details can be found at the end of Section 5.4.1 and in Refs. [333, 340, 341].

4. Electroweak radiative corrections—real emission effects

4.1. Infrared divergences in real electroweak corrections

In gauge theories involving massless gauge bosons or massive gauge bosons in their high-energy limit, virtual corrections to particle scattering processes in general contain mass singularities originating from the exchange of soft or collinear massless or light particles. In Section 5.4 we discuss those virtual effects for energies well above the EW scale in some detail. In the following, we focus on energies of the order of the EW scale and refer to the occurring soft and/or collinear mass singularities—following the usual terminology in QCD—globally as infrared (IR) singularities. In one-loop corrections, *soft* singularities arise from the exchange of a massless gauge boson (gluon or photon), while *collinear* singularities occur whenever a massless external particle (gluon, photon, or light fermion in the massless limit) splits into two massless lines in a loop diagram [365]. These IR divergences cancel in predictions for observables after combining *virtual* corrections with *real* corrections that involve the emission of additional massless particles. At NLO, the real emission of one extra particle is relevant. The counterpart to soft virtual corrections is the emission (*bremsstrahlung*) of one massless gauge boson (gluon or photon). Within QED, summing virtual corrections and photonic bremsstrahlung corrections already leads to IR-finite corrections to all perturbative orders—this is the statement of the *Bloch–Nordsieck theorem* [366]. In the limit of a small fermion mass m_f , those IR-finite corrections involve logarithmic terms of the form $\ln(m_f/Q)$, where Q is any kinematical quantity such as the scattering energy. Such logarithms originate from collinear particle exchange in loops and from the collinear splitting of fermions and photons in real emission corrections.

Collinear singularities require special attention and treatment for several reasons: Firstly, whenever quarks or gluons are involved in those singularities, the incomplete cancellation of IR singularities is a sign of non-perturbative physics of strong interactions at low energy scales. This is also the case if the singularities are formally arising as logarithms of light quark masses, because those masses do not represent perturbatively well-defined quantities. In such cases, the definition of observables either has to be refined in such a way that IR singularities systematically cancel (like in jets), or the IR-singular non-perturbative part has to be isolated properly and eventually extracted from experimental data (like in parton distribution or fragmentation functions). To achieve this cancellation, the *Kinoshita–Lee–Nauenberg theorem (KLN)* [365, 367] is crucial, which predicts the cancellation of singularities in observables that are sufficiently inclusive w.r.t. energy-degenerate particle configurations. The second type of collinear singularities concerns leptons and photons. The corresponding corrections can be calculated perturbatively, because lepton masses are well-defined parameters and measured to good precision, but at present-day collider energies the mentioned logarithms lead to corrections of the form $[\alpha \ln(m_l/Q)]^n$ at the n -loop level. Since those corrections can get very large at NLO ($n = 1$), at least their dominating effects in higher orders should be known. A third reason why collinear singularities require some special treatment is of technical nature. Even if physical observables are free of IR singularities, such divergences appear in different ingredients of the calculation, so that suitable techniques for their treatment are required.

In the following, we first review the structure of soft and collinear singularities appearing in *real* NLO EW corrections, then turn to frequently used techniques to isolate and calculate them, and subsequently discuss their absorption in parton distribution and fragmentation functions of hadronic systems. Finally, we add some brief discussion of enhanced EW corrections beyond NLO in lepton–photon systems that are connected to higher-order collinear singularities.

4.1.1. Soft singularities

In QED, the asymptotic form of soft-photon singularities as well as their cancellation was worked out in the classic paper of Yennie, Frautschi, and Suura [368]. The results carry over to the full SM and even apply to all electrically charged particles (such as W bosons), because soft photons are blind to the spin of charged particles. A soft photon

(outgoing momentum k) only couples to the *eikonal current* J_{eik}^μ generated by the charges Q_n of all particles (momenta p_n) taking part in the considered process,

$$J_{\text{eik}}^\mu = - \sum_n \sigma_n Q_n e \frac{p_n^\mu}{p_n k}. \quad (257)$$

The momenta p_n might be incoming or outgoing. The sign factors $\sigma_n = \pm 1$ are determined by the physical charge flow in the process. We define $\sigma_n = +1$ for an incoming particle and outgoing antiparticle, and $\sigma_n = -1$ for an outgoing particle and incoming antiparticle. Charge conservation for some process, thus, implies

$$\sum_n Q_n \sigma_n = 0. \quad (258)$$

In the calculation of NLO EW corrections, one-photon bremsstrahlung is relevant. Denoting the amplitudes for the bremsstrahlung process and for the underlying hard process without photon emission by \mathcal{M}_1 and \mathcal{M}_0 , respectively, the asymptotic behaviour of $|\mathcal{M}_1|^2$, summed over photon polarizations λ_γ , in the soft-photon limit $k \rightarrow 0$ is given by

$$\sum_{\lambda_\gamma} |\mathcal{M}_1|^2 \underset{k \rightarrow 0}{\sim} -J_{\text{eik}}^\mu J_{\text{eik},\mu}^* |\mathcal{M}_0|^2 = - \sum_{n,n'} Q_n \sigma_n Q_{n'} \sigma_{n'} e^2 \frac{p_n p_{n'}}{(p_n k)(p_{n'} k)} |\mathcal{M}_0|^2. \quad (259)$$

Integrating this squared amplitude over the soft-photon phase space, leads to a logarithmic singularity which can be either regularized by an infinitesimal photon mass m_γ or by dimensional regularization (DR) in $D = 4 - 2\epsilon$ dimensions, where the singularity shows up as $1/\epsilon$ pole. As long as all charged particles have non-vanishing masses, there is a simple universal correspondence between the soft divergences in the two regularizations schemes,

$$\ln m_\gamma^2 \leftrightarrow \frac{(4\pi\mu^2)^\epsilon \Gamma(1+\epsilon)}{\epsilon} + \mathcal{O}(\epsilon) = \frac{(4\pi\mu^2)^\epsilon}{\epsilon \Gamma(1-\epsilon)} + \mathcal{O}(\epsilon), \quad (260)$$

where μ is the arbitrary reference mass scale of DR. If at least one radiating particle is truly massless, DR should be used; the interplay between soft and collinear singularities then leads to $1/\epsilon^2$ poles. The correspondence between such IR-singular terms in DR and the corresponding logarithms of small mass parameters is more complicated and is discussed in Section 4.2 for light fermions.

4.1.2. Collinear singularities

In the SM at experimentally relevant energy scales, collinear singularities involving photons only appear in connection with light fermions (W bosons should be treated with their full mass dependence), so that we restrict our discussion to fermions in the following. Figure 1 depicts the various cases in which such collinear singularities can appear in scattering processes. In the first two cases, the collinear splittings happen in the final state, i.e. after the hard scattering process. In the remaining three cases, an initial-state particle is splitting, so that only a reduced momentum flows into the hard scattering process. For later convenience we introduce the complete set of relevant splitting functions $P_{ab}(z)$ already here,

$$\begin{aligned} P_{ff}(z) &= \left(\frac{1+z^2}{1-z} \right)_+, & \hat{P}_{ff}(z) &= \frac{1+z^2}{1-z}, \\ P_{f\gamma}(z) &= z^2 + (1-z)^2, & P_{\gamma f}(z) &= \frac{1+(1-z)^2}{z}, & P_{\gamma\gamma}(z) &= -\frac{2}{3}\delta(1-z), \end{aligned} \quad (261)$$

which determine the probability to find parton a in parton b . Note, in particular, the two different variants P_{ff} and \hat{P}_{ff} , which are related by the $(\dots)_+$ distribution, defined by

$$\int_0^1 dx [f(x)]_+ g(x) = \int_0^1 dx f(x) [g(x) - g(1)], \quad (262)$$

with g representing some test function. The kinematical region that develops the collinear singularity for two external light particles of momenta p_1 and p_2 is characterized by $\mathcal{O}(p_1 p_2) = \mathcal{O}(m_f^2) \ll Q^2$, i.e. the squared mass of the fermion

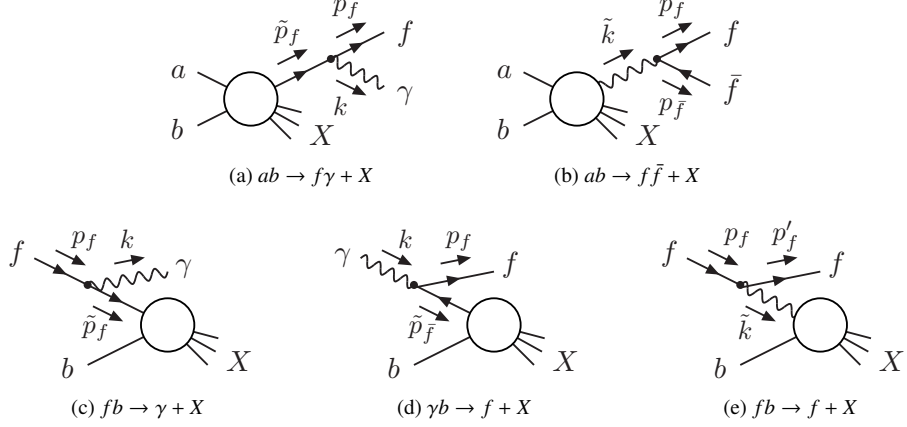


Figure 1: Structural diagrams illustrating the various fermion–photon splittings leading to collinear singularities in scattering processes.

f participating in the splitting and the virtuality $(p_1 + p_2)^2$ of the splitting propagator are much smaller than the typical (squared) energy scale Q^2 of the hard process. Using the momentum assignments defined in Fig. 1, the unpolarized squared matrix elements (spin-averaged for the initial and spin-summed for the final states) $\langle |\mathcal{M}_1^{\cdot\cdot\cdot}|^2 \rangle$ asymptotically behave as follows in the collinear limits,

$$\langle |\mathcal{M}_1^{ab \rightarrow f\gamma X}(p_f, k)|^2 \rangle \underset{p_f k \rightarrow 0}{\sim} Q_f^2 e^2 h_{f\gamma}(p_f, k) \langle |\mathcal{M}_0^{ab \rightarrow fX}(\tilde{p}_f)|^2 \rangle, \quad (263)$$

$$\langle |\mathcal{M}_1^{ab \rightarrow f\bar{f}X}(p_f, p_{\bar{f}})|^2 \rangle \underset{p_f p_{\bar{f}} \rightarrow 0}{\sim} N_C^f Q_f^2 e^2 h_{f\bar{f}}^{\mu\nu}(p_f, p_{\bar{f}}) \langle T_{0,\mu}^{ab \rightarrow \gamma X}(\tilde{k}) (T_{0,\nu}^{ab \rightarrow \gamma X}(\tilde{k}))^* \rangle, \quad (264)$$

$$\langle |\mathcal{M}_1^{fb \rightarrow \gamma X}(p_f, k)|^2 \rangle \underset{p_f k \rightarrow 0}{\sim} Q_f^2 e^2 h^{f\gamma}(p_f, k) \langle |\mathcal{M}_0^{fb \rightarrow X}(\tilde{p}_f)|^2 \rangle, \quad (265)$$

$$\langle |\mathcal{M}_1^{\gamma b \rightarrow fX}(k, p_f)|^2 \rangle \underset{p_f k \rightarrow 0}{\sim} Q_f^2 e^2 h^{\gamma f}(k, p_f) \langle |\mathcal{M}_0^{\bar{f}b \rightarrow X}(\tilde{p}_f)|^2 \rangle, \quad (266)$$

$$\langle |\mathcal{M}_1^{fb \rightarrow fX}(p_f, p'_f)|^2 \rangle \underset{p_f p'_f \rightarrow 0}{\sim} N_C^f Q_f^2 e^2 h^{ff,\mu\nu}(p_f, p'_f) \langle T_{0,\mu}^{fb \rightarrow X}(\tilde{k}) (T_{0,\nu}^{fb \rightarrow X}(\tilde{k}))^* \rangle, \quad (267)$$

where N_C^f is the colour multiplicity of f (i.e. 1 or 3 if f is a lepton or a quark, respectively). Here $\langle |\mathcal{M}_0^{\cdot\cdot\cdot}|^2 \rangle$ are the unpolarized squared matrix elements of the hard scattering processes, and $T_{0,\mu}^{\cdot\cdot\cdot}$ the amplitudes of the hard processes with photon polarization vector $\epsilon^\mu(\tilde{k})$ truncated,

$$\mathcal{M}_0^{ab \rightarrow \gamma X}(\tilde{k}) = \epsilon^\mu(\tilde{k})^* T_{0,\mu}^{ab \rightarrow \gamma X}(\tilde{k}), \quad \mathcal{M}_0^{\gamma b \rightarrow X}(\tilde{k}) = \epsilon^\mu(\tilde{k}) T_{0,\mu}^{\gamma b \rightarrow X}(\tilde{k}). \quad (268)$$

All squared matrix elements $\langle |\mathcal{M}_k^{\cdot\cdot\cdot}|^2 \rangle$ are colour summed, but summed over outgoing and averaged over incoming polarizations, where the number of polarizations for fermions and the photon are 2 and $D-2 = 2(1-\epsilon)$, respectively.²⁷ If the incoming fermion turns into a photon or vice versa, this leads to additional ϵ -terms in the radiator functions $h^{\cdot\cdot\cdot}(p_1, p_2)$ which are given by

$$\begin{aligned} h_{f\gamma}(p_f, k) &= \frac{1}{p_f k} \left[\hat{P}_{ff}(z) - \epsilon(1-z) - \frac{m_f^2}{p_f k} \right], \\ h_{f\bar{f}}^{\mu\nu}(p_f, p_{\bar{f}}) &= \frac{2}{(p_f + p_{\bar{f}})^2} \left[-g^{\mu\nu} + 4z(1-z) \frac{k_\perp^\mu k_\perp^\nu}{k_\perp^2 - m_f^2} \right], \\ h^{f\gamma}(p_f, k) &= \frac{1}{x(p_f k)} \left[\hat{P}_{ff}(x) - \epsilon(1-x) - \frac{x m_f^2}{p_f k} \right], \end{aligned}$$

²⁷The spin average on the right-hand side of Eq. (267) is for the incoming fermion f and not yet for the incoming photon, i.e. it yields a factor 1/2.

$$\begin{aligned}
h^{\gamma f}(k, p_f) &= \frac{1}{x(kp_f)} \left[P_{f\gamma}(x) - \frac{1}{1-\epsilon} \left(2\epsilon x(1-x) - \frac{xm_f^2}{kp_f} \right) \right], \\
h^{ff,\mu\nu}(p_f, p'_f) &= \frac{-2}{(p_f - p'_f)^2} \left[-g^{\mu\nu} - \frac{4(1-x)}{x^2} \frac{k_\perp^\mu k_\perp^\nu}{k_\perp^2 - x^2 m_f^2} \right]. \tag{269}
\end{aligned}$$

Here and in the following, we give results for unpolarized particles that are both valid in DR and mass regularization (MR), which are obtained upon combining the results given in Refs. [55, 369, 370]. Results valid for polarized hard particles (in MR) can be found in Refs. [55, 369]. With the momentum assignments in $h_{ii'}(p_1, p_2)$ and $h^{aa'}(p_1, p_2)$, the dimensionless variables z and x are given by

$$z = \frac{p_1^0}{p_1^0 + p_2^0}, \quad x = \frac{p_1^0 - p_2^0}{p_1^0}, \tag{270}$$

i.e. z is the energy fraction taken by particle i in a final-state splitting $\tilde{i} \rightarrow i + i'$ and x is the energy fraction carried into the hard process by particle \tilde{a} resulting from the splitting $a \rightarrow a' + \tilde{a}$. The momentum k_\perp is the orthogonal component of the momenta p_1 and p_2 in their *Sudakov parametrization* around some collinear axis \tilde{p} ($\tilde{p}k_\perp = 0$). Following Ref. [370] (Sect. 4.2), a parametrization appropriate for a final-state splitting is given by

$$p_1^\mu = z\tilde{p}^\mu + k_\perp^\mu - \frac{k_\perp^2 + z^2 m^2 - m_1^2}{z} \frac{n^\mu}{2\tilde{p}n}, \quad p_2^\mu = (1-z)\tilde{p}^\mu - k_\perp^\mu - \frac{k_\perp^2 + (1-z)^2 m^2 - m_2^2}{1-z} \frac{n^\mu}{2\tilde{p}n}, \tag{271}$$

with the squared masses $p_1^2 = m_1^2$, $p_2^2 = m_2^2$, $\tilde{p}^2 = m^2$, and n^μ denoting an auxiliary light-like vector ($n^2 = nk_\perp = 0$). Depending on the specific splitting, the masses m_1 , m_2 , and m are either m_f or zero. Owing to

$$(p_1 + p_2)^2 = -\frac{k_\perp^2}{z(1-z)} + \frac{m_1^2}{z} + \frac{m_2^2}{1-z}, \tag{272}$$

we have $\mathcal{O}((p_1 + p_2)^2) = \mathcal{O}(k_\perp^2) = \mathcal{O}(m_f^2)$ in the collinear limit. A Sudakov parametrization for an initial-state splitting can be obtained analogously.

The momenta \tilde{p}_f , $\tilde{p}_{\bar{f}}$, \tilde{k} in the hard matrix elements \mathcal{M}_0 , T_0 (263)–(267) correspond to the collinear axes, i.e. to \tilde{p} in the case of a final-state splitting. Note that those momenta have to fulfil the corresponding OS conditions (i.e. they are not identical with $p_1 \pm p_2$ as suggested by momentum conservation in Fig. 1), otherwise the hard matrix element would be ill-defined and in general gauge dependent.

Let us further inspect the terms of the form $\langle k_{\perp\mu}^\mu T_{0,\mu} k_{\perp\nu}^\nu (T_{0,\nu})^* \rangle$ in the asymptotics of $\langle |\mathcal{M}_1|^2 \rangle$ for splittings with an external photon in the hard scattering process, Eqs. (264) and (267). These terms express correlations between the polarization of the hard photon and the azimuthal angle ϕ of the nearly collinear momenta around the collinear axis. Assuming inclusiveness w.r.t. ϕ in the final state, $\langle |\mathcal{M}_1|^2 \rangle$ can be averaged over ϕ (which is equivalent to a spin average of the splitting particle), so that the asymptotics of Eqs. (264) and (267) further simplifies and shows factorization from the squared hard matrix elements $\langle |\mathcal{M}_0|^2 \rangle$,

$$\langle |\mathcal{M}_1^{ab \rightarrow f\bar{f}X}(p_f, p_{\bar{f}})|^2 \rangle_\phi \underset{p_f p_{\bar{f}} \rightarrow 0}{\widetilde{}} N_C^f Q_f^2 e^2 h_{f\bar{f}}(p_f, p_{\bar{f}}) \langle |\mathcal{M}_0^{ab \rightarrow \gamma X}(\tilde{k})|^2 \rangle, \tag{273}$$

$$\langle |\mathcal{M}_1^{fb \rightarrow fX}(p_f, p'_f)|^2 \rangle_\phi \underset{p_f p'_f \rightarrow 0}{\widetilde{}} N_C^f Q_f^2 e^2 h^{ff}(p_f, p'_f) \langle |\mathcal{M}_0^{\gamma b \rightarrow X}(\tilde{k})|^2 \rangle, \tag{274}$$

where the azimuthal average is indicated as $\langle \cdots \rangle_\phi$. The radiator functions simplify to

$$\begin{aligned}
h_{f\bar{f}}(p_f, p_{\bar{f}}) &= \frac{2}{(p_f + p_{\bar{f}})^2} \left[P_{f\gamma}(z) + \frac{2}{1-\epsilon} \left(-\epsilon z(1-z) + \frac{m_f^2}{(p_f + p_{\bar{f}})^2} \right) \right], \\
h^{ff}(p_f, p'_f) &= \frac{-2}{x(p_f - p'_f)^2} \left[P_{\gamma f}(x) - \epsilon x + \frac{2xm_f^2}{(p_f - p'_f)^2} \right]. \tag{275}
\end{aligned}$$

For the other splittings, $\langle |\mathcal{M}_1|^2 \rangle$ and $\langle |\mathcal{M}_1|^2 \rangle_\phi$ are identical. Integrating the asymptotic forms of all $\langle |\mathcal{M}_1|^2 \rangle_\phi$ over small emission angles in the collinear regions produces mass-singular corrections proportional to $\alpha \ln(m_f/Q) P_{ab}(\xi)$ with $\xi = x, z$.

In the following we describe two different techniques how the singular contributions to real NLO corrections originating from soft or collinear regions can be extracted from the full phase-space integral, integrated with regularization parameters, and eventually combined with the remaining non-singular contributions.

4.2. Techniques for calculating real electroweak corrections

An analytical calculation of real radiative corrections is typically only aimed at for fully inclusive quantities, such as total cross sections or decay widths (if they are simple enough), while real corrections to differential quantities are mostly evaluated numerically. Phase-space cuts and event-selection procedures such as jet algorithms render an analytical treatment in general impossible. Apart from feasibility, flexibility is another motivation for the numerical approach, because analytical calculations—if possible at all—are tied to idealized setups, while numerical phase-space integrations can deliver many differential distributions simultaneously and for arbitrary (physically reasonable) event selections. On the other hand, it is desirable to obtain the IR-singular contributions originating from soft and/or collinear phase-space regions in analytic form, in order to properly cancel the singularities against their counterparts in the virtual corrections. This means that we need flexible, general procedures that allow for a numerical evaluation of real-emission contributions without any regulators in the regular phase-space regions, but provide an analytical treatment of the phase-space integration at least over the subspaces containing the IR-singular contributions in the presence of IR regulators, such as phase spaces with $D \neq 4$ dimensions or small mass parameters. Among such procedures, two fundamentally different approaches are used in applications: *phase-space slicing* and *subtraction methods*.

In *slicing* approaches, the singular regions are cut away from phase space in the numerical integration and treated separately. Employing general factorization properties of squared amplitudes in the soft or collinear regions, the singular integrations can be carried out analytically. In the limit of small technical slicing cut parameters the sum of the two contributions reproduces the full phase-space integral. There is a trade-off between residual technical cut dependences and numerical integration errors which increase with decreasing slicing cuts; in practice, one is forced to search for a plateau in the integrated result within integration errors by varying the slicing cut parameters. Technically, mostly two different slicing approaches are in use: *one-cutoff* [52, 371, 372] and *two-cutoff slicing* (see, for instance, Refs. [51, 373]). One-cutoff slicing excludes the IR-singular regions by cuts $s_{ij} > s_{\min}$ on the invariant masses s_{ij} of particle pairs ij that can develop an IR singularity, so that the separation between regular and singular regions is ruled by a single parameter $s_{\min} \ll Q^2$, which is small w.r.t. any relevant scale Q^2 in the considered process. By construction, this method is particularly appealing in QCD calculations that employ colour-ordered amplitudes. Without colour ordering, the separation of soft and collinear singularities involves subtleties in disentangling the overlap between different cut conditions $s_{ij} > s_{\min}$, as discussed in Ref. [374] in detail. Since there is no analogue to colour ordering for electric charges, one-cutoff slicing does not seem to be the method of choice for real EW corrections. Two-cutoff slicing, which is frequently used in NLO EW calculations, separates soft and collinear regions by two different types of cuts. Singularities from soft-photon (or gluon) emission are excluded by a cut $E_\gamma > \Delta E$ on the photon energy E_γ with $\Delta E \ll Q$, and collinear singularities are excluded by angular cuts $\theta_{ij} > \Delta\theta$ ($\Delta\theta \ll 1$), where θ_{ij} is the angle between the directions of two particles that can develop a collinear singularity. Note that all individual cross-section contributions have to be calculated in the same frame of reference, since the cut procedure is based on energies and angles, which are not Lorentz invariant. Finally, we mention another type of a slicing procedure, called (by some misleading naming) *jettiness subtraction* [375], which employs the event-shape variable *jettiness* [376] to separate IR-singular regions. To our knowledge, jettiness subtraction was not yet used in EW higher-order calculations.

Subtraction techniques are based on the idea of subtracting a simple auxiliary function from the singular integrand and adding this contribution again. The auxiliary function has to be chosen in such a way that it cancels all singularities of the original integrand so that the phase-space integration of the difference can be performed numerically, even over the singular regions of the original integrand. In this difference the original matrix element can be evaluated without regulators for soft or collinear singularities. The auxiliary function has to be simple enough so that it can be integrated over the singular regions (ideally analytically) with the help of regulators, before the subtracted contribution is added again. This singular analytical integration can be done once and for all in a process-independent way because

of the general factorization properties of squared amplitudes in the singular regions. At NLO several subtraction variants have been proposed and worked out in the literature, first within QCD [53, 54, 370, 377–380] and subsequently for photonic corrections [55, 328, 369, 374, 381]. The most frequently used variants are *FKS subtraction* and *dipole subtraction*, which have their roots in the papers of Frixione, Kunszt, Signer [53] and Catani, Seymour [54, 378], respectively. While dipole subtraction for EW corrections, including its formulation in MR, is described in the literature very explicitly [55, 369, 374, 381]. FKS subtraction for EW corrections [328] mostly follows the literal translation of its formulation in QCD. The application of FKS subtraction to the EW corrections to Drell–Yan processes is, for example, described in Refs. [382, 383] in some detail. At NNLO, several approaches [384–390], some of them based on numerical procedures, have been suggested and successfully used in QCD calculations. In principle, the latter procedures could be used in the calculation of real EW corrections as well, the only caveat might be the fact that MR is not supported in most cases. On the other hand, a generalization of the FKS method [53] to real NNLO QED corrections (and beyond) with truly massive charged particles, i.e. in the case where only soft IR singularities exist, was proposed in Ref. [391] recently. We will not consider the issue of real corrections beyond NLO in this review.

By experience, subtraction techniques are often superior to slicing approaches in the sense that integration errors in cross-section predictions are typically much smaller if a comparable amount of statistics is used in the numerics within two comparable calculations. On the other hand, subtraction techniques produce events in Monte Carlo integrations with (even unbounded) negative weights, because the difference between the original integrand and the auxiliary function is not positive definite, even if the original integrand is. This problem is tricky to handle in Monte Carlo event generation and less delicate in slicing approaches.

In the following, we describe two very popular techniques for handling IR singularities in real NLO EW corrections in quite some detail: *two-cutoff slicing* and *dipole subtraction*. To keep the presentation transparent, we restrict it to the case of IR (soft and/or collinear) singularities appearing in processes involving light, unpolarized fermions only. For an account of massive or polarized particles, and for a description of the other techniques, we refer to the original papers quoted above. We do not consider the separation of mass singularities related to particle masses at the EW scale, which e.g. appear for W-boson bremsstrahlung at energies way above the EW scale. Those issues are still under discussion and corresponding methods under construction.

4.2.1. Two-cutoff slicing

As already indicated, two-cutoff slicing employs two different types of phase-space cuts to separate IR singularities. Soft singularities from soft-photon (or gluon) emission are excluded from the full photon emission phase space upon demanding $E_\gamma > \Delta E$, where $E_\gamma = k_0$ is the energy of the emitted photon of momentum k . The other IR-singular splittings described in Section 4.1, which do not involve real photons in the final state, do not lead to soft singularities. Collinear singularities are separated by the cuts $\theta_{ij} > \Delta\theta$ on the emission angles θ_{ij} between the two particles i, j whose collinear splitting leads to a singularity. In total, the cross-section contribution of the real NLO EW corrections is split into three parts,

$$d\sigma^{\text{real}} = d\sigma^{\text{hard}}|_{E_\gamma > \Delta E, \text{all } \theta_{ij} > \Delta\theta} + d\sigma^{\text{soft}}|_{E_\gamma < \Delta E} + \sum_{\text{pairs } ij} d\sigma_{ij}^{\text{coll}}|_{E_\gamma > \Delta E, \theta_{ij} < \Delta\theta}. \quad (276)$$

In the *hard* contribution $d\sigma^{\text{hard}}$ the dependence on the cut parameters ΔE and $\Delta\theta$ emerges from the numerical phase-space integration which extends rather deeply into the IR region owing to $\Delta E \ll Q$ and $\Delta\theta \ll 1$ and is, thus, rather CPU expensive in practice.

The *soft* contribution $d\sigma^{\text{soft}}$ corresponding to the cross section for a process $ab \rightarrow X + \gamma$ involves only an integration over the soft-photon region, which can be separated from the full phase-space integral according to

$$\int_{E_\gamma < \Delta E} d\Phi_{ab \rightarrow X + \gamma} = \int d\Phi_{ab \rightarrow X} \mu^{4-D} \int_{E_\gamma < \Delta E} \frac{d^{D-1}\mathbf{k}}{2E_\gamma (2\pi)^{D-1}} \Bigg|_{E_\gamma = \sqrt{|\mathbf{k}|^2 + m_\gamma^2}}. \quad (277)$$

Here we have left open whether we want to apply DR with $D \neq 4$ or MR with an infinitesimal photon mass m_γ . Using the asymptotic behaviour (259) of the squared matrix element $|\mathcal{M}_1|^2$ for a process involving external charged particles with charges Q_n and momenta p_n , the soft contribution fully factorizes from the differential LO cross section $d\sigma^{\text{LO}}$,

$$d\sigma^{\text{soft}} = \delta^{\text{soft}} d\sigma^{\text{LO}}, \quad (278)$$

and the soft-photon factor can be calculated to

$$\begin{aligned}\delta^{\text{soft}} &= -\frac{\alpha}{4\pi^2} \sum_{n,n'} \sigma_n Q_n \sigma_{n'} Q_{n'} (2\pi\mu)^{4-D} \int_{E_\gamma < \Delta E} \frac{d^{D-1}\mathbf{k}}{E_\gamma} \frac{p_n p_{n'}}{(p_n k)(p_{n'} k)} \Big|_{E_\gamma = \sqrt{|\mathbf{k}|^2 + m_\gamma^2}} \\ &= \frac{\alpha}{2\pi} \sum_{\substack{n,n' \\ n < n'}} \sigma_n Q_n \sigma_{n'} Q_{n'} [I_{nn} + I_{n'n'} - 2I_{nn'}],\end{aligned}\quad (279)$$

where we have used charge conservation (258) and introduced the basic integrals

$$I_{nn'} = \frac{(2\pi\mu)^{4-D}}{2\pi} \int_{E_\gamma < \Delta E} \frac{d^{D-1}\mathbf{k}}{E_\gamma} \frac{p_n p_{n'}}{(p_n k)(p_{n'} k)} \Big|_{E_\gamma = \sqrt{|\mathbf{k}|^2 + m_\gamma^2}}, \quad (280)$$

in which $p_n^0, p_{n'}^0 > 0$ is assumed. Explicit expressions for the integrals $I_{nn'}$ for $D = 4$ but arbitrary non-vanishing mass parameters $p_n^2 = m_n^2, p_{n'}^2 = m_{n'}^2$ can be found in Refs. [40, 392]. Here we just give the solutions for small masses $m_n, m_{n'}$, which still obey the hierarchy $m_\gamma \ll m_n, m_{n'} \ll Q$,

$$I_{nn} \Big|_{\text{MR}} = 2 \ln \left(\frac{2\Delta E}{m_\gamma} \right) + 2 \ln \left(\frac{m_n}{2p_n^0} \right), \quad (281)$$

$$I_{nn'} \Big|_{\text{MR}} = 2 \ln \left(\frac{2\Delta E}{m_\gamma} \right) \ln \left(\frac{s_{nn'}}{m_n m_{n'}} \right) - \ln^2 \left(\frac{m_n}{2p_n^0} \right) - \ln^2 \left(\frac{m_{n'}}{2p_{n'}^0} \right) - \frac{\pi^2}{3} - \text{Li}_2 \left(1 - \frac{4p_n^0 p_{n'}^0}{s_{nn'}} \right), \quad (282)$$

with $s_{nn'} = 2p_n p_{n'} \gg m_n^2, m_{n'}^2$. In DR with $p_n^2 = p_{n'}^2 = k^2 = 0$ these integrals read

$$I_{nn} \Big|_{\text{DR}} = 0, \quad (283)$$

$$\begin{aligned}I_{nn'} \Big|_{\text{DR}} &= \frac{(4\pi)^\epsilon}{\epsilon^2 \Gamma(1-\epsilon)} \left[1 + \epsilon \ln \left(\frac{\mu^2}{4\Delta E^2} \right) + \epsilon \ln \left(\frac{4p_n^0 p_{n'}^0}{s_{nn'}} \right) + \frac{\epsilon^2}{2} \ln^2 \left(\frac{\mu^2}{4\Delta E^2} \right) \right. \\ &\quad \left. + \epsilon^2 \ln \left(\frac{\mu^2}{4\Delta E^2} \right) \ln \left(\frac{4p_n^0 p_{n'}^0}{s_{nn'}} \right) - \epsilon^2 \text{Li}_2 \left(1 - \frac{4p_n^0 p_{n'}^0}{s_{nn'}} \right) - \epsilon^2 \frac{\pi^2}{6} \right] + O(\epsilon).\end{aligned}\quad (284)$$

The integration over the *collinear* phase-space regions is straightforward as well, although the necessary phase-space factorization is somewhat more complicated than Eq. (277). One way of carrying out the integrals is to employ the phase-space factorization of the dipole subtraction formalism (see next section) and restricting it to the collinear regions, as e.g. described in Ref. [369]. The resulting cross-section contributions (in the same order as shown in Fig. 1) can be written as

$$\begin{aligned}\int d\sigma_{ab \rightarrow f\gamma X}^{\text{coll}}(p_f, k) &= \frac{Q_f^2 \alpha}{2\pi} \int d\sigma_{ab \rightarrow fX}^{\text{LO}}(\tilde{p}_f) \int_0^1 dz \left\{ H_{f\gamma}(\tilde{p}_f^0) \delta(1-z) + [\bar{H}_{f\gamma}(\tilde{p}_f^0, z)]_+ \right\} \\ &\quad \times \Theta_{\text{cut}}(p_f = z\tilde{p}_f, k = (1-z)\tilde{p}_f),\end{aligned}\quad (285)$$

$$\begin{aligned}\int d\sigma_{ab \rightarrow f\bar{f}X}^{\text{coll}}(p_f, p_{\bar{f}}) &= N_C^f \frac{Q_f^2 \alpha}{2\pi} \int d\sigma_{ab \rightarrow \gamma X}^{\text{LO}}(\tilde{k}) \int_0^1 dz \left\{ H_{f\bar{f}}(\tilde{k}^0) \delta(1-z) + [\bar{H}_{f\bar{f}}(\tilde{k}^0, z)]_+ \right\} \\ &\quad \times \Theta_{\text{cut}}(p_f = z\tilde{k}, p_{\bar{f}} = (1-z)\tilde{k}),\end{aligned}\quad (286)$$

$$\int d\sigma_{fb \rightarrow \gamma X}^{\text{coll}}(p_f, k) = \frac{Q_f^2 \alpha}{2\pi} \int_0^1 dx \int d\sigma_{fb \rightarrow X}^{\text{LO}}(\tilde{p}_f = xp_f) \left\{ H^{f\gamma}(p_f^0) \delta(1-x) + [\mathcal{H}^{f\gamma}(p_f^0, x)]_+ \right\}, \quad (287)$$

$$\int d\sigma_{\gamma b \rightarrow fX}^{\text{coll}}(k, p_f) = N_C^f \frac{Q_f^2 \alpha}{2\pi} \int_0^1 dx \int d\sigma_{\bar{f}b \rightarrow X}^{\text{LO}}(\tilde{p}_{\bar{f}} = xk) \mathcal{H}^{\gamma f}(k^0, x), \quad (288)$$

$$\int d\sigma_{fb \rightarrow fX}^{\text{coll}}(p_f, p_f') = \frac{Q_f^2 \alpha}{2\pi} \int_0^1 dx \int d\sigma_{\gamma b \rightarrow X}^{\text{LO}}(\tilde{k} = xp_f) \mathcal{H}^{ff}(p_f^0, x), \quad (289)$$

where the momenta p_1 and p_2 that get collinear are indicated as arguments in $d\sigma^{\text{coll}}(p_1, p_2)$ on the l.h.s. of the equations. The relations between $p_{1,2}$ and the momentum \tilde{p} playing the role of $p_1 \pm p_2$ in the hard LO cross section $d\sigma^{\text{LO}}(\tilde{p})$ are made explicit on the r.h.s., where the step functions Θ_{cut} (being 1 or 0) show which momenta are subject to possible phase-space cuts in the case of final-state splittings (for initial-state splittings the collinear particles are assumed to escape in the beam pipe). Note that the hard cross section does not depend on the splitting variable z for final-state splittings (first two equations). For initial-state splittings, however, it depends on the variable x , since the hard kinematics is initiated by the reduced incoming momentum xp_1 and the CM frame of the hard scattering is boosted in the direction opposite to \mathbf{p}_1 by the velocity $(1-x)/(1+x)$ in the CM frame of the two original incoming momenta. The cross-section contributions take the form of convolutions of the hard LO cross sections over the splitting variables z and x with radiator functions $\bar{\mathcal{H}}$, \mathcal{H} , and H describing the radiation pattern. In some of the cases it is appropriate to separate the *endpoint contributions*, which correspond to the LO kinematics, from the continuum contributions to the convolution by employing $(\dots)_+$ distributions. For the splittings $f \rightarrow f\gamma$ with real photon emission, this procedure isolates the soft-singular contributions in the endpoint contributions, which facilitates the cancellation of soft singularities. The continuum parts $\bar{\mathcal{H}}$, \mathcal{H} of the radiator functions, thus do not depend on ΔE .

Before moving on to the explicit results on the radiator function $\bar{\mathcal{H}}_{f\gamma}$, etc., we want to emphasize a subtlety in the use of the $(\dots)_+$ distributions introduced above. Definition (262) does not make the fact explicit that in general some kinematical variable Q (such as \tilde{p}_f^0 etc.) appears inside the $(\dots)_+$ symbol in addition to the integration variable x , i.e. we have to evaluate a distribution like $[f(x, Q)]_+$, where $Q = Q(\tilde{\Phi}(x))$ is a function on the phase space $\tilde{\Phi}(x)$ of the hard scattering process. In the analytical calculation of the endpoint contribution proportional to $\delta(1-x)$, the value of Q is kept fixed in the integration over x . In the numerical evaluation, the integral appears in the form

$$\begin{aligned} & \int_0^1 dx \int d\tilde{\Phi}(x) [f(x, Q(\tilde{\Phi}(x)))]_+ |\mathcal{M}(\tilde{\Phi}(x))|^2 \\ &= \int_0^1 dx \left[\int d\tilde{\Phi}(x) f(x, Q(\tilde{\Phi}(x))) |\mathcal{M}(\tilde{\Phi}(x))|^2 - \int d\tilde{\Phi}(1) f(x, Q(\tilde{\Phi}(1))) |\mathcal{M}(\tilde{\Phi}(1))|^2 \right], \end{aligned} \quad (290)$$

i.e. the variable Q inside $[f(x, Q)]_+$ has to be equal to the Q value in the corresponding matrix element $|\mathcal{M}(\tilde{\Phi})|^2$ (see also related discussion at the end of Sect. 5.2.3 and in App. B of Ref. [370]).

In MR, i.e. for small fermion masses $m_f \ll \tilde{p}_f^0$, the radiator functions read

$$\bar{\mathcal{H}}_{f\gamma}(\tilde{p}_f^0, z) \Big|_{\text{MR}} = \hat{P}_{ff}(z) \left[2 \ln \left(\frac{\tilde{p}_f^0 \Delta \theta}{m_f} \right) + 2 \ln z - 1 \right] + 1 - z, \quad (291)$$

$$\bar{\mathcal{H}}_{f\bar{f}}(\tilde{k}^0, z) \Big|_{\text{MR}} = 2P_{f\gamma}(z) \left[\ln \left(\frac{\tilde{k}^0 \Delta \theta}{m_f} \right) + \ln z + \ln(1-z) \right] + 2z(1-z), \quad (292)$$

$$\mathcal{H}^{f\gamma}(p_f^0, x) \Big|_{\text{MR}} = \hat{P}_{ff}(x) \left[2 \ln \left(\frac{p_f^0 \Delta \theta}{m_f} \right) - 1 \right] + 1 - x, \quad (293)$$

$$\mathcal{H}^{\gamma f}(k^0, x) \Big|_{\text{MR}} = 2P_{f\gamma}(x) \left[\ln \left(\frac{k^0 \Delta \theta}{m_f} \right) + \ln(1-x) \right] + 2x(1-x), \quad (294)$$

$$\mathcal{H}^{ff}(p_f^0, x) \Big|_{\text{MR}} = P_{\gamma f}(x) \left[2 \ln \left(\frac{p_f^0 \Delta \theta}{m_f} \right) + 2 \ln(1-x) - 2 \ln x - 1 \right] + x. \quad (295)$$

The corresponding endpoint parts are given by

$$H_{f\gamma}(\tilde{p}_f^0) \Big|_{\text{MR}} = - \left[2 \ln \left(\frac{\Delta E}{\tilde{p}_f^0} \right) + \frac{3}{2} \right] \left[2 \ln \left(\frac{\tilde{p}_f^0 \Delta \theta}{m_f} \right) - 1 \right] + 3 - \frac{2\pi^2}{3}, \quad (296)$$

$$H_{f\bar{f}}(\tilde{k}^0) \Big|_{\text{MR}} = \frac{4}{3} \ln \left(\frac{\tilde{k}^0 \Delta \theta}{m_f} \right) - \frac{23}{9}, \quad (297)$$

$$H^{f\gamma}(p_f^0)|_{\text{MR}} = - \left[2 \ln \left(\frac{\Delta E}{p_f^0} \right) + \frac{3}{2} \right] \left[2 \ln \left(\frac{p_f^0 \Delta \theta}{m_f} \right) - 1 \right] + \frac{1}{2}. \quad (298)$$

The radiator functions in DR can be obtained by substituting the mass-singular terms appropriately. For all splittings that do not involve soft singularities, the logarithm $\ln m_f$ turns into the usual $1/\epsilon$ pole according to the correspondence

$$\ln m_f^2 \leftrightarrow \frac{(4\pi\mu^2)^\epsilon}{\epsilon\Gamma(1-\epsilon)} = \frac{1}{\epsilon\Gamma(1-\epsilon)} + \ln(4\pi) + \ln\mu^2 + O(\epsilon) = \Delta + \ln\mu^2 + O(\epsilon), \quad (299)$$

with the same formal definition of Δ as for UV singularities in Eq. (169), but in general some finite terms change as well. For the case at hand, the correspondence (299) is exact including finite terms for $\bar{\mathcal{H}}_{f\bar{f}}$ in Eq. (292), $\mathcal{H}^{\gamma f}$ in Eq. (294), and $H_{f\bar{f}}$ in Eq. (297). For \mathcal{H}^{ff} of Eq. (295), the transition to DR changes also some finite terms:

$$\mathcal{H}^{ff}(p_f^0, x)|_{\text{DR}} = P_{\gamma f}(x) \left[-\frac{(4\pi)^\epsilon}{\epsilon\Gamma(1-\epsilon)} + 2 \ln \left(\frac{p_f^0 \Delta \theta}{\mu} \right) + 2 \ln(1-x) \right] + x. \quad (300)$$

For the soft-singular $f \rightarrow f\gamma$ splittings with real-photon emission the translation to DR is somewhat more complicated owing to the interplay between the soft and collinear singularities. Those radiator functions can, for instance, be easily obtained in DR upon integrating the factorization formulae of Ref. [378] with the slicing cuts (see also Refs. [51, 172]). The results for the continuum parts read

$$\bar{\mathcal{H}}_{f\gamma}(\tilde{p}_f^0, z)|_{\text{DR}} = \hat{P}_{ff}(z) \left[-\frac{(4\pi)^\epsilon}{\epsilon\Gamma(1-\epsilon)} + 2 \ln \left(\frac{\tilde{p}_f^0 \Delta \theta}{\mu} \right) + 2 \ln(1-z) + 2 \ln z \right] + 1-z, \quad (301)$$

$$\mathcal{H}^{f\gamma}(p_f^0, x)|_{\text{DR}} = \hat{P}_{ff}(x) \left[-\frac{(4\pi)^\epsilon}{\epsilon\Gamma(1-\epsilon)} + 2 \ln \left(\frac{p_f^0 \Delta \theta}{\mu} \right) + 2 \ln(1-x) \right] + 1-x, \quad (302)$$

and the corresponding (soft-singular) endpoint parts are given by

$$H_{f\gamma}(\tilde{p}_f^0)|_{\text{DR}} = \left[2 \ln \left(\frac{\Delta E}{\tilde{p}_f^0} \right) + \frac{3}{2} \right] \left[\frac{(4\pi)^\epsilon}{\epsilon\Gamma(1-\epsilon)} + 2 \ln \left(\frac{\mu}{\tilde{p}_f^0 \Delta \theta} \right) \right] - \frac{2\pi^2}{3} + \frac{13}{2} - 2 \ln^2 \left(\frac{\Delta E}{\tilde{p}_f^0} \right), \quad (303)$$

$$H^{f\gamma}(p_f^0)|_{\text{DR}} = \left[2 \ln \left(\frac{\Delta E}{p_f^0} \right) + \frac{3}{2} \right] \left[\frac{(4\pi)^\epsilon}{\epsilon\Gamma(1-\epsilon)} + 2 \ln \left(\frac{\mu}{p_f^0 \Delta \theta} \right) \right] + 4 - 2 \ln^2 \left(\frac{\Delta E}{p_f^0} \right). \quad (304)$$

We end our discussion of two-cutoff slicing by considering the convolutions (285)–(289) in more detail. For the final-state splittings (285) and (286), the integrations over z do not involve the hard cross section $d\sigma^{\text{LO}}$, but only depend on the event selection encoded in Θ_{cut} . If the two collinear particles are not resolved, but clustered into a single “quasiparticle” (e.g. as part of a jet or electromagnetic shower), only the sum of the two momenta enters the event selection, and $\Theta_{\text{cut}} \equiv 1$ for all z . In this case, the continuum parts $\bar{\mathcal{H}}$ integrate to zero because of their appearance inside $(\dots)_+$ distributions. This observation is in line with the statement of the KLN theorem which predicts the cancellation of all mass-singular contributions related to the considered final-state splitting if all energy-degenerate configurations of the two collinear particles are integrated over. For the $\gamma \rightarrow f\bar{f}$ splitting, the singularity in the collinear endpoint part (297) cancels against its counterpart in the one-loop correction to the photon production process $ab \rightarrow \gamma + X$; for the $f \rightarrow f\gamma$ splitting the cancellation occurs between the endpoint part (296), corresponding soft-photon contributions in $d\sigma^{\text{soft}}$, and one-loop corrections involving photons coupling to the external fermion line. Observables in which collinear final-state singularities cancel are called *collinear-safe*, and *non-collinear-safe* otherwise. This issue frequently occurs in the identification of charged leptons which copiously radiate photons in their direction of flight. We further elaborate on this point in Section 4.5.

In contrast to collinear singularities from final-state splittings, those originating from initial-state splittings do not cancel in cross-section predictions, as can be seen explicitly in the convolutions (287)–(289) by the fact that the hard cross sections depend on the convolution variable x . We discuss the role of those singularities in the description of hadronic collisions in the QCD-improved parton model in Section 4.3, and in the predictions for leptonic collisions in Section 4.5.

4.2.2. Dipole subtraction

Dipole subtraction is one of the standard methods to treat IR singularities in both NLO QCD and EW calculations. It was continuously extended since its original formulation for massless QCD in Refs. [54, 378]. The step towards the inclusion of massive particles was first done for photonic corrections [55] and subsequently for QCD with massive quarks [370, 379]. For a comprehensive treatment of NLO EW corrections to scattering processes, further generalizations towards the treatment of non-collinear-safe observables and all possible mass-singular fermion–photon splittings were described in Ref. [369]; the modification for decay processes was described in Ref. [374]. Dipole subtraction has been successfully automated for generic applications in NLO calculations in various variants [381, 393–397] and is part of several multipurpose Monte Carlo generators.²⁸ The origin of the name *dipole subtraction* roots in the construction of the subtraction function which resembles the singularity structure of the squared matrix element $\langle |\mathcal{M}_1|^2 \rangle$ of real-emission corrections. In the EW case, photon emission amplitudes possess the most complicated IR structure, since they are the only ones with soft *and* collinear singularities. In detail, each light charged particle with momentum p_n participating in some bremsstrahlung process defines the axis of some collinear cone around \mathbf{p}_n , in which potential photon emission is ruled by the factorization formulae (263) and (265). Constructing a subtraction function $|\mathcal{M}_{\text{sub}}|^2$ from a sum over those radiating particles seems natural, but the fact that all collinear cones for photon radiation meet in the soft region of small photon momentum complicates the construction. The requirement that all contributions resembling the asymptotics in the collinear cones conspire to reproduce the soft asymptotics given in Eq. (259) is a rather non-trivial constraint. Dipole subtraction employs partial fractioning

$$\frac{p_n p_{n'}}{(p_n k)(p_{n'} k)} = \frac{p_n p_{n'}}{p_n k + p_{n'} k} \frac{1}{p_n k} + \frac{p_n p_{n'}}{p_n k + p_{n'} k} \frac{1}{p_{n'} k} \quad (305)$$

to the individual terms with $n \neq n'$ in Eq. (259), so that each of the two terms on the r.h.s. can be attributed to a single collinear cone. Splitting the contributions with $n = n'$ with the help of Eq. (258) expressing charge conservation, the asymptotic form (259) of the soft correction can be written as a sum over all (ordered) charged-particle pairs nn' with $n \neq n'$ as follows

$$\begin{aligned} - \sum_{n,n'} Q_n \sigma_n Q_{n'} \sigma_{n'} e^2 \frac{p_{n'} p_n}{(p_{n'} k)(p_n k)} &= - \sum_{\substack{n,n' \\ n \neq n'}} Q_n \sigma_n Q_{n'} \sigma_{n'} e^2 \frac{p_{n'} p_n}{(p_{n'} k)(p_n k)} - \sum_n Q_n^2 \sigma_n^2 e^2 \frac{m_n^2}{(p_n k)^2} \\ &= - \sum_{\substack{n,n' \\ n \neq n'}} Q_n \sigma_n Q_{n'} \sigma_{n'} e^2 \frac{1}{p_n k} \left[\frac{2(p_n p_{n'})}{p_n k + p_{n'} k} - \frac{m_n^2}{p_n k} \right]. \end{aligned} \quad (306)$$

In this double sum, particle n defines a particular collinear cone, while n' is needed to balance charge and to get the soft limit in the correct way. The subtraction function, thus, can be constructed from a sum over all ordered pairs nn' called *dipoles*, where n is called *emitter* and n' *spectator*.

Finally, we mention another role of the spectator in the construction of $|\mathcal{M}_{\text{sub}}|^2$. In all collinear limits (263)–(267), the original matrix element \mathcal{M}_1 on the l.h.s. and the hard LO matrix elements \mathcal{M}_0 (or partial matrix element T_0^μ) on the r.h.s. are defined on different phase spaces. If \mathcal{M}_1 involves $N + 1$ particles, then \mathcal{M}_0 involves only N particles where the two particles i, i' getting collinear in \mathcal{M}_1 are merged to one “quasiparticle” \tilde{i} with momentum \tilde{p}_i . To define $|\mathcal{M}_{\text{sub}}|^2$ on the phase space of \mathcal{M}_1 , we, thus, have to find appropriate phase-space mappings from the $(N + 1)$ -particle phase space Φ_1 with emitter i and spectator j to the N -particle phase space $\tilde{\Phi}_{0,ij}$ with the property that $p_i \pm p'_i$ (the sign depending on the splitting type) asymptotically approaches \tilde{p}_i in the collinear limit $p_i p'_i \rightarrow 0$. Moreover, the consistency of the N -particle matrix elements requires that the mappings respect overall momentum conservation and all OS conditions including $\tilde{p}_i^2 = m_i^2$. These constraints on the mappings can only be respected if more than the two momenta p_i and p'_i of Φ_1 are distorted. In the construction described below, in most cases it is sufficient to modify the spectator momentum in addition, leaving all other momenta unchanged.

The construction of $|\mathcal{M}_{\text{sub}}|^2$ resembling the collinear asymptotics of the remaining splittings that are not of bremsstrahlung type actually do not require a construction via a sum over all emitter–spectator pairs. For each collinear configuration represented by an emitter, it is sufficient to choose one spectator particle from the initial or final state.

²⁸The automation of FKS subtraction [53] has been accomplished as well [328, 380] and represents the underlying IR subtraction method of the **MADGRAPH5_AMC@NLO** [68] and **POWHEG** [398, 399] Monte Carlo programs.

In the following, we give a brief account of all dipole subtraction functions needed in NLO EW calculations for scattering processes with external light, unpolarized, charged fermions, following closely Refs. [55, 369]. For the treatment of massive or polarized radiating particles we refer to those papers. Again, we support both MR and DR in the results. For a process $ab \rightarrow \gamma + X$ of bremsstrahlung type, the subtraction function reads

$$|\mathcal{M}_{\text{sub}}^{ab \rightarrow \gamma X}(\Phi_1)|^2 = - \sum_{\substack{f, f' \\ f \neq f'}} Q_f \sigma_f Q_{f'} \sigma_{f'} e^2 g_{ff'}^{(\text{sub})}(p_f, p_{f'}, k) \langle |\mathcal{M}_0^{ab \rightarrow X}(\tilde{\Phi}_{0,ff'})|^2 \rangle, \quad (307)$$

with f and f' denoting all emitter and spectator fermions, respectively. For processes not of bremsstrahlung type, no soft singularities occur, and the subtraction function can be obtained as a single sum over all external particles of the hard scattering process that can undergo a collinear splitting. Nevertheless, a spectator parton is required for all splittings to preserve momentum conservation and mass-shell conditions, but it is possible to select any other external particle as spectator. The corresponding contributions to the subtraction function can be constructed from the following building blocks,

$$|\mathcal{M}_{\text{sub},j}^{ab \rightarrow f \bar{f} X}(\Phi_1)|^2 = N_C^f Q_f^2 e^2 h_{f\bar{f},j}^{\mu\nu}(p_f, p_{\bar{f}}, p_j) \langle T_{0,\mu}^{ab \rightarrow \gamma X}(\tilde{\Phi}_{0,fj}) (T_{0,\nu}^{ab \rightarrow \gamma X}(\tilde{\Phi}_{0,fj}))^* \rangle, \quad (308)$$

$$|\mathcal{M}_{\text{sub},j}^{\gamma b \rightarrow f X}(\Phi_1)|^2 = Q_f^2 e^2 h_j^{\gamma f}(k, p_f, p_j) \langle |\mathcal{M}_0^{\bar{f} b \rightarrow X}(\tilde{\Phi}_{0,\gamma j})|^2 \rangle, \quad (309)$$

$$|\mathcal{M}_{\text{sub},j}^{fb \rightarrow f X}(\Phi_1)|^2 = N_C^f Q_f^2 e^2 h_j^{ff,\mu\nu}(p_f, p_{f'}, p_j) \langle T_{0,\mu}^{\gamma b \rightarrow X}(\tilde{\Phi}_{0,fj}) (T_{0,\nu}^{\gamma b \rightarrow X}(\tilde{\Phi}_{0,fj}))^* \rangle, \quad (310)$$

where each of the terms stands for one specific splitting type. Here we specifically chose a spectator particle j from the final state. Choosing an initial-state spectator a does not change the form of those definitions, but only the index position; by convention, the lower spectator index j just turns into an upper index a in the subtraction kernels h_{\dots}^{\dots} .

Once the full subtraction function is constructed, the difference $\langle |\mathcal{M}_1| \rangle^2 - |\mathcal{M}_{\text{sub}}|^2$ can be numerically integrated over the full real-emission phase space Φ_1 without any regulators, because $\langle |\mathcal{M}_1| \rangle^2 \sim |\mathcal{M}_{\text{sub}}|^2$ in all IR-singular limits by construction. To obtain the complete real corrections, we have to add back the integral of $|\mathcal{M}_{\text{sub}}|^2$ over Φ_1 , which contains the IR singularities. If $|\mathcal{M}_{\text{sub}}|^2$ is chosen sufficiently simple, the integration over the degrees of freedom in Φ_1 leading to the singularities can be done analytically in some regularization scheme. To this end, the phase-space measure $d\Phi_1$ is split into the one of each hard subspace, $d\tilde{\Phi}_{0,ij}$, and an effective one-particle part $[dp']$ parametrizing the splitting process. The full cross-section contribution of the real corrections in the dipole subtraction approach can, thus, be schematically summarized as follows,

$$\int d\sigma^{\text{real}} = \frac{1}{2s} \int d\Phi_1 \langle |\mathcal{M}_1|^2 \rangle = \int d\sigma^{\text{real-sub}} + \int d\sigma^{\text{sub}} \quad (311)$$

with

$$\int d\sigma^{\text{real-sub}} = \frac{1}{2s} \int d\Phi_1 \left(\langle |\mathcal{M}_1|^2 \rangle - |\mathcal{M}_{\text{sub}}|^2 \right), \quad (312)$$

$$\int d\sigma^{\text{sub}} = \frac{1}{2s} \int d\tilde{\Phi}_0 \otimes \left(\int [dp'] |\mathcal{M}_{\text{sub}}|^2 \right), \quad (313)$$

where $1/(2s)$ is the flux factor for massless incoming particles with CM energy \sqrt{s} . The symbol \otimes indicates that the phase-space factorization is not necessarily an ordinary product, but might still involve convolutions or summations. The detailed prescription to evaluate the r.h.s. of Eq. (313) depends on the emitter–spectator configuration and will become clear in the results below. Details on the construction of the whole formalism can be found in the original papers [54, 55, 369, 370]; in this review we just outline the basic concepts and quote some final results, following the original notation, but omitting unnecessary clutter as much as possible.

We now go through the explicit construction of the subtraction kernels $g_{\dots}^{(\text{sub})}$, h_{\dots}^{\dots} , and their integrated counterparts for the four different cases with emitter and spectator from the final or initial state. In detail, the functions $g_{\dots}^{(\text{sub})}$, h_{\dots}^{\dots} coincide with the respective quantities of Refs. [55, 369] in the limit of light fermions. In all cases but one, those results are directly related to the QCD results of Refs. [54, 370], from which at least the results in DR can be obtained

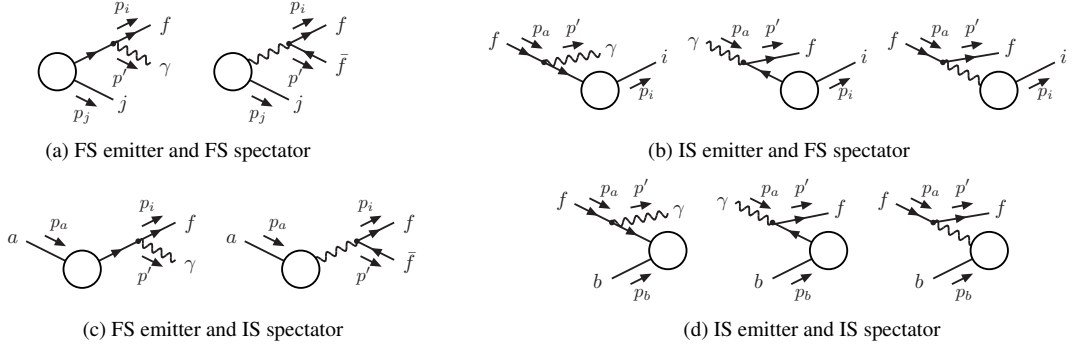


Figure 2: Diagrams illustrating the EW dipole terms with emitters and spectators in the final state (FS) or initial state (IS).

by an appropriate substitution (*abelianization*) of the QCD couplings by its QED counterparts, as described at the end of this section.²⁹

(a) *Final-state emitter and final-state spectator*

The subtraction kernels $g_{ij}^{(\text{sub})}$ and $h_{f\bar{f},j}^{\mu\nu}$ with emitter $i = f$ and spectator j in the final state are graphically illustrated in Fig. 2a and defined by

$$g_{ij}^{(\text{sub})}(p_i, p_j, k = p') = \frac{1}{(p_i p')(1-y)} \left[\frac{2}{1-z(1-y)} - 1 - z \right], \quad (314)$$

$$h_{f\bar{f},j}^{\mu\nu}(p_f = p_i, p_{\bar{f}} = p', p_j) = \frac{1}{p_i p'} \left[-g^{\mu\nu} - \frac{2}{p_i p'} (z p_i - \bar{z} p')^\mu (z p_i - \bar{z} p')^\nu \right], \quad (315)$$

where the variables y and z are given by

$$y = \frac{p_i p'}{p_i p_j + p_i p' + p_j p'}, \quad z = 1 - \bar{z} = \frac{p_i p_j}{p_i p_j + p_j p'}. \quad (316)$$

It is straightforward to check that the functions $g_{ij}^{(\text{sub})}$ and $h_{f\bar{f},j}^{\mu\nu}$ have the required asymptotic behaviour in the soft ($p' \rightarrow 0$) and collinear ($p_i p' \rightarrow 0$) limits, in which $y \rightarrow 0$ and z plays the role of the splitting variable z defined in Eq. (270). Note that we did not include explicit mass terms or terms of $\mathcal{O}(\epsilon)$ in the form of $g_{ij}^{(\text{sub})}$ and $h_{f\bar{f},j}^{\mu\nu}$ given above, because those terms do not contribute in the (IR-finite) phase-space integral of the difference $\langle |\mathcal{M}_1|^2 - |\mathcal{M}_{\text{sub}}|^2 \rangle$. Note, however, that those mass and ϵ terms are essential in the full construction and integration of the subtraction function over the singular degrees of freedom in $[dp']$.

For the evaluation of $|\mathcal{M}_0^{ab \rightarrow X}(\tilde{\Phi}_{0,ij})|^2$ and $T_{0,\mu}^{ab \rightarrow \gamma X}(\tilde{\Phi}_{0,fj})$ we have to define the mapping $\tilde{\Phi}_{0,ij}$ from Φ_1 to Φ_0 . For i and j both in the final state, it is possible to redefine only the momenta p_i , p' , and p_j , leaving all other momenta k_n in the process unaffected, $\tilde{k}_n = k_n$. The momenta \tilde{p}_i and \tilde{p}_j are chosen as

$$\tilde{p}_i^\mu = p_i^\mu + p'^\mu - \frac{y}{1-y} p_j^\mu, \quad \tilde{p}_j^\mu = \frac{1}{1-y} p_j^\mu, \quad (317)$$

where \tilde{p}_i is the momentum of the quasiparticle \tilde{i} replacing the collinear particle pair i, i' . Obviously, the new momenta have the required behaviour $\tilde{p}_i^\mu \rightarrow p_i^\mu + p'^\mu$ and $\tilde{p}_j^\mu \rightarrow p_j^\mu$ in the IR limits, and the momentum

$$P_{ij} = p_i + p_j + p' = \tilde{p}_i + \tilde{p}_j \quad (318)$$

²⁹The only exception, in which the definitions of Refs. [55, 369] and Refs. [54, 370] differ in the massless limit, is the bremsstrahlung case of final–final type. To be precise, the factor $(1-y)^{-1}$ in the function $g_{ij}^{(\text{sub})}$ of Eq. (314) is absent in the counterparts given in Refs. [54, 370], which leads to different non-singular terms in the corresponding integrated dipole functions. Marking the quantities corresponding to the definition of Refs. [54, 370] by CS, those are related to the quantities of this work by $g_{ij}^{(\text{sub})}|_{\text{CS}} = (1-y)g_{ij}^{(\text{sub})}$, $\tilde{G}_{ij}^{(\text{sub})}|_{\text{CS}} = \tilde{G}_{ij}^{(\text{sub})} + 2 \ln(1-z)/z + 1 + z$, $G_{ij}^{(\text{sub})}|_{\text{CS}} = G_{ij}^{(\text{sub})} - \pi^2/3 + 3/2$, which modifies the relations (314), (321), (322), and (326).

is left invariant by the phase-space mapping. In particular, the 3-particle invariant mass $P_{ij}^2 \geq 0$ is not affected by the mapping. The above definitions comprise all ingredients for the evaluation of the ij contribution to the difference $\langle |\mathcal{M}_1|^2 - |\mathcal{M}_{\text{sub}}|^2 \rangle$.

The second step in the subtraction procedure consists in adding back the contribution $d\sigma^{\text{sub}}$ of Eq. (313), analytically integrated over $[dp']$. This integration implicitly involves an integration over the azimuthal angle ϕ around the collinear axis, so that $h_{f\bar{f},j}^{\mu\nu}$ can be replaced by its ϕ -averaged form, as explained already in our discussion of the asymptotics in the collinear limit in the transition from Eq. (264) to Eq. (273). The singular integration with regulators is quite complicated in general, but has to be done only once owing to the process independence of the integration over the singular degrees of freedom in $[dp']$. We therefore refer to the original papers for the details and just quote the final results,

$$\int d\sigma_{ab \rightarrow f\gamma X}^{\text{sub},ij} = -\frac{\alpha}{2\pi} Q_i \sigma_i Q_j \sigma_j \int d\sigma_{ab \rightarrow fX}^{\text{LO}}(\tilde{\Phi}_{0,ij}) \int_0^1 dz \left\{ G_{ij}^{(\text{sub})}(P_{ij}^2) \delta(1-z) + [\bar{\mathcal{G}}_{ij}^{(\text{sub})}(P_{ij}^2, z)]_+ \right\} \times \Theta_{\text{cut}}(p_i = z\tilde{p}_i, p' = (1-z)\tilde{p}_i, \tilde{p}_j), \quad (319)$$

$$\int d\sigma_{ab \rightarrow f\bar{f}X}^{\text{sub},fj} = N_C^f \frac{Q_f^2 \alpha}{2\pi} \int d\sigma_{ab \rightarrow \gamma X}^{\text{LO}}(\tilde{\Phi}_{0,fj}) \int_0^1 dz \left\{ H_{f\bar{f},j}(P_{ij}^2) \delta(1-z) + [\bar{\mathcal{H}}_{f\bar{f},j}(P_{ij}^2, z)]_+ \right\} \times \Theta_{\text{cut}}(p_f = z\tilde{p}_i, p_{\bar{f}} = (1-z)\tilde{p}_i, \tilde{p}_j). \quad (320)$$

The arguments of the cut functions Θ_{cut} again indicate which momenta are subject to phase-space cuts and, in particular, show how the collinear momentum of the splitting particle is shared by the two particles resulting from the splitting. As explained already in Section 4.2.1, this momentum assignment is essential in the calculation of non-collinear-safe observables, where cuts (or histogram boundaries in differential distributions) restrict the z integration in a non-trivial way, so that the continuum parts quantified by $\bar{\mathcal{G}}_{ij}^{(\text{sub})}$ and $\bar{\mathcal{H}}_{f\bar{f},j}$ do not integrate to zero in general. In this context we emphasize that the cut functions Θ_{cut} are implicitly also part of the differential subtraction functions (307) and (308), i.e. in the subtraction terms the momenta in the arguments of Θ_{cut} are subject to the phase-space cuts, not the original momenta p_i , p' , and p_j of Φ_1 . The treatment of non-collinear-safe observables is described in detail in Ref. [369].

In MR, the integrated subtraction kernels $\bar{\mathcal{G}}_{ij}^{(\text{sub})}$, $G_{ij}^{(\text{sub})}$, $\bar{\mathcal{H}}_{f\bar{f},j}$, and $H_{f\bar{f},j}$ are explicitly given by

$$\bar{\mathcal{G}}_{ij}^{(\text{sub})}(P^2, z)|_{\text{MR}} = \hat{P}_{ff}(z) \left[\ln \left(\frac{P^2}{m_i^2} \right) + \ln z - 1 \right] + (1+z) \ln(1-z) + 1 - z, \quad (321)$$

$$G_{ij}^{(\text{sub})}(P^2)|_{\text{MR}} = \mathcal{L}(P^2, m_i^2)|_{\text{MR}} - \frac{\pi^2}{3} + \frac{3}{2}, \quad (322)$$

$$\bar{\mathcal{H}}_{f\bar{f},j}(P^2, z)|_{\text{MR}} = P_{f\gamma}(z) \left[\ln \left(\frac{P^2}{m_f^2} \right) + \ln z + \ln(1-z) - 1 \right] + 2z(1-z), \quad (323)$$

$$H_{f\bar{f},j}(P^2)|_{\text{MR}} = \frac{2}{3} \ln \left(\frac{P^2}{m_f^2} \right) - \frac{16}{9}, \quad (324)$$

where we have introduced the auxiliary function

$$\mathcal{L}(P^2, m^2)|_{\text{MR}} = \ln \left(\frac{m^2}{P^2} \right) \ln \left(\frac{m_\gamma^2}{P^2} \right) + \ln \left(\frac{m_\gamma^2}{P^2} \right) - \frac{1}{2} \ln^2 \left(\frac{m^2}{P^2} \right) + \frac{1}{2} \ln \left(\frac{m^2}{P^2} \right). \quad (325)$$

For the subtraction kernels $\bar{\mathcal{H}}_{f\bar{f},j}$ and $H_{f\bar{f},j}$ of the $\gamma \rightarrow f\bar{f}$ splitting, the transition from MR to DR follows the simple correspondence (299) including finite terms. For $\bar{\mathcal{G}}_{ij}^{(\text{sub})}$ the result in DR reads

$$\bar{\mathcal{G}}_{ij}^{(\text{sub})}(P^2, z)|_{\text{DR}} = \hat{P}_{ff}(z) \left[-\frac{(4\pi)^\epsilon}{\epsilon \Gamma(1-\epsilon)} + \ln \left(\frac{P^2}{\mu^2} \right) + \ln z + 2 \ln(1-z) \right] + (1+z) \ln(1-z) + 1 - z. \quad (326)$$

The result for $G_{ij}^{(\text{sub})}$ takes the same form as in Eq. (322), but the auxiliary function \mathcal{L} in DR is given by (see, e.g., appendix of Ref. [374])

$$\begin{aligned}\mathcal{L}(P^2, 0) \Big|_{\text{DR}} &= \Gamma(1 + \epsilon) \left(\frac{4\pi\mu^2}{P^2} \right)^\epsilon \left(\frac{1}{\epsilon^2} + \frac{3}{2\epsilon} \right) + 2 \\ &= \frac{(4\pi)^\epsilon}{\Gamma(1 - \epsilon)} \left[\frac{1}{\epsilon^2} + \frac{3}{2\epsilon} + \frac{1}{\epsilon} \ln \left(\frac{\mu^2}{P^2} \right) \right] + \frac{1}{2} \ln^2 \left(\frac{\mu^2}{P^2} \right) + \frac{3}{2} \ln \left(\frac{\mu^2}{P^2} \right) + \frac{\pi^2}{6} + 2.\end{aligned}\quad (327)$$

(b) *Initial-state emitter and final-state spectator*

The subtraction kernels $g_{ai}^{(\text{sub})}$, $h_i^{\gamma f}$, and $h_i^{ff,\mu\nu}$ with an initial-state emitter a and a final-state spectator i , are graphically illustrated in Fig. 2b and defined by

$$g_{ai}^{(\text{sub})}(p_a, p_i, k = p') = \frac{1}{(p_a p') x} \left[\frac{2}{2 - x - z} - 1 - x \right], \quad (328)$$

$$h_i^{\gamma f}(k = p_a, p_f = p', p_i) = \frac{P_{f\gamma}(x)}{(p_a p') x}, \quad (329)$$

$$h_i^{ff,\mu\nu}(p_f = p_a, p'_f = p', p_i) = \frac{1}{p_a p'} \left[-g^{\mu\nu} + \frac{2}{(p_a p') x^2 z} (z p' - \bar{z} p_i)^\mu (z p' - \bar{z} p_i)^\nu \right], \quad (330)$$

with the kinematical variables

$$x = \frac{p_a p_i + p_a p' - p_i p'}{p_a p_i + p_a p'}, \quad z = 1 - \bar{z} = \frac{p_a p_i}{p_a p_i + p_a p'}.\quad (331)$$

In the soft ($p' \rightarrow 0$) and collinear ($p_a p' \rightarrow 0$) limits, $z \rightarrow 1$ and x plays the role of the splitting variable x defined in Eq. (270). The momentum mapping from Φ_1 to the reduced phase space $\tilde{\Phi}_{0,ia}$ is given by

$$\tilde{p}_i^\mu = p_i^\mu + p'^\mu - (1 - x) p_a^\mu, \quad \tilde{p}_a^\mu = x p_a^\mu, \quad (332)$$

with all other momenta of the process left unchanged. This momentum redefinition changes the initial state, so that the original CM frame and the one of the hard process (with $x p_a$ as incoming momentum) are related by a boost along the beam axis with the relative velocity $(1 - x)/(1 + x)$. The OS relations $\tilde{p}_i^2 = \tilde{p}_a^2 = 0$ as well as momentum conservation,

$$P_{ia} = p_i + p' - p_a = \tilde{p}_i - \tilde{p}_a, \quad (333)$$

are easily seen to hold, and the virtuality $P_{ia}^2 < 0$ is left unchanged by the momentum mapping. Together with the hard scattering amplitudes \mathcal{M}_0 (or partial amplitudes T_0^μ), these ingredients define the considered contributions to $|\mathcal{M}_{\text{sub}}|^2$ completely, so that the contribution to $d\sigma^{\text{real-sub}}$ of Eq. (312) can be evaluated numerically.

In order to evaluate the contribution to $d\sigma^{\text{sub}}$ of Eq. (313), the subtraction kernels have to be analytically integrated over the $[dp']$. In view of this, the same comments as made for the previous case of final-state emitter and spectator apply, up to one point. Now the hard LO cross section depends on x , so that the $[dp']$ integration cannot be carried out completely analytically. The process-dependent x integration has to be left for a numerical treatment. Since the x integration is soft singular near its endpoint at $x \rightarrow 1$ for the $f \rightarrow f\gamma$ splitting with a real photon, it is convenient to split off this endpoint contribution by a $(\dots)_+$ prescription. The resulting cross-section contributions read

$$\int d\sigma_{fb \rightarrow \gamma X}^{\text{sub},ai} = -\frac{\alpha}{2\pi} Q_a \sigma_a Q_i \sigma_i \int_0^1 dx \int d\sigma_{fb \rightarrow X}^{\text{LO}}(\tilde{\Phi}_{0,ai}(x)) \left\{ \left[\mathcal{G}_{ai}^{(\text{sub})}(P_{ia}^2, x) \right]_+ + \delta(1 - x) G_{ai}^{(\text{sub})}(P_{ia}^2) \right\}, \quad (334)$$

$$\int d\sigma_{\gamma b \rightarrow f X}^{\text{sub},\gamma i} = N_C^f \frac{Q_f^2 \alpha}{2\pi} \int_0^1 dx \int d\sigma_{fb \rightarrow X}^{\text{LO}}(\tilde{\Phi}_{0,ai}(x)) \mathcal{H}_i^{\gamma f}(P_{ia}^2, x), \quad (335)$$

$$\int d\sigma_{fb \rightarrow f X}^{\text{sub},fi} = \frac{Q_f^2 \alpha}{2\pi} \int_0^1 dx \int d\sigma_{\gamma b \rightarrow X}(\tilde{\Phi}_{0,ai}(x)) \mathcal{H}_i^{ff}(P_{ia}^2, x), \quad (336)$$

with the mass-regularized integrated subtraction kernels

$$\mathcal{G}_{ai}^{(\text{sub})}(P^2, x) \Big|_{\text{MR}} = \hat{P}_{ff}(x) \left[\ln \left(\frac{-P^2}{m_f^2} \right) - \ln x - 1 \right] - \frac{2 \ln(2-x)}{1-x} + (1+x) \ln(1-x) + 1-x, \quad (337)$$

$$G_{ai}^{(\text{sub})}(P^2) \Big|_{\text{MR}} = \mathcal{L}(-P^2, m_f^2) \Big|_{\text{MR}} + \frac{\pi^2}{6} - 1, \quad (338)$$

$$\mathcal{H}_i^{\gamma f}(P^2, x) \Big|_{\text{MR}} = P_{f\gamma}(x) \left[\ln \left(\frac{-P^2}{m_f^2} \right) + \ln(1-x) - \ln x \right] + 2x(1-x), \quad (339)$$

$$\mathcal{H}_i^{ff}(P^2, x) \Big|_{\text{MR}} = P_{\gamma f}(x) \left[\ln \left(\frac{-P^2}{m_f^2} \right) + \ln(1-x) - 3 \ln x - 1 \right] + x. \quad (340)$$

The subtraction kernel $\mathcal{H}_i^{\gamma f}$ translates into DR according to Eq. (299) including finite terms. In DR, the kernels $\mathcal{G}_{ai}^{(\text{sub})}$ and \mathcal{H}_i^{ff} read

$$\mathcal{G}_{ai}^{(\text{sub})}(P^2, x) \Big|_{\text{DR}} = \hat{P}_{ff}(x) \left[-\frac{(4\pi)^\epsilon}{\epsilon \Gamma(1-\epsilon)} + \ln \left(\frac{-P^2}{\mu^2} \right) - \ln x + 2 \ln(1-x) \right] - \frac{2 \ln(2-x)}{1-x} + (1+x) \ln(1-x) + 1-x, \quad (341)$$

$$\mathcal{H}_i^{ff}(P^2, x) \Big|_{\text{DR}} = P_{\gamma f}(x) \left[-\frac{(4\pi)^\epsilon}{\epsilon \Gamma(1-\epsilon)} + \ln \left(\frac{-P^2}{\mu^2} \right) + \ln(1-x) - \ln x \right] + x, \quad (342)$$

and $G_{ai}^{(\text{sub})}$ is evaluated as in Eq. (338), but with \mathcal{L} given in Eq. (327).

(c) *Final-state emitter and initial-state spectator*

The subtraction kernels $g_{ia}^{(\text{sub})}$ and $h_{f\bar{f}}^{a,\mu\nu}$ with a final-state emitter i and an initial-state spectator a are graphically illustrated in Fig. 2c and defined by

$$g_{ia}^{(\text{sub})}(p_i, p_a, k = p') = \frac{1}{(p_i p') x} \left[\frac{2}{2-x-z} - 1 - z \right], \quad (343)$$

$$h_{f\bar{f}}^{a,\mu\nu}(p_f = p_i, p_{\bar{f}} = p', p_a) = \frac{1}{p_i p'} \left[-g^{\mu\nu} - \frac{2}{p_i p'} (z p_i - \bar{z} p')^\mu (z p_i - \bar{z} p')^\nu \right], \quad (344)$$

with the kinematical variables defined in Eq. (331). The whole kinematical construction of new momenta \tilde{p}_a and \tilde{p}_i is the same as in the previous case, since only the roles of a and i as emitter or spectator are interchanged, i.e. Eqs. (332) and (333) remain valid. The interpretation of the variables x and z , however, changes. In the soft ($p' \rightarrow 0$) and collinear ($p_i p' \rightarrow 0$) limits with i as emitter, $x \rightarrow 1$ and z plays the role of the splitting variable defined in Eq. (270).

The contributions to $d\sigma^{\text{sub}}$ of Eq. (313) can be worked out in a way similar to the previous case where the roles of emitter and spectator are interchanged. The results take the form of a convolution over x , and for the $f \rightarrow f\gamma$ splitting with a real photon the soft-singular endpoint contribution is again separated by a $(\dots)_+$ prescription. In order to cover the case of non-collinear-safe observables, however, a new feature arises, since the information on both the variable x and the splitting variable z , which rules the momentum share in the configuration of the collinear particle pair, should be made accessible in the numerical evaluation. However, the z integration is soft singular at its endpoint at $z \rightarrow 1$, which renders a plain numerical integration over z rather inconvenient. The solution to this problem is again to introduce a $(\dots)_+$ prescription in the z integration as well. The resulting distribution $(\dots)_+^{(x,z)}$ for the double integral is defined as

$$\int_0^1 dx \int_0^1 dz \left[f(x, z) \right]_+^{(x,z)} g(x, z) = \int_0^1 dx \int_0^1 dz f(x, z) [g(x, z) - g(x, 1) - g(1, z) + g(1, 1)], \quad (345)$$

where $g(x, z)$ is some test function of two independent variables. Further details on the introduction and the evaluation of this distribution can be found in Ref. [369]. Using this prescription, the cross-section contributions to $d\sigma^{\text{sub}}$ can be written as

$$\begin{aligned} \int d\sigma_{ab \rightarrow f\gamma X}^{\text{sub},ia} = & -\frac{\alpha}{2\pi} Q_a \sigma_a Q_i \sigma_i \int_0^1 dx \int d\sigma_{ab \rightarrow fX}^{\text{LO}}(\tilde{\Phi}_{0,ia}(x)) \int_0^1 dz \left\{ \left[\bar{g}_{ia}^{\text{(sub)}}(x, z) \right]_+^{(x,z)} \right. \\ & + \delta(1-z) \left[\mathcal{G}_{ia}^{\text{(sub)}}(P_{ia}^2, x) \right]_+ + \delta(1-x) \left[\bar{\mathcal{G}}_{ia}^{\text{(sub)}}(P_{ia}^2, z) \right]_+ + \delta(1-x) \delta(1-z) G_{ia}^{\text{(sub)}}(P_{ia}^2) \left. \right\} \\ & \times \Theta_{\text{cut}}(p_f = z \tilde{p}_i(x), k = (1-z) \tilde{p}_i(x)), \end{aligned} \quad (346)$$

$$\begin{aligned} \int d\sigma_{ab \rightarrow f\bar{f}X}^{\text{sub},fa} = & N_C^f \frac{Q_f^2 \alpha}{2\pi} \int_0^1 dx \int d\sigma_{ab \rightarrow \gamma X}^{\text{LO}}(\tilde{\Phi}_{0,ia}(x)) \int_0^1 dz \left\{ \left[\bar{h}_{f\bar{f}}^a(x, z) \right]_+^{(x,z)} \right. \\ & + \delta(1-z) \left[\mathcal{H}_{f\bar{f}}^a(P_{ia}^2, x) \right]_+ + \delta(1-x) \left[\bar{\mathcal{H}}_{f\bar{f}}^a(P_{ia}^2, z) \right]_+ + \delta(1-x) \delta(1-z) H_{f\bar{f}}^a(P_{ia}^2) \left. \right\} \\ & \times \Theta_{\text{cut}}(p_f = z \tilde{p}_i(x), p_{\bar{f}} = (1-z) \tilde{p}_i(x)), \end{aligned} \quad (347)$$

where the arguments of the step function Θ_{cut} again indicate which momenta resulting from the final-state splitting are subject to phase-space cuts.

Using MR, the various subtraction kernels are given by

$$\bar{g}_{ia}^{\text{(sub)}}(x, z) \Big|_{\text{MR}} = \frac{1}{1-x} \left(\frac{2}{2-x-z} - 1 - z \right), \quad (348)$$

$$\mathcal{G}_{ia}^{\text{(sub)}}(P^2, x) \Big|_{\text{MR}} = \frac{1}{1-x} \left[2 \ln \left(\frac{2-x}{1-x} \right) - \frac{3}{2} \right], \quad (349)$$

$$\bar{\mathcal{G}}_{ia}^{\text{(sub)}}(P^2, z) \Big|_{\text{MR}} = \hat{P}_{ff}(z) \left[\ln \left(\frac{-P^2}{m_f^2} \right) + \ln z - 1 \right] - \frac{2 \ln(2-z)}{1-z} + (1+z) \ln(1-z) + 1 - z, \quad (350)$$

$$G_{ia}^{\text{(sub)}}(P_{ia}^2) \Big|_{\text{MR}} = \mathcal{L}(-P^2, m_f^2) \Big|_{\text{MR}} - \frac{\pi^2}{2} + \frac{3}{2}, \quad (351)$$

$$\bar{h}_{f\bar{f}}^a(x, z) \Big|_{\text{MR}} = \frac{x}{1-x} P_{f\gamma}(z), \quad (352)$$

$$\mathcal{H}_{f\bar{f}}^a(P^2, x) \Big|_{\text{MR}} = \frac{2x}{3(1-x)}, \quad (353)$$

$$\bar{\mathcal{H}}_{f\bar{f}}^a(P^2, z) \Big|_{\text{MR}} = P_{f\gamma}(z) \left[\ln \left(\frac{-P^2}{m_f^2} \right) + \ln z + \ln(1-z) - 1 \right] + 2z(1-z), \quad (354)$$

$$H_{f\bar{f}}^a(P^2) \Big|_{\text{MR}} = \frac{2}{3} \ln \left(\frac{-P^2}{m_f^2} \right) - \frac{16}{9}. \quad (355)$$

In the transition to DR, the non-singular functions remain unchanged. The mass-singular integrated $\gamma \rightarrow f\bar{f}$ splitting kernels $\bar{\mathcal{H}}_{f\bar{f}}^a$ and $H_{f\bar{f}}^a$ translate into DR according to Eq. (299). For the mass-singular $f \rightarrow f\gamma$ splitting kernels the translation is more complicated; in DR $\bar{\mathcal{G}}_{ia}^{\text{(sub)}}$ reads

$$\bar{\mathcal{G}}_{ia}^{\text{(sub)}}(P^2, z) \Big|_{\text{DR}} = \hat{P}_{ff}(z) \left[-\frac{(4\pi)^\epsilon}{\epsilon \Gamma(1-\epsilon)} + \ln \left(\frac{-P^2}{\mu^2} \right) + \ln z + 2 \ln(1-z) \right] - \frac{2 \ln(2-z)}{1-z} + (1+z) \ln(1-z) + 1 - z, \quad (356)$$

and $G_{ia}^{\text{(sub)}}$ has to be evaluated as in Eq. (351) but with \mathcal{L} given in Eq. (327).

(d) *Initial-state emitter and initial-state spectator*

The subtraction kernels $g_{ab}^{(\text{sub})}$, $h^{\gamma f,a}$, and $h^{ff,a\mu\nu}$ with emitter a and spectator b in the initial state are graphically illustrated in Fig. 2d and defined by

$$g_{ab}^{(\text{sub})}(p_a, p_b, k = p') = \frac{1}{(p_a p')x} \left[\frac{2}{1-x} - 1 - x \right], \quad (357)$$

$$h^{\gamma f,b}(k = p_a, p_f = p', p_b) = \frac{P_{f\gamma}(x)}{(p_a p')x}, \quad (358)$$

$$h^{ff,b,\mu\nu}(p_f = p_a, p'_f = p', p_b) = \frac{1}{p_a p'} \left[-g^{\mu\nu} + \frac{2(1-x)}{(p' p_b)x^2 y} (p' - y p_b)^\mu (p' - y p_b)^\nu \right], \quad (359)$$

with the kinematical variables

$$x = \frac{p_a p_b - p_a p' - p_b p'}{p_a p_b}, \quad y = \frac{p_a p'}{p_a p_b}. \quad (360)$$

In the soft ($p' \rightarrow 0$) and collinear ($p_a p' \rightarrow 0$) limits, $y \rightarrow 0$ and x takes over the role of the splitting variable of Eq. (331). If both emitter and spectator are from the initial state, a mere modification of the emitter and spectator momenta in the mapping $\Phi_1 \rightarrow \tilde{\Phi}_0$ would change the direction of the beam axis, so that it is more appropriate to modify only the emitter momentum p_a and all outgoing momenta k_n , while keeping the spectator momentum p_b fixed. Defining the new incoming momenta according to

$$\tilde{p}_a^\mu = x p_a^\mu, \quad \tilde{p}_b^\mu = p_b^\mu, \quad (361)$$

the total outgoing momentum for the hard scattering process (i.e. without p' from the splitting) before and after the momentum mapping is

$$P_{ab} = p_a + p_b - p' = \sum_n k_n, \quad \tilde{P}_{ab}^\mu = x_{ab} p_a^\mu + p_b^\mu = \sum_n \tilde{k}_n, \quad (362)$$

respectively. Obviously, the OS conditions $\tilde{p}_a^2 = \tilde{p}_b^2 = 0$ are fulfilled. Moreover, by construction the invariant mass squared of the produced particles, $P_{ab}^2 > 0$, does not change by the momentum mapping, $P_{ab}^2 = \tilde{P}_{ab}^2$, so that the mapping of all k_n to \tilde{k}_n can be accomplished by a Lorentz transformation

$$\tilde{k}_n^\mu = \Lambda^\mu_\nu k_n^\nu \quad (363)$$

with

$$\Lambda^\mu_\nu = g^\mu_\nu - \frac{(P_{ab} + \tilde{P}_{ab})^\mu (P_{ab} + \tilde{P}_{ab})_\nu}{P_{ab}^2 + P_{ab} \tilde{P}_{ab}} + \frac{2 \tilde{P}_{ab}^\mu P_{ab,\nu}}{P_{ab}^2}, \quad (364)$$

and all outgoing particles from the hard process stay on their mass shell, $\tilde{k}_n^2 = k_n^2$. This completes the construction of the respective contributions to the subtraction function $|\mathcal{M}_{\text{sub}}|^2$ needed for the numerical evaluation of Eq. (312).

The contributions to $d\sigma^{\text{sub}}$ of Eq. (313) can be worked out without further complications and take the form of one-dimensional convolutions over x , and the soft-singular endpoint contribution of the $f \rightarrow f\gamma$ splitting with a real photon is again separated by a $(\cdots)_+$ prescription. The corresponding results are

$$\int d\sigma_{fb \rightarrow \gamma X}^{\text{sub},ab} = -\frac{\alpha}{2\pi} Q_a \sigma_a Q_b \sigma_b \int_0^1 dx \int d\sigma_{fb \rightarrow X}^{\text{LO}}(\tilde{\Phi}_{0,ab}(x)) \left\{ \left[\mathcal{G}_{ab}^{(\text{sub})}(s, x) \right]_+ + \delta(1-x) G_{ab}^{(\text{sub})}(s) \right\}, \quad (365)$$

$$\int d\sigma_{\gamma b \rightarrow f X}^{\text{sub},\gamma b} = N_C^f \frac{Q_f^2 \alpha}{2\pi} \int_0^1 dx \int d\sigma_{\bar{f}b \rightarrow X}^{\text{LO}}(\tilde{\Phi}_{0,ab}(x)) \mathcal{H}^{\gamma f,b}(s, x), \quad (366)$$

$$\int d\sigma_{fb \rightarrow f X}^{\text{sub},fb} = \frac{Q_f^2 \alpha}{2\pi} \int_0^1 dx \int d\sigma_{\gamma b \rightarrow X}^{\text{LO}}(\tilde{\Phi}_{0,ab}(x)) \mathcal{H}^{ff,b}(s, x), \quad (367)$$

where $s = (p_a + p_b)^2$ is the squared CM energy in the original process.

In MR the corresponding integrated subtraction kernels are given by

$$\mathcal{G}_{ab}^{(\text{sub})}(s, x) \Big|_{\text{MR}} = \hat{P}_{ff}(x) \left[\ln \left(\frac{s}{m_f^2} \right) - 1 \right] + 1 - x, \quad (368)$$

$$G_{ab}^{(\text{sub})}(s) \Big|_{\text{MR}} = \mathcal{L}(s, m_f^2) \Big|_{\text{MR}} - \frac{\pi^2}{3} + 2, \quad (369)$$

$$\mathcal{H}^{\gamma f, b}(s, x) \Big|_{\text{MR}} = P_{f\gamma}(x) \left[\ln \left(\frac{s}{m_f^2} \right) + 2 \ln(1 - x) \right] + 2x(1 - x), \quad (370)$$

$$\mathcal{H}^{ff, b}(s, x) \Big|_{\text{MR}} = P_{\gamma f}(x) \left[\ln \left(\frac{s}{m_f^2} \right) + 2 \ln(1 - x) - 2 \ln x - 1 \right] + x. \quad (371)$$

In DR, $\mathcal{H}^{\gamma f, b}$ can be obtained by the correspondence (299) including finite terms, while $\mathcal{G}_{ab}^{(\text{sub})}$ and $\mathcal{H}^{ff, b}$ are given by

$$\mathcal{G}_{ab}^{(\text{sub})}(s, x) \Big|_{\text{DR}} = \hat{P}_{ff}(x) \left[-\frac{(4\pi)^\epsilon}{\epsilon \Gamma(1 - \epsilon)} + \ln \left(\frac{s}{\mu^2} \right) + 2 \ln(1 - x) \right] + 1 - x, \quad (372)$$

$$\mathcal{H}^{ff, b}(s, x) \Big|_{\text{DR}} = P_{\gamma f}(x) \left[-\frac{(4\pi)^\epsilon}{\epsilon \Gamma(1 - \epsilon)} + \ln \left(\frac{s}{\mu^2} \right) + 2 \ln(1 - x) \right] + x, \quad (373)$$

and $G_{ab}^{(\text{sub})}$ has to be evaluated as in Eq. (369), but with the dimensionally regularized version of \mathcal{L} given in Eq. (327).

We end this brief introduction to dipole subtraction by mentioning a byproduct of the formalism. The subtraction function $|\mathcal{M}_{\text{sub}}|^2$ resembles all IR singularities in the squared real-emission amplitudes, so that $d\sigma^{\text{sub}}$ of Eq. (313) comprises all IR-singular real corrections to cross sections. As stated by the KLN theorem, all IR-singular (virtual + real) corrections to differential cross sections cancel for processes with neutral initial-state particles if final-state particles are treated in a collinear-safe way. This implies that the IR-singular contributions of the virtual corrections $d\sigma^{\text{virt}}$ are the same as in $-d\sigma^{\text{sub}}$ for processes with neutral initial-state particles. The generalization of this statement on $d\sigma^{\text{virt}}$ to processes with charged initial-state particles can be obtained via *crossing*, i.e. for a given process first consider all particles outgoing to derive the virtual IR singularities and then apply crossing relations to the result in order to restore the original initial state. This strategy was used in Ref. [400] to predict the complete IR structure of virtual NLO QCD corrections in DR or MR for any generic process. It is straightforward to transfer this result to NLO EW corrections by “abelianization”. Using the notation of Ref. [400] for QCD amplitudes, the mass-singular NLO EW corrections can be obtained by the substitutions

$$g_s \rightarrow e, \quad \alpha_s \rightarrow \alpha, \quad \mathbf{T}_j \cdot \mathbf{T}_k \rightarrow Q_j \sigma_j Q_k \sigma_k, \quad C_A \rightarrow 0, \quad C_F \rightarrow Q_f^2, \quad T_R \rightarrow N_C^f Q_f^2. \quad (374)$$

Note, however, that this procedure only produces all mass-singular terms that have a counterpart in real-emission processes. For instance, potentially mass-singular contributions resulting from electric charge renormalization are not concerned.

4.3. Electromagnetic corrections to parton distribution functions

4.3.1. Factorization of photonic initial-state singularities

In quantum field theory, the cancellation of IR divergences is generally ruled by the KLN theorem [365, 367]. The key feature for the cancellation is the necessary level of inclusiveness in the particle configuration w.r.t. the degeneracy in energy. For soft singularities, the degeneracy concerns states with different numbers of soft massless particles, i.e. gluons or photons. For NLO EW corrections this means that soft singularities always cancel between virtual EW and real photonic corrections in physical (IR-finite) observables, a statement that is analogous to the Bloch–Nordsieck theorem of QED [366]. For collinear singularities, a complete compensation only takes place if the collinear configurations of massless (or light) particles or partons are treated inclusively in the event selection.

Phrased in more simple words, distributing the total momentum of the collinear many-particle state to the individual collinear particles differently should not shift the considered event over any phase-space cut or histogram boundary in a cross-section calculation.

According to the parton model (see standard textbooks such as Refs. [83, 86, 87, 93, 401]), a parton (quark, gluon, etc.) inside a hadron h of momentum p is characterized by its flavour a , its momentum xp , with x denoting the momentum fraction of the parton, and by its parton distribution function (PDF) $f_a^{(h)}(x)$, which—naively interpreted—is the probability density to find a inside h with momentum fraction x . In the case of collinear initial-state radiation, where the parton momentum xp is further reduced by some factor ξ , the process is effectively initiated by the momentum ξxp with a weight depending on ξ non-trivially. This implies that IR singularities from collinear initial-state radiation remain after summing virtual and real corrections, since inclusiveness w.r.t. all ξ values is missing. This flaw of the *naive parton model* is cured within the *QCD-improved parton model by factorization*, which absorbs the uncancelled collinear singularities into redefined PDFs. In other words, the effects of collinear initial-state radiation are considered as a property of the hadron rather than of the hard scattering process. The proof of the universality (process independence) of the collinear singularities, however, is non-trivial; a detailed discussion of this issue can, for instance, be found in Ref. [402]. The PDF redefinition effectively separates the long-distance effects caused by collinear radiation from the short-distance physics going on in the hard scattering process, a procedure that introduces the so-called *factorization scale* μ_F , which is widely ambiguous. After their redefinition, the PDFs inherit a dependence on μ_F , which is controlled by the famous Dokshitzer–Gribov–Lipatov–Altarelli–Parisi (DGLAP) equations [403–405]. Likewise the hard partonic scattering process receives some explicit μ_F dependence from the subtraction of the collinear singularities, but physically observable hadronic cross sections σ must not depend on μ_F . In practice, some μ_F dependence, however, remains in predictions owing to the necessary truncation of the perturbative series on which the calculation of the hard partonic cross section $\hat{\sigma}$ is based. Such residual scale dependences are part of the overall theoretical uncertainty of the prediction. We exemplify the calculation of a hadronic cross section from the scattering of two hadrons h_1 and h_2 (e.g. protons at the LHC):

$$\int d\sigma_{h_1 h_2}(p_1, p_2) = \sum_{a,b} \int_0^1 dx_1 \int_0^1 dx_2 f_a^{(h_1)}(x_1, \mu_F^2) f_b^{(h_2)}(x_2, \mu_F^2) \int d\hat{\sigma}_{ab}(x_1 p_1, x_2 p_2, \mu_F^2), \quad (375)$$

where a and b are all relevant partons in h_1 and h_2 , respectively. If h is not explicitly written in $f_a^{(h)}(x, \mu_F^2)$ in the following, $h = p$ = proton is assumed by default.

The calculation of EW corrections to hadronic scattering processes requires the generalization of the concept of QCD factorization and PDF redefinition to QED, i.e. to the inclusion of the photon as parton. Fortunately, this generalization is straightforward. The generic size of the collinear QED singularities is controlled by α instead of α_s , so that the corresponding QED-driven PDF evolution effects, factorization-scale dependences, etc., are typically much smaller than in QCD. Another important difference is due to the fact that photons do not self-interact.

Since we have worked out the general form of NLO EW collinear singularities for all possible splittings involving light charged fermions and photons in the previous section, we can immediately identify the contributions of QED singularities from collinear initial-state splittings to cross sections. Starting from a hadronic cross section in the form (375), but calculated from *bare PDFs* $f_a^{(h)}(x)$, the following PDF redefinition for (anti)quarks and photons removes all QED initial-state singularities from $\sigma_{h_1 h_2}$,

$$\begin{aligned} f_{q/\bar{q}}^{(h)}(x) &\rightarrow f_{q/\bar{q}}^{(h)}(x, \mu_F^2) - \frac{\alpha Q_q^2}{2\pi} \int_x^1 \frac{d\xi}{\xi} f_{q/\bar{q}}^{(h)}\left(\frac{x}{\xi}, \mu_F^2\right) \left\{ -\frac{(4\pi)^\epsilon}{\Gamma(1-\epsilon)} \left(\frac{\mu^2}{\mu_F^2}\right)^\epsilon \frac{1}{\epsilon} P_{ff}(\xi) + C_{ff}(\xi) \right\} \\ &\quad - N_C^q \frac{\alpha Q_q^2}{2\pi} \int_x^1 \frac{d\xi}{\xi} f_\gamma^{(h)}\left(\frac{x}{\xi}, \mu_F^2\right) \left\{ -\frac{(4\pi)^\epsilon}{\Gamma(1-\epsilon)} \left(\frac{\mu^2}{\mu_F^2}\right)^\epsilon \frac{1}{\epsilon} P_{f\gamma}(\xi) + C_{f\gamma}(\xi) \right\}, \end{aligned} \quad (376)$$

$$\begin{aligned} f_\gamma^{(h)}(x) &\rightarrow f_\gamma^{(h)}(x, \mu_F^2) - N_C^q \frac{\alpha}{2\pi} \int_x^1 \frac{d\xi}{\xi} f_\gamma^{(h)}\left(\frac{x}{\xi}, \mu_F^2\right) \sum_{a=q} Q_a^2 \left\{ -\frac{(4\pi)^\epsilon}{\Gamma(1-\epsilon)} \left(\frac{\mu^2}{\mu_F^2}\right)^\epsilon \frac{1}{\epsilon} P_{\gamma\gamma}(\xi) + C_{\gamma\gamma}(\xi) \right\} \\ &\quad - \frac{\alpha}{2\pi} \sum_{a=q, \bar{q}} Q_a^2 \int_x^1 \frac{d\xi}{\xi} f_a^{(h)}\left(\frac{x}{\xi}, \mu_F^2\right) \left\{ -\frac{(4\pi)^\epsilon}{\Gamma(1-\epsilon)} \left(\frac{\mu^2}{\mu_F^2}\right)^\epsilon \frac{1}{\epsilon} P_{\gamma f}(\xi) + C_{\gamma f}(\xi) \right\}. \end{aligned} \quad (377)$$

The gluon PDF is not redefined at NLO EW, since it does not have any EW coupling. The splitting functions P_{ab} are the ones introduced in Eq. (261). Up to the different coupling factors, they are the same as for the quark–gluon system, with the only exception of $P_{\gamma\gamma}(\xi)$, which is entirely due to some “hard contact term” $\propto \delta(1 - \xi)$. This term is needed in the sum rules

$$\int_0^1 d\xi P_{ff}(\xi) = 0, \quad \int_0^1 d\xi \xi [P_{ff}(\xi) + P_{\gamma f}(\xi)] = 0, \quad \int_0^1 d\xi \xi [2P_{f\gamma}(\xi) + P_{\gamma\gamma}(\xi)] = 0, \quad (378)$$

which guarantee charge and momentum conservation when μ_F is changed.

Note that the replacements (376) and (377) are to be applied in the strict NLO sense, i.e. after the PDF replacements only linear contributions of relative order $O(\alpha)$ are kept, while $O(\alpha^2)$ terms are dropped. This effectively leads to an additional NLO contribution—also known as *collinear counterterm*—to the partonic cross section, cancelling the initial-state collinear singularities of the virtual one-loop and real emission corrections. The full NLO partonic cross section, thus, is given by the sum

$$d\hat{\sigma}_{ab} = d\hat{\sigma}_{ab}^0 + d\hat{\sigma}_{ab}^{\text{virt}} + d\hat{\sigma}_{ab}^{\text{real}} + d\hat{\sigma}_{ab}^{\text{coll-ct}}, \quad (379)$$

where $d\hat{\sigma}_{ab}^0$, $d\hat{\sigma}_{ab}^{\text{virt}}$, $d\hat{\sigma}_{ab}^{\text{real}}$, and $d\hat{\sigma}_{ab}^{\text{coll-ct}}$ refer to the lowest-order, virtual one-loop, real emission, and collinear counterterm contributions, respectively.

The PDF redefinitions (376) and (377) are formulated in DR, which corresponds to the common standard in QCD. Recall that μ is the reference mass scale of DR without any physical meaning; it is neither identical to the renormalization scale μ_R nor to μ_F . Many NLO EW calculations, however, employ MR with small fermion masses as regulators for mass singularities. Regularizing initial-state collinear singularities with small quark masses m_q , the PDF redefinitions read

$$\begin{aligned} f_{q/\bar{q}}^{(h)}(x) &\rightarrow f_{q/\bar{q}}^{(h)}(x, \mu_F^2) - \frac{\alpha Q_q^2}{2\pi} \int_x^1 \frac{d\xi}{\xi} f_{q/\bar{q}}^{(h)}\left(\frac{x}{\xi}, \mu_F^2\right) \left\{ \ln\left(\frac{\mu_F^2}{m_q^2}\right) P_{ff}(\xi) - \left[\hat{P}_{ff}(\xi) (2 \ln(1 - \xi) + 1) \right]_+ + C_{ff}(\xi) \right\} \\ &\quad - N_C^q \frac{\alpha Q_q^2}{2\pi} \int_x^1 \frac{d\xi}{\xi} f_\gamma^{(h)}\left(\frac{x}{\xi}, \mu_F^2\right) \left\{ \ln\left(\frac{\mu_F^2}{m_q^2}\right) P_{f\gamma}(\xi) + C_{f\gamma}(\xi) \right\}, \end{aligned} \quad (380)$$

$$\begin{aligned} f_\gamma^{(h)}(x) &\rightarrow f_\gamma^{(h)}(x, \mu_F^2) - N_C^q \frac{\alpha}{2\pi} \int_x^1 \frac{d\xi}{\xi} f_\gamma^{(h)}\left(\frac{x}{\xi}, \mu_F^2\right) \sum_{a=q} Q_a^2 \left\{ \ln\left(\frac{\mu_F^2}{m_a^2}\right) P_{\gamma\gamma}(\xi) + C_{\gamma\gamma}(\xi) \right\} \\ &\quad - \frac{\alpha}{2\pi} \sum_{a=q,\bar{q}} Q_a^2 \int_x^1 \frac{d\xi}{\xi} f_a^{(h)}\left(\frac{x}{\xi}, \mu_F^2\right) \left\{ \ln\left(\frac{\mu_F^2}{m_a^2}\right) P_{\gamma f}(\xi) - P_{\gamma f}(\xi) (2 \ln \xi + 1) + C_{\gamma f}(\xi) \right\}. \end{aligned} \quad (381)$$

Obviously the standard collinear divergence $\Delta + \ln(\mu^2)$ in DR corresponds to the mass-singular term $\ln m_q^2$, as expressed by the correspondence (299), but it should be realized that the correspondence involves non-trivial IR-finite contributions for the parts involving the splitting functions P_{ff} and $P_{\gamma f}$. The precise form of those terms can be obtained by comparing the collinear singularities in the functions $\mathcal{H}^{f\gamma}$ and \mathcal{H}^{ff} in MR, i.e. Eqs. (293) and (295), with their counterparts in DR, Eqs. (302) and (300). The differences between the functions in the two regularization schemes can be calculated either taking the results for two-cutoff slicing given in Section 4.2.1 or the ones for dipole subtraction, where $\mathcal{H}^{f\gamma}$ is replaced by \mathcal{G}^{ab} , given in Section 4.2.2. Translating the PDF redefinitions between regularization schemes in this way guarantees that the *coefficient functions* $C_{ab}(\xi)$, which define the *factorization scheme*, are identical in the two regularization schemes. Nowadays, practically all hadronic cross sections are calculated within the *MS factorization scheme*, which corresponds to

$$C_{ab}^{\overline{\text{MS}}}(\xi) = 0. \quad (382)$$

The *DIS scheme* [401, 406], which absorbs all corrections to the structure function F_2 of deep-inelastic electron–proton scattering into the PDFs, is hardly in use anymore.

In the PDF redefinitions at NLO EW, we did not yet make the precise form of the electromagnetic coupling α explicit. Taking the formalism of the QCD-improved parton model literally, the running coupling $\alpha(\mu_F^2)$ as dictated by the employed factorization scheme should be used. In NLO EW calculations (or in higher EW orders), however, the

choice of α is typically adjusted to the specific process, in order to minimize universal corrections of higher order (cf. Section 5.1). Note that this is not a contradiction. It simply means that the explicit α appearing in Eqs. (376), (377), (380), and (381) has to be identified with the α used to calculate all matrix elements; otherwise the cancellation of the initial-state collinear singularities would be incomplete. The mismatch between the α used in the PDF evolution and in the matrix elements only concerns effects of NNLO EW or higher. *Leading* universal corrections beyond NLO EW can still be controlled. We will come back to the issue of schemes to set α in the discussion of photon-induced processes below.

Finally, we comment on the role of charged leptons l in the context of mass singularities from collinear splittings in the partonic initial state. Initial-state photons can split according to $\gamma \rightarrow l\bar{l}^*/\bar{l}l^*$, where \bar{l}^*/l^* initiates the hard scattering process. This leads to collinear singularities if the outgoing lepton l/\bar{l} gets lost in the beam direction. If such initial-state singularities are absorbed into the photon PDF, the DGLAP formalism demands also PDFs for charged leptons [407]. Since the introduction and evolution of lepton PDFs indirectly proceeds via the photon PDF, which is already suppressed, PDFs of charged leptons are usually not considered. Moreover, mass singularities of leptons can be treated perturbatively.

4.3.2. QED-corrected PDFs and photon distribution function

The inclusion of EW $O(\alpha)$ corrections in the DGLAP evolution has an influence on all PDFs [408–410], but owing to the hierarchy $\alpha \ll \alpha_s$ the impact is quite small. For $\mu_F \sim M_W$, which is typical for many LHC processes, quark and antiquark PDFs are changed at the level of 0.3% (1%) for $x \lesssim 0.1$ (0.4). This influences also the gluon PDF via the momentum sum rule for the proton. Moreover, including the photon in the list of partons, a photon distribution function appears. The latter is similar to the gluon PDF in shape, but relatively suppressed by roughly a factor of $\langle Q_q^2 \rangle \alpha / \alpha_s \sim 10^{-2}$ for not too high x values, where $\langle Q_q^2 \rangle$ stands for some average squared quark charge. It should also be realized that the photon PDF actually consists of both inelastic and elastic components, where the latter corresponds to the situation when the proton (or the considered hadron) does not break up in the scattering process.

The first global PDF set including QED corrections was MRST2004qed [411] where the photon PDF was based on some simple modelling and a fit to deep-inelastic ep scattering data; an error estimate in a later version of this PDF set confirmed the initial expectation that the photon PDF was good within roughly 20%. About ten years later, the NNPDF group supported QED corrections and photon PDFs in the NNPDF23qed [412] and NNPDF30qed [413] PDF sets, which were derived from experimental data (DIS, Drell–Yan-like W/Z production). Since photon-induced contributions are generically small in standard candle processes used in PDF fits, the so-obtained photon PDF involved very large uncertainties with up to 100% in the high- x range. The photon PDF of the CT14qed PDF set [414], on the other hand, combined model assumptions and experimental input from $ep \rightarrow ey + X$ data, achieving an accuracy at the level of 10–20%. The situation was drastically improved in 2016 with the advent of the LUXqed photon PDF [415, 416], which was derived by exploiting the observation that hadronic collisions mediated by only virtual photons can be equivalently described by using a photon PDF or by the parametrization of the hadronic tensor in terms of the structure functions F_2 and F_L . In this way, it is possible to derive a relation between the photon PDF $f_\gamma(x, \mu^2)$ and the structure functions,

$$xf_\gamma(x, \mu^2) = \frac{1}{2\pi\alpha(\mu^2)} \int_x^1 \frac{d\xi}{\xi} \left\{ \int_{x^2 m_p^2 / (1-\xi)}^{\mu^2 / (1-\xi)} \frac{dQ^2}{Q^2} \left(\alpha(Q^2) \right)^2 \left[\left(\xi P_{\gamma f}(\xi) + \frac{2x^2 m_p^2}{Q^2} \right) F_2\left(\frac{x}{\xi}, Q^2\right) - \xi^2 F_L\left(\frac{x}{\xi}, Q^2\right) \right] - \left(\alpha(\mu^2) \right)^2 \xi^2 F_2\left(\frac{x}{\xi}, \mu^2\right) \right\}, \quad (383)$$

where m_p is the proton mass. Based on Eq. (383), $f_\gamma(x, \mu^2)$ can be numerically evaluated from data on $F_2(x, Q^2)$ and $F_L(x, Q^2)$, leading to an extremely accurate result for the photon PDF. The l.h.s. of Fig. 3 illustrates the coverage of the (x, Q^2) plane by data from different experiments. Note that the region at $x = 1$ contains the contribution from elastic scattering, where the proton does not break up in the collision. The r.h.s., finally, shows the comparison of the mentioned determinations of the photon PDF, normalized to LUXqed, with respective error bands. The LUXqed photon PDF is good within 1–2% in the typical x range of LHC physics and, thus, even the best known of all PDFs.

Other approaches to extract the photon PDF from DIS and LHC data were described in Refs. [417, 418]. Nowadays, several PDF sets, which are publically available via LHAPDF [419], include QED corrections and a photon PDF.

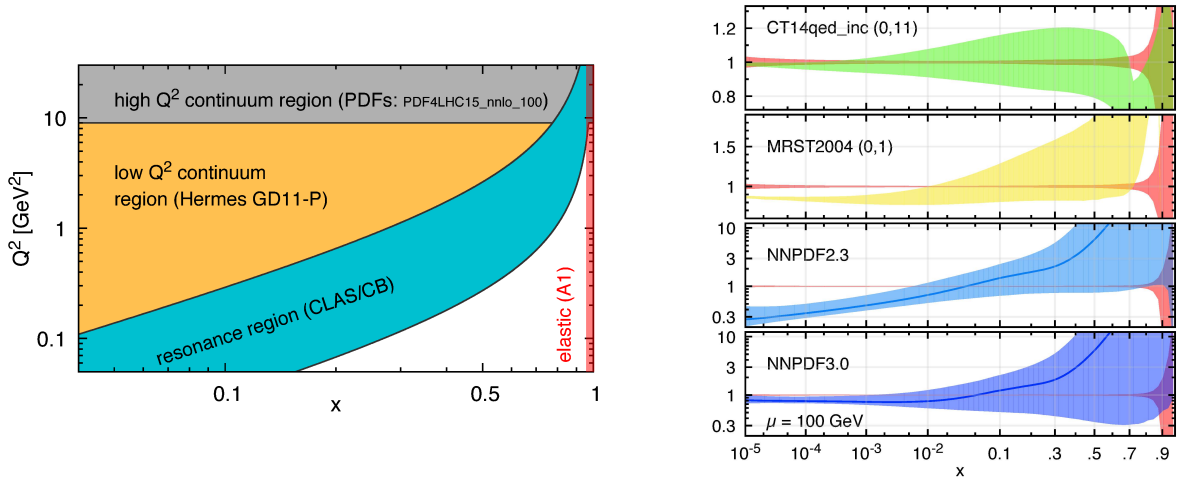


Figure 3: Left: breakup of the (x, Q^2) plane in terms of the $F_2(x, Q^2)$ and $F_L(x, Q^2)$ data used in Eq. (383). Right: ratio of photon PDFs from some common PDF sets (with uncertainty bands) to the LUXqed photon PDF (uncertainty band in red). (Taken from Ref. [415].)

4.3.3. Photon-induced processes

The inclusion of the photon in the set of partons leads to so-called photon-induced processes, i.e. partonic channels with photons in the initial state. At NLO EW, photon-induced channels always result as crossed counterparts of photonic bremsstrahlung corrections. For instance, quark-initiated $q\bar{q}$, $q\bar{q}$, $\bar{q}\bar{q}$ channels always receive (real) $\mathcal{O}(\alpha)$ corrections from $q\gamma$ and/or $\bar{q}\gamma$ scattering, where the additional q or \bar{q} in the final state leads to an additional jet with respect to the LO signature, similar to real NLO QCD corrections. For specific final states with charged particles, but without net electric charge, there is also a contribution from $\gamma\gamma$ scattering with LO kinematics and without additional partons in the final state. This, for instance, happens in the case for $\mu^+\mu^-$ or W^+W^- production.

If photonic channels already exist in LO predictions, the redefinition of the photon PDF becomes relevant at NLO EW. At this point, special attention has to be paid to the term $\propto P_{\gamma\gamma}(\xi) \sum_{a=q} Q_a^2 \ln m_a^2$ in Eq. (381), or its counterpart in Eq. (377).³⁰ Owing to $P_{\gamma\gamma}(\xi) \propto \delta(1-\xi)$, the corresponding contribution to the NLO cross section is proportional to the photon-induced LO cross section and has some impact on the issue of the EW input-parameter scheme for photon-induced processes, as pointed out in Refs. [332, 420]. In detail, for processes with one or two incoming photons the partonic cross-section contribution is given by

$$d\hat{\sigma}_{a\gamma}^{\text{coll-ct}} = \left[\Delta\alpha_{\text{had}}^{(5)}(\mu_F^2) + \dots \right] d\hat{\sigma}_{a\gamma}^0, \quad d\hat{\sigma}_{\gamma\gamma}^{\text{coll-ct}} = 2 \left[\Delta\alpha_{\text{had}}^{(5)}(\mu_F^2) + \dots \right] d\hat{\sigma}_{\gamma\gamma}^0, \quad (384)$$

where a denotes an incoming parton different from a photon, and the dots stand for non-singular constant terms. The quantity $\Delta\alpha(Q^2)$, which is defined in Section 5.1.1, controls the running of the electromagnetic coupling α , and the subscript ‘had’ indicates that only light-quark loops (all but the top-quark loop) are taken into account in $\Delta\alpha_{\text{had}}^{(5)}(Q^2)$. Recall that $\Delta\alpha_{\text{had}}^{(5)}(Q^2)$ receives non-perturbative effects from all hadronic resonances of mass $\sqrt{Q^2}$ lying between the Thomson limit at $\sqrt{Q^2} = 0$ and some high value of $\sqrt{Q^2}$, which results in the appearance of the light quark masses in the perturbative result (418) for $\Delta\alpha(Q^2)$. As discussed in Section 5.1.1, a sound way to account for those effects in perturbation theory is provided by their absorption into an appropriately defined input value for α , i.e. by a properly chosen input-parameter scheme. For an NLO EW amplitude with an initial-state photon, there are four sources for terms involving $\Delta\alpha_{\text{had}}^{(5)}(Q^2)$: (i) the charge renormalization constant δZ_e , (ii) the photon wave-function renormalization constant δZ_{AA} , (iii) the hadronic contribution to $-\Delta\alpha(M_Z^2)$ in the $\alpha(M_Z^2)$ or the G_μ scheme, and (iv) the contribution from the photon PDF redefinition discussed above. For the charge factor e of each initial-state photon the $\Delta\alpha$ parts in (i) and (ii) cancel in the sum $2\delta Z_e + \delta Z_{AA}$, so that the mass-singular contribution $\Delta\alpha_{\text{had}}^{(5)}(\mu_F^2)$ of type (iv)

³⁰In early calculations of photon-induced processes, those terms were often disregarded, a procedure that was acceptable, because early QED-corrected PDFs did not make use of a consistent QED factorization scheme in all ingredients of the PDF determination. Present-day QED-corrected PDF sets, however, employ $\overline{\text{MS}}$ factorization consistently, so that also all terms in the PDF redefinition have to be taken into account properly.

should be compensated by a term $-\Delta\alpha(M_Z^2)$ of type (iii) in order to avoid large logarithmic corrections sensitive to non-perturbative physics. This means that the electromagnetic coupling for initial-state photons in hadronic collisions should be renormalized in some input-parameter scheme with α defined at some high momentum transfer, such as in the $\alpha(M_Z^2)$ or the G_μ scheme. The fact that mass logarithms of leptons still survive in the difference $\Delta\alpha_{\text{had}}^{(5)}(\mu_F^2) - \Delta\alpha(M_Z^2)$ is not harmful, since they can be safely calculated in perturbation theory.

For processes where the diagrams of the $q\gamma$ -induced corrections have direct counterparts in the qg channels of the NLO QCD corrections, the $q\gamma$ channels typically contribute at the percent level to the hadronic cross section, or even less, which is a direct consequence of the suppression of the photon PDF w.r.t. gluon PDF by roughly 10^{-2} . A similar statement holds for $\gamma\gamma$ channels whenever similar $g\gamma$ or gg channels exist. More significant contributions from photon-induced processes can arise if the photonic channels involve diagrams without QCD counterparts, i.e. diagrams where the photon couples to colour-neutral charged particles like muons or W bosons. Typical examples for enhanced $\gamma\gamma$ contributions are the channels $\gamma\gamma \rightarrow l^+l^-$ [421–423] and $\gamma\gamma \rightarrow W^+W^-$ [355–357, 424, 425], where the $\gamma\gamma$ channels comprise more than 10% of the differential cross sections in certain regions of phase space. An extreme case for large $q\gamma$ contributions is provided by WW production at the LHC [343, 358–360], where photon-induced channels deliver 5–10% of the integrated cross section, strongly depending on the event selection (in particular on possible jet vetoes).

4.4. Photon–jet systems

The perturbative treatment of final-state configurations with collinear photons and light quarks in general leads to mass singularities in the quark masses, similar to quark–gluon systems in QCD. In principle those singularities could be removed from predictions by consistently considering the photon as another QCD parton, which takes part in all clustering procedures of jet algorithms just like gluons and quarks. This procedure, however, would merge all processes with hard photons in the final state with corresponding processes with jet activity, i.e. this procedure is blind to any processes with tagged hard photon production. Since processes with hard photons are certainly interesting to analyze, we need a procedure to separate photon from jet production.

In the following we distinguish two different collinear photon–quark configurations which deserve some special treatment:

- Quark-to-photon splittings $q \rightarrow q\gamma$: This subprocess (see Fig. 1a with f being a quark) intertwines QCD and EW corrections in predictions for the production of a specific final state F in association with a hard jet or a hard photon. Specifically, the real corrections to $F + \text{jet}$ and $F + \gamma$ production both involve $F + \text{jet} + \gamma$ final states, which contribute to the NLO EW corrections to $F + \text{jet}$ production and to the NLO QCD corrections to $F + \gamma$ production at the same time. A consistent isolation of $F + \text{jet}$ from $F + \gamma$ signatures at full (QCD+EW) NLO accuracy requires a photon–jet separation that guarantees a proper cancellation of all IR (soft and collinear) singularities on the theory side and that is experimentally feasible at the particle level.
- Photon-to-quark splittings $\gamma \rightarrow q\bar{q}$: Low-virtuality photons creating quark–antiquark pairs (see Fig. 1b with f representing a quark) lead to hadronic final states. The perturbative treatment of this splitting leads to mass singularities in cross-section predictions that would be cancelled against loop corrections to the underlying hard process with a photon in the final state instead of the $q\bar{q}$ pair. Assuming that hadronic activity can be experimentally distinguished from a hard photon, we need a procedure to treat the effect of the low-virtuality $q\bar{q}$ pair in a non-perturbative way.

4.4.1. Photon–jet separation

Since calorimetric information is decisive for the reconstruction of jets and photons, it is natural to take the electromagnetic energy fraction inside some hadronic/electromagnetic shower as criterion to decide whether it is called a jet or a photon. Note that this criterion, however, necessarily leads to an incomplete cancellation of collinear singularities for photon emission off (anti)quarks. This can be explicitly seen by inspecting the mass-singular contributions from photon radiation off final-state quarks, as spelled out for two-cutoff slicing in Eq. (285) with Eq. (291) and for dipole subtraction in Eqs. (319) and (346) with Eqs. (321) and (350). Separating jets from photons via their energy flow, cuts into the integration over the splitting variable z , so that the cancellation of collinear final-state singularities is destroyed, which would require the integration over the full z -range. Two different methods have been suggested in the literature to cope with this situation: One method introduces a phenomenological *quark-to-photon fragmentation*

function [426] that absorbs the collinear singularity in the same way as PDFs absorb collinear singularities from the initial state. Another method, known as *Frixione isolation* [427], shifts the complete collinear singularity to the jet side upon designing a specially adapted definition of the allowed hadronic energy fraction in a photonic shower:

(a) *Quark-to-photon fragmentation function*

The quark-to-photon fragmentation function $D_{q \rightarrow \gamma}(z_\gamma)$ describes the probability of a quark fragmenting into a jet containing a photon carrying the fraction z_γ of the total jet energy. Since fragmentation is a long-distance process, it cannot be calculated entirely in perturbation theory, but receives two types of contributions: (i) the perturbatively calculable radiation of a photon off a quark, which contains a collinear divergence; (ii) the non-perturbative production of a photon during the hadronization of the quark, which is described by a bare non-perturbative fragmentation function $D_{q \rightarrow \gamma}^{\text{bare}}(z_\gamma)$. The latter contributes to the photon-emission cross section as

$$d\sigma_{ab \rightarrow \gamma X}^{\text{frag}}(z_{\text{cut}}) = d\sigma_{ab \rightarrow qX}^{\text{LO}} \int_{z_{\text{cut}}}^1 dz_\gamma D_{q \rightarrow \gamma}^{\text{bare}}(z_\gamma), \quad (385)$$

where z_{cut} is the smallest photon energy fraction required in the collinear photon–quark system to be identified as a photon. The perturbative and non-perturbative (bare) contributions to the fragmentation function are sensitive to the soft dynamics inside the quark jet and can a priori not be separated from each other in a unique way. Since the IR singularity present in the perturbative contribution must be balanced by a divergent piece in the bare fragmentation function, $D_{q \rightarrow \gamma}^{\text{bare}}(z_\gamma)$ can be decomposed at a factorization scale μ_F into a universal divergent piece and a phenomenological contribution $D_{q \rightarrow \gamma}(z_\gamma, \mu_F^2)$, which has to be taken from experiment. The precise form of this separation, including the choice of the IR-finite contributions in the perturbative part, determines the *factorization scheme* in which $D_{q \rightarrow \gamma}$ is defined. The $\overline{\text{MS}}$ factorization scheme, which removes only the singular parts as defined in DR from $D_{q \rightarrow \gamma}^{\text{bare}}$, is the most common choice [426]:

$$D_{q \rightarrow \gamma}^{\text{bare}}(z_\gamma) \Big|_{\text{DR}} = \frac{\alpha Q_q^2}{2\pi} \frac{(4\pi)^\epsilon}{\Gamma(1-\epsilon)} \left(\frac{\mu^2}{\mu_F^2} \right)^\epsilon \frac{1}{\epsilon} \hat{P}_{ff}(1-z_\gamma) + D_{q \rightarrow \gamma}(z_\gamma, \mu_F^2). \quad (386)$$

The respective result for MR with a small quark mass m_q , which corresponds to the same phenomenological contribution $D_{q \rightarrow \gamma}$, reads [428]

$$D_{q \rightarrow \gamma}^{\text{bare}}(z_\gamma) \Big|_{\text{MR}} = \frac{\alpha Q_q^2}{2\pi} \left[\ln \left(\frac{m_q^2}{\mu_F^2} z_\gamma^2 \right) + 1 \right] \hat{P}_{ff}(1-z_\gamma) + D_{q \rightarrow \gamma}(z_\gamma, \mu_F^2). \quad (387)$$

In Refs. [426, 429] a method was proposed how to measure $D_{q \rightarrow \gamma}(z_\gamma, \mu_F^2)$ upon analyzing the process $e^+e^- \rightarrow n \text{jets} + \text{photon}$. The key feature of the proposed method is the democratic clustering of both hadrons and photons into jets, while keeping track of the photonic energy fraction in the jet, i.e. technically one has to deal with identified particles in the final state that lead to non-collinear-safe observables. The combination of the various ingredients in such a calculation based on one-cutoff phase-space slicing or dipole subtraction is described in Refs. [426, 429] and [428], respectively. The first determination of $D_{q \rightarrow \gamma}(z, \mu_F^2)$ was performed by the ALEPH collaboration [430] using the ansatz

$$D_{q \rightarrow \gamma}^{\text{ALEPH}}(z_\gamma, \mu_F^2) = \frac{\alpha Q_q^2}{2\pi} \left[\hat{P}_{ff}(1-z_\gamma) \ln \left(\frac{\mu_F^2}{\mu_0^2} \frac{1}{(1-z_\gamma)^2} \right) + C \right], \quad (388)$$

with two fitting parameters, $C = -12.1$ and $\mu_0 = 0.22 \text{ GeV}$.

(b) *Frixione isolation*

This procedure defines isolated hard photons by the requirement that only soft partons can become collinear to the photon. In detail, the total transverse energy $\sum_i E_{T,i}$ of all partons i with small distances $R_{iy} = \sqrt{(\eta_i - \eta_\gamma)^2 + \Delta\phi_{iy}^2}$ to the photon in the pseudo-rapidity–azimuthal-angle plane is required to go to zero with the maximally allowed distance R_{iy} , i.e.

$$\sum_i E_{T,i} \theta(\delta - R_{iy}) \leq X(\delta) \quad \text{for all } \delta \leq \delta_0, \quad (389)$$

where δ_0 is a measure for the size of the cone around the photon, in which the criterion is used. The sum on the l.h.s. of Eq. (389) receives contributions only from hadrons with a distance to the photon smaller or equal to δ . In Eq. (389), $X(\delta)$ is an appropriate function with $X(\delta) \rightarrow 0$ for $\delta \rightarrow 0$. Specifically, the form

$$X(\delta) = E_{T,\gamma} \epsilon_\gamma \left(\frac{1 - \cos \delta}{1 - \cos \delta_0} \right)^n \quad (390)$$

is suggested in Ref. [427] for a photon of transverse energy $E_{T,\gamma}$, where the two parameters ϵ_γ and n can be taken to be 1. While we here reproduce the definitions for a hadron collider, for lepton colliders the transverse energies should be replaced by the ordinary energies in Eqs. (389) and (390). The condition (389) excludes any hard jet activity collinear to the photon, but still takes into account soft jet activity at a sufficiently inclusive level to guarantee the proper cancellation of IR singularities when calculating NLO QCD corrections to $F + \gamma$ production with γ being the isolated photon. Taking the inverse procedure to define $F +$ jet production, i.e. interpreting $F +$ jet + γ production as photonic EW correction to $F +$ jet if condition (389) is not fulfilled, formally shifts the complete contribution of the quark-to-photon fragmentation function to $F +$ jet production. Whether this means that $F + \gamma$ production is really insensitive to non-perturbative corrections is not proven and sometimes under debate. Moreover, the implementation of condition (389) at the experimental level raises issues, in particular concerning shower effects on the hard photon kinematics and the realizability at the apex of the cone.

At the LHC, a prominent example for photon-jet separation is given by W/Z production in association with a jet or a photon, where the NLO EW corrections to $W/Z +$ jet production and the NLO QCD corrections to $W/Z + \gamma$ production overlap. For $W/Z +$ jet and $W/Z + \gamma$ production, NLO QCD+EW results obtained with the quark-to-photon fragmentation function were discussed in Refs. [431–433] and Refs. [434, 435]; NLO QCD results based on Frixione isolation can, for instance, be obtained with the program MCFM [436]. Comparing results on $Z + \gamma$ production obtained with the two separation procedures, reveals differences at the level of $\sim 1\%$ only [435], if the separation parameters of the two methods are matched as far as possible.³¹ Note, however, that it is not possible to make generic, process-independent statements on such differences.

4.4.2. Photon-to-jet conversion

The phase-space integral over squared amplitudes that involve some $\gamma^* \rightarrow q\bar{q}$ splitting process contains a mass singularity for light quarks q , originating from the collinear region (i.e. low-virtuality photons). As discussed in Section 4.1, the structure of this singularity is universal in the sense that the underlying squared matrix elements factorize into a universal radiator function and the square of the hard matrix element of the underlying process with a real photon instead of the $q\bar{q}$ pair. Note, however, that the physical final state is still a jet, or at least some hadronic activity, emerging from the photon initiating the splitting. Perturbatively, the mass-singular cross-section contribution can be calculated in a straightforward way, e.g. via two-cutoff slicing or dipole subtraction, as outlined in Section 4.2. The singular contributions show up as $1/\epsilon$ poles in DR or as logarithms $\ln m_q$ in small quark masses m_q in MR. Either way, the resulting singular contribution is not yet described in a physically meaningful way, since the splitting contains non-perturbative contributions, which have to be taken from experiment.

The non-perturbative cross-section contribution can be combined with the perturbative part by means of a *photon-to-quark conversion function* $D_{\gamma \rightarrow \text{jet}}^{\text{bare}}$ similar to the concept of fragmentation functions for identified-particle production [437],

$$d\sigma_{ab \rightarrow \text{jet}+X}^{\text{conv}} = d\sigma_{ab \rightarrow \gamma X}^{\text{LO}} \int_0^1 dz D_{\gamma \rightarrow \text{jet}}^{\text{bare}}(z). \quad (391)$$

Here $D_{\gamma \rightarrow \text{jet}}^{\text{bare}}(z)$ is the *bare* $\gamma \rightarrow$ jet conversion function, which depends on the variable z describing the fraction of the photon momentum \tilde{k} transferred to one of the jets ($p_{\text{jet}} = z\tilde{k}$). The bare conversion function contains singular contributions so that the sum of the conversion part $d\sigma^{\text{conv}}$ and the remaining perturbative cross-section contribution is non-singular. The extraction of the singular contribution from $D_{\gamma \rightarrow \text{jet}}^{\text{bare}}(z)$ at some factorization scale μ_F requires a

³¹Using $R_{\gamma \text{jet}} \sim R_0$ for the critical events, the two parameters z_{cut} and ϵ_γ can be related by $z_{\text{cut}} \approx 1/(1 + \epsilon_\gamma)$.

factorization scheme, for which we take the $\overline{\text{MS}}$ scheme following common practice. In DR, $D_{\gamma \rightarrow \text{jet}}^{\text{bare}}(z)$ is decomposed into a singular and a phenomenological part $D_{\gamma \rightarrow \text{jet}}(z, \mu_F^2)$ as follows,

$$D_{\gamma \rightarrow \text{jet}}^{\text{bare}}(z) \Big|_{\text{DR}} = \sum_q N_C^q \frac{Q_q^2 \alpha}{2\pi} \frac{(4\pi)^\epsilon}{\Gamma(1-\epsilon)} \left(\frac{\mu^2}{\mu_F^2} \right)^\epsilon \frac{1}{\epsilon} P_{f\gamma}(z) + D_{\gamma \rightarrow \text{jet}}(z, \mu_F^2). \quad (392)$$

In MR, this splitting reads

$$D_{\gamma \rightarrow \text{jet}}^{\text{bare}}(z) \Big|_{\text{MR}} = \sum_q N_C^q \frac{Q_q^2 \alpha}{2\pi} \ln \left(\frac{m_q^2}{\mu_F^2} \right) P_{f\gamma}(z) + D_{\gamma \rightarrow \text{jet}}(z, \mu_F^2), \quad (393)$$

where the finite non-perturbative part $D_{\gamma \rightarrow \text{jet}}(z, \mu_F^2)$ is the same in the two versions.

The non-perturbative contributions to $D_{\gamma \rightarrow \text{jet}}(z, \mu_F^2)$ have to be extracted from experimental data. Ideally, this information would come from an accurate differential measurement of a jet production cross section (with low jet invariant mass) and of its corresponding prompt-photon counterpart, i.e. experimental information that is not available at present.

In Ref. [437] it was shown that at least the inclusive z -integral over $D_{\gamma \rightarrow \text{jet}}(z, \mu_F^2)$ can be obtained from a dispersion integral for the R ratio of the cross sections for $e^+e^- \rightarrow \text{hadrons}/\mu^+\mu^-$. This dispersion integral, in turn, can be tied to the quantity $\Delta\alpha_{\text{had}}^{(5)}(M_Z^2)$, which is fitted to experimental data (see also Section 5.1.1). Based on this feature, it is possible to predict the following form of $D_{\gamma \rightarrow \text{jet}}(z, \mu_F^2)$,

$$D_{\gamma \rightarrow \text{jet}}(z, \mu_F^2) = \Delta\alpha_{\text{had}}^{(5)}(M_Z^2) + \sum_q N_C^q \frac{Q_q^2 \alpha}{2\pi} \left[\ln \left(\frac{\mu_F^2}{M_Z^2} \right) + \frac{5}{3} \right] P_{f\gamma}(z), \quad (394)$$

which is valid up to z -dependent terms that integrate to zero. Here the sum over q runs over all quarks but the top quark. Since mostly the inclusive integral over z is needed in predictions for cross sections, and since the impact of $D_{\gamma \rightarrow \text{jet}}(z)$ is quite small in general, this result should be sufficient for all phenomenological purposes.

4.5. Radiation effects in lepton–photon systems

4.5.1. Prominent features of radiation effects

Collinear photon radiation off massive fermions f (mass m_f , electric charge Q_f) or collinear photons splitting into massive fermion–antifermion pairs $f\bar{f}$ lead to real radiative corrections $\propto Q_f^2 \alpha \ln(m_f^2/Q^2)$ that are enhanced by mass logarithms if a typical energy scale Q of the underlying process is much larger than the fermion mass m_f , i.e. $Q \gg m_f$, a fact that is already known for a long time [438]. In contrast to light quarks, whose masses are perturbatively not well defined, the masses of charged leptons l are physical and measured to very high precision. Leptonic mass-singular corrections are, thus, perturbatively calculable and are often dominating EW corrections to cross sections involving charged leptons in the initial or final state.

At NLO, the methods outlined in Section 4.2 are suitable to calculate those corrections. Technically, it is not favourable to employ the full lepton mass dependence in real-emission amplitudes. Rather, it is more appropriate to neglect the lepton masses wherever possible and to keep them only as regulators in the mass-singular logarithms. The lepton masses can be neglected in all real-emission amplitudes, and non-vanishing masses are only required in the phase-space integration over the regions of collinear emission and splittings, which are isolated via slicing or subtraction techniques. This procedure significantly increases efficiency, speed, and stability in the phase-space integration of cross sections.

Phenomenologically, the most important situations in which collinear enhancements in corrections occur are:

(a) Photonic initial-state radiation (ISR):

Since the factorization property of collinear photon emission off light fermions is universal, the corresponding mass-singular corrections originating from each incoming charged-lepton line take the form of a convolution of the underlying LO cross section σ^{LO} with a universal *structure function* $\Gamma_{ll}^{\text{LL}}(x, Q^2)$, where “LL” indicates the leading-logarithmic approximation. For a process with two incoming charged leptons of momenta p_1 and p_2 this convolution is given by

$$\int d\sigma^{\text{LL,ISR}} = \int_0^1 dx_1 \int_0^1 dx_2 \Gamma_{ll}^{\text{LL}}(x_1, Q^2) \Gamma_{ll}^{\text{LL}}(x_2, Q^2) \int d\sigma^{\text{LO}}(x_1 p_1, x_2 p_2), \quad (395)$$

where the integration variables x_k are the momentum fractions of the leptons initiating the hard scattering process. From the analysis of the collinear limit in Section 4.2 we can directly read off the form of $\Gamma_{ll}^{\text{LL}}(x, Q^2)$ at NLO,³²

$$\Gamma_{ll}^{\text{LL}}(x, Q^2) = \delta(1-x) + \frac{\beta_l}{4} P_{ff}(x) + \mathcal{O}(\alpha^2) \quad (396)$$

$$= \delta(1-x) \left[1 + \frac{\beta_l}{4} \left(\frac{3}{2} + 2 \ln \epsilon \right) \right] + \frac{\beta_l}{4} \theta(1-x-\epsilon) \hat{P}_{ff}(x) \Big|_{\epsilon \rightarrow 0+} + \mathcal{O}(\alpha^2), \quad (397)$$

where the difference between the two forms is only of technical nature. The large logarithmic enhancement is contained in the parameter

$$\beta_l = \frac{2Q_l^2 \alpha}{\pi} \left(\ln \frac{Q^2}{m_l^2} - 1 \right), \quad (398)$$

where the non-logarithmic term is motivated from the soft-photon limit [368]. The generic energy scale Q of the process is not uniquely determined in LL approximation; in a full NLO EW correction the dependence on Q completely cancels against the remaining NLO EW contributions, from which the LL contribution of $\sigma^{\text{LL,ISR}}$ has to be subtracted to avoid double counting. If not the full NLO EW corrections are included in the prediction, or more generally, if the accuracy in $\sigma^{\text{LL,ISR}}$ goes beyond the order of the remaining completely calculated corrections, some residual Q dependence remains. For lepton–lepton annihilation processes at a centre-of-mass energy \sqrt{s} , the scale $Q^2 = s = (p_1 + p_2)^2$ often is a reasonable choice, and varying Q by some numerical factor illustrates part of the theoretical uncertainty from missing higher-order corrections.

Apart from the enhancement by the large correction factor β_l , ISR is distinguished by the fact that it effectively reduces the energy that is available for the hard scattering process after ISR. Neglecting m_l in the kinematics, the squared CM energy s is reduced to $x_1 x_2 s$ for the ISR contribution in Eq. (395). The reduction of the CM energy in $d\sigma^{\text{LO}}(x_1 p_1, x_2 p_2)$ can have a large impact if σ^{LO} has a strong energy dependence below the nominal scattering energy \sqrt{s} . The most prominent case is an s -channel resonance with mass smaller than \sqrt{s} which can be reached by an ISR reduction of the available scattering energy—a phenomenon known as *radiative return*. This effect, for example, leads to a significant distortion of the Z-boson line shape [42, 44, 82, 439–444] as observed at LEP1 [18] via $e^+e^- \rightarrow \gamma^*/Z \rightarrow f\bar{f}$ and to radiative corrections of $\mathcal{O}(100\%)$ well above the Z-boson resonance [445], as illustrated on the l.h.s. of Fig. 4. W-boson pair production near the pair production threshold at $\sqrt{s} = 2M_W$ provides another example where ISR corrections of $\mathcal{O}(10\text{--}20\%)$ are the by far dominating EW higher-order effects (see also Section 6.5.5), which have to be controlled with high precision in order to achieve a sound confrontation between theory and experiment.

Obviously, a pure NLO treatment of the logarithmically enhanced ISR corrections is often insufficient. We consider the inclusion of radiation effects beyond NLO further below.

(b) *Photonic final-state radiation (FSR):*

At the LL level, the universal factorization property of collinear photon emission is identical for initial- and final-state fermions. Nevertheless there are characteristic differences in the impact of the corresponding corrections on cross sections which are mainly due to the different momentum flow: ISR photons reduce the effective scattering energy of the hard process, but FSR photons do not. The LL approximation for the inclusion of FSR off a single lepton l schematically reads

$$\int d\sigma^{\text{LL,FSR}(l)} = \int_0^1 dz \Gamma_{ll}^{\text{LL}}(z, Q^2) \int d\sigma^{\text{LO}}(\hat{p}_l) \Theta_{\text{cut}}(p_l = z\hat{p}_l, k = (1-z)\hat{p}_l), \quad (399)$$

where the structure function $\Gamma_{ll}^{\text{LL}}(z, Q^2)$ is the same as for ISR in LL approximation and \hat{p}_l is the hard lepton momentum before FSR. The theta function Θ_{cut} indicates that the collinear lepton and photon momenta p_l and k are relevant for

³²The mass-singular logarithms of $\Gamma_{ll}^{\text{LL}}(x, Q^2)$ can, e.g., be read from the sum of the continuum parts $[G_{ai}^{(\text{sub})}(P^2, x)|_{\text{MR}}]_+$ and $[G_{ab}^{(\text{sub})}(s, x)|_{\text{MR}}]_+$ of dipole subtraction with a massive initial-state emitter, as given in Eqs. (337) and (368), since the sum of the respective endpoint parts $G_{ai}^{(\text{sub})}(P^2, x)|_{\text{MR}}$ and $G_{ab}^{(\text{sub})}(s, x)|_{\text{MR}}$ cancels against the corresponding mass singularities of the virtual corrections by virtue of the KLN theorem.

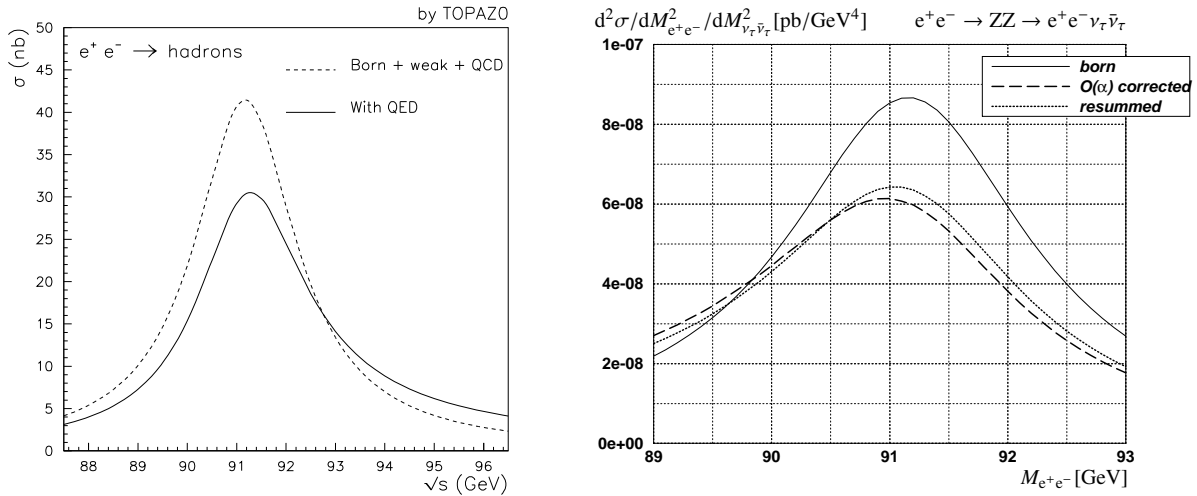


Figure 4: Resonance distortion due to ISR (left) and FSR (right). Left: Cross-section prediction for $e^+e^- \rightarrow \gamma^*/Z \rightarrow \text{hadrons}$ as function of the CM energy \sqrt{s} from TOPAZ0 [446, 447], in which “with QED” refers to photonic ISR (taken from Ref. [448]). Right: Differential cross section for $e^+e^- \rightarrow ZZ \rightarrow e^+e^-\nu_\tau\bar{\nu}_\tau$ in the invariant mass $M_{e^+e^-}$ of the final-state e^+e^- pair for $M_{\nu_\tau\bar{\nu}_\tau} = M_Z$, in which “ $O(\alpha)$ corrected” refers to photonic FSR and “resummed” to the corresponding effect of soft-photon resummation (taken from Ref. [449]).

the event selection that defines the measurable cross section. Note that only Γ_{ll}^{LL} and Θ_{cut} depend on the momentum fraction z which controls the momentum share of lepton and photon after FSR, while the LO cross section $d\sigma^{\text{LO}}$ is z independent. The scale Q plays the same role as for ISR discussed above.

The KLN theorem [365, 367] guarantees that the mass-singular FSR corrections to cross sections cancel if collinear lepton–photon systems are treated fully inclusively, i.e. if the z integral in Eq. (399) is carried out over the full domain with $\Theta_{\text{cut}} \equiv 1$. A total cross section, defined without any phase-space cuts, is an obvious observable of this kind. The NLO approximation of Γ_{ll}^{LL} given in Eq. (396) makes this property of FSR very explicit by the appearance of the $(\dots)_+$ distribution. Observables that are sufficiently inclusive so that FSR mass singularities cancel are called *collinear safe*, as already discussed in Section 4.2.1.

In the presence of phase-space cuts and in differential cross sections, in general, mass-singular contributions survive, leading to enhanced FSR effects. The r.h.s. of Fig. 4 illustrates those FSR effects in the e^+e^- invariant-mass distribution of the process $e^+e^- \rightarrow ZZ \rightarrow e^+e^-\nu_\tau\bar{\nu}_\tau$, where collinear FSR effectively reduces the invariant mass after the resonant production of the e^+e^- pair, leading to large positive corrections for $M_{e^+e^-} \lesssim M_Z$ known as *radiative tail*. Examples of this kind also show up in hadron-collider observables for processes involving final-state leptons, which are copiously produced in any process of W- or Z-boson production. Considering, e.g., the distribution in the l^+l^- invariant-mass $M_{l^+l^-}$ from Drell–Yan-like Z-boson production (see in particular Section 6.5.4), the spectrum receives FSR corrections of several tens of percent for $M_{l^+l^-}$ values below the Z resonance peak at $M_{l^+l^-} = M_Z$.

For differential observables the level of inclusiveness necessary for collinear safety can be restored by a procedure known as *photon recombination*, which treats collinear lepton–photon systems as one quasi-particle. This procedure is similar to the application of a jet algorithm in QCD. For final-state electrons, photon recombination automatically is involved in their experimental reconstruction from electromagnetic showers detected in calorimeters. Muons, on the other hand, can be observed as *bare* leptons from their tracks in the muon chambers, but in order to reduce large FSR corrections, observed muons are sometimes also reconstructed as *dressed* muons via photon recombination, as e.g. described in Ref. [450] for an ATLAS analysis. Working with dressed leptons, where mass-singular FSR effects cancel, has the advantage that the resulting cross section does not depend on the mass (and thus on the flavour) of the charged lepton, i.e. the reconstructed lepton looks universal (at least for electrons and muons).

(c) Photon processes in ee collisions:

The complementary process to photonic ISR with subsequent ee scattering is the process where the radiated photon instead of the e^\pm is initiating the hard scattering process (see Fig. 1e with f representing an e^\pm). Similar to the

LL approximation for ISR and FSR, the universal factorization of the collinear singularity in the $l \rightarrow l\gamma^*$ splitting can be employed to calculate the hard photon scattering contribution in leptonic collisions—a procedure known as *Weizsäcker–Williams* or *equivalent photon approximation (EPA)* [451, 452]. For the $\gamma\gamma$ contribution to a high-energy e^+e^- scattering cross section, the EPA reads

$$\int d\sigma_{ee}^{\text{EPA}} = \int_0^1 dx_1 \int_0^1 dx_2 \Gamma_{\gamma l}^{\text{LL}}(x_1, Q^2) \Gamma_{\gamma l}^{\text{LL}}(x_2, Q^2) \int d\sigma_{\gamma\gamma}^{\text{LO}}(x_1 p_1, x_2 p_2), \quad (400)$$

with $\sigma_{\gamma\gamma}^{\text{LO}}$ denoting the LO cross section for hard $\gamma\gamma$ scattering into any targeted final state. The leading contribution to the corresponding structure function $\Gamma_{\gamma l}^{\text{LL}}$, which describes the probability to find a photon with momentum fraction x in a lepton, can be read off from the results of Section 4.2,³³

$$\Gamma_{\gamma l}^{\text{LL}}(x, Q^2) = \frac{Q_l^2 \alpha}{2\pi} \left[P_{\gamma f}(x) \ln \left(\frac{Q^2(1-x)}{m_l^2 x^2} \right) - \frac{2(1-x)}{x} \right] + \mathcal{O}(\alpha^2). \quad (401)$$

Here we have included finite terms beyond LL approximation in such a way that choosing $Q^2 = (1-x)E^2\Delta\theta^2$ reproduces the cross section for incoming leptons with energy E and outgoing leptons with scattering angle from 0 to $\Delta\theta \gg m_l/E$ [453] in the centre-of-mass frame of the process.

Since the physics of photon–photon collisions is more characterized by the strong rather than the EW interaction, we will not consider it any further in this review and instead refer to Refs. [453–455] for more details.

4.5.2. QED structure functions to higher orders

As already indicated in the phenomenological examples mentioned in the previous section, radiative corrections from collinear photon emission off leptons can be rather large, so that NLO EW precision for those corrections often is not sufficient to achieve percent accuracy (or beyond). In such cases, at least the dominant ISR or FSR corrections beyond NLO should be better taken into account. Since those corrections are tied to IR singularities of a system of light fermions and photons, many field-theoretical statements of perturbative QCD on systems of light quarks and gluons can be adapted to the QED case. Although many simplifications occur in the transition from non-abelian QCD to abelian QED, some care has to be taken, because leptons and photons are not confined, i.e. in the QED case observables are typically not based on objects at the same level of inclusiveness as jets in QCD.

In QCD, *IR evolution equations* can be used to resum IR-singular contributions to cross sections, the most famous example being the DGLAP equations for PDFs. Generically, those equations are consistency relations expressing the fact that physical observables cannot depend on some *factorization scale* μ_F which is introduced in the theory to separate *soft* (i.e. IR-sensitive) and *hard* interaction effects. Both soft and hard contributions to an observable depend on μ_F , but only the effects from the hard interactions are perturbatively calculable. The soft effects are absorbed into some non-perturbative quantity like a PDF, which in most cases is fitted to experimental data. In spite of its non-perturbative nature, however, the μ_F dependence of the quantity comprising the soft, IR-sensitive physics is controlled by perturbation theory via IR evolution equations. Thorough treatments of these concepts and of the formal construction can be found in many text books on quantum field theory, such as Refs. [83, 86, 87, 93, 101, 402].

In the following we sketch the application of IR evolution equations to the LL QED structure functions $\Gamma_{ab}^{\text{LL}}(x, \mu_F^2)$ as introduced in Eq. (395) for photonic ISR. These functions are the precise counterparts to the PDFs of QCD partons, but now formulated for a system of leptons and photons. We first consider the case of one lepton flavour and a photon and comment on the generalization to more leptons below. In detail, $\Gamma_{ab}^{\text{LL}}(x, \mu_F^2)$ is the generalized (i.e. not necessarily positive) probability density to find the lepton, antilepton, or photon $a = l, \bar{l}, \gamma$ with momentum fraction x inside some lepton, antilepton, or photon $b = l, \bar{l}, \gamma$. Identifying $\Gamma_{ab}^{\text{LL}}(x, \mu_F^2)$ with the parton density $f_a^{(b)}(x, \mu_F^2)$ of Eq. (376) or Eq. (380), upon taking the derivative w.r.t. $\ln \mu_F^2$ we get the evolution equations

$$\frac{\partial}{\partial \ln \mu_F^2} \begin{pmatrix} \Gamma_{lb}^{\text{LL}}(x, \mu_F^2) \\ \Gamma_{\bar{l}b}^{\text{LL}}(x, \mu_F^2) \\ \Gamma_{\gamma b}^{\text{LL}}(x, \mu_F^2) \end{pmatrix} = \frac{Q_l^2 \alpha(0)}{2\pi} \int_x^1 \frac{d\xi}{\xi} \begin{pmatrix} P_{ff} \left(\frac{x}{\xi} \right) & 0 & P_{f\gamma} \left(\frac{x}{\xi} \right) \\ 0 & P_{ff} \left(\frac{x}{\xi} \right) & P_{f\gamma} \left(\frac{x}{\xi} \right) \\ P_{\gamma f} \left(\frac{x}{\xi} \right) & P_{\gamma f} \left(\frac{x}{\xi} \right) & P_{\gamma\gamma} \left(\frac{x}{\xi} \right) \end{pmatrix} \begin{pmatrix} \Gamma_{lb}^{\text{LL}}(\xi, \mu_F^2) \\ \Gamma_{\bar{l}b}^{\text{LL}}(\xi, \mu_F^2) \\ \Gamma_{\gamma b}^{\text{LL}}(\xi, \mu_F^2) \end{pmatrix}, \quad (402)$$

³³The result for $\Gamma_{\gamma l}^{\text{LL}}(x_1, Q^2)$ with $Q^2 = (1-x)(p_l^0)^2 \Delta\theta^2$ can be directly read from $\mathcal{H}^{ff}(p_f^0, x)|_{\text{MR}}$ as given in the slicing approach in Eq. (295).

which are valid in LL accuracy with the splitting functions given in Eq. (261).

At LO the structure functions are given by

$$\Gamma_{ab}^{\text{LL}}(x, \mu_F^2) \Big|_{\alpha^0} = \delta_{ab} \delta(1 - x). \quad (403)$$

This simply states that without any interaction a lepton stays a lepton, an antilepton stays an antilepton, and a photon stays a photon. Given Γ_{ab}^{LL} at LO, the evolution equations can be solved iteratively by integrating them over $\ln \mu_F^2$. The upper limit in this integration is set by the target scale μ_F^2 , the lower limit is set by the IR mass scale of the chosen IR regularization scheme. Since lepton masses are physically meaningful, we make use of MR where the lower limit in the integration over $\ln \mu_F^2$ is given by $\ln m_l^2$. In LL approximation, the IR evolution equations do not contain any additional information beyond the coefficients of the logarithms $[\alpha \ln(\mu_F^2/m_l^2)]^n$. Integrating Eq. (402) and inserting Eq. (403) on the r.h.s. leads to

$$\begin{aligned} \begin{pmatrix} \Gamma_{ll}^{\text{LL}} & \Gamma_{l\bar{l}}^{\text{LL}} & \Gamma_{l\gamma}^{\text{LL}} \\ \Gamma_{\bar{l}l}^{\text{LL}} & \Gamma_{\bar{l}\bar{l}}^{\text{LL}} & \Gamma_{\bar{l}\gamma}^{\text{LL}} \\ \Gamma_{\gamma l}^{\text{LL}} & \Gamma_{\gamma \bar{l}}^{\text{LL}} & \Gamma_{\gamma\gamma}^{\text{LL}} \end{pmatrix}(x, \mu_F^2) &= \delta(1 - x) \mathbb{1}_3 + \frac{Q_l^2 \alpha(0)}{2\pi} \int_{\ln m_l^2}^{\ln \mu_F^2} d \ln \mu^2 \int_x^1 \frac{d\xi}{\xi} \\ &\times \begin{pmatrix} P_{ff}\left(\frac{x}{\xi}\right) & 0 & P_{f\gamma}\left(\frac{x}{\xi}\right) \\ 0 & P_{ff}\left(\frac{x}{\xi}\right) & P_{f\gamma}\left(\frac{x}{\xi}\right) \\ P_{\gamma f}\left(\frac{x}{\xi}\right) & P_{\gamma f}\left(\frac{x}{\xi}\right) & P_{\gamma\gamma}\left(\frac{x}{\xi}\right) \end{pmatrix} \begin{pmatrix} \Gamma_{ll}^{\text{LL}} & \Gamma_{l\bar{l}}^{\text{LL}} & \Gamma_{l\gamma}^{\text{LL}} \\ \Gamma_{\bar{l}l}^{\text{LL}} & \Gamma_{\bar{l}\bar{l}}^{\text{LL}} & \Gamma_{\bar{l}\gamma}^{\text{LL}} \\ \Gamma_{\gamma l}^{\text{LL}} & \Gamma_{\gamma \bar{l}}^{\text{LL}} & \Gamma_{\gamma\gamma}^{\text{LL}} \end{pmatrix}(\xi, \mu^2) + O(\alpha^2) \end{aligned} \quad (404)$$

$$= \delta(1 - x) \mathbb{1}_3 + L_l \begin{pmatrix} P_{ff}(x) & 0 & P_{f\gamma}(x) \\ 0 & P_{ff}(x) & P_{f\gamma}(x) \\ P_{\gamma f}(x) & P_{\gamma f}(x) & P_{\gamma\gamma}(x) \end{pmatrix} + O(\alpha^2) \quad (405)$$

$$= \begin{pmatrix} \text{Diagram 1} & 0 & \text{Diagram 2} \\ 0 & \text{Diagram 3} & \text{Diagram 4} \\ \text{Diagram 5} & \text{Diagram 6} & \text{Diagram 7} \end{pmatrix} \quad (406)$$

with

$$L_l = \frac{Q_l^2 \alpha(0)}{2\pi} \ln\left(\frac{\mu_F^2}{m_l^2}\right). \quad (407)$$

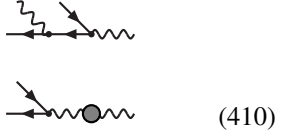
This, in particular, confirms the NLO results for $\Gamma_{ll}^{\text{LL}}(x, q^2)$ and $\Gamma_{\gamma l}^{\text{LL}}(x, q^2)$ of the previous section up to terms that are beyond the LL approximation. The diagrammatic illustration in the last line shows the individual contributions to each structure function Γ_{ab}^{LL} with b coming in from the right, a going out on the left. For more than one lepton species, each lepton and antilepton just behaves as l and \bar{l} at NLO, respectively; in $\Gamma_{\gamma\gamma}^{\text{LL}}$ the sum over all lepton types has to be taken.

Iterating this procedure by inserting the results for the structure functions into the r.h.s. of Eq. (404), higher-order LL contributions to Γ_{ab}^{LL} can be calculated. The NNLO contribution is still easy to calculate and reads

$$\begin{aligned} \Gamma_{ll}^{\text{LL}}(x, \mu_F^2) \Big|_{\alpha^2} &= \frac{L_l^2}{2} \left\{ \hat{P}_{ff}(x) [4 \ln(1 - x) + 3] - \frac{1 + 3x^2}{1 - x} \ln x - 2 + 2x \right\}_+ \\ &+ \frac{L_l^2}{2} \left\{ \frac{1 - x}{3x} (4 + 7x + 4x^2) + 2(1 + x) \ln x \right\}, \end{aligned} \quad (408)$$

$$\Gamma_{\bar{l}\bar{l}}^{\text{LL}}(x, \mu_F^2) \Big|_{\alpha^2} = \frac{L_l^2}{2} \left\{ \frac{1 - x}{3x} (4 + 7x + 4x^2) + 2(1 + x) \ln x \right\}, \quad (409)$$

$$\Gamma_{l\gamma}^{\text{LL}}(x, \mu_F^2) \Big|_{\alpha^2} = \frac{L_l^2}{2} \left\{ 2P_{f\gamma}(x) \ln(1-x) - (1-2x+4x^2) \ln x - \frac{1}{2} + 2x \right\} - \frac{L_l^2}{3} P_{f\gamma}(x),$$



(410)

$$\Gamma_{\bar{l}l}^{\text{LL}}(x, \mu_F^2) \Big|_{\alpha^2} = \Gamma_{l\bar{l}}^{\text{LL}}(x, \mu_F^2) \Big|_{\alpha^2},$$



(411)

$$\Gamma_{\bar{l}l}^{\text{LL}}(x, \mu_F^2) \Big|_{\alpha^2} = \Gamma_{l\bar{l}}^{\text{LL}}(x, \mu_F^2) \Big|_{\alpha^2},$$



(412)

$$\Gamma_{l\gamma}^{\text{LL}}(x, \mu_F^2) \Big|_{\alpha^2} = \Gamma_{\gamma l}^{\text{LL}}(x, \mu_F^2) \Big|_{\alpha^2},$$



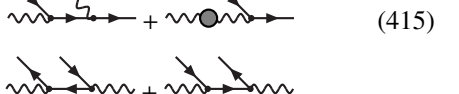
(413)

$$\Gamma_{\gamma l}^{\text{LL}}(x, \mu_F^2) \Big|_{\alpha^2} = \frac{L_l^2}{2} \left\{ 2P_{\gamma f}(x) \ln(1-x) + (2-x) \ln x + 2 - \frac{x}{2} \right\} - \frac{L_l^2}{3} P_{\gamma f}(x),$$



(414)

$$\Gamma_{\gamma\bar{l}}^{\text{LL}}(x, \mu_F^2) \Big|_{\alpha^2} = \Gamma_{\gamma l}^{\text{LL}}(x, \mu_F^2) \Big|_{\alpha^2},$$



(415)

$$\Gamma_{\gamma\gamma}^{\text{LL}}(x, \mu_F^2) \Big|_{\alpha^2} = L_l^2 \left\{ \frac{1-x}{3x} (4+7x+4x^2) + 2(1+x) \ln x \right\} - \frac{L_l^2}{3} P_{\gamma\gamma}(x).$$



(416)

The diagrams illustrate the splitting processes contributing to Γ_{ab}^{LL} with b coming in from the right, a going out on the left, and the diagonal lines showing the particles being radiated off. In the case of more than one lepton type, the structural diagrams determine by charge and flavour conservation which types of processes can take place. Note that at NNLO, some new structure functions appear, such as $\Gamma_{ll'}^{\text{LL}}$ for $l \neq l'$ or $\Gamma_{\bar{l}\bar{l}'}^{\text{LL}}$. In $\Gamma_{\gamma\gamma}^{\text{LL}}$ the sum over all possible lepton types has to be taken for each $P_{\gamma\gamma}$ insertion, and all possible $l\bar{l}$ and $\bar{l}l$ emissions have to be taken into account.

Instead of working out higher iterations explicitly, we concentrate on the important special cases of genuine photonic ISR and FSR, i.e. on the phenomenological situation in which any further (anti)lepton emission during ISR or FSR (or hadronic activity via quarks) can be vetoed in the event selection. In this case, only the splitting $l \rightarrow l\gamma$ (splitting function P_{ff}) with real γ emission is relevant, i.e. diagrammatically the initial- or final-state lepton line goes into the hard process without conversion to intermediate photons [first term in Eq. (408)]. Explicit analytical results are known in the soft-photon region ($x \rightarrow 1$) to all orders in α [403] and for arbitrary x values even up to order α^5 [456–458]. Here we just quote a frequently used form of the LL structure function which combines the full LL correction up to order α^3 with the LL soft-photon exponentiation and is sufficient for many practical purposes [459],

$$\begin{aligned} \Gamma_{ll}^{\text{LL},\gamma\text{-rad}}(x, \mu_F^2) = & \frac{\exp\left(-\frac{1}{2}\beta_l\gamma_E + \frac{3}{8}\beta_l\right)\beta_l}{\Gamma\left(1 + \frac{1}{2}\beta_l\right)} \frac{\beta_l}{2} (1-x)^{\frac{\beta_l}{2}-1} - \frac{\beta_l}{4} (1+x) \\ & - \frac{\beta_l^2}{32} \left\{ \frac{1+3x^2}{1-x} \ln x + 4(1+x) \ln(1-x) + 5 + x \right\} \\ & - \frac{\beta_l^3}{384} \left\{ (1+x) \left[6\text{Li}_2(x) + 12 \ln^2(1-x) - 3\pi^2 \right] + \frac{1}{1-x} \left[\frac{3}{2}(1+8x+3x^2) \ln x \right. \right. \\ & \left. \left. + 6(x+5)(1-x) \ln(1-x) + 12(1+x^2) \ln x \ln(1-x) - \frac{1}{2}(1+7x^2) \ln^2 x \right. \right. \\ & \left. \left. + \frac{1}{4}(39-24x-15x^2) \right] \right\}, \end{aligned} \quad (417)$$

where β_l is defined in Eq. (398) and γ_E denotes the Euler–Mascheroni constant.

Finally, we recall that the full series of powers L_l^n with L_l given in Eq. (407) does not comprise all logarithmically enhanced QED corrections, but defines the *leading logarithmic* (LL) accuracy. The *next-to-leading logarithmic* (NLL) order scales like αL_l^{n-1} and involves one logarithmic enhancement factor less than the LL level in each given order α^n . The QED structure functions Γ^{NLL} were calculated recently in Refs. [460, 461].

4.5.3. QED structure functions versus parton showers

While analytical results for structure functions are quite easy to implement in predictions, they also have some shortcomings, which are due to the fact that the kinematics of the emitted particles is integrated over up to their total energy fraction $(1 - x)$. In particular, all information on transverse momenta from nearly collinear splittings is lost, and no information on the momentum share between emitted particles from multiple emissions is kept. In this respect, a probabilistic parton-shower approach is doing better. Parton showers are based on the universal factorization properties of emission processes as well, and as such also limited to some (leading or subleading) logarithmic approximation, but they provide the fully differential information on all emitted particles, which can be important if decaying particles have to be reconstructed to very high precision. For this reason, multi-purpose event generators typically employ QED parton showers to account for photonic radiation effects, as described in the program descriptions of HERWIG [462, 463], PYTHIA [464], and SHERPA [465, 466] in more detail. A standalone QED parton shower is, e.g., provided by the program PHOTOS [467–469], which can be linked to any Monte Carlo program providing cross-section predictions. Finally, applications and further developments of QED parton showers have been described in the context of predictions for specific processes, such as for Drell–Yan-like processes with the Monte Carlo generators HORACE [470–473], WGRAD [474], and WINHAC [475].

In complete analogy to higher-order QCD calculations, a consistent combination of NLO (or even higher-order) calculations with parton showers is non-trivial and has to carefully avoid double-counting of fixed-order contributions, in order not to destroy NLO (or higher) accuracy. Note that this combination is quite simple if higher-order QED effects are included via LL structure functions, where double-counting can be avoided easily due to the analytic knowledge of all higher-order effects. For a consistent matching of NLO EW corrections with QED parton showers mostly the POWHEG [398, 399] approach was employed, as, for instance, described for Drell–Yan production in Refs. [383, 473, 474]. For many important processes with leptons analyzed at the LHC with high precision, such as EW diboson production, this step is still to be done.

More generally, also the W and Z bosons should be included in PDFs and EW parton showers. While this will become relevant at very-high-energy colliders, it is presently work in progress. PDFs for transverse and longitudinal EW gauge bosons were computed in terms of deep-inelastic scattering structure functions, following the LUXqed method to determine the photon PDF [476]. LO evolution of parton fragmentation functions for all the SM fermions and bosons were studied in Ref. [477]. The inclusion of the emission of W and Z bosons in a traditional QCD + QED shower was investigated in Ref. [478] and the emission of collinear W-bosons in jets in Ref. [479]. EW collinear splitting functions for the complete SM were derived and implemented in a comprehensive, practical EW showering scheme in Ref. [480].

5. Electroweak radiative corrections—general features

5.1. Input-parameter schemes

In order to perform consistent higher-order calculations in the SM, a set of input parameters together with the corresponding numerical values has to be specified. It is crucial to stick to a set of independent parameters in order to guarantee gauge independence and consistency in the results. Moreover, the input-parameter set should be chosen in a phenomenologically sensible way, i.e. precisely known and well-defined parameters should be preferred. Since this is the case for the electromagnetic coupling and many of the masses, these are often used as input parameters. Such input-parameter schemes that are suited for on-shell (OS) renormalization schemes are presented in Section 5.1.1. In Section 5.1.2 we discuss $\overline{\text{MS}}$ renormalization schemes, which are sometimes used as an alternative to OS renormalization schemes and require different or at least converted input parameters.

5.1.1. The $\alpha(0)$, $\alpha(M_Z^2)$, and G_μ schemes

An obvious choice for the input parameters of the SM consists of the electromagnetic coupling $\alpha = e^2/(4\pi)$, the strong coupling $\alpha_s = g_s^2/(4\pi)$, the weak gauge-boson masses M_W and M_Z , the Higgs-boson mass M_H , the fermion masses m_f , and the CKM matrix V .

In the EW sector of the SM, the masses of the particles are conveniently defined as *pole masses*, fixed by the locations of the particle poles in the respective propagators. Since the non-perturbative strong interaction at the scale of the quark masses renders the definition of pole masses problematic, for quarks it is often useful to switch to a running mass at some appropriate scale [90, 481, 482]. Properly defined observables and their predictions should be insensitive to the perturbatively problematic light quark masses, as discussed below in more detail. The Yukawa couplings do not represent independent parameters, but are fixed by the fermion masses and the other EW input parameters. Disturbing the relation between Yukawa couplings and fermion masses, violates EW gauge invariance and can lead to inconsistent and wrong predictions, especially in the calculation of EW corrections.

As discussed in Section 3.1.5, the definition of the CKM matrix in the presence of EW corrections is a non-trivial task. However, apart from applications in flavour physics, for high-energy scattering the approximation of taking all quarks other than the top quark and possibly the bottom quark massless and ignoring mixing with the third generation is an appropriate procedure. In this approximation, the CKM matrix can only become relevant in charged-current processes that are not democratic w.r.t. quark flavours so that the unitarity relations $\sum_k V_{ik} V_{kj}^* = \delta_{ij}$ are disturbed. This is, for instance, the case in charged-current quark-antiquark-annihilation channels, such as Drell-Yan-like W-boson production, where it leads to global factors $|V_{ij}|^2$ in partonic cross sections with $q_i \bar{q}_j$ or $q_j \bar{q}_i$ initial states. This statement holds at the level of NLO EW corrections as well because of the mass degeneracy in the first two quark generations where the mixing takes place.

For the boson masses M_W , M_Z , and M_H , real OS masses are usually employed. Details about different schemes that become relevant if the instability of those bosons matters are discussed in Section 6. Here, we emphasize that the weak mixing angle θ_w is not an independent input parameter. The most common choice in EW physics follows the OS prescription [36] which defines $c_w = \cos \theta_w = M_W/M_Z$ and $s_w = \sqrt{1 - c_w^2}$ via the OS W- and Z-boson masses. Taking s_w as independent parameter in addition to M_W and M_Z , e.g. by setting it to some ad hoc value or to the sine of the effective weak mixing angle measured at the Z pole, in general breaks gauge invariance, destroys gauge cancellations, and can lead to totally wrong results, even at LO.

For the electromagnetic coupling constant α basically three different input values are used: the fine-structure constant $\alpha(0) \approx 1/137$ ($\alpha(0)$ scheme), the effective value $\alpha(M_Z^2) \approx 1/129$ ($\alpha(M_Z^2)$ scheme), where $\alpha(0)$ is evolved via renormalization-group equations from $Q^2 = 0$ to the Z pole, and an effective value derived from the Fermi constant G_μ leading to $\alpha_{G_\mu} = \sqrt{2}G_\mu M_W^2(1 - M_W^2/M_Z^2)/\pi \approx 1/132$, defining the so-called G_μ scheme. The various choices for α differ by 2–6% and represent an important part of the *input-parameter scheme*. In practice, the most appropriate scheme depends on the nature of the process under consideration. In any case, it is crucial that a common coupling factor α^n is used in complete gauge-invariant subsets of diagrams, otherwise important consistency relations (compensation of divergences, unitarity cancellations, etc.) are destroyed. Note that this does not necessarily mean that there is only one value of α , but that all factors α have to be global factors to gauge-invariant pieces of amplitudes.

In the following we describe the input-parameter schemes appropriate for a contribution to a cross section (or squared matrix element) whose LO contribution is proportional to a fixed order $\alpha_s^m \alpha^n$, i.e. NLO EW contributions scale like $\alpha_s^m \alpha^{n+1}$. Corrections to LO contributions scaling with different powers m or n belong to disjoint gauge-invariant contributions, which can be treated independently. The standard QED definition of α (see Section 3.1.4) employs an OS renormalization condition in the Thomson limit (photon momentum transfer $Q^\mu = 0$), leading to the renormalized value $\alpha = \alpha(0)$ of the $\alpha(0)$ scheme. When applied to processes at energies of the scale of the EW gauge bosons or above, this scheme leads to large logarithmic corrections involving the ratios of the light fermion masses and the gauge-boson masses. It turns out that these logarithmic corrections are related to the running of the electromagnetic coupling from low ($Q^2 = 0$) to high ($|Q^2| \gtrsim M_W^2$) scales Q^2 . Thus, they can be absorbed upon using a suitable input scheme for α .³⁴

³⁴There are additional logarithmic corrections involving fermion masses. These originate from collinear singularities that can be linked to the external lines of the process under consideration. For (anti)quarks they are absorbed in parton distribution functions or fragmentation functions, for leptons those contributions can be safely calculated in perturbation theory and, if needed, supplemented by leading corrections beyond NLO. These issues are discussed in Section 4.

Let us first consider a process without external photons in the initial or final state. In the $\alpha(0)$ scheme with OS charge renormalization, each of the n EW couplings leads to a relative correction $2\delta Z_e$ to the cross section. The charge renormalization constant δZ_e contains mass-singular terms of the form $\alpha \ln m_f$ from each light fermion f that remain uncancelled in the EW corrections. These terms are contained in the quantity

$$\Delta\alpha(M_Z^2) = \Pi_{f \neq t}^{AA}(0) - \text{Re} \left\{ \Pi_{f \neq t}^{AA}(M_Z^2) \right\} = \frac{\alpha(0)}{3\pi} \sum_{f \neq t} N_C^f Q_f^2 \left[\ln \frac{M_Z^2}{m_f^2} - \frac{5}{3} \right] + \mathcal{O}(m_f^2/M_Z^2), \quad (418)$$

with $\Pi_{f \neq t}^{AA}$ denoting the photonic vacuum polarization induced by all fermions f (with charge Q_f) other than the top quark (see also Ref. [40]), and $N_C^l = 1$ and $N_C^q = 3$ are the colour multiplicities for leptons and quarks, respectively. The vacuum polarization is related to the transverse part of the photon self-energy defined in Section 3.1.7 according to,

$$\Pi^{AA}(Q^2) = \frac{\Sigma_T^{AA}(Q^2)}{Q^2}. \quad (419)$$

The correction $\Delta\alpha(M_Z^2) \approx 6\%$ quantifies the running of α from $Q^2 = 0$ to the high scale $Q^2 = M_Z^2$ induced by vacuum polarization effects of the light fermions,

$$\alpha(M_Z^2) = \frac{\alpha(0)}{1 - \Delta\alpha(M_Z^2)}, \quad (420)$$

a quantity that is non-perturbative, as signalled by its sensitivity to the light-quark masses. The appearance of $\Delta\alpha(M_Z^2)$ in the denominator results from a resummation of the large logarithms [483, 484]. The numerical value for the hadronic contribution $\Delta\alpha_{\text{had}}^{(5)}(M_Z^2)$ to $\Delta\alpha(M_Z^2)$ and thus to $\alpha(M_Z^2)$ is obtained from an experimental analysis of e^+e^- annihilation into hadrons and hadronic τ decays at low energies below the Z -boson resonance, combined with theoretical arguments using dispersion relations [485]. Eliminating $\alpha(0)$ in favour of $\alpha(M_Z^2)$ in the LO prediction, i.e. turning to the $\alpha(M_Z^2)$ scheme, effectively subtracts the $\Delta\alpha(M_Z^2)$ terms from the EW corrections and thus cancels all light-fermion logarithms resulting from charge renormalization in the EW corrections. This cancellation happens at each loop order in α , i.e. employing the $\alpha(M_Z^2)$ scheme resums the dominant effects from the running of α and, at the same time, removes the (perturbatively unpleasant) light-quark masses, which should have been taken from a fit to $\text{Re} \Pi_{f \neq t}^{AA}(Q^2) - \Pi_{f \neq t}^{AA}(0)$ otherwise. For high-energy processes without external photons the $\alpha(M_Z^2)$ scheme is appropriate from this point of view. Practically, the $\alpha(M_Z^2)$ scheme can be implemented by using $\alpha(M_Z^2)$ as electromagnetic coupling and replacing the charge renormalization constant (153) by

$$\delta Z_e|_{\alpha(M_Z^2)} = \frac{1}{2} \Pi^{AA}(0) - \frac{s_w}{c_w} \frac{\Sigma_T^{AZ}(0)}{M_Z^2} - \frac{1}{2} \Delta\alpha(M_Z^2). \quad (421)$$

Note that the same value of $\alpha = \alpha(M_Z^2)$ should be used in all terms of Eq. (421) to guarantee the complete cancellation of the fermion-mass logarithms. While all terms involving logarithms of fermion masses are absorbed into $\Delta\alpha(M_Z^2)$ or $\alpha(M_Z^2)$ (and parton distribution and fragmentation functions), a non-logarithmic dependence on the small quark masses remains. These contributions are suppressed as m_q^2/E^2 and thus negligible at sufficiently high energies E .

For processes with l external photons ($l \leq n$), however, the relative EW corrections contain l times the photonic wave-function renormalization constant δZ_{AA} , which exactly cancels the light-fermion mass logarithms appearing in $2\delta Z_e$. This statement expresses the fact that external, i.e. real, photons effectively couple with the scale $Q^2 = 0$. Consequently, the coupling factor α^n in the LO cross section should be parametrized as $\alpha(0)^l \alpha(M_Z^2)^{n-l}$, and the corresponding $\Delta\alpha(M_Z^2)$ terms should be subtracted only $(n-l)$ times from the EW correction, in order to absorb the large effects from $\Delta\alpha(M_Z^2)$ into the LO prediction. For $l = n$, this scaling corresponds to the pure $\alpha(0)$ scheme, but for $l < n$ to a mixed scheme. Thus, if the appropriate definition of α is used, large logarithms are avoided and the hadronic vacuum polarization is not required as input. On the other hand, $\alpha(M_Z^2)$ is needed as input parameter in this case. This is valid if photons truly act as external states, either in the preparation of initial states or in their detection. Exceptions are initial-state photons in photon-induced processes in hadronic collisions (see Section 4.3.2) and final-state photons as parts of electromagnetic showers of photons and leptons (see Section 4.5.3).

The G_μ scheme, finally, offers the possibility to absorb some significant universal corrections connected with the renormalization of the weak mixing angle into LO contributions. At NLO, the G_μ and $\alpha(0)$ schemes are related according to

$$\alpha_{G_\mu} = \frac{\sqrt{2}G_\mu M_W^2}{\pi} \left(1 - \frac{M_W^2}{M_Z^2}\right) = \alpha(0) \left(1 + \Delta r^{(1)}\right) + \mathcal{O}(\alpha^3), \quad (422)$$

where $\Delta r^{(1)}$ is the NLO EW correction to muon decay [36, 40, 82, 145], which can be written as

$$\Delta r^{(1)} = \Pi^{AA}(0) - \frac{c_W^2}{s_W^2} \left(\frac{\Sigma_T^{ZZ}(M_Z^2)}{M_Z^2} - \frac{\Sigma_T^W(M_W^2)}{M_W^2} \right) + \frac{\Sigma_T^W(0) - \Sigma_T^W(M_W^2)}{M_W^2} + 2 \frac{c_W}{s_W} \frac{\Sigma_T^{AZ}(0)}{M_Z^2} + \frac{\alpha(0)}{4\pi s_W^2} \left(6 + \frac{7 - 4s_W^2}{2s_W^2} \ln c_W^2 \right). \quad (423)$$

The last term as well as part of the term involving $\Sigma_T^{AZ}(0)$ result from vertex and box corrections. The quantity $\Delta r^{(1)}$ can be decomposed according to

$$\Delta r^{(1)} = \Delta\alpha(M_Z^2) - \Delta\rho^{(1)} c_W^2 / s_W^2 + \Delta r_{\text{rem}} \quad (424)$$

with $\Delta\alpha(M_Z^2)$ from Eq. (418), the universal (top-mass-enhanced) correction to the ρ parameter [130, 486, 487]

$$\Delta\rho^{(1)} = \frac{3\alpha(0)m_t^2}{16\pi s_W^2 M_W^2} \quad (425)$$

and a small remainder Δr_{rem} . In view of the running of α , the G_μ scheme corresponds to an α at the EW scale similar to the $\alpha(M_Z^2)$ scheme, since $\Delta r^{(1)}$ contains exactly one unit of $\Delta\alpha(M_Z^2)$. The G_μ scheme is thus similar to the $\alpha(M_Z^2)$ scheme as far as the running of α is concerned, i.e. it is preferable over the $\alpha(0)$ scheme except for the case of external photons. The choice between the G_μ or $\alpha(M_Z^2)$ scheme is driven by the appearance of s_W in the EW couplings. Whenever s_W (or c_W) is involved in an EW coupling, the corresponding EW correction receives a contribution from $\Delta\rho^{(1)}$ according to $s_W^2 \rightarrow s_W^2 + \Delta\rho^{(1)} c_W^2$ originating from the OS renormalization of the weak mixing angle. Using Eq. (422), it is easy to see that the combination α_{G_μ}/s_W^2 , which corresponds to the $SU(2)_W$ gauge coupling, does not receive this universal correction, since the $\Delta\rho^{(1)}$ terms from $\Delta r^{(1)}$ and the correction associated with s_W^2 cancel. In other words, in the G_μ scheme the leading correction to the ρ parameter is absorbed into the LO $SU(2)_W$ gauge coupling. This statement holds also at the two-loop level [488]. The G_μ scheme is thus most appropriate for describing couplings of W bosons. For Z bosons this scheme absorbs at least part of the $\Delta\rho^{(1)}$ corrections because of additional c_W factors in the coupling from the weak mixing, while the scheme is actually not appropriate for photonic couplings. However, also here it should be kept in mind that a fixed scheme with a global definition of couplings has to be employed within gauge-invariant subsets of diagrams. In most cases, it is advisable to use the G_μ scheme for couplings that involve weak bosons, although the gauge-invariant subsets of diagrams, in general, also contain internal photons. Practically, the G_μ scheme can be implemented by substituting the charge renormalization constant (153) by

$$\delta Z_e|_{G_\mu} = \frac{1}{2} \Pi^{AA}(0) - \frac{s_W}{c_W} \frac{\Sigma_T^{AZ}(0)}{M_Z^2} - \frac{1}{2} \Delta r^{(1)}, \quad (426)$$

and the r.h.s. should involve a common factor of $\alpha = \alpha_{G_\mu}$.

5.1.2. \overline{MS} scheme and running couplings

Besides the OS scheme, the \overline{MS} scheme is sometimes used for the renormalization of the EW gauge couplings. While masses could also be renormalized in the \overline{MS} scheme, a hybrid scheme where masses are defined on shell and couplings via \overline{MS} subtraction is more customary [489] and used for instance by the Particle Data Group [90]. In this section we follow the convention of Refs. [90, 489] to denote \overline{MS} parameters with a caret (not to be confused with the carets used in the BFM above).

Inspecting the UV divergences and the top-quark contributions in the OS charge renormalization constant (153),³⁵ we obtain the charge renormalization constant in the \overline{MS} scheme as

$$\delta Z_e(\mu_R^2) = -\frac{\hat{\alpha}(\mu_R^2)}{4\pi} \left[\left(\frac{7}{2} - \frac{2}{3} \sum_f N_C^f Q_f^2 \right) \left(\Delta + \ln \frac{\mu^2}{\mu_R^2} \right) - 2\theta(m_t^2 - \mu_R^2) Q_t^2 \ln \frac{\mu_R^2}{m_t^2} \right], \quad (427)$$

³⁵Explicit expressions for the 1PI contributions to the one-loop self-energies can, e.g., be found in Ref. [40].

where $\hat{\alpha} = \hat{e}^2/(4\pi)$ with the renormalized coupling \hat{e} in the $\overline{\text{MS}}$ scheme, $\sum_f N_C^f Q_f^2 = 8$, μ is the mass parameter of DR, and μ_R the renormalization scale. Here the contributions of all degrees of freedom lighter than μ_R are renormalized in the $\overline{\text{MS}}$ scheme, while the top-quark contribution is subtracted at zero momentum transfer for $m_t^2 > \mu_R^2$ to ensure decoupling.

The OS and $\overline{\text{MS}}$ couplings are related via the bare coupling by

$$(1 + \delta Z_e)e = e_0 = \left[1 + \delta Z_e(\mu_R^2)\right] \hat{e}(\mu_R^2). \quad (428)$$

This can be solved for the running $\overline{\text{MS}}$ coupling, yielding

$$\hat{\alpha}(\mu_R^2) = \frac{\alpha(0)}{1 - \Delta\hat{\alpha}(\mu_R^2)} \quad (429)$$

up to two-loop terms with

$$\begin{aligned} \Delta\hat{\alpha}(\mu_R^2) = 2 \left[\delta Z_e - \delta Z_e(\mu_R^2) \right] &= \Pi_{q \neq t}^{AA}(0) - \text{Re} \Pi_{q \neq t}^{AA}(M_Z^2) + \frac{\alpha(0)}{\pi} \left[\sum_{q \neq t} Q_q^2 \left(\frac{5}{3} - \ln \frac{M_Z^2}{\mu_R^2} \right) \right. \\ &\quad \left. - \frac{1}{3} \sum_l Q_l^2 \ln \frac{m_l^2}{\mu_R^2} - Q_t^2 \ln \frac{m_t^2}{\mu_R^2} \theta(\mu_R^2 - m_t^2) + \frac{7}{4} \ln \frac{M_W^2}{\mu_R^2} - \frac{1}{6} \right]. \end{aligned} \quad (430)$$

Here we have substituted

$$\Pi_{q \neq t}^{AA}(0) = \left[\Pi_{q \neq t}^{AA}(0) - \text{Re} \Pi_{q \neq t}^{AA}(M_Z^2) \right] + \text{Re} \Pi_{q \neq t}^{AA}(M_Z^2) \quad (431)$$

and used the perturbative one-loop expressions for the contributions of the leptons and the top quark as well as for the contribution $\text{Re} \Pi_{q \neq t}^{AA}(M_Z^2)$ of the light quarks to the vacuum polarization in the limit $\mu_R^2, M_Z^2 \gg m_f^2$. The difference $\left[\Pi_{q \neq t}^{AA}(0) - \text{Re} \Pi_{q \neq t}^{AA}(M_Z^2) \right]$ can be determined experimentally as described in Section 5.1.1. Since the top quark is decoupled for $\mu_R^2 < m_t^2$, Eq. (429) allows us to compute the running coupling $\hat{\alpha}(\mu_R^2)$ independently of m_t in this case. A similar procedure can be applied to other unknown heavy particles.

The difference between Eqs. (430) and (418) for $\mu_R^2 = M_Z^2$ is given by

$$\Delta\hat{\alpha}(M_Z^2) - \Delta\alpha(M_Z^2) = \frac{\alpha(0)}{\pi} \left[\frac{100}{27} - \frac{1}{6} - \frac{7}{4} \ln \frac{M_Z^2}{M_W^2} \right]. \quad (432)$$

Contributions of higher-order corrections to Eqs. (418) and (430) or (432) can be found in Refs. [90, 489] and references therein.³⁶

In the OS scheme, the weak mixing angle is defined according to Eq. (154) [36]. Alternatively, it can be defined in the $\overline{\text{MS}}$ scheme [483, 489–492], which is useful for comparing with predictions of grand unification. In this scheme, the weak mixing angle is related to the running electromagnetic $\hat{e}^2(\mu_R^2)$ and SU(2)_w gauge coupling $\hat{g}_2(\mu_R^2)$ as follows,

$$\hat{s}_w^2(\mu_R^2) \equiv \sin^2 \hat{\theta}_w(\mu_R^2) = \frac{\hat{e}^2(\mu_R^2)}{\hat{g}_2^2(\mu_R^2)}. \quad (433)$$

If $\hat{s}_w^2(\mu_R^2)$ is used as free parameter in a calculation, only one of the masses M_W and M_Z can be treated as a free parameter, while the other one plays the role of a derived parameter. Otherwise the parameter set would be overdetermined leading to potential gauge-invariance violation in predictions.

The pure $\overline{\text{MS}}$ counterterm $\delta\hat{s}_w^2$ can be determined from any definition of the weak mixing angle. Extracting the UV-divergent part of the OS definition (156) yields

$$\delta\hat{s}_w^2(\mu_R^2) = \hat{c}_w^2 \left[\frac{\Sigma_T^{ZZ}(M_Z^2)}{M_Z^2} - \frac{\Sigma_T^W(M_W^2)}{M_W^2} \right]_{\text{UV}} = \frac{\hat{\alpha}(\mu_R^2)}{4\pi} \left[\frac{11}{3} \hat{s}_w^2 + \frac{19}{6} \right] \left(\Delta + \ln \frac{\mu^2}{\mu_R^2} \right), \quad (434)$$

³⁶The quantity $\Delta\hat{\alpha}(M_Z^2)$ is called $(\alpha/\pi)\Delta_\gamma$ in Ref. [489].

where the UV-divergent part involves all singular terms in the form $\Delta + \ln(\mu^2/\mu_R^2)$. The running $\hat{s}_w^2(\mu_R^2)$ satisfies the renormalization-group equation

$$\mu_R^2 \frac{\partial}{\partial \mu_R^2} \hat{s}_w^2(\mu_R^2) = -\mu_R^2 \frac{\partial}{\partial \mu_R^2} \delta \hat{s}_w^2(\mu_R^2) = \frac{\hat{\alpha}(\mu_R^2)}{4\pi} \left[\frac{11}{3} \hat{s}_w^2 + \frac{19}{6} \right] + \text{higher orders.} \quad (435)$$

The running of $\hat{s}_w^2(\mu_R^2)$, as determined by Eqs. (434) and (435), receives contributions from bosonic and fermionic loops, with equal contributions from all three fermion generations. With this definition, however, the effects of a heavy top quark do in general not decouple in EW corrections. To decouple heavy-top-quark contributions several modifications in the definition of $\hat{s}_w^2(\mu_R^2)$ have been proposed in the literature. A standard choice [489] is to use the neutral-current interaction of the Z boson with a massless fermion which has the general form [492, 493]

$$\begin{aligned} \langle 0 | J_Z^\mu | \bar{f}(\bar{p}) f(p) \rangle &= V_f(q^2) \bar{v}(\bar{p}) \gamma^\mu [I_{w,f}^3 \omega_- - Q_f \hat{\kappa}_f(q^2) \hat{s}_w^2(q^2)] u(p) \\ &= V_f(q^2) \bar{v}(\bar{p}) \gamma^\mu [I_{w,f}^3 \omega_- - Q_f \kappa_f(q^2) s_w^2] u(p), \end{aligned} \quad (436)$$

where $V_f(q^2)$, $\hat{\kappa}_f(q^2)$ and its OS counterpart $\kappa_f(q^2)$ are EW form factors and $q^2 = (\bar{p} + p)^2$ is the invariant mass of the Z boson. The form factors $\hat{\kappa}_f(q^2)$ or $\kappa_f(q^2)$ get contributions from vertex corrections and from the photon-Z-boson mixing energy, and the $\overline{\text{MS}}$ counterterm can be written as [490]

$$\delta \hat{s}_w^2(\mu_R^2) = \frac{\hat{c}_w \hat{s}_w}{M_Z^2} [\Sigma_T^{AZ}(M_Z^2) + \Sigma_T^{AZ}(0)]_{\text{UV}}. \quad (437)$$

Decoupling of the top quark for $\mu_R^2 < m_t^2$ (and analogously for other heavy particles) can be incorporated by including the full top-quark contribution to $\Sigma_T^{AZ}(q^2)/q^2$ in Eq. (437) for $q^2 \rightarrow 0$ instead of using $\Sigma_T^{AZ}(M_Z^2)|_{\text{UV}}/M_Z^2$. This leads to the following counterterm [491],

$$\delta \hat{s}_w^2(\mu_R^2) = \frac{\alpha}{4\pi} \left(\Delta + \ln \frac{\mu^2}{\mu_R^2} \right) \left[\frac{11}{3} \hat{s}_w^2 + \frac{19}{6} \right] + \frac{\alpha}{\pi} \ln \frac{m_t}{\mu_R} \left[\frac{1}{3} - \frac{8}{9} \hat{s}_w^2 \right] \theta(m_t^2 - \mu_R^2). \quad (438)$$

For higher-order corrections to $\delta \hat{s}_w^2(\mu_R^2)$ we refer to Refs. [90, 489] and references therein. The scale μ_R is conveniently chosen to be M_Z for many EW processes.

The derivation of the $\overline{\text{MS}}$ renormalization constants, including their modifications for decoupling a heavy top quark, is formally significantly simplified if the background-field vertex functions are used, owing to the connection between gauge-field and gauge-coupling renormalization constants as given in Eq. (158) for the EWSM. The divergences of the gauge-coupling renormalization constants can, thus, be obtained directly from the derivatives of the relevant BFM self-energies at zero momentum transfer,

$$\delta Z_e(\mu_R^2) = \frac{1}{2} \Sigma_T'^{\hat{A}\hat{A}}(0)|_{\overline{\text{UV}}}, \quad \delta \hat{s}_w^2(\mu_R^2) = \hat{c}_w \hat{s}_w \frac{\Sigma_T'^{\hat{A}\hat{Z}}(M_Z^2)|_{\overline{\text{UV}}}}{M_Z^2} = \hat{c}_w \hat{s}_w \Sigma_T'^{\hat{A}\hat{Z}}(0)|_{\overline{\text{UV}}}, \quad (439)$$

where $\overline{\text{UV}}$ here means to include besides all UV-divergent parts the full top-quark loops to ensure decoupling. In the last equation we used the fact that $\Sigma_T'^{\hat{A}\hat{Z}}(q^2)$ vanishes for $q^2 = 0$ and that its divergent part is proportional to q^2 . This procedure directly reproduces the results given in Eqs. (427) and (438).

Finally, we point out that the relation between the muon decay constant and the SM parameters somewhat changes in the $\overline{\text{MS}}$ scheme [494],

$$\sqrt{2} G_\mu = \frac{\pi \alpha(0)}{M_W^2 \hat{s}_w^2(M_Z^2)(1 - \Delta \hat{r}_W)} \quad (440)$$

with the modified EW correction $\Delta \hat{r}_W$. Moreover, the modified relation between the weak mixing angle and the OS gauge-boson masses leads to a non-trivial ρ parameter [495],

$$\hat{\rho} = \frac{c_w^2}{\hat{c}_w^2(M_Z^2)} = \frac{M_W^2}{\hat{c}_w^2(M_Z^2) M_Z^2}. \quad (441)$$

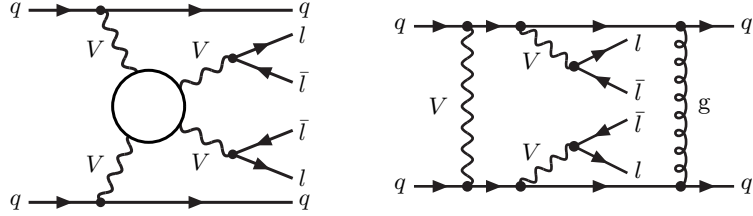


Figure 5: Structure of vector-boson scattering at hadron colliders (left) and an example for a loop diagram for $qq \rightarrow qq\bar{l}\bar{l}l\bar{l}$ (right).

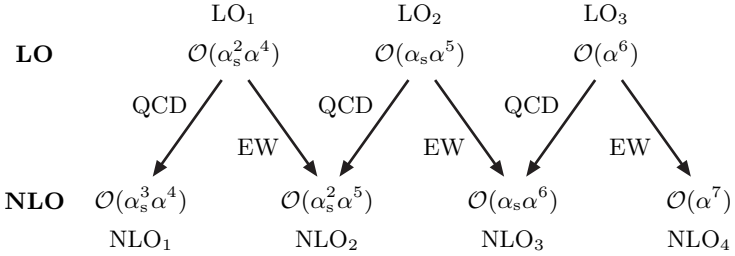


Figure 6: Contributing orders at LO and NLO for the processes $pp \rightarrow 2 \text{ jets} + 4 \text{ leptons} + X$.

5.2. The structure of NLO electroweak corrections

5.2.1. EW and QCD corrections for general processes

The LO of simple processes receives contributions of a single power in the strong and EW couplings, i.e. the LO cross section is proportional to $\alpha_s^n \alpha^m$ with unique n and m . In this case, the NLO corrections can be trivially separated into NLO QCD corrections and NLO EW corrections of the orders $\alpha_s^{n+1} \alpha^m$ and $\alpha_s^n \alpha^{m+1}$, respectively. Since both contributions are characterized by complete contributions to physical matrix elements in the corresponding orders of the couplings, they are individually gauge invariant.

For general processes, however, the LO matrix element gets contributions of different orders in the strong and EW couplings. While the different sizes of the strong and EW coupling constants suggest a hierarchy of contributions, this is not always respected in specific processes. Moreover, in some cases a formally subleading contribution is of specific interest in view of a particular physical ingredient.

An example in this respect is provided by vector-boson scattering (VBS), i.e. processes of the form $pp \rightarrow 2 \text{ jets} + 4 \text{ leptons} + X$. The LO matrix element receives purely EW contributions of order $\mathcal{O}(e^6)$ as well as QCD-induced contributions of order $\mathcal{O}(g_s^2 e^4)$. While the former involve the physically interesting VBS diagrams (cf. Fig. 5 left), the latter dominate the complete cross section for most final states. The LO cross section, derived from squared matrix elements, then receives contributions of three different orders, the EW contributions of $\mathcal{O}(\alpha^6)$, the QCD-induced contributions of $\mathcal{O}(\alpha^4 \alpha_s^2)$, and the interference contributions of $\mathcal{O}(\alpha^5 \alpha_s)$.

This tower of contributions proliferates at higher orders as illustrated in Fig. 6. There are QCD corrections of relative order $\mathcal{O}(\alpha_s)$ and EW corrections of relative order $\mathcal{O}(\alpha)$ to each LO contribution, leading to four different NLO contributions: $\mathcal{O}(\alpha^7)$, $\mathcal{O}(\alpha_s \alpha^6)$, $\mathcal{O}(\alpha_s^2 \alpha^5)$, and $\mathcal{O}(\alpha_s^3 \alpha^4)$. The order $\mathcal{O}(\alpha^7)$ contributions are the NLO EW corrections to the EW-induced LO processes [333, 340]. The order $\mathcal{O}(\alpha_s^3 \alpha^4)$ contributions furnish the QCD corrections to the QCD-induced process [496–500]. For the orders $\mathcal{O}(\alpha_s \alpha^6)$ and $\mathcal{O}(\alpha_s^2 \alpha^5)$, a simple separation of the EW-induced process and the QCD-induced process is not possible anymore, and only the complete orders are gauge independent. In fact, there are loop diagrams, like the one in the right of Fig. 5, that cannot be attributed to one of these processes. Thus, the order $\mathcal{O}(\alpha_s \alpha^6)$ contains QCD corrections to the VBS process as well as EW corrections to the LO interference. The QCD corrections were originally computed in the VBS approximation in Refs. [500–506], where the s -channel diagrams as well as the interference of t - and u -channel diagrams are neglected. In this approximation, the interferences of the LO VBS and QCD-induced contributions are neglected, and the order $\mathcal{O}(\alpha_s \alpha^6)$ contains only QCD corrections. Similarly to the $\mathcal{O}(\alpha_s \alpha^6)$, also the order $\mathcal{O}(\alpha_s^2 \alpha^5)$ contains EW corrections to the QCD-induced contribution as well as QCD corrections to the LO interference.

Other examples where a tower of contributions appears at LO and NLO are dijet production [362, 507] and top–antitop production processes [328].

The treatment of simultaneous expansions in the two coupling constants α_s and α in `MADGRAPH5_AMC@NLO` is discussed in Ref. [68]. In Refs. [327, 328, 362] the notation LO_x and NLO_x for the different contributions was introduced. Here LO_1 stands for the LO contribution with highest power in the strong coupling, say the contribution of order $\alpha_s^n \alpha^m$. Then, LO_x indicates the contribution of order $\alpha_s^{n+1-x} \alpha^{m+x-1}$ and NLO_x the one of order $\alpha_s^{n+2-x} \alpha^{m+x-1}$. For the process $\text{pp} \rightarrow t\bar{t}t\bar{t} + X$ [364] five different coupling orders show up at LO ($\text{LO}_1, \dots, \text{LO}_5$), leading to six different coupling combinations at NLO ($\text{NLO}_1, \dots, \text{NLO}_6$).

5.2.2. Disentangling weak and electromagnetic corrections

For phenomenological applications and the understanding of the structure of the EW corrections it is useful to split NLO amplitudes of a given order $\alpha_s^n \alpha^m$ further into gauge-invariant parts as far as possible. We restrict the following discussion to the one-loop level.

For arbitrary processes, the subset of diagrams (loop diagrams and counterterms) that involve a closed fermion loop form a gauge-invariant subset, often called *fermionic* NLO corrections. This is evident from the fact that adding further fermion generations to the SM (in the absence of generation mixing) would not violate its gauge invariance. The remaining NLO corrections are called *bosonic*.

It is often desirable to split the bosonic NLO corrections further into an *electromagnetic* (or photonic) part and a purely *weak* part. In a gauge-invariant way this is possible for processes that proceed in LO via neutral-current interactions only, but not for processes that involve W bosons (and charged would-be Goldstone bosons) at LO. This fact can, for instance, be seen as follows. Removing the W bosons and charged would-be Goldstone bosons from the SM Lagrangian results in a Lagrangian for a spontaneously broken $U(1)_{\text{em}} \times U(1)_Z$ gauge theory with the same fermion content, the same electromagnetic couplings, the same neutral-current couplings, and the same neutral Higgs couplings as in the SM. Here, $U(1)_{\text{em}}$ refers to the electromagnetic gauge group with the photon as massless gauge boson and $U(1)_Z$ to an abelian gauge symmetry with the Z boson as gauge boson and the associated weak charges of the (left- and right-handed) fermions and neutral scalars (H, χ) given by

$$Q_Z = \frac{I_w^3}{c_w s_w} - \frac{s_w}{c_w} Q. \quad (442)$$

The resulting Lagrangian defines a consistent and renormalizable field theory and, thus, isolates gauge-invariant subsets of SM contributions to arbitrary gauge-invariant quantities. In particular, it provides a gauge-invariant subset of the full SM corrections for processes involving only fermions, photons, Z bosons, and neutral scalar bosons. Since the $U(1)_{\text{em}} \times U(1)_Z$ gauge group is abelian and the photon couples only to fermions, the photon–fermion couplings can be modified arbitrarily within this theory (while keeping all other couplings fixed) without destroying its gauge invariance. Thus, gauge-invariant subsets can be further classified according to independent powers of the fermion–photon couplings. In particular, for processes involving no charged scalar or vector bosons at LO, this implies that the bosonic corrections of the full SM can be split into three gauge-invariant subsets: 1) contributions resulting from photon exchange between fermions (i.e. the QED corrections), 2) corrections resulting from Z-, χ -, or Higgs-boson exchange, and 3) corrections that involve W- or ϕ -boson exchange. The photonic corrections can be further split into smaller gauge-invariant subsets by considering the coefficients of the global charge factors $Q_1 Q_2$ of different fermions.

In practice, the gauge-invariant decomposition of the bosonic NLO EW corrections $\Delta\sigma_{\text{NLO}}$ into a purely weak part $\Delta\sigma_{\text{NLO}}^{\text{weak}}$ and a photonic part $\Delta\sigma_{\text{NLO}}^{\text{phot}}$ can be performed as follows for a process that does not involve charged-current interactions at LO. The virtual photonic part is defined as the set of all diagrams with at least one photon in the loop coupling to the (charged) fermion lines. These diagrams are obtained upon inserting one additional photon line into a LO diagram and do not contain W bosons. The weak contribution is then the set of all remaining bosonic one-loop diagrams, which may also involve W bosons. The contributions to the renormalization constants have to be split accordingly.

As an example we consider the production of two different lepton–antilepton pairs in proton–proton scattering [508], assuming massless leptons and massless incoming quarks. Out of the eight diagrams shown in Fig. 7 only the first pair with exclusively Z bosons in the loop belongs to the weak corrections while the three other pairs with one or two photons in the loop are part of the electromagnetic corrections. Note that the criterion for the splitting considers

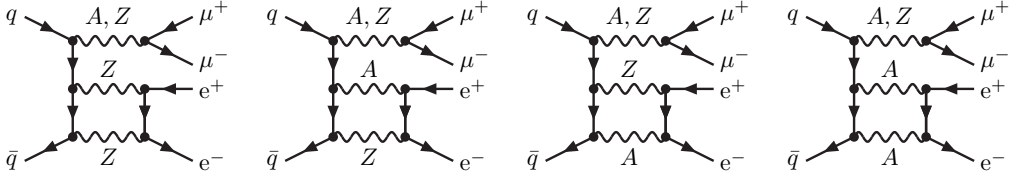


Figure 7: Illustration of the splitting of EW corrections into purely weak (first diagram) and photonic (2nd-4th diagrams) contributions for a sample process that proceeds via neutral-current interactions at tree level.

only the vector bosons in the loop, while it does not refer to the tree-level part of the diagram. The contributions to the field renormalization constants of the fermions are decomposed in an analogous manner. Note that the photon-exchange contributions to the renormalization constants for the W-boson mass and the weak mixing angle count as weak corrections. Since only loops with internal photons coupling to fermions lead to soft and collinear divergences, the purely weak contribution is IR finite. The IR singularities of the virtual photonic corrections are cancelled by the real photonic corrections, which are purely photonic corrections.

5.3. Goldstone-boson equivalence theorem

An important consequence of the Slavnov–Taylor identities in spontaneously broken gauge theories is the *Goldstone-boson equivalence theorem* [509–511]. It states that the amplitudes for reactions involving high-energetic, longitudinal vector bosons are asymptotically proportional to the amplitudes where those vector bosons are replaced by their associated would-be Goldstone bosons. The practical virtue of the Goldstone-boson equivalence theorem is twofold. First of all, it facilitates the calculation of cross sections for reactions with longitudinal vector bosons at high energies, as the amplitudes for external scalars are much easier to evaluate. On the other hand, it might allow us to derive information on the mechanism of spontaneous symmetry breaking from the experimental study of longitudinal vector bosons.

The Goldstone-boson equivalence theorem can be derived starting from the Slavnov–Taylor identities (47) and (48) (see for instance Ref. [83, 512]). For the case of one external W boson the corresponding equation (47) reads

$$0 = \left\langle T(\partial^\mu W_\mu^\mp \pm i M_W \xi'_W \phi^\mp) \prod_l \Psi_{I_l}^{\text{on-shell,phys.}} \right\rangle. \quad (443)$$

This identity holds for unrenormalized quantities, but also for renormalized quantities in the renormalization scheme, where the linear gauge-fixing functions are not renormalized.

In order to obtain relations for S -matrix elements, one truncates the external legs of the considered longitudinal vector bosons and transforms to momentum space. In Ref. [513] it was realized that the truncation leads to non-trivial proportionality factors originating from higher-order corrections. The resulting relation for a W boson can be written as [83]

$$k^\nu \left\langle T \underline{W}_\nu^\pm \prod_l \Psi_{I_l}^{\text{on-shell,phys.}} \right\rangle = \pm M_W A^W(k^2) \left\langle T \underline{\phi}^\pm \prod_l \Psi_{I_l}^{\text{on-shell,phys.}} \right\rangle, \quad (444)$$

where $\langle T \underline{W}^\pm(k) \dots \rangle$ and $\langle T \underline{\phi}^\pm(k) \dots \rangle$ denote Green functions with the W and ϕ legs truncated, respectively. We recall our conventions from Appendix B that the fields in Eq. (443) are outgoing, but the underlined field labels for the truncated lines in Eq. (444) correspond to incoming fields; the momentum k is incoming. Analogous equations can be derived for the Z-boson sector.

At LO the correction factors $A^V(k^2)$ are equal to one; at higher orders they depend on the gauge and the renormalization of the unphysical sector [512]. To derive explicit expressions for $A^V(k^2)$ (see, e.g., Ref. [83]), the matrix-valued propagator for the external vector–scalar system of V and its corresponding Goldstone field S is truncated from the full (reducible, connected) Green functions; for the Z-boson this system includes the mixing to the photon as well. Subsequently $A^V(k^2)$ can be directly read off in terms of propagator functions G^{ab} of the VS system and expressed in terms of 2-point vertex functions Γ^{ab} , which result from the inverse of the matrix (G^{ab}) . Using the Slavnov–Taylor

identities (50) for the propagators G^{ab} , helps to bring the factors $A^V(k^2)$ into a simple final form. In terms of unrenormalized Γ^{ab} in the 't Hooft gauge, the $A^V(k^2)$ read

$$\begin{aligned} A^W(k^2) &= \frac{k^2/\xi_W + \Gamma_L^{WW}(k^2)}{M_W(M_W + \Gamma^{W\phi}(k^2))} = r_H \frac{k^2/\xi_W + \Gamma_{1PI,L}^{WW}(k^2)}{M_W(M_W + \Gamma_{1PI}^{W\phi}(k^2))}, \\ A^Z(k^2) &= \frac{k^2/\xi_Z + \Gamma_L^{ZZ}(k^2)}{M_Z(M_Z - i\Gamma^{Z\chi}(k^2))} = r_H \frac{k^2/\xi_Z + \Gamma_{1PI,L}^{ZZ}(k^2)}{M_Z(M_Z - i\Gamma_{1PI}^{Z\chi}(k^2))}, \end{aligned} \quad (445)$$

where the factor r_H depends on the tadpole scheme (see Section 3.1.6):

$$r_H^{\text{PRTS}} = 1, \quad r_H^{\text{FJTS}} = 1 + \frac{T^H}{M_H^2 v}. \quad (446)$$

This difference originates from the fact that the unrenormalized vertex functions are derived from the bare Lagrangian and do include besides the explicit loop contributions also contributions from tadpole counterterms, as already pointed out in Eq. (141) for the 2-point vertex functions and the corresponding definition of the self-energies Σ . The Lorentz decompositions of the vector–vector 2-point functions are given in Eq. (105), those for the vector–scalar 2-point functions read

$$\Gamma_\mu^{W^\pm\phi^\mp}(k, -k) = \pm k_\mu \Gamma^{W\phi}(k^2), \quad \Gamma_\mu^{Z\chi}(k, -k) = k_\mu \Gamma^{Z\chi}(k^2). \quad (447)$$

Note that the first equality in Eq. (445) for each $A^V(k^2)$ holds to all orders, but the second equality is restricted to the one-loop approximation with respect to the tadpole contribution T^H . Splitting the vertex functions into LO contributions and self-energies Σ according to

$$\Gamma_L^{VV}(k^2) = M_V^2 - \frac{k^2}{\xi_V} - \Sigma_L^{VV}, \quad \Gamma^{W\phi}(k^2) = \Sigma^{W\phi}(k^2), \quad \Gamma^{Z\chi}(k^2) = \Sigma^{Z\chi}(k^2), \quad (448)$$

the unrenormalized correction factors at the one-loop level read

$$\begin{aligned} A^W(k^2) &= 1 - \frac{\Sigma_L^{WW}(k^2)}{M_W^2} - \frac{\Sigma^{W\phi}(k^2)}{M_W} = r_H - \frac{\Sigma_{1PI,L}^{WW}(k^2)}{M_W^2} - \frac{\Sigma_{1PI}^{W\phi}(k^2)}{M_W}, \\ A^Z(k^2) &= 1 - \frac{\Sigma_L^{ZZ}(k^2)}{M_Z^2} + i \frac{\Sigma^{Z\chi}(k^2)}{M_Z} = r_H - \frac{\Sigma_{1PI,L}^{ZZ}(k^2)}{M_Z^2} + i \frac{\Sigma_{1PI}^{Z\chi}(k^2)}{M_Z}. \end{aligned} \quad (449)$$

In the renormalization scheme where the gauge-fixing functions are not renormalized, the renormalized correction factors $A_R^V(k^2)$ are given by

$$A_R^W(k^2) = \frac{k^2/\xi_W + \Gamma_{R,L}^{WW}(k^2)}{M_W(M_W + \Gamma_R^{W\phi}(k^2))}, \quad A_R^Z(k^2) = \frac{k^2/\xi_Z + \Gamma_{R,L}^{ZZ}(k^2)}{M_Z(M_Z - i\Gamma_R^{Z\chi}(k^2))}. \quad (450)$$

Inserting the decomposition of the renormalized vertex functions into one-loop self-energies and counterterms, we get

$$A_R^W(k^2) = A^W(k^2) + \frac{1}{2}\delta Z_W - \frac{1}{2}\delta Z_\phi + \frac{\delta M_W^2}{2M_W^2}, \quad A_R^Z(k^2) = A^Z(k^2) + \frac{1}{2}\delta Z_{ZZ} - \frac{1}{2}\delta Z_\chi + \frac{\delta M_Z^2}{2M_Z^2} \quad (451)$$

in one-loop approximation, where δZ_ϕ and δZ_χ are field renormalization constants for the would-be Goldstone fields that render Green functions involving these fields as well as the factors $A_R^V(k^2)$ finite. Note that the tadpole counterterms are already contained in the unrenormalized functions $A^V(k^2)$. The renormalized correction factors are independent of the tadpole scheme, since all tadpole contributions cancel in the sum of the unrenormalized factors $A^V(k^2)$ and the contributions of the mass counterterms δM_V^2 .

Upon expressing the external momentum of the vector boson that appears explicitly in the identity Eq. (444) by the corresponding longitudinal polarization vector $\epsilon_L^\mu(k)$ using

$$\epsilon_L^\mu(k) = \frac{k^\mu}{M_W} + O\left(\frac{M_W}{k^0}\right), \quad (452)$$

for the case of a single external longitudinal W boson, one arrives at

$$\langle \dots | S | W_L^\pm(k) \dots \rangle = \pm A_R^W(M_W^2) \langle T \underline{\phi}^\pm(k) \dots \rangle + O\left(\frac{M_W}{k^0}\right), \quad (453)$$

and similarly for a single external longitudinal Z boson

$$\langle \dots | S | Z_L(k) \dots \rangle = i A_R^Z(M_Z^2) \langle T \underline{\chi}(k) \dots \rangle + O\left(\frac{M_Z}{k^0}\right), \quad (454)$$

where the left-hand sides represent S -matrix elements. All quantities are renormalized in the complete OS scheme as defined in Section 3.1.3, so that no wave-function renormalization corrections for the external vector bosons appear, because all corrections to the propagator residues and all mixing effects of OS particles are absorbed by the field renormalization. The $O(M_V/k^0)$ terms in Eqs. (453) and (454) describe mass-suppressed terms relative to the leading canonical mass dimension of the inspected Green function, i.e. if the explicit terms on the r.h.s. of Eqs. (453) and (454) are already mass suppressed, the r.h.s. does not predict the leading term explicitly.

The relations (453) and (454) can be generalized to S -matrix elements with more longitudinal vector bosons, e.g. for n charged W bosons:

$$\langle \dots | S | \left(\prod_n W_L^\pm(k_n) \right) \dots \rangle = \left(\prod_n [\pm A_R^W(M_W^2)] \right) \langle T \left(\prod_n \underline{\phi}^\pm(k_n) \right) \dots \rangle + O\left(\frac{M_W}{k_n^0}\right). \quad (455)$$

The inclusion of longitudinal Z bosons is obtained via an obvious generalization. The relations (455) and their generalization constitute the Goldstone-boson equivalence theorem. It relates S -matrix elements involving longitudinal gauge bosons to matrix elements involving the corresponding would-be Goldstone-boson fields in the high-energy limit.

Finally, we briefly consider the derivation of the Goldstone-boson equivalence theorem within the BFM, which was discussed in detail in Ref. [115]. The major result of that paper is that the renormalized correction factors reduce to one,

$$A_R^{\hat{V}}(k^2) \Big|_{\text{BFM}} = 1, \quad \hat{V} = \hat{W}, \hat{Z}, \quad (456)$$

in all orders of perturbation theory if the BFM renormalization scheme [107] is employed that preserves all BFM Ward identities for renormalized vertex functions, as outlined in Section 3.2. In Ref. [115], this fact was proven within the PRTS, but the all-order result (456) does not depend on the tadpole treatment. It should, however, be realized that the final form of Eqs. (453)–(455) for S -matrix elements receives another UV-finite correction originating from the fact that the employed BFM renormalization scheme does not normalize the residues of the W and Z propagators to one. In detail, each factor $A_R^{\hat{V}}(k^2)$ has to be replaced by the wave-function correction factor $R_{\hat{V}}^{1/2}$, where $R_{\hat{V}}$ in one-loop approximation is given by

$$R_{\hat{V}} = 1 - \widetilde{\text{Re}} \left. \frac{\partial \Sigma_{R,T}^{\hat{V}\hat{V}}(k^2)}{\partial k^2} \right|_{k^2=M_V^2}. \quad (457)$$

The generalization of this factor beyond one loop is described in Ref. [115] as well.

5.4. Electroweak corrections at high energies

At energies that are large compared to the masses of the EW gauge bosons, the EW corrections can become large due to the appearance of large logarithms that result from the virtual exchange of soft and/or collinear massive weak

gauge bosons [514–522]. The leading contributions from the soft–collinear limit are known as *Sudakov logarithms* [523]. At NLO, the leading and subleading terms are of the form $(\alpha/s_W^2) \ln^2(Q^2/M_W^2)$ and $(\alpha/s_W^2) \ln(Q^2/M_W^2)$, respectively, where Q denotes the energy scale of the hard scattering process, which is typically determined by the centre-of-mass energy \sqrt{s} of the partonic process. In QED and QCD the corresponding double logarithms resulting from virtual photons and gluons are cancelled against the related real-emission corrections, and the remaining single logarithms can be absorbed into parton distribution and fragmentation functions. However, since the masses of the W and Z bosons provide a physical cutoff and since the EW charges are not confined, the radiated real W or Z bosons can be experimentally reconstructed to a large extent. Consequently, real massive vector-boson radiation needs not be included in the definition of cross sections, and typically only a small fraction that remains unresolved compensates for part of the virtual corrections [524]. Thus, at high scales $Q \gg M_W$, which are accessible at the LHC and future colliders, the Sudakov logarithms can produce large corrections. Since the real corrections that would cancel the enhanced virtual corrections in fully inclusive quantities result from separate process classes (with their own squared matrix elements $|\mathcal{M}|^2$) and are thus positive, the latter are negative. In the TeV range these negative corrections typically amount to tens of percent rendering the EW corrections very significant.³⁷

The *Sudakov regime* is characterized by the situation that all invariants $s_{ij} = (p_i + p_j)^2$ formed from pairs of external particles’ four-momenta p_i (taken all incoming) become large ($|s_{ij}| \gg M_W^2$). In this limit, the large logarithms are associated with soft and/or collinear singularities arising if the masses are small compared to the relevant energies. Since these singularities are associated with external particles of the scattering processes and thus universal [365], this allows us to derive general process-independent results for the EW high-energy logarithms. We note that this applies to processes that are not mass suppressed, i.e. the corresponding matrix elements scale with the scattering energy according to their mass dimension. For mass-suppressed processes, like Higgs production in vector-boson fusion or Higgs-strahlung off a vector boson, the EW logarithms may have a different structure.

The structure of EW corrections in the Sudakov regime has been investigated in detail at $\mathcal{O}(\alpha)$ and beyond by several groups (see e.g. Refs. [520–522, 525–535] and references therein). As described for example in Refs. [527, 528, 532, 535], the leading EW logarithmic corrections, which are enhanced by large factors $L = \ln(s_{ij}/M_W^2)$, can be divided into an $SU(2)_W \times U(1)_Y$ -symmetric part, an electromagnetic part related to the running of EW couplings below M_W , and a subleading part induced by the mass difference between W and Z bosons. The leading (Sudakov) logarithms $\propto (\alpha L^2)^n$ of electromagnetic origin cancel between virtual and real (soft) photonic bremsstrahlung corrections, so that the only source of leading logarithms is the symmetric EW part, which can be characterized by comprising W bosons, Z bosons, and photons of a common mass M_W . These leading EW Sudakov corrections can be obtained to all orders from the respective NLO result via exponentiation [520]. For the subleading EW high-energy logarithms, corresponding resummations are not rigorously proven, but the corrections are expected to obey *IR evolution equations* [521, 536], a statement that is backed by explicit two-loop calculations [532, 535, 537].

A general result for the large logarithmic contributions at one loop was derived in Refs. [527, 528], and a general method for the resummation of these logarithms was developed in Refs. [538, 539] based on *soft–collinear effective theory* [540–543]. Owing to these results, the resummed EW corrections to all hard scattering processes that are not mass suppressed and do not involve kinematic scales of the order of M_W , such as processes with intermediate resonances, are known explicitly at next-to-leading logarithmic (NLL) order [544–546] and can be incorporated into LHC cross-section calculations.

We note that the EW logarithmic corrections are independent of the quark-mixing matrix, because in the high-energy limit, the masses of the light quarks are irrelevant, so that the quark-mixing matrix can be replaced by the unit matrix. Consequently, quark mixing only enters the underlying LO matrix elements, while the relative correction factors to these do not depend on it.

5.4.1. General results for one-loop electroweak logarithmic corrections

At the one-loop level, the single and double EW logarithms result from soft and/or collinear singularities and, thus, have a universal form. General results for processes that are not mass suppressed were presented in Ref. [527], and the factorization of these logarithms in the EWSM was proven in Ref. [528]. These results were derived in the

³⁷The fact that EW corrections at energies above the EW scale are dominated by large single and double logarithms has been observed in the 1990s in various calculations. See, for instance, Refs. [514–519].

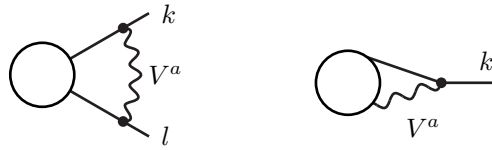


Figure 8: The types of Feynman diagrams leading to double-logarithmic corrections (left) and single-logarithmic corrections (right).

't Hooft–Feynman gauge in the broken phase of the EW theory, i.e. with fields in the physical basis. Upon choosing the mass scale μ of DR of the order of the energy of the scattering process, only mass-singular logarithms of the form $\ln(\mu^2/M^2)$ or $\ln(s/M^2)$ are large, where M is of the order of M_W . Field renormalization is fixed in such a way that no separate wave-function renormalization is required (see Section 3.1.3), and for parameter renormalization the OS scheme is adopted. The fact that the polarization vector of longitudinal gauge bosons involves the gauge-boson mass in the denominator complicates the extraction of the logarithmic corrections in the massless limit. This problem is circumvented by using the Goldstone-boson equivalence theorem [509–511] taking into account correction factors from higher-order contributions [513], as discussed in Section 5.3. All external particles are considered as on shell and incoming. Outgoing particles are obtained via crossing symmetry.

In this setup, EW logarithms are due to the following contributions:

- Double-logarithmic contributions result from loop diagrams where soft–collinear gauge bosons are exchanged between pairs of external legs (see Fig. 8 left). These contributions can be obtained within the *eikonal approximation*, i.e. in the approximation where the momenta of the soft–collinear gauge bosons can be neglected everywhere but in the singular propagators. In fact, the eikonal approximation includes already all contributions associated with soft singularities, i.e. singularities related to the vanishing of a gauge-boson loop momentum. The soft contributions associated with single external lines are treated separately together with the collinear contributions in the field renormalization constants.
- Single-logarithmic contributions result from the emission of virtual collinear gauge bosons from external lines [365] (see Fig. 8 right). These contributions are extracted in the collinear limit by means of Ward identities and are found to factorize into the LO amplitude times collinear factors [528].
- Additional single-logarithmic contributions originating from soft or collinear regions are contained in the field renormalization constants.
- Single-logarithmic contributions of UV origin show up in the parameter renormalization constants, i.e. the renormalization of the electromagnetic coupling, the weak mixing angle, the Yukawa couplings, and the scalar self-coupling. The corresponding logarithms are controlled by the renormalization-group equations and associated to the running of the couplings.

In the following, we summarize the results of Ref. [527] on the structure of EW high-energy logarithms at NLO. We concentrate on logarithms that involve the ratio of the high-energy scale \sqrt{s} and a generic EW mass for which we choose M_W , since these logarithms give rise to the most important corrections at high energies for many processes. These EW logarithms could directly be derived in the symmetric basis with a subsequent transformation to the physical basis. This is, however, not the case for the electromagnetic logarithms and terms involving $\ln(M_W/M_Z)$, which can be found in Ref. [527] as well, but are not reproduced here. While the former cancel to a large extent against similar logarithms in the real electromagnetic corrections, the latter are of the order of the finite terms. We do not consider enhanced logarithms from real corrections in this section either.

The LO matrix element for the generic process

$$\varphi_{i_1}(p_1) \dots \varphi_{i_n}(p_n) \rightarrow 0 \quad (458)$$

is denoted as $\mathcal{M}_0^{i_1 \dots i_n}(p_1, \dots, p_n)$. The particles (or antiparticles) φ_{i_k} correspond to the components of the various multiplets φ present in the SM. Chiral fermions and antifermions are represented by f^κ and \bar{f}^κ , respectively, with the chirality $\kappa = R, L$. The gauge bosons are denoted by $V^a = A, Z, W^\pm$, and can be transversely (T) or longitudinally (L) polarized. The components Φ_i of the scalar doublet correspond to the physical Higgs particle H and the would-be Goldstone bosons χ, ϕ^\pm , which are used to describe the longitudinally polarized massive gauge bosons Z_L and W_L^\pm .

with help of the Goldstone-boson equivalence theorem (see Section 5.3). In logarithmic approximation, the correction $\delta\mathcal{M}$ to a matrix element takes the form

$$\delta\mathcal{M}^{i_1 \dots i_n}(p_1, \dots, p_n) = \mathcal{M}_0^{i'_1 \dots i'_n}(p_1, \dots, p_n) \delta_{i'_1 i_1 \dots i'_n i_n}, \quad (459)$$

i.e. it can be written as a matrix product of the LO matrix element and a relative correction δ . The latter is split into various contributions according to their origin:

$$\delta = \delta^{\text{LSC}} + \delta^{\text{SSC}} + \delta^{\text{C}} + \delta^{\text{PR}}. \quad (460)$$

The leading and subleading soft-collinear logarithms are denoted by δ^{LSC} and δ^{SSC} , respectively, the collinear logarithms by δ^{C} , and the logarithms resulting from parameter renormalization by δ^{PR} . Note that in Eq. (459) and in the following equations, sums over $i'_1 \dots i'_n$ are understood.

Considering the diagrams of the form shown in the left of Fig. 8, using the eikonal approximation and neglecting all terms proportional to masses, the soft-collinear one-loop corrections read

$$\begin{aligned} \delta^{\text{eik}} \mathcal{M}^{i_1 \dots i_n} &= \sum_{k,l=1}^n \sum_{\substack{V^a=A,Z,W^\pm \\ l < k}} (-4ie^2)(p_k p_l) I_{i'_k i_k}^{V^a}(k) I_{i'_l i_l}^{\bar{V}^a}(l) \mathcal{M}_0^{i_1 \dots i'_k \dots i'_l \dots i_n} \\ &\quad \times \int \frac{d^4 q}{(2\pi)^4} \frac{1}{(q^2 - M_{V^a}^2)[(q + p_k)^2 - m_k^2][(q - p_l)^2 - m_l^2]} \\ &= \sum_{k,l=1}^n \sum_{\substack{V^a=A,Z,W^\pm \\ l < k}} \frac{e^2}{4\pi^2} (p_k p_l) I_{i'_k i_k}^{V^a}(k) I_{i'_l i_l}^{\bar{V}^a}(l) \mathcal{M}_0^{i_1 \dots i'_k \dots i'_l \dots i_n} C_0(p_k, -p_l, M_{V^a}^2, m_k^2, m_l^2) \\ &\sim \frac{1}{2} \sum_{\substack{k,l=1 \\ l \neq k}}^n \sum_{\substack{V^a=A,Z,W^\pm}} I_{i'_k i_k}^{V^a}(k) I_{i'_l i_l}^{\bar{V}^a}(l) \mathcal{M}_0^{i_1 \dots i'_k \dots i'_l \dots i_n} \frac{\alpha}{4\pi} \left[\ln^2 \frac{s_{kl}}{M_{V^a}^2} - \delta_{V^a A} \ln^2 \frac{m_k^2}{m_\gamma^2} \right]. \end{aligned} \quad (461)$$

While in the last line all potentially large logarithms in the Sudakov regime are kept, in the following we only retain terms involving logarithms of ratios of large energy scales $s_{kl} = (p_k + p_l)^2$ and the W-boson mass squared. The couplings of the external fields φ_i to the gauge bosons V^a in the eikonal approximation are denoted by $ieI_{ii'}^{V^a}(\varphi)$. To be precise, these couplings correspond to the $V^a \bar{\varphi}_i \varphi_{i'}$ vertex, where all fields are considered incoming, and $\bar{\varphi}$ denotes the charge conjugate of φ . The couplings of antiparticles are related to the couplings of the particles as

$$ieI_{ii'}^{\bar{V}^a}(\bar{\varphi}) = (ieI_{ii'}^{V^a}(\varphi))^*. \quad (462)$$

Furthermore, C_0 is the scalar 3-point function as defined in Section 3.4.3. In the last step in Eq. (461) the high-energy expansion of the scalar integral [547] is inserted with the (infinitesimal) photon mass m_γ as regulator.

The single collinear logarithms result from the type of diagrams shown on the right of Fig. 8 and from the field renormalization constants, which are calculated separately. In order to avoid double counting, the contributions of the field renormalization constants and those in the soft-collinear corrections have to be subtracted as illustrated here:

$$\begin{aligned} \sum_{V^a=A,Z,W^\pm} \left\{ \begin{array}{c} \text{Diagram: } \text{circle} \text{---} \text{line} \text{---} k \\ \text{with } V^a \text{ label} \end{array} - \begin{array}{c} \text{Diagram: } \text{circle} \text{---} \text{line} \text{---} k \\ \text{with } V^a \text{ label} \end{array} \right. \\ \left. - \sum_{l \neq k} \left[\begin{array}{c} \text{Diagram: } \text{circle} \text{---} \text{line} \text{---} k \\ \text{with } V^a \text{ label} \\ \text{---} \text{line} \text{---} l \end{array} \right]_{\text{eik. appr.}} \right\}_{\text{coll.}} = \delta^{\text{coll}}(k) \begin{array}{c} \text{Diagram: } \text{circle} \text{---} k \end{array}. \end{aligned} \quad (463)$$

Using Ward identities resulting from the BRS invariance of the complete EWSM, the factorization of the collinear logarithms is proven, and the collinear factors $\delta^{\text{coll}}(k)$ are determined for the various fields of the EWSM in Ref. [528].

(a) *Leading soft-collinear contributions*

The leading soft-collinear contributions are the double-logarithmic contributions, arising from Eq. (461) with the different kinematical invariants replaced by one high-energy scale s . Upon using $SU(2)_W \times U(1)_Y$ invariance,

$$0 = ie \sum_{k=1}^n I_{i'_k i_k}^{V^a}(k) \mathcal{M}^{i_1 \dots i'_k \dots i_n}, \quad (464)$$

the leading soft-collinear contributions can be cast into a single sum over external legs,

$$\delta^{\text{LSC}} \mathcal{M}^{i_1 \dots i_n} = \sum_{k=1}^n \delta_{i'_k i_k}^{\text{LSC}}(k) \mathcal{M}_0^{i_1 \dots i'_k \dots i_n}, \quad (465)$$

with the correction factors

$$\delta_{i'_k i_k}^{\text{LSC}}(k) = -\frac{1}{2} C_{i'_k i_k}^{\text{EW}}(k) L(s), \quad (466)$$

involving the double logarithm

$$L(s) = \frac{\alpha}{4\pi} \ln^2 \frac{s}{M_W^2}. \quad (467)$$

The EW Casimir operator C^{EW} is defined from the eikonal couplings $I^{V^a}(\varphi)_{ii'}$ of the external fields φ_i to the gauge bosons V^a as

$$C^{\text{EW}} = \sum_{V^a=A,Z,W^\pm} I^{V^a} I^{\bar{V}^a} = \frac{1}{c_w^2} \left(\frac{Y_w}{2} \right)^2 + \frac{1}{s_w^2} I_w (I_w + 1) \quad (468)$$

with the weak hypercharge Y_w and the weak isospin I_w defined in Section 2.1.1. For most of the fields, C^{EW} is diagonal and given by:

$$\begin{array}{cccccccccc} \varphi & W^\pm, W^3 & B & \Phi, H, \chi, \phi^\pm & \nu^L, \bar{\nu}^L, l^L, \bar{l}^L & l^R, \bar{l}^R & u^L, \bar{u}^L, d^L, \bar{d}^L & u^R, \bar{u}^R & d^R, \bar{d}^R \\ \hline C^{\text{EW}} & \frac{2}{s_w^2} & 0 & \frac{1+2c_w^2}{4s_w^2 c_w^2} & \frac{1+2c_w^2}{4s_w^2 c_w^2} & \frac{1}{c_w^2} & \frac{1+26c_w^2}{36s_w^2 c_w^2} & \frac{4}{9c_w^2} & \frac{1}{9c_w^2} \end{array} \quad (469)$$

For the neutral gauge bosons, C^{EW} becomes non-diagonal owing to the mixing between photon and Z boson, and the Casimir matrix entries read

$$C_{AA}^{\text{EW}} = 2, \quad C_{AZ}^{\text{EW}} = C_{ZA}^{\text{EW}} = -2 \frac{c_w}{s_w}, \quad C_{ZZ}^{\text{EW}} = 2 \frac{c_w^2}{s_w^2}. \quad (470)$$

(b) *Subleading soft-collinear contributions*

The subleading soft-collinear contributions result from Eq. (461) after subtracting the leading double-logarithmic contributions. Upon using

$$\ln^2 \frac{s_{ij}}{M^2} = \ln^2 \frac{s}{M^2} + 2 \ln \frac{s}{M^2} \ln \frac{s_{ij}}{s} + \ln^2 \frac{s_{ij}}{s}, \quad (471)$$

the angular-dependent part of the form $\ln \frac{s}{M^2} \ln \frac{s_{ij}}{s}$ furnishes the subleading soft-collinear contributions, which can be written as

$$\delta^{\text{SSC}} \mathcal{M}^{i_1 \dots i_n} = \sum_{\substack{k,l=1 \\ l < k}}^n \delta_{i'_k i_k i'_l i_l}^{\text{SSC}}(k, l) \mathcal{M}_0^{i_1 \dots i'_k \dots i'_l \dots i_n}, \quad (472)$$

with

$$\delta_{i'_k i_k i'_l i_l}^{\text{SSC}}(k, l) = 2l(s) \ln \frac{s_{kl}}{s} \sum_{V^a=A,Z,W^\pm} I_{i'_k i_k}^{V^a}(k) I_{i'_l i_l}^{\bar{V}^a}(l) \quad (473)$$

and the single logarithm

$$l(s) = \frac{\alpha}{4\pi} \ln \frac{s}{M_W^2}. \quad (474)$$

In the physical basis the couplings are given by

$$I^A = -Q, \quad I^Z = \frac{I_w^3 - s_w^2 Q}{s_w c_w}, \quad I^\pm = \frac{I_w^\pm}{s_w} = \frac{I_w^1 \pm i I_w^2}{\sqrt{2} s_w} \quad (475)$$

with the generators of electric charge and weak isospin as defined in Section 2.1.1. Specifically, for gauge bosons, charged would-be Goldstone bosons, and fermions the diagonal couplings to photons and Z bosons are obtained to:

φ	W^\pm	A, Z	ϕ^\pm	$\nu^L, \bar{\nu}^L$	l^L, \bar{l}^L	l^R, \bar{l}^R	u^L, \bar{u}^L	d^L, \bar{d}^L	u^R, \bar{u}^R	d^R, \bar{d}^R
$I^A(\varphi)$	∓ 1	0	∓ 1	0	± 1	± 1	$\mp \frac{2}{3}$	$\pm \frac{1}{3}$	$\mp \frac{2}{3}$	$\pm \frac{1}{3}$
$I^Z(\varphi)$	$\pm \frac{c_w}{s_w}$	0	$\pm \frac{1-2s_w^2}{2c_w s_w}$	$\pm \frac{1}{2c_w s_w}$	$\mp \frac{1-2s_w^2}{2c_w s_w}$	$\pm \frac{s_w}{c_w}$	$\pm \frac{3-4s_w^2}{6c_w s_w}$	$\mp \frac{3-2s_w^2}{6c_w s_w}$	$\mp \frac{2s_w}{3c_w}$	$\pm \frac{s_w}{3c_w}$

The non-vanishing couplings of the gauge bosons to the charged gauge bosons are given by

$$I_{AW^\pm}^{W^\pm} = -I_{W^\pm A}^{W^\pm} = \mp 1, \quad I_{ZW^\pm}^{W^\pm} = -I_{W^\pm Z}^{W^\pm} = \pm \frac{c_w}{s_w}, \quad (477)$$

and the non-vanishing couplings of left-handed fermions to the W^\pm bosons by

$$\begin{aligned} I_{ud}^{W^+}(Q^L) &= -I_{\bar{d}u}^{W^+}(\bar{Q}^L) = I_{du}^{W^-}(Q^L) = -I_{\bar{u}d}^{W^-}(\bar{Q}^L) = \frac{1}{\sqrt{2} s_w}, \\ I_{\nu l}^{W^+}(L^L) &= -I_{\bar{l}\nu}^{W^+}(\bar{L}^L) = I_{l\nu}^{W^-}(L^L) = -I_{\bar{\nu}l}^{W^-}(\bar{L}^L) = \frac{1}{\sqrt{2} s_w}, \end{aligned} \quad (478)$$

while those to right-handed fermions vanish. In the physical basis, the couplings of the neutral scalar fields to the gauge bosons become non-diagonal. All couplings of neutral scalars to the photon field vanish, while the non-vanishing couplings to the Z-boson field read

$$I_{H\chi}^Z = -I_{\chi H}^Z = \frac{-i}{2s_w c_w}. \quad (479)$$

The non-vanishing eikonal couplings of the scalar fields to the charged W bosons read

$$I_{H\phi^\pm}^{W^\pm} = -I_{\phi^\pm H}^{W^\pm} = \mp \frac{1}{2s_w}, \quad I_{\chi\phi^\pm}^{W^\pm} = -I_{\phi^\pm \chi}^{W^\pm} = -\frac{i}{2s_w}. \quad (480)$$

(c) Collinear and soft single logarithms

The complete single-logarithmic contributions originating from soft or collinear regions can be written as a sum over the external legs,

$$\delta^C \mathcal{M}^{i_1 \dots i_n} = \sum_{k=1}^n \delta_{i'_k i_k}^C(k) \mathcal{M}_0^{i_1 \dots i'_k \dots i_n} \quad (481)$$

with

$$\delta_{i'_k i_k}^C(k) = \delta_{i'_k i_k}^{\text{coll}}(k) + \frac{1}{2} \delta Z_{i'_k i_k}^\varphi \Big|_{\mu^2 = s}, \quad (482)$$

where δZ^φ are the field renormalization constants in the OS renormalization scheme [see Eqs. (144) and (145)] in logarithmic approximation. The collinear factors $\delta^{\text{coll}}(k)$ and the corrections $\delta^C(k)$ depend on the quantum numbers of the external fields φ_{i_k} .

The correction factor for the fermions is diagonal and reads

$$\delta_{ff}^C(f^\kappa) = \left[\frac{3}{2} C_{f^\kappa}^{\text{EW}} - \frac{1}{8s_w^2} \left((1 + \delta_{\kappa R}) \frac{m_f^2}{M_W^2} + \delta_{\kappa L} \frac{m_{\tilde{f}}^2}{M_W^2} \right) \right] l(s), \quad (483)$$

where \tilde{f} denotes the isospin partner of the fermion f , $\kappa = L, R$, and $\delta_{\kappa L}, \delta_{\kappa R}$ are Kronecker deltas. The fermion-mass-dependent Yukawa contributions are only relevant for top and bottom quarks.

While the correction factor for the charged transverse gauge bosons is diagonal

$$\delta_{W^\pm W^\pm}^C(V_T) = \frac{1}{2} b_W^{\text{EW}} l(s), \quad (484)$$

those for the neutral transverse gauge bosons involve non-diagonal terms,

$$\delta_{AA}^C(V_T) = \frac{1}{2} b_{AA}^{\text{EW}} l(s), \quad \delta_{ZZ}^C(V_T) = \frac{1}{2} b_{ZZ}^{\text{EW}} l(s), \quad \delta_{AZ}^C(V_T) = b_{AZ}^{\text{EW}} l(s), \quad \delta_{ZA}^C(V_T) = 0. \quad (485)$$

The coefficients b^{EW} are proportional to the one-loop coefficients in the β functions of the EW couplings and explicitly read

$$b_W^{\text{EW}} = \frac{19}{6s_w^2}, \quad b_{AA}^{\text{EW}} = -\frac{11}{3}, \quad b_{AZ}^{\text{EW}} = -\frac{19 + 22s_w^2}{6s_w c_w}, \quad b_{ZZ}^{\text{EW}} = \frac{19 - 38s_w^2 - 22s_w^4}{6s_w^2 c_w^2}. \quad (486)$$

The correction factors for the longitudinal gauge bosons are extracted with the help of the Goldstone-boson equivalence theorem taking into account higher-order corrections [513]

$$\delta_{W^\pm W^\pm}^C(V_L) = \delta_{ZZ}^C(V_L) = \left[2C_\Phi^{\text{EW}} - \frac{N_C^t}{4s_w^2} \frac{m_t^2}{M_W^2} \right] l(s), \quad (487)$$

where the m_t^2 term accounts for the enhanced coupling to the top quark.

Finally, the correction factor for the Higgs boson reads

$$\delta_{HH}^C(\Phi) = \left[2C_\Phi^{\text{EW}} - \frac{N_C^t}{4s_w^2} \frac{m_t^2}{M_W^2} \right] l(s). \quad (488)$$

(d) Logarithms from parameter renormalization

Additional EW logarithms result from the renormalization of dimensionless parameters at scales small compared to $\mu^2 = s$. We here only give contributions related to the running of the couplings from M_W^2 to s . Further contributions from the running of the electromagnetic coupling from zero to M_W^2 result from the renormalization of the electric charge. In the $\alpha(0)$ scheme, those contributions appear as $\Delta\alpha(M_W^2)$ terms, as explicitly given in Ref. [527]; in other EW input-parameter schemes those terms are different (cf. Section 5.1).

While neglecting light fermion masses, it is convenient to choose the four dimensionless parameters

$$e, \quad c_w^2, \quad g_t = \frac{e}{\sqrt{2}s_w} \frac{m_t}{M_W}, \quad \lambda = \frac{e^2}{2s_w^2} \frac{M_H^2}{M_W^2} \quad (489)$$

for the renormalization transformation. Then, the UV logarithms are obtained from the LO matrix element $\mathcal{M}_0 = \mathcal{M}_0(e, c_w^2, g_t, \lambda)$ in the high-energy limit by

$$\delta^{\text{PR}} \mathcal{M} = \frac{\delta \mathcal{M}_0}{\delta e} \delta e + \frac{\delta \mathcal{M}_0}{\delta c_w^2} \delta c_w^2 + \frac{\delta \mathcal{M}_0}{\delta g_t} \delta g_t + \frac{\delta \mathcal{M}_0}{\delta \lambda} \delta \lambda \Big|_{\mu^2=s}. \quad (490)$$

In the case of processes with longitudinal gauge bosons, these logarithms should be determined from the matrix elements for external Goldstone bosons according to the equivalence theorem. Note that the correction factors $A_V(k^2)$ in Eqs. (453) and (454) do not give rise to logarithmic corrections.

The leading-logarithmic contributions to the counterterms read for the charge renormalization

$$\delta Z_e = -\frac{1}{2} b_{AA}^{\text{EW}} l(\mu^2), \quad (491)$$

for the renormalization of the weak mixing angle

$$\frac{\delta c_w^2}{c_w^2} = \frac{s_w}{c_w} b_{AZ}^{\text{EW}} l(\mu^2), \quad (492)$$

for the renormalization of the top-quark Yukawa coupling

$$\frac{\delta g_t}{g_t} = \left[-\frac{3}{4s_w^2} - \frac{3}{8s_w^2 c_w^2} + \frac{3}{2c_w^2} Q_t - \frac{3}{c_w^2} Q_t^2 + \frac{3+2N_C^t}{8s_w^2} \frac{m_t^2}{M_W^2} \right] l(\mu^2) = \left[-\frac{17+10c_w^2}{24c_w^2 s_w^2} + \frac{9}{8s_w^2} \frac{m_t^2}{M_W^2} \right] l(\mu^2), \quad (493)$$

and for the renormalization of the scalar self-coupling

$$\frac{\delta \lambda}{\lambda} = \frac{3}{2s_w^2} \left[\frac{M_W^2}{M_H^2} \left(2 + \frac{1}{c_w^4} \right) - \left(2 + \frac{1}{c_w^2} \right) + \frac{M_H^2}{M_W^2} \right] l(\mu^2) + \frac{N_C^t}{s_w^2} \frac{m_t^2}{M_W^2} \left(1 - 2 \frac{m_t^2}{M_H^2} \right) l(\mu^2). \quad (494)$$

We note that the counterterms for the dimensionless parameters are independent of the tadpole scheme.

While the collinear and soft logarithms involve β -function coefficients b^{EW} with a positive sign for external transverse gauge bosons, the logarithms from the renormalization of the electromagnetic coupling contain such terms with negative sign leading to partial cancellation of single EW logarithms for processes with external transverse gauge bosons. For the particular case of processes with exactly one external fermion–antifermion pair and only external transverse gauge bosons (but no other external fields) all these contributions cancel. This feature is a consequence of Ward identities.

(e) Application to scattering processes

The formulae given above are applicable to arbitrary scattering processes subject to the condition that all kinematic invariants are large compared to M_W^2 . This is, however, not directly the case for processes that involve the production of unstable particles with their subsequent decays. The above results can nevertheless be applied in such cases within the pole approximation (cf. Section 6.5), since then the conditions are fulfilled for the production subprocesses while no large logarithms appear in the corrections to decay subprocesses where the scale is set by the mass of the decaying resonance [548].

An interesting physical example is the scattering of EW vector bosons, which occurs as subprocess in partonic processes such as $qq \rightarrow qq\bar{l}\bar{l}\bar{l}\bar{l}$. In this case, the double-pole approximation for the produced gauge bosons can be combined [549] with the effective vector-boson approximation [550–552] for the incoming vector bosons, and the dominant contributions result from diagrams with the generic form shown in the left of Fig. 5 on page 102. While the effective vector-boson approximation yields only a crude approximation for the matrix elements in the very-high-energy limit [549, 553], it provides a reasonable basis for an approximation for the relative corrections. Within this approach, the logarithmic approximation can, for instance, be applied to the subprocess $W^+W^+ \rightarrow W^+W^+$, while the emission of the W bosons from the quark lines and the decay of the W bosons do not give rise to large EW logarithms. Disregarding the angular-dependent subleading soft–collinear corrections, but including the leading soft–collinear corrections, the single soft and collinear logarithms for the dominant transverse polarization of the scattering W bosons, as well as the EW logarithms from parameter renormalization for the dominant transverse vector bosons, one finds a simple approximation for the corrections to the cross section for the process $pp \rightarrow \mu^+\nu_\mu e^+\nu_e jj + X$ [340]

$$\sigma_{\text{LL,T}} = \sigma_{\text{LO}} \left[1 - \frac{\alpha}{4\pi} 4C_W^{\text{ew}} \ln^2 \frac{Q^2}{M_W^2} + \frac{\alpha}{4\pi} 2b_W^{\text{ew}} \ln \frac{Q^2}{M_W^2} \right], \quad (495)$$

where σ_{LO} is the full LO cross section. Using $\langle M_{4l} \rangle \sim 390 \text{ GeV}$ as a typical scale Q for the vector-boson scattering subprocess, which can be determined from a LO calculation, leads to an EW correction of about -16% in remarkably good agreement with the full calculation of the NLO EW corrections [340, 341]. Using $Q = M_{4l}$ on an event-by-event basis results in a correction of about -15% . Since the self-interaction of EW gauge bosons is only due to the $SU(2)_w$ interaction, the result (495) is valid for arbitrary scattering processes of EW vector bosons. This can be derived either in the symmetric phase of the EW theory or using the results given above together with the fact that LO matrix elements for $VV \rightarrow VV$ scattering in the high-energy limit differ only by factors $-c_w/s_w$ if a photon field is replaced by a Z -boson field. While the effective scale $\langle M_{4l} \rangle$ depends somewhat on the considered process and the event selection, the EW corrections are expected to be of the same order of magnitude for all scattering processes of EW gauge bosons. This has been confirmed for $WZ \rightarrow WZ$ scattering, where relative EW corrections of -16% were found in nice agreement with the approximation (495) [333].

The angular-dependent subleading soft-collinear corrections, on the other hand, depend on the considered scattering process $VV \rightarrow VV$, and the corresponding correction factor to the integrated cross section requires a non-trivial integration over the scattering angle. The correction factors for the differential cross sections can be easily constructed from the results of Ref. [549] [see also Eqs. (472)–(480)]. They depend on the polarization of the vector bosons and on the various LO matrix elements with different intermediate vector bosons. Using the high-energy relations between the LO matrix elements, the result for the dominant contribution of purely transverse W^+W^+ scattering reads

$$d\sigma_{SSC,T} = d\sigma_{LO} \frac{\alpha}{\pi s_w^2} 2 \ln \left(\frac{Q^2}{M_W^2} \right) \left[\ln \frac{s_{12}}{Q^2} - \left(1 - \frac{s_{13}}{s_{12}} \right) \ln \frac{s_{13}}{Q^2} - \left(1 - \frac{s_{23}}{s_{12}} \right) \ln \frac{s_{23}}{Q^2} \right], \quad (496)$$

where s_{ij} are the Mandelstam variables of the vector-boson scattering subprocess. When integrating over the phase space, the angular-dependent corrections (496) average out to a large extent such that the resulting contribution is only of the order of one percent.

The generic results of Ref. [527] were used to calculate the one-loop logarithmic corrections to various processes including vector-boson pair production at the LHC [548, 554], vector-boson scattering in electron–positron annihilation [549], and $V + j$ production at the LHC [555–557]. In Section 5.4.4 below, we consider the evaluation of the leading EW logarithms to the Drell–Yan-like W - and Z -boson production. The results of Ref. [527] have been implemented in the event generator ALPGEN [558] and applied to the production of jets with missing energy [559].

5.4.2. Resummation of EW double-logarithmic corrections

Since the EW high-energy logarithmic corrections can grow to several tens of percent in the TeV range for typical scattering processes, EW logarithms beyond NLO can become relevant as well. These can be taken into account via appropriate resummation methods. The resummation of the leading EW logarithms (double soft-collinear logarithms) was studied in a pioneering paper by Fadin et al. [520]. There, the *IR evolution equations* [560], describing the dependence of amplitudes on some IR cutoff μ_{IR} of the virtual particle transverse momenta, were used to perform the resummation. In the following we basically follow the arguments of Ref. [520].

We start with a generic non-abelian gauge theory and consider an arbitrary amplitude, where all invariants s_{ij} are large and of the same order $|s_{ij}| \sim s$. We extract the virtual particle with the smallest value of transverse momentum $|\mathbf{q}_\perp|$ in such a way that the transverse momenta $|\mathbf{q}'_\perp|$ of the other virtual particles are much bigger,

$$\mathbf{q}'_\perp^2 \gg \mathbf{q}_\perp^2 \gg \mu_{IR}^2. \quad (497)$$

For the other particles, \mathbf{q}_\perp^2 plays the role of the initial IR cutoff μ_{IR}^2 . The Sudakov double logarithms result from the exchange of soft-collinear gauge bosons (see Fig. 8 left on page 108). In this case, the integral over the momentum q of the soft virtual boson with smallest \mathbf{q}_\perp can be extracted based on the non-abelian generalization of the Gribov theorem [561–563]. This leads, via a generalization of the one-loop results (461), to the IR evolution equation

$$\begin{aligned} \mathcal{M}^{i_1 \dots i_n}(p_1, \dots, p_n, \mu_{IR}^2) &= \mathcal{M}_0^{i_1 \dots i_n}(p_1, \dots, p_n) + \frac{i}{2} g^2 \sum_{\substack{k, l=1 \\ l \neq k}}^n \sum_a T_{i'_k i_k}^a(k) T_{i'_l i_l}^a(l) \\ &\times \int_{s > \mathbf{q}_\perp^2 > \mu_{IR}^2} \frac{d^4 q}{(2\pi)^4} \frac{-4p_k p_l}{(q^2 - M^2 + i\epsilon)[(q + p_k)^2 - m_k^2][(q - p_l)^2 - m_l^2]} \mathcal{M}^{i_1 \dots i'_k \dots i'_l \dots i_n}(p_1, \dots, p_n, \mathbf{q}_\perp^2), \end{aligned} \quad (498)$$

where M is the mass of the exchanged gauge boson, the external particles are on their mass shell ($p_l^2 = m_l^2$, $p_k^2 = m_k^2$). In the double logarithmic approximation m_l and m_k are only needed for photon exchange, where they are equal, while they are negligible for W - or Z -boson exchange. Moreover, g denotes the non-abelian gauge coupling and $T^a(l)$ the representation of the generators of the gauge group corresponding to the external particle l . In Eq. (498), \mathbf{q}_\perp represents the component of the gauge-boson 3-momentum \mathbf{q} transverse to the particles k and l coupling to this boson, defined in the CM frame of the two momenta p_k, p_l . In the limit of small masses m_k, m_l and small virtuality q^2 , it can be expressed in Lorentz-invariant form according to

$$\mathbf{q}_\perp^2 = 2 \min_{k \neq l} \left| \frac{(q p_l)(q p_k)}{p_k p_l} \right|. \quad (499)$$

Equation (498) is valid in a covariant gauge for the gauge boson with momentum q , but can be written in a gauge-invariant way upon including the term with $k = l$ in the sum (which does not give a double-logarithmic term).

In order to evaluate the integral in Eq. (498), the Sudakov parametrization

$$q = -x \left(p_k - \frac{m_k^2}{2p_k p_l} p_l \right) + y \left(p_l - \frac{m_l^2}{2p_k p_l} p_k \right) + q_\perp, \quad p_k q_\perp = p_l q_\perp = 0, \quad (500)$$

is used, where here and in the following terms of order m_k^4 , m_l^4 , $m_k^2 m_l^2$, which are irrelevant in double-logarithmic approximation, are neglected. In the CM frame of p_k, p_l , we have $q_\perp^0 = 0$, so that $q_\perp^2 = -\mathbf{q}_\perp^2 < 0$. The integral in Eq. (498) can be rewritten as

$$\begin{aligned} I &= \int_{s > \mathbf{q}_\perp^2 > \mu_{\text{IR}}^2} \frac{d^4 q}{(2\pi)^4} \frac{-4p_k p_l}{(q^2 - M^2 + i\epsilon)[(q + p_k)^2 - m_k^2][(q - p_l)^2 - m_l^2]} \\ &\sim -(p_k p_l) |p_k p_l| \frac{4\pi}{(2\pi)^4} \int_{\mu_{\text{IR}}^2}^s d\mathbf{q}_\perp^2 \int dx \int dy \left[-2xy(p_k p_l) - \mathbf{q}_\perp^2 - M^2 + i\epsilon \right]^{-1} \\ &\quad \times \left[2(1-x)y(p_k p_l) - \mathbf{q}_\perp^2 - xm_k^2 \right]^{-1} \left[2x(1-y)(p_k p_l) - \mathbf{q}_\perp^2 - ym_l^2 \right]^{-1}, \end{aligned} \quad (501)$$

where the asymptotic equality \sim here and in the following refers to double-logarithmic approximation. To evaluate I , it is convenient to apply a *sector decomposition* which separates the two types of collinear singularities w.r.t. p_k or p_l by assuming a hierarchy between $|x|$ and $|y|$,

$$I = I_{|x| > |y|} + I_{|x| < |y|}. \quad (502)$$

In the following we evaluate $I_{|x| > |y|}$, which contains the collinear singularity w.r.t. p_k , and get $I_{|x| < |y|}$ from $I_{|x| > |y|}$ upon interchanging k and l . Using

$$\frac{1}{2xy(p_k p_l) + \mathbf{q}_\perp^2 + M^2 - i\epsilon} = i\pi \delta(2xy(p_k p_l) + \mathbf{q}_\perp^2 + M^2) + \text{PV} \frac{1}{2xy(p_k p_l) + \mathbf{q}_\perp^2 + M^2} \quad (503)$$

for the gauge-boson propagator, only the part with the δ function but not the principle-value (PV) part contributes in the double-logarithmic approximation. Performing the y integration in the $|x| > |y|$ sector of Eq. (501) with the help of the δ function in Eq. (503), results in

$$I_{|x| > |y|} \sim -\frac{i\pi^2}{(2\pi)^4} \int_{\mu_{\text{IR}}^2}^s d\mathbf{q}_\perp^2 \int_{x^2 > \frac{\mathbf{q}_\perp^2 + M^2}{|2p_k p_l|}} dx \frac{1}{\mathbf{q}_\perp^2 + M^2(1-x) + x^2 m_k^2} \frac{4|x|(p_k p_l)^2}{4x^2(p_k p_l)^2 + 2x(p_k p_l)M^2 + m_l^2(\mathbf{q}_\perp^2 + M^2)}. \quad (504)$$

The restriction on the x -integration originates from the combination of the requirements $|x| > |y|$ and that the argument of the δ function in Eq. (503) has to vanish. Owing to this restriction the mass term m_l^2 in the integral never regularizes a singularity, so that we can set $m_l = 0$ in the integral $I_{|x| > |y|}$. Substituting $\mathbf{q}_\perp^2 \rightarrow \mathbf{q}_\perp^2 - M^2$, we get

$$\begin{aligned} I_{|x| > |y|} &\sim -\frac{i\pi^2}{(2\pi)^4} \int_{\mu_{\text{IR}}^2 + M^2}^s d\mathbf{q}_\perp^2 \int_{x^2 > \frac{\mathbf{q}_\perp^2}{|2p_k p_l|}} dx \frac{1}{\mathbf{q}_\perp^2 - xM^2 + x^2 m_k^2} \frac{2(p_k p_l)}{2|x|(p_k p_l) + \text{sgn}(x)M^2} \\ &\sim -\frac{i\pi^2}{(2\pi)^4} \int_{\max\{\mu_{\text{IR}}^2, M^2\}}^s d\mathbf{q}_\perp^2 \int_{x^2 > \frac{\mathbf{q}_\perp^2}{s}} dx \frac{1}{|x| \frac{\mathbf{q}_\perp^2}{s} + x^2 m_k^2}, \end{aligned} \quad (505)$$

where the second form is valid, because the M^2 terms in the integrand of the first form do not regularize a singularity. Moreover, we have modified the integration boundaries in a way that does not change the integral in double-logarithmic approximation. Finally, we translate the m_k^2 term in the integrand into an effective upper bound of the x -integration: For $m_k = 0$, the upper limit of x can be set to any number of $O(1)$ that does not lead to an enhanced logarithm; for $m_k \neq 0$, the m_k^2 term truncates the logarithmic contribution for $x^2 \gtrsim \mathbf{q}_\perp^2/m_k^2$. Thus, the double logarithmic contribution from the sector $|x| > |y|$ is obtained as

$$I_{|x| > |y|} \sim -\frac{2i\pi^2}{(2\pi)^4} \int_{\max\{\mu_{\text{IR}}^2, M^2\}}^s \frac{d\mathbf{q}_\perp^2}{\mathbf{q}_\perp^2} \int_{|\mathbf{q}_\perp|/\sqrt{s}}^{\min\{1, |\mathbf{q}_\perp|/m_k\}} \frac{dx}{x} = -\frac{i\pi^2}{(2\pi)^4} \int_{\max\{\mu_{\text{IR}}^2, M^2\}}^s \frac{d\mathbf{q}_\perp^2}{\mathbf{q}_\perp^2} \ln \frac{s}{\max\{\mathbf{q}_\perp^2, m_k^2\}}$$

$$\equiv -\frac{i\pi^2}{(2\pi)^4} J(\mu_{\text{IR}}^2, M^2, m_k^2), \quad (506)$$

where a factor 2 results from combining regions of positive and negative x . Adding the contribution of the sector $|x| < |y|$, the full result for I in double-logarithmic approximation is given by

$$I \sim -\frac{i\pi^2}{(2\pi)^4} [J(\mu_{\text{IR}}^2, M^2, m_k^2) + J(\mu_{\text{IR}}^2, M^2, m_l^2)] \quad (507)$$

with

$$J(\mu_{\text{IR}}^2, M^2, m^2) = \begin{cases} \frac{1}{2} \ln^2 \frac{s}{\max\{\mu_{\text{IR}}^2, M^2\}} & \text{for } \max\{\mu_{\text{IR}}^2, M^2\} > m^2, \\ \frac{1}{2} \ln^2 \frac{s}{m^2} + \ln \frac{s}{m^2} \ln \frac{m^2}{\max\{\mu_{\text{IR}}^2, M^2\}} & \text{for } m^2 > \max\{\mu_{\text{IR}}^2, M^2\}. \end{cases} \quad (508)$$

Each contribution for $|x| > |y|$ or $|y| < |x|$ depends on the mass and momentum of only one of the external legs. Using the above results as well as charge conservation

$$\sum_k T_{i'_k i_k}^a(k) \mathcal{M}_0^{i_1 \dots i'_k \dots i_n}(p_1, \dots, p_n) = 0, \quad (509)$$

the IR evolution equation (498) can be transformed to

$$\begin{aligned} \mathcal{M}^{i_1 \dots i_n}(p_1, \dots, p_n, \mu_{\text{IR}}^2) &= \mathcal{M}_0^{i_1 \dots i_n}(p_1, \dots, p_n) \\ &- \frac{g^2}{(4\pi)^2} \sum_{k=1}^n \int_{\max\{\mu_{\text{IR}}^2, M^2\}}^s \frac{d\mathbf{q}_\perp^2}{\mathbf{q}_\perp^2} \ln \frac{s}{\max\{\mathbf{q}_\perp^2, m_k^2\}} C_{i'_k i_k}(k) \mathcal{M}^{i_1 \dots i'_k \dots i_n}(p_1, \dots, p_n, \mathbf{q}_\perp^2), \end{aligned} \quad (510)$$

with the Casimir operator $C_{i'_k i_k}(l) = \sum_a [T^a(l) T^a(l)]_{i'_k i_k}$ of the generic non-abelian gauge group.

The differential form of the evolution equation then reads

$$\frac{\partial \mathcal{M}^{i_1 \dots i_n}(p_1, \dots, p_n, \mu_{\text{IR}}^2)}{\partial \ln(\mu_{\text{IR}}^2)} = -\frac{g^2}{(4\pi)^2} \sum_{k=1}^n C_{i'_k i_k}(k) \frac{\partial J(\mu_{\text{IR}}^2, M^2, m_k^2)}{\partial \ln(\mu_{\text{IR}}^2)} \prod_{\substack{l=1 \\ l \neq k}}^n \delta_{i'_l i_l} \mathcal{M}^{i'_1 \dots i'_n}(p_1, \dots, p_n, \mu_{\text{IR}}^2), \quad (511)$$

with

$$\frac{\partial J(\mu_{\text{IR}}^2, M^2, m_k^2)}{\partial \ln(\mu_{\text{IR}}^2)} = -\theta(\mu_{\text{IR}}^2 - M^2) \ln \frac{s}{\max\{\mu_{\text{IR}}^2, m_k^2\}}. \quad (512)$$

Since there are no large logarithms for large cutoff scale $\mu_{\text{IR}}^2 = s$, we have the initial condition

$$\mathcal{M}^{i_1 \dots i_n}(p_1, \dots, p_n, \mu_{\text{IR}}^2 = s) = \mathcal{M}_0^{i_1 \dots i_n}(p_1, \dots, p_n). \quad (513)$$

Using the fact that for unbroken gauge theories the Casimir operators are diagonal, $C_{i'_k i_k}(k) = C(k) \delta_{i'_k i_k}$, the evolution equation (511) can be solved as

$$\mathcal{M}^{i_1 \dots i_n}(p_1, \dots, p_n, \mu_{\text{IR}}^2) = \mathcal{M}_0^{i_1 \dots i_n}(p_1, \dots, p_n) \exp \left(-\frac{g^2}{(4\pi)^2} \sum_{k=1}^n C(k) J(\mu_{\text{IR}}^2, M^2, m_k^2) \right), \quad (514)$$

i.e. the Sudakov double logarithms exponentiate in the non-abelian case in the same way as in the abelian case.

The method based on the IR evolution equations is also applicable to broken gauge theories like the EWSM. To double-logarithmic accuracy all heavy masses can be considered equal,

$$M_Z \sim M_W \sim M_H \sim m_t \sim M, \quad (515)$$

and the energy should be much larger, $\sqrt{s} \gg M$. For $\sqrt{s} > \mu_{\text{IR}} > M$, effects of spontaneous symmetry breaking and gauge-boson masses can be neglected, and the evolution equation can be studied in the unbroken phase. If the

equation is formulated in the broken phase, the photon contributions have to be taken into account in order not to violate gauge invariance. For $\mu_{\text{IR}} \ll M$ only the photon exchange drives the running in μ_{IR} as in QED.

If we assume for simplicity that all charged particles have masses $m_k \lesssim M$, the IR evolution equation reads for $\sqrt{s} > \mu_{\text{IR}} > M$

$$\frac{\partial \mathcal{M}^{i_1 \dots i_n}(p_1, \dots, p_n, \mu_{\text{IR}}^2)}{\partial \ln(\mu_{\text{IR}}^2)} = \frac{e^2}{(4\pi)^2} \ln \frac{s}{\mu_{\text{IR}}^2} \sum_{k=1}^n C_{i'_k i_k}^{\text{EW}}(k) \mathcal{M}^{i_1 \dots i'_k \dots i_n}(p_1, \dots, p_n, \mu_{\text{IR}}^2) \quad (516)$$

with the EW Casimir operator defined in Eq. (468). In the symmetric basis, i.e. diagonal EW Casimir operators, the solution of Eq. (516) is given by

$$\mathcal{M}^{i_1 \dots i_n}(p_1, \dots, p_n, \mu_{\text{IR}}^2) = \mathcal{M}_0^{i_1 \dots i_n}(p_1, \dots, p_n) \exp \left[-\frac{e^2}{2(4\pi)^2} \ln^2 \frac{s}{\mu_{\text{IR}}^2} \sum_{k=1}^n C^{\text{EW}}(k) \right]. \quad (517)$$

The corresponding results in the physical basis can be easily obtained by transforming the matrix elements or by using the matrices for the Casimir operators in the exponential function.

Choosing the cutoff μ_{IR} in the region $\mu_{\text{IR}} < M$, only the photon contribution remains. In order to carry over the above results to this new situation, the IR regulator mass previously called M is now the infinitesimal photon mass $m_\gamma \ll m_k$. The corresponding IR evolution equation then reads

$$\frac{\partial \mathcal{M}^{i_1 \dots i_n}(p_1, \dots, p_n, \mu_{\text{IR}}^2)}{\partial \ln(\mu_{\text{IR}}^2)} = \mathcal{M}^{i_1 \dots i_n}(p_1, \dots, p_n, \mu_{\text{IR}}^2) \frac{e^2}{(4\pi)^2} \sum_{k=1}^n Q_k^2 \ln \frac{s}{\max\{\mu_{\text{IR}}^2, m_k^2\}}. \quad (518)$$

The appropriate initial condition is given by Eq. (517) evaluated at the matching point $\mu_{\text{IR}} = M$, and the solution is

$$\begin{aligned} \mathcal{M}^{i_1 \dots i_n}(p_1, \dots, p_n, \mu_{\text{IR}}^2) &= \mathcal{M}_0^{i_1 \dots i_n}(p_1, \dots, p_n) \exp \left[-\frac{e^2}{2(4\pi)^2} \ln^2 \frac{s}{M^2} \sum_{k=1}^n C^{\text{EW}}(k) \right] \\ &\times \exp \left[-\frac{e^2}{(4\pi)^2} \sum_{k=1}^n Q_k^2 \left(J(\mu_{\text{IR}}^2, m_\gamma^2, m_k^2) - J(M^2, m_\gamma^2, m_k^2) \right) \right], \end{aligned} \quad (519)$$

which takes the following explicit form in the region $m_\gamma < \mu_{\text{IR}} < m_k < M$,

$$\begin{aligned} \mathcal{M}^{i_1 \dots i_n}(p_1, \dots, p_n, \mu_{\text{IR}}^2) &= \mathcal{M}_0^{i_1 \dots i_n}(p_1, \dots, p_n) \exp \left[-\frac{e^2}{2(4\pi)^2} \ln^2 \frac{s}{M^2} \sum_{k=1}^n C^{\text{EW}}(k) \right] \\ &\times \exp \left[-\frac{e^2}{(4\pi)^2} \sum_{k=1}^n Q_k^2 \left(\ln \frac{s}{m_k^2} \ln \frac{M^2}{\mu_{\text{IR}}^2} - \frac{1}{2} \ln^2 \frac{m_k^2}{M^2} \right) \right], \end{aligned} \quad (520)$$

The results (517) and (519) are applicable for processes involving chiral fermions, transverse gauge bosons, and Higgs bosons, provided that all invariants of order s are large compared to M^2 . For longitudinal gauge bosons, the equivalence theorem (see Section 5.3) has to be used. When expanded to one-loop accuracy, the results of Ref. [527] including the electromagnetic logarithms are reproduced upon substituting m_γ (called λ in Ref. [527]) for μ_{IR} . It has been shown for specific processes that the exponentiation of the EW double logarithms is in agreement with explicit two-loop calculations of these contributions [526, 531, 564].

IR evolution equations have also been used to sum subleading EW Sudakov logarithms (see Refs. [529, 530, 533] and references therein). To this end, the evolution equations have been taken over from QCD [565–567] and applied to the EWSM. This approach has been extended to the NLL and next-to-next-to-leading logarithmic ($N^2\text{LL}$) approximation [521, 536]. Starting with the $N^3\text{LL}$ approximation, the corrections become sensitive to the details of the gauge-boson mass generation [533]. This method has been applied to sum the EW logarithms to the vector form factor and neutral-current 4-fermion amplitudes at the NLL [521], $N^2\text{LL}$ [536], and $N^3\text{LL}$ level [533], and for W-pair production at the ILC and LHC at the $N^2\text{LL}$ level [568, 569]. Various explicit two-loop calculations have been performed to verify the resummation of the subleading logarithms [532, 535, 537].

5.4.3. EW logarithmic corrections from Soft–Collinear Effective Theory

The computation of EW corrections in the high-energy domain can be greatly simplified by using effective field theory (EFT) methods, specifically *Soft–Collinear Effective field Theory (SCET)* [538, 539, 544]. In the SCET approach [540–543] factorization of physics at different scales is assumed. As a result, the hard scattering amplitude can be written as a product of process-independent one-particle collinear functions depending on external particle energies and a universal soft function depending only on external particle directions [544].

The treatment of EW corrections within the SCET approach (SCET_{EW}) [538, 539, 544–546, 570] is summarized in Ref. [571] as follows:

- At a high scale μ_h of order \sqrt{s} , the scattering amplitudes are matched onto $SU(3)_c \times SU(2)_w \times U(1)_Y$ gauge-invariant local operators O_k with Wilson coefficients C_k which can be computed perturbatively in terms of a power series in the three gauge coupling constants $\alpha_i(\mu_h^2)$ of the SM. As an example, for $g(p_1) + g(p_2) \rightarrow q(p_3) + \bar{q}(p_4)$ the operators read

$$O_1 = \bar{q}_4 q_3 G_2^A G_1^A, \quad O_2 = d^{ABC} \bar{q}_4 T^C q_3 G_2^A G_1^B, \quad O_3 = i f^{ABC} \bar{q}_4 T^C q_3 G_2^A G_1^B, \quad (521)$$

which represent the possible colour structures of the amplitude. The subscripts 1, 2, 3, 4 label the different external particles.

- The Wilson coefficients C_i are evolved using renormalization-group equations (RGEs) down to a low scale μ_l of order M_W . The anomalous dimensions can be computed in the unbroken $SU(3)_c \times SU(2)_w \times U(1)_Y$ theory.
- At the scale μ_l , the fields of the EW gauge bosons W and Z, the Higgs field, and the top-quark field are integrated out. This calculation must be performed in the broken theory. A single gauge-invariant operator breaks up into different components, because the weak gauge symmetry is broken. For example, each of the operators O_i in Eq. (521) splits into an $SU(3)_c$ -invariant $gg \rightarrow t\bar{t}$ and $gg \rightarrow b\bar{b}$ operator, if q is an EW doublet (t_L, b_L).
- The operators in the theory below μ_l are used to compute the scattering cross sections.

As final result, the scattering amplitudes \mathcal{M} can be written in resummed form

$$\mathcal{M} = \exp [D_C(\mu_l, L_M, \bar{n}p)] d_S(\mu_l, L_M) P \exp \left[\int_{\mu_h}^{\mu_l} \frac{d\mu}{\mu} \gamma(\mu) \right] C(\mu_h, L_Q). \quad (522)$$

The operator P denotes path ordering so that the values of μ increase from left to right. The ingredients in Eq. (522), for which explicit formulas are given in Ref. [545], are discussed in the following.

The *high-scale matching* $C(\mu_h, L_Q)$ is an n -dimensional column vector with a perturbative expansion in $\alpha_i(\mu_h^2)$, with $i = 1, 2, 3$ being the respective $U(1)_Y$, $SU_w(2)$, and $SU(3)_c$ gauge couplings. For the example (521), we have $n = 3$, since there are 3 gauge-invariant amplitudes. The high-scale matching depends on $L_Q = \ln s/\mu_h^2$, which is not a large logarithm if one chooses $\mu_h^2 \sim s$, and is computed from graphs of the full theory, setting all small scales such as the gauge-boson and fermion masses to zero. It can be calculated in the unbroken theory without worrying about mass effects and EW mixing. In an NLO calculation, the high-scale matching corresponds to the finite non-logarithmic corrections in the high-energy limit. The high-scale matching does not obey the factorization structure of the EFT amplitude and cannot be calculated using EFT results. For processes including a small number of external particles it is known [539].

The *SCET anomalous dimension* $\gamma(\mu)$ determines the running of the amplitude between the high scale $\mu_h \sim \sqrt{s}$ and the low scale $\mu_l \sim M_W$. It is an $n \times n$ anomalous-dimension matrix which can be written as the sum of a collinear and a soft part,

$$\gamma(\mu) = \gamma_C(\mu, \bar{n}p) + \gamma_S(\mu, \{n\}), \quad (523)$$

where the collinear part is proportional to a unit matrix in colour space,

$$\gamma_C(\mu, \bar{n}p) = \mathbb{1} \sum_r \left[A_r(\mu) \ln \frac{2E_r}{\mu} + B_r(\mu) \right], \quad (524)$$

and linear in $\ln(\bar{n}_r p_r) = \ln(2E_r)$ to all orders in perturbation theory [544, 572], with E_r denoting the energy of parton r . For incoming particles, $n_r = (1, \mathbf{n}_r)$ and $\bar{n}_r = (1, -\mathbf{n}_r)$, where \mathbf{n}_r , with $|\mathbf{n}_r| = 1$, points into the direction of motion

of parton r ; for outgoing particles $n_r = -(1, \mathbf{n}_r)$ and $\bar{n}_r = -(1, -\mathbf{n}_r)$. The sum over r comprises all partons in the scattering process, and $A_r(\mu)$, the *cusp anomalous dimension*, and $B_r(\mu)$, the *non-cusp anomalous dimension*, have a perturbative expansion in $\alpha_i(\mu^2)$. The one-loop expressions for the SM fields are given in Table 1 of Ref. [545]. They are in one-to-one correspondence with the corresponding results of Ref. [527]. The results for γ_C in Table 1 of Ref. [545] summarize the leading soft-collinear contributions [terms containing $L_p = \ln(\bar{n}p/\mu)$], the collinear factors δ^{coll} (explicit constant terms $\propto T \cdot T$), and the contributions from field renormalization constants γ_ϕ from Ref. [527]. At one-loop order, the soft part reads

$$\gamma_S(\mu, \{n\}) = - \sum_{i=1}^3 \sum_{\text{pairs } r,s} \frac{\alpha_i(\mu^2)}{\pi} T_r^{(i)} \cdot T_s^{(i)} \ln \frac{-n_r n_s - i\epsilon}{2}, \quad (525)$$

where the sum is over all parton pairs r, s , and $T_r^{(i)}$ is the gauge generator for the i th gauge group acting on parton r . The soft part γ_S corresponds to the subleading soft-collinear contributions of Ref. [527]. The anomalous dimension $\gamma(\mu)$ is independent of the low-energy scales and can be computed in the unbroken gauge theory. The \bar{n} dependence (Lorentz-frame dependence) cancels between the collinear and soft functions. The renormalization-group evolution governed by the SCET anomalous dimension sums the Sudakov double logarithms which provide the dominant effect of the EW corrections.

The *low-scale matching* consists of a collinear part D_C and a soft part d_S . The soft part d_S is an $m \times n$ matrix, where m is the number of amplitudes produced after $SU(2)_W \times U(1)_Y$ breaking. In $gg \rightarrow q\bar{q}$, if q is an EW doublet of left-handed quarks (t_L, b_L), the operators in Eq. (521) give rise to $m = 6$ operators after $SU(2)_W \times U(1)_Y$ breaking, where $\bar{q}_4 q_3 = \bar{t}_4 t_3$ or $\bar{q}_4 q_3 = \bar{b}_4 b_3$. If q in Eq. (521) is an EW singlet, such as b_R or t_R , then $m = 3$. The collinear matching D_C is proportional to an $m \times m$ unit matrix and given by

$$[D_C(\mu_1, \bar{n}p, L_M)]_{ii} = \sum_r \left[J_r(\mu_1, L_M) \ln \frac{2E_r}{\mu_1} + H_r(\mu_1, L_M) \right]. \quad (526)$$

The sum over r includes all particles in the operator O_i produced after EW symmetry breaking, and D_C is linear in $\ln(\bar{n}p)$ to all orders in perturbation theory [544, 572]. The collinear contributions D_C [and also γ_C in Eq. (524)] are process independent. The soft part $d_S(\mu_1, \{n\}, L_M)$ and the functions J_r and H_r of the collinear part have an expansion in $\alpha_{s,w,em}(\mu_1)$, i.e. in the couplings of the broken theory, and depend on μ_1 and on masses of the order of the EW scale via dimensionless ratios such as M_W/M_Z and $L_M = \ln(M_Z/\mu_1)$. The one-loop contribution to the soft part has the structure of Eq. (525) with an additional logarithm of the gauge-boson mass. These logarithms are small if one chooses $\mu_1 \sim M_Z$. The low-scale matching has to be computed in the broken EW theory. It translates the amplitudes for the fields of the unbroken theory to those of the broken theory [545]. Since all light lepton and quark masses can be neglected, the quark-mixing matrix does not enter the SCET computation. Once the EW corrections are computed, one can introduce the quark-mixing matrix by transforming to the mass-eigenstate basis.

The exponent in Eq. (522) contains at most a double (Sudakov) logarithm resulting from integrating the $A_r(\mu)$ terms in the collinear anomalous dimension. The high-scale matching is by two powers of logarithms less important than the leading Sudakov logarithms. The low-scale matching contains a single-logarithmic term. This is a new feature of SCET_{EW} with respect to SCET_{QCD} first pointed out in Ref. [538]. One can show that the low-scale matching contains at most a single logarithm to all orders in perturbation theory [538, 545]. As a consequence, resummed perturbation theory remains valid even at high energy, because $\alpha_i^k \ln(s/M_W^2) \ll 1$ for sufficiently large k .

The logarithmic term in the matching (526) is needed for a proper factorization of scales. A typical Sudakov double-logarithmic term at one loop has the form (suppressing coupling factors)

$$\ln^2 \frac{Q^2}{M^2} = \ln^2 \frac{Q^2}{\mu_h^2} + \left[\ln^2 \frac{Q^2}{\mu_1^2} - \ln^2 \frac{Q^2}{\mu_h^2} \right] + \left[\ln^2 \frac{M^2}{\mu_1^2} - 2 \ln \frac{Q^2}{\mu_1^2} \ln \frac{M^2}{\mu_1^2} \right]. \quad (527)$$

The first term on the r.h.s. belongs to the high-scale matching C , the second term arises from integrating the $\ln(Q^2/\mu^2)$ anomalous dimension from μ_h to μ_1 , and the third term enters the low-scale matching D_C . The existence of the logarithmic term in the low-scale matching also follows from the consistency condition that the theory is independent of μ_1 . Since changes in the running between μ_h and μ_1 contain a single logarithm from the anomalous dimension, there must be a single logarithm in the matching.

The resummed EW corrections can be grouped into LL, NLL, etc., in the usual way; the precise definition for SCET_{EW} can be found in Ref. [544]. The LL series is determined by the one-loop cusp anomalous dimension $A_r(\mu)$. The NLL series is determined by the two-loop cusp anomalous dimension and the one-loop values of $B_r(\mu)$ and $J_r(\mu, L_M)$. All terms needed for an NLL computation are known, so that *all* processes can be computed to resummed NLL order. In Refs. [545, 546] the one-loop d_S and C terms were computed for all $2 \rightarrow 2$ processes. The three-loop cusp anomalous dimension $A_r(\mu)$ and the two-loop non-cusp anomalous dimension $B_r(\mu)$ are available in the literature, except for the scalar Higgs contributions, which are numerically small. The two-loop contribution to D_C has not been calculated yet. The NNLL results are known, with the exception of these terms.

Based on the SCET_{EW} results, one can compute radiative corrections in the EFT to all partonic hard scattering processes at the LHC with an arbitrary number of external particles, if the high-scale matching is known. These calculations are valid in the Sudakov region and neglect power corrections of the form $M_{W,Z}^2/s$ and m_f^2/s in the one-loop and higher-order radiative corrections. In this regard, we expect that the results do not apply to processes that are mass-suppressed at LO. For the Sudakov form factor, the mass-suppressed one-loop corrections are 2% for $M_W/Q \sim 1$ and decrease fast with increasing Q [544]. How this translates to general processes is not obvious. In this respect it might be interesting to note that for Higgs production processes in e^+e^- annihilation and at hadron colliders bosonic EW corrections at the level of 5% have been found that could not be attributed to a known source of enhanced corrections [573–577].

5.4.4. EW logarithmic corrections for practical calculations

The detailed knowledge of the tower of EW high-energy logarithms is important for a deeper understanding of EW dynamics, but making use of it in predictions is a subject that deserves care:

- It is certainly advisable to make use of full NLO EW corrections, i.e. without applying expansions for high energies, whenever possible for a given process. Non-logarithmic corrections are process specific and typically amount to some percent, depending on the kinematical domain and the process under consideration. After including finite, non-logarithmic terms in the high-energy approximation, power-suppressed terms are still missing. A safe assessment of the quality of high-energy approximations requires the comparison to full NLO results [516, 555, 556, 578].
- Beyond NLO, the knowledge of higher-order EW logarithms can be very useful to improve pure NLO predictions. However, particular care has to be taken if the EW logarithms show large cancellations between leading and subleading terms, as for instance observed in the case of neutral-current fermion–antifermion scattering [533]. If the full tower of logarithms of a fixed perturbative order is not known, it is not clear to which accuracy truncated towers approximate the full correction. However, the known part of the tower can at least deliver estimates for the size of missing corrections and be used in the assessment of theoretical uncertainties.
- Since the EW high-energy logarithmic corrections are associated with virtual soft and/or collinear weak-boson or photon exchange, they all have counterparts in real weak-boson or photon-emission processes which can partially cancel the large negative virtual corrections. This cancellation is incomplete [525], since $SU(2)_W$ doublets are in general not treated inclusively in EW corrections—a fact that is by some abuse of language called *Bloch–Nordsieck violation*.³⁸ To which extent the cancellation occurs depends on the experimental capabilities to separate final states with or without weak bosons or photons. Logarithmic approximations, as implemented in the PYTHIA shower [478] can deliver first estimates, but solid predictions have to be based on complete matrix elements. The general issue and specific examples were discussed in Refs. [524, 544, 559, 571, 579–582]. For instance, the numerical analysis [524] of neutral-current Drell–Yan production demonstrates the effect of real weak-boson emission in the distributions in the transverse lepton momentum $p_{T,l}$ and in the invariant mass M_{ll} of the lepton pair. At the LHC, at $M_{ll} = 2 \text{ TeV}$ the EW corrections are reduced from about -11% to -8% by weak-boson emission. At $p_{T,l} = 1 \text{ TeV}$ the corresponding reduction from about -10% to -3% is somewhat larger. A framework to perform an all-order resummation of EW logarithms for inclusive scattering processes at energies much above the EW scale was developed in Ref. [583].

While the analytical structure of EW corrections was studied in the literature in detail in the Sudakov regime, there is only little knowledge on EW corrections beyond NLO in more general kinematical situations where not

³⁸The Bloch–Nordsieck theorem [366] simply does not apply to non-abelian gauge theories.

$M_{T,\nu_l}/\text{GeV}$	50–∞	100–∞	200–∞	500–∞	1000–∞	2000–∞
σ_0/pb	4495.7(2)	27.589(2)	1.7906(1)	0.084697(4)	0.0065222(4)	0.00027322(1)
$\delta_{q\bar{q}}^{\mu^+\nu_\mu}/\%$	−2.9(1)	−5.2(1)	−8.1(1)	−14.8(1)	−22.6(1)	−33.2(1)
$\delta_{q\bar{q}}^{\text{rec}}/\%$	−1.8(1)	−3.5(1)	−6.5(1)	−12.7(1)	−20.0(1)	−29.6(1)
$\delta_{\text{EWdlog}}^{(1)}/\%$	0.0005	0.5	−1.9	−9.5	−18.5	−29.7
$\delta_{\text{EWslog}}^{(1)}/\%$	0.008	0.9	2.3	3.8	4.8	5.9
$\delta_{\text{EWdlog}}^{(2)}/\%$	−0.0002	−0.023	−0.082	0.21	1.3	3.8

Table 5: Integrated LO cross sections for $\text{pp} \rightarrow l^+\nu_l + X$ at the LHC for $\sqrt{s} = 14 \text{ TeV}$ for different ranges in the transverse mass M_{T,ν_l} and corresponding relative corrections (results taken from Ref. [585] and extended).

M_{ll}/GeV	50–∞	100–∞	200–∞	500–∞	1000–∞	2000–∞
σ_0/pb	738.733(6)	32.7236(3)	1.48479(1)	0.0809420(6)	0.00679953(3)	0.000303744(1)
$\delta_{q\bar{q},\text{phot}}^{\text{rec}}/\%$	−1.81	−4.71	−2.92	−3.36	−4.24	−5.66
$\delta_{q\bar{q},\text{weak}}^{\text{rec}}/\%$	−0.71	−1.02	−0.14	−2.38	−5.87	−11.12
$\delta_{\text{EWdlog}}^{(1)}/\%$	0.27	0.54	−1.43	−7.93	−15.52	−25.50
$\delta_{\text{EWdlog}}^{(2)}/\%$	−0.00046	−0.0067	−0.035	0.23	1.14	3.38

Table 6: Integrated LO cross sections for $\text{pp} \rightarrow l^+l^- + X$ at the LHC for $\sqrt{s} = 14 \text{ TeV}$ for different ranges in the invariant mass M_{ll} and corresponding relative corrections (results taken from Ref. [422] and extended)).

all invariants s_{ij} are large. Note that there are many cross sections that are in fact not dominated by the Sudakov regime in the high-energy limit, including all processes that are dominated by t -channel diagrams. For example, unless specifically designed cuts are applied, reactions like W-boson pair production via e^+e^- , pp, or $\gamma\gamma$ collisions receive sizeable contributions from the *Regge limit*, where the Mandelstam variable t remains small while s gets large. Moreover, it often depends on the specific observable which regime is probed in high-energy tails of kinematical distributions. Taking neutral-current Drell–Yan processes (see, e.g., Refs. [422, 584]) and dijet production [507] at the LHC as examples, differential distributions in the transverse momenta of the produced leptons or jets probe the Sudakov regime in the high-momentum tails. On the other hand, the dilepton or dijet invariant-mass distributions of these processes are not dominated by this regime at high scales, so that the EW high-energy logarithms derived in the Sudakov regime do not approximate the EW corrections well in those observables.

In Ref. [585] the full EW corrections for the process $\text{pp} \rightarrow l^+\nu_l + X$, where l is a massless lepton, were compared to the double-logarithmic approximation for the LHC with $\sqrt{s} = 14 \text{ TeV}$. In Table 5 we show the LO cross section for different cuts on the transverse mass M_{T,ν_l} of the produced W boson. We list the EW corrections for bare muon final states $\delta_{q\bar{q}}^{\mu^+\nu_\mu}$ and with photon recombination applied $\delta_{q\bar{q}}^{\text{rec}}$, as well as the NLO corrections due to EW double logarithms $\delta_{\text{EWdlog}}^{(1)}$ and EW single logarithms $\delta_{\text{EWslog}}^{(1)}$ as derived from Eqs. (465), (472), and (481), (490) respectively,

$$\delta_{\text{EWdlog}}^{(1)} = -C_{\bar{d}u \rightarrow l^+\nu}^{\text{EW}} L(\hat{s}) + 4l_{\bar{d}u \rightarrow l^+\nu}(\hat{s}, \hat{t}, \hat{u}) l(\hat{s}), \quad (528)$$

$$\delta_{\text{EWslog}}^{(1)} = 3C_{\bar{d}u \rightarrow l^+\nu}^{\text{EW}} l(\hat{s}) + p_{\bar{d}u \rightarrow l^+\nu} l(\hat{s}), \quad (529)$$

with the large logarithms $L(\hat{s})$ and $l(\hat{s})$ defined in Eqs. (467) and (474) and

$$\begin{aligned} C_{\bar{d}u \rightarrow l^+\nu}^{\text{EW}} &= C^{\text{EW}}(d^L) + C^{\text{EW}}(u^L) + C^{\text{EW}}(l^L) + C^{\text{EW}}(v^L) = \frac{3}{s_w^2} + \frac{5}{9c_w^2}, \\ l_{\bar{d}u \rightarrow l^+\nu}(\hat{s}, \hat{t}, \hat{u}) &= -\frac{1}{s_w^2} \ln\left(\frac{\hat{t}\hat{u}}{\hat{s}^2}\right) + \frac{1}{3c_w^2} \ln\left(\frac{\hat{t}}{\hat{u}}\right), \\ p_{\bar{d}u \rightarrow l^+\nu}(\hat{s}, \hat{t}, \hat{u}) &= 2\left(\frac{c_w}{s_w} b_{AZ}^{\text{EW}} - b_{AA}^{\text{EW}}\right) = -\frac{19}{3s_w^2}. \end{aligned} \quad (530)$$

Here, $\hat{s}, \hat{t}, \hat{u}$ are the usual Mandelstam variables of the partonic process $\bar{d}u \rightarrow l^+ \nu$, i.e. $\hat{s} = (p_{\bar{d}} + p_u)^2$, $\hat{t} = (p_{\bar{d}} - p_{l^+})^2$, and $\hat{u} = (p_{\bar{d}} - p_{\nu})^2$. Moreover, we include an estimate $\delta_{\text{EWdlog}}^{(2)}$ of the NNLO EW logarithms based on the first two leading two-loop logarithms obtained from $\delta_{\text{EWdlog}}^{(1)}$ by exponentiation,

$$\delta_{\text{EWdlog}}^{(2)} = C_{\bar{d}u \rightarrow l^+ \nu}^{\text{EW}} L(\hat{s}) \left[\frac{1}{2} C_{\bar{d}u \rightarrow l^+ \nu}^{\text{EW}} L(\hat{s}) - 4 l_{\bar{d}u \rightarrow l^+ \nu}(\hat{s}, \hat{t}, \hat{u}) l(\hat{s}) \right]. \quad (531)$$

We observe that the relative NLO EW corrections are apparently well reproduced for large $M_{T,l\nu}$ by $\delta_{\text{EWdlog}}^{(1)}$, i.e. by the leading and subleading EW logarithms of types LSC and SSC. However, the perfect match is accidental, since the single EW logarithms $\delta_{\text{EWslog}}^{(1)}$ from collinear singularities and parameter renormalization contribute at the level of 5%. Logarithmic contributions from real radiation, which are not included in $\delta_{\text{EWdlog}}^{(1)} + \delta_{\text{EWslog}}^{(1)}$, and terms involving constants or pure angular-dependent logarithms are at the level of a few percent (as also demonstrated for $W\gamma$ production at the LHC in Ref. [578]). Thus, a generic uncertainty of a few per cent should be attributed to an approximation based on enhanced logarithmic contributions only. Within this uncertainty margin, the logarithmic approximation works well for the considered case. This is due to the fact that demanding large values of $M_{T,l\nu}$ by a cut enforces large Mandelstam invariants $\hat{s}, |\hat{t}|$, and $|\hat{u}|$ in the underlying partonic process, which corresponds to the Sudakov domain.

As a further example we consider the neutral current Drell–Yan process $pp \rightarrow l^+ l^- + X$ at $\sqrt{s} = 14 \text{ TeV}$ as investigated in Ref. [422]. The corresponding cross section and EW corrections for different cuts on the lepton-pair invariant mass M_{ll} are shown in Table 6. The table shows the complete EW corrections, the gauge-invariant weak corrections as well as the double-logarithmic EW corrections at NLO (types LSC and SSC) and NNLO as defined in the previous case, i.e. which are calculated as in Eqs. (528) and (531). However, for the partonic neutral-current process $\bar{q}^\sigma q^\sigma \rightarrow l^{+\tau} l^\tau$ the factors (see also Ref. [527])

$$\begin{aligned} C_{\bar{q}^\sigma q^\sigma \rightarrow l^{+\tau} l^\tau}^{\text{EW}} &= 2C^{\text{EW}}(q^\sigma) + 2C^{\text{EW}}(l^\tau) = \frac{2}{s_w^2} \left[I_{w,q^\sigma}(I_{w,q^\sigma} + 1) + I_{w,l^\tau}(I_{w,l^\tau} + 1) \right] + \frac{1}{2c_w^2} \left[(Y_{w,q^\sigma})^2 + (Y_{w,l^\tau})^2 \right], \\ l_{\bar{q}^\sigma q^\sigma \rightarrow l^{+\tau} l^\tau}(\hat{s}, \hat{t}, \hat{u}) &= 2 \left(\frac{I_{w,q^\sigma}^3 I_{w,l^\tau}^3}{s_w^2} + \frac{Y_{w,q^\sigma} Y_{w,l^\tau}}{4c_w^2} \right) \ln \left(\frac{\hat{u}}{\hat{t}} \right) - \frac{2}{s_w^2} \frac{4c_w^2 I_{w,q^\sigma}^3 I_{w,l^\tau}^3}{4c_w^2 I_{w,q^\sigma}^3 I_{w,l^\tau}^3 + s_w^2 Y_{w,q^\sigma} Y_{w,l^\tau}} \ln \left(\frac{|\hat{r}_{\sigma\tau}|}{\hat{s}} \right), \\ \hat{r}_{\sigma\tau} &= \begin{cases} \hat{t}, & I_{w,q^\sigma}^3 I_{w,l^\tau}^3 > 0, \\ \hat{u}, & I_{w,q^\sigma}^3 I_{w,l^\tau}^3 < 0, \end{cases} \\ p_{\bar{q}^\sigma q^\sigma \rightarrow l^{+\tau} l^\tau} &= 2 \left(\frac{4c_w^4 I_{w,q^\sigma}^3 I_{w,l^\tau}^3 - s_w^4 Y_{w,q^\sigma} Y_{w,l^\tau}}{c_w s_w (4c_w^2 I_{w,q^\sigma}^3 I_{w,l^\tau}^3 + s_w^2 Y_{w,q^\sigma} Y_{w,l^\tau})} b_{AZ}^{\text{EW}} - b_{AA}^{\text{EW}} \right), \end{aligned} \quad (532)$$

depend on the chiralities $\sigma, \tau = \text{R/L} = +/ -$. In this case, the EW logarithms fail to approximate the full EW corrections, as can already be concluded from the significant discrepancy between the double-logarithmic correction $\delta_{\text{EWdlog}}^{(1)}$ and the full correction. The failure is a consequence of the different event selection: The cut demanding large M_{ll} values enforces only large values of \hat{s} (which is equal to M_{ll}^2 in LO kinematics), but not large values of $|\hat{t}|$ and $|\hat{u}|$, which would be required in the Sudakov regime. Instead, the cross section still receives large contributions from regions where \hat{s} is large, but either $|\hat{t}|$ or $|\hat{u}|$ small, where the EW corrections are less pronounced.

6. Issues with unstable particles

6.1. Unstable particles and resonances

Since most of the elementary degrees of freedom (fermions, Higgs and gauge bosons) of the SM are unstable, the appearance of unstable particles in high-energy particle reactions is more the rule than an exception. Apart from rare exceptions, such as muons or B mesons, unstable states do not exist long enough to leave directly accessible traces in detectors, but rather appear as resonances that can only be reconstructed from their decay products. The lifetime τ_P of such a resonance P can, thus, not be determined in a time-of-flight measurement, but only indirectly from its total decay width $\Gamma_P = 1/\tau_P$, which is accessible via the width of the resonance if the experimental resolution in

the reconstruction is good enough.³⁹ In an ideal situation, Γ_P is obtained from the Breit–Wigner-like resonance in the invariant-mass distribution of its decay products, but also other distributions (e.g. transverse-mass or transverse-momentum distributions) might be useful.

Theoretically, resonance processes lead to complications in standard perturbation theory which requires stable asymptotic states in S -matrix elements. Strictly speaking, an unstable particle P (mass M_P) should only appear as intermediate state, i.e. on internal lines in Feynman diagrams. However, there it might happen that the pole at invariant mass $p^2 = M_P^2$ in a propagator $\propto (p^2 - M_P^2)^{-1}$ of P is hit for some physical momentum transfer p , leading to a singularity at any fixed order in perturbation theory. This artificially introduced singularity is only lifted if at least the imaginary parts of self-energy corrections near the singularity are *Dyson summed*. Denoting the renormalized self-energy $\Sigma_R(p^2)$ of P graphically by a dark grey blob,⁴⁰

$$\Sigma_R(p^2) = \text{---} \bullet \text{---} = \text{---} \bullet \text{---} (1) + \text{---} \bullet \text{---} (2) + \text{---} \bullet \text{---} (2) + \text{---} \bullet \text{---} (1) + \dots, \quad (533)$$

where the numbers represent the loop orders in the light grey 1PI blobs on the right-hand side, the Dyson summation modifies the LO propagator $G_{0,P}(p^2) = i/(p^2 - M_P^2)$ to

$$\begin{aligned} \bullet \text{---} \bullet &= \text{---} \bullet \text{---} + \text{---} \bullet \text{---} (1) + \text{---} \bullet \text{---} (2) + \dots \\ G_P(p^2) &= \frac{i}{p^2 - M_P^2} + \frac{i}{p^2 - M_P^2} i \Sigma_R(p^2) \frac{i}{p^2 - M_P^2} + \frac{i}{p^2 - M_P^2} i \Sigma_R(p^2) \frac{i}{p^2 - M_P^2} i \Sigma_R(p^2) \frac{i}{p^2 - M_P^2} + \dots \\ &= \frac{i}{p^2 - M_P^2 + \Sigma_R(p^2)}. \end{aligned} \quad (534)$$

The difference between a stable and an unstable particle of mass $M_P > 0$ rests in the fact that the pole of the propagator lies on the positive real axis or strictly below it in the complex p^2 plane, respectively.

The *optical theorem*, which is a consequence of the unitarity of the S -matrix, yields the relation

$$\text{Im } \Sigma_R(M_P^2) = \text{Im} \left\{ \text{---} \bullet \text{---} \right\} \Big|_{p^2=M_P^2} = \frac{1}{2} \sum_X \text{---} \bullet \text{---} (0) X \text{---} (0) \text{---} = \frac{1}{2} \sum_X \int d\Phi_X |\mathcal{M}_{P \rightarrow X}|^2 = M_P \Gamma_P \quad (535)$$

in one-loop approximation (see for instance Refs. [86, 87]). Since moreover $\text{Re } \Sigma_R(M_P^2) = 0$ for the on-shell (OS)-renormalized mass M_P , the propagator of an unstable particle behaves like $[p^2 - M_P^2 + iM_P \Gamma_P]^{-1}$ with $\Gamma_P > 0$ near the pole, so that its singularity turns into the shape of a Breit–Wigner resonance after squaring it. The sign of Γ_P is determined by causality, i.e. already fixed by Feynman’s $i\epsilon$ prescription for propagators, and guarantees that the intermediate resonance P exponentially decays in forward time direction with the lifetime $\tau_P = 1/\Gamma_P$.

In a quantum field theory with stable particles only, the unitarity of the S -matrix can be expressed in terms of *Cutkosky’s cutting rules* [586], which relate imaginary parts of Feynman integrals with corresponding *cut diagrams*. Those cut diagrams result from the original diagram by replacing the propagators (with momentum p) on the cut by *cut propagators* of the form $2\pi\theta(p_0)\delta(p^2 - M_P^2)$, which correspond to physical OS intermediate states, and replacing the propagators and vertices on one side of the cut by their complex conjugates. Following common practice, the complex-conjugated part of the cut diagram is indicated in Eq. (535) by a shadow on the right side of the cut. Obviously, the cut relations require modification in the presence of unstable particles, which cannot appear as intermediate states with real mass values. Already in 1963 Veltman showed for a generic scalar field theory that unitarity is still respected and that the cutting relations can be restored if cuts through intermediate lines of unstable particles are omitted [587]. Veltman’s proof, however, consistently makes use of Dyson-summed propagators and all-order properties of amplitudes, so that the arguments do not easily carry over to calculations in practice. Unitarity within the *complex-mass scheme (CMS)*, which is presented in Section 6.6 below in detail, was investigated in Ref. [588].

³⁹When restoring Planck’s constant \hbar , which equals one in the natural units that we use, the relation between width and lifetime reads $\tau_P = \hbar/\Gamma_P$.

⁴⁰For a scalar field, Σ is the usual self-energy as defined in Eq. (141), for a vector field Σ stands for the transverse part Σ_T , and for fermionic fields Σ is effectively formed by some combination of self-energies corresponding to the various covariants spanning the 2-point function.

Technically, the Dyson summation is straightforward, but conceptually it bears some issues in combination with the truncation of the perturbative series, which is necessary in practice for corrections that are not of self-energy type, so that perturbative orders are only partially included starting from some loop level. However, consistency relations, such as the gauge independence of S -matrix elements or cutting relations expressing unitarity, are typically formulated order by order in perturbation theory, so that those relations are in general disturbed if some perturbative orders are not taken into account completely. Without taking special measures, this can totally destroy the consistency and reliability of predictions. Before introducing and discussing solutions to this problem at tree and loop level, we first look into the form of resonance propagators and naive approaches that ignore issues connected with their embedding in full matrix elements, in order to put into context simple approximations and to clarify some details in the definition of mass and width of an unstable particle.

6.2. Narrow-width approximation and naive width schemes

The simplest, but somewhat crude way to describe the production of an unstable particle P is to employ the *narrow-width approximation (NWA)*, which treats P as “stable intermediate state”, i.e. the full process is decomposed into the production of an OS particle P and its decay to some final state X . This decomposition results from the limit $\Gamma_P \rightarrow 0$ in the squared matrix element of the full resonance process, where the squared propagator with momentum transfer p behaves like

$$\frac{1}{|p^2 - M_P^2 + iM_P\Gamma_P|^2} \xrightarrow{\Gamma_P \rightarrow 0} \frac{\pi}{M_P\Gamma_P} \delta(p^2 - M_P^2). \quad (536)$$

The $1/\Gamma_P$ factor on the r.h.s. is part of the well-known *branching ratio*

$$\text{BR}_{P \rightarrow X} = \frac{\Gamma_{P \rightarrow X}}{\Gamma_P}, \quad \Gamma_P = \sum_X \Gamma_{P \rightarrow X}, \quad (537)$$

which emerges after the inclusive integration over the $P \rightarrow X$ decay phase space and is the probability that P chooses the final state X in its decay. The quantity $\Gamma_{P \rightarrow X}$ is the *partial decay width* for this channel, which is calculable in perturbation theory similar to a cross section from the $P \rightarrow X$ matrix elements. This pattern repeats for each resonance if several unstable particles are produced. By construction, the NWA fails to describe observables that resolve the invariant mass of the resonance, i.e. it is restricted to observables in which the resonances are integrated over.

For unstable particles with spin, in general effects of spin correlations between production and decay or between various decaying particles appear if cuts are imposed on the decay products, or if distributions in kinematical variables of those are considered. The naive NWA, which employs unpolarized production cross sections and decay widths, can be easily improved to include these correlations by properly combining production and decay parts for definite polarization states of the unstable particle.

The NWA is also useful in a first approximate calculation of radiative corrections to cross sections for unstable-particle production. The NWA can accommodate corrections to the production cross section and to the relevant branching ratio, but neglects off-shell effects of $\mathcal{O}(\Gamma_P/M_P)$ for each resonating particle P . These off-shell effects, which are due to the off-shell tails of the resonances and *background diagrams* with fewer or no resonances, have to be added to NWA predictions, e.g., to get full NLO accuracy in cross-section predictions [589, 590]. Moreover, we note that naive estimates often underestimate the theoretical uncertainties of the NWA, as e.g. discussed in Refs. [591, 592]. Specifically, in decays near some kinematical boundary or in scenarios with cascade decays, which are quite common in non-standard models, the NWA can even fail completely, as demonstrated in Refs. [593, 594].

In view of EW physics at colliders, the most important resonances are the ones of W and Z bosons, which decay into lepton–antilepton or quark–antiquark pairs at LO. The decay widths Γ_V ($V = W, Z$) formally count as $\mathcal{O}(\alpha)$ in the electromagnetic coupling α . In numbers, we get $\mathcal{O}(\Gamma_V/M_V) \sim 3\%$, which is the expected order of relative uncertainty of NWA predictions at LO, which start from the approximation of OS W/Z bosons in production and decay. NLO corrections of relative order $\mathcal{O}(\alpha)$ do not only comprise virtual one-loop and real emission corrections to OS W/Z production and decays, but also off-shell effects in LO amplitudes. Including the latter goes beyond a pure NWA calculation, but nevertheless the NLO accuracy achieved by this improved description [590] of the resonance process is restricted to the resonance region and to observables in which the resonances are not resolved, i.e. completely integrated over.

$e^+e^- \rightarrow u\bar{d}\mu^-\bar{\nu}_\mu$ (no phase-space cuts applied)				
\sqrt{s}/GeV	189	500	2000	10000
$\sigma(\text{FW})/\text{fb}$	703.5(3)	237.4(1)	13.99(2)	0.624(3)
$\sigma(\text{RW})/\text{fb}$	703.4(3)	238.9(1)	34.39(3)	498.8(1)
$\sigma(\text{CMS})/\text{fb}$	703.1(3)	237.3(1)	13.98(2)	0.624(3)

$e^+e^- \rightarrow u\bar{d}\mu^-\bar{\nu}_\mu + \gamma$ (separation cuts for γ applied)				
\sqrt{s}/GeV	189	500	2000	10000
$\sigma(\text{FW})/\text{fb}$	224.0(4)	83.4(3)	6.98(5)	0.457(6)
$\sigma(\text{RW})/\text{fb}$	224.6(4)	84.2(3)	19.2(1)	368(6)
$\sigma(\text{CMS})/\text{fb}$	223.9(4)	83.3(3)	6.98(5)	0.460(6)

$e^+e^- \rightarrow \nu_e\bar{\nu}_e\mu^-\bar{\nu}_\mu u\bar{d}$ (phase-space cuts applied)				
\sqrt{s}/GeV	500	800	2000	10000
$\sigma(\text{FW})/\text{fb}$	1.633(1)	4.105(4)	11.74(2)	26.38(6)
$\sigma(\text{RW})/\text{fb}$	1.640(1)	4.132(4)	12.88(1)	12965(12)
$\sigma(\text{CMS})/\text{fb}$	1.633(1)	4.104(3)	11.73(1)	26.39(6)

Table 7: Some LO predictions for cross sections based on different schemes to treat the EW gauge-boson resonances: fixed-width (FW), running-width (RW), and complex-mass scheme (CMS). (Results taken from Refs. [58, 596]).

A detailed description of a resonance process, keeping the full differential information of the kinematics of the decay products, has to be based on complete matrix elements for the full process, including both resonant and non-resonant diagrams. Early LO calculations based on full matrix elements proceeded in a minimalist way and merely modified propagators of unstable particles P upon including an approximation for the imaginary part of the Dyson-summed self-energies,

$$P_P(p^2) = \frac{1}{p^2 - M_P^2 + iM_P\Gamma_P(p^2)}, \quad (538)$$

where $\Gamma_P(p^2)$ plays the role of the width of P in the vicinity of the resonance. Two frequently used versions are:

- *Fixed width (FW):* $\Gamma_P(p^2) = \Gamma_P = \text{const.}$

In this parametrization, the complex squared mass

$$\mu_P^2 = M_P^2 - iM_P\Gamma_P \quad (539)$$

plays the role of the location of the pole in the propagator in the complex p^2 plane.

- *Running width (RW):*

$$\Gamma_P(p^2) = \Gamma_P \times p^2 / M_P^2 \times \theta(p^2). \quad (540)$$

The function $\Gamma_P(p^2)$ resembles the p^2 dependence of the imaginary part of the one-loop self-energy of a vector particle P that exclusively decays into pairs of massless fermions. To good approximation this applies to W and Z bosons. The intention in this scheme is to come closer to the off-shell behaviour of the full propagator, in particular by including the factor $\theta(p^2)$ which switches off the imaginary part below the kinematical decay threshold, as demanded by causality and unitarity. The running-width scheme has, in particular, been used for the analysis of the Z-boson resonance at LEP1/SLC (see Ref. [18] and references therein).

We note, however, that none of these naive width schemes is satisfactory even at LO, because both versions introduce a gauge dependence in matrix elements. While the FW scheme for W/Z nevertheless delivers reasonable LO results by experience, (see, e.g., Refs. [58, 595, 596]), the RW scheme often fails completely, since the p^2 factor in the off-shell regions is prone to enhance gauge-invariance-breaking terms by orders of magnitude [597]. We illustrate these facts in Table 7, where we show the high-energy behaviour of some LO cross sections featuring WW production, WW γ production, and WW scattering in e^+e^- annihilation. The FW and RW schemes are compared with the CMS, which fully respects gauge-invariance requirements and is explained in detail in Section 6.6 below. While the results from the FW and CMS nicely agree, the RW scheme totally fails in the high-energy regime.

6.3. The issue of gauge invariance

Gauge invariance implies two crucial properties of amplitudes that are required for consistency: independence of the gauge-fixing procedure employed in the quantization of the gauge theory and the validity of *Ward identities*. The first property obviously ensures that amplitudes do not depend on gauge parameters, the second deserves somewhat more explanation. With Ward identities we mean the Slavnov–Taylor identities discussed in Section 2.2 applied to truncated Green functions with external lines that are either physical states, would-be Goldstone bosons, or gauge-boson legs that are contracted with their momenta. Consider, for instance, an amplitude \mathcal{M} with an outgoing gauge boson V of outgoing momentum p , i.e.

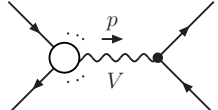
$$\mathcal{M} = \varepsilon_V^\mu(p)^* T_\mu^V(p), \quad V = W^\pm, Z, A, \quad (541)$$

where $\varepsilon^\mu(p)^*$ is the polarization vector of V . Then electromagnetic $U(1)_{\text{em}}$ and $SU(2)_w$ gauge invariance imply the relations

$$p^\mu T_\mu^{W^\pm}(p) = \pm M_W T_\mu^{\phi^\pm}(p), \quad p^\mu T_\mu^Z(p) = -i M_Z T_\mu^X(p), \quad p^\mu T_\mu^A(p) = 0, \quad (542)$$

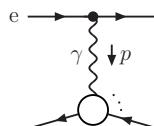
which are equivalent to the relations (47) of Section 2.2 or to Eq. (70) within the BFM. Disturbing these relations can lead to unphysical behaviour of the corresponding amplitudes. Violating, for instance, the $SU(2)_w$ relations for W and Z bosons, has a direct impact on the longitudinal polarizations owing to the Goldstone-boson equivalence theorem, which was described in Section 5.3. This can easily result in a totally wrong high-energy behaviour of amplitudes and cross sections.

Note that the Ward identities (542) are not only relevant in the case of external gauge bosons V , but also for subamplitudes in many-particle processes. The most important case arises in the situation where an external fermion–antifermion current $\bar{u}_{f_1}(p_1)\gamma^\mu\omega_\sigma v_{f_2}(p_2)$ becomes asymptotically proportional to its total momentum p , which is $p = p_1 + p_2$ if p_1 and p_2 are outgoing. In the subamplitude where the $f_1\bar{f}_2$ current is connected to the rest of the diagram by a V propagator, the Ward identities (542) are crucial for the correct behaviour of the amplitude in this kinematic limit. For W and Z bosons this situation occurs, e.g., in the high-energy limit of V production and subsequent decay, which is diagrammatically illustrated by



$$\sim \frac{\text{const.}}{p^2 - M_V^2 + i M_V \Gamma_V} p^\mu T_\mu^V(p) \quad \text{for } p^0 \gg M_V, \quad (543)$$

where the dots stand for any other produced particles. It is the violation of the corresponding Ward identities for W bosons that leads to the bad high-energy behaviour of the cross sections shown in Table 7 of the previous section in the case of the RW scheme. More such examples can be found in Ref. [598]. For photons an analogous situation occurs, e.g., in forward scattering of light fermions such as electrons,



$$\sim \frac{\text{const.}}{p^2} p^\mu T_\mu^A(p) \quad \text{for } |p^2| \rightarrow O(m_e^2) \ll (p^0)^2, \quad (544)$$

where the validity of the Ward identity is required to guarantee a decent behaviour of the amplitude in the limit of low photon virtuality p^2 . In practice, this situation, for instance, occurs in single- W production in e^+e^- annihilation, as discussed in detail in Refs. [595, 597–599].

6.4. Mass and width of unstable particles

Before we can describe schemes to treat resonances beyond LO, we have to consider mass renormalization for unstable particles to properly identify the definition of mass and width that parametrize the resonances that are analyzed experimentally. We compare the two most common renormalization schemes: (i) the OS scheme that closely follows the mass renormalization for stable particles described in Section 3.1.3 and (ii) the scheme that introduces the complex pole location μ_P^2 of Eq. (539) to define a renormalized mass M_P . Running masses, as e.g. defined in the $\overline{\text{MS}}$ scheme, are not suited to parametrize resonances and, thus, not considered in the following. We denote the previously

used *bare mass* $M_{0,P}$ of the unstable particle and add the subscript OS to quantities defined in the OS scheme. The OS renormalization condition fixes $M_{P,OS}^2$ as the zero of the real part of the inverse P propagator,

$$M_{P,OS}^2 - M_{0,P}^2 + \text{Re}\{\Sigma(M_{P,OS}^2)\} = 0, \quad (545)$$

while the condition that identifies μ_P^2 with the complex location of the propagator pole reads

$$\mu_P^2 - M_{0,P}^2 + \Sigma(\mu_P^2) = 0, \quad (546)$$

where $\Sigma(p^2)$ denotes the unrenormalized self-energy of P . The determination of OS renormalization constants works as for stable particles, which is described in Section 3.1.7; the procedure for complex masses is described in Section 6.6 below. Here we are concerned with the relation between mass and width parameters in the two schemes. Eliminating the bare mass from the propagator factors in either scheme, the corresponding leading resonance behaviour of $P_P(p^2)$ is given by

$$P_{P,OS}(p^2) = \frac{1}{p^2 - M_{P,OS}^2 + \Sigma(p^2) - \text{Re}\{\Sigma(M_{P,OS}^2)\}} \xrightarrow{p^2 \rightarrow M_{P,OS}^2} \frac{1}{(p^2 - M_{P,OS}^2)[1 + \text{Re}\{\Sigma'(M_{P,OS}^2)\}] + i\text{Im}\{\Sigma(p^2)\} + \dots}, \quad (547)$$

$$P_P(p^2) = \frac{1}{p^2 - \mu_P^2 + \Sigma(p^2) - \Sigma(\mu_P^2)} \xrightarrow{p^2 \rightarrow \mu_P^2} \frac{1}{(p^2 - \mu_P^2)[1 + \Sigma'(\mu_P^2)] + \dots}, \quad (548)$$

where the expansions in the denominators are correct up to $\mathcal{O}((p^2 - M_{P,OS}^2)^2)$ and $\mathcal{O}((p^2 - \mu_P^2)^2)$, respectively. Comparing Eq. (547) near the resonance pole $p^2 \sim M_{P,OS}^2$ with the standard form $1/(p^2 - M_P^2 + iM_P\Gamma_P)$, we can associate

$$\Gamma_{P,OS} = \frac{\text{Im}\{\Sigma(M_{P,OS}^2)\}}{M_{P,OS}[1 + \text{Re}\{\Sigma'(M_{P,OS}^2)\}]} \quad (549)$$

with the width in the OS scheme. A similar comparison of Eq. (548) yields the *pole mass* M_P and the *pole width* Γ_P in the scheme with μ_P from Eq. (539) as renormalized parameter. Since the pole location μ_P^2 is an intrinsic property of the S -matrix, the definition of M_P and Γ_P is gauge independent [600, 601] in the sense that the complex mass renormalization constant and the parametrization of S -matrix elements in terms of μ_P^2 are gauge independent. On the other hand, the OS scheme involves gauge dependences starting from the two-loop level [602].

For W and Z bosons the form of the propagator in the OS scheme (547) is compatible with the form Eq. (538) with the running width (540) for massless decay products. Historically, the W and Z masses and widths were experimentally determined at LEP, Tevatron, and the LHC in the OS scheme, even though the (gauge-independent) pole definitions are theoretically preferred. Fortunately, the conversion from the OS to the pole definitions can be easily obtained from Eqs. (539), (545), (546), and (549) upon using the form Eq. (540) via an order-by-order expansion of Σ , leading to [595, 603]

$$M_V = \frac{M_{V,OS}}{\sqrt{1 + \Gamma_{V,OS}^2/M_{V,OS}^2}}, \quad \Gamma_V = \frac{\Gamma_{V,OS}}{\sqrt{1 + \Gamma_{V,OS}^2/M_{V,OS}^2}}. \quad (550)$$

This implies

$$M_{W,OS} - M_W \approx 27 \text{ MeV}, \quad M_{Z,OS} - M_Z \approx 34 \text{ MeV}, \quad (551)$$

i.e. the scheme differences are much larger than the corresponding experimental uncertainties on the W and Z masses, which are currently [90] 12 MeV and 2.1 MeV, respectively.

6.5. Pole scheme and pole approximation

6.5.1. Pole scheme—general idea and subtleties

The *pole scheme* is a prescription for a construction of gauge-independent cross sections including resonances, exploiting the fact that both the location of the P propagator pole and its residue in amplitudes are gauge-independent

quantities. The idea [56, 57] is to first isolate the residue R of each resonance in the considered amplitude \mathcal{M} and subsequently to introduce a finite decay width Γ_P only in the gauge-independent resonant part,

$$\mathcal{M} = \frac{R(p^2)}{p^2 - M_P^2} + N(p^2) = \underbrace{\frac{R(M_P^2)}{p^2 - M_P^2} + \frac{R(p^2) - R(M_P^2)}{p^2 - M_P^2}}_{\text{resonant}} + N(p^2) \rightarrow \underbrace{\frac{\tilde{R}(\mu_P^2)}{p^2 - \mu_P^2}}_{\text{resonant}} + \underbrace{\frac{R(p^2) - R(M_P^2)}{p^2 - M_P^2} + \tilde{N}(p^2)}_{\text{non-resonant}}. \quad (552)$$

Here, $R(p^2)$ summarizes all contributions developing resonant parts in the P propagator with virtuality p^2 , and $N(p^2)$ the remaining non-resonant contributions. The replacement, thus, dresses the propagator denominator $p^2 - M_P^2$ with the contribution $iM_P\Gamma_P$ from the finite decay width, i.e. partially takes into account Dyson summation of propagator corrections. Note, however, that in the resonance region $p^2 \sim M_P^2$, the width contribution $iM_P\Gamma_P$ becomes part of the leading term, although Γ_P accounts for a correction according to the counting in the off-shell region. Thus, if radiative corrections are to be included, the Γ_P value inserted here has to include corrections one order higher than the rest of the matrix-element calculation. Moreover, double-counting has to be carefully avoided. The tilde on the symbols \tilde{R} and \tilde{N} indicates that there are some modifications of those terms in the course of replacing $M_P^2 \rightarrow \mu_P^2$, in order to avoid double counting. If done carefully the prescription (552) respects gauge invariance and can be used to make uniform predictions in resonant and non-resonant phase-space regions.

Although the general idea seems quite simple and appealing, we emphasize that Eq. (552) is a generic formula that involves several subtleties in practice:

- There is some freedom in the actual implementation of the scheme, because the resonant part of an amplitude is not uniquely determined by the propagator structure alone, but depends on a specific phase-space parameterization and in most cases also on the separation of polarization-dependent parts (spinors, polarization vectors).
- Taking the pole prescription literally, the scattering amplitude on the resonance pole (i.e. with μ_P^2 being complex) involves matrix elements with complex kinematical variables, which is a subtle issue [604].⁴¹ For narrow resonances such as the weak gauge bosons $V = W, Z$, or the SM Higgs boson, the complex kinematics can be avoided by suitable expansions in Γ_V/M_V .
- Taking into account higher-order corrections, the resonance does not appear as a pure pole structure in the amplitude, but rather as branch point in the complex p^2 plane. The exchange of massless particles such as photons or gluons with the resonance or between production and decay subprocesses leads to correction terms involving factors like $\ln(p^2 - M_P^2)$. For such terms the concept of taking the residue, $R(p^2) \rightarrow R(\mu_P^2)$, is ill-defined and has to be generalized. Since all non-analytic terms in $R(p^2)$ can be uniquely isolated, a possible generalization consists in the substitution $\ln(p^2 - M_P^2) \rightarrow \ln(p^2 - \mu_P^2)$ while we set $p^2 \rightarrow \mu_P^2$ in all regular terms.
- In the case of multiple resonances further generalizations are necessary. Massless particle (i.e. photon or gluon) exchange that involves more than one resonance leads to deviations from the pole structure $K_P(p, M_P)^{-1} = (p^2 - M_P^2)^{-1}$ for each resonance. For the case of two resonances P_1 and P_2 , for instance, in addition to the pattern $K_{P_1}(p_1, M_{P_1})^{-1}K_{P_2}(p_2, M_{P_2})^{-1}$ also doubly-resonant terms of the form $[a_{11}K_{P_1}^2 + a_{12}K_{P_1}K_{P_2} + a_{22}K_{P_2}^2]^{-1}$ arise, where a_{ij} depend on further kinematical invariants [606–608]. Again, such terms should be uniquely isolated (in order to avoid gauge dependences) and subsequently regularized by $K_{P_i}(p_i, M_{P_i}) \rightarrow K_{P_i}(p_i, \mu_{P_i})$.
- If the pole scheme is applied to higher-order corrections, it should be kept in mind that both virtual and real corrections have to be handled, including a consistent matching of IR singularities. On the side of the real corrections, this means that real-photon (or real-gluon) emission might appear before, during, or after the resonant production of an unstable particle P . If P is electrically (or colour neutral), there is a gauge-invariant separation of radiation effects into emission from the production or decay processes in matrix elements, so that the procedure outlined in Eq. (552) is applicable, though being quite cumbersome in complicated cases. If P is charged, however, the problem of overlapping resonances occurs. In this case, radiation off the resonating particle leads to propagator

⁴¹This *complex pole scheme* was, e.g., applied to Higgs production via gluon fusion at the LHC in Ref. [605], with particular emphasis on a heavy, i.e. very broad, Higgs boson.

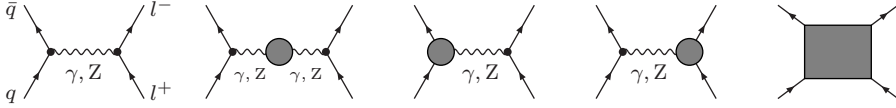


Figure 9: LO and generic one-loop diagrams for the process $q\bar{q} \rightarrow l^- l^+$, where the grey blobs and the grey box stand for self-energy, vertex, and box corrections.

tor products $K_P(p+k, M_P)^{-1} K_P(p, M_P)^{-1}$ with k denoting the momentum of the radiated photon (or gluon). In principle, the partial fractioning

$$\frac{1}{K_P(p+k, M_P) K_P(p, M_P)} = \frac{1}{(2pk) K_P(p, M_P)} - \frac{1}{(2pk) K_P(p+k, M_P)} \quad (553)$$

offers a separation into emission after or before the resonance, where the double slash on a propagator line indicates which momentum is set on its mass shell in the rest of the diagram (but not on the slashed line itself). However, the $1/(2pk)$ factors on the r.h.s. induce spurious soft singularities in this decomposition, because this factor mimics photon radiation off an OS state.

To our knowledge, a full pole-scheme calculation including all non-resonant terms for multiple resonances or for processes with charged resonances has not been carried out in the literature yet, which is certainly due to the subtleties and problems explained above.

Nevertheless, for cases where the pole scheme can be applied, it certainly offers various virtues. For instance, it provides a well-defined separation between resonant and non-resonant parts of a cross section, i.e. in some sense a definition of *signal* and *background* for the production of a resonance. This scheme is, thus, well suited for a parametrization of a resonance by so-called *pseudo-observables*, such as total and partial decay widths, peak cross sections, effective couplings, etc. Moreover, the consistent separation of signal and background contributions is an ideal starting point to further improve the description of the signal by higher-order corrections, a point that is particularly important if the signal dominates over the background and, thus, deserves higher precision.

6.5.2. Weak corrections to Drell–Yan-like Z-boson production in the pole scheme

As an example for the successful implementation of the pole scheme, we consider the calculation of NLO weak corrections to Z-boson production at hadron colliders, as presented in Ref. [422]. Photonic corrections, which comprise all contributions from virtual exchange and real emission of photons between or off the external fermions, are separated in a gauge-invariant way, following the procedure outlined in Section 5.2.2. At NLO the weak corrections, thus, comprise all remaining virtual one-loop diagrams with W/Z- or Higgs-boson exchange or closed fermion-loop corrections. The weak corrections do not involve any real radiation effects, nor IR divergences.

In detail, we consider the partonic processes $q(p_1)\bar{q}(p_2) \rightarrow l^-(k_1)l^+(k_2)$ with massless quarks q and leptons l , the momenta of which are indicated in parentheses. The corresponding LO diagrams and the generic one-loop diagrams are shown in Fig. 9. The LO matrix elements can be written in the generic way

$$\mathcal{M}_{q\bar{q}}^{\text{LO},\sigma\tau} = -\frac{e^2}{\hat{s}} \sum_{V=A,Z} g_{qV}^\sigma g_{lV}^\tau \chi_V(\hat{s}) \mathcal{A}^{\sigma\tau} = f_{q\bar{q}}^{\text{LO},\sigma\tau} \mathcal{A}^{\sigma\tau}, \quad (554)$$

where $\sigma = \pm$ and $\tau = \pm$ denote the chiralities on the quark and lepton lines, respectively, and g_{fV}^σ are the chiral couplings of the fermions f to the vector bosons V ,

$$g_{ffA}^\pm = -Q_f, \quad g_{ffZ}^+ = -\frac{s_w}{c_w} Q_f, \quad g_{ffZ}^- = \frac{I_{w,f}^3 - s_w^2 Q_f}{s_w c_w}. \quad (555)$$

The quantities

$$\mathcal{A}^{\sigma\tau} = [\bar{v}_q(p_2) \gamma^\mu \omega_\sigma u_q(p_1)] [\bar{u}_l(k_1) \gamma_\mu \omega_\tau v_l(k_2)], \quad (556)$$

are *standard matrix elements* (with an obvious notation for Dirac spinors $u_{q,l}, v_{q,l}$) containing the spin information of the fermions, which are functions of the usual Mandelstam variables

$$\hat{s} = (p_1 + p_2)^2, \quad \hat{t} = (p_1 - k_1)^2, \quad \hat{u} = (p_1 - k_2)^2. \quad (557)$$

The functions

$$\chi_A(\hat{s}) = 1, \quad \chi_Z(\hat{s}) = \frac{\hat{s}}{\hat{s} - \mu_Z^2}, \quad (558)$$

describe the propagation of V and contain the Z -boson resonance, which is regularized by writing the complex mass μ_Z instead of the real mass M_Z .

The NLO weak corrections receive contributions from self-energy, vertex, and (irreducible) box corrections, which are generically illustrated in Fig. 9. The weak correction factor $f_{q\bar{q},\text{weak}}^{\text{virt},\sigma\tau}$ in the weak one-loop matrix element

$$\mathcal{M}_{q\bar{q}}^{\text{weak},\sigma\tau} = f_{q\bar{q},\text{weak}}^{\text{virt},\sigma\tau} \mathcal{A}^{\sigma\tau}, \quad f_{q\bar{q},\text{weak}}^{\text{virt},\sigma\tau} = f_{q\bar{q},\text{weak}}^{\text{self},\sigma\tau}(\hat{s}) + f_{q\bar{q},\text{weak}}^{\text{vert},\sigma\tau}(\hat{s}) + f_{q\bar{q},\text{weak}}^{\text{box},\sigma\tau}(\hat{s}, \hat{t}), \quad (559)$$

is decomposed into respective contributions accordingly. The self-energy and vertex correction factors contain resonant contributions, but depend only on \hat{s} ; the box contribution depends both on \hat{s} and \hat{t} , but does not contain resonant parts. This means that only the former need modifications for the resonance treatment in the pole scheme. For the vertex corrections this procedure is very simple. The contributions involving Z -boson exchange, $f_{q\bar{q}}^{\text{vert},Z,\sigma\tau}$, are modified as follows,

$$\begin{aligned} f_{q\bar{q},\text{weak}}^{\text{vert},Z,\sigma\tau}(\hat{s}) &= -e^2 \frac{g_{qqZ}^\sigma g_{llZ}^\tau}{\hat{s} - M_Z^2} \left[F_{R,qqZ,\text{weak}}^\sigma(\hat{s}) + F_{R,llZ,\text{weak}}^\tau(\hat{s}) \right] \\ &\rightarrow -e^2 g_{qqZ}^\sigma g_{llZ}^\tau \left[\frac{F_{R,qqZ,\text{weak}}^\sigma(M_Z^2) + F_{R,llZ,\text{weak}}^\tau(M_Z^2)}{\hat{s} - \mu_Z^2} \right. \\ &\quad \left. + \frac{F_{R,qqZ,\text{weak}}^\sigma(\hat{s}) - F_{R,qqZ,\text{weak}}^\sigma(M_Z^2) + F_{R,llZ,\text{weak}}^\tau(\hat{s}) - F_{R,llZ,\text{weak}}^\tau(M_Z^2)}{\hat{s} - M_Z^2} \right], \end{aligned} \quad (560)$$

while the non-resonant contributions involving photon exchange are kept unchanged. Off resonance the introduction of the finite Z -decay width Γ_Z in the denominator of the vertex corrections changes the amplitude only in $\mathcal{O}(\alpha^2)$ relative to LO, i.e. the effect is beyond NLO. The explicit form of the renormalized one-loop vertex form factors $F_{R,ffV,\text{weak}}^\sigma$ can be found in Ref. [422]. The treatment of the self-energy corrections is somewhat more involved, since it involves more propagator factors $(\hat{s} - M_Z^2)^{-1}$ and care has to be taken that no double-counting is introduced in the modification of the sum of LO and NLO matrix elements,

$$\begin{aligned} f_{q\bar{q}}^{\text{LO},\sigma\tau} + f_{q\bar{q},\text{weak}}^{\text{self},\sigma\tau} &= -e^2 \left\{ \frac{Q_q Q_l}{\hat{s}} \left[1 - \frac{\Sigma_{R,T}^{AA}(\hat{s})}{\hat{s}} \right] + \frac{g_{qqZ}^\sigma g_{llZ}^\tau}{\hat{s} - M_Z^2} \left[1 - \frac{\Sigma_{R,T}^{ZZ}(\hat{s})}{\hat{s} - M_Z^2} \right] + \frac{Q_l g_{qqZ}^\sigma + Q_q g_{llZ}^\tau \Sigma_{R,T}^{AZ}(\hat{s})}{\hat{s}} \frac{\Sigma_{R,T}^{AZ}(\hat{s})}{\hat{s} - M_Z^2} \right\} \\ &= -e^2 \left\{ \frac{Q_q Q_l}{\hat{s}} \left[1 - \frac{\Sigma_{R,T}^{AA}(\hat{s})}{\hat{s}} \right] + \frac{g_{qqZ}^\sigma g_{llZ}^\tau}{\hat{s} - M_Z^2} \left[1 - \frac{\Sigma_{R,T}^{ZZ}(M_Z^2)}{\hat{s} - M_Z^2} \right. \right. \\ &\quad \left. \left. - \Sigma_{R,T}^{\prime ZZ}(M_Z^2) - \frac{\Sigma_{R,T}^{ZZ}(\hat{s}) - \Sigma_{R,T}^{ZZ}(M_Z^2) - (\hat{s} - M_Z^2) \Sigma_{R,T}^{\prime ZZ}(M_Z^2)}{\hat{s} - M_Z^2} \right] \right. \\ &\quad \left. + \frac{Q_l g_{qqZ}^\sigma + Q_q g_{llZ}^\tau}{\hat{s}} \left[\frac{\Sigma_{R,T}^{AZ}(M_Z^2)}{\hat{s} - M_Z^2} + \frac{\Sigma_{R,T}^{AZ}(\hat{s}) - \Sigma_{R,T}^{AZ}(M_Z^2)}{\hat{s} - M_Z^2} \right] \right\} \\ &\rightarrow -e^2 \left\{ \frac{Q_q Q_l}{\hat{s}} \left[1 - \frac{\Sigma_{R,T}^{AA}(\hat{s})}{\hat{s}} \right] + g_{qqZ}^\sigma g_{llZ}^\tau \left[\frac{1 - \Sigma_{R,T}^{\prime ZZ}(M_Z^2)}{\hat{s} - \mu_Z^2} \right. \right. \\ &\quad \left. \left. - \frac{\Sigma_{R,T}^{ZZ}(\hat{s}) - \Sigma_{R,T}^{ZZ}(M_Z^2) - (\hat{s} - M_Z^2) \Sigma_{R,T}^{\prime ZZ}(M_Z^2)}{(\hat{s} - M_Z^2)^2} \right] \right\} \end{aligned}$$

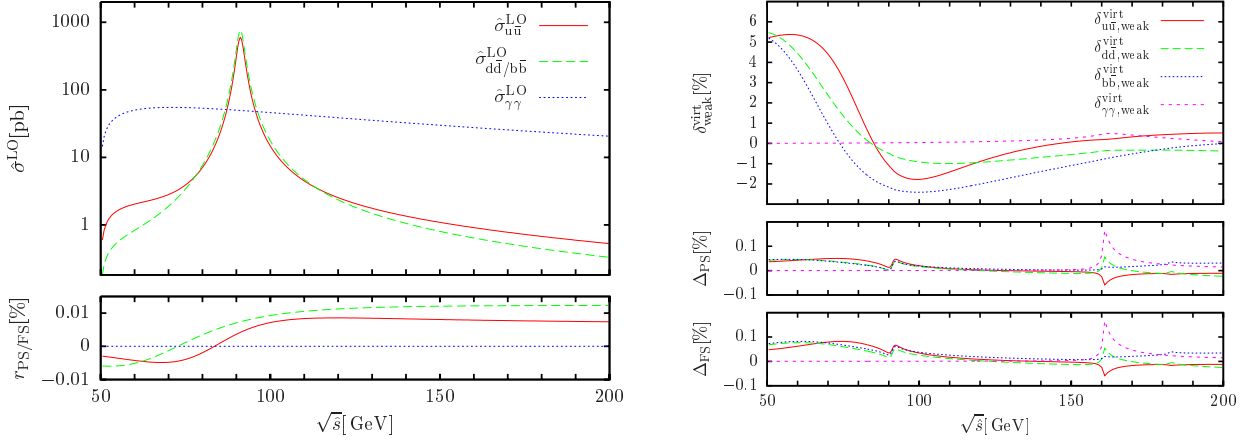


Figure 10: LO cross sections $\hat{\sigma}^{\text{LO}}$ (top left) for the partonic processes $q\bar{q}/\gamma\gamma \rightarrow l^- l^+$ as function of the partonic CM energy \sqrt{s} and corresponding weak corrections $\delta_{\text{weak}}^{\text{virt}}$ (top right), indicating the partonic channels as subscripts. The lower panels show the relative deviations $\tau_X = \hat{\sigma}^{\text{LO}}|_X / \hat{\sigma}^{\text{LO}}|_{\text{CMS}} - 1$ of the LO cross sections and the differences $\Delta_X = \delta_{\text{weak}}^{\text{virt}}|_X - \delta_{\text{weak}}^{\text{virt}}|_{\text{CMS}}$ between scheme X and the CMS for treating the Z resonance, where PS stands for pole scheme and FS for factorization scheme. (Plots taken from Ref. [422].)

$$+ \left(Q_l g_{qqZ}^\sigma + Q_q g_{llZ}^\tau \right) \left[\frac{1}{\hat{s} - \mu_Z^2} \frac{\Sigma_{\text{R,T}}^{AZ}(M_Z^2)}{M_Z^2} + \frac{1}{\hat{s} - M_Z^2} \left(\frac{\Sigma_{\text{R,T}}^{AZ}(\hat{s})}{\hat{s}} - \frac{\Sigma_{\text{R,T}}^{AZ}(M_Z^2)}{M_Z^2} \right) \right] \right\}. \quad (561)$$

Here we have used the fact that in the OS renormalization scheme the renormalized Z-boson self-energy fulfills $\text{Re } \Sigma_{\text{R,T}}^{ZZ}(M_Z^2) = 0$ and that the resummed terms account for some imaginary parts via the optical theorem (535), $\text{Im } \Sigma_{\text{R,T}}^{ZZ}(M_Z^2) = M_Z \Gamma_Z$, which holds in $\mathcal{O}(\alpha)$.

Figure 10 shows some numerical results of Ref. [422] on the application of the pole scheme to the LO and NLO contributions to the partonic scattering channels of the Drell–Yan process in the broad neighbourhood of the Z-boson resonance. The pole scheme (PS) results are compared to two further schemes that were applied to uniformly describe the resonance processes in resonant and non-resonant phase-space regions: the CMS described in Section 6.6 and a *factorization scheme (FS)* briefly sketched in Section 6.7. The central result from this comparison is the excellent level of agreement between NLO results from the various schemes, leaving uncertainties from the resonance treatment that are well below the impact of missing corrections beyond the NLO level.

6.5.3. Pole approximation

A *pole approximation (PA)*—in contrast to a full pole-scheme calculation—results from a resonant amplitude defined in the pole scheme upon neglecting non-resonant parts. The general concept as well as specific applications have been introduced and described by several authors in different contexts (see, e.g., Refs. [56, 57, 195, 606–611]). Typically, the PA is applied to higher-order corrections where full off-shell calculations are too difficult to carry out or not needed in view of the aimed precision tag. In this context, we recall the interplay between different perturbative orders on and off resonance: To achieve NLO precision in the resonance region of a cross section, both off-shell and finite-width effects have to be included at least in LO along with the NLO corrections on resonance, and likewise in higher orders. In the following, we describe the structure of NLO calculations in PA, which are combined with complete LO calculations including off-shell effects. Such predictions deliver NLO accuracy only in the neighbourhood of resonances, but only LO precision in off-shell tails. The corresponding inclusive cross sections integrated over the resonances, however, possess NLO accuracy. Let us make this counting more quantitative for the case of the resonant production of a weakly decaying particle P , such as a W or a Z boson. In this case, LO off-shell effects are of $\mathcal{O}(\Gamma_P/M_P) \sim \mathcal{O}(\alpha)$ relative to the leading resonant contribution and, thus, of the same generic order as NLO EW corrections on resonance. In PA at NLO, the largest missing EW contributions are the off-shell NLO EW effects which are of the typical size $\alpha/(\pi s_w^2) \times \Gamma_P/M_P$ times some possible enhancement factor. Taking the latter at most to ~ 10 , still offers an uncertainty estimate of $\lesssim 0.5\%$ for observables that are dominated by resonant

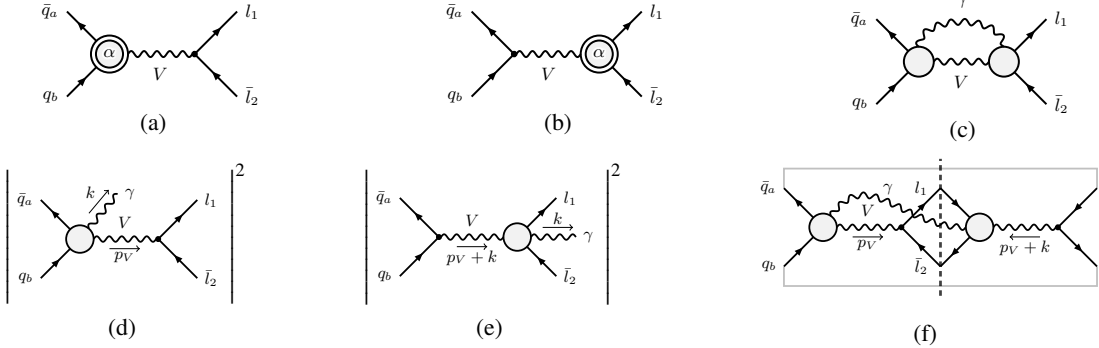


Figure 11: Generic diagrams for NLO EW corrections in PA for the resonance process $\bar{q}_a q_b \rightarrow V \rightarrow l_1 \bar{l}_2$, with q and l denoting generic quarks and leptons: (a/b) virtual factorizable corrections to production/decay, (c) virtual non-factorizable corrections, (d/e) real factorizable corrections to production/decay, and (f) real non-factorizable corrections. The “squared diagrams” (d) and (e) and the “interference diagram” (f) are direct contributions to the squared amplitude $|\mathcal{M}|^2$. The empty blobs stand for all relevant tree structures, the ones with “ α ” for one-loop corrections of $\mathcal{O}(\alpha)$. (Adapted from Ref. [611].)

contributions, which is good enough for most phenomenological purposes for a wide class of processes. We will further elaborate on the applicability, reliability, and limitations of such NLO calculations in PA below.

In the simple generic form (552) of a resonance amplitude, the PA is defined by taking only the resonant part $\tilde{R}(\mu_P^2)/(p^2 - \mu_P^2)$ into account. However, as mentioned already above, whenever the resonance is involved in (virtual or real) photon or gluon exchange, or if the resonance is “bridged over” by a photon or a gluon, this form is oversimplified. In those cases, the resonance singularity is a branch point rather than a pole, and resonant terms in addition to the ones proportional to $\tilde{R}(\mu_P^2)$ arise. More precisely, the $\tilde{R}(\mu_P^2)$ terms define the so-called *factorizable corrections*, which include all resonant contributions that can be written as a product of production and decay matrix elements with the intermediate particle P set on shell multiplied with the off-shell propagator $(p^2 - \mu_P^2)^{-1}$. The remaining resonant contributions define the so-called *non-factorizable corrections*, where the non-factorizability refers to the resonance structure which deviates from the $(p^2 - \mu_P^2)^{-1}$ factor. The various types of corrections appearing in an NLO calculation in PA for a generic $2 \rightarrow 2$ -particle process with a vector resonance V are illustrated in Fig. 11. We describe the characteristic features of factorizable and non-factorizable corrections in the following.

The calculation of factorizable corrections can be done widely independent for the production and decay subprocesses for specific resonance patterns. Some care has to be taken in the following points:

- To properly take into account spin correlations between different subprocesses, the same polarization basis has to be taken both in production and decay of each resonance.
- The evaluation of the subamplitudes in the factorizable corrections requires kinematical variables or momenta that consistently respect the on-shellness of the resonance, in order to be theoretically consistent (gauge independence, etc.). On the other hand, the factorizable contributions should be evaluated on the original off-shell phase space. This problem is solved by introducing an *on-shell projection* of off-shell momenta, which deforms external momenta in such a way that the intermediate resonant particle P becomes on shell. In the vicinity of the resonance, momenta are only changed by terms of $\mathcal{O}(\Gamma_P/M_P)$ relative to their original momenta, i.e. NLO corrections of $\mathcal{O}(\alpha)$ are formally changed at the NNLO level, so that NLO precision in the resonance region is maintained. Comparing results obtained with different OS projections, can, thus, help to assess theoretical uncertainties in NLO predictions in PA.
- The factorizable corrections have the usual IR structure of OS production and decay of the resonating particles. Note that this IR structure in general is not the same as for the full off-shell amplitude, because additional IR divergences connected with a resonating charged particle are introduced by setting its momentum on shell.

By definition, the non-factorizable corrections are the resonant remnants of the difference between the full off-shell amplitude and its factorizable parts, which result from going on shell with the kinematics of the resonating particle(s) in the production and decay subamplitudes. This difference can be inspected graph by graph:

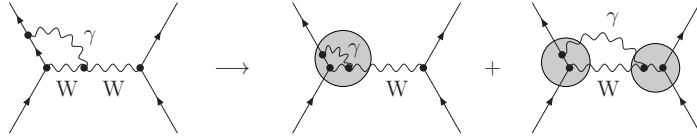


Figure 12: An example for the splitting of a diagram with photon exchange of a resonance (left) into factorizable (middle) and non-factorizable (right) contributions.

- Loop diagrams with explicit resonance factors $(p^2 - \mu_P^2)^{-1}$ originating from tree-like resonance propagators obviously contribute to the factorizable corrections. They also contribute to the non-factorizable corrections only if the process of setting the resonance momentum on shell in a subamplitude leads to an IR divergence (cf. Refs. [195, 608]). This only happens in the case where a photon or gluon of a loop is attached to the resonance. In those cases, the non-factorizable contribution entirely stems from soft photon or gluon exchange with the resonance(s). Formally the diagrams that contain both factorizable and non-factorizable parts can be split into the respective contributions via the partial fractioning given in Eq. (553). This is illustrated in Fig. 12, where photon exchange between an initial-state fermion and a charged resonance ($V = W$) leads to factorizable and non-factorizable contributions which contribute to the corrections of types (a) and (c) in Fig. 11, respectively.
- Loop diagrams with no tree-like resonance line, or more generally with less tree-like resonance lines than the leading resonance pattern, obviously do not possess factorizable parts, but still might deliver non-factorizable resonant contributions. Loop integrals can only deliver resonance enhancements if the loop contains a propagator of the potentially resonating particle and if the loop momentum corresponding to the resonance at the same time leads to an IR divergence. This is exactly the case if a soft photon or gluon bridges over the resonance (or over several resonances), i.e. the corresponding diagrams lead only to contributions of type (c) of Fig. 11.
- Real non-factorizable corrections are classified and constructed accordingly, but instead of considering graphs with photon exchange contributing to the amplitude \mathcal{M} , interference contributions of the type $\mathcal{M}_{\gamma,1}\mathcal{M}_{\gamma,2}^*$ have to be considered, where $\mathcal{M}_{\gamma,1}$ and $\mathcal{M}_{\gamma,2}$ are contributions to the amplitude \mathcal{M}_γ resulting from \mathcal{M} by adding an extra photon emission. Interference diagrams in which the photon in $\mathcal{M}_{\gamma,1}$ and $\mathcal{M}_{\gamma,2}$ is emitted from one and the same subprocess (production or decay) obviously lead to factorizable corrections to the corresponding subprocess; those contributions are of type (d) or (e) of Fig. 11. But diagrams with one of the photons coupling to the resonance and the other to an external leg or to a resonance lead to non-factorizable contributions as well. Again, this is due to the fact that the process of going on shell with the kinematics of the resonance in subamplitudes leads to new IR divergences in the factorizable contributions. Finally, photon exchange between different production or decay subprocesses entirely contributes to non-factorizable corrections. The generic structure of non-factorizable corrections is sketched in Fig. 11(f).

Since the non-factorizable corrections are due to the exchange or emission of soft massless particles, they can be evaluated using modified eikonal currents [cf. Eq. (257) for their original form] applied to LO matrix elements [608, 612]. Ordinary eikonal currents describe only the coupling of soft photons or gluons to external OS states. The modification necessary for the calculation of non-factorizable corrections concerns the inclusion of the couplings to the internal resonance lines and the corresponding momentum flow. To this end, for a single resonance P the eikonal current J_{eik}^μ for the full process is decomposed into currents for the production and decay subprocesses of P according to

$$J_{\text{eik}}^\mu = J_{\text{eik,prod},P}^\mu + J_{\text{eik,dec},P}^\mu, \quad (562)$$

where the radiation off P contributes to $J_{\text{eik,prod},P}^\mu$ and $J_{\text{eik,dec},P}^\mu$. The two contributions result from splitting all diagrams with photon radiation off P via partial fractioning the product of the two P propagators before and after the resonance, as shown in Eq. (305). Note that the two contributions involve different P momenta in the P propagators. If p is the P momentum after photon emission off P , $J_{\text{eik,prod},P}^\mu$ involves a P propagator with momentum p and $J_{\text{eik,dec},P}^\mu$ one with momentum $p + k$. The current $J_{\text{eik,prod},P}^\mu$ is, thus, constructed from all charged external states of the production process as described in Eq. (257), including the resonance if it is charged. The current $J_{\text{eik,dec},P}^\mu$ is constructed analogously, but receives an additional global factor $(p^2 - M_P^2)/[(p + k)^2 - M_P^2]$ accounting for the momentum shift in the resonance when the photon is radiated after the resonance has formed. In spite of the modified eikonal factors, the factorization

property of soft-photon corrections remains, so that non-factorizable corrections take the form of a differential, but universal correction factors to LO cross sections, which depend only on the resonance pattern and the external states of the process. On the side of the virtual corrections, the loop integration leads to a non-factorizable correction factor to the LO cross section. On the side of the real corrections, however, the non-factorizable corrections depend on details of the event selection, i.e. whether or how “semi-soft” photons or gluons with energies of the size of the width(s) of the resonance(s) are recombined into jets or dressed leptons.

In spite of the restriction of its validity to resonance regions, the PA has several virtues:

- In comparison to the application of the full pole scheme including the calculation of non-resonant contributions, the PA is conceptually much simpler to apply. Non-resonant diagrams can be omitted from the beginning, reducing the number of graphs drastically.
- Issues with artificially created IR singularities, which were mentioned for the pole scheme, are conceptually solved by the systematic extraction and evaluation of non-factorizable corrections. By definition, the combination of the non-factorizable and factorizable corrections reproduces the IR structure of the full process in the neighbourhood of the resonances. Owing to the universal structure of the non-factorizable corrections widely generic results for those exist in the literature [554, 606–608, 612, 613].
- The PA, similar to the pole scheme, decomposes amplitudes into production and decay subprocesses and non-factorizable contributions. As explained, the latter factorize from the underlying LO cross sections. Predictions in PA, thus, are ideal as basis for *improved Born approximations* to parametrize cross sections near resonances in terms of appropriate pseudo-observables, such as mass, width, and effective couplings of the resonating particle. Moreover, matrix elements in PA can be used to define cross sections for polarized unstable particle production [614, 615].
- Finally, calculations in PA can be pushed to higher orders much more easily than full off-shell calculations. Since off-shell contributions of higher orders are further suppressed with respect to the dominating resonant contribution, including higher-order corrections in PA often is a reasonable first step towards higher-order predictions.

Pole approximations for processes with one or two resonances were worked out by several groups for many processes. In the following we pick two prominent examples from EW gauge-boson production where both results in PA and with full off-shell effects are available.

6.5.4. NLO EW corrections to Drell–Yan-like Z-boson production in the pole approximation

Technically, the application of the PA to single-resonance processes is rather simple. As an example, we consider again the neutral-current Drell–Yan process of Z-boson production at the LHC following closely Ref. [611], making use of the basic definitions given in Section 6.5.2, where we have described the calculation of the purely weak corrections in the pole scheme. Here, we take into account the full NLO EW corrections, which consist of both weak virtual contributions and photonic virtual and real contributions.

The structure of the matrix element $\mathcal{M}_{q\bar{q},\text{fact}}^{\text{EW},\sigma\tau}$ of the factorizable virtual EW corrections can be obtained from Eq. (559) by replacing the weak one-loop contributions with the full EW one-loop contributions and performing the OS limit $\hat{s} \rightarrow M_Z^2$ in the vertex form factors $F_{R,fZ,\text{EW}}^\sigma(\hat{s})$ and the bosonic self-energies $\Sigma_{R,T}^{AZ}(\hat{s})$ and $\Sigma_{R,T}^{ZZ}(\hat{s})$. The irreducible box contributions do not exhibit an explicit resonance factor $(\hat{s} - \mu_Z^2)^{-1}$ from a tree-like resonance propagator and do not contribute to the factorizable corrections, which read

$$\begin{aligned} \mathcal{M}_{q\bar{q},\text{fact}}^{\text{EW},\sigma\tau} &= f_{q\bar{q},\text{EW,fact}}^{\text{virt},\sigma\tau} \mathcal{A}^{\sigma\tau}, \\ f_{q\bar{q},\text{EW,fact}}^{\text{virt},\sigma\tau} &= -e^2 g_{qqZ}^\sigma g_{llZ}^\tau \frac{F_{R,qqZ,\text{EW}}^\sigma(M_Z^2) + F_{R,llZ,\text{EW}}^\tau(M_Z^2)}{\hat{s} - \mu_Z^2} \\ &\quad + e^2 g_{qqZ}^\sigma g_{llZ}^\tau \frac{\Sigma_{R,T}^{ZZ}(M_Z^2)}{\hat{s} - \mu_Z^2} - e^2 (Q_l g_{qqZ}^\sigma + Q_q g_{llZ}^\tau) \frac{\Sigma_{R,T}^{AZ}(M_Z^2)}{(\hat{s} - \mu_Z^2) M_Z^2}. \end{aligned} \quad (563)$$

Note that the self-energy contributions in the last line vanish in the complete OS renormalization scheme, underlining the simplicity of the PA. The standard matrix elements $\mathcal{A}^{\sigma\tau}$ can still be evaluated on the off-shell phase space, where $\hat{s} = -\hat{t} - \hat{u} \neq M_Z^2$ off resonance, or alternatively with the OS-projected kinematics, where $\hat{s} = -\hat{t} - \hat{u} = M_Z^2$. In the latter case, the OS limit $\hat{s} \rightarrow M_Z^2$ is taken while keeping the scattering angle in the partonic CM frame fixed.

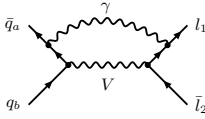


Figure 13: Example for a manifestly non-factorizable box diagram for Drell–Yan-like W- or Z-boson production.

Since the Z boson is electrically neutral, there are no one-loop graphs with photons coupling to the resonance, so that there are no graphs that contribute to both factorizable and non-factorizable corrections. The non-factorizable corrections entirely result from box diagrams with photon and Z-boson exchange between initial and final states (cf. Fig. 13) and take the simple form

$$\mathcal{M}_{q\bar{q},\text{nf}}^{\text{EW},\sigma\tau} = \delta_{\text{nf}}^{q\bar{q}} \mathcal{M}_{q\bar{q},\text{PA}}^{\text{LO},\sigma\tau}, \quad \delta_{\text{nf}}^{q\bar{q}} = \frac{\alpha}{\pi} Q_q Q_l \left\{ \left[\Delta - 2 \ln \left(\frac{\mu_Z^2 - \hat{s}}{\mu M_Z} \right) \right] \ln \left(\frac{\hat{t}}{\hat{u}} \right) + \text{Li}_2 \left(1 + \frac{M_Z^2}{\hat{t}} \right) - \text{Li}_2 \left(1 + \frac{M_Z^2}{\hat{u}} \right) \right\}, \quad (564)$$

where the subscript PA in $\mathcal{M}_{q\bar{q},\text{PA}}^{\text{LO},\sigma\tau}$ indicates that the non-resonant photon contribution is not included here. In $\delta_{\text{nf}}^{q\bar{q}}$, the divergent contribution Δ , defined in Eq. (169), originates from the soft IR divergence in DR. Note that this IR singularity comes along with the non-analytic contribution proportional to $\ln(\mu_Z^2 - \hat{s})$, which shows that $\hat{s} = \mu_Z^2$ is a branch point in the complex \hat{s} plane. As explained above, by construction the sum of factorizable and non-factorizable corrections has the same IR structure as the full off-shell EW one-loop amplitude.

For a full NLO prediction in PA, we still have to add the real-photonic corrections, which can either be based on the full LO prediction for $q\bar{q} \rightarrow l\bar{l}\gamma$ or on a corresponding result in PA. Figure 14 shows the comparison [611] of the NLO EW corrections for Z production based on the PA for virtual and real corrections with full off-shell results based on the CMS, described in Section 6.6. The distribution in the dilepton invariant mass M_{ll} shows the resonance near $M_{ll} \sim M_Z$, but the distribution in the lepton transverse momentum $p_{T,l}$ is dominated by resonant contributions for the whole range of $p_{T,l} \lesssim M_Z/2$. The results clearly show that the difference in the relative EW correction between full off-shell result and PA is only some 0.1% whenever the resonance dominates the distribution. In more detail, the plots also show the individual contributions to the PA from (real+virtual) factorizable corrections to production (“fact,ini”) and decay (“fact,fin”) of the Z boson and from the (real+virtual) non-factorizable corrections (“non-fact”), which turn out to be negligibly small.

More results and further details on the NLO EW corrections in PA, including the corresponding charged-current process of W-boson production, can be found in Ref. [611]. Moreover, the generalization of the concept of the PA to NNLO QCD×EW corrections of $\mathcal{O}(\alpha_s \alpha)$ as well as the calculation of the non-factorizable corrections at this order are given there. The factorizable $\mathcal{O}(\alpha_s \alpha)$ corrections can be further decomposed into pure production or decay contributions and cross-talk between production and decay. The latter are dominant and discussed in Ref. [616], while the pure decay corrections are negligibly small [616]. The pure production corrections are only known to NNLO QCD×QED yet [617, 618].

6.5.5. Multiple resonances in pole approximation and gauge-boson pair production in double-pole approximation

The PA concept can be applied to any resonance structure, as long as resonances are kinematically well separated.⁴² The factorizable corrections are calculated as for single-resonance processes. Merely the OS projection of the kinematics becomes somewhat more complicated. As indicated already above, the calculation of the non-factorizable corrections, however, is more involved in the case of multiple resonances. For the class of processes with several “parallel resonances” (i.e. cascade decays are not included), generic results on virtual one-loop EW non-factorizable corrections were given in Refs. [548, 612]. These results were obtained by generalizing the corresponding corrections to EW gauge-boson pair production processes first derived for W-pair production [606–608, 613]. In the following, we briefly review some features of W-pair production in e^+e^- annihilation in *double-pole approximation (DPA)*, which was worked out for cross-section predictions for LEP2 in different variants by various groups [195, 610, 619–623] (see also Ref. [46]). Finally, we show a comparison of the DPA with results from the full off-shell calculation for $e^+e^- \rightarrow 4 \text{ fermions}$ [59, 196].

⁴²The necessary separation is, for instance, not given in processes with cascade decays such as $ab \rightarrow P_1 + X_1 \rightarrow P_2 + X_2 + X_1 \rightarrow X_3 + X_2 + X_1$, where the mass gap $M_{P_1} - M_{P_2}$ between the two resonances P_1 and P_2 is not large w.r.t. the widths Γ_{P_1} and Γ_{P_2} .

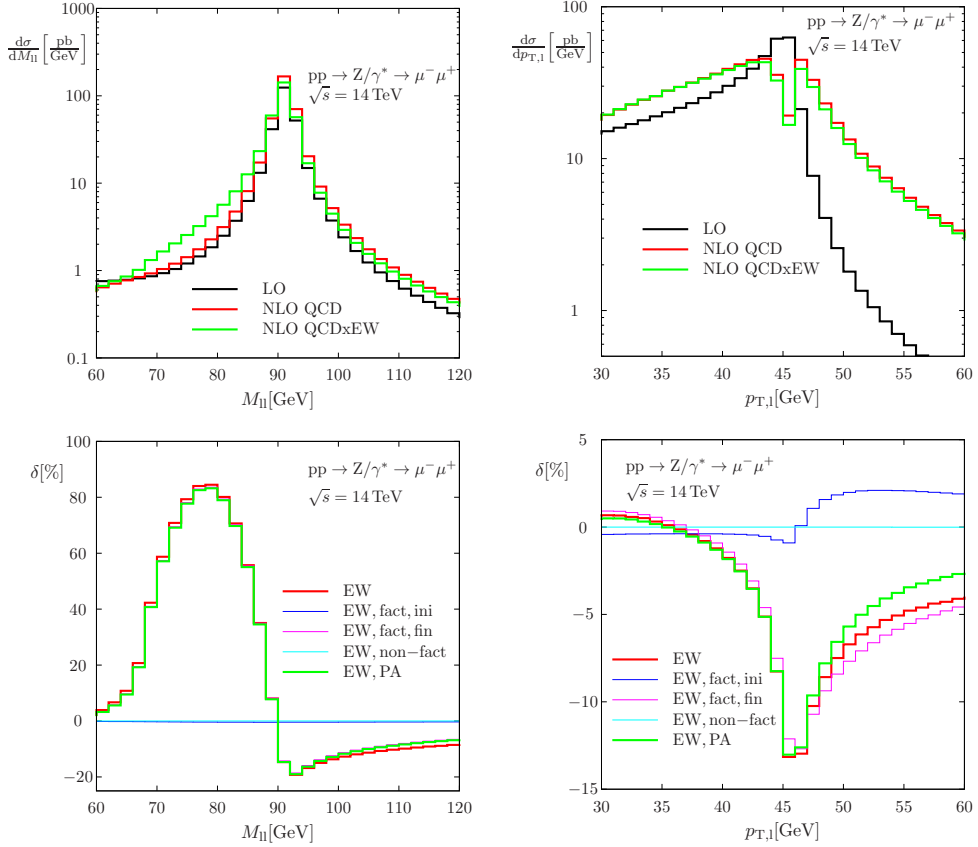


Figure 14: LO and NLO distributions in the invariant dilepton-mass M_{ll} and in the transverse-lepton-momentum $p_{T,l}$ for Drell–Yan-like Z production $pp \rightarrow Z/\gamma^* \rightarrow \mu^-\mu^+ + X$ at the LHC (upper panels) and corresponding relative EW corrections (lower panels), where the corrections both show the full NLO EW results as well as the individual contributions (and their sum) in pole approximation (PA). (Plots taken from Ref. [611].)

Figure 15 shows the LO *signal diagrams* containing the double-pole structure as well as a typical *background diagram* with only one W resonance, which are all needed to describe W-pair production near the resonances at NLO accuracy. Recall that the DPA is only applied to NLO corrections, since its application at LO would introduce errors of the order of $\mathcal{O}(\Gamma_P/M_P) \sim \mathcal{O}(\alpha)$. The generic diagram for the virtual factorizable corrections of the DPA as well as a typical one-loop diagram beyond DPA are depicted in Fig. 16. Finally, Figure 17 illustrates the types of diagrams contributing to the non-factorizable corrections in the DPA, where the diagrams in the first line deliver both factorizable and non-factorizable parts, while the diagrams in the second line exclusively contribute to the non-factorizable corrections.

NLO calculations in DPA can be set up in different ways as far as the application of the DPA to virtual and/or real corrections is concerned:

- If both virtual and real corrections are treated in DPA, it is possible to separately discuss factorizable and non-factorizable corrections, which are gauge independent each. Both types receive IR-divergent virtual and real contributions, but the two sums of virtual and real parts are each IR finite. A numerical evaluation of the non-factorizable corrections alone, as presented in Refs. [608, 613], reveals that those are very small and phenomenologically unimportant.⁴³ This observation is in line with the known property that the sum of virtual and real non-factorizable corrections cancels in observables that are inclusive with respect to the resonance [609, 625, 626], i.e. if the invariant mass of the resonating particle is fully integrated over the resonance region.

⁴³This was also observed for Z-pair production at LEP2 [624].

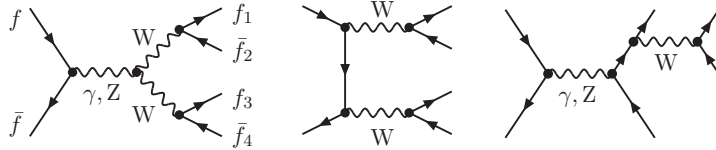


Figure 15: Doubly-resonant *signal diagrams* (left and middle) as well as an example for a singly-resonant *background diagram* (right) for the charged-current 4-fermion production process $f\bar{f} \rightarrow WW \rightarrow 4\text{ fermions}$.

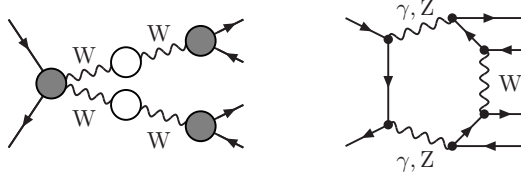


Figure 16: Structural diagram for the virtual factorizable corrections of the DPA (left) as well as an example for an irreducible diagram type which is not included in the DPA (right) for $f\bar{f} \rightarrow WW \rightarrow 4\text{ fermions}$.

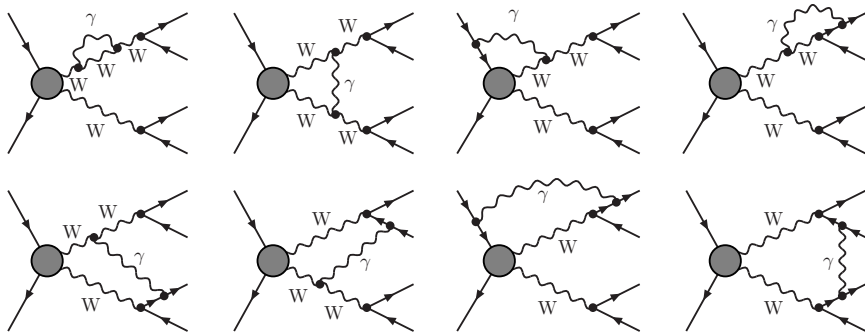


Figure 17: A representative set of diagrams for the virtual non-factorizable corrections to the process $f\bar{f} \rightarrow WW \rightarrow 4\text{ fermions}$, where the grey blobs stand for any tree-like structures.

- An alternative “hybrid version” of the DPA was implemented in the Monte Carlo generator **RacoonWW** [195, 621, 622] for $e^+e^- \rightarrow WW \rightarrow 4\text{ fermions}$, which applies the DPA only to the virtual corrections, but employs complete LO matrix elements for $e^+e^- \rightarrow 4f + \gamma$ in the real radiation part. In this way, it was possible to check that the splitting of real radiation off resonating W bosons into production and decay contributions, as formally done via the partial fractioning (553) for real photons, does not introduce additional uncertainties if the two W resonances overlap (i.e. if the photon energy $k^0 \sim \Gamma_W$).

A detailed comparison [46] between the various results in DPA [195, 610, 619–623] as well as several uncertainty estimates within the different approaches confirmed the validity of the DPA within a precision margin of $\lesssim 0.5\%$ for W-pair production in the energy range $170\text{ GeV} \lesssim \sqrt{s} \lesssim 300\text{ GeV}$, which in particular covers the energy range of LEP2 where W-pair production was accessible within good precision. Note that the DPA necessarily breaks down near the threshold energy $\sqrt{s} = 2M_W$, because at least one of the two W bosons is shifted out of resonance below threshold. For $\sqrt{s} \lesssim 2M_W + n\Gamma_W$ with $n \sim 2\text{--}3$ the calculation of the W-pair cross section is based on an *improved Born approximation (IBA)* [627, 628], which includes only universal corrections such as leading-logarithmic initial-state radiation, running-coupling effects, and the Coulomb singularity.

Finally, the reliability of the DPA for W-pair production was ultimately checked after the completion of the full NLO EW corrections to the charged-current processes $e^+e^- \rightarrow 4f$ [59, 196] in the CMS, which is described in Section 6.6. Figure 18 shows a comparison of predictions for the inclusive W-pair production cross section for CM energies ranging from the LEP2 energy range up to 2 TeV. The predictions include NLO EW corrections based on an IBA and the DPA of **RacoonWW** and the full off-shell calculation of Refs. [59, 196] as implemented in the extension **Racoon4F** of **RacoonWW**, as well as leading higher-order effects from initial-state radiation in all versions, as described in Section 4.5.2. In the LEP2 energy range, the IBA, the DPA, and the full off-shell calculations nicely

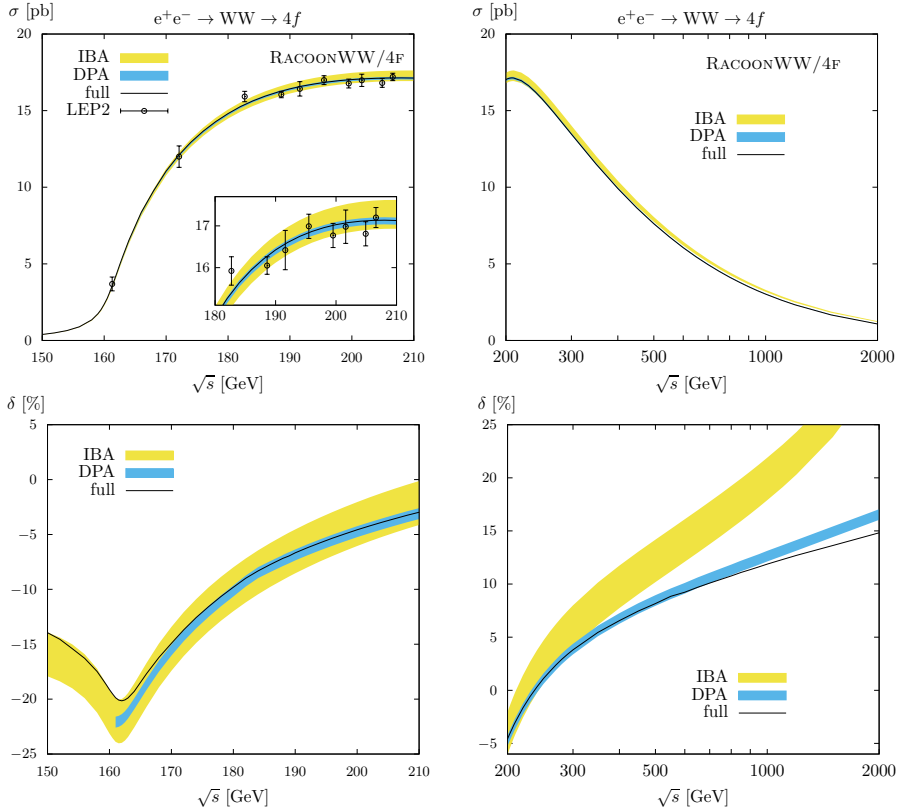


Figure 18: Inclusive W-pair production cross section in e^+e^- annihilation as provided by RacoonWW/4F, including NLO EW corrections in IBA, in DPA, and obtained from the “full” off-shell calculation in the CMS. All predictions include leading higher-order effects from initial-state radiation. The IBA and DPA bands illustrate the uncertainty bands of $\pm 2\%$ and $\pm 0.5\%$, as assessed for the LEP2 energy range. The cross-section measurements of LEP2 [60] are shown as data points. (Results taken from Refs. [59, 196].)

agree within the assessed error margins.⁴⁴ Note that a proper confrontation of LEP2 data [60], which are included in the plot, with theory predictions in fact required the inclusion of non-universal EW corrections, as provided by the DPA. For energies above the LEP2 energy range, the error assessments of $\pm 2\%$ and $\pm 0.5\%$ for IBA and DPA, respectively, start to fail. For $\sqrt{s} \gtrsim 300$ –400 GeV, the onset of the enhanced negative high-energy EW corrections from soft/collinear W/Z exchange (cf. Section 5.4) can be observed, an effect that is not accounted for by the IBA, but still by the DPA. Those corrections grow to $\sim -10\%$ and more in the TeV range for the total cross sections and are even larger in differential distributions. The difference of some percent between DPA and full off-shell result, on the other hand, is due to the increasing contribution of background diagrams, which are included in the DPA calculation only at LO (see last diagram in Fig. 15), but not at NLO (see second diagram in Fig. 16). More details and results from this comparison can be found in Refs. [59, 196].

Predictions for EW gauge-boson production in DPA were worked out for other channels and collider types as well, for instance for WW production at a $\gamma\gamma$ collider [629, 630] and WW [356] and WZ [631] production at the LHC. Complete NLO EW corrections with fully off-shell gauge bosons were presented for WW [332, 357], WZ [632], and ZZ [508, 633] production at the LHC.

Recently, the concept of the pole approximation was also applied to triple-W production at the LHC in Ref. [360], defining a *triple pole approximation (TPA)*. Similar to the findings for W-pair production, the TPA is able to reproduce the NLO corrections to the full off-shell $2 \rightarrow 6$ particle reaction with W-boson decays whenever the W resonances dominate the cross section, as shown in Ref. [360] for leptonically decaying W bosons.

⁴⁴Note that the central prediction of the IBA, as provided by RacoonWW, includes also some fitted terms to come closer to the DPA, which accounts for non-universal NLO EW corrections.

6.6. Complex-mass scheme

6.6.1. LO procedure and general properties

The *complex-mass scheme (CMS)* was introduced in Ref. [58] for LO calculations with W/Z resonances and generalized to NLO in Refs. [59, 634] for arbitrary SM particles.⁴⁵ In this approach the mass squared of each unstable particle P is consistently identified with the complex value μ_P^2 as defined in Eq. (539), not only in the P -propagators, but also in the couplings, which therefore become complex. In particular, couplings involve a complex weak mixing angle fixed via

$$c_w^2 = 1 - s_w^2 = \mu_W^2 / \mu_Z^2. \quad (565)$$

The CMS does not change the theory at all, but only rearranges its perturbative expansion, so that in particular no double counting of terms occurs. At LO, the above prescription already describes the full procedure. At NLO, the scheme requires some changes in the NLO machinery, since the imaginary parts in the complex masses correspond to higher-order contributions in the perturbative expansion in the formalism for stable particles. The necessary changes in the renormalization procedure are described below, otherwise the usual perturbative calculus with Feynman rules and counterterms works without modification. Generalizations beyond NLO have not yet been described in the literature, but should be straightforward.

LO and NLO calculations in the CMS have the following virtues:

- All relations following from gauge invariance are respected, because the gauge-boson masses are modified only by an analytic continuation. This concerns both the gauge independence in the parametrization of S -matrix elements in terms of renormalized input parameters and the validity of all Ward or Slavnov–Taylor identities of the related Green functions. This, in particular, implies that so-called unitarity cancellations within amplitudes remain intact, since those are a consequence of gauge invariance.
- NLO calculations deliver uniform predictions with NLO accuracy everywhere in phase space, i.e. both in resonant and non-resonant regions (if the widths of the unstable particles have NLO accuracy).
- Amplitudes involve spurious, i.e. artificially introduced, imaginary parts (in space-like propagators and complex couplings). As a consequence, amplitudes do not exactly obey the standard cutting relations [586] which express unitarity, because these relations involve complex conjugation. However, the spurious terms spoiling unitarity are unproblematic, since they are of (N)NLO in an (N)LO calculation, i.e. of higher order, without any unnatural amplification, because unitarity cancellations are respected. Modified cutting rules for the CMS were formulated, and the unitarity within this scheme investigated in Ref. [588].

6.6.2. Complex renormalization

Let us consider the modified renormalization procedure in detail in 't Hooft–Feynman gauge, following closely its original introduction presented in Ref. [59]. Further below we comment on the procedure in the framework of the background-field method. In the following, we assume a unit quark-mixing matrix.

We start by considering the gauge-boson sector. The squares of the (real) bare W, Z masses, $M_{0,W}^2$ and $M_{0,Z}^2$, are split into complex renormalized mass squares μ_W^2 , μ_Z^2 and complex counterterms $\delta\mu_W^2$, $\delta\mu_Z^2$,

$$M_{0,W}^2 = \mu_W^2 + \delta\mu_W^2, \quad M_{0,Z}^2 = \mu_Z^2 + \delta\mu_Z^2, \quad (566)$$

and the field renormalization transformation is carried out in the same way as in the OS renormalization for stable particles described in Section 3.1,

$$W_0^\pm = \left(1 + \frac{1}{2}\delta\mathcal{Z}_W\right) W^\pm, \quad \begin{pmatrix} Z_0 \\ A_0 \end{pmatrix} = \begin{pmatrix} 1 + \frac{1}{2}\delta\mathcal{Z}_{ZZ} & \frac{1}{2}\delta\mathcal{Z}_{ZA} \\ \frac{1}{2}\delta\mathcal{Z}_{AZ} & 1 + \frac{1}{2}\delta\mathcal{Z}_{AA} \end{pmatrix} \begin{pmatrix} Z \\ A \end{pmatrix}. \quad (567)$$

To make the changes transparent, we denote the field renormalization constants in the CMS by calligraphic letters. The renormalized transverse (T) gauge-boson self-energies now read

$$\Sigma_{R,T}^W(k^2) = \Sigma_T^W(k^2) - \delta\mu_W^2 + (k^2 - \mu_W^2)\delta\mathcal{Z}_W, \quad \Sigma_{R,T}^{ZZ}(k^2) = \Sigma_T^{ZZ}(k^2) - \delta\mu_Z^2 + (k^2 - \mu_Z^2)\delta\mathcal{Z}_{ZZ},$$

⁴⁵Here and in Refs. [58, 59, 634] all external particles are assumed to be stable. Generalizations to external unstable particles have been discussed in the literature as well (see, e.g., Ref. [635–637]). In this case, it is convenient to introduce different wave-function renormalization constants for incoming and outgoing particles [636, 637].

$$\Sigma_{R,T}^{AA}(k^2) = \Sigma_T^{AA}(k^2) + k^2 \delta \mathcal{Z}_{AA}, \quad \Sigma_{R,T}^{AZ}(k^2) = \Sigma_T^{AZ}(k^2) + k^2 \frac{1}{2} \delta \mathcal{Z}_{AZ} + (k^2 - \mu_Z^2) \frac{1}{2} \delta \mathcal{Z}_{ZA}. \quad (568)$$

Note that the renormalized complex masses μ_W and μ_Z are used everywhere, i.e. also within the self-energies.

The counterterms are fixed by generalizing the renormalization conditions of the complete OS scheme [40, 117] for stable particles to

$$\Sigma_{R,T}^W(\mu_W^2) = 0, \quad \Sigma_{R,T}^{ZZ}(\mu_Z^2) = 0, \quad (569)$$

$$\begin{aligned} \Sigma_{R,T}^{AZ}(0) &= 0, & \Sigma_{R,T}^{AZ}(\mu_Z^2) &= 0, \\ \Sigma_{R,T}'^W(\mu_W^2) &= 0, & \Sigma_{R,T}'^{ZZ}(\mu_Z^2) &= 0, & \Sigma_{R,T}'^{AA}(0) &= 0, \end{aligned} \quad (570)$$

where the prime on $\Sigma_{R,T}'^V(p^2)$ denotes differentiation with respect to the argument p^2 . The conditions (569) fix the mass counterterms in such a way that the squared renormalized masses are equal to the location of the corresponding propagator pole in the complex plane. The conditions (570) fix the field renormalization constants. In contrast to OS renormalization for stable particles described in Section 3.1.7, the imaginary parts of the self-energies are kept in the renormalization conditions, so that both mass and field renormalization constants become complex. This, in particular, implies that the renormalized Z-boson field is not real anymore and that the renormalized W^\pm fields are not complex conjugates of each other. Thus, the renormalized Lagrangian, i.e. the Lagrangian in terms of renormalized fields without counterterms, is not hermitean, but the total Lagrangian (which is equal to the bare Lagrangian) of course is.

The renormalization conditions (569) and (570) have the solutions

$$\delta \mu_W^2 = \Sigma_T^W(\mu_W^2), \quad \delta \mu_Z^2 = \Sigma_T^{ZZ}(\mu_Z^2), \quad (571)$$

$$\begin{aligned} \delta \mathcal{Z}_{ZA} &= \frac{2}{\mu_Z^2} \Sigma_T^{AZ}(0), & \delta \mathcal{Z}_{AZ} &= -\frac{2}{\mu_Z^2} \Sigma_T^{AZ}(\mu_Z^2), \\ \delta \mathcal{Z}_W &= -\Sigma_T'^W(\mu_W^2), & \delta \mathcal{Z}_{ZZ} &= -\Sigma_T'^{ZZ}(\mu_Z^2), & \delta \mathcal{Z}_{AA} &= -\Sigma_T'^{AA}(0), \end{aligned} \quad (572)$$

which require to calculate the self-energies for complex squared momenta.

Owing to its definition (565), the renormalization of the complex weak mixing angle is determined by

$$\frac{\delta s_w}{s_w} = -\frac{c_w^2}{s_w^2} \frac{\delta c_w}{c_w} = -\frac{c_w^2}{2s_w^2} \left(\frac{\delta \mu_W^2}{\mu_W^2} - \frac{\delta \mu_Z^2}{\mu_Z^2} \right). \quad (573)$$

The electric charge is fixed in the OS scheme by requiring that there are no higher-order corrections to the eey vertex in the Thomson limit. In the CMS this condition reads

$$\delta Z_e = \frac{\delta e}{e} = \frac{1}{2} \Sigma'^{AA}(0) - \frac{s_w}{c_w} \frac{\Sigma_T^{AZ}(0)}{\mu_Z^2}. \quad (574)$$

Because of the explicit and implicit presence of the complex masses and couplings in the expressions on the r.h.s. of Eq. (574), the charge renormalization constant and thus the renormalized charge become complex. Since the imaginary part of the bare charge vanishes, the imaginary part of the charge renormalization constant is directly fixed by the imaginary part of self-energies. As further discussed in Section 6.6.4 below, the imaginary part of the renormalized charge is not relevant in a one-loop calculation, but has to be taken into account at the two-loop level.

For the Higgs boson the renormalization proceeds along the same lines as for the gauge bosons above. The complex Higgs mass squared

$$\mu_H^2 = M_H^2 - i M_H \Gamma_H = M_{0,H}^2 - \delta \mu_H^2 \quad (575)$$

is defined as the location of the zero in k^2 in the renormalized Higgs-boson self-energy

$$\Sigma_R^H(k^2) = \Sigma^H(k^2) - \delta \mu_H^2 + (k^2 - \mu_H^2) \delta \mathcal{Z}_H. \quad (576)$$

Fixing the Higgs field renormalization on shell, we obtain the renormalization constants

$$\delta \mu_H^2 = \Sigma^H(\mu_H^2), \quad \delta \mathcal{Z}_H = -\Sigma'^H(\mu_H^2). \quad (577)$$

To complete the renormalization in the scalar sector, the field renormalization for the would-be Goldstone bosons can simply be set equal to the Higgs field renormalization constant δZ_H , which is sufficient to cancel all UV divergences in vertex functions. In the case of the CMS, the same tadpole schemes can be used as discussed for the OS scheme in Section 3.1.6. In particular, the tadpole counterterm δt can be introduced to cancel explicitly occurring tadpole graphs, i.e. we set $\delta t = -T^H$, where $\Gamma_{\text{1Pl}}^H(0) = T^H$ is the one-loop contribution to the 1-point vertex function for the Higgs boson at one loop. The linear 't Hooft gauge-fixing term need not be renormalized.

Among the fermions of the SM, only very few appear as high-energy resonance (mainly the top quark and the τ lepton). In the following we nevertheless formulate the CMS for a generic unstable fermion f and comment on the treatment of stable fermions further below. For the unstable fermion f , the complex mass and its renormalization constant are introduced via

$$\mu_f^2 = m_f^2 - i m_f \Gamma_f, \quad m_{0,f} = \mu_f + \delta \mu_f. \quad (578)$$

The field renormalization constants become complex, but as for the bosons the fermion fields f_i^σ ($\sigma = \text{R, L}$) and their adjoint counterparts \bar{f}_i^σ both are rescaled by the same field renormalization factor,

$$f_{0,i}^\sigma = \left(1 + \frac{1}{2} \delta Z^{f,\sigma}\right) f_i^\sigma, \quad \bar{f}_{0,i}^\sigma = \left(1 + \frac{1}{2} \delta Z^{f,\sigma}\right) \bar{f}_i^\sigma, \quad (579)$$

so that $(f_i^\sigma)^\dagger \gamma_0$ and \bar{f}_i^σ are not identical, but differ by spurious imaginary parts. The renormalized fermion self-energy reads

$$\Sigma_R^f(p) = \left[\Sigma^{f,\text{R}}(p^2) + \delta Z^{f,\text{R}} \right] \not{p} \omega_+ + \left[\Sigma^{f,\text{L}}(p^2) + \delta Z^{f,\text{L}} \right] \not{p} \omega_- + \mu_f \left[\Sigma^{f,\text{S}}(p^2) - \frac{1}{2} (\delta Z^{f,\text{R}} + \delta Z^{f,\text{L}}) - \frac{\delta \mu_f}{\mu_f} \right]. \quad (580)$$

Generalizing the OS renormalization conditions to complex renormalization as

$$\begin{aligned} \delta \mu_f &= \frac{\mu_f}{2} \left[\Sigma^{f,\text{R}}(\mu_f^2) + \Sigma^{f,\text{L}}(\mu_f^2) + 2 \Sigma^{f,\text{S}}(\mu_f^2) \right], \\ \delta Z^{f,\sigma} &= -\Sigma^{f,\sigma}(\mu_f^2) - \mu_f^2 \left[\Sigma'^{f,\text{R}}(\mu_f^2) + \Sigma'^{f,\text{L}}(\mu_f^2) + 2 \Sigma'^{f,\text{S}}(\mu_f^2) \right], \quad \sigma = \text{R, L}, \end{aligned} \quad (581)$$

fixes μ_f^2 as the location of the complex pole in the fermion propagator.

Typically, only a few of the fields considered above develop resonances in interesting processes at a time, so that the complex renormalization is not needed and often also not wanted for all unstable particles. Concerning such a mix of real and complex renormalization conditions, the following points should be respected:

- The masses of all initial- and final-state particles of a resonance process should be taken real, i.e. those states are considered as stable.
- Even the mass and field renormalization constants of stable (or supposed to be stable) particles become complex quantities if at least one mass is renormalized according to the CMS, because the complex mass enters in general all self-energies that appear in the renormalization. The imaginary parts in all renormalization constants have to be kept in order to guarantee a full cancellation of UV divergences in amplitudes, i.e. no real parts of self-energies should be taken in the calculation of renormalization constants. However, the absorptive parts resulting from the self-energies of fields that are treated as stable have to be discarded. Thus, if some unstable particles are treated as stable, the operator Re (see Section 3.1.3) should be introduced with the understanding that it only eliminates the absorptive parts of the loop integrals appearing in all field and mass renormalization constants of the particles that are treated as stable, while it does not affect complex couplings and masses.
- One and the same particle should not appear as external stable state and internal resonance within the same process, because their simultaneous appearance would mean two different types of renormalization for one and the same particle. Any attempt to allow for this asymmetric treatment would necessarily face issues with gauge invariance.
- Even if only the W or only the Z boson develops a resonance in the considered process, it is advisable to treat both W and Z bosons in the CMS, although complex renormalization for only one of those would formally work as well. The reason for this advice is more of practical nature, because the spurious imaginary parts in couplings, which result from the complex weak mixing angle, are numerically smaller if both μ_W and μ_Z are used in Eq. (565) to calculate c_w .

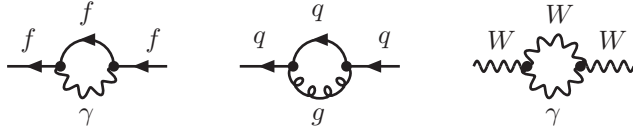


Figure 19: Typical one-loop diagrams that lead to a non-analytic behaviour in the self-energies for charged fermions f , quarks q , and W bosons at OS momentum, where the singularity in the virtuality p^2 becomes a logarithmic branch point.

6.6.3. Simplified version of the complex renormalization

Renormalization in the CMS requires to calculate the self-energies for complex squared momenta. This demands an analytic continuation of the 2-point functions entering the self-energies in the momentum variable to the unphysical Riemann sheet (cf. Ref. [604]). This complication can be avoided by expanding the self-energies appearing in the renormalization constants about real arguments in such a way that one-loop accuracy is retained.

We schematically illustrate the procedure for a scalar resonance P with pole mass M_P and pole width Γ_P , i.e. the location of the complex pole in the propagator is $\mu_P^2 = M_P^2 - iM_P\Gamma_P$. The one-loop self-energy correction to an amplitude in the CMS is proportional to

$$f(k^2) = \frac{\Sigma(k^2) - \Sigma(\mu_P^2)}{k^2 - \mu_P^2} + \delta\mathcal{Z}_P = \frac{\Sigma(k^2) - \Sigma(\mu_P^2)}{k^2 - \mu_P^2} - \Sigma'(\mu_P^2), \quad (582)$$

where we used the OS counterterms

$$\delta\mu_P^2 = \Sigma(\mu_P^2), \quad \delta\mathcal{Z}_P = -\Sigma'(\mu_P^2). \quad (583)$$

Note that the pole at $k^2 = \mu_P^2$ cancels exactly in Eq. (582), and $f(k^2)$ is well-behaved in the vicinity of the resonance ($k^2 \approx M_P^2$), where $k^2 - \mu_P^2 \approx iM_P\Gamma_P$ is of one-loop order, as the width Γ_P . When approximating $f(k^2)$ we have to make sure that the approximation is NLO correct in the vicinity of the resonance.

If the self-energy can be expanded as

$$\begin{aligned} \Sigma(\mu_P^2) &= \Sigma(M_P^2) + (\mu_P^2 - M_P^2)\Sigma'(M_P^2) + \mathcal{O}((\mu_P^2 - M_P^2)^2) \\ &= \Sigma(M_P^2) - iM_P\Gamma_P\Sigma'(M_P^2) + \mathcal{O}((M_P\Gamma_P)^2), \end{aligned} \quad (584)$$

we can approximate the mass and wave-function renormalization counterterms by

$$\delta\mu_P^2 = \Sigma(M_P^2) + (\mu_P^2 - M_P^2)\Sigma'(M_P^2) + \mathcal{O}(\alpha^3), \quad \delta\mathcal{Z}_P = -\Sigma'(M_P^2) + \mathcal{O}(\alpha^2), \quad (585)$$

and the resulting approximation

$$\begin{aligned} f(k^2) &= \frac{\Sigma(k^2) - \Sigma(M_P^2) - (\mu_P^2 - M_P^2)\Sigma'(M_P^2)}{k^2 - \mu_P^2} - \Sigma'(M_P^2) + \mathcal{O}(\alpha^2) \\ &= \frac{\Sigma(k^2) - \Sigma(M_P^2) - (k^2 - M_P^2)\Sigma'(M_P^2)}{k^2 - \mu_P^2} + \mathcal{O}(\alpha^2) \end{aligned} \quad (586)$$

is correct at NLO accuracy. The $\mathcal{O}(\alpha^2)$ and $\mathcal{O}(\alpha^3)$ contributions in Eqs. (585) and (586) result from products of terms $\Sigma = \mathcal{O}(\alpha)$ and $(\mu_P^2 - M_P^2) = \mathcal{O}(\alpha)$ and are UV finite by construction at the one-loop level.

While the expansion (584) holds true for a neutral and colourless field, it breaks down for charged or coloured fields in the presence of photon or gluon exchange due to the contributions with a branch point at $k^2 = \mu_P^2$. The corresponding types of one-loop diagrams are depicted in Fig. 19. We explicitly see this by considering

$$\Sigma(k^2) = a \left(\frac{\mu_P^2}{k^2} - 1 \right) \ln \left(1 - \frac{k^2}{\mu_P^2} \right) + \text{regular terms near } k^2 \sim \mu_P^2 \quad (587)$$

with a constant a , which is the typical functional form for a self-energy diagram with P emitting and reabsorbing a photon or gluon. In this case, the difference between the exact self-energy and the expansion is given by

$$\left[\Sigma(M_P^2) - iM_P\Gamma_P\Sigma'(M_P^2) \right] - \Sigma(\mu_P^2) = ia \frac{\Gamma_P}{M_P} + a \mathcal{O}(\Gamma_P^2 \ln \Gamma_P) \quad (588)$$

in the limit $\Gamma_P \ll M_P$, i.e. it is of two-loop order and thus of one order higher than nominally required. Substituting Eq. (588) into Eq. (586) shows that $f(k^2)$ does not have one-loop accuracy anymore. The failure of the expansion can be easily corrected by adding the missing term back to the expanded counterterm:

$$\begin{aligned}\Sigma(\mu_P^2) &= \Sigma(M_P^2) + (\mu_P^2 - M_P^2) \left[\Sigma'(M_P^2) + \frac{a}{M_P^2} \right] + \mathcal{O}((\mu_P^2 - M_P^2)^2) \\ &= \Sigma(M_P^2) - iM_P\Gamma_P\Sigma'(M_P^2) - ia\frac{\Gamma_P}{M_P} + \mathcal{O}((M_P\Gamma_P)^2).\end{aligned}\quad (589)$$

In this way the counterterms can be consistently expressed in terms of self-energies at real momentum arguments.

The described procedure can be applied to the CMS in the SM as follows. The gauge-boson self-energies at the complex pole positions can be approximated as

$$\begin{aligned}\Sigma_T^W(\mu_W^2) &= \Sigma_T^W(M_W^2) + (\mu_W^2 - M_W^2)\Sigma'_T^W(M_W^2) + c_T^W + \mathcal{O}(\alpha^3), \\ \Sigma_T^{ZZ}(\mu_Z^2) &= \Sigma_T^{ZZ}(M_Z^2) + (\mu_Z^2 - M_Z^2)\Sigma'_T^{ZZ}(M_Z^2) + \mathcal{O}(\alpha^3), \\ \frac{1}{\mu_Z^2}\Sigma_T^{AZ}(\mu_Z^2) &= \frac{1}{\mu_Z^2}\Sigma_T^{AZ}(0) + \frac{1}{M_Z^2}\Sigma_T^{AZ}(M_Z^2) - \frac{1}{M_Z^2}\Sigma_T^{AZ}(0) + \mathcal{O}(\alpha^2).\end{aligned}\quad (590)$$

The constant

$$c_T^W = \frac{i\alpha}{\pi}M_W\Gamma_W = \frac{\alpha}{\pi}(M_W^2 - \mu_W^2) \quad (591)$$

compensates for the failure of the expansion of the photon-exchange diagram in the W-boson self-energy as described above.

By neglecting the $\mathcal{O}(\alpha^2)$ terms in the expansion of the mixing energy and the $\mathcal{O}(\alpha^3)$ terms in the diagonal self-energies in Eq. (590), we can replace Eqs. (571) and (572) by

$$\begin{aligned}\delta\mu_W^2 &= \Sigma_T^W(M_W^2) + (\mu_W^2 - M_W^2)\Sigma'_T^W(M_W^2) + c_T^W, \\ \delta\mu_Z^2 &= \Sigma_T^{ZZ}(M_Z^2) + (\mu_Z^2 - M_Z^2)\Sigma'_T^{ZZ}(M_Z^2),\end{aligned}\quad (592)$$

$$\begin{aligned}\delta\mathcal{Z}_{ZA} &= \frac{2}{\mu_Z^2}\Sigma_T^{AZ}(0), & \delta\mathcal{Z}_{AZ} &= -\frac{2}{M_Z^2}\Sigma_T^{AZ}(M_Z^2) + \left(\frac{\mu_Z^2}{M_Z^2} - 1 \right) \delta\mathcal{Z}_{ZA}, \\ \delta\mathcal{Z}_W &= -\Sigma'_T^W(M_W^2), & \delta\mathcal{Z}_{ZZ} &= -\Sigma'_T^{ZZ}(M_Z^2).\end{aligned}\quad (593)$$

The missing $\mathcal{O}(\alpha^2)$ terms in $\delta\mathcal{Z}_W$, $\delta\mathcal{Z}_{ZZ}$, and $\delta\mathcal{Z}_{AZ}$ do not influence our results, since the gauge-boson field renormalization constants drop out as there is no external unstable gauge boson allowed when using the CMS, and the missing (finite) $\mathcal{O}(\alpha^3)$ terms in the mass counterterms are beyond the accuracy of a one-loop calculation. The counterterms (592) and (593) involve only functions that appear also in the usual OS renormalization scheme [40, 117], but consistently take into account the imaginary parts.

After inserting the counterterms (592) and (593) into Eq. (568), we can rewrite the renormalized self-energies in the CMS as

$$\begin{aligned}\Sigma_{R,T}^W(k^2) &= \Sigma_T^W(k^2) - \delta M_W^2 + (k^2 - M_W^2)\delta Z_W - c_T^W, \\ \Sigma_{R,T}^{ZZ}(k^2) &= \Sigma_T^{ZZ}(k^2) - \delta M_Z^2 + (k^2 - M_Z^2)\delta Z_{ZZ}, \\ \Sigma_{R,T}^{AA}(k^2) &= \Sigma_T^{AA}(k^2) + k^2\delta Z_{AA}, \\ \Sigma_{R,T}^{AZ}(k^2) &= \Sigma_T^{AZ}(k^2) + k^2\frac{1}{2}\delta Z_{AZ} + (k^2 - M_Z^2)\frac{1}{2}\delta Z_{ZA}\end{aligned}\quad (594)$$

with

$$\begin{aligned}\delta M_W^2 &= \Sigma_T^W(M_W^2), & \delta M_Z^2 &= \Sigma_T^{ZZ}(M_Z^2), \\ \delta Z_{ZA} &= \frac{2}{M_Z^2}\Sigma_T^{AZ}(0), & \delta Z_{AZ} &= -\frac{2}{M_Z^2}\Sigma_T^{AZ}(M_Z^2),\end{aligned}$$

$$\delta Z_W = -\Sigma'_T^W(M_W^2), \quad \delta Z_{ZZ} = -\Sigma'_T^{ZZ}(M_Z^2), \quad \delta Z_{AA} = -\Sigma'_T^{AA}(0). \quad (595)$$

Apart from the terms c_T^W , Eq. (594) with Eq. (595) have exactly the form of the renormalized self-energies in the usual OS scheme, but without taking the real parts of the counterterms. While in the OS scheme for stable particles the self-energies are calculated in terms of the real renormalized masses M_Z^2 and M_W^2 , in Eqs. (594) and (595) the self-energies are to be calculated in terms of the complex internal masses μ_Z^2 and μ_W^2 , although with real squared momenta. Note that this difference between usual OS and complex renormalization also changes the form of the IR divergence appearing in the W-field renormalization constant δZ_W . In the former scheme, it appears as logarithm $\ln m_\gamma$ of an infinitesimally small photon mass [or as the related $1/(4 - D)$ pole in DR]; in the latter, the W width regularizes the singularity via $\ln \Gamma_W$.

The renormalization of the complex weak mixing angle is given by Eq. (573) with mass counterterms from Eq. (592). The renormalization of the electric charge stays the same as in Eq. (574).

For the (neutral and colourless) Higgs boson, the approximate renormalization works as for the generic scalar P discussed above. The renormalization constants can be approximated as

$$\delta \mu_H^2 = \Sigma^H(M_H^2) + (\mu_H^2 - M_H^2) \Sigma'^H(M_H^2) + O(\alpha^3), \quad \delta Z_H = -\Sigma'^H(M_H^2) + O(\alpha^2), \quad (596)$$

so that the renormalized Higgs-boson self-energy up to finite $O(\alpha^2)$ terms can be written as

$$\Sigma_R^H(k^2) = \Sigma^H(k^2) - \delta M_H^2 + (k^2 - M_H^2) \delta Z_H \quad (597)$$

with

$$\delta M_H^2 = \Sigma^H(M_H^2), \quad \delta Z_H = -\Sigma'^H(M_H^2). \quad (598)$$

For a SM Higgs boson with mass $M_H = 125$ GeV, as determined by the LHC experiments, the expansion parameter is $\Gamma_H/M_H \sim 3 \times 10^{-5}$ and, thus, extremely small. Note, however, that for large Higgs-boson masses ($M_H \gtrsim 400$ GeV) the Higgs-boson width grows drastically, so that the expansion of the mass counterterm for $\Gamma_H/M_H \rightarrow 0$ would not be justified anymore.

Expanding the self-energies appearing in the renormalization constants (581) for an unstable fermion f about m_f^2 and neglecting (UV-finite) terms of order $O(\alpha^3)$ in the mass counterterm and of order $O(\alpha^2)$ in the field renormalization constant, the renormalized fermion self-energy can be expressed as

$$\begin{aligned} \Sigma_R^f(p) = & \left\{ \Sigma^{f,R}(p^2) + \delta Z^{f,R} \right\} \not{p} \omega_+ + \left\{ \Sigma^{f,L}(p^2) + \delta Z^{f,L} \right\} \not{p} \omega_- \\ & + \mu_f \left\{ \Sigma^{f,S}(p^2) - \frac{1}{2}(\delta Z^{f,R} + \delta Z^{f,L}) - \frac{\delta m_f}{m_f} + i m_f \Gamma_f \left[\frac{1}{2} \Sigma'^{f,R}(m_f^2) + \frac{1}{2} \Sigma'^{f,L}(m_f^2) + \Sigma'^{f,S}(m_f^2) \right] - c^f \right\} \end{aligned} \quad (599)$$

with

$$\begin{aligned} \delta m_f = & \frac{m_f}{2} \left[\Sigma^{f,R}(m_f^2) + \Sigma^{f,L}(m_f^2) + 2 \Sigma^{f,S}(m_f^2) \right], \\ \delta Z^{f,\sigma} = & -\Sigma^{f,\sigma}(m_f^2) - m_f^2 \left[\Sigma'^{f,R}(m_f^2) + \Sigma'^{f,L}(m_f^2) + 2 \Sigma'^{f,S}(m_f^2) \right], \quad \sigma = R, L. \end{aligned} \quad (600)$$

Note that for QCD corrections, in case f is a quark q , the neglected terms are of order $O(\alpha_s^3)$ or $O(\alpha_s^2)$, respectively. The constant c^f again originates from the non-analytic terms from photon and gluon exchange, as explained above. Taking EW and QCD corrections into account, it reads

$$c^f = \frac{i \alpha Q_f^2}{\pi} \frac{\Gamma_f}{m_f} + \frac{i \alpha_s C_F}{\pi} \frac{\Gamma_f}{m_f} \delta_{fq} \quad (601)$$

with the electric charge Q_f , the constant $C_F = 4/3$, and δ_{fq} is 0 or 1 if f is a lepton or a quark, respectively.

In summary, the calculation of self-energies with complex momentum arguments can be avoided by carefully expanding these about real values. In case of charged or coloured particles, extra constants must be added to the expanded self-energies in order not to spoil the one-loop accuracy of the results. All the mass arguments of the self-energies are complex, and no real parts should be taken.

6.6.4. Input parameters to the complex-mass scheme

In the above description we did not yet clarify how the width of an unstable particle P should be chosen in the CMS. Note that the width Γ_P is part of the renormalized parameter μ_P , but not an independent parameter of the theory. It is rather determined by the theory and thus calculable, either from the decay processes of P or equivalently via unitarity cuts from the imaginary part of its self-energy,

$$M_P \Gamma_P = \text{Im} \left\{ \Sigma(M_P^2 - i M_P \Gamma_P) \right\}. \quad (602)$$

In principle, this equation can be iteratively solved for Γ_P , but the result would only be of LO accuracy if Σ is of NLO, because imaginary parts of one-loop self-energies contain only tree-level information about particle widths via unitarity cuts. In order to obtain full NLO accuracy in the cross section near the resonance, however, NLO corrections to Γ_P are required. This is obvious, because near resonance the offshellness of the propagator with virtuality k^2 and the width part are of the same size, $|k^2 - M_P^2| = \mathcal{O}(M_P \Gamma_P)$. Equation (602) should, thus, be solved for Γ_P using self-energy contributions up to the two-loop level, or alternatively Γ_P can be calculated directly from decay amplitudes at NLO.

This asymmetry in the loop level between input preparation and matrix-element calculation in the CMS deserves further justification: For each unstable particle mass, in the CMS we add and subtract the same imaginary part in the Lagrangian. One of these terms provides the imaginary part for the mass parameter and becomes part of the free propagator, while the other becomes part of a counterterm vertex. Thus, the first term is resummed, but the second is not. Independently of the imaginary part that is added and subtracted, this procedure does not spoil the algebraic relations that govern gauge invariance, and unitarity cancellations (not to be confused with the full cut equations expressing unitarity) are exactly respected. In practice, this means that we can insert values for the particle widths that are not directly related to the loop order to which the amplitudes of the process are calculated. We could even go beyond NLO in the calculation of the widths or take an empirical value. On the other hand, the validity of the cut equations at NLO requires to use the NLO decay widths [588].

Note that this argument generalizes to all (independent) input parameters, real or complex in the CMS: Changing the input parameter or the corresponding counterterm by terms that affect amplitude calculations beyond NLO precision, is a legal procedure in the sense that it does not introduce any inconsistencies such as violating gauge invariance or unitarity cancellations.

Similarly, the numerical setting of the electromagnetic coupling deserves some care. Owing to the use of complex masses in the loop corrections that enter the charge renormalization constant and the fact that the bare elementary charge is real, the renormalized electromagnetic coupling e actually becomes complex. The imaginary part of e is not a free input parameter, but determined by the charge renormalization constant, i.e. it could be iteratively calculated. Note, however, that the imaginary part of e is entirely due to spurious terms, since the charge renormalization constant only involves self-energies at zero momentum transfer, which do not develop imaginary parts for real internal masses. The imaginary parts in e are, thus, of formal two-loop order. Following the above argument, we conclude that it is consistent within NLO accuracy to set the imaginary parts in e to zero. We also remark that using a complex electromagnetic coupling e would disturb the cancellation of IR divergences between virtual and real EW corrections, because those two types of corrections only involve exactly the same power e^n in the contributions to squared amplitudes if e is real, while the powers $e^{n_1} (e^*)^{n_2}$ for a complex e would be different in spite of the same values of $n = n_1 + n_2$.

The situation does not change much if the coupling α is not fixed to the fine-structure constant $\alpha(0)$, but derived from a high-energy value $\alpha(Q^2)$ or from the Fermi constant G_μ in the G_μ scheme as described in Section 5.1.1. In the latter case, the input value α_{G_μ} should be calculated from the real W and Z masses to avoid spurious terms of $\mathcal{O}(\alpha)$ in α_{G_μ} . In this way the input conversion is done in the same way as in the real OS scheme for stable particles, and the quantity Δr , which modifies the charge renormalization constant δZ_e , is calculated from real input parameters as well. Again, following the above general argument about changing input parameters or corresponding renormalization constants beyond NLO, it would also be legal to calculate Δr from complex masses, etc. (but keeping α_{G_μ} real), because the corresponding change in Δr is of two-loop order.

6.6.5. Complex renormalization—background-field method

Using the background-field method, the gauge-boson field renormalization constants can be determined in terms of the parameter renormalization in such a way that Ward identities possess the same form before and after renormalization [107], as explained in Section 2.3.2. Real parameters have to be substituted by the corresponding complex

parameters everywhere when the complex renormalization is employed. The complex parameter renormalization is fixed as above in Eqs. (571), (573), (574), (577), and (581) or likewise by their simplified versions described in Section 6.6.3. Note that $\Sigma_T^{AZ}(0)$ vanishes in the background-field method as a consequence of the background-field gauge invariance of the effective action, which in particular simplifies the charge renormalization constant (574).

Since the gauge-boson field renormalization constants drop out in the S -matrix elements without external gauge-boson fields, we can also use the definitions in Eq. (593) in the calculation of S -matrix elements.

6.7. Further schemes for unstable particles

To our experience, pole scheme, pole approximation, and CMS are the most frequently used methods to describe resonance processes beyond the NWA, especially as far as the calculation of EW corrections is concerned. There are also other methods to deal with unstable-particle effects in resonance processes with different strengths and weaknesses which were suggested and used in the literature. In the following we briefly sketch some of those alternative approaches, without claiming to be exhaustive.

(a) Factorization schemes

Different variants of factorizing resonance structures from amplitudes have been proposed in the literature, but they all share the idea to separate a simple resonance factor from complete (gauge-invariant) amplitudes or from gauge-invariant subsets of diagrams. For pure LO predictions, this idea can be implemented easily: For each potentially resonant propagator factor $(p^2 - M_P^2)^{-1}$ of a resonance P , multiply the amplitude with the *fudge factor* $f_P(p^2) = (p^2 - M_P^2)/(p^2 - \mu_P^2)$. In the resonance region, this factor restores the correct Breit–Wigner factor. On resonance the non-resonant terms are put to zero and off resonance, where $|p^2 - M_P^2| \gg M_P \Gamma_P$, the amplitude is modified by a factor $f_P = 1 + O(\Gamma_P/M_P)$, which changes the result only at formal NLO level. LO results on W-pair production in e^+e^- annihilation based on this scheme can, for instance, be found in Refs. [597, 599].

Beyond LO, however, it can be quite non-trivial to guarantee the aimed precision (e.g. NLO) everywhere in phase space and to match virtual and real corrections. Simply modifying LO cross sections with fudge factors containing decay widths for resonances in general introduces spurious $O(\Gamma_P/M_P)$ terms destroying NLO accuracy. The most simple example in which the method works perfectly well is the case where the LO amplitude receives only contributions with a common resonance structure without any non-resonant or subleading background diagrams. In such cases, the relative correction to the LO amplitude does not involve any resonance factors. The Drell–Yan-like production of W bosons at hadron colliders is such a fortunate case; the first calculation of NLO EW corrections to this process was based on the factorization scheme [584]. Owing to the non-resonant background by photon exchange, the application of the factorization scheme to Drell–Yan-like Z-boson production is already more complicated. For NLO weak corrections such a calculation was described in Ref. [422], and corresponding results were already included in the comparison of schemes in Section 6.5.2 above.

(b) Schemes based on resummation and the fermion-loop scheme

As discussed at the very beginning of this section, standard perturbation theory cannot describe particle resonances in any finite order, but requires at least some partial Dyson summation of self-energy contributions in the propagators of unstable particles. Although it would be straightforward to consistently construct all amplitudes from Dyson-summed propagators, the necessary truncation of the perturbative series when calculating irreducible vertex functions at some finite order in general invalidates this procedure, because consistency relations from gauge invariance and unitarity usually hold order by order and get violated in perturbative orders that are not completely taken into account.

In view of this situation, it seems natural to look for the technical possibility to reconcile Dyson summation and constraints from gauge invariance and unitarity. In the case of unstable particles that exclusively decay into fermion–antifermion pairs at LO—a case that in particular includes W and Z bosons—such a procedure is provided by the *fermion-loop scheme* [595, 598, 599], which was suggested and used to describe W- and Z-boson pair production processes at LEP2. In this scheme, all one-loop corrections induced by closed fermion loops are Dyson summed to all orders, but no other corrections are taken into account. This procedure obviously introduces all necessary finite-width effects in propagators of unstable particles decaying only into fermion–antifermion pairs. Taking into account *all* closed fermion loops, i.e. also in vertex corrections etc., however, preserves all Ward identities in amplitudes and subamplitudes even in the presence of resummed propagators and does not introduce any dependence on gauge

parameters. This statement is quite non-trivial and originates from the fact that closed fermion loops always provide gauge-invariant subsets of radiative corrections in each perturbative order (see Section 5.2.2).⁴⁶ Predictions based on the fermion-loop scheme, thus, provide fully consistent cross sections at LO accuracy improved by the higher-order effects induced by closed fermion loops, such as running effects in the electromagnetic coupling or leading corrections in the ρ -parameter.

Promoting those results to full NLO precision, however, is highly non-trivial and has not yet been accomplished. Some steps or field-theoretical statements of such a procedure are known though. For example, in Ref. [115] it was shown that even the full $\mathcal{O}(\alpha)$ one-loop corrections to amplitudes can be Dyson summed without violating Ward identities if the field theory is quantized within the background-field method (see Section 2.3), which is a straightforward consequence of the gauge invariance of the background-field effective action. This feature also lifts the restriction of the method to unstable particles decaying only into fermion–antifermion pairs.⁴⁷

The most serious show-stopper in the Dyson-summation approach towards complete higher orders seems to be the fact that the introduction of widths via imaginary parts of self-energies lags behind by one perturbative order. Even taking into account the full set of $\mathcal{O}(\alpha)$ corrections in Dyson-summed amplitudes lacks the $\mathcal{O}(\alpha)$ corrections to total decay widths in propagator denominators. Moreover, the cancellation of IR singularities against real-emission corrections might require a non-trivial modification in such calculations.

(c) Effective field theories

Effective field theories (EFTs) generically can describe physical systems consisting of two or more components that are characterized by different energy scales μ_i obeying some hierarchy $\mu_1 \ll \mu_2 \ll \dots$. Field theories with one or more narrow resonances P with $\Gamma_P \ll M_P$ fulfil this requirement, rendering the formulation of EFTs for unstable particles possible [638–640]. In the EFT approach to describe an unstable particle P , an effective Lagrangian is constructed that separates hard, collinear, and soft degrees of freedom in the fields. The splitting of modes corresponds to the different momentum regions in Feynman diagrams of the full theory as defined by the *strategy of regions* [641, 642]. Particles with hard momenta (high-energetic, non-resonant, or massive particles of some energy scale $|q^\mu| \sim M_P$) do not represent dynamical degrees of freedom in the EFT. They are “integrated out”, so that their effect is included through the Wilson coefficients of the operators describing P production and decay. The soft momentum region, on the other hand, accounts for off-shell modes of P ($|p^2 - M_P^2| \sim M_P \Gamma_P$) and the exchange or emission of soft massless gauge bosons ($|q^\mu| \sim \Gamma_P$). The domains of collinear momenta (with a non-trivial hierarchy of its light-cone components in terms of Γ_P) are needed to consistently include the interaction of massless gauge bosons with light high-energetic particles (such as quarks or leptons). The contributions of the different momentum regions involve artificial UV and IR divergences which in their sum combine to a systematic expansion of amplitudes in powers of Γ_P/M_P , similar to the result of a direct pole expansion of Feynman diagrams. In particular, the leading contribution of the soft momentum region corresponds to non-factorizable corrections in the PA.

In summary, the EFTs of Refs. [638–640] deliver a field-theoretically elegant way to carry out pole expansions owing to their formulation via effective actions. Like the PA, their validity is restricted to the resonance region, but they offer the combination with further expansions, e.g. around thresholds, and suggest better possibilities to carry out dedicated resummations of higher-order effects. The EFT shows limitations or complications if detailed information on differential properties of observables is needed, since experimental degrees of freedom do not correspond to the degrees of freedom of the EFT. For e^+e^- collisions the EFT approach was, for instance, used to evaluate NLO EW corrections to the W-pair production cross section near the WW threshold [643, 644], including leading EW higher-order effects beyond NLO.

⁴⁶One possibility to establish the validity of the Ward identities for amplitudes with propagators based on Dyson-summed closed-fermion-loop corrections is to start from the background-field Ward identities for connected Green functions established in Ref. [115] and to reduce the $\mathcal{O}(\alpha)$ corrections to the closed fermion loops, which can be separated in a gauge-invariant way and which are identical in the conventional and background-field approaches.

⁴⁷Recall that irreducible vertex functions in the BFM still depend on some quantum gauge parameter ξ , although BFM vertex functions fulfil the simple BFM Ward identities exactly. The dependence on ξ drops out in complete amplitudes order by order. If Dyson-summed propagators are used, however, the cancellation of the ξ dependence only happens within completely calculated orders, i.e. a corresponding NLO calculation based on resummed propagators still shows some ξ dependence of formal NNLO level. If ξ is not taken “artificially large”, this residual dependence should not be too harmful. Since Ward identities are fulfilled exactly, there are no systematic enhancements of those artifacts by violation of unitarity cancellations.

7. Conclusions

After the discovery of a Higgs boson at the CERN LHC in 2012, the full particle content of the SM of particle physics is experimentally established. Moreover, all particle phenomena of the strong and electroweak interactions observed at colliders are nicely described by the SM without truly significant deviations. In other words, any effects of physics beyond the SM—if accessible at all by current and future collider experiments—are small and subtle, putting the aspect of precision at the forefront of experimental analyses and theory predictions. The inclusion of perturbative corrections in predictions for present and future collider experiments is at the heart of this task on the theory side. Besides the indispensable corrections of the strong interaction, *electroweak radiative corrections* must be taken into account as well. While their generic size is at the level of a few percent and thus roughly comparable to the NNLO QCD corrections, they can be enhanced via different mechanisms. The inclusion of NLO electroweak corrections is becoming standard in the experimental analyses.

This review gives an overview of the most important, established techniques that are presently used in the calculation of electroweak corrections. While we have included some discussion on the resummation of the leading logarithmic corrections in the high-energy limit, in parton distribution functions, and structure functions for photonic interactions, we mainly focus on the methods for NLO electroweak calculations. In this realm, a set of agreed-upon, well-developed, and efficient approaches exists both for the calculation of virtual and real contributions. On the other hand, the calculation of NNLO corrections, in particular for the electroweak parts, is still in an exploratory phase.

The aim of this review is to provide a coherent introduction to the well-established and most frequently used concepts and techniques for the calculation of NLO electroweak corrections. In detail, we have spelled out the renormalization of the SM in the on-shell scheme and discussed frequently used input-parameter schemes as well as the structure of the NLO electroweak corrections. An overview over the modern techniques for the calculation of electroweak one-loop corrections and the available automated tools is given. As far as real corrections are concerned, slicing and subtraction techniques for the treatment of infrared singularities are described in some detail, and applications to the electromagnetic corrections to parton distribution functions, peculiarities of photon–jet systems, as well as real radiation effects in lepton–photon systems are discussed. Moreover, a section is devoted to the treatment of unstable particles in quantum field theory, in particular in connection with the calculation of NLO electroweak corrections—a subject that is to our knowledge not covered in such a coherent form in the literature yet. Finally, the appendix contains a complete list of Feynman rules with counterterms for the SM both in the conventional and in the background-field formalism, which might be helpful for practitioners.

While this review is primarily targeted to the description of the basic concepts and calculational techniques, we have included typical phenomenological applications for illustration of generic features whenever appropriate. A comprehensive account of the status of electroweak corrections for collider processes is, however, way beyond the scope of this review. Moreover, extrapolating the great progress of recent years in the field, such an account would be outdated very soon. Regular compilations and updates of important precision calculations for collider processes may be found in workshop proceedings such as those of the bi-annual *Les Houches workshop on Physics at TeV Colliders*.

We end this review with a brief assessment of the current state of the art concerning the calculation of electroweak corrections for high-energy colliders and possible future directions. With the present techniques, NLO calculations for processes with up to six particles in the final state are achieved. We expect that further refinements of the methods will allow us to push this limit even somewhat further. A more pressing issue is, however, to provide interfaces of NLO electroweak calculations with general-purpose Monte Carlo generators including electromagnetic or even electroweak parton showers, to bring electroweak precision more directly into the analyses of experimental data. Another line of development, but also beyond the reach of this review, concerns electroweak precision in the search for physics beyond the SM which is currently pushed forward in two different directions. On the one hand, electroweak corrections are calculated in various specific extensions of the SM, a task that is technically straightforward, but requires great care in the formulation of phenomenologically sound renormalization and input-parameter schemes. On the other hand, physics beyond the SM is searched for in the more model-independent framework of effective field theories, which poses new challenges in the renormalization procedure because of the lack of renormalizability. Currently, the field of electroweak precision calculations develops rapidly in both directions.

Looking further ahead, potential future high-energy colliders will implicate new theoretical challenges on the electroweak precision frontier. If high-energy electron–positron colliders are realized, electroweak corrections at the NNLO level and higher will be required. At present, such results are only available for selected low-multiplicity

processes, such as pseudo-observables at the Z-boson resonance, but for future e^+e^- colliders electroweak two-loop calculations have to become standard for the most important processes. In particular, this program requires considerable advancements in the calculation of multi-loop integrals with many scales, where the most promising road presently seems to be numerical integration. If multi-TeV colliders, such as future circular hadron colliders, become reality, the higher scattering energies bring in further challenges. Extrapolating the large electroweak corrections appearing in the TeV range even to higher energies, makes it clear that electroweak effects have to be controlled way beyond NLO accuracy. In particular, electroweak corrections from multiple W- and Z-boson radiation will become more and more important, rendering it more and more difficult to isolate different types of hard scattering processes. Eventually, we might face the problem of refining the definition of appropriate observables.

In summary, looking back at the previous decades and looking ahead to future challenges, the hunt for higher precision in collider physics goes hand in hand with the need for a deeper understanding of quantum field theory, which is part of the charm that pushes us forward.

Appendix A. Feynman rules

In this appendix we list the Feynman rules for the SM both in the conventional and in the background-field formalism. We provide the complete set of propagators and vertices by listing possible actual insertions for generic Feynman rules. In the vertices all momenta and fields are defined as incoming. For brevity we use the shorthand notation

$$c = c_w = \cos \theta_w, \quad s = s_w = \sin \theta_w. \quad (\text{A.1})$$

Feynman rules for QCD

In the following we list the Feynman rules for QCD in the conventional formalism in the R_ξ gauge including the counterterms resulting from the renormalization of parameters, gluon fields, and quark fields. We do not include counterterms from the gauge-fixing term, which does not need to be renormalized in linear gauges, and do not provide counterterms for the vertices involving Faddeev–Popov fields as these are not needed to render one-loop S -matrix elements finite.

Propagators

- gluons (A, B are colour indices of the adjoint representation)

$$G_\mu^A \bullet \text{---} \overset{k}{\text{---}} \bullet G_\nu^B = -i \left[\left(g_{\mu\nu} - \frac{k_\mu k_\nu}{k^2} \right) + \xi \frac{k_\mu k_\nu}{k^2} \right] \frac{\delta^{AB}}{k^2 + i\epsilon} \quad (\text{A.2})$$

- Faddeev–Popov ghosts

$$\bar{u}^A \bullet \text{---} \overset{k}{\text{---}} \bullet u^B = \frac{i\delta^{AB}}{k^2 + i\epsilon} \quad (\text{A.3})$$

- quarks (α, β are colour indices of the fundamental representation)

$$\bar{q}_\beta \bullet \overset{k}{\text{---}} \bullet q_\alpha = \frac{i\delta_{\alpha\beta}(\not{k} + m_q)}{k^2 - m_q^2 + i\epsilon} \quad (\text{A.4})$$

Vertices

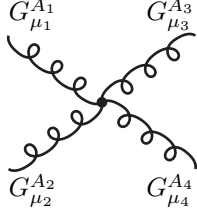
- GG vertex

$$\text{---} \overset{G_\mu^A, k}{\text{---}} \times \text{---} \overset{G_\nu^B}{\text{---}} = i \left(-g_{\mu\nu} k^2 + k_\mu k_\nu \right) \delta^{AB} \delta Z_G \quad (\text{A.5})$$

- $\bar{q}q$ vertex

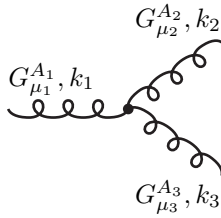
$$\begin{array}{c} q_\beta, k \\ \xrightarrow{\quad \times \quad} \end{array} \bar{q}_\alpha = i[(\not{k} - m_q)\delta Z_q - \delta m_q]\delta_{\alpha\beta} \quad (\text{A.6})$$

- $GGGG$ vertex



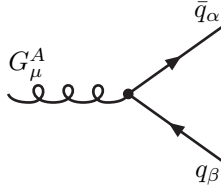
$$= -ig_s^2 (1 + 2\delta Z_{g_s} + 2\delta Z_G) \left[f^{A_1 A_2 B} f^{A_3 A_4 B} (g_{\mu_1 \mu_3} g_{\mu_2 \mu_4} - g_{\mu_1 \mu_4} g_{\mu_2 \mu_3}) + f^{A_1 A_3 B} f^{A_4 A_2 B} (g_{\mu_1 \mu_4} g_{\mu_3 \mu_2} - g_{\mu_1 \mu_2} g_{\mu_3 \mu_4}) + f^{A_1 A_4 B} f^{A_2 A_3 B} (g_{\mu_1 \mu_2} g_{\mu_4 \mu_3} - g_{\mu_1 \mu_3} g_{\mu_4 \mu_2}) \right] \quad (\text{A.7})$$

- GGG vertex



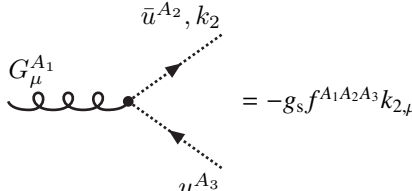
$$= g_s (1 + \delta Z_{g_s} + \frac{3}{2} \delta Z_G) f^{A_1 A_2 A_3} \left[g_{\mu_1 \mu_2} (k_1 - k_2)_{\mu_3} + g_{\mu_2 \mu_3} (k_2 - k_3)_{\mu_1} + g_{\mu_3 \mu_1} (k_3 - k_1)_{\mu_2} \right] \quad (\text{A.8})$$

- $G\bar{q}q$ vertex



$$= ig_s (1 + \delta Z_{g_s} + \frac{1}{2} \delta Z_G + \delta Z_q) \gamma_\mu T_{\alpha\beta}^A \quad (\text{A.9})$$

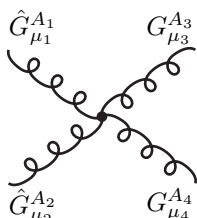
- $G\bar{U}U$ vertex



$$= -g_s f^{A_1 A_2 A_3} k_{2,\mu} \quad (\text{A.10})$$

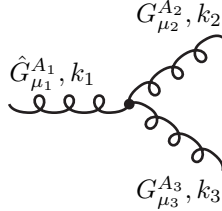
Next we list the Feynman rules for QCD in the background-field formalism. The Feynman rules involving only background fields are identical to those in the conventional formalism given in Eqs. (A.2)–(A.10) including the counterterms. Only the Feynman rules involving Faddeev–Popov fields or exactly two quantum gluon fields differ from those of the conventional formalism. In the quantum R_ξ gauge these read:

- $\hat{G}\hat{G}GG$ vertex



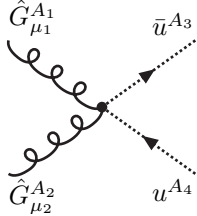
$$= -ig_s^2 \left[f^{A_1 A_2 B} f^{A_3 A_4 B} (g_{\mu_1 \mu_3} g_{\mu_2 \mu_4} - g_{\mu_1 \mu_4} g_{\mu_2 \mu_3}) + f^{A_1 A_3 B} f^{A_4 A_2 B} (g_{\mu_1 \mu_4} g_{\mu_3 \mu_2} - g_{\mu_1 \mu_2} g_{\mu_3 \mu_4} - g_{\mu_1 \mu_3} g_{\mu_2 \mu_4}/\xi) + f^{A_1 A_4 B} f^{A_2 A_3 B} (g_{\mu_1 \mu_2} g_{\mu_4 \mu_3} - g_{\mu_1 \mu_3} g_{\mu_4 \mu_2} + g_{\mu_1 \mu_4} g_{\mu_3 \mu_2}/\xi) \right] \quad (\text{A.11})$$

- $\hat{G}GG$ vertex



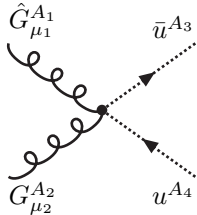
$$= g_s f^{A_1 A_2 A_3} \left[g_{\mu_1 \mu_2} (2k_1 + k_3 (1 - 1/\xi))_{\mu_3} + g_{\mu_2 \mu_3} (k_2 - k_3)_{\mu_1} - g_{\mu_3 \mu_1} (2k_1 + k_2 (1 - 1/\xi))_{\mu_2} \right] \quad (\text{A.12})$$

- $\hat{G}\hat{G}\bar{U}U$ vertex



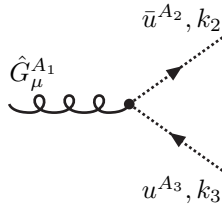
$$= i g_s^2 (f^{A_1 A_3 B} f^{A_2 A_4 B} + f^{A_1 A_4 B} f^{A_2 A_3 B}) g_{\mu_1 \mu_2} \quad (\text{A.13})$$

- $\hat{G}G\bar{U}U$ vertex



$$= i g_s^2 f^{A_1 A_3 B} f^{A_2 A_4 B} g_{\mu_1 \mu_2} \quad (\text{A.14})$$

- $\hat{G}\bar{U}U$ vertex



$$= -g_s f^{A_1 A_2 A_3} (k_2 - k_3)_{\mu} \quad (\text{A.15})$$

Feynman rules for the EWSM in the conventional formalism

We provide the Feynman rules in a general 't Hooft gauge with a gauge-fixing term as defined in Eqs. (27) and (28) with $\xi'_W = \xi_W$, $\xi'_Z = \xi_Z$. In this gauge all propagators are diagonal. We include the one-loop contributions of the counterterms from the renormalization of parameters and fields in the physical basis, but do not include counterterms from the renormalization of unphysical fields and counterterms due to the gauge-fixing terms. The tadpole counterterms δt are given both in the Fleischer–Jegerlehner tadpole scheme (FJTS) [147, 169, 170] and in the (PRTS) scheme of Ref. [40], as described in Section 3.1.6. The respective tadpole terms are called δt_{FJTS} or δt_{PRTS} ; whenever δt is written without subscript FJTS or PRTS, this term contributes in both schemes. We do not provide counterterms for the vertices involving Faddeev–Popov fields, as these are not needed for S -matrix elements at the one-loop level.

If the following Feynman rules are used in the CMS described in Section 6.6, only minor modifications are required. All parameters and renormalizations constants have to be substituted by their complex counterparts. In this context, one should recall that spinors and corresponding adjoint spinors are rescaled by the same field renormalization constants [cf. Eq. (579)], so that both $\delta Z^{f,\sigma}$ and $(\delta Z^{f,\sigma})^{\dagger}$ are represented by $\delta Z^{f,\sigma}$. Recall that we assume a unit quark mixing matrix in the CMS.

Propagators

- gauge bosons $V = A, Z, W$ ($M_A = 0$):

$$V_\mu^\dagger \bullet \overset{k}{\text{wavy line}} \bullet V_\nu = \frac{-ig_{\mu\nu}}{k^2 - M_V^2 + i\epsilon} + \frac{i(1 - \xi_V)k_\mu k_\nu}{(k^2 - M_V^2 + i\epsilon)(k^2 - \xi_V M_V^2 + i\epsilon)} \quad (\text{A.16})$$

- Faddeev–Popov ghosts $U = u^A, u^Z, u^\pm$ ($M_{u^A} = 0, M_{u^Z} = \sqrt{\xi_Z} M_Z, M_{u^\pm} = \sqrt{\xi_W} M_W$),

$$\bar{U} \bullet \overset{k}{\text{dotted line}} \bullet U = \frac{i}{k^2 - M_U^2 + i\epsilon} \quad (\text{A.17})$$

- scalar fields $S = H, \chi, \phi$ ($M_\chi = \sqrt{\xi_Z} M_Z, M_\phi = \sqrt{\xi_W} M_W$),

$$S^\dagger \bullet \overset{k}{\text{dash-dot line}} \bullet S = \frac{i}{k^2 - M_S^2 + i\epsilon} \quad (\text{A.18})$$

- fermion fields F ,

$$\bar{f}_i \bullet \overset{k}{\text{solid line}} \bullet f_i = \frac{i(\not{k} + m_{f,i})}{k^2 - m_{f,i}^2 + i\epsilon} \quad (\text{A.19})$$

Vertices and counterterms

- tadpole

$$\cancel{\times} \text{---} \overset{H}{\text{---}} = i\delta t \quad (\text{A.20})$$

- VV counterterm

$$\overset{V_{1,\mu}, k}{\text{wavy line}} \cancel{\times} \overset{V_{2,\nu}}{\text{wavy line}} = i[(-g_{\mu\nu}k^2 + k_\mu k_\nu)C_1 + g_{\mu\nu}C_2] \quad (\text{A.21})$$

$$\begin{array}{lll} V_1 V_2 & C_1 & C_2 \\ \hline W^+ W^- & \delta Z_W & \delta Z_W M_W^2 + \delta M_W^2 - \frac{e M_W}{s M_H^2} \delta t_{\text{FJTS}} \\ ZZ & \delta Z_{ZZ} & \delta Z_{ZZ} M_Z^2 + \delta M_Z^2 - \frac{e M_Z}{s c M_H^2} \delta t_{\text{FJTS}} \\ AZ & \frac{1}{2} \delta Z_{AZ} + \frac{1}{2} \delta Z_{ZA} & \frac{1}{2} \delta Z_{ZA} M_Z^2 \\ AA & \delta Z_{AA} & 0 \end{array} \quad (\text{A.22})$$

- VS counterterm

$$\overset{V_\mu, k}{\text{wavy line}} \cancel{\times} \text{---} \overset{S}{\text{---}} = i k_\mu C \quad (\text{A.23})$$

$$\begin{array}{ll} VS & C \\ \hline W^\pm \phi^\mp & \pm \frac{1}{2} \left(\delta Z_W + \frac{\delta M_W^2}{M_W^2} - \frac{e}{s M_H^2 M_W} \delta t_{\text{FJTS}} \right) M_W \\ Z\chi & i \frac{1}{2} \left(\delta Z_{ZZ} + \frac{\delta M_Z^2}{M_Z^2} - \frac{e}{s M_H^2 M_W} \delta t_{\text{FJTS}} \right) M_Z \\ A\chi & i \frac{1}{2} \delta Z_{ZA} M_Z \end{array} \quad (\text{A.24})$$

- SS counterterm

$$\overset{S_1, k}{\text{---}} \cancel{\times} \text{---} \overset{S_2}{\text{---}} = i[C_1 k^2 - C_2] \quad (\text{A.25})$$

$$\begin{array}{ccc}
V_1 V_2 & C_1 & C_2 \\
\hline
HH & \delta Z_H & \delta Z_H M_H^2 + \delta M_H^2 - \frac{3e}{2sM_W} \delta t_{\text{FJTS}} \\
\chi\chi \} & 0 & -\frac{e}{2sM_W} \delta t
\end{array} \tag{A.26}$$

• $F\bar{F}$ counterterm

$$\begin{array}{ccc}
f_j, k & \xrightarrow{\quad \times \quad} & \bar{f}_i \\
\hline
\end{array} = i[C_L \not{k} \omega_- + C_R \not{k} \omega_+ - C_S^- \omega_- - C_S^+ \omega_+] \tag{A.27}$$

$$\begin{aligned}
C_L &= \frac{1}{2} (\delta Z_{ij}^{f,L} + \delta Z_{ij}^{f,L\dagger}), & C_R &= \frac{1}{2} (\delta Z_{ij}^{f,R} + \delta Z_{ij}^{f,R\dagger}) \\
C_S^- &= m_{f,i} \frac{1}{2} \delta Z_{ij}^{f,L} + \frac{1}{2} \delta Z_{ij}^{f,R\dagger} m_{f,j} + \delta_{ij} \left(\delta m_{f,i} - m_{f,i} \frac{e}{2sM_H^2 M_W} \delta t_{\text{FJTS}} \right) \\
C_S^+ &= m_{f,i} \frac{1}{2} \delta Z_{ij}^{f,R} + \frac{1}{2} \delta Z_{ij}^{f,L\dagger} m_{f,j} + \delta_{ij} \left(\delta m_{f,i} - m_{f,i} \frac{e}{2sM_H^2 M_W} \delta t_{\text{FJTS}} \right)
\end{aligned} \tag{A.28}$$

• $VVVV$ vertex:

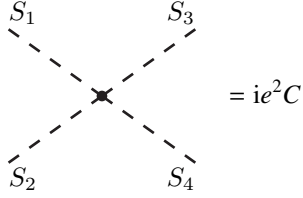
$$\begin{array}{ccc}
V_{1,\mu} & & V_{3,\rho} \\
\swarrow & & \searrow \\
& \text{---} & \\
V_{2,\nu} & & V_{4,\sigma} \\
\searrow & & \swarrow \\
\hline
V_1 V_2 V_3 V_4 & C & \\
\hline
W^+ W^+ W^- W^- & \frac{1}{s^2} \left[1 + 2\delta Z_e - 2\frac{\delta s}{s} + 2\delta Z_W \right] \\
W^+ W^- ZZ & -\frac{c^2}{s^2} \left[1 + 2\delta Z_e - 2\frac{1}{c^2} \frac{\delta s}{s} + \delta Z_W + \delta Z_{ZZ} \right] + \frac{c}{s} \delta Z_{AZ} \\
W^+ W^- AZ & \frac{c}{s} \left[1 + 2\delta Z_e - \frac{1}{c^2} \frac{\delta s}{s} + \delta Z_W + \frac{1}{2} \delta Z_{ZZ} + \frac{1}{2} \delta Z_{AA} \right] - \frac{1}{2} \delta Z_{AZ} - \frac{1}{2} \frac{c^2}{s^2} \delta Z_{ZA} \\
W^+ W^- AA & - \left[1 + 2\delta Z_e + \delta Z_W + \delta Z_{AA} \right] + \frac{c}{s} \delta Z_{ZA}
\end{array} \tag{A.29}$$

• VVV vertex:

$$\begin{array}{ccc}
V_{2,\nu}, k_2 & & \\
\swarrow & & \searrow \\
V_{1,\mu}, k_1 & \text{---} & V_{3,\rho}, k_3 \\
\searrow & & \swarrow \\
\hline
V_1 V_2 V_3 & C & \\
\hline
\end{array} = i e C \left[g_{\mu\nu} (k_1 - k_2)_\rho + g_{\nu\rho} (k_2 - k_3)_\mu + g_{\rho\mu} (k_3 - k_1)_\nu \right] \tag{A.31}$$

$$\begin{array}{ccc}
V_1 V_2 V_3 & C & \\
\hline
AW^+ W^- & 1 + \delta Z_e + \delta Z_W + \frac{1}{2} \delta Z_{AA} - \frac{1}{2} \frac{c}{s} \delta Z_{ZA} \\
ZW^+ W^- & -\frac{c}{s} (1 + \delta Z_e - \frac{1}{c^2} \frac{\delta s}{s} + \delta Z_W + \frac{1}{2} \delta Z_{ZZ}) + \frac{1}{2} \delta Z_{AZ}
\end{array} \tag{A.32}$$

- $SSSS$ vertex:

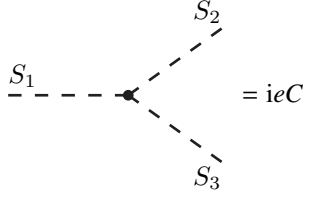


$$= ie^2 C \quad (A.33)$$

$S_1 S_2 S_3 S_4 \quad C$	$\frac{3}{4s^2} \frac{M_H^2}{M_W^2} \left[1 + 2\delta Z_e - 2\frac{\delta s}{s} + \frac{\delta M_H^2}{M_H^2} + \frac{e}{2sM_H^2 M_W} \delta t_{\text{PRTS}} - \frac{\delta M_W^2}{M_W^2} + 2\delta Z_H \right]$
$HHHH$	$-\frac{1}{4s^2} \frac{M_H^2}{M_W^2} \left[1 + 2\delta Z_e - 2\frac{\delta s}{s} + \frac{\delta M_H^2}{M_H^2} + \frac{e}{2sM_H^2 M_W} \delta t_{\text{PRTS}} - \frac{\delta M_W^2}{M_W^2} + \delta Z_H \right]$
$HH\chi\chi \quad \left. \begin{array}{l} HH\phi\phi \end{array} \right\}$	$-\frac{3}{4s^2} \frac{M_H^2}{M_W^2} \left[1 + 2\delta Z_e - 2\frac{\delta s}{s} + \frac{\delta M_H^2}{M_H^2} + \frac{e}{2sM_H^2 M_W} \delta t_{\text{PRTS}} - \frac{\delta M_W^2}{M_W^2} \right]$
$\chi\chi\chi\chi$	$-\frac{1}{4s^2} \frac{M_H^2}{M_W^2} \left[1 + 2\delta Z_e - 2\frac{\delta s}{s} + \frac{\delta M_H^2}{M_H^2} + \frac{e}{2sM_H^2 M_W} \delta t_{\text{PRTS}} - \frac{\delta M_W^2}{M_W^2} \right]$
$\chi\chi\phi\phi$	$-\frac{1}{2s^2} \frac{M_H^2}{M_W^2} \left[1 + 2\delta Z_e - 2\frac{\delta s}{s} + \frac{\delta M_H^2}{M_H^2} + \frac{e}{2sM_H^2 M_W} \delta t_{\text{PRTS}} - \frac{\delta M_W^2}{M_W^2} \right]$
$\phi\phi\phi\phi$	$-\frac{1}{2s^2} \frac{M_H^2}{M_W^2} \left[1 + 2\delta Z_e - 2\frac{\delta s}{s} + \frac{\delta M_H^2}{M_H^2} + \frac{e}{2sM_H^2 M_W} \delta t_{\text{PRTS}} - \frac{\delta M_W^2}{M_W^2} \right]$

$$(A.34)$$

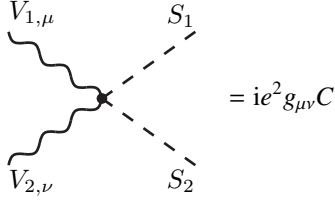
- SSS vertex:



$$= ieC \quad (A.35)$$

$S_1 S_2 S_3 \quad C$	$-\frac{3}{2s} \frac{M_H^2}{M_W^2} \left[1 + \delta Z_e - \frac{\delta s}{s} + \frac{\delta M_H^2}{M_H^2} + \frac{e}{2sM_H^2 M_W} (\delta t_{\text{PRTS}} - \delta t_{\text{FJTS}}) - \frac{1}{2} \frac{\delta M_W^2}{M_W^2} + \frac{3}{2} \delta Z_H \right]$
HHH	$-\frac{1}{2s} \frac{M_H^2}{M_W^2} \left[1 + \delta Z_e - \frac{\delta s}{s} + \frac{\delta M_H^2}{M_H^2} + \frac{e}{2sM_H^2 M_W} (\delta t_{\text{PRTS}} - \delta t_{\text{FJTS}}) - \frac{1}{2} \frac{\delta M_W^2}{M_W^2} + \frac{1}{2} \delta Z_H \right]$
$H\chi\chi \quad \left. \begin{array}{l} H\phi\phi \end{array} \right\}$	$(A.36)$

- $VVSS$ vertex:



$$= ie^2 g_{\mu\nu} C \quad (A.37)$$

$V_1 V_2 S_1 S_2 \quad C$	$W^+ W^- HH \quad \frac{1}{2s^2} \left[1 + 2\delta Z_e - 2\frac{\delta s}{s} + \delta Z_W + \delta Z_H \right]$
$W^+ W^- \chi\chi \quad \left. \begin{array}{l} W^+ W^- \phi^+ \phi^- \end{array} \right\}$	$\frac{1}{2s^2} \left[1 + 2\delta Z_e - 2\frac{\delta s}{s} + \delta Z_W \right]$
$ZZ\phi^+ \phi^-$	$\frac{(s^2 - c^2)^2}{2s^2 c^2} \left[1 + 2\delta Z_e + \frac{2}{(s^2 - c^2)c^2} \frac{\delta s}{s} + \delta Z_{ZZ} \right] + \frac{s^2 - c^2}{sc} \delta Z_{AZ}$
$Z A \phi^+ \phi^-$	$\frac{s^2 - c^2}{sc} \left[1 + 2\delta Z_e + \frac{1}{(s^2 - c^2)c^2} \frac{\delta s}{s} + \frac{1}{2} \delta Z_{ZZ} + \frac{1}{2} \delta Z_{AA} \right] + \frac{(s^2 - c^2)^2}{2s^2 c^2} \frac{1}{2} \delta Z_{ZA} + \delta Z_{AZ}$

$$\begin{aligned}
AA\phi^+\phi^- & 2\left[1 + 2\delta Z_e + \delta Z_{AA}\right] + \frac{s^2-c^2}{sc}\delta Z_{ZA} \\
ZZHH & \frac{1}{2s^2c^2}\left[1 + 2\delta Z_e + 2\frac{s^2-c^2}{c^2}\frac{\delta s}{s} + \delta Z_{ZZ} + \delta Z_H\right] \\
ZZ\chi\chi & \frac{1}{2s^2c^2}\left[1 + 2\delta Z_e + 2\frac{s^2-c^2}{c^2}\frac{\delta s}{s} + \delta Z_{ZZ}\right] \\
ZAH\bar{H} \quad \left. \begin{array}{l} \\ \end{array} \right\} & \frac{1}{2s^2c^2}\frac{1}{2}\delta Z_{ZA} \\
WA\phi^+H & -\frac{1}{2c}\left[1 + 2\delta Z_e - \frac{\delta c}{c} + \frac{1}{2}\delta Z_W + \frac{1}{2}\delta Z_H + \frac{1}{2}\delta Z_{ZZ}\right] - \frac{1}{2s}\frac{1}{2}\delta Z_{AZ} \\
WA\phi^+H & -\frac{1}{2s}\left[1 + 2\delta Z_e - \frac{\delta s}{s} + \frac{1}{2}\delta Z_W + \frac{1}{2}\delta Z_H + \frac{1}{2}\delta Z_{AA}\right] - \frac{1}{2c}\frac{1}{2}\delta Z_{ZA} \\
W^{\pm}Z\phi^{\mp}\chi & \mp\frac{i}{2c}\left[1 + 2\delta Z_e - \frac{\delta c}{c} + \frac{1}{2}\delta Z_W + \frac{1}{2}\delta Z_{ZZ}\right] \mp\frac{i}{2s}\frac{1}{2}\delta Z_{AZ} \\
W^{\pm}A\phi^{\mp}\chi & \mp\frac{i}{2s}\left[1 + 2\delta Z_e - \frac{\delta s}{s} + \frac{1}{2}\delta Z_W + \frac{1}{2}\delta Z_{AA}\right] \mp\frac{i}{2c}\frac{1}{2}\delta Z_{ZA}
\end{aligned} \tag{A.38}$$

• VSS vertex:

$$\begin{array}{c}
\text{---} \quad S_1, k_1 \\
\text{---} \quad V_\mu \quad \text{---} \\
\text{---} \quad S_2, k_2
\end{array} = ieC(k_1 - k_2)_\mu \tag{A.39}$$

$$\begin{array}{c}
VS_1S_2 \quad C \\
\hline
A\chi H & -\frac{i}{2cs}\frac{1}{2}\delta Z_{ZA} \\
Z\chi H & -\frac{i}{2cs}\left[1 + \delta Z_e + \frac{s^2-c^2}{c^2}\frac{\delta s}{s} + \frac{1}{2}\delta Z_H + \frac{1}{2}\delta Z_{ZZ}\right] \\
A\phi^+\phi^- & -\left[1 + \delta Z_e + \frac{1}{2}\delta Z_{AA} + \frac{s^2-c^2}{2sc}\frac{1}{2}\delta Z_{ZA}\right] \\
Z\phi^+\phi^- & -\frac{s^2-c^2}{2sc}\left[1 + \delta Z_e + \frac{1}{(s^2-c^2)c^2}\frac{\delta s}{s} + \frac{1}{2}\delta Z_{ZZ}\right] - \frac{1}{2}\delta Z_{AZ} \\
W^{\pm}\phi^+H & \mp\frac{1}{2s}\left[1 + \delta Z_e - \frac{\delta s}{s} + \frac{1}{2}\delta Z_W + \frac{1}{2}\delta Z_H\right] \\
W^{\pm}\phi^+\chi & -\frac{i}{2s}\left[1 + \delta Z_e - \frac{\delta s}{s} + \frac{1}{2}\delta Z_W\right]
\end{array} \tag{A.40}$$

• SVV vertex:

$$\begin{array}{c}
V_{1,\mu} \\
\text{---} \quad S \quad \text{---} \\
\text{---} \quad V_{2,\nu}
\end{array} = ie g_{\mu\nu} C \tag{A.41}$$

$S V_1 V_2$	C	
$HW^+ W^-$	$M_W \frac{1}{s} \left[1 + \delta Z_e - \frac{\delta s}{s} + \frac{1}{2} \frac{\delta M_W^2}{M_W^2} - \frac{e}{2s M_H^2 M_W} \delta t_{\text{FJTS}} + \frac{1}{2} \delta Z_H + \delta Z_W \right]$	
HZZ	$M_W \frac{1}{sc^2} \left[1 + \delta Z_e + \frac{2s^2 - c^2}{c^2} \frac{\delta s}{s} + \frac{1}{2} \frac{\delta M_W^2}{M_W^2} - \frac{e}{2s M_H^2 M_W} \delta t_{\text{FJTS}} + \frac{1}{2} \delta Z_H + \delta Z_{ZZ} \right]$	
HZA	$M_W \frac{1}{sc^2} \frac{1}{2} \delta Z_{ZA}$	
$\phi^\pm W^\mp Z$	$-M_W \frac{s}{c} \left[1 + \delta Z_e + \frac{1}{c^2} \frac{\delta s}{s} + \frac{1}{2} \frac{\delta M_W^2}{M_W^2} - \frac{e}{2s M_H^2 M_W} \delta t_{\text{FJTS}} + \frac{1}{2} \delta Z_W + \frac{1}{2} \delta Z_{ZZ} \right] - M_W \frac{1}{2} \delta Z_{AZ}$	(A.42)
$\phi^\pm W^\mp A$	$-M_W \left[1 + \delta Z_e + \frac{1}{2} \frac{\delta M_W^2}{M_W^2} - \frac{e}{2s M_H^2 M_W} \delta t_{\text{FJTS}} + \frac{1}{2} \delta Z_W + \frac{1}{2} \delta Z_{AA} \right] - M_W \frac{s}{c} \frac{1}{2} \delta Z_{ZA}$	

• $V\bar{F}F$ vertex:



$V\bar{F}_1 F_2$	C_R, C_L	
$A \bar{f}_i f_j$	$\begin{cases} C_R = -Q_f \left[\delta_{ij} \left(1 + \delta Z_e + \frac{1}{2} \delta Z_{AA} \right) + \frac{1}{2} \left(\delta Z_{ij}^{f,R} + \delta Z_{ij}^{f,R\dagger} \right) \right] + \delta_{ij} g_f^+ \frac{1}{2} \delta Z_{ZA} \\ C_L = -Q_f \left[\delta_{ij} \left(1 + \delta Z_e + \frac{1}{2} \delta Z_{AA} \right) + \frac{1}{2} \left(\delta Z_{ij}^{f,L} + \delta Z_{ij}^{f,L\dagger} \right) \right] + \delta_{ij} g_f^- \frac{1}{2} \delta Z_{ZA} \end{cases}$	
$Z \bar{f}_i f_j$	$\begin{cases} C_R = g_f^+ \left[\delta_{ij} \left(1 + \frac{\delta g_f^+}{g_f^+} + \frac{1}{2} \delta Z_{ZZ} \right) + \frac{1}{2} \left(\delta Z_{ij}^{f,R} + \delta Z_{ij}^{f,R\dagger} \right) \right] - \delta_{ij} Q_f \frac{1}{2} \delta Z_{AZ} \\ C_L = g_f^- \left[\delta_{ij} \left(1 + \frac{\delta g_f^-}{g_f^-} + \frac{1}{2} \delta Z_{ZZ} \right) + \frac{1}{2} \left(\delta Z_{ij}^{f,L} + \delta Z_{ij}^{f,L\dagger} \right) \right] - \delta_{ij} Q_f \frac{1}{2} \delta Z_{AZ} \end{cases}$	
$W^+ \bar{u}_i d_j$	$C_R = 0, \quad C_L = \frac{1}{\sqrt{2}s} \left[V_{ij} \left(1 + \delta Z_e - \frac{\delta s}{s} + \frac{1}{2} \delta Z_W \right) + \delta V_{ij} + \frac{1}{2} \sum_k \left(\delta Z_{ik}^{u,L\dagger} V_{kj} + V_{ik} \delta Z_{kj}^{u,L} \right) \right]$	
$W^- \bar{d}_j u_i$	$C_R = 0, \quad C_L = \frac{1}{\sqrt{2}s} \left[V_{ji}^\dagger \left(1 + \delta Z_e - \frac{\delta s}{s} + \frac{1}{2} \delta Z_W \right) + \delta V_{ji}^\dagger + \frac{1}{2} \sum_k \left(\delta Z_{jk}^{d,L\dagger} V_{ki}^\dagger + V_{jk}^\dagger \delta Z_{ki}^{u,L} \right) \right]$	
$W^+ \bar{\nu}_i l_j$	$C_R = 0, \quad C_L = \frac{1}{\sqrt{2}s} \delta_{ij} \left[1 + \delta Z_e - \frac{\delta s}{s} + \frac{1}{2} \delta Z_W + \frac{1}{2} \left(\delta Z_{ii}^{v,L\dagger} + \delta Z_{ii}^{l,L} \right) \right]$	
$W^- \bar{l}_j \nu_i$	$C_R = 0, \quad C_L = \frac{1}{\sqrt{2}s} \delta_{ij} \left[1 + \delta Z_e - \frac{\delta s}{s} + \frac{1}{2} \delta Z_W + \frac{1}{2} \left(\delta Z_{ii}^{l,L\dagger} + \delta Z_{ii}^{v,L} \right) \right]$	(A.44)

where

$$\begin{aligned} g_f^+ &= -\frac{s}{c} Q_f, & \delta g_f^+ &= -\frac{s}{c} Q_f \left[\delta Z_e + \frac{1}{c^2} \frac{\delta s}{s} \right], \\ g_f^- &= \frac{I_{W,f}^3 - s^2 Q_f}{sc}, & \delta g_f^- &= \frac{I_{W,f}^3}{sc} \left[\delta Z_e + \frac{s^2 - c^2}{c^2} \frac{\delta s}{s} \right] + \delta g_f^+. \end{aligned} \quad (\text{A.45})$$

The vector and axial-vector couplings of the Z -boson are given by

$$v_f = \frac{1}{2} (g_f^- + g_f^+) = \frac{I_{W,f}^3 - 2s^2 Q_f}{2sc}, \quad a_f = \frac{1}{2} (g_f^- - g_f^+) = \frac{I_{W,f}^3}{2sc}. \quad (\text{A.46})$$

• $S\bar{F}F$ vertex:



$S \bar{F}_1 F_2$	C_R, C_L
$H \bar{f}_i f_j$	
$\left\{ \begin{array}{l} C_R = -\frac{1}{2s} \frac{1}{M_W} \left[\delta_{ij} m_{f,i} \left(1 + \delta Z_e - \frac{\delta s}{s} + \frac{\delta m_{f,i}}{m_{f,i}} - \frac{1}{2} \frac{\delta M_W^2}{M_W^2} + \frac{1}{2} \delta Z_H \right) + \frac{1}{2} \left(m_{f,i} \delta Z_{ij}^{f,R} + \delta Z_{ij}^{f,L\dagger} m_{f,j} \right) \right] \\ C_L = -\frac{1}{2s} \frac{1}{M_W} \left[\delta_{ij} m_{f,i} \left(1 + \delta Z_e - \frac{\delta s}{s} + \frac{\delta m_{f,i}}{m_{f,i}} - \frac{1}{2} \frac{\delta M_W^2}{M_W^2} + \frac{1}{2} \delta Z_H \right) + \frac{1}{2} \left(m_{f,i} \delta Z_{ij}^{f,L} + \delta Z_{ij}^{f,R\dagger} m_{f,j} \right) \right] \end{array} \right.$	
$\chi \bar{f}_i f_j$	
$\left\{ \begin{array}{l} C_R = i \frac{1}{2s} 2I_{W,f}^3 \frac{1}{M_W} \left[\delta_{ij} m_{f,i} \left(1 + \delta Z_e - \frac{\delta s}{s} + \frac{\delta m_{f,i}}{m_{f,i}} - \frac{1}{2} \frac{\delta M_W^2}{M_W^2} \right) + \frac{1}{2} \left(m_{f,i} \delta Z_{ij}^{f,R} + \delta Z_{ij}^{f,L\dagger} m_{f,j} \right) \right] \\ C_L = -i \frac{1}{2s} 2I_{W,f}^3 \frac{1}{M_W} \left[\delta_{ij} m_{f,i} \left(1 + \delta Z_e - \frac{\delta s}{s} + \frac{\delta m_{f,i}}{m_{f,i}} - \frac{1}{2} \frac{\delta M_W^2}{M_W^2} \right) + \frac{1}{2} \left(m_{f,i} \delta Z_{ij}^{f,L} + \delta Z_{ij}^{f,R\dagger} m_{f,j} \right) \right] \end{array} \right.$	
$\phi^+ \bar{u}_i d_j$	
$\left\{ \begin{array}{l} C_R = -\frac{1}{\sqrt{2}s} \frac{1}{M_W} \left[V_{ij} m_{d,j} \left(1 + \delta Z_e - \frac{\delta s}{s} + \frac{\delta m_{d,j}}{m_{d,j}} - \frac{1}{2} \frac{\delta M_W^2}{M_W^2} \right) + \delta V_{ij} m_{d,j} \right. \\ \quad \left. + \frac{1}{2} \sum_k \left(\delta Z_{ik}^{u,L\dagger} V_{kj} m_{d,j} + V_{ik} m_{d,k} \delta Z_{kj}^{d,R} \right) \right] \\ C_L = \frac{1}{\sqrt{2}s} \frac{1}{M_W} \left[m_{u,i} V_{ij} \left(1 + \delta Z_e - \frac{\delta s}{s} + \frac{\delta m_{u,i}}{m_{u,i}} - \frac{1}{2} \frac{\delta M_W^2}{M_W^2} \right) + m_{u,i} \delta V_{ij} \right. \\ \quad \left. + \frac{1}{2} \sum_k \left(\delta Z_{ik}^{u,R\dagger} m_{u,k} V_{kj} + m_{u,i} V_{ik} \delta Z_{kj}^{d,L} \right) \right] \end{array} \right.$	
$\phi^- \bar{d}_j u_i$	
$\left\{ \begin{array}{l} C_R = \frac{1}{\sqrt{2}s} \frac{1}{M_W} \left[V_{ji}^\dagger m_{u,i} \left(1 + \delta Z_e - \frac{\delta s}{s} + \frac{\delta m_{u,i}}{m_{u,i}} - \frac{1}{2} \frac{\delta M_W^2}{M_W^2} \right) + \delta V_{ji}^\dagger m_{u,i} \right. \\ \quad \left. + \frac{1}{2} \sum_k \left(\delta Z_{jk}^{d,L\dagger} V_{ki}^\dagger m_{u,i} + V_{jk}^\dagger m_{u,k} \delta Z_{ki}^{u,R} \right) \right] \\ C_L = -\frac{1}{\sqrt{2}s} \frac{1}{M_W} \left[m_{d,j} V_{ji}^\dagger \left(1 + \delta Z_e - \frac{\delta s}{s} + \frac{\delta m_{d,j}}{m_{d,j}} - \frac{1}{2} \frac{\delta M_W^2}{M_W^2} \right) + m_{d,j} \delta V_{ji}^\dagger \right. \\ \quad \left. + \frac{1}{2} \sum_k \left(\delta Z_{jk}^{d,R\dagger} m_{d,k} V_{ki}^\dagger + m_{d,j} V_{jk}^\dagger \delta Z_{ki}^{u,L} \right) \right] \end{array} \right.$	
$\phi^+ \bar{v}_i l_j$	$C_R = -\frac{1}{\sqrt{2}s} \frac{m_{l,i}}{M_W} \delta_{ij} \left[1 + \delta Z_e - \frac{\delta s}{s} + \frac{\delta m_{l,i}}{m_{l,i}} - \frac{1}{2} \frac{\delta M_W^2}{M_W^2} + \frac{1}{2} \left(\delta Z_{ii}^{v,L\dagger} + \delta Z_{ii}^{l,R} \right) \right], \quad C_L = 0$
$\phi^- \bar{l}_j v_i$	$C_R = 0, \quad C_L = -\frac{1}{\sqrt{2}s} \frac{m_{l,i}}{M_W} \delta_{ij} \left[1 + \delta Z_e - \frac{\delta s}{s} + \frac{\delta m_{l,i}}{m_{l,i}} - \frac{1}{2} \frac{\delta M_W^2}{M_W^2} + \frac{1}{2} \left(\delta Z_{ii}^{l,R\dagger} + \delta Z_{ii}^{v,L} \right) \right]$

• $V \bar{U} U$ vertex:

(A.49)

$V \bar{U}_1 U_2$	C	$V \bar{U}_1 U_2$	C
$A \bar{u}^\pm u^\pm, W^\mp \bar{u}^\mp u^A, W^\pm \bar{u}^A u^\mp$	± 1	$A \bar{u}^\pm u^\pm, W^\mp \bar{u}^\mp u^Z, W^\pm \bar{u}^Z u^\mp$	$\mp \frac{c}{s}$

• $S \bar{U} U$ vertex:

(A.51)

$S \bar{U}_1 U_2$	C	$S \bar{U}_1 U_2$	C	$S \bar{U}_1 U_2$	C
$H \bar{u}^Z u^Z$	$-\frac{1}{2sc} M_W \xi_Z$	$\chi \bar{u}^\pm u^\pm$	$\mp i \frac{1}{2s} M_W \xi_W$	$\phi^\pm \bar{u}^\pm u^Z$	$-\frac{s^2 - c^2}{2sc} M_W \xi_W$
$H \bar{u}^\pm u^\pm$	$-\frac{1}{2s} M_W \xi_W$	$\phi^\pm \bar{u}^Z u^\mp$	$\frac{1}{2sc} M_W \xi_Z$	$\phi^\pm \bar{u}^\pm u^A$	$M_W \xi_W$

Feynman rules for the EWSM in the background-field formalism

We provide the Feynman rules in the BFM 't Hooft gauge, as given in Eqs. (56) and (57), for an arbitrary quantum gauge parameter $\xi = \xi_W = \xi_B$. In this gauge all propagators are diagonal. We neglect quark mixing as in Ref. [107], but include the one-loop contributions of the counterterms from the renormalization of physical parameters and fields in the vertices that involve only background fields. While the Feynman rules for these vertices are equivalent to those of the conventional formalism, the counterterms have a much simpler structure. We do not include counterterms for vertices involving quantum fields, as these are not required for one-loop calculations. Furthermore, we assume $\delta Z^{f,L} = (\delta Z^{f,L})^\dagger$ and $\delta Z^{f,R} = (\delta Z^{f,R})^\dagger$. Note that these conditions are not needed in the complex renormalization as carried out in the CMS in Section 6.6, because we rescale spinors and corresponding adjoint spinors by the same field renormalization constants, so that complex conjugated field renormalization constants never appear in counterterms [cf. Eq. (579)].

The tadpole counterterms δt are given both in the FJTS [147, 169, 170] and in the (PRTS) scheme of Ref. [40], as described in Section 3.1.6. The respective tadpole terms are called δt_{FJTS} or δt_{PRTS} ; whenever δt is written without subscript FJTS or PRTS, this term contributes in both schemes. We note that the following Feynman rules do not only involve explicit δt_{FJTS} terms, but also implicit δt_{FJTS} terms contained in the renormalization constant $\delta Z_{\hat{H}}$ defined in Eq. (158). Whenever the $\delta Z_{\hat{H}}$ term does not entirely originate from external Higgs or would-be Goldstone fields, the explicit δt_{FJTS} term does not exactly correspond to its counterterm in the conventional Feynman rules listed above.

We do not list Feynman rules for the propagators of the background fields and assume that the vertices are not affected by the gauge fixing for the background fields, which holds for linear gauges. The gauge fixing for the background fields can be chosen independently from the gauge-fixing of the quantum fields. In a background 't Hooft gauge, the background-field propagators take the same form as the propagators in the conventional gauge, given in Eqs. (A.16)–(A.19), with ξ_V replaced by the background gauge parameter $\hat{\xi}_V$. Note, however, that it is sometimes preferable to use a more convenient gauge for the background fields like the unitary gauge.

The propagators for the quantum field have the same form as those in the conventional formalism given in Eqs. (A.16)–(A.19) with ξ_V replaced by the quantum gauge parameter ξ .

Vertices between background fields and symmetric counterterms

- tadpole

$$\cancel{\times} - - \frac{\hat{H}}{\text{---}} = i\delta t \quad (\text{A.53})$$

- $\hat{V}\hat{V}$ counterterm

$$\cancel{\text{---}}^{\hat{V}_{1,\mu}, k} \cancel{\times} \cancel{\text{---}}^{\hat{V}_{2,\nu}} = i[(-g_{\mu\nu}k^2 + k_\mu k_\nu)C_1 + g_{\mu\nu}C_2] \quad (\text{A.54})$$

$$\begin{array}{ccccc} \hat{V}_1 \hat{V}_2 & \hat{W}^+ \hat{W}^- & \hat{Z} \hat{Z} & \hat{A} \hat{Z} & \hat{A} \hat{A} \\ \hline C_1 & \delta Z_{\hat{W}} & \delta Z_{\hat{Z} \hat{Z}} & \frac{1}{2} \delta Z_{\hat{A} \hat{Z}} & \delta Z_{\hat{A} \hat{A}} \\ C_2 & \delta Z_{\hat{H}} M_W^2 & \delta Z_{\hat{H}} M_Z^2 & 0 & 0 \end{array} \quad (\text{A.55})$$

- $\hat{V}\hat{S}$ counterterm

$$\cancel{\text{---}}^{\hat{V}_\mu, k} \cancel{\times} - - - \frac{\hat{S}}{\text{---}} = i k_\mu C \delta Z_{\hat{H}} \quad (\text{A.56})$$

$$\begin{array}{ccc} \hat{V}\hat{S} & \hat{W}^\pm \hat{\phi}^\mp & \hat{Z} \hat{\chi} \\ \hline C & \pm M_W & i M_Z \end{array} \quad (\text{A.57})$$

- $\hat{S}\hat{S}$ counterterm

$$\cancel{\text{---}}^{\hat{S}_1, k} - - - \cancel{\times} - - - \frac{\hat{S}_2}{\text{---}} = i[\delta Z_{\hat{H}} k^2 - C] \quad (\text{A.58})$$

$$\frac{\hat{S}_1 \hat{S}_2}{C} \frac{\hat{H} \hat{H}}{\delta Z_{\hat{H}} M_H^2 + \delta M_H^2 - \frac{3e}{2sM_W} \delta t_{\text{FJTS}}} \frac{\hat{\chi} \hat{\chi}, \hat{\phi} \hat{\phi}}{-\frac{e}{2s} \frac{\delta t}{M_W}} \quad (\text{A.59})$$

- $F\bar{F}$ counterterm

$$f, k \xrightarrow{\times} \bar{f} = i[\delta Z^{f,\text{L}} \not{k} \omega_- + \delta Z^{f,\text{R}} \not{k} \omega_+ - C_S] \quad (\text{A.60})$$

$$C_S = \frac{1}{2} (\delta Z^{f,\text{L}} + \delta Z^{f,\text{R}}) m_f + \delta m_f - m_f \frac{e}{2sM_H^2 M_W} \delta t_{\text{FJTS}} \quad (\text{A.61})$$

- $\hat{V}\hat{V}\hat{V}\hat{V}$ vertex:

$$\begin{array}{c} \hat{V}_{1,\mu} \quad \hat{V}_{3,\rho} \\ \swarrow \quad \searrow \\ \text{---} \quad \text{---} \\ \hat{V}_{2,\nu} \quad \hat{V}_{4,\sigma} \end{array} = ie^2 C [2g_{\mu\nu}g_{\rho\sigma} - g_{\mu\sigma}g_{\nu\rho} - g_{\mu\rho}g_{\nu\sigma}] (1 + \delta Z_{\hat{W}}) \quad (\text{A.62})$$

$$\frac{\hat{V}_1 \hat{V}_2 \hat{V}_3 \hat{V}_4}{C} \frac{\hat{W}^+ \hat{W}^+ \hat{W}^- \hat{W}^-}{\frac{1}{s^2}} \frac{\hat{W}^+ \hat{W}^- \hat{Z} \hat{Z}}{-\frac{c^2}{s^2}} \frac{\hat{W}^+ \hat{W}^- \hat{A} \hat{Z}}{\frac{c}{s}} \frac{\hat{W}^+ \hat{W}^- \hat{A} \hat{A}}{-1} \quad (\text{A.63})$$

- $\hat{V}\hat{V}\hat{V}$ vertex:

$$\begin{array}{c} \hat{V}_{2,\nu}, k_2 \\ \swarrow \quad \searrow \\ \hat{V}_{1,\mu}, k_1 \\ \text{---} \quad \text{---} \\ \hat{V}_{3,\rho}, k_3 \end{array} = ieC [g_{\mu\nu}(k_1 - k_2)_\rho + g_{\nu\rho}(k_2 - k_3)_\mu + g_{\rho\mu}(k_3 - k_1)_\nu] (1 + \delta Z_{\hat{W}}) \quad (\text{A.64})$$

$$\frac{\hat{V}_1 \hat{V}_2 \hat{V}_3}{C} \frac{\hat{A} \hat{W}^+ \hat{W}^-}{1} \frac{\hat{Z} \hat{W}^+ \hat{W}^-}{-\frac{c}{s}} \quad (\text{A.65})$$

- $\hat{S}\hat{S}\hat{S}\hat{S}$ vertex:

$$\begin{array}{c} \hat{S}_1 \quad \hat{S}_3 \\ \text{---} \quad \text{---} \\ \text{---} \quad \text{---} \\ \hat{S}_2 \quad \hat{S}_4 \end{array} = ie^2 C \left[1 + \frac{\delta M_H^2}{M_H^2} + \frac{e}{2sM_W M_H^2} (\delta t_{\text{PRTS}} - 2\delta t_{\text{FJTS}}) + \delta Z_{\hat{H}} \right] \quad (\text{A.66})$$

$$\frac{\hat{S}_1 \hat{S}_2 \hat{S}_3 \hat{S}_4}{C} \frac{\hat{H} \hat{H} \hat{H} \hat{H}}{-\frac{3}{4s^2} \frac{M_H^2}{M_W^2}} \frac{\hat{\chi} \hat{\chi} \hat{\chi} \hat{\chi}}{-\frac{1}{4s^2} \frac{M_H^2}{M_W^2}} \frac{\hat{H} \hat{H} \hat{\phi}^+ \hat{\phi}^-}{-\frac{1}{2s^2} \frac{M_H^2}{M_W^2}} \quad (\text{A.67})$$

- $\hat{S}\hat{S}\hat{S}$ vertex:

$$\begin{array}{c} \hat{S}_2 \\ \text{---} \quad \text{---} \\ \hat{S}_1 \quad \text{---} \quad \text{---} \\ \text{---} \quad \text{---} \quad \text{---} \\ \hat{S}_3 \end{array} = ieC \left[1 + \frac{\delta M_H^2}{M_H^2} + \frac{e}{2sM_W M_H^2} (\delta t_{\text{PRTS}} - 2\delta t_{\text{FJTS}}) + \delta Z_{\hat{H}} \right] \quad (\text{A.68})$$

$$\frac{\hat{S}_1 \hat{S}_2 \hat{S}_3}{C} \quad \frac{\hat{H} \hat{H} \hat{H}}{-\frac{3}{2s} \frac{M_H^2}{M_W}} \quad \frac{\hat{H} \hat{\chi} \hat{\chi}, \hat{H} \hat{\phi}^+ \hat{\phi}^-}{-\frac{1}{2s} \frac{M_H^2}{M_W}} \quad (A.69)$$

• $\hat{V} \hat{V} \hat{S} \hat{S}$ vertex:

$$\begin{array}{c} \hat{V}_{1,\mu} \quad \hat{S}_1 \\ \text{---} \quad \text{---} \\ \hat{V}_{2,\nu} \quad \hat{S}_2 \end{array} = ie^2 g_{\mu\nu} C (1 + \delta Z_{\hat{H}}) \quad (A.70)$$

$$\begin{array}{ccccccc} \hat{V}_1 \hat{V}_2 \hat{S}_1 \hat{S}_2 & \hat{Z} \hat{Z} \hat{H} \hat{H}, \hat{Z} \hat{Z} \hat{\chi} \hat{\chi} & \hat{W}^+ \hat{W}^- \hat{H} \hat{H}, \hat{W}^+ \hat{W}^- \hat{\phi}^+ \hat{\phi}^- & \hat{W}^+ \hat{W}^- \hat{\chi} \hat{\chi} & \hat{A} \hat{A} \hat{\phi}^+ \hat{\phi}^- & \hat{Z} \hat{A} \hat{\phi}^+ \hat{\phi}^- & \hat{Z} \hat{Z} \hat{\phi}^+ \hat{\phi}^- \\ \hline C & \frac{1}{2c^2 s^2} & \frac{1}{2s^2} & 2 & -\frac{c^2 - s^2}{cs} & \frac{(c^2 - s^2)^2}{2c^2 s^2} \\ \hat{V}_1 \hat{V}_2 \hat{S}_1 \hat{S}_2 & \hat{W}^\pm \hat{A} \hat{\phi}^\mp \hat{H} & \hat{W}^\pm \hat{A} \hat{\phi}^\mp \hat{\chi} & \hat{W}^\pm \hat{Z} \hat{\phi}^\mp \hat{H} & \hat{W}^\pm \hat{Z} \hat{\phi}^\mp \hat{\chi} \\ \hline C & -\frac{1}{2s} & \mp \frac{i}{2s} & -\frac{1}{2c} & \mp \frac{i}{2c} \end{array} \quad (A.71)$$

• $\hat{V} \hat{S} \hat{S}$ vertex:

$$\begin{array}{c} \hat{S}_1, k_1 \\ \text{---} \\ \hat{S}_2, k_2 \end{array} = ie C (k_1 - k_2)_\mu (1 + \delta Z_{\hat{H}}) \quad (A.72)$$

$$\begin{array}{cccccc} \hat{V}_1 \hat{S}_1 \hat{S}_2 & \hat{Z} \hat{\chi} \hat{H} & \hat{A} \hat{\phi}^+ \hat{\phi}^- & \hat{Z} \hat{\phi}^+ \hat{\phi}^- & \hat{W}^\pm \hat{\phi}^\mp \hat{H} & \hat{W}^\pm \hat{\phi}^\mp \hat{\chi} \\ \hline C & -\frac{i}{2cs} & -1 & \frac{c^2 - s^2}{2cs} & \mp \frac{1}{2s} & -\frac{i}{2s} \end{array} \quad (A.73)$$

• $\hat{S} \hat{V} \hat{V}$ vertex:

$$\begin{array}{c} \hat{V}_{1,\mu} \\ \text{---} \\ \hat{V}_{2,\nu} \end{array} = ie g_{\mu\nu} C (1 + \delta Z_{\hat{H}}) \quad (A.74)$$

$$\begin{array}{ccccc} \hat{S} \hat{V}_1 \hat{V}_2 & \hat{H} \hat{Z} \hat{Z} & \hat{H} \hat{W}^+ \hat{W}^- & \hat{\phi}^\pm \hat{W}^\mp \hat{A} & \hat{\phi}^\pm \hat{W}^\mp \hat{Z} \\ \hline C & \frac{1}{c^2 s} M_W & \frac{1}{s} M_W & -M_W & -\frac{s}{c} M_W \end{array} \quad (A.75)$$

• $\hat{V} \bar{F} F$ vertex:

$$\begin{array}{c} \hat{V}_\mu \\ \text{---} \\ \text{---} \end{array} = ie \gamma_\mu [C_L \omega_- (1 + \delta Z^{F_1, L}) + C_R \omega_+ (1 + \frac{1}{2} (\delta Z^{F_1, R} + \delta Z^{F_2, R}))] \quad (A.76)$$

$$\begin{array}{cccc} \hat{V}\bar{F}_1F_2 & \hat{A}\bar{f}f & \hat{Z}\bar{f}f & \hat{W}^+\bar{f}_uf_d, \hat{W}^-\bar{f}_df_u \\ \hline C_L & -Q_f & \frac{I_{w,f}^3 - s^2 Q_f}{cs} & \frac{1}{\sqrt{2}s} \\ C_R & -Q_f & -\frac{s}{c}Q_f & 0 \end{array} \quad (A.77)$$

- $\hat{S}\bar{F}F$ vertex:



$$= ie \left[C_L \omega_- \left(1 + \frac{\delta m_{F_1}}{m_{F_1}} + \frac{1}{2} \delta Z^{F_2, L} + \frac{1}{2} \delta Z^{F_1, R} - \frac{e}{2sM_W M_H} \delta t_{\text{FJTS}} \right) + C_R \omega_+ \left(1 + \frac{\delta m_{F_2}}{m_{F_2}} + \frac{1}{2} \delta Z^{F_1, L} + \frac{1}{2} \delta Z^{F_2, R} - \frac{e}{2sM_W M_H} \delta t_{\text{FJTS}} \right) \right] \quad (\text{A.78})$$

$$\begin{array}{ccccc}
\hat{S} \bar{F}_1 F_2 & \hat{H} \bar{f} f & \hat{\chi} \bar{f} f & \hat{\phi}^+ \bar{f}_u f_d & \hat{\phi}^- \bar{f}_d f_u \\
\hline
C_L & -\frac{1}{2s} \frac{m_f}{M_W} & -i \frac{1}{2s} 2I_{w,f}^3 \frac{m_f}{M_W} & + \frac{1}{\sqrt{2}s} \frac{m_{fu}}{M_W} & - \frac{1}{\sqrt{2}s} \frac{m_{fd}}{M_W} \\
C_R & -\frac{1}{2s} \frac{m_f}{M_W} & +i \frac{1}{2s} 2I_{w,f}^3 \frac{m_f}{M_W} & - \frac{1}{\sqrt{2}s} \frac{m_{fd}}{M_W} & + \frac{1}{\sqrt{2}s} \frac{m_{fu}}{M_W}
\end{array} \tag{A.79}$$

In contrast to the conventional formalism, no counterterms are present for the $\hat{Z}\hat{A}\hat{H}\hat{H}$, $\hat{Z}\hat{A}\hat{\chi}\hat{\chi}$, $\hat{A}\hat{\chi}\hat{H}$, and $\hat{H}\hat{Z}\hat{A}$ couplings.

Vertices involving quantum fields

We provide the Feynman rules for vertices containing quantum fields in lowest order, i.e. we do not list the corresponding counterterms. All lowest-order vertices involving fermions have the usual form and are not separately listed. Since the gauge-fixing term is quadratic in the quantum fields, only vertices containing exactly two quantum fields or containing ghost fields differ from the conventional ones. In the following, we list only those couplings for which the generic form or actual insertion differ from the results in the conventional formalism. The vertices of types $\hat{V}\hat{V}SS$, $\hat{S}\hat{S}VV$, $\hat{V}SS$, $\hat{S}VV$, $V\bar{U}U$, and $S\bar{U}U$ have the usual Feynman rules (with $\xi_Z, \xi_W \rightarrow \xi$). Note that some of the insertions appearing in the conventional couplings have no counterparts here; we list only the non-vanishing insertions.

- $\hat{V}\hat{V}VV$ vertex: Here two types of Feynman rules exist.

$$\begin{array}{cccccc}
\hat{V}_1 \hat{V}_2 V_3 V_4 & \hat{W}^\pm \hat{W}^\pm W^\mp W^\mp & \hat{Z} \hat{Z} W^+ W^- & \hat{W}^+ \hat{W}^- ZZ & \hat{A} \hat{Z} W^+ W^- & \hat{A} \hat{A} W^+ W^- & \hat{W}^+ \hat{W}^- AA \\
\hline
C & \frac{1}{s^2} & -\frac{c^2}{s^2} & \frac{c}{s} & & -1 & \\
\end{array} \quad (A.81)$$



$$= i e^2 C \left[2g_{\mu\rho}g_{\nu\sigma} - g_{\mu\nu}g_{\rho\sigma} - g_{\mu\sigma}g_{\nu\rho} \left(1 + \frac{1}{\xi} \right) \right] \quad (\text{A.82})$$

$$\begin{array}{ccccc} \hat{V}_1 \hat{V}_2 V_3 V_4 & \hat{W}^+ \hat{W}^- W^+ W^- & \hat{W}^\pm \hat{Z} W^\mp Z & \hat{W}^\pm \hat{A} W^\mp Z, \hat{W}^\pm \hat{Z} W^\mp A & \hat{W}^\pm \hat{A} W^\mp A \\ \hline C & \frac{1}{s^2} & -\frac{c^2}{s^2} & \frac{c}{s} & -1 \end{array} \quad (\text{A.83})$$

- $\hat{V}VV$ vertex:

$$\begin{array}{c}
 \text{Diagram: } \hat{V}_{1,\mu, k_1} \text{ (wavy line)} \text{ and } \hat{V}_{2,\nu, k_2} \text{ (wavy line)} \text{ and } \hat{V}_{3,\rho, k_3} \text{ (wavy line)} \\
 \text{Equation: } = -ieC \left[g_{\nu\rho}(k_3 - k_2)_\mu + g_{\mu\nu} \left(k_2 - k_1 + \frac{k_3}{\xi} \right)_\rho + g_{\rho\mu} \left(k_1 - k_3 - \frac{k_2}{\xi} \right)_\nu \right]
 \end{array} \quad (\text{A.84})$$

$$\begin{array}{cccc}
 \hat{V}_1 V_2 V_3 & \hat{A} W^+ W^- & \hat{W}^+ W^- A & \hat{W}^- A W^+ \\
 \hline
 C & 1 & & -\frac{c}{s}
 \end{array} \quad (\text{A.85})$$

- $\hat{S} \hat{S} S S$ vertex:

$$\begin{array}{c}
 \text{Diagram: } \hat{S}_1 \text{ (dashed line)} \text{ and } S_3 \text{ (dashed line)} \\
 \text{Equation: } = ie^2 C
 \end{array} \quad (\text{A.86})$$

$$\begin{array}{ccccc}
 \hat{S}_1 \hat{S}_2 S_3 S_4 & \hat{H} \hat{H} H H & \hat{H} \hat{H} \chi \chi & \hat{H} \hat{\chi} H \chi & \hat{\phi}^+ \hat{\phi}^- H H, \hat{H} \hat{H} \phi^+ \phi^- \\
 \hat{\chi} \hat{\chi} \chi \chi & \hat{\chi} \hat{\chi} H H & & & \hat{\phi}^+ \hat{\phi}^- \chi \chi, \hat{\chi} \hat{\chi} \phi^+ \phi^- \\
 \hline
 C & -\frac{3}{4s^2} \frac{M_H^2}{M_W^2} & -\frac{1}{4s^2} \frac{M_H^2}{M_W^2} - \frac{\xi}{2c^2 s^2} & -\frac{1}{4s^2} \frac{M_H^2}{M_W^2} + \frac{\xi}{4c^2 s^2} & -\frac{1}{4s^2} \frac{M_H^2}{M_W^2} - \frac{\xi}{2s^2} \\
 \hat{S}_1 \hat{S}_2 S_3 S_4 & \hat{\phi}^\pm \hat{H} \phi^\mp H & \hat{\phi}^+ \hat{\phi}^- \phi^+ \phi^- & \hat{\phi}^\pm \hat{\phi}^\pm \phi^\mp \phi^\mp & \hat{\phi}^\pm \hat{H} \phi^\mp \chi \\
 \hat{\phi}^\pm \hat{\chi} \phi^\mp \chi & & & & \hat{\phi}^\mp \hat{\chi} \phi^\pm H \\
 \hline
 C & -\frac{1}{4s^2} \frac{M_H^2}{M_W^2} + \frac{\xi}{4s^2} & -\frac{1}{2s^2} \frac{M_H^2}{M_W^2} - \frac{\xi}{4c^2 s^2} & -\frac{1}{2s^2} \frac{M_H^2}{M_W^2} + \frac{\xi}{2c^2 s^2} & \mp \frac{i\xi}{4c^2}
 \end{array} \quad (\text{A.87})$$

- $\hat{S} S S$ vertex:

$$\begin{array}{c}
 \text{Diagram: } \hat{S}_1 \text{ (dashed line)} \text{ and } S_2 \text{ (dashed line)} \\
 \text{Equation: } = ieC
 \end{array} \quad (\text{A.88})$$

$$\begin{array}{ccccccc}
 \hat{S}_1 S_2 S_3 & \hat{H} H H & \hat{H} \chi \chi & \hat{\chi} H \chi & \hat{H} \phi^+ \phi^- & \hat{\phi}^\pm \phi^\mp H & \hat{\phi}^\pm \phi^\mp \chi \\
 \hline
 C & -\frac{3}{2s} \frac{M_H^2}{M_W^2} & -\frac{1}{2s} \frac{M_H^2}{M_W^2} - \xi \frac{M_W}{c^2 s} & -\frac{1}{2s} \frac{M_H^2}{M_W^2} + \xi \frac{M_W}{2c^2 s} & -\frac{1}{2s} \frac{M_H^2}{M_W^2} - \xi \frac{M_W}{s} & -\frac{1}{2s} \frac{M_H^2}{M_W^2} + \xi \frac{M_W}{2s} & \mp i\xi M_W \frac{s}{2c^2}
 \end{array} \quad (\text{A.89})$$

- $\hat{V}V\hat{S} S$ vertex:

$$\begin{array}{c}
 \text{Diagram: } \hat{V}_{1,\mu, k_1} \text{ (wavy line)} \text{ and } \hat{S}_1 \text{ (dashed line)} \\
 \text{Equation: } = ie^2 g_{\mu\nu} C
 \end{array} \quad (\text{A.90})$$

$$\begin{array}{cccccccc}
 \hat{V}_1 V_2 \hat{S}_1 S_2 & \hat{Z} Z \hat{H} H & \hat{W}^\pm W^\mp \hat{H} H & \hat{W}^\pm W^\mp \hat{\phi}^\mp \phi^\pm & \hat{A} A \hat{\phi}^\pm \phi^\mp & \hat{Z} A \hat{\phi}^\pm \phi^\mp & \hat{Z} Z \hat{\phi}^\pm \phi^\mp & \hat{W}^\pm A \hat{H} \phi^\mp \\
 \hat{Z} Z \hat{\chi} \chi & \hat{W}^\pm W^\mp \hat{\chi} \chi & & & & \hat{A} Z \hat{\phi}^\pm \phi^\mp & & \hat{A} W^\pm \hat{\phi}^\mp H \\
 \hline
 C & \frac{1}{2c^2 s^2} & \frac{1}{2s^2} & \frac{1}{s^2} & 2 & -\frac{c^2 - s^2}{cs} & \frac{(c^2 - s^2)^2}{2c^2 s^2} & -\frac{1}{s}
 \end{array}$$

$$\begin{array}{ccccccc}
\hat{V}_1 V_2 \hat{S}_1 S_2 & \hat{W}^\pm A \hat{\chi} \phi^\mp & \hat{W}^\pm Z \hat{\phi}^\mp H & \hat{W}^\pm Z \hat{\phi}^\mp \chi & \hat{W}^\pm Z \hat{H} \phi^\mp & \hat{W}^\pm Z \hat{\chi} \phi^\mp & \hat{W}^\pm W^\mp \hat{\chi} H \\
\hat{A} W^\pm \hat{\phi}^\mp \chi & \hat{Z} W^\pm \hat{H} \phi^\mp & \hat{Z} W^\pm \hat{\chi} \phi^\mp & \hat{Z} W^\pm \hat{\phi}^\mp H & \hat{Z} W^\pm \hat{\phi}^\mp \chi & \hat{Z} W^\pm \hat{\chi} \phi^\mp & \hat{W}^\mp W^\pm \hat{H} \chi
\end{array} \quad (A.91)$$

• $\hat{V} \hat{V} S S$ vertex and $V V \hat{S} \hat{S}$: Feynman rules coincide with Eqs. (A.70) and (A.71) (apart from counterterms).

• $V \hat{S} S$ vertex:

$$\begin{array}{c}
\text{Diagram: } V_\mu \text{ (wavy line)} \text{ connects to } \hat{S}_1, k_1 \text{ (dashed line)} \text{ which connects to } S_2, k_2. \\
\text{Equation: } = i2eCk_{1\mu} \\
\hline
V \hat{S}_1 S_2 & Z \hat{\chi} H & Z \hat{H} \chi & A \hat{\phi}^\pm \phi^\mp & Z \hat{\phi}^\pm \phi^\mp & W^\pm \hat{\phi}^\mp H, W^\mp \hat{H} \phi^\pm & W^\pm \hat{\phi}^\mp \chi & W^\pm \hat{\chi} \phi^\mp
\end{array} \quad (A.92)$$

$$\begin{array}{ccccccc}
C & -\frac{i}{2cs} & \frac{i}{2cs} & \mp 1 & \pm \frac{c^2-s^2}{2cs} & \mp \frac{1}{2s} & -\frac{i}{2s} & \frac{i}{2s}
\end{array} \quad (A.93)$$

• $\hat{V} S S$ vertex: Feynman rules coincide with Eqs. (A.72) and (A.73) (apart from counterterms).

• $S \hat{V} V$ vertex:

$$\begin{array}{c}
\text{Diagram: } S \text{ (dashed line)} \text{ connects to } \hat{V}_{1,\mu} \text{ (wavy line)} \text{ which connects to } V_{2,\nu} \text{ (wavy line).} \\
\text{Equation: } = i e g_{\mu\nu} C \\
\hline
S \hat{V}_1 V_2 & H \hat{Z} Z & H \hat{W}^\pm W^\mp & \chi \hat{W}^\pm W^\mp & \phi^\pm \hat{W}^\mp A & \phi^\pm \hat{W}^\mp Z & \phi^\pm \hat{Z} W^\mp
\end{array} \quad (A.94)$$

$$\begin{array}{ccccccc}
C & \frac{1}{c^2 s} M_W & \frac{1}{s} M_W & \mp \frac{i}{s} M_W & -2 M_W & \frac{c^2-s^2}{c s} M_W & -\frac{1}{c s} M_W
\end{array} \quad (A.95)$$

• $\hat{S} V V$ vertex: Feynman rules coincide with Eqs. (A.74) and (A.75) (apart from counterterms).

• $\hat{V} \bar{U} U$ vertex:

$$\begin{array}{c}
\text{Diagram: } \hat{V}_\mu \text{ (wavy line)} \text{ connects to } \bar{U}_1, k_1 \text{ (dotted line)} \text{ which connects to } U_2, k_2. \\
\text{Equation: } = i e (k_1 - k_2)_\mu C
\end{array} \quad (A.96)$$

$$\begin{array}{ccc}
\hat{V} \bar{U}_1 U_2 & \hat{A} \bar{u}^\pm u^\pm, \hat{W}^\pm \bar{u}^A u^A, \hat{W}^\mp \bar{u}^\mp u^A & \hat{Z} \bar{u}^\pm u^\pm, \hat{W}^\pm \bar{u}^Z u^A, \hat{W}^\mp \bar{u}^\mp u^Z \\
C & \pm 1 & \mp \frac{c}{s}
\end{array} \quad (A.97)$$

• $V \bar{U} U$ vertex: Feynman rules coincide with Eqs. (A.49) and (A.50).

• $\hat{V} \hat{V} \bar{U} U$ vertex:

$$\begin{array}{c}
\text{Diagram: } \hat{V}_{1,\mu} \text{ (wavy line)} \text{ connects to } \bar{U}_1 \text{ (dotted line)} \text{ which connects to } U_2. \\
\text{Equation: } = i e^2 g_{\mu\nu} C
\end{array} \quad (A.98)$$

$\hat{V}_1 \hat{V}_2 \bar{U}_1 U_2$	$\hat{W}^\pm \hat{W}^\pm \bar{u}^\pm u^\mp$	$\hat{W}^+ \hat{W}^- \bar{u}^A u^A$	$\hat{W}^+ \hat{W}^- \bar{u}^A u^Z, \hat{A} \hat{Z} \bar{u}^\pm u^\pm$	$\hat{W}^+ \hat{W}^- \bar{u}^Z u^Z$
$\hat{A} \hat{A} \bar{u}^\pm u^\pm$	$\hat{W}^+ \hat{W}^- \bar{u}^Z u^A$			$\hat{Z} \hat{Z} \bar{u}^\pm u^\pm$
C	$-\frac{2}{s^2}$	2	$-2\frac{c}{s}$	$2\frac{c^2}{s^2}$
$\hat{V}_1 \hat{V}_2 \bar{U}_1 U_2$	$\hat{W}^+ \hat{W}^- \bar{u}^\pm u^\pm$	$\hat{A} \hat{W}^\pm \bar{u}^\pm u^A$	$\hat{Z} \hat{W}^\pm \bar{u}^\pm u^A, \hat{A} \hat{W}^\pm \bar{u}^\pm u^Z$	$\hat{Z} \hat{W}^\pm \bar{u}^\pm u^Z$
$\hat{A} \hat{W}^\pm \bar{u}^A u^\mp$	$\hat{Z} \hat{W}^\pm \bar{u}^A u^\mp$		$\hat{A} \hat{W}^\pm \bar{u}^Z u^\mp$	$\hat{Z} \hat{W}^\pm \bar{u}^Z u^\mp$
C	$\frac{1}{s^2}$	-1	$\frac{c}{s}$	$-\frac{c^2}{s^2}$

(A.99)

• $\hat{V}V\bar{U}U$ vertex:



$\hat{V}_1 V_2 \bar{U}_1 U_2$	$\hat{W}^\pm W^\pm \bar{u}^\pm u^\mp$	$\hat{W}^\pm W^\mp \bar{u}^A u^A$	$\hat{W}^\pm W^\mp \bar{u}^A u^Z, \hat{A} \hat{Z} \bar{u}^\pm u^\pm$	$\hat{W}^\pm W^\mp \bar{u}^Z u^Z$
$\hat{A} \hat{A} \bar{u}^\pm u^\pm$	$\hat{W}^\pm W^\mp \bar{u}^Z u^A$			$\hat{Z} \hat{Z} \bar{u}^\pm u^\pm$
C	$-\frac{1}{s^2}$	1	$-\frac{c}{s}$	$\frac{c^2}{s^2}$
$\hat{V}_1 V_2 \bar{U}_1 U_2$	$\hat{W}^\pm W^\mp \bar{u}^\pm u^\pm$	$\hat{A} \hat{W}^\pm \bar{u}^\pm u^A$	$\hat{Z} \hat{W}^\pm \bar{u}^\pm u^A, \hat{A} \hat{W}^\pm \bar{u}^\pm u^Z$	$\hat{Z} \hat{W}^\pm \bar{u}^\pm u^Z$
$\hat{W}^\pm A \bar{u}^A u^\mp$	$\hat{W}^\pm Z \bar{u}^A u^\mp$		$\hat{W}^\pm Z \bar{u}^Z u^\mp$	$\hat{W}^\pm Z \bar{u}^Z u^\mp$
C	$\frac{1}{s^2}$	-1	$\frac{c}{s}$	$-\frac{c^2}{s^2}$

(A.101)

• $\hat{S}\bar{U}U$ vertex:



$\hat{S} \bar{U}_1 U_2$	$\hat{H} \bar{u}^Z u^Z$	$\hat{H} \bar{u}^\pm u^\pm$	$\hat{\phi}^\pm \bar{u}^\pm u^A, \hat{\phi}^\pm \bar{u}^A u^\mp$	$\hat{\phi}^\pm \bar{u}^\pm u^Z, \hat{\phi}^\pm \bar{u}^Z u^\mp$
C	$-\frac{1}{c^2 s} M_W$	$-\frac{1}{s} M_W$	M_W	$\frac{s}{c} M_W$

(A.103)

• $S\bar{U}U$ vertex: Feynman rules coincide with Eqs. (A.51) and (A.52) after setting $\xi_{W,Z} \rightarrow \xi$.

• $\hat{S}\hat{S}\bar{U}U$ vertex:

\hat{S}_1	\bar{U}_1				
\hat{S}_2	U_2				
$\hat{S}_1 \hat{S}_2 \bar{U}_1 U_2$	$\hat{H} \hat{H} \bar{u}^Z u^Z$	$\hat{H} \hat{H} \bar{u}^\pm u^\pm, \hat{\phi}^+ \hat{\phi}^- \bar{u}^\pm u^\pm$	$\hat{\phi}^+ \hat{\phi}^- \bar{u}^A u^A$	$\hat{\phi}^+ \hat{\phi}^- \bar{u}^A u^Z$	$\hat{\phi}^+ \hat{\phi}^- \bar{u}^Z u^Z$
$\hat{\chi} \hat{\chi} \bar{u}^Z u^Z$	$\hat{\chi} \hat{\chi} \bar{u}^\pm u^\pm$			$\hat{\phi}^+ \hat{\phi}^- \bar{u}^Z u^A$	
C	$-\frac{1}{2c^2 s^2}$	$-\frac{1}{2s^2}$	-2	$\frac{c^2 - s^2}{cs}$	$-\frac{(c^2 - s^2)^2}{2c^2 s^2}$

(A.104)

$\hat{S}_1 \hat{S}_2 \bar{U}_1 U_2$	$\hat{H} \hat{\phi}^\pm \bar{u}^\pm u^A$	$\hat{\chi} \hat{\phi}^\pm \bar{u}^\pm u^A$	$\hat{H} \hat{\phi}^\pm \bar{u}^\pm u^Z$	$\hat{\chi} \hat{\phi}^\pm \bar{u}^\pm u^Z$
	$\hat{\phi}^\pm \hat{H} \bar{u}^A u^\mp$	$\hat{\phi}^\pm \hat{\chi} \bar{u}^A u^\mp$	$\hat{\phi}^\pm \hat{H} \bar{u}^Z u^\mp$	$\hat{\phi}^\pm \hat{\chi} \bar{u}^Z u^\mp$
C	$\frac{1}{2s}$	$\mp \frac{i}{2s}$	$\frac{1}{2c}$	$\mp \frac{i}{2c}$

(A.105)

• $\hat{S} S \bar{U} U$ vertex:



$\hat{S}_1 \hat{S}_2 \bar{U}_1 U_2$	$\hat{H} H \bar{u}^Z u^Z$	$\hat{H} H \bar{u}^\pm u^\pm$	$\hat{\phi}^\pm \phi^\mp \bar{u}^\pm u^\pm$	$\hat{\phi}^\pm \phi^\mp \bar{u}^A u^A$	$\hat{\phi}^\pm \phi^\mp \bar{u}^A u^Z$	$\hat{\phi}^\pm \phi^\mp \bar{u}^Z u^Z$	$\hat{H} \phi^\pm \bar{u}^\pm u^A$
	$\hat{\chi} \chi \bar{u}^Z u^Z$	$\hat{\chi} \chi \bar{u}^\pm u^\pm$		$\hat{\phi}^\pm \phi^\mp \bar{u}^A u^A$			$\hat{\phi}^\pm \phi^\mp \bar{u}^A u^Z$
C	$-\frac{1}{4c^2 s^2}$	$-\frac{1}{4s^2}$	$-\frac{1}{2s^2}$	-1	$\frac{c^2 - s^2}{2cs}$	$-\frac{(c^2 - s^2)^2}{4c^2 s^2}$	$\frac{1}{2s}$
$\hat{S}_1 S_2 \bar{U}_1 U_2$	$\hat{\chi} \phi^\pm \bar{u}^\pm u^A$	$\hat{H} \phi^\pm \bar{u}^\pm u^Z$	$\hat{H} \phi^\pm \bar{u}^Z u^\mp$	$\hat{\chi} \phi^\pm \bar{u}^\pm u^Z$	$\hat{\chi} \phi^\pm \bar{u}^Z u^\mp$	$\hat{H} \chi \bar{u}^\pm u^\pm$	
	$\hat{\phi}^\pm \chi \bar{u}^A u^\mp$	$\hat{\phi}^\pm H \bar{u}^Z u^\mp$	$\hat{\phi}^\pm H \bar{u}^\pm u^Z$	$\hat{\phi}^\pm \chi \bar{u}^Z u^\mp$	$\hat{\phi}^\pm \chi \bar{u}^\pm u^Z$	$\hat{\chi} H \bar{u}^\mp u^\mp$	
C	$\mp \frac{i}{2s}$	$-\frac{c^2 - s^2}{4cs^2}$	$\frac{1}{4c s^2}$	$\pm i \frac{c^2 - s^2}{4cs^2}$	$\mp \frac{i}{4cs^2}$	$\mp \frac{i}{4s^2}$	

(A.107)

Appendix B. Green functions and their generating functionals

In order to define our conventions for Green functions we use generic charged bosonic fields ϕ with adjoints ϕ^\dagger and generic fermionic fields ψ with adjoints $\bar{\psi}$. General Green functions, defined via vacuum-expectation values of time-ordered products of field operators in the canonical formalism, are denoted as

$$G^{\phi\phi^\dagger\dots}(x, y, \dots) = \langle T\phi(x)\phi^\dagger(y)\dots \rangle = \frac{\delta}{i\delta J_\phi(x)} \frac{\delta}{i\delta J_{\phi^\dagger}(y)} \dots T[J_\phi, J_{\phi^\dagger}] \Big|_{J_\phi, J_{\phi^\dagger}, \dots \equiv 0} = \text{Diagram with a circle and arrows for } \phi(x) \text{ and } \phi^\dagger(y), \quad (\text{B.1})$$

where $T[J_\phi, J_{\phi^\dagger}]$ is the *generating functional of Green functions* represented by the functional integral

$$T[J_\phi, J_{\phi^\dagger}] = N \int \mathcal{D}\phi \int \mathcal{D}\phi^\dagger \exp \left\{ i \int d^4x [\mathcal{L}(x) + J_\phi(x)\phi(x) + J_{\phi^\dagger}(x)\phi^\dagger(x)] \right\}, \quad T[0, 0] = 1, \quad (\text{B.2})$$

and J_ϕ and J_{ϕ^\dagger} are the sources corresponding to ϕ and ϕ^\dagger , respectively. Because the field operator ϕ creates antiparticles and annihilates particles, the particles and thus the fields in $\langle T\phi(x)\phi^\dagger(y)\dots \rangle$ have to be considered as outgoing. The order of the field indices equals the order of fields in the vacuum expectation value and the order of corresponding derivatives. In the diagrams, the arrows indicate the flow of the particles, which is opposite to the flow of antiparticles.

The transformation to momentum space is defined as

$$G^{\phi\phi^\dagger\dots}(x, y, \dots) = \int \frac{d^4p}{(2\pi)^4} \int \frac{d^4q}{(2\pi)^4} \dots \exp \{i(px + qy + \dots)\} (2\pi)^4 \delta^{(4)}(p + q + \dots) G^{\phi\phi^\dagger\dots}(p, q, \dots), \quad (\text{B.3})$$

where the momenta p, q are incoming and the momentum-conservation δ -function is extracted from the *momentum-space Green functions*.

The *generating functional for connected Green functions* $G_c^{\phi\phi^\dagger\dots}(x, y, \dots)$ is defined as

$$T_c[J_\phi, J_{\phi^\dagger}] = \ln T[J_\phi, J_{\phi^\dagger}]. \quad (\text{B.4})$$

Truncated Green functions, which appear in the calculation of S -matrix elements, are denoted as

$$G_{\text{trunc}}^{\phi^\dagger \phi \dots}(x, y, \dots) = G^{\phi^\dagger \phi \dots}(x, y, \dots) = \langle T \underline{\phi}(x) \underline{\phi}^\dagger(y) \dots \rangle = \text{Diagram with a circle and two external lines labeled } \phi^\dagger(x) \text{ and } \phi(y) \text{ (B.5)}$$

Underlining is also used to indicate truncation of single lines,

$$G^{\dots \phi \dots}(\dots, x, \dots) = \int d^4y \sum_{\phi'} G^{\phi \phi'}(x, y) G^{\dots \phi' \dots}(\dots, y, \dots), \quad (\text{B.6})$$

where the r.h.s. involves a sum over all fields ϕ' that can mix with ϕ^\dagger . Note that the field indices in truncated Green functions denote incoming particles or fields, i.e. ϕ^\dagger is one of the fields ϕ' (but ϕ in general not).

The *generating functional of vertex functions* $\Gamma[\phi, \phi^\dagger]$, also known as *effective action*, is defined by

$$\begin{aligned} i\Gamma[\phi, \phi^\dagger] &= T_c[J_\phi, J_{\phi^\dagger}] - i \int d^4x [J_\phi(x)\phi(x) + J_{\phi^\dagger}(x)\phi^\dagger(x)], \\ \phi(x) &= \frac{\delta T_c[J_\phi, J_{\phi^\dagger}]}{i\delta J_\phi(x)}, \quad \phi^\dagger(x) = \frac{\delta T_c[J_\phi, J_{\phi^\dagger}]}{i\delta J_{\phi^\dagger}(x)}, \end{aligned} \quad (\text{B.7})$$

and generates the vertex functions via

$$\Gamma^{\phi^\dagger \dots}(x, y, \dots) = \frac{\delta}{\delta\phi(x)} \frac{\delta}{\delta\phi^\dagger(y)} \dots \delta\Gamma[\phi, \phi^\dagger] \Big|_{\phi, \phi^\dagger, \dots \equiv 0}. \quad (\text{B.8})$$

In the vertex functions, as in truncated Green functions, the field arguments denote incoming quanta. The Fourier transformation of truncated functions or vertex functions is as in Eq. (B.3), i.e. all momenta are incoming.

Specifically, the 2-point functions are given by

$$\begin{aligned} G^{\phi \phi^\dagger}(x, y) &= \langle T\phi(x)\phi^\dagger(y) \rangle = \frac{\delta^2 T[J_\phi, J_{\phi^\dagger}]}{i\delta J_\phi(x)i\delta J_{\phi^\dagger}(y)} \Big|_{J_\phi, J_{\phi^\dagger}, \dots \equiv 0}, \\ \Gamma^{\phi^\dagger \phi}(x, y) &= \frac{\delta^2 \Gamma[\phi, \phi^\dagger]}{\delta\phi^\dagger(x)\delta\phi(y)} \Big|_{\phi, \phi^\dagger, \dots \equiv 0} \end{aligned} \quad (\text{B.9})$$

and obey the relations

$$\int d^4z \sum_{\phi'} i\Gamma^{\phi^\dagger \phi'}(x, z) G^{\phi' \phi''}(z, y) = -\delta^{(4)}(x - y) \delta_{\phi^\dagger, \phi''}, \quad \sum_{\phi'} i\Gamma^{\phi^\dagger \phi'}(k, -k) G^{\phi' \phi''}(k, -k) = -\delta_{\phi^\dagger, \phi''}, \quad (\text{B.10})$$

where the sum over the intermediate fields ϕ' appears in case of mixing.

For Grassmann fields extra minus signs appear. The order of labels corresponds to the order of left derivatives, and interchange of labels of the Green functions leads to sign changes. The Green functions for fermion fields ψ and $\bar{\psi}$ are defined as

$$\begin{aligned} G^{\psi \dots}(x, \dots) &= \langle T\psi(x) \dots \rangle = +\frac{\delta}{i\delta J_\psi(x)} \dots T[J_\psi, J_{\bar{\psi}}] \Big|_{J_\psi, \dots \equiv 0}, \\ G^{\bar{\psi} \dots}(x, \dots) &= \langle T\bar{\psi}(x) \dots \rangle = -\frac{\delta}{i\delta J_{\bar{\psi}}(x)} \dots T[J_\psi, J_{\bar{\psi}}] \Big|_{J_{\bar{\psi}}, \dots \equiv 0}, \end{aligned} \quad (\text{B.11})$$

i.e. each derivative with respect to $J_{\bar{\psi}}$ gets a minus sign, and the source terms to be added to the Lagrangian have the form $J_\psi \psi + \bar{\psi} J_{\bar{\psi}}$.

Truncation of Grassman fields is defined according to

$$\begin{aligned} G^{\psi\psi\cdots}(\dots, x, \dots) &= \int d^4y \sum_{\psi'} G^{\psi\bar{\psi}'}(x, y) G^{\psi'\bar{\psi}'\cdots}(\dots, y, \dots), \\ G^{\bar{\psi}\bar{\psi}\cdots}(\dots, x, \dots) &= \int d^4y \sum_{\psi'} G^{\psi'\bar{\psi}'}(\dots, y, \dots) G^{\psi'\bar{\psi}}(y, x). \end{aligned} \quad (\text{B.12})$$

The functionals are related via

$$\begin{aligned} i\Gamma[\psi, \bar{\psi}] &= T_c[J_\psi, J_{\bar{\psi}}] - i \int d^4x [J_\psi(x)\psi(x) + \bar{\psi}(x)J_{\bar{\psi}}(x)], \\ \psi(x) &= \frac{\delta T_c[J_\psi, J_{\bar{\psi}}]}{i\delta J_\psi(x)}, \quad \bar{\psi}(x) = -\frac{\delta T_c[J_\psi, J_{\bar{\psi}}]}{i\delta J_{\bar{\psi}}(x)}, \end{aligned} \quad (\text{B.13})$$

and the vertex functions are defined by

$$\Gamma^{\psi\cdots}(x, \dots) = -\frac{\delta}{\delta\psi(x)} \cdots \Gamma[\psi, \bar{\psi}] \Big|_{\psi\cdots\equiv 0}, \quad \Gamma^{\bar{\psi}\cdots}(x, \dots) = +\frac{\delta}{\delta\bar{\psi}(x)} \cdots \Gamma[\psi, \bar{\psi}] \Big|_{\bar{\psi}\cdots\equiv 0}, \quad (\text{B.14})$$

i.e. each derivative with respect to ψ gets a minus sign. In this way the tree-level vertex functions correspond to the usual Feynman rules.

The fermionic 2-point functions are given by

$$\begin{aligned} G^{\psi\bar{\psi}}(x, y) &= \langle T\psi(x)\bar{\psi}(y) \rangle = -\frac{\delta^2 T[J_\psi, J_{\bar{\psi}}]}{i\delta J_\psi(x)i\delta J_{\bar{\psi}}(y)} \Big|_{J_\psi, J_{\bar{\psi}}, \dots\equiv 0}, \\ \Gamma^{\bar{\psi}\psi}(x, y) &= -\frac{\delta^2 \Gamma[\psi, \bar{\psi}]}{\delta\bar{\psi}(x)\delta\psi(y)} \Big|_{\psi, \bar{\psi}, \dots\equiv 0} \end{aligned} \quad (\text{B.15})$$

and obey the relations

$$\begin{aligned} \int d^4z \sum_{\psi'} i\Gamma^{\bar{\psi}\psi'}(x, z) G^{\psi'\bar{\psi}''}(z, y) &= -\delta^{(4)}(x - y)\delta_{\bar{\psi}\psi''}, \quad \sum_{\psi'} i\Gamma^{\bar{\psi}\psi'}(k, -k) G^{\psi'\bar{\psi}''}(k, -k) = -\delta_{\bar{\psi}\psi''}, \\ \int d^4z \sum_{\bar{\psi}'} G^{\psi\bar{\psi}'}(x, z) i\Gamma^{\bar{\psi}'\psi''}(z, y) &= -\delta^{(4)}(x - y)\delta_{\psi\psi''}, \quad \sum_{\bar{\psi}'} G^{\psi\bar{\psi}'}(k, -k) i\Gamma^{\bar{\psi}'\psi''}(k, -k) = -\delta_{\psi\psi''}, \end{aligned} \quad (\text{B.16})$$

again with a sum over ψ' or $\bar{\psi}'$ in case of mixing.

With these definitions, the lowest-order 2-point functions for fermions read

$$\begin{aligned} \Gamma_{0,\alpha\beta}^{\bar{\psi}\psi}(-p, p) &= (\not{p} - m)_{\alpha\beta} = -\Gamma_{0,\beta\alpha}^{\psi\bar{\psi}}(p, -p), \\ G_{0,\alpha\beta}^{\psi\bar{\psi}}(-p, p) &= \frac{i(\not{p} + m)_{\alpha\beta}}{p^2 - m^2 - i\epsilon} = -G_{0,\beta\alpha}^{\bar{\psi}\psi}(p, -p). \end{aligned} \quad (\text{B.17})$$

The conventions for Faddeev–Popov ghosts are equivalent to those for the fermions.

Appendix C. Ward identity for the on-shell $A\bar{f}f$ vertex

In this appendix we give a derivation of the Ward identity (152) for the on-shell $A\bar{f}f$ vertex in the SM that can be used to fix the charge renormalization constant from self-energies at the one-loop level. While this Ward identity is often used in the literature, it has to the best of our knowledge not been derived from the symmetries of the EWSM, but only verified via direct calculation of the one-loop diagrams. We recall the situation in the BFM where the QED-like

relation (160) automatically fixes the charge renormalization constant in terms of the background photon self-energy to all orders, so that this complicated derivation is not required.

We start from the *Lee identities* [28, 645, 646] for the EWSM as given in Ref. [83] (see also Ref. [117]).⁴⁸ The Lee identities for the vertex functional are a consequence of the invariance of the theory under BRS transformations (45). They can be derived from the Slavnov–Taylor identities for the functional of connected Green functions via Legendre transformation to the effective action Γ .

For linear *gauge-fixing functionals* like in Eq. (27), or in the more generic form ($a = A, Z, \pm$, $V^A = A$, $V^Z = Z$, $V^\pm = W^\pm$, $\phi^Z = \chi$)

$$C^a = \partial_\mu V^{a,\mu}(x) + \sum_{b=Z,\pm} \Phi^{ab} \phi^b(x), \quad (\text{C.1})$$

the Lee identities read

$$0 = \int d^4x \left[\sum_{a=A,Z,\pm} \left(\frac{\delta \tilde{\Gamma}}{\delta V_\mu^a} \frac{\delta \tilde{\Gamma}}{\delta K_V^{a,\mu}} + \frac{\delta \tilde{\Gamma}}{\delta u^a} \frac{\delta \tilde{\Gamma}}{\delta K_u^a} \right) + \sum_{a=Z,\pm} \frac{\delta \tilde{\Gamma}}{\delta \phi^a} \frac{\delta \tilde{\Gamma}}{\delta K_\phi^a} + \frac{\delta \tilde{\Gamma}}{\delta H} \frac{\delta \tilde{\Gamma}}{\delta K_H} + \sum_i \left(\frac{\delta \tilde{\Gamma}}{\delta K_{\bar{\psi}}^i} \frac{\delta \tilde{\Gamma}}{\delta \bar{\psi}_i} + \frac{\delta \tilde{\Gamma}}{\delta \psi_i} \frac{\delta \tilde{\Gamma}}{\delta K_\psi^i} \right) \right], \quad (\text{C.2})$$

$$0 = \partial^\mu \frac{\delta \tilde{\Gamma}}{\delta K_V^{a,\mu}} + \sum_{b=Z,\pm} \Phi^{ab} \frac{\delta \tilde{\Gamma}}{\delta K_\phi^b} + \frac{\delta \tilde{\Gamma}}{\delta u^a}, \quad (\text{C.3})$$

where

$$\tilde{\Gamma} = \Gamma + \int d^4x \left(\frac{1}{2\xi_A} C^A C^A + \frac{1}{2\xi_Z} C^Z C^Z + \frac{1}{\xi_W} C^+ C^- \right) \quad (\text{C.4})$$

is the vertex functional with the gauge-fixing term (28) subtracted, and i runs over all fermion fields denoted generically by ψ_i . The terms involving the sources K of the BRS-transformed fields are given by

$$\mathcal{L}_{\text{BRS-sources}} = \sum_{a=A,Z,\pm} \left(K_V^{a,\mu} s V_\mu^a + K_u^a s u^a \right) + \sum_{a=Z,\pm} K_\phi^a s \phi^a + K_H s H + \sum_i K_{\bar{\psi}}^i s \psi_i + \sum_i (s \bar{\psi}_i) K_{\bar{\psi}}^i, \quad (\text{C.5})$$

and the sources for the charged gauge-boson, Faddeev–Popov ghost, and would-be Goldstone fields are related to the sources in the canonical $SU(2)_W$ basis via $K^\pm = (K^1 \pm iK^2)/\sqrt{2}$. Note that the sources $K_V^{a,\mu}$, K_ϕ^a , K_H are Grassmann-odd functions, while K_u^a , $K_{\bar{\psi}}^i$, $K_{\bar{\psi}}^i$ are Grassmann even. If functional derivatives w.r.t. the K 's are taken, we label the corresponding Green functions and vertex functions as follows,

$$G^{K^{\dots}}(x, \dots) = \frac{\delta}{i\delta K(x)} \cdots T|_{K_{\dots} \equiv 0}, \quad \Gamma^{K^{\dots}}(x, \dots) = \frac{\delta}{\delta K(x)} \cdots \Gamma|_{K_{\dots} \equiv 0}. \quad (\text{C.6})$$

The sign choice for $\Gamma^{K^{\dots}}(x, \dots)$ ensures that the tree-level contributions of those functions can be read from the Lagrangian in the same way as for ordinary vertex functions, where the tree-level parts coincide with the corresponding Feynman rules (using the conventions of Appendix B). Denoting tree-level parts with subscript zero, we give the tree-level parts of some $\Gamma^{K^{\dots}}(x, \dots)$ in momentum space for later convenience,

$$\begin{aligned} \tilde{\Gamma}_{0,\mu}^{K_V^A u^A}(-k, k) &= -ik_\mu, & \tilde{\Gamma}_{0,\mu}^{K_V^Z u^A}(-k, k) &= 0, & \tilde{\Gamma}_0^{K_\chi u^A}(-k, k) &= \tilde{\Gamma}_0^{K_H u^A}(-k, k) = 0, \\ \tilde{\Gamma}_0^{\bar{\psi}_l K_{\bar{\psi}}^k u^A}(\bar{p}, p, k) &= \tilde{\Gamma}_0^{K_\psi^l \psi_k u^A}(\bar{p}, p, k) = -iQ_l e \delta_{lk}, \end{aligned} \quad (\text{C.7})$$

which simply follow from inserting the respective BRS variations Eq. (45) into Eq. (C.5).

We start by taking functional derivatives of the Lee identity (C.2) with respect to $\bar{\psi}_k$, ψ_k , and u^A , where $\bar{\psi}_k$ and ψ_k correspond to the same fermion species. After transformation to momentum space, we obtain

$$0 = \sum_{a=A,Z} \tilde{\Gamma}_\mu^{V^a \bar{\psi}_k \psi_k}(k, \bar{p}, p) \tilde{\Gamma}^{K_V^a u^A, \mu}(-k, k) + \sum_{S=\chi,H} \tilde{\Gamma}^S \bar{\psi}_k \psi_k(k, \bar{p}, p) \tilde{\Gamma}^{K_S u^A}(-k, k)$$

⁴⁸Alternatively, we could also derive Eq. (152) starting from the BRS invariance of the Green function $\langle T\bar{u}^A(x)\psi_f(x)\bar{\psi}_f(z) \rangle$, which produces a Slavnov–Taylor identity for $\langle T\partial_\mu^a A_\mu(x)\psi_f(x)\bar{\psi}_f(z) \rangle$. The derivation proceeds similarly to the one described in the following, involves a smaller number of unphysical quantities, but is more cumbersome in the truncation of external lines.

$$- \sum_i \tilde{\Gamma}^{\bar{\psi}_k K_\psi^i u^A}(\bar{p}, p, k) \tilde{\Gamma}^{\bar{\psi}_i \psi_k}(-p, p) + \sum_i \tilde{\Gamma}^{\bar{\psi}_k \psi_i}(\bar{p}, -\bar{p}) \tilde{\Gamma}^{K_\psi^i \psi_k u^A}(\bar{p}, p, k), \quad (\text{C.8})$$

where $K_\chi = K_\phi^Z$ and all quantities $\tilde{\Gamma}^{\dots}(\{p_i\})$ represent bare vertex functions derived from the functional (C.4), transformed to momentum space with momentum-conservation δ -functions split off, and with incoming momenta and labels denoting incoming fields. Since $\tilde{\Gamma}^{\dots} = \Gamma^{\dots}$ for vertex functions involving fermion fields or sources K , we omit the tilde in the following whenever possible. Note that we do not get terms involving the tadpole term $\Gamma^H(0)$ by definition, since we include tadpole counterterms, which render $\Gamma^H(0)$ zero, in our definition of unrenormalized vertex functions, as made explicit in Eq. (141) for self-energies. The tadpole counterterms can be generated via a shift of the Higgs field, which does not affect the Lee identities. In Refs. [83, 117] the identity (C.8) is used for the renormalized vertex functions in order to proof charge universality in the EWSM, i.e. the fact that the (renormalized) on-shell coupling of the photon to charged particles is independent of the particle species. Here we use this identity for bare vertex functions in order to derive an identity between the charge renormalization constant and self-energies.

We insert the covariant decompositions

$$\Gamma_\mu^{K_V^a u^b}(-k, k) = -k_\mu \Gamma_V^{K_V^a u^b}(k^2), \quad \Gamma^{K_S u^b}(-k, k) = \Gamma^{K_S u^b}(k^2), \quad S = \chi, H, \quad (\text{C.9})$$

take the derivative of Eq. (C.8) with respect to k^μ for p^μ fixed and $\bar{p}^\mu = -p^\mu - k^\mu$, put $k_\mu = 0$, sandwich the result between spinors $\bar{u}_k(p) \dots u_k(p)$, and obtain:

$$\begin{aligned} 0 = & - \sum_{a=A,Z} \bar{u}_k(p) \Gamma_\mu^{V^a \bar{\psi}_k \psi_k}(0, -p, p) u_k(p) \Gamma^{K_V^a u^A}(0) \\ & + \sum_{S=\chi,H} \bar{u}_k(p) \left[\frac{\partial}{\partial k^\mu} \Gamma^{S \bar{\psi}_k \psi_k}(k, -p - k, p) \right]_{k=0} u_k(p) \Gamma^{K_S u^A}(0) \\ & - \sum_i \bar{u}_k(p) \left[\frac{\partial}{\partial k^\mu} \Gamma^{\bar{\psi}_k K_\psi^i u^A}(-p - k, p, k) \right]_{k=0} \Gamma^{\bar{\psi}_i \psi_k}(-p, p) u_k(p) \\ & + \sum_i \bar{u}_k(p) \Gamma^{\bar{\psi}_k \psi_i}(-p, p) \left[\frac{\partial}{\partial k^\mu} \Gamma^{K_\psi^i \psi_k u^A}(-p - k, p, k) \right]_{k=0} u_k(p) \\ & + \sum_i \bar{u}_k(p) \left[\frac{\partial}{\partial p^\mu} \Gamma^{\bar{\psi}_k \psi_i}(-p, p) \right] \Gamma^{K_\psi^i \psi_k u^A}(-p, p, 0) u_k(p). \end{aligned} \quad (\text{C.10})$$

We have used the fact that the derivative of the functions $\Gamma^{K_S u^A}(k^2)$ with respect to k_μ vanishes for $k_\mu = 0$. In the following we evaluate Eq. (C.10) in one-loop approximation line by line:

- Defining the one-loop correction $\Lambda^{A \bar{\psi}_k \psi_k}$ to the $A \bar{\psi}_k \psi_k$ vertex as in Eq. (150), the one-loop approximation of the first line of Eq. (C.10) reads

$$\begin{aligned} \bar{u}_k(p) & \left[e Q_k \gamma_\mu \Gamma^{K_V^A u^A}(0) - e \Lambda_\mu^{A \bar{\psi}_k \psi_k}(0, -p, p) \Gamma_0^{K_V^A u^A}(0) - e \gamma_\mu (v_k - a_k \gamma_5) \Gamma^{K_V^Z u^A}(0) \right] u_k(p) \\ & = e \bar{u}_k(p) \left[-\Lambda_\mu^{A \bar{\psi}_k \psi_k}(0, -p, p) \Gamma_0^{K_V^A u^A}(0) + Q_k \gamma_\mu \left(\Gamma^{K_V^A u^A}(0) + \frac{S_w}{C_w} \Gamma^{K_V^Z u^A}(0) \right) - 2 a_k \gamma_\mu \omega_- \Gamma^{K_V^Z u^A}(0) \right] u_k(p), \end{aligned} \quad (\text{C.11})$$

where we have inserted the tree-level $V^a \bar{\psi}_k \psi_k$ couplings and employed the vector and axial-vector couplings v_k and a_k defined in Eq. (A.46). This can be further simplified by using $\Gamma_0^{K_V^A u^A}(0) = i$ from Eq. (C.7) and by exploiting the all-order relation

$$c_w \Gamma^{K_V^A u^A}(k^2) + s_w \Gamma^{K_V^Z u^A}(k^2) = i c_w. \quad (\text{C.12})$$

This identity follows from the fact that B_μ is an abelian gauge field: Using $s B_\mu = \partial_\mu (c_w u^A + s_w u^Z)$, which can be read from Eq. (45), we can write

$$G^{K_V^B \bar{u}^a \mu}(x, y) = \langle T s B^\mu(x) \bar{u}^a(y) \rangle = \partial_x^\mu \left(c_w G^{u^A \bar{u}^a}(x, y) + s_w G^{u^Z \bar{u}^a}(x, y) \right). \quad (\text{C.13})$$

Truncating the outgoing antighost field \bar{u}^a and going over to momentum space,

$$\Gamma_\mu^{K_V^B u^b}(-k, k) = - \sum_a G_\mu^{K_V^B \bar{u}^a}(-k, k) i \Gamma^{\bar{u}^a u^b}(-k, k), \quad (\text{C.14})$$

with the help of Eq. (B.16) directly produces Eq. (C.12). Inserting Eq. (C.12) into Eq. (C.11), leads to

$$e \bar{u}_k(p) \left[-i \Lambda_\mu^{A \bar{\psi}_k \psi_k}(0, -p, p) + i Q_k \gamma_\mu - 2 a_k \gamma_\mu \omega_- \Gamma^{K_V^Z u^A}(0) \right] u_k(p). \quad (\text{C.15})$$

The last term with $\Gamma^{K_V^Z u^A}(0)$ will be combined with other terms below.

- The second line of Eq. (C.10) does not contribute in one-loop approximation. According to Eq. (C.7), $\Gamma^{K_S u^A}(0)$ is of one-loop order, so that $\Gamma^{S \bar{\psi}_k \psi_k}$ is only needed at tree level. Since the tree-level part $\Gamma_0^{S \bar{\psi}_k \psi_k}$ is constant, the whole contribution is at least of two-loop order.
- Lines three and four of Eq. (C.10) do not contribute at one loop either, because the fermionic 2-point functions project the external wave function $u_k(p)$ and $\bar{u}_k(p)$ to zero at tree level,

$$\Gamma_0^{\bar{\psi}_i \psi_k}(-p, p) u_k(p) = 0, \quad \bar{u}_k(p) \Gamma_0^{\bar{\psi}_k \psi_i}(-p, p) = 0. \quad (\text{C.16})$$

Since the tree-level parts $\Gamma_0^{\bar{\psi}_k K_\psi^i u^A}$ and $\Gamma_0^{K_\psi^i \bar{\psi}_k u^A}$ are constant according to Eq. (C.7), the whole contributions are again zero at one loop.

- The fifth and last line of Eq. (C.10) produces a non-trivial contribution. In order to derive it, we go back to Eq. (C.8), set $k = 0$, $p^2 = m_k^2$, and multiply it with $u_k(p)$ from the right. Following the same reasoning as in the previous items and splitting the fermionic 2-point functions into tree-level and one-loop parts,

$$\Gamma^{\bar{\psi}_i \psi_j}(-p, p) = \Gamma_0^{\bar{\psi}_i \psi_j}(-p, p) + \Sigma^{\bar{\psi}_i \psi_j}(-p, p) = (\not{p} - m_i) \delta_{ij} + \Sigma^{\bar{\psi}_i \psi_j}(-p, p), \quad (\text{C.17})$$

at one loop this leads to

$$\begin{aligned} 0 &= \Gamma_0^{\chi \bar{\psi}_k \psi_k} u_k(p) \Gamma^{K_\chi u^A}(0) + \Gamma_0^{H \bar{\psi}_k \psi_k} u_k(p) \Gamma^{K_H u^A}(0) \\ &\quad - \sum_i \Gamma_0^{\bar{\psi}_k K_\psi^i u^A}(-p, p, 0) \Gamma_0^{\bar{\psi}_i \psi_k}(-p, p) u_k(p) + \sum_i \Gamma_0^{\bar{\psi}_k \psi_i}(-p, p) \Gamma_0^{K_\psi^i \bar{\psi}_k u^A}(-p, p, 0) u_k(p) \\ &\quad - \sum_i \Gamma_0^{\bar{\psi}_k K_\psi^i u^A} \Sigma^{\bar{\psi}_i \psi_k}(-p, p) u_k(p) + \sum_i \Sigma^{\bar{\psi}_k \psi_i}(-p, p) \Gamma_0^{K_\psi^i \bar{\psi}_k u^A} u_k(p). \end{aligned} \quad (\text{C.18})$$

In this relation, the last two terms trivially cancel each other, and the third term is zero according to Eq. (C.16). The second is zero as well, since it is the only term left after multiplying Eq. (C.18) with $\bar{u}_k(p)$ from the left and using $\bar{u}_k(p) \gamma_5 u_k(p) = 0$. Since $\bar{u}_k(p) \Gamma_0^{H \bar{\psi}_k \psi_k} u_k(p) \neq 0$, we get

$$\Gamma^{K_H u^A}(0) = 0. \quad (\text{C.19})$$

With these simplifications and inserting the explicit form of

$$\Gamma_0^{\chi \bar{\psi}_k \psi_k} = 2 i e a_k \frac{m_k}{M_Z} \gamma_5, \quad (\text{C.20})$$

Eq. (C.18) reads

$$0 = 2 i e a_k \frac{m_k}{M_Z} \gamma_5 u_k(p) \Gamma^{K_\chi u^A}(0) + (\not{p} - m_k) \Gamma_0^{K_\psi^k \bar{\psi}_k u^A}(-p, p, 0) u_k(p). \quad (\text{C.21})$$

The function $\Gamma_0^{K_\psi^k \bar{\psi}_k u^A}(\bar{p}, p, k)$ receives one-loop contributions from the graphs shown in Fig. C.20. Inspecting

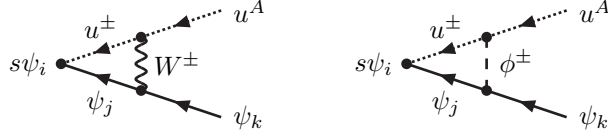


Figure C.20: One-loop Feynman diagrams contributing to $\Gamma_0^{K\psi\psi_k u^A}$.

the BRS variations of fermions given in Eq. (45), we see that the graphs in Fig. C.20 all involve a chirality projection factor ω_- on the left, so that Lorentz invariance admits us to write

$$\Gamma^{K\psi\psi_k u^A}(-p, p, 0) u_k(p) = [-iQ_k e + \omega_- i e \Lambda^{K\psi\psi_k u^A}] u_k(p) \quad (\text{C.22})$$

where $\Lambda^{K\psi\psi_k u^A}$ is a scalar constant, since $\Gamma^{K\psi\psi_k u^A}(-p, p, 0)$ can only depend on \not{p} and is projected on the spinor. Inserting this into Eq. (C.21), we can calculate $\Lambda^{K\psi\psi_k u^A}$ to

$$\Lambda^{K\psi\psi_k u^A} = -\frac{2a_k}{M_Z} \Gamma^{K\chi u^A}(0). \quad (\text{C.23})$$

With this result we can evaluate the last line of Eq. (C.10) to

$$\begin{aligned} \bar{u}_k(p) \gamma_\mu \Gamma^{K\psi\psi_k u^A}(-p, p, 0) u_k(p) &+ \sum_i \bar{u}_k(p) \left[\frac{\partial}{\partial p^\mu} \Sigma^{\bar{\psi}_k \psi_i}(-p, p) \right] \Gamma_0^{K\psi\psi_k u^A} u_k(p) \\ &= -ie \bar{u}_k(p) \left[Q_k \gamma_\mu + \frac{2a_k}{M_Z} \Gamma^{K\chi u^A}(0) \gamma_\mu \omega_- + Q_k \left(\frac{\partial}{\partial p^\mu} \Sigma^{\bar{\psi}_k \psi_k}(-p, p) \right) \right] u_k(p). \end{aligned} \quad (\text{C.24})$$

In summary, the r.h.s. of Eq. (C.10) is given by the sum of Eqs. (C.15) and (C.24), so that the full identity reads

$$0 = ie \bar{u}_k(p) \left[-\Lambda_\mu^{A\bar{\psi}_k \psi_k}(0, -p, p) + \frac{2a_k}{M_Z} \left(iM_Z \Gamma^{K_V^Z u^A}(0) - \Gamma^{K\chi u^A}(0) \right) \gamma_\mu \omega_- - Q_k \left(\frac{\partial}{\partial p^\mu} \Sigma^{\bar{\psi}_k \psi_k}(-p, p) \right) \right] u_k(p). \quad (\text{C.25})$$

In a final non-trivial step, we express the combination of $\Gamma^{K\chi u^A}$ vertex functions in terms of gauge-boson 2-point functions. To this end, we take functional derivatives of Eq. (C.2) w.r.t. a neutral gauge-boson field V_ν^b and a neutral ghost field u^c to obtain

$$0 = \sum_{a=A,Z} \tilde{\Gamma}_{\mu\nu}^{V^a V^b}(k, -k) \Gamma^{K_V^a u^c, \mu}(-k, k) + \tilde{\Gamma}_\nu^{V^b}(k, -k) \Gamma^{K\chi u^c}(-k, k). \quad (\text{C.26})$$

Note that we have to keep the tilde on the 2-point vertex functions without K fields. Specializing these relations to $b = Z$ and $c = A$ and introducing the covariant decompositions (105), (447), and (C.9), leads to the one-loop relation

$$0 = \Gamma_L^{AZ}(k^2) \Gamma_0^{K_V^A u^A}(k^2) + \tilde{\Gamma}_{L,0}^{ZZ}(k^2) \Gamma^{K_V^Z u^A}(k^2) + \tilde{\Gamma}_0^{\chi Z}(k^2) \Gamma^{K\chi u^A}(k^2), \quad (\text{C.27})$$

which can be further simplified with the tree-level results

$$\Gamma_0^{K_V^A u^A}(k^2) = i, \quad \tilde{\Gamma}_{L,0}^{ZZ}(k^2) = M_Z^2, \quad \tilde{\Gamma}_0^{\chi Z}(k^2) = iM_Z. \quad (\text{C.28})$$

With the identification $\Gamma_L^{AZ}(k^2) = -\Sigma_L^{AZ}(k^2)$, we finally get

$$\Sigma_L^{AZ}(k^2) = M_Z \left(-iM_Z \Gamma^{K_V^Z u^A}(k^2) + \Gamma^{K\chi u^A}(k^2) \right). \quad (\text{C.29})$$

For $k^2 = 0$ this relation, together with the identity $\Sigma_L^{AZ}(0) = \Sigma_T^{AZ}(0)$ resulting from the analyticity of $\Gamma^{AZ}(k, -k)$ at $k = 0$, can be used to bring Eq. (C.25) into its final form

$$0 = \bar{u}_k(p) \left[\Lambda_\mu^{A\bar{\psi}_k \psi_k}(0, -p, p) + \frac{2a_k}{M_Z^2} \Sigma_T^{AZ}(0) \gamma_\mu \omega_- + Q_k \left(\frac{\partial}{\partial p^\mu} \Sigma^{\bar{\psi}_k \psi_k}(-p, p) \right) \right] u_k(p), \quad (\text{C.30})$$

which is the Ward identity quoted in Eq. (152).

Upon inserting the Lorentz decompositions for the fermion self-energy defined as in Eq. (105) and for the vertex function Eq. (151) and using the Gordon identities and the definition (145) of the fermion field renormalization constants $\delta Z_{kk}^{\psi,\sigma}$ in the OS scheme, this gives rise to the relations [40, 83]:

$$\begin{aligned} 0 &= \Lambda_V(0) + \Lambda_S(0) + \frac{a_k}{M_Z^2} \Sigma_T^{AZ}(0) - \frac{1}{2} Q_k (\delta Z_{kk}^{\psi,L} + \delta Z_{kk}^{\psi,R}), \\ 0 &= \Lambda_A(0) + \frac{a_k}{M_Z^2} \Sigma_T^{AZ}(0) - \frac{1}{2} Q_k (\delta Z_{kk}^{\psi,L} - \delta Z_{kk}^{\psi,R}), \end{aligned} \quad (C.31)$$

which link the vertex form factors at zero momentum transfer to quantities defined in terms of self-energies.

For the derivation of the identities (C.30) and (C.31) we just have used the Lee identities of the $SU(2)_W \times U(1)_Y$ gauge symmetry within a general 't Hooft gauge and Lorentz invariance. The arguments do not change if additional fermions or scalars are added to the SM. As long as the gauge sector is not modified, the identity (C.30) and thus the relation (153) between the renormalization of the electromagnetic coupling and the gauge-boson self-energies in Section 3.1.7 are valid.

Acknowledgements

AD acknowledges financial support by the German Federal Ministry for Education and Research (BMBF) under contracts no. 05H15WWCA1 and 05H18WWCA1 and the German Research Foundation (DFG) under reference numbers DE 623/5-1 and DE 623/6-1. SD gratefully acknowledges support by the BMBF under contracts no. 05H15VFCA1 and 05H18VFCA1, by the DFG under reference numbers DI 784/3-2 and DI 784/4-1, and by the DFG Research Training Group GRK 2044. In the course of writing this review, we have profited from many stimulating discussions and fruitful collaborations with Th. Hahn, V. Hirschi, W. Hollik, A. Huss, A. Kabelschacht, J.N. Lang, A. Mück, G. Passarino, S. Pozzorini, Ch. Schwinn, H. Spiesberger, S. Uccirati, and G. Weiglein. We thank Th. Hahn, G. Heinrich, V. Hirschi, Ph. Maierhöfer, R. Pittau, and S. Pozzorini for feedback on a draft version of parts of Section 3.

References

- [1] H. Fritzsch, M. Gell-Mann, H. Leutwyler, Advantages of the Color Octet Gluon Picture, *Phys. Lett.* **47B** (1973) 365–368. [doi:10.1016/0370-2693\(73\)90625-4](https://doi.org/10.1016/0370-2693(73)90625-4).
- [2] D. J. Gross, F. Wilczek, Asymptotically Free Gauge Theories I, *Phys. Rev. D8* (1973) 3633–3652. [doi:10.1103/PhysRevD.8.3633](https://doi.org/10.1103/PhysRevD.8.3633).
- [3] H. D. Politzer, Reliable Perturbative Results for Strong Interactions?, *Phys. Rev. Lett.* **30** (1973) 1346–1349. [doi:10.1103/PhysRevLett.30.1346](https://doi.org/10.1103/PhysRevLett.30.1346).
- [4] D. J. Gross, F. Wilczek, Asymptotically Free Gauge Theories II, *Phys. Rev. D9* (1974) 980–993. [doi:10.1103/PhysRevD.9.980](https://doi.org/10.1103/PhysRevD.9.980).
- [5] S. L. Glashow, Partial Symmetries of Weak Interactions, *Nucl. Phys.* **22** (1961) 579–588. [doi:10.1016/0029-5582\(61\)90469-2](https://doi.org/10.1016/0029-5582(61)90469-2).
- [6] S. Weinberg, A Model of Leptons, *Phys. Rev. Lett.* **19** (1967) 1264–1266. [doi:10.1103/PhysRevLett.19.1264](https://doi.org/10.1103/PhysRevLett.19.1264).
- [7] A. Salam, Weak and Electromagnetic Interactions, in: N. Svartholm (Ed.), *Elementary Particle Theory*, Almqvist and Wiksell, Stockholm, Vol. C680519, 1968, pp. 367–377. [doi:10.1142/9789812795915_0034](https://doi.org/10.1142/9789812795915_0034).
- [8] F. Englert, R. Brout, Broken Symmetry and the Mass of Gauge Vector Mesons, *Phys. Rev. Lett.* **13** (1964) 321–323. [doi:10.1103/PhysRevLett.13.321](https://doi.org/10.1103/PhysRevLett.13.321).
- [9] P. W. Higgs, Broken Symmetries and the Masses of Gauge Bosons, *Phys. Rev. Lett.* **13** (1964) 508–509. [doi:10.1103/PhysRevLett.13.508](https://doi.org/10.1103/PhysRevLett.13.508).
- [10] P. W. Higgs, Broken symmetries, massless particles and gauge fields, *Phys. Lett.* **12** (1964) 132–133. [doi:10.1016/0031-9116\(64\)91136-9](https://doi.org/10.1016/0031-9116(64)91136-9).
- [11] G. S. Guralnik, C. R. Hagen, T. W. B. Kibble, Global Conservation Laws and Massless Particles, *Phys. Rev. Lett.* **13** (1964) 585–587. [doi:10.1103/PhysRevLett.13.585](https://doi.org/10.1103/PhysRevLett.13.585).
- [12] P. W. Higgs, Spontaneous Symmetry Breakdown without Massless Bosons, *Phys. Rev.* **145** (1966) 1156–1163. [doi:10.1103/PhysRev.145.1156](https://doi.org/10.1103/PhysRev.145.1156).
- [13] B. T. Cleveland, et al., Measurement of the solar electron neutrino flux with the Homestake chlorine detector, *Astrophys. J.* **496** (1998) 505–526. [doi:10.1086/305343](https://doi.org/10.1086/305343).
- [14] Y. Fukuda, et al., Evidence for oscillation of atmospheric neutrinos, *Phys. Rev. Lett.* **81** (1998) 1562–1567. [arXiv:hep-ex/9807003](https://arxiv.org/abs/hep-ex/9807003), [doi:10.1103/PhysRevLett.81.1562](https://doi.org/10.1103/PhysRevLett.81.1562).
- [15] Q. R. Ahmad, et al., Direct evidence for neutrino flavor transformation from neutral current interactions in the Sudbury Neutrino Observatory, *Phys. Rev. Lett.* **89** (2002) 011301. [arXiv:nucl-ex/0204008](https://arxiv.org/abs/nucl-ex/0204008), [doi:10.1103/PhysRevLett.89.011301](https://doi.org/10.1103/PhysRevLett.89.011301).

[16] S. L. Glashow, J. Iliopoulos, L. Maiani, Weak Interactions with Lepton-Hadron Symmetry, *Phys. Rev. D* (1970) 1285–1292. doi:10.1103/PhysRevD.2.1285.

[17] D. Decamp, et al., Determination of the Number of Light Neutrino Species, *Phys. Lett. B* 231 (1989) 519–529. doi:10.1016/0370-2693(89)90704-1.

[18] S. Schael, et al., Precision electroweak measurements on the Z resonance, *Phys. Rept.* 427 (2006) 257–454. arXiv:hep-ex/0509008, doi:10.1016/j.physrep.2005.12.006.

[19] N. Cabibbo, Unitary Symmetry and Leptonic Decays, *Phys. Rev. Lett.* 10 (1963) 531–533. doi:10.1103/PhysRevLett.10.531.

[20] M. Kobayashi, T. Maskawa, CP Violation in the Renormalizable Theory of Weak Interaction, *Prog. Theor. Phys.* 49 (1973) 652–657. doi:10.1143/PTP.49.652.

[21] G. 't Hooft, Renormalization of Massless Yang-Mills Fields, *Nucl. Phys. B* 33 (1971) 173–199. doi:10.1016/0550-3213(71)90395-6.

[22] G. 't Hooft, Renormalizable Lagrangians for Massive Yang-Mills Fields, *Nucl. Phys. B* 35 (1971) 167–188. doi:10.1016/0550-3213(71)90139-8.

[23] G. 't Hooft, M. J. G. Veltman, Regularization and Renormalization of Gauge Fields, *Nucl. Phys. B* 44 (1972) 189–213. doi:10.1016/0550-3213(72)90279-9.

[24] G. 't Hooft, M. J. G. Veltman, Combinatorics of gauge fields, *Nucl. Phys. B* 50 (1972) 318–353. doi:10.1016/S0550-3213(72)80021-X.

[25] B. W. Lee, J. Zinn-Justin, Spontaneously Broken Gauge Symmetries Part 1: Preliminaries, *Phys. Rev. D* 5 (1972) 3121–3137. doi:10.1103/PhysRevD.5.3121.

[26] B. W. Lee, J. Zinn-Justin, Spontaneously Broken Gauge Symmetries Part 2: Perturbation Theory and Renormalization, *Phys. Rev. D* 5 (1972) 3137–3155, [Erratum: *Phys. Rev. D* 8 (1973) 4654]. doi:10.1103/PhysRevD.5.3137, 10.1103/PhysRevD.8.4654.

[27] B. W. Lee, J. Zinn-Justin, Spontaneously Broken Gauge Symmetries Part 4: General Gauge Formulation, *Phys. Rev. D* 7 (1973) 1049–1056. doi:10.1103/PhysRevD.7.1049.

[28] B. W. Lee, Renormalization of gauge theories: unbroken and broken, *Phys. Rev. D* 9 (1974) 933–946. doi:10.1103/PhysRevD.9.933.

[29] G. Arnison, et al., Experimental observation of isolated large transverse energy electrons with associated missing energy at $\sqrt{s} = 540$ GeV, *Phys. Lett. B* 122 (1983) 103–116. doi:10.1016/0370-2693(83)91177-2.

[30] M. Banner, et al., Observation of single isolated electrons of high transverse momentum in events with missing transverse energy at the CERN $\bar{p}p$ collider, *Phys. Lett. B* 122 (1983) 476–485. doi:10.1016/0370-2693(83)91605-2.

[31] G. Arnison, et al., Experimental observation of lepton pairs of invariant mass around $95\text{ GeV}/c^2$ at the CERN SPS collider, *Phys. Lett. B* 126 (1983) 398–410. doi:10.1016/0370-2693(83)90188-0.

[32] P. Bagnaia, et al., Evidence for $Z^0 \rightarrow e^+e^-$ at the CERN $\bar{p}p$ collider, *Phys. Lett. B* 129 (1983) 130–140. doi:10.1016/0370-2693(83)90744-X.

[33] G. 't Hooft, M. J. G. Veltman, Scalar one-loop integrals, *Nucl. Phys. B* 153 (1979) 365–401. doi:10.1016/0550-3213(79)90605-9.

[34] G. Passarino, M. J. G. Veltman, One-loop corrections for e^+e^- annihilation into $\mu^+\mu^-$ in the Weinberg model, *Nucl. Phys. B* 160 (1979) 151. doi:10.1016/0550-3213(79)90234-7.

[35] D. A. Ross, J. C. Taylor, Renormalization of a unified theory of weak and electromagnetic interactions, *Nucl. Phys. B* 51 (1973) 125–144, [Erratum: *Nucl. Phys. B* 58 (1973) 643]. doi:10.1016/0550-3213(73)90608-1, 10.1016/0550-3213(73)90505-1.

[36] A. Sirlin, Radiative Corrections in the $SU(2)_L \times U(1)$ Theory: A Simple Renormalization Framework, *Phys. Rev. D* 22 (1980) 971–981. doi:10.1103/PhysRevD.22.971.

[37] K.-i. Aoki, et al., Electroweak Theory: Framework of On-Shell Renormalization and Study of Higher Order Effects, *Prog. Theor. Phys. Suppl.* 73 (1982) 1–225. doi:10.1143/PTPS.73.1.

[38] M. Böhm, H. Spiesberger, W. Hollik, On the 1-Loop Renormalization of the Electroweak Standard Model and its Application to Leptonic Processes, *Fortsch. Phys.* 34 (1986) 687–751. doi:10.1002/prop.19860341102.

[39] F. Jegerlehner, Renormalizing the standard model, in: Testing the Standard Model - TASI-90: Theoretical Advanced Study Inst. in Elementary Particle Physics, Boulder, Colorado, June 3–29, 1990, Vol. C900603, 1990, pp. 476–590.

[40] A. Denner, Techniques for the Calculation of Electroweak Radiative Corrections at the One-Loop Level and Results for W-physics at LEP200, *Fortsch. Phys.* 41 (1993) 307–420. arXiv:0709.1075, doi:10.1002/prop.2190410402.

[41] G. Altarelli, R. Kleiss, C. Verzegnassi (Eds.), Z physics at LEP 1. Vol. 1: Standard Physics, CERN, Geneva, 1989, CERN-89-08. doi:10.5170/CERN-1989-008-V-1.
URL <http://www.slac.stanford.edu/spires/find/books/www?cl=QCD161:L39:1989>

[42] D. Yu. Bardin, et al., Electroweak working group report, in: D. Bardin, W. Hollik, G. Passarino (Ed.), Reports of the Working Group on Precision Calculations for the Z Resonance, 1995, pp. 7–162, CERN-95-03. arXiv:hep-ph/9709229, doi:10.5170/CERN-1995-003.
URL <http://doc.cern.ch/cernrep/1995/95-03/95-03.html>

[43] D. Yu. Bardin, G. Passarino, The standard model in the making: Precision study of the electroweak interactions, Clarendon Press, Oxford, UK, 1999.

[44] D. Yu. Bardin, M. Grünwald, G. Passarino, Precision calculation project report (1999). arXiv:hep-ph/9902452.

[45] D. Yu. Bardin, et al., Event generators for WW physics, in: G. Altarelli, T. Sjöstrand, F. Zwirner (Ed.), Physics at LEP2, Vol. 2, 1997, pp. 3–101, CERN-96-01. arXiv:hep-ph/9709270.
URL http://doc.cern.ch/cernrep/1996/96-01_v2/96-01_v2.html

[46] M. W. Grünwald, et al., Four fermion production in electron–positron collisions, in: S. Jadach, G. Passarino, R. Pittau (Ed.), Reports of the Working Groups on Precision Calculations for LEP2 Physics, CERN, 2000, pp. 1–135, CERN-2000-009. arXiv:hep-ph/0005309, doi:10.5170/CERN-2000-009.1.

[47] F. A. Berends, P. H. Daverveldt, R. Kleiss, Complete lowest-order calculations for four-lepton final states in electron-positron collisions, *Nucl. Phys. B* 253 (1985) 441–463. doi:10.1016/0550-3213(85)90541-3.

[48] J. Hilgart, R. Kleiss, F. Le Diberder, An electroweak Monte Carlo for four fermion production, *Comput. Phys. Commun.* 75 (1993) 191–218. doi:10.1016/0010-4655(93)90175-C.

[49] F. A. Berends, R. Pittau, R. Kleiss, All electroweak four fermion processes in electron–positron collisions, *Nucl. Phys.* **B424** (1994) 308–342. [arXiv:hep-ph/9404313](https://arxiv.org/abs/hep-ph/9404313), doi:10.1016/0550-3213(94)90297-6.

[50] R. Kleiss, R. Pittau, Weight optimization in multichannel Monte Carlo, *Comput. Phys. Commun.* **83** (1994) 141–146. [arXiv:hep-ph/9405257](https://arxiv.org/abs/hep-ph/9405257), doi:10.1016/0010-4655(94)90043-4.

[51] B. W. Harris, J. F. Owens, Two cutoff phase space slicing method, *Phys. Rev. D65* (2002) 094032. [arXiv:hep-ph/0102128](https://arxiv.org/abs/hep-ph/0102128), doi:10.1103/PhysRevD.65.094032.

[52] W. T. Giele, E. W. N. Glover, Higher-order corrections to jet cross sections in e^+e^- annihilation, *Phys. Rev. D46* (1992) 1980–2010. doi:10.1103/PhysRevD.46.1980.

[53] S. Frixione, Z. Kunszt, A. Signer, Three jet cross-sections to next-to-leading order, *Nucl. Phys.* **B467** (1996) 399–442. [arXiv:hep-ph/9512328](https://arxiv.org/abs/hep-ph/9512328), doi:10.1016/0550-3213(96)00110-1.

[54] S. Catani, M. H. Seymour, A general algorithm for calculating jet cross-sections in NLO QCD, *Nucl. Phys.* **B485** (1997) 291–419, [Erratum: *Nucl. Phys.* **B510** (1998) 503]. [arXiv:hep-ph/9605323](https://arxiv.org/abs/hep-ph/9605323), doi:10.1016/S0550-3213(96)00589-5, 10.1016/S0550-3213(98)81022-5.

[55] S. Dittmaier, A general approach to photon radiation off fermions, *Nucl. Phys.* **B565** (2000) 69–122. [arXiv:hep-ph/9904440](https://arxiv.org/abs/hep-ph/9904440), doi:10.1016/S0550-3213(99)00563-5.

[56] R. G. Stuart, Gauge invariance, analyticity and physical observables at the Z^0 resonance, *Phys. Lett. B262* (1991) 113–119. doi:10.1016/0370-2693(91)90653-8.

[57] A. Aeppli, G. J. van Oldenborgh, D. Wyler, Unstable particles in one loop calculations, *Nucl. Phys.* **B428** (1994) 126–146. [arXiv:hep-ph/9312212](https://arxiv.org/abs/hep-ph/9312212), doi:10.1016/0550-3213(94)90195-3.

[58] A. Denner, S. Dittmaier, M. Roth, D. Wackerlo, Predictions for all processes $e^+e^- \rightarrow 4$ fermions + γ , *Nucl. Phys.* **B560** (1999) 33–65. [arXiv:hep-ph/9904472](https://arxiv.org/abs/hep-ph/9904472), doi:10.1016/S0550-3213(99)00437-X.

[59] A. Denner, S. Dittmaier, M. Roth, L. H. Wieders, Electroweak corrections to charged-current $e^+e^- \rightarrow 4$ fermion processes: Technical details and further results, *Nucl. Phys.* **B724** (2005) 247–294, [Erratum: *Nucl. Phys.* **B854** (2012) 504]. [arXiv:hep-ph/0505042](https://arxiv.org/abs/hep-ph/0505042), doi:10.1016/j.nuclphysb.2011.09.001, 10.1016/j.nuclphysb.2005.06.033.

[60] S. Schael, et al., Electroweak Measurements in Electron-Positron Collisions at W-Boson-Pair Energies at LEP, *Phys. Rept.* **532** (2013) 119–244. [arXiv:1302.3415](https://arxiv.org/abs/1302.3415), doi:10.1016/j.physrep.2013.07.004.

[61] J. Erler, M. Schott, Electroweak Precision Tests of the Standard Model after the Discovery of the Higgs Boson, *Prog. Part. Nucl. Phys.* **106** (2019) 68–119. [arXiv:1902.05142](https://arxiv.org/abs/1902.05142), doi:10.1016/j.ppnp.2019.02.007.

[62] G. Aad, et al., Observation of a new particle in the search for the Standard Model Higgs boson with the ATLAS detector at the LHC, *Phys. Lett. B716* (2012) 1–29. [arXiv:1207.7214](https://arxiv.org/abs/1207.7214), doi:10.1016/j.physletb.2012.08.020.

[63] S. Chatrchyan, et al., Observation of a new boson at a mass of 125 GeV with the CMS experiment at the LHC, *Phys. Lett. B716* (2012) 30–61. [arXiv:1207.7235](https://arxiv.org/abs/1207.7235), doi:10.1016/j.physletb.2012.08.021.

[64] S. Dittmaier, C. Mariotti, G. Passarino, R. Tanaka (Eds.), Handbook of LHC Higgs Cross Sections: 1. Inclusive observables, CERN, Geneva, 2011, CERN-2011-002. [arXiv:1101.0593](https://arxiv.org/abs/1101.0593), doi:10.5170/CERN-2011-002.

[65] S. Dittmaier, C. Mariotti, G. Passarino, R. Tanaka (Eds.), Handbook of LHC Higgs Cross Sections: 2. Differential Distributions, CERN, Geneva, 2012, CERN-2012-002. [arXiv:1201.3084](https://arxiv.org/abs/1201.3084), doi:10.5170/CERN-2012-002.

[66] S. Heinemeyer, C. Mariotti, G. Passarino, R. Tanaka (Eds.), Handbook of LHC Higgs Cross Sections: 3. Higgs Properties, CERN, Geneva, 2013, CERN-2013-004. [arXiv:1307.1347](https://arxiv.org/abs/1307.1347), doi:10.5170/CERN-2013-004.

[67] D. de Florian, et al. (Eds.), Handbook of LHC Higgs Cross Sections: 4. Deciphering the nature of the Higgs sector, CERN, Geneva, 2016, CERN-2017-002-M. [arXiv:1610.07922](https://arxiv.org/abs/1610.07922), doi:10.23731/CYRM-2017-002.

[68] J. Alwall, et al., The automated computation of tree-level and next-to-leading order differential cross sections, and their matching to parton shower simulations, *JHEP* **07** (2014) 079. [arXiv:1405.0301](https://arxiv.org/abs/1405.0301), doi:10.1007/JHEP07(2014)079.

[69] F. Cascioli, P. Maierhöfer, S. Pozzorini, Scattering amplitudes with Open Loops, *Phys. Rev. Lett.* **108** (2012) 111601. [arXiv:1111.5206](https://arxiv.org/abs/1111.5206), doi:10.1103/PhysRevLett.108.111601.

[70] S. Kallweit, et al., NLO electroweak automation and precise predictions for W+multijet production at the LHC, *JHEP* **04** (2015) 012. [arXiv:1412.5157](https://arxiv.org/abs/1412.5157), doi:10.1007/JHEP04(2015)012.

[71] F. Buccioni, et al., OpenLoops 2, *Eur. Phys. J.* **C79** (2019) 866. [arXiv:1907.13071](https://arxiv.org/abs/1907.13071), doi:10.1140/epjc/s10052-019-7306-2.

[72] S. Actis, et al., Recursive generation of one-loop amplitudes in the Standard Model, *JHEP* **1304** (2013) 037. [arXiv:1211.6316](https://arxiv.org/abs/1211.6316), doi:10.1007/JHEP04(2013)037.

[73] S. Actis, et al., RECOLA: RECURsive COMPUTation of One-Loop Amplitudes, *Comput. Phys. Commun.* **214** (2017) 140–173. [arXiv:1605.01090](https://arxiv.org/abs/1605.01090), doi:10.1016/j.cpc.2017.01.004.

[74] J. R. Andersen, et al., Les Houches 2013: Physics at TeV Colliders: Standard Model Working Group Report, 2014. [arXiv:1405.1067](https://arxiv.org/abs/1405.1067).

[75] J. R. Andersen, et al., Les Houches 2015: Physics at TeV Colliders Standard Model Working Group Report, 2016. [arXiv:1605.04692](https://arxiv.org/abs/1605.04692).

[76] J. R. Andersen, et al., Les Houches 2017: Physics at TeV Colliders Standard Model Working Group Report, 2018. [arXiv:1803.07977](https://arxiv.org/abs/1803.07977).

[77] A. Djouadi, The anatomy of electro-weak symmetry breaking. I: The Higgs boson in the standard model, *Phys. Rept.* **457** (2008) 1–216. [arXiv:hep-ph/0503172](https://arxiv.org/abs/hep-ph/0503172), doi:10.1016/j.physrep.2007.10.004.

[78] S. Dittmaier, M. Schumacher, The Higgs Boson in the Standard Model – From LEP to LHC: Expectations, Searches, and Discovery of a Candidate, *Prog. Part. Nucl. Phys.* **70** (2013) 1–54. [arXiv:1211.4828](https://arxiv.org/abs/1211.4828), doi:10.1016/j.ppnp.2013.02.001.

[79] T. Schörner-Sadenius (Ed.), The Large Hadron Collider, Springer, Berlin, 2015. doi:10.1007/978-3-319-15001-7. URL <http://www.springer.com/gb/book/9783319150017>

[80] M. Spira, Higgs Boson Production and Decay at Hadron Colliders, *Prog. Part. Nucl. Phys.* **95** (2017) 98–159. [arXiv:1612.07651](https://arxiv.org/abs/1612.07651), doi:10.1016/j.ppnp.2017.04.001.

[81] J. Campbell, J. Huston, F. Krauss, The Black Book of Quantum Chromodynamics, Oxford University Press, Oxford, 2017. doi:10.1093/oso/9780199652747.001. URL <https://global.oup.com/academic/product/the-black-book-of-quantum-chromodynamics-9780199652747>

[82] W. F. L. Hollik, Radiative Corrections in the Standard Model and their Role for Precision Tests of the Electroweak Theory, *Fortsch. Phys.* 38 (1990) 165–260. doi:10.1002/prop.2190380302.

[83] M. Böhm, A. Denner, H. Joos, *Gauge theories of the strong and electroweak interaction*, Teubner, Stuttgart, Germany, 2001. doi:10.1007/978-3-322-80160-9.

[84] J. F. Gunion, H. E. Haber, G. L. Kane, S. Dawson, The Higgs Hunter’s Guide, *Front. Phys.* 80 (2000) 1–404.

[85] B. Grzadkowski, M. Iskrzynski, M. Misiak, J. Rosiek, Dimension-Six Terms in the Standard Model Lagrangian, *JHEP* 1010 (2010) 085. arXiv:1008.4884, doi:10.1007/JHEP10(2010)085.

[86] M. E. Peskin, D. V. Schroeder, *An introduction to quantum field theory*, Addison-Wesley, Reading, USA, 1995. doi:10.1201/9780429503559. URL <http://www.slac.stanford.edu/~mpeskin/QFT.html>

[87] M. D. Schwartz, *Quantum Field Theory and the Standard Model*, Cambridge University Press, Cambridge, UK, 2014. doi:10.1080/00107514.2014.970232. URL <http://www.cambridge.org/us/academic/subjects/physics/theoretical-physics-and-mathematical-physics/quantum-field-theory-and-the-standard-model>

[88] S. M. Bilenky, Neutrino in Standard Model and beyond, *Phys. Part. Nucl.* 46 (2015) 475–496. arXiv:1501.00232, doi:10.1134/S1063779615040024.

[89] P. Hernandez, Neutrino Physics, in: *Proceedings, 8th CERN–Latin-American School of High-Energy Physics (CLASHEP2015)*: Ibarra, Ecuador, March 05–17, 2015, 2016, pp. 85–142. arXiv:1708.01046, doi:10.51170/CERN-2016-005.85.

[90] M. Tanabashi, et al., Review of Particle Physics, *Phys. Rev. D*98 (2018) 030001. doi:10.1103/PhysRevD.98.030001.

[91] B. Pontecorvo, Inverse beta processes and nonconservation of lepton charge, *Sov. Phys. JETP* 7 (1958) 172–173, [Zh. Eksp. Teor. Fiz. 34 (1957) 247].

[92] Z. Maki, M. Nakagawa, S. Sakata, Remarks on the unified model of elementary particles, *Prog. Theor. Phys.* 28 (1962) 870–880. doi:10.1143/PTP.28.870.

[93] G. F. Sterman, *An introduction to quantum field theory*, Cambridge University Press, Cambridge, UK, 1993. doi:10.1017/CBO9780511622618.

[94] S. Weinberg, *The quantum theory of fields. Vol. 2: Modern applications*, Cambridge University Press, Cambridge, UK, 2013.

[95] M. Dine, TASI lectures on the strong CP problem, in: *Flavor physics for the millennium: Theoretical Advanced Study Institute in elementary particle physics, TASI 2000*, Boulder, USA, June 4–30, 2000, 2000, pp. 349–369. arXiv:hep-ph/0011376.

[96] K. Fujikawa, Path-Integral Measure for Gauge-Invariant Fermion Theories, *Phys. Rev. Lett.* 42 (1979) 1195–1198. doi:10.1103/PhysRevLett.42.1195.

[97] J. Dragos, et al., Confirming the Existence of the strong CP Problem in Lattice QCD with the Gradient Flow (2019). arXiv:1902.03254.

[98] J. M. Pendlebury, et al., Revised experimental upper limit on the electric dipole moment of the neutron, *Phys. Rev. D*92 (2015) 092003. arXiv:1509.04411, doi:10.1103/PhysRevD.92.092003.

[99] B. Graner, Y. Chen, E. G. Lindahl, B. R. Heckel, Reduced Limit on the Permanent Electric Dipole Moment of Hg199, *Phys. Rev. Lett.* 116 (2016) 161601, [Erratum: *Phys. Rev. Lett.* 119 (2017) 119901]. arXiv:1601.04339, doi:10.1103/PhysRevLett.119.119901, 10.1103/PhysRevLett.116.161601.

[100] C. Becchi, A. Rouet, R. Stora, Renormalization of the Abelian Higgs-Kibble Model, *Commun. Math. Phys.* 42 (1975) 127–162. doi:10.1007/BF01614158.

[101] J. C. Collins, *Renormalization*, Cambridge Monographs on Mathematical Physics, Cambridge University Press, Cambridge, UK, 1986. doi:10.1017/CBO9780511622656.

[102] B. S. DeWitt, Quantum Theory of Gravity. 2. The Manifestly Covariant Theory, *Phys. Rev.* 162 (1967) 1195–1239. doi:10.1103/PhysRev.162.1195.

[103] B. S. DeWitt, A gauge invariant effective action, in: *Oxford Conference on Quantum Gravity* Oxford, England, April 15–19, 1980, 1980, pp. 449–487.

[104] G. ’t Hooft, The Background Field Method in Gauge Field Theories, in: *Functional and Probabilistic Methods in Quantum Field Theory. Proceedings, 12th Winter School of Theoretical Physics, Karpacz, Feb 17–March 2, 1975*, 1975, pp. 345–369.

[105] D. G. Boulware, Gauge Dependence of the Effective Action, *Phys. Rev. D*23 (1981) 389. doi:10.1103/PhysRevD.23.389.

[106] L. F. Abbott, The Background Field Method Beyond One Loop, *Nucl. Phys.* B185 (1981) 189–203. doi:10.1016/0550-3213(81)90371-0.

[107] A. Denner, G. Weiglein, S. Dittmaier, Application of the Background Field Method to the electroweak Standard Model, *Nucl. Phys.* B440 (1995) 95–128. arXiv:hep-ph/9410338, doi:10.1016/0550-3213(95)00037-S.

[108] A. Denner, G. Weiglein, S. Dittmaier, Gauge invariance of Green functions: Background field method versus pinch technique, *Phys. Lett.* B333 (1994) 420–426. arXiv:hep-ph/9406204, doi:10.1016/0370-2693(94)90162-7.

[109] J. M. Cornwall, Dynamical Mass Generation in Continuum QCD, *Phys. Rev. D*26 (1982) 1453. doi:10.1103/PhysRevD.26.1453.

[110] J. M. Cornwall, J. Papavassiliou, Gauge Invariant Three Gluon Vertex in QCD, *Phys. Rev. D*40 (1989) 3474. doi:10.1103/PhysRevD.40.3474.

[111] J. Papavassiliou, Gauge Invariant Proper Selfenergies and Vertices in Gauge Theories with Broken Symmetry, *Phys. Rev. D*41 (1990) 3179. doi:10.1103/PhysRevD.41.3179.

[112] L. F. Abbott, Introduction to the Background Field Method, *Acta Phys. Polon.* B13 (1982) 33.

[113] L. F. Abbott, M. T. Grisaru, R. K. Schaefer, The Background Field Method and the S Matrix, *Nucl. Phys.* B229 (1983) 372–380. doi:10.1016/0550-3213(83)90337-1.

[114] A. Rebhan, G. Wirthmer, On the Equivalence of the Background Field Method, *Z. Phys. C*28 (1985) 269. doi:10.1007/BF01575734.

[115] A. Denner, S. Dittmaier, Dyson summation without violating Ward identities and the Goldstone-boson equivalence theorem, *Phys. Rev. D*54 (1996) 4499–4514. arXiv:hep-ph/9603341, doi:10.1103/PhysRevD.54.4499.

[116] A. Denner, S. Dittmaier, J.-N. Lang, Renormalization of mixing angles, *JHEP* 11 (2018) 104. arXiv:1808.03466, doi:10.1007/JHEP11(2018)104.

[117] K.-i. Aoki, et al., Electroweak Radiative Corrections to High Energy νe Scatterings, *Prog. Theor. Phys.* **65** (1981) 1001. doi:10.1143/PTP.65.1001.

[118] W. Buchmüller, D. Wyler, Effective Lagrangian Analysis of New Interactions and Flavor Conservation, *Nucl. Phys. B* **268** (1986) 621. doi:10.1016/0550-3213(86)90262-2.

[119] G. F. Giudice, C. Grojean, A. Pomarol, R. Rattazzi, The Strongly-Interacting Light Higgs, *JHEP* **06** (2007) 045. arXiv:hep-ph/0703164, doi:10.1088/1126-6708/2007/06/045.

[120] F. Bonnet, M. B. Gavela, T. Ota, W. Winter, Anomalous Higgs couplings at the LHC, and their theoretical interpretation, *Phys. Rev. D* **85** (2012) 035016. arXiv:1105.5140, doi:10.1103/PhysRevD.85.035016.

[121] T. Corbett, O. J. P. Eboli, J. Gonzalez-Fraile, M. C. Gonzalez-Garcia, Constraining anomalous Higgs interactions, *Phys. Rev. D* **86** (2012) 075013. arXiv:1207.1344, doi:10.1103/PhysRevD.86.075013.

[122] F. Bonnet, T. Ota, M. Rauch, W. Winter, Interpretation of precision tests in the Higgs sector in terms of physics beyond the Standard Model, *Phys. Rev. D* **86** (2012) 093014. arXiv:1207.4599, doi:10.1103/PhysRevD.86.093014.

[123] G. Passarino, NLO Inspired Effective Lagrangians for Higgs Physics, *Nucl. Phys. B* **868** (2013) 416–458. arXiv:1209.5538, doi:10.1016/j.nuclphysb.2012.11.018.

[124] T. Corbett, O. J. P. Eboli, J. Gonzalez-Fraile, M. C. Gonzalez-Garcia, Robust Determination of the Higgs Couplings: Power to the Data, *Phys. Rev. D* **87** (2013) 015022. arXiv:1211.4580, doi:10.1103/PhysRevD.87.015022.

[125] R. Contino, et al., Effective Lagrangian for a light Higgs-like scalar, *JHEP* **07** (2013) 035. arXiv:1303.3876, doi:10.1007/JHEP07(2013)035.

[126] I. Brivio, M. Trott, The Standard Model as an Effective Field Theory, *Phys. Rept.* **793** (2019) 1–98. arXiv:1706.08945, doi:10.1016/j.physrep.2018.11.002.

[127] S. Weinberg, Baryon and Lepton Nonconserving Processes, *Phys. Rev. Lett.* **43** (1979) 1566–1570. doi:10.1103/PhysRevLett.43.1566.

[128] R. Alonso, E. E. Jenkins, A. V. Manohar, M. Trott, Renormalization Group Evolution of the Standard Model Dimension Six Operators III: Gauge Coupling Dependence and Phenomenology, *JHEP* **04** (2014) 159. arXiv:1312.2014, doi:10.1007/JHEP04(2014)159.

[129] G. Passarino, M. Trott, The Standard Model Effective Field Theory and Next to Leading Order (2016). arXiv:1610.08356.

[130] D. A. Ross, M. J. G. Veltman, Neutral Currents in Neutrino Experiments, *Nucl. Phys. B* **95** (1975) 135–147. doi:10.1016/0550-3213(75)90485-X.

[131] E. E. Jenkins, A. V. Manohar, M. Trott, Renormalization group evolution of the standard model dimension six operators I: formalism and λ dependence, *JHEP* **10** (2013) 087. arXiv:1308.2627, doi:10.1007/JHEP10(2013)087.

[132] E. E. Jenkins, A. V. Manohar, M. Trott, Renormalization group evolution of the standard model dimension six operators II: Yukawa dependence, *JHEP* **01** (2014) 035. arXiv:1310.4838, doi:10.1007/JHEP01(2014)035.

[133] M. Ghezzi, R. Gomez-Ambrosio, G. Passarino, S. Uccirati, NLO Higgs effective field theory and κ -framework, *JHEP* **07** (2015) 175. arXiv:1505.03706, doi:10.1007/JHEP07(2015)175.

[134] G. M. Pruna, A. Signer, The $\mu \rightarrow e\gamma$ decay in a systematic effective field theory approach with dimension 6 operators, *JHEP* **10** (2014) 014. arXiv:1408.3565, doi:10.1007/JHEP10(2014)014.

[135] C. Hartmann, M. Trott, Higgs Decay to Two Photons at One Loop in the Standard Model Effective Field Theory, *Phys. Rev. Lett.* **115** (2015) 191801. arXiv:1507.03568, doi:10.1103/PhysRevLett.115.191801.

[136] C. Hartmann, M. Trott, On one-loop corrections in the standard model effective field theory; the $\Gamma(h \rightarrow \gamma\gamma)$ case, *JHEP* **07** (2015) 151. arXiv:1505.02646, doi:10.1007/JHEP07(2015)151.

[137] J. Baglio, S. Dawson, I. M. Lewis, NLO effects in EFT fits to W^+W^- production at the LHC, *Phys. Rev. D* **99** (2019) 035029. arXiv:1812.00214, doi:10.1103/PhysRevD.99.035029.

[138] J. M. Cullen, B. D. Pecjak, D. J. Scott, NLO corrections to $h \rightarrow b\bar{b}$ decay in SMEFT, *JHEP* **08** (2019) 173. arXiv:1904.06358, doi:10.1007/JHEP08(2019)173.

[139] C. Hartmann, W. Shepherd, M. Trott, The Z decay width in the SMEFT: y_t and λ corrections at one loop, *JHEP* **03** (2017) 060. arXiv:1611.09879, doi:10.1007/JHEP03(2017)060.

[140] S. Dawson, A. Ismail, Standard model EFT corrections to Z boson decays, *Phys. Rev. D* **98** (2018) 093003. arXiv:1808.05948, doi:10.1103/PhysRevD.98.093003.

[141] S. Dawson, P. P. Giardino, Electroweak corrections to Higgs boson decays to $\gamma\gamma$ and W^+W^- in standard model EFT, *Phys. Rev. D* **98** (2018) 095005. arXiv:1807.11504, doi:10.1103/PhysRevD.98.095005.

[142] S. Dawson, P. P. Giardino, Electroweak and QCD Corrections to Z and W pole observables in the SMEFT (2019). arXiv:1909.02000.

[143] T. Martini, M. Schulze, Electroweak Loops as a Probe of New Physics in $t\bar{t}$ Production at the LHC (2019). arXiv:1911.11244.

[144] I. Brivio, et al., Computing Tools for the SMEFT, 2019. arXiv:1910.11003.

[145] W. J. Marciano, A. Sirlin, Radiative corrections to neutrino-induced neutral-current phenomena in the $SU(2)_L \times U(1)$ theory, *Phys. Rev. D* **22** (1980) 2695, [Erratum: *Phys. Rev. D* **31** (1985) 213]. doi:10.1103/PhysRevD.31.213, 10.1103/PhysRevD.22.2695.

[146] D. Yu. Bardin, P. K. Khristova, O. M. Fedorenko, On the lowest order electroweak corrections to spin 1/2 fermion scattering. (I). The one-loop diagrammar, *Nucl. Phys. B* **175** (1980) 435–461. doi:10.1016/0550-3213(80)90021-8.

[147] J. Fleischer, F. Jegerlehner, Radiative corrections to Higgs-boson decays in the Weinberg-Salam Model, *Phys. Rev. D* **23** (1981) 2001–2026. doi:10.1103/PhysRevD.23.2001.

[148] S. Sakakibara, Radiative corrections to the neutral-current interactions in the Weinberg-Salam model, *Phys. Rev. D* **24** (1981) 1149. doi:10.1103/PhysRevD.24.1149.

[149] A. Sirlin, W. J. Marciano, Radiative Corrections to $\nu_\mu + N \rightarrow \mu^- + X$ and their effect on the determination of ρ^2 and $\sin^2 \theta_W$, *Nucl. Phys. B* **189** (1981) 442–460. doi:10.1016/0550-3213(81)90574-5.

[150] D. Yu. Bardin, P. K. Khristova, O. M. Fedorenko, On the lowest order electroweak corrections to Spin-1/2 fermion scattering. 2. The one-loop amplitudes, *Nucl. Phys. B* **197** (1982) 1–44. doi:10.1016/0550-3213(82)90152-3.

[151] W. E. Thirring, Radiative corrections in the nonrelativistic limit, *Phil. Mag. Ser. 7* **41** (1950) 1193–1194.

[152] S. Dittmaier, Thirring's low-energy theorem and its generalizations in the electroweak Standard Model, *Phys. Lett. B* 409 (1997) 509–516. [arXiv:hep-ph/9704368](https://arxiv.org/abs/hep-ph/9704368), doi:10.1016/S0370-2693(97)00888-5.

[153] A. Freitas, W. Hollik, W. Walter, G. Weiglein, Electroweak two-loop corrections to the M_W – M_Z mass correlation in the Standard Model, *Nucl. Phys. B* 632 (2002) 189–218, [Erratum: *Nucl. Phys. B* 666 (2003) 305]. [arXiv:hep-ph/0202131](https://arxiv.org/abs/hep-ph/0202131), doi:10.1016/S0550-3213(03)00500-5, 10.1016/S0550-3213(02)00243-2.

[154] M. Awramik, M. Czakon, A. Onishchenko, O. Veretin, Bosonic corrections to Δr at the two-loop level, *Phys. Rev. D* 68 (2003) 053004. [arXiv:hep-ph/0209084](https://arxiv.org/abs/hep-ph/0209084), doi:10.1103/PhysRevD.68.053004.

[155] S. Actis, A. Ferroglia, M. Passera, G. Passarino, Two-Loop Renormalization in the Standard Model. Part I: Prolegomena, *Nucl. Phys. B* 777 (2007) 1–34. [arXiv:hep-ph/0612122](https://arxiv.org/abs/hep-ph/0612122), doi:10.1016/j.nuclphysb.2007.04.021.

[156] S. Actis, G. Passarino, Two-Loop Renormalization in the Standard Model Part II: Renormalization Procedures and Computational Techniques, *Nucl. Phys. B* 777 (2007) 35–99. [arXiv:hep-ph/0612123](https://arxiv.org/abs/hep-ph/0612123), doi:10.1016/j.nuclphysb.2007.03.043.

[157] S. Actis, G. Passarino, Two-Loop Renormalization in the Standard Model Part III: Renormalization Equations and their Solutions, *Nucl. Phys. B* 777 (2007) 100–156. [arXiv:hep-ph/0612124](https://arxiv.org/abs/hep-ph/0612124), doi:10.1016/j.nuclphysb.2007.04.027.

[158] C. Jarlskog, Commutator of the Quark Mass Matrices in the Standard Electroweak Model and a Measure of Maximal CP Violation, *Phys. Rev. Lett.* 55 (1985) 1039. doi:10.1103/PhysRevLett.55.1039.

[159] C. Jarlskog, A Basis Independent Formulation of the Connection Between Quark Mass Matrices, CP Violation and Experiment, *Z. Phys. C* 29 (1985) 491–497. doi:10.1007/BF01565198.

[160] A. Denner, T. Sack, Renormalization of the quark mixing matrix, *Nucl. Phys. B* 347 (1990) 203–216. doi:10.1016/0550-3213(90)90557-T.

[161] P. Gambino, P. A. Grassi, F. Madrigal, Fermion mixing renormalization and gauge invariance, *Phys. Lett. B* 454 (1999) 98–104. [arXiv:hep-ph/9811470](https://arxiv.org/abs/hep-ph/9811470), doi:10.1016/S0370-2693(99)00321-4.

[162] C. Balzereit, T. Mannel, B. Plümper, The renormalization group evolution of the CKM matrix, *Eur. Phys. J. C* 9 (1999) 197–211. [arXiv:hep-ph/9810350](https://arxiv.org/abs/hep-ph/9810350), doi:10.1007/s100520050524.

[163] K. P. O. Diener, B. A. Kniehl, On mass shell renormalization of fermion mixing matrices, *Nucl. Phys. B* 617 (2001) 291–307. [arXiv:hep-ph/0109110](https://arxiv.org/abs/hep-ph/0109110), doi:10.1016/S0550-3213(01)00453-9.

[164] Y. Yamada, Gauge dependence of the on-shell renormalized mixing matrices, *Phys. Rev. D* 64 (2001) 036008. [arXiv:hep-ph/0103046](https://arxiv.org/abs/hep-ph/0103046), doi:10.1103/PhysRevD.64.036008.

[165] A. Pilaftsis, Gauge and scheme dependence of mixing matrix renormalization, *Phys. Rev. D* 65 (2002) 115013. [arXiv:hep-ph/0203210](https://arxiv.org/abs/hep-ph/0203210), doi:10.1103/PhysRevD.65.115013.

[166] A. Denner, E. Kraus, M. Roth, Physical renormalization condition for the quark mixing matrix, *Phys. Rev. D* 70 (2004) 033002. [arXiv:hep-ph/0402130](https://arxiv.org/abs/hep-ph/0402130), doi:10.1103/PhysRevD.70.033002.

[167] B. A. Kniehl, A. Sirlin, Simple On-Shell Renormalization Framework for the Cabibbo-Kobayashi-Maskawa Matrix, *Phys. Rev. D* 74 (2006) 116003. [arXiv:hep-th/0612033](https://arxiv.org/abs/hep-th/0612033), doi:10.1103/PhysRevD.74.116003.

[168] B. A. Kniehl, A. Sirlin, A Novel Formulation of Cabibbo-Kobayashi-Maskawa Matrix Renormalization, *Phys. Lett. B* 673 (2009) 208–210. [arXiv:0901.0114](https://arxiv.org/abs/0901.0114), doi:10.1016/j.physletb.2009.02.024.

[169] M. Krause, et al., Gauge-independent Renormalization of the 2-Higgs-Doublet Model, *JHEP* 09 (2016) 143. [arXiv:1605.04853](https://arxiv.org/abs/1605.04853), doi:10.1007/JHEP09(2016)143.

[170] A. Denner, L. Jenniches, J.-N. Lang, C. Sturm, Gauge-independent \overline{MS} renormalization in the 2HDM, *JHEP* 09 (2016) 115. [arXiv:1607.07352](https://arxiv.org/abs/1607.07352), doi:10.1007/JHEP09(2016)115.

[171] G. Degrassi, A. Vicini, Two loop renormalization of the electric charge in the standard model, *Phys. Rev. D* 69 (2004) 073007. [arXiv:hep-ph/0307122](https://arxiv.org/abs/hep-ph/0307122), doi:10.1103/PhysRevD.69.073007.

[172] W. Beenakker, et al., NLO QCD corrections to $t\bar{t}H$ production in hadron collisions, *Nucl. Phys. B* 653 (2003) 151–203. [arXiv:hep-ph/0211352](https://arxiv.org/abs/hep-ph/0211352), doi:10.1016/S0550-3213(03)00044-0.

[173] L. M. Brown, R. P. Feynman, Radiative corrections to Compton scattering, *Phys. Rev.* 85 (1952) 231–244. doi:10.1103/PhysRev.85.231.

[174] G. Ossola, C. G. Papadopoulos, R. Pittau, Reducing full one-loop amplitudes to scalar integrals at the integrand level, *Nucl. Phys. B* 763 (2007) 147–169. [arXiv:hep-ph/0609007](https://arxiv.org/abs/hep-ph/0609007), doi:10.1016/j.nuclphysb.2006.11.012.

[175] C. G. Bollini, J. J. Giambiagi, Dimensional Renormalization: The Number of Dimensions as a Regularizing Parameter, *Nuovo Cim.* B12 (1972) 20–26. doi:10.1007/BF02895558.

[176] G. Leibbrandt, Introduction to the technique of dimensional regularization, *Rev. Mod. Phys.* 47 (1975) 849. doi:10.1103/RevModPhys.47.849.

[177] S. Dittmaier, Separation of soft and collinear singularities from one loop N point integrals, *Nucl. Phys. B* 675 (2003) 447–466. [arXiv:hep-ph/0308246](https://arxiv.org/abs/hep-ph/0308246), doi:10.1016/j.nuclphysb.2003.10.003.

[178] O. Piguet, Construction of a Strictly Renormalizable Effective Lagrangian for the Massive Abelian Higgs Model, *Commun. Math. Phys.* 37 (1974) 19. doi:10.1007/BF01646031.

[179] A. Denner, S. Dittmaier, Scalar one-loop 4-point integrals, *Nucl. Phys. B* 844 (2011) 199–242. [arXiv:1005.2076](https://arxiv.org/abs/1005.2076), doi:10.1016/j.nuclphysb.2010.11.002.

[180] C. Gnendiger, et al., To d , or not to d : recent developments and comparisons of regularization schemes, *Eur. Phys. J. C* 77 (2017) 471. [arXiv:1705.01827](https://arxiv.org/abs/1705.01827), doi:10.1140/epjc/s10052-017-5023-2.

[181] F. Jegerlehner, Facts of life with γ_5 , *Eur. Phys. J. C* 18 (2001) 673–679. [arXiv:hep-th/0005255](https://arxiv.org/abs/hep-th/0005255), doi:10.1007/s100520100573.

[182] D. A. Akyeampong, R. Delbourgo, Dimensional regularization, abnormal amplitudes and anomalies, *Nuovo Cim.* A17 (1973) 578–586. doi:10.1007/BF02786835.

[183] P. Breitenlohner, D. Maison, Dimensional Renormalization and the Action Principle, *Commun. Math. Phys.* 52 (1977) 11–38. doi:10.1007/BF01609069.

[184] G. Bonneau, Consistency in dimensional regularization with γ_5 , *Phys. Lett.* **96B** (1980) 147–150. [doi:10.1016/0370-2693\(80\)90232-4](https://doi.org/10.1016/0370-2693(80)90232-4).

[185] S. A. Larin, The renormalization of the axial anomaly in dimensional regularization, *Phys. Lett.* **B303** (1993) 113–118. [arXiv:hep-ph/9302240](https://arxiv.org/abs/hep-ph/9302240), [doi:10.1016/0370-2693\(93\)90053-K](https://doi.org/10.1016/0370-2693(93)90053-K).

[186] M. S. Chanowitz, M. Furman, I. Hinchliffe, The axial current in dimensional regularization, *Nucl. Phys.* **B159** (1979) 225–243. [doi:10.1016/0550-3213\(79\)90333-X](https://doi.org/10.1016/0550-3213(79)90333-X).

[187] S. L. Adler, Axial vector vertex in spinor electrodynamics, *Phys. Rev.* **177** (1969) 2426–2438. [doi:10.1103/PhysRev.177.2426](https://doi.org/10.1103/PhysRev.177.2426).

[188] J. S. Bell, R. Jackiw, A PCAC puzzle: $\pi^0 \rightarrow \gamma\gamma$ in the σ model, *Nuovo Cim.* **A60** (1969) 47–61. [doi:10.1007/BF02823296](https://doi.org/10.1007/BF02823296).

[189] S. L. Adler, Perturbation theory anomalies, in: S. D. Deser, M. T. Grisaru, H. Pendleton (Eds.), *Proceedings of the 13th Brandeis University Summer Institute in Theoretical Physics, Lectures On Elementary Particles and Quantum Field Theory*, MIT, Cambridge, MA, USA, 1970.

[190] D. Kreimer, The γ_5 problem and anomalies: A Clifford algebra approach, *Phys. Lett.* **B237** (1990) 59–62. [doi:10.1016/0370-2693\(90\)90461-E](https://doi.org/10.1016/0370-2693(90)90461-E).

[191] J. G. Körner, D. Kreimer, K. Schilcher, A practicable γ_5 scheme in dimensional regularization, *Z. Phys.* **C54** (1992) 503–512. [doi:10.1007/BF01559471](https://doi.org/10.1007/BF01559471).

[192] D. Kreimer, The Rôle of γ_5 in Dimensional Regularization (1993). [arXiv:hep-ph/9401354](https://arxiv.org/abs/hep-ph/9401354).

[193] M. Lemoine, M. J. G. Veltman, Radiative Corrections to $e^+e^- \rightarrow W^+W^-$ in the Weinberg Model, *Nucl. Phys.* **B164** (1980) 445–483. [doi:10.1016/0550-3213\(80\)90521-0](https://doi.org/10.1016/0550-3213(80)90521-0).

[194] J. Fleischer, F. Jegerlehner, Radiative corrections to Higgs production by $e^+e^- \rightarrow ZH$ in the Weinberg-Salam model, *Nucl. Phys.* **B216** (1983) 469–492. [doi:10.1016/0550-3213\(83\)90296-1](https://doi.org/10.1016/0550-3213(83)90296-1).

[195] A. Denner, S. Dittmaier, M. Roth, D. Wackerlo, Electroweak radiative corrections to $e^+e^- \rightarrow WW \rightarrow 4$ fermions in double pole approximation: The RACOONWW approach, *Nucl. Phys.* **B587** (2000) 67–117. [arXiv:hep-ph/0006307](https://arxiv.org/abs/hep-ph/0006307), [doi:10.1016/S0550-3213\(00\)00511-3](https://doi.org/10.1016/S0550-3213(00)00511-3).

[196] A. Denner, S. Dittmaier, M. Roth, L. H. Wieders, Complete electroweak $\mathcal{O}(\alpha)$ corrections to charged-current $e^+e^- \rightarrow 4$ fermion processes, *Phys. Lett.* **B612** (2005) 223–232. [arXiv:hep-ph/0502063](https://arxiv.org/abs/hep-ph/0502063).

[197] G. Ossola, C. G. Papadopoulos, R. Pittau, On the rational terms of the one-loop amplitudes, *JHEP* **05** (2008) 004. [arXiv:0802.1876](https://arxiv.org/abs/0802.1876), [doi:10.1088/1126-6708/2008/05/004](https://doi.org/10.1088/1126-6708/2008/05/004).

[198] M. V. Garzelli, I. Malamos, R. Pittau, Feynman rules for the rational part of the electroweak 1-loop amplitudes in the R_ξ gauge and in the unitary gauge, *JHEP* **01** (2011) 029. [arXiv:1009.4302](https://arxiv.org/abs/1009.4302), [doi:10.1007/JHEP01\(2011\)029](https://doi.org/10.1007/JHEP01(2011)029).

[199] H.-S. Shao, Y.-J. Zhang, K.-T. Chao, Feynman Rules for the Rational Part of the Standard Model One-loop Amplitudes in the 't Hooft-Veltman γ_5 Scheme, *JHEP* **09** (2011) 048. [arXiv:1106.5030](https://arxiv.org/abs/1106.5030), [doi:10.1007/JHEP09\(2011\)048](https://doi.org/10.1007/JHEP09(2011)048).

[200] T. Binoth, J. P. Guillet, G. Heinrich, Algebraic evaluation of rational polynomials in one-loop amplitudes, *JHEP* **02** (2007) 013. [arXiv:hep-ph/0609054](https://arxiv.org/abs/hep-ph/0609054), [doi:10.1088/1126-6708/2007/02/013](https://doi.org/10.1088/1126-6708/2007/02/013).

[201] A. Bredenstein, A. Denner, S. Dittmaier, S. Pozzorini, NLO QCD corrections to $t\bar{t}b\bar{b}$ production at the LHC: 1. Quark–antiquark annihilation, *JHEP* **08** (2008) 108. [arXiv:0807.1248](https://arxiv.org/abs/0807.1248), [doi:10.1088/1126-6708/2008/08/108](https://doi.org/10.1088/1126-6708/2008/08/108).

[202] A. Denner, S. Dittmaier, Reduction schemes for one-loop tensor integrals, *Nucl. Phys.* **B734** (2006) 62–115. [arXiv:hep-ph/0509141](https://arxiv.org/abs/hep-ph/0509141), [doi:10.1016/j.nuclphysb.2005.11.007](https://doi.org/10.1016/j.nuclphysb.2005.11.007).

[203] A. Denner, S. Dittmaier, Reduction of one-loop tensor 5-point integrals, *Nucl. Phys.* **B658** (2003) 175–202. [arXiv:hep-ph/0212259](https://arxiv.org/abs/hep-ph/0212259).

[204] G. J. van Oldenborgh, J. A. M. Vermaasen, New algorithms for one-loop integrals, *Z. Phys.* **C46** (1990) 425–438. [doi:10.1007/BF01621031](https://doi.org/10.1007/BF01621031).

[205] Y. Ezawa, et al., Brown–Feynman reduction of one-loop Feynman diagrams to scalar integrals with orthonormal basis tensors, *Comput. Phys. Commun.* **69** (1992) 15–45. [doi:10.1016/0010-4655\(92\)90125-I](https://doi.org/10.1016/0010-4655(92)90125-I).

[206] G. Belanger, et al., Automatic calculations in high energy physics and Grace at one-loop, *Phys. Rept.* **430** (2006) 117–209. [arXiv:hep-ph/0308080](https://arxiv.org/abs/hep-ph/0308080), [doi:10.1016/j.physrep.2006.02.001](https://doi.org/10.1016/j.physrep.2006.02.001).

[207] A. I. Davydychev, A simple formula for reducing Feynman diagrams to scalar integrals, *Phys. Lett.* **B263** (1991) 107–111. [doi:10.1016/0370-2693\(91\)91715-8](https://doi.org/10.1016/0370-2693(91)91715-8).

[208] O. V. Tarasov, Connection between Feynman integrals having different values of the space-time dimension, *Phys. Rev.* **D54** (1996) 6479–6490. [arXiv:hep-th/9606018](https://arxiv.org/abs/hep-th/9606018), [doi:10.1103/PhysRevD.54.6479](https://doi.org/10.1103/PhysRevD.54.6479).

[209] Z. Bern, L. J. Dixon, D. A. Kosower, Dimensionally regulated one-loop integrals, *Phys. Lett.* **B302** (1993) 299–308, [Erratum: *Phys. Lett.* **B318** (1993) 649]. [arXiv:hep-ph/9212308](https://arxiv.org/abs/hep-ph/9212308), [doi:10.1016/0370-2693\(93\)90469-X](https://doi.org/10.1016/0370-2693(93)90469-X), [10.1016/0370-2693\(93\)90400-C](https://doi.org/10.1016/0370-2693(93)90400-C).

[210] T. Binoth, J. P. Guillet, G. Heinrich, Reduction formalism for dimensionally regulated one-loop N -point integrals, *Nucl. Phys.* **B572** (2000) 361–386. [arXiv:hep-ph/9911342](https://arxiv.org/abs/hep-ph/9911342), [doi:10.1016/S0550-3213\(00\)00040-7](https://doi.org/10.1016/S0550-3213(00)00040-7).

[211] G. Duplancic, B. Nizic, Reduction method for dimensionally regulated one-loop N -point Feynman integrals, *Eur. Phys. J.* **C35** (2004) 105–118. [arXiv:hep-ph/0303184](https://arxiv.org/abs/hep-ph/0303184), [doi:10.1140/epjc/s2004-01723-7](https://doi.org/10.1140/epjc/s2004-01723-7).

[212] W. T. Giele, E. W. N. Glover, A calculational formalism for one-loop integrals, *JHEP* **04** (2004) 029. [arXiv:hep-ph/0402152](https://arxiv.org/abs/hep-ph/0402152), [doi:10.1088/1126-6708/2004/04/029](https://doi.org/10.1088/1126-6708/2004/04/029).

[213] W. Giele, E. W. N. Glover, G. Zanderighi, Numerical evaluation of one-loop diagrams near exceptional momentum configurations, *Nucl. Phys. Proc. Suppl.* **135** (2004) 275–279. [arXiv:hep-ph/0407016](https://arxiv.org/abs/hep-ph/0407016), [doi:10.1016/j.nuclphysbps.2004.09.028](https://doi.org/10.1016/j.nuclphysbps.2004.09.028).

[214] T. Binoth, et al., An algebraic/numerical formalism for one-loop multi-leg amplitudes, *JHEP* **10** (2005) 015. [arXiv:hep-ph/0504267](https://arxiv.org/abs/hep-ph/0504267), [doi:10.1088/1126-6708/2005/10/015](https://doi.org/10.1088/1126-6708/2005/10/015).

[215] D. B. Melrose, Reduction of Feynman diagrams, *Nuovo Cim.* **40** (1965) 181–213. [doi:10.1007/BF02832919](https://doi.org/10.1007/BF02832919).

[216] J. M. Campbell, E. W. N. Glover, D. J. Miller, One-loop tensor integrals in dimensional regularization, *Nucl. Phys.* **B498** (1997) 397–442. [arXiv:hep-ph/9612413](https://arxiv.org/abs/hep-ph/9612413), [doi:10.1016/S0550-3213\(97\)00268-X](https://doi.org/10.1016/S0550-3213(97)00268-X).

[217] W. L. van Neerven, J. A. M. Vermaasen, Large loop integrals, *Phys. Lett.* **137B** (1984) 241–244. [doi:10.1016/0370-2693\(84\)90237-5](https://doi.org/10.1016/0370-2693(84)90237-5).

[218] G. Belanger, et al., Full one-loop electroweak radiative corrections to single Higgs production in e^+e^- , *Phys. Lett.* **B559** (2003) 252–262. [arXiv:hep-ph/0212261](https://arxiv.org/abs/hep-ph/0212261), [doi:10.1016/S0370-2693\(03\)00339-3](https://doi.org/10.1016/S0370-2693(03)00339-3).

[219] J. Fleischer, T. Riemann, A complete algebraic reduction of one-loop tensor Feynman integrals, *Phys. Rev. D* 83 (2011) 073004. [arXiv:1009.4436](https://arxiv.org/abs/1009.4436), doi:10.1103/PhysRevD.83.073004.

[220] J. Fleischer, T. Riemann, A solution for tensor reduction of one-loop N -point functions with $N \geq 6$, *Phys. Lett. B* 707 (2012) 375–380. [arXiv:1111.5821](https://arxiv.org/abs/1111.5821), doi:10.1016/j.physletb.2011.12.060.

[221] T. Hahn, M. Perez-Victoria, Automatized one-loop calculations in four and D dimensions, *Comput. Phys. Commun.* 118 (1999) 153–165. [arXiv:hep-ph/9807565](https://arxiv.org/abs/hep-ph/9807565), doi:10.1016/S0010-4655(98)00173-8.

[222] G. J. van Oldenborgh, FF: A package to evaluate one-loop Feynman diagrams, *Comput. Phys. Commun.* 66 (1991) 1–15. doi:10.1016/0010-4655(91)90002-3.

[223] T. Hahn, S. Paßehr, C. Schappacher, FormCalc 9 and Extensions, *PoS LL2016* (2016) 068, [*J. Phys. Conf. Ser.* 762 (2016) 012065]. [arXiv:1604.04611](https://arxiv.org/abs/1604.04611), doi:10.22323/1.260.0068, 10.1088/1742-6596/762/1/012065.

[224] D. T. Nhungh, L. D. Ninh, D0C : A code to calculate scalar one-loop four-point integrals with complex masses, *Comput. Phys. Commun.* 180 (2009) 2258–2267. [arXiv:0902.0325](https://arxiv.org/abs/0902.0325), doi:10.1016/j.cpc.2009.07.012.

[225] T. Binoth, et al., Golem95: A numerical program to calculate one-loop tensor integrals with up to six external legs, *Comput. Phys. Commun.* 180 (2009) 2317–2330. [arXiv:0810.0992](https://arxiv.org/abs/0810.0992), doi:10.1016/j.cpc.2009.06.024.

[226] G. Cullen, et al., Golem95C: A library for one-loop integrals with complex masses, *Comput. Phys. Commun.* 182 (2011) 2276–2284. [arXiv:1101.5595](https://arxiv.org/abs/1101.5595), doi:10.1016/j.cpc.2011.05.015.

[227] J. P. Guillet, G. Heinrich, J. F. von Soden-Fraunhofen, Tools for NLO automation: extension of the golem95C integral library, *Comput. Phys. Commun.* 185 (2014) 1828–1834. [arXiv:1312.3887](https://arxiv.org/abs/1312.3887), doi:10.1016/j.cpc.2014.03.009.

[228] A. Denner, S. Dittmaier, L. Hofer, COLLIER - A fortran library for one-loop integrals, *PoS LL2014* (2014) 071. [arXiv:1407.0087](https://arxiv.org/abs/1407.0087).

[229] A. Denner, S. Dittmaier, L. Hofer, COLLIER: a fortran-based Complex One-Loop Library in Extended Regularizations, *Comput. Phys. Commun.* 212 (2017) 220–238. [arXiv:1604.06792](https://arxiv.org/abs/1604.06792), doi:10.1016/j.cpc.2016.10.013.

[230] J. Fleischer, T. Riemann, V. Yundin, PJFry: A C++ package for tensor reduction of one-loop Feynman integrals, *Tech. rep.*, DESY (2011).

[231] H. H. Patel, Package-X: A Mathematica package for the analytic calculation of one-loop integrals, *Comput. Phys. Commun.* 197 (2015) 276–290. [arXiv:1503.01469](https://arxiv.org/abs/1503.01469), doi:10.1016/j.cpc.2015.08.017.

[232] H. H. Patel, Package-X 2.0: A Mathematica package for the analytic calculation of one-loop integrals, *Comput. Phys. Commun.* 218 (2017) 66–70. [arXiv:1612.00009](https://arxiv.org/abs/1612.00009), doi:10.1016/j.cpc.2017.04.015.

[233] F. del Aguila, R. Pittau, Recursive numerical calculus of one-loop tensor integrals, *JHEP* 07 (2004) 017. [arXiv:hep-ph/0404120](https://arxiv.org/abs/hep-ph/0404120), doi:10.1088/1126-6708/2004/07/017.

[234] R. Pittau, Formulae for a numerical computation of one-loop tensor integrals, in: *Linear colliders. Proceedings, International Conference, LCWS 2004*, Paris, 2004. [arXiv:hep-ph/0406105](https://arxiv.org/abs/hep-ph/0406105).

[235] F. Buccioni, S. Pozzorini, M. Zoller, On-the-fly reduction of open loops, *Eur. Phys. J. C* 78 (2018) 70. [arXiv:1710.11452](https://arxiv.org/abs/1710.11452), doi:10.1140/epjc/s10052-018-5562-1.

[236] A. van Hameren, J. Vollinga, S. Weinzierl, Automated computation of one-loop integrals in massless theories, *Eur. Phys. J. C* 41 (2005) 361–375. [arXiv:hep-ph/0502165](https://arxiv.org/abs/hep-ph/0502165), doi:10.1140/epjc/s2005-02229-6.

[237] P. Mastrolia, G. Ossola, C. G. Papadopoulos, R. Pittau, Optimizing the reduction of one-loop amplitudes, *JHEP* 06 (2008) 030. [arXiv:0803.3964](https://arxiv.org/abs/0803.3964), doi:10.1088/1126-6708/2008/06/030.

[238] P. Mastrolia, E. Mirabella, T. Peraro, Integrand reduction of one-loop scattering amplitudes through Laurent series expansion, *JHEP* 06 (2012) 095, [Erratum: *JHEP* 11 (2012) 128]. [arXiv:1203.0291](https://arxiv.org/abs/1203.0291), doi:10.1007/JHEP11(2012)128, 10.1007/JHEP06(2012)095.

[239] G. Ossola, C. G. Papadopoulos, R. Pittau, CutTools: a program implementing the OPP reduction method to compute one-loop amplitudes, *JHEP* 0803 (2008) 042. [arXiv:0711.3596](https://arxiv.org/abs/0711.3596), doi:10.1088/1126-6708/2008/03/042.

[240] G. Ossola, C. G. Papadopoulos, R. Pittau, Numerical evaluation of six-photon amplitudes, *JHEP* 07 (2007) 085. [arXiv:0704.1271](https://arxiv.org/abs/0704.1271), doi:10.1088/1126-6708/2007/07/085.

[241] P. Draggiotis, M. V. Garzelli, C. G. Papadopoulos, R. Pittau, Feynman rules for the rational part of the QCD 1-loop amplitudes, *JHEP* 04 (2009) 072. [arXiv:0903.0356](https://arxiv.org/abs/0903.0356), doi:10.1088/1126-6708/2009/04/072.

[242] M. V. Garzelli, I. Malamos, R. Pittau, Feynman rules for the rational part of the electroweak 1-loop amplitudes, *JHEP* 01 (2010) 040, [Erratum: *JHEP* 10 (2010) 097]. [arXiv:0910.3130](https://arxiv.org/abs/0910.3130), doi:10.1007/JHEP10(2010)097, 10.1007/JHEP01(2010)040.

[243] R. Pittau, Primary Feynman rules to calculate the ϵ -dimensional integrand of any 1-loop amplitude, *JHEP* 02 (2012) 029. [arXiv:1111.4965](https://arxiv.org/abs/1111.4965), doi:10.1007/JHEP02(2012)029.

[244] H.-S. Shao, Y.-J. Zhang, Feynman Rules for the Rational Part of One-loop QCD Corrections in the MSSM, *JHEP* 06 (2012) 112. [arXiv:1205.1273](https://arxiv.org/abs/1205.1273), doi:10.1007/s13130-012-4240-2.

[245] B. Page, R. Pittau, R_2 vertices for the effective ggH theory, *JHEP* 09 (2013) 078. [arXiv:1307.6142](https://arxiv.org/abs/1307.6142), doi:10.1007/JHEP09(2013)078.

[246] Z. Bern, L. J. Dixon, D. A. Kosower, Bootstrapping multi-parton loop amplitudes in QCD, *Phys. Rev. D* 73 (2006) 065013. [arXiv:hep-ph/0507005](https://arxiv.org/abs/hep-ph/0507005), doi:10.1103/PhysRevD.73.065013.

[247] Z. Bern, L. J. Dixon, D. A. Kosower, One-loop amplitudes for e^+e^- to four partons, *Nucl. Phys. B* 513 (1998) 3–86. [arXiv:hep-ph/9708239](https://arxiv.org/abs/hep-ph/9708239), doi:10.1016/S0550-3213(97)00703-7.

[248] C. Anastasiou, et al., d -dimensional unitarity cut method, *Phys. Lett. B* 645 (2007) 213–216. [arXiv:hep-ph/0609191](https://arxiv.org/abs/hep-ph/0609191), doi:10.1016/j.physletb.2006.12.022.

[249] C. Anastasiou, et al., Unitarity cuts and reduction to master integrals in d dimensions for one-loop amplitudes, *JHEP* 03 (2007) 111. [arXiv:hep-ph/0612277](https://arxiv.org/abs/hep-ph/0612277), doi:10.1088/1126-6708/2007/03/111.

[250] W. T. Giele, Z. Kunszt, K. Melnikov, Full one-loop amplitudes from tree amplitudes, *JHEP* 0804 (2008) 049. [arXiv:0801.2237](https://arxiv.org/abs/0801.2237), doi:10.1088/1126-6708/2008/04/049.

[251] S. D. Badger, Direct extraction of one loop rational terms, *JHEP* 01 (2009) 049. [arXiv:0806.4600](https://arxiv.org/abs/0806.4600), doi:10.1088/1126-6708/2009/01/049.

[252] P. Mastrolia, G. Ossola, T. Reiter, F. Tramontano, Scattering amplitudes from unitarity-based reduction algorithm at the integrand-level, *JHEP* 1008 (2010) 080. [arXiv:1006.0710](https://arxiv.org/abs/1006.0710), doi:10.1007/JHEP08(2010)080.

[253] T. Peraro, Ninja: Automated Integrand Reduction via Laurent Expansion for One-Loop Amplitudes, *Comput. Phys. Commun.* 185 (2014) 2771–2797. [arXiv:1403.1229](https://arxiv.org/abs/1403.1229), doi:10.1016/j.cpc.2014.06.017.

[254] R. K. Ellis, W. T. Giele, Z. Kunszt, A numerical unitarity formalism for evaluating one-loop amplitudes, *JHEP* 0803 (2008) 003. [arXiv:0708.2398](https://arxiv.org/abs/0708.2398), doi:10.1088/1126-6708/2008/03/003.

[255] A. Denner, U. Nierste, R. Scharf, A compact expression for the scalar one-loop four-point function, *Nucl. Phys.* B367 (1991) 637–656.

[256] J. Fleischer, F. Jegerlehner, O. V. Tarasov, A new hypergeometric representation of one-loop scalar integrals in d dimensions, *Nucl. Phys.* B672 (2003) 303–328. [arXiv:hep-ph/0307113](https://arxiv.org/abs/hep-ph/0307113), doi:10.1016/j.nuclphysb.2003.09.004.

[257] W. Beenakker, A. Denner, Infrared divergent scalar box integrals with applications in the Electroweak Standard Model, *Nucl. Phys.* B338 (1990) 349–370.

[258] Z. Bern, L. J. Dixon, D. A. Kosower, Dimensionally regulated pentagon integrals, *Nucl. Phys.* B412 (1994) 751–816. [arXiv:hep-ph/9306240](https://arxiv.org/abs/hep-ph/9306240), doi:10.1016/0550-3213(94)90398-0.

[259] G. Duplancic, B. Nizic, Dimensionally regulated one-loop box scalar integrals with massless internal lines, *Eur. Phys. J. C20* (2001) 357–370. [arXiv:hep-ph/0006249](https://arxiv.org/abs/hep-ph/0006249), doi:10.1007/s100520100675.

[260] G. Duplancic, B. Nizic, IR finite one-loop box scalar integral with massless internal lines, *Eur. Phys. J. C24* (2002) 385–391. [arXiv:hep-ph/0201306](https://arxiv.org/abs/hep-ph/0201306), doi:10.1007/s100520200943.

[261] R. K. Ellis, G. Zanderighi, Scalar one-loop integrals for QCD, *JHEP* 02 (2008) 002. [arXiv:0712.1851](https://arxiv.org/abs/0712.1851), doi:10.1088/1126-6708/2008/02/002.

[262] J. P. Guillet, E. Pilon, Y. Shimizu, M. S. Zidi, A novel approach to the computation of one-loop three- and four-point functions. I - The real mass case, *Progress of Theoretical and Experimental Physics* 2019 (2019) 113B05. [arXiv:1811.03550](https://arxiv.org/abs/1811.03550), doi:10.1093/ptep/ptz114.

[263] J. P. Guillet, E. Pilon, Y. Shimizu, M. S. Zidi, A novel approach to the computation of one-loop three- and four-point functions. II - The complex mass case (2018). [arXiv:1811.03917](https://arxiv.org/abs/1811.03917).

[264] J. P. Guillet, E. Pilon, Y. Shimizu, M. S. Zidi, A novel approach to the computation of one-loop three- and four-point functions. III - The infrared divergent case (2018). [arXiv:1811.07760](https://arxiv.org/abs/1811.07760).

[265] A. van Hameren, OneLoop: for the evaluation of one-loop scalar functions, *Comput. Phys. Commun.* 182 (2011) 2427–2438. [arXiv:1007.4716](https://arxiv.org/abs/1007.4716), doi:10.1016/j.cpc.2011.06.011.

[266] S. Carrazza, R. K. Ellis, G. Zanderighi, QCDLoop: A comprehensive framework for one-loop scalar integrals, *Comput. Phys. Commun.* 209 (2016) 134–143. [arXiv:1605.03181](https://arxiv.org/abs/1605.03181), doi:10.1016/j.cpc.2016.07.033.

[267] A. Freitas, Numerical multi-loop integrals and applications, *Prog. Part. Nucl. Phys.* 90 (2016) 201–240. [arXiv:1604.00406](https://arxiv.org/abs/1604.00406), doi:10.1016/j.ppnp.2016.06.004.

[268] A. Ferroglia, M. Passera, G. Passarino, S. Uccirati, All purpose numerical evaluation of one-loop multi-leg Feynman diagrams, *Nucl. Phys.* B650 (2003) 162–228. [arXiv:hep-ph/0209219](https://arxiv.org/abs/hep-ph/0209219), doi:10.1016/S0550-3213(02)01070-2.

[269] I. N. Bernshein, The analytic continuation of generalized functions with respect to a parameter, *Functional Analysis and Its Applications* 6 (1972) 273–285. doi:10.1007/BF01077645.

[270] F. V. Tkachov, Algebraic algorithms for multiloop calculations. The first 15 years. What's next?, *Nucl. Instrum. Meth. A389* (1997) 309–313. [arXiv:hep-ph/9609429](https://arxiv.org/abs/hep-ph/9609429), doi:10.1016/S0168-9002(97)00110-1.

[271] S. Actis, G. Passarino, C. Sturm, S. Uccirati, NLO Electroweak Corrections to Higgs Boson Production at Hadron Colliders, *Phys. Lett.* B670 (2008) 12–17. [arXiv:0809.1301](https://arxiv.org/abs/0809.1301), doi:10.1016/j.physletb.2008.10.018.

[272] G. Passarino, C. Sturm, S. Uccirati, Complete Two-Loop Corrections to $H \rightarrow \gamma\gamma$, *Phys. Lett.* B655 (2007) 298–306. [arXiv:0707.1401](https://arxiv.org/abs/0707.1401), doi:10.1016/j.physletb.2007.09.002.

[273] S. Actis, G. Passarino, C. Sturm, S. Uccirati, NNLO Computational Techniques: The Cases $H \rightarrow \gamma\gamma$ and $H \rightarrow gg$, *Nucl. Phys.* B811 (2009) 182–273. [arXiv:0809.3667](https://arxiv.org/abs/0809.3667), doi:10.1016/j.nuclphysb.2008.11.024.

[274] Z. Nagy, D. E. Soper, General subtraction method for numerical calculation of one-loop QCD matrix elements, *JHEP* 09 (2003) 055. [arXiv:hep-ph/0308127](https://arxiv.org/abs/hep-ph/0308127), doi:10.1088/1126-6708/2003/09/055.

[275] S. Becker, C. Reuschle, S. Weinzierl, Numerical NLO QCD calculations, *JHEP* 12 (2010) 013. [arXiv:1010.4187](https://arxiv.org/abs/1010.4187), doi:10.1007/JHEP12(2010)013.

[276] S. Becker, et al., NLO results for five, six and seven jets in electron-positron annihilation, *Phys. Rev. Lett.* 108 (2012) 032005. [arXiv:1111.1733](https://arxiv.org/abs/1111.1733), doi:10.1103/PhysRevLett.108.032005.

[277] D. Götz, C. Reuschle, C. Schwan, S. Weinzierl, NLO corrections to Z production in association with several jets, *PoS LL2014* (2014) 009. [arXiv:1407.0203](https://arxiv.org/abs/1407.0203), doi:10.22323/1.211.0009.

[278] S. Catani, et al., From loops to trees by-passing Feynman's theorem, *JHEP* 09 (2008) 065. [arXiv:0804.3170](https://arxiv.org/abs/0804.3170), doi:10.1088/1126-6708/2008/09/065.

[279] Z. Capatti, V. Hirschi, D. Kermanschah, B. Ruijl, Loop Tree Duality for multi-loop numerical integration, *Phys. Rev. Lett.* 123 (2019) 151602. [arXiv:1906.06138](https://arxiv.org/abs/1906.06138), doi:10.1103/PhysRevLett.123.151602.

[280] M. Consoli, One-loop corrections to $e^+e^- \rightarrow e^+e^-$ in the Weinberg model, *Nucl. Phys.* B160 (1979) 208–252. doi:10.1016/0550-3213(79)90235-9.

[281] H. Strubbe, Manual for Schoonschip: A CDC 6000 / 7000 program for symbolic evaluation of algebraic expressions, *Comput. Phys. Commun.* 8 (1974) 1–30. doi:10.1016/0010-4655(74)90081-2.

[282] G. J. van Oldenborgh, J. A. M. Vermaasen, The formula manipulation program Form, in: *New computing techniques in physics research. Proceedings, 1st International Workshop on Software Engineering, Artificial Intelligence and Expert Systems in High-Energy and Nuclear Physics*, Lyon, France, March 19–24, 1990, 1990, pp. 545–553.

[283] B. Ruijl, T. Ueda, J. Vermaseren, FORM version 4.2 (2017). [arXiv:1707.06453](https://arxiv.org/abs/1707.06453).

[284] R. Mertig, M. Böhm, A. Denner, Feyn Calc: Computer algebraic calculation of Feynman amplitudes, *Comput. Phys. Commun.* 64 (1991) 345–359. doi:10.1016/0010-4655(91)90130-D.

[285] V. Shtabovenko, R. Mertig, F. Orellana, New Developments in FeynCalc 9.0, *Comput. Phys. Commun.* 207 (2016) 432–444. [arXiv:1601.01167](https://arxiv.org/abs/1601.01167), doi:10.1016/j.cpc.2016.06.008.

[286] S. Dittmaier, Weyl-van der Waerden formalism for helicity amplitudes of massive particles, *Phys. Rev. D* 59 (1998) 016007. [arXiv:hep-ph/9805445](https://arxiv.org/abs/hep-ph/9805445), doi:10.1103/PhysRevD.59.016007.

[287] H. Murayama, I. Watanabe, K. Hagiwara, HELAS: HELicity Amplitude Subroutines for Feynman diagram evaluations, KEK-91-11 (1992).

[288] T. Stelzer, W. F. Long, Automatic generation of tree level helicity amplitudes, *Comput. Phys. Commun.* 81 (1994) 357–371. [arXiv:hep-ph/9401258](https://arxiv.org/abs/hep-ph/9401258), doi:10.1016/0010-4655(94)90084-1.

[289] P. de Aquino, et al., ALOHA: Automatic Libraries Of Helicity Amplitudes for Feynman Diagram Computations, *Comput. Phys. Commun.* 183 (2012) 2254–2263. [arXiv:1108.2041](https://arxiv.org/abs/1108.2041), doi:10.1016/j.cpc.2012.05.004.

[290] C. Degrande, et al., UFO - The Universal FeynRules Output, *Comput. Phys. Commun.* 183 (2012) 1201–1214. [arXiv:1108.2040](https://arxiv.org/abs/1108.2040), doi:10.1016/j.cpc.2012.01.022.

[291] T. Hahn, Generating Feynman diagrams and amplitudes with FeynArts 3, *Comput. Phys. Commun.* 140 (2001) 418–431. [arXiv:hep-ph/0012260](https://arxiv.org/abs/hep-ph/0012260), doi:10.1016/S0010-4655(01)00290-9.

[292] J. Küblbeck, M. Böhm, A. Denner, Feyn Arts: Computer Algebraic Generation of Feynman Graphs and Amplitudes, *Comput. Phys. Commun.* 60 (1990) 165–180. doi:10.1016/0010-4655(90)90001-H.

[293] P. Nogueira, Automatic Feynman graph generation, *J. Comput. Phys.* 105 (1993) 279–289. doi:10.1006/jcph.1993.1074.

[294] M. Tentyukov, J. Fleischer, A Feynman diagram analyzer DIANA, *Comput. Phys. Commun.* 132 (2000) 124–141. [arXiv:hep-ph/9904258](https://arxiv.org/abs/hep-ph/9904258), doi:10.1016/S0010-4655(00)00147-8.

[295] N. D. Christensen, C. Duhr, FeynRules - Feynman rules made easy, *Comput. Phys. Commun.* 180 (2009) 1614–1641. [arXiv:0806.4194](https://arxiv.org/abs/0806.4194), doi:10.1016/j.cpc.2009.02.018.

[296] A. Alloul, et al., FeynRules 2.0 - A complete toolbox for tree-level phenomenology, *Comput. Phys. Commun.* 185 (2014) 2250–2300. [arXiv:1310.1921](https://arxiv.org/abs/1310.1921), doi:10.1016/j.cpc.2014.04.012.

[297] A. Belyaev, N. D. Christensen, A. Pukhov, CalcHEP 3.4 for collider physics within and beyond the Standard Model, *Comput. Phys. Commun.* 184 (2013) 1729–1769. [arXiv:1207.6082](https://arxiv.org/abs/1207.6082), doi:10.1016/j.cpc.2013.01.014.

[298] G. Cullen, et al., Automated one-loop calculations with GoSam, *Eur. Phys. J. C* 72 (2012) 1889. [arXiv:1111.2034](https://arxiv.org/abs/1111.2034), doi:10.1140/epjc/s10052-012-1889-1.

[299] G. Cullen, et al., GoSAM-2.0: a tool for automated one-loop calculations within the Standard Model and beyond, *Eur. Phys. J. C* 74 (2014) 3001. [arXiv:1404.7096](https://arxiv.org/abs/1404.7096), doi:10.1140/epjc/s10052-014-3001-5.

[300] J. Alwall, et al., MadGraph 5: going beyond, *JHEP* 06 (2011) 128. [arXiv:1106.0522](https://arxiv.org/abs/1106.0522), doi:10.1007/JHEP06(2011)128.

[301] T. Gleisberg, et al., Event generation with SHERPA 1.1, *JHEP* 02 (2009) 007. [arXiv:0811.4622](https://arxiv.org/abs/0811.4622), doi:10.1088/1126-6708/2009/02/007.

[302] M. Moretti, T. Ohl, J. Reuter, O'Mega: An optimizing matrix element generator, in: Physics and Experimentation at a Linear Electron-Positron Collider, 2nd ECFA/DESY Study, 1998-2001, Vol. 1-3, 2001, pp. 1981–2009. [arXiv:hep-ph/0102195](https://arxiv.org/abs/hep-ph/0102195).

[303] W. Kilian, T. Ohl, J. Reuter, WHIZARD: Simulating Multi-Particle Processes at LHC and ILC, *Eur. Phys. J. C* 71 (2011) 1742. [arXiv:0708.4233](https://arxiv.org/abs/0708.4233), doi:10.1140/epjc/s10052-011-1742-y.

[304] N. D. Christensen, et al., Introducing an interface between WHIZARD and FeynRules, *Eur. Phys. J. C* 72 (2012) 1990. [arXiv:1010.3251](https://arxiv.org/abs/1010.3251), doi:10.1140/epjc/s10052-012-1990-5.

[305] A. Semenov, LanHEP – A package for automatic generation of Feynman rules from the Lagrangian. Version 3.2, *Comput. Phys. Commun.* 201 (2016) 167–170. [arXiv:1412.5016](https://arxiv.org/abs/1412.5016), doi:10.1016/j.cpc.2016.01.003.

[306] E. Boos, et al., CompHEP 4.4: Automatic computations from Lagrangians to events, *Nucl. Instrum. Meth. A* 534 (2004) 250–259. [arXiv:hep-ph/0403113](https://arxiv.org/abs/hep-ph/0403113), doi:10.1016/j.nima.2004.07.096.

[307] F. A. Berends, W. T. Giele, Recursive calculations for processes with n gluons, *Nucl. Phys. B* 306 (1988) 759–808. doi:10.1016/0550-3213(88)90442-7.

[308] F. Caravaglios, M. Moretti, An algorithm to compute Born scattering amplitudes without Feynman graphs, *Phys. Lett. B* 358 (1995) 332–338. [arXiv:hep-ph/9507237](https://arxiv.org/abs/hep-ph/9507237), doi:10.1016/0370-2693(95)00971-M.

[309] A. Kanaki, C. G. Papadopoulos, HELAC: A package to compute electroweak helicity amplitudes, *Comput. Phys. Commun.* 132 (2000) 306–315. [arXiv:hep-ph/0002082](https://arxiv.org/abs/hep-ph/0002082), doi:10.1016/S0010-4655(00)00151-X.

[310] F. J. Dyson, The S matrix in quantum electrodynamics, *Phys. Rev.* 75 (1949) 1736–1755. doi:10.1103/PhysRev.75.1736.

[311] J. S. Schwinger, On the Green's functions of quantized fields. 1., *Proc. Nat. Acad. Sci.* 37 (1951) 452–455. doi:10.1073/pnas.37.7.452.

[312] J. S. Schwinger, On the Green's functions of quantized fields. 2., *Proc. Nat. Acad. Sci.* 37 (1951) 455–459. doi:10.1073/pnas.37.7.455.

[313] Z. Bern, L. J. Dixon, D. C. Dunbar, D. A. Kosower, One-loop n -point gauge theory amplitudes, unitarity and collinear limits, *Nucl. Phys. B* 425 (1994) 217–260. [arXiv:hep-ph/9403226](https://arxiv.org/abs/hep-ph/9403226), doi:10.1016/0550-3213(94)90179-1.

[314] Z. Bern, L. J. Dixon, D. C. Dunbar, D. A. Kosower, Fusing gauge theory tree amplitudes into loop amplitudes, *Nucl. Phys. B* 435 (1995) 59–101. [arXiv:hep-ph/9409265](https://arxiv.org/abs/hep-ph/9409265), doi:10.1016/0550-3213(94)00488-Z.

[315] R. Britto, F. Cachazo, B. Feng, Generalized unitarity and one-loop amplitudes in $\mathcal{N} = 4$ super-Yang-Mills, *Nucl. Phys. B* 725 (2005) 275–305. [arXiv:hep-th/0412103](https://arxiv.org/abs/hep-th/0412103), doi:10.1016/j.nuclphysb.2005.07.014.

[316] R. K. Ellis, W. T. Giele, Z. Kunszt, K. Melnikov, Masses, fermions and generalized D -dimensional unitarity, *Nucl. Phys. B* 822 (2009) 270–282. [arXiv:0806.3467](https://arxiv.org/abs/0806.3467), doi:10.1016/j.nuclphysb.2009.07.023.

[317] A. van Hameren, Multi-gluon one-loop amplitudes using tensor integrals, *JHEP* 07 (2009) 088. [arXiv:0905.1005](https://arxiv.org/abs/0905.1005), doi:10.1088/1126-6708/2009/07/088.

[318] A. van Hameren, C. G. Papadopoulos, R. Pittau, Automated one-loop calculations: A proof of concept, *JHEP* 0909 (2009) 106. [arXiv:0903.4665](https://arxiv.org/abs/0903.4665), doi:10.1088/1126-6708/2009/09/106.

[319] G. Bevilacqua, et al., HELAC-NLO, *Comput. Phys. Commun.* 184 (2013) 986–997. [arXiv:1110.1499](https://arxiv.org/abs/1110.1499), doi:10.1016/j.cpc.2012.10.033.

[320] C. F. Berger, et al., An automated implementation of on-shell methods for one-loop amplitudes, *Phys. Rev. D* 78 (2008) 036003. [arXiv:0803.4180](https://arxiv.org/abs/0803.4180), doi:10.1103/PhysRevD.78.036003.

[321] Z. Bern, et al., Next-to-leading order $W + 5$ -jet production at the LHC, *Phys. Rev.* D88 (2013) 014025. [arXiv:1304.1253](https://arxiv.org/abs/1304.1253), doi:10.1103/PhysRevD.88.014025.

[322] F. R. Anger, F. Febres Cordero, H. Ita, V. Sotnikov, NLO QCD predictions for $Wb\bar{b}$ production in association with up to three light jets at the LHC, *Phys. Rev.* D97 (2018) 036018. [arXiv:1712.05721](https://arxiv.org/abs/1712.05721), doi:10.1103/PhysRevD.97.036018.

[323] S. Badger, B. Biedermann, P. Uwer, V. Yundin, Numerical evaluation of virtual corrections to multi-jet production in massless QCD, *Comput. Phys. Commun.* 184 (2013) 1981–1998. [arXiv:1209.0100](https://arxiv.org/abs/1209.0100), doi:10.1016/j.cpc.2013.03.018.

[324] S. Badger, B. Biedermann, P. Uwer, *NGluon*: a package to calculate one-loop multi-gluon amplitudes, *Comput. Phys. Commun.* 182 (2011) 1674–1692. [arXiv:1011.2900](https://arxiv.org/abs/1011.2900), doi:10.1016/j.cpc.2011.04.008.

[325] S. Badger, B. Biedermann, P. Uwer, V. Yundin, Next-to-leading order QCD corrections to five jet production at the LHC, *Phys. Rev.* D89 (2014) 034019. [arXiv:1309.6585](https://arxiv.org/abs/1309.6585), doi:10.1103/PhysRevD.89.034019.

[326] M. Chiesa, N. Greiner, F. Tramontano, Automation of electroweak corrections for LHC processes, *J. Phys. G43* (2016) 013002. [arXiv:1507.08579](https://arxiv.org/abs/1507.08579), doi:10.1088/0954-3899/43/1/013002.

[327] S. Frixione, et al., Electroweak and QCD corrections to top-pair hadroproduction in association with heavy bosons, *JHEP* 06 (2015) 184. [arXiv:1504.03446](https://arxiv.org/abs/1504.03446), doi:10.1007/JHEP06(2015)184.

[328] R. Frederix, et al., The automation of next-to-leading order electroweak calculations, *JHEP* 07 (2018) 185. [arXiv:1804.10017](https://arxiv.org/abs/1804.10017), doi:10.1007/JHEP07(2018)185.

[329] S. Honeywell, S. Quackenbush, L. Reina, C. Reuschle, *NLOX*, a one-loop provider for Standard Model processes (2018). [arXiv:1812.11925](https://arxiv.org/abs/1812.11925).

[330] D. Figueroa, et al., Electroweak and QCD corrections to Z -boson production with one b jet in a massive five-flavor scheme, *Phys. Rev.* D98 (2018) 093002. [arXiv:1805.01353](https://arxiv.org/abs/1805.01353), doi:10.1103/PhysRevD.98.093002.

[331] S. Kallweit, et al., NLO QCD+EW predictions for V -jets including off-shell vector-boson decays and multijet merging, *JHEP* 04 (2016) 021. [arXiv:1511.08692](https://arxiv.org/abs/1511.08692), doi:10.1007/JHEP04(2016)021.

[332] S. Kallweit, J. M. Lindert, S. Pozzorini, M. Schönherr, NLO QCD+EW predictions for $2\ell 2\nu$ diboson signatures at the LHC, *JHEP* 11 (2017) 120. [arXiv:1705.00598](https://arxiv.org/abs/1705.00598), doi:10.1007/JHEP11(2017)120.

[333] A. Denner, et al., QCD and electroweak corrections to WZ scattering at the LHC, *JHEP* 06 (2019) 067. [arXiv:1904.00882](https://arxiv.org/abs/1904.00882), doi:10.1007/JHEP06(2019)067.

[334] F. Granata, J. M. Lindert, C. Oleari, S. Pozzorini, NLO QCD+EW predictions for HV and HV +jet production including parton-shower effects, *JHEP* 09 (2017) 012. [arXiv:1706.03522](https://arxiv.org/abs/1706.03522), doi:10.1007/JHEP09(2017)012.

[335] T. Ježo, P. Nason, On the Treatment of Resonances in Next-to-Leading Order Calculations Matched to a Parton Shower, *JHEP* 12 (2015) 065. [arXiv:1509.09071](https://arxiv.org/abs/1509.09071), doi:10.1007/JHEP12(2015)065.

[336] S. Alioli, P. Nason, C. Oleari, E. Re, A general framework for implementing NLO calculations in shower Monte Carlo programs: the *POWHEG BOX*, *JHEP* 06 (2010) 043. [arXiv:1002.2581](https://arxiv.org/abs/1002.2581), doi:10.1007/JHEP06(2010)043.

[337] C. Gütschow, J. M. Lindert, M. Schönherr, Multi-jet merged top-pair production including electroweak corrections, *Eur. Phys. J.* C78 (2018) 317. [arXiv:1803.00950](https://arxiv.org/abs/1803.00950), doi:10.1140/epjc/s10052-018-5804-2.

[338] A. Denner, M. Pellen, NLO electroweak corrections to off-shell top-antitop production with leptonic decays at the LHC, *JHEP* 08 (2016) 155. [arXiv:1607.05571](https://arxiv.org/abs/1607.05571), doi:10.1007/JHEP08(2016)155.

[339] A. Denner, J.-N. Lang, M. Pellen, S. Uccirati, Higgs production in association with off-shell top-antitop pairs at NLO EW and QCD at the LHC, *JHEP* 02 (2017) 053. [arXiv:1612.07138](https://arxiv.org/abs/1612.07138), doi:10.1007/JHEP02(2017)053.

[340] B. Biedermann, A. Denner, M. Pellen, Large electroweak corrections to vector-boson scattering at the Large Hadron Collider, *Phys. Rev. Lett.* 118 (2017) 261801. [arXiv:1611.02951](https://arxiv.org/abs/1611.02951), doi:10.1103/PhysRevLett.118.261801.

[341] B. Biedermann, A. Denner, M. Pellen, Complete NLO corrections to W^+W^+ scattering and its irreducible background at the LHC, *JHEP* 10 (2017) 124. [arXiv:1708.00268](https://arxiv.org/abs/1708.00268), doi:10.1007/JHEP10(2017)124.

[342] M. Chiesa, A. Denner, J.-N. Lang, M. Pellen, An event generator for same-sign W -boson scattering at the LHC including electroweak corrections, *Eur. Phys. J.* C79 (2019) 788. [arXiv:1906.01863](https://arxiv.org/abs/1906.01863), doi:10.1140/epjc/s10052-019-7290-6.

[343] M. Schönherr, Next-to-leading order electroweak corrections to off-shell $WW\bar{W}$ production at the LHC, *JHEP* 07 (2018) 076. [arXiv:1806.00307](https://arxiv.org/abs/1806.00307), doi:10.1007/JHEP07(2018)076.

[344] C. Degrande, V. Hirschi, O. Mattelaer, Automated Computation of One-Loop Amplitudes, *Ann. Rev. Nucl. Part. Sci.* 68 (2018) 291–312. doi:10.1146/annurev-nucl-101917-020959.

[345] A. Bredenstein, A. Denner, S. Dittmaier, S. Pozzorini, NLO QCD corrections to $t\bar{t}b\bar{b}$ production at the LHC: 2. full hadronic results, *JHEP* 03 (2010) 021. [arXiv:1001.4006](https://arxiv.org/abs/1001.4006), doi:10.1007/JHEP03(2010)021.

[346] A. Denner, S. Dittmaier, S. Kallweit, S. Pozzorini, NLO QCD corrections to off-shell top-antitop production with leptonic decays at hadron colliders, *JHEP* 1210 (2012) 110. [arXiv:1207.5018](https://arxiv.org/abs/1207.5018), doi:10.1007/JHEP10(2012)110.

[347] G. 't Hooft, A Planar Diagram Theory for Strong Interactions, *Nucl. Phys.* B72 (1974) 461. doi:10.1016/0550-3213(74)90154-0.

[348] A. Kanaki, C. G. Papadopoulos, *HELAC-PHEGAS*: Automatic computation of helicity amplitudes and cross-sections, in: Proceedings, 7th International Workshop on Advanced Computing and Analysis Techniques in Physics Research (ACAT 2000), 2000, p. 169, [AIP Conf. Proc. 583 (2001) 169]. [arXiv:hep-ph/0012004](https://arxiv.org/abs/hep-ph/0012004), doi:10.1063/1.1405294.

[349] F. Maltoni, K. Paul, T. Stelzer, S. Willenbrock, Color flow decomposition of QCD amplitudes, *Phys. Rev.* D67 (2003) 014026. [arXiv:hep-ph/0209271](https://arxiv.org/abs/hep-ph/0209271), doi:10.1103/PhysRevD.67.014026.

[350] A. Denner, J.-N. Lang, S. Uccirati, *Recola2*: REcursive Computation of One-Loop Amplitudes 2, *Comput. Phys. Commun.* 224 (2018) 346–361. [arXiv:1711.07388](https://arxiv.org/abs/1711.07388), doi:10.1016/j.cpc.2017.11.013.

[351] A. Denner, J.-N. Lang, S. Uccirati, NLO electroweak corrections in extended Higgs Sectors with *RECOLA2*, *JHEP* 07 (2017) 087. [arXiv:1705.06053](https://arxiv.org/abs/1705.06053), doi:10.1007/JHEP07(2017)087.

[352] V. Hirschi, et al., Automation of one-loop QCD corrections, *JHEP* 1105 (2011) 044. [arXiv:1103.0621](https://arxiv.org/abs/1103.0621), doi:10.1007/JHEP05(2011)044.

[353] C. Degrande, Automatic evaluation of UV and R_2 terms for beyond the Standard Model Lagrangians: a proof-of-principle, *Comput. Phys. Commun.* 197 (2015) 239–262. [arXiv:1406.3030](#), doi:10.1016/j.cpc.2015.08.015.

[354] V. Hirschi, O. Mattelaer, Automated event generation for loop-induced processes, *JHEP* 10 (2015) 146. [arXiv:1507.00020](#), doi:10.1007/JHEP10(2015)146.

[355] J. Baglio, L. D. Ninh, M. M. Weber, Massive gauge boson pair production at the LHC: a next-to-leading order story, *Phys. Rev.* D88 (2013) 113005, [Erratum: *Phys. Rev.* D94 (2016) 099902]. [arXiv:1307.4331](#), doi:10.1103/PhysRevD.94.099902, 10.1103/PhysRevD.88.113005.

[356] M. Billoni, S. Dittmaier, B. Jäger, C. Speckner, Next-to-leading order electroweak corrections to $pp \rightarrow W^+W^- \rightarrow 4$ leptons at the LHC in double-pole approximation, *JHEP* 12 (2013) 043. [arXiv:1310.1564](#), doi:10.1007/JHEP12(2013)043.

[357] B. Biedermann, et al., Next-to-leading-order electroweak corrections to $pp \rightarrow W^+W^- \rightarrow 4$ leptons at the LHC, *JHEP* 06 (2016) 065. [arXiv:1605.03419](#), doi:10.1007/JHEP06(2016)065.

[358] Y.-B. Shen, et al., NLO QCD and electroweak corrections to WWW production at the LHC, *Phys. Rev.* D95 (2017) 073005. [arXiv:1605.00554](#), doi:10.1103/PhysRevD.95.073005.

[359] S. Dittmaier, A. Huss, G. Knippen, Next-to-leading-order QCD and electroweak corrections to WWW production at proton-proton colliders, *JHEP* 09 (2017) 034. [arXiv:1705.03722](#), doi:10.1007/JHEP09(2017)034.

[360] S. Dittmaier, G. Knippen, C. Schwan, Next-to-leading-order QCD and electroweak corrections to triple-W production with leptonic decays at the LHC (2019). [arXiv:1912.04117](#).

[361] D. T. Nhungh, L. D. Ninh, M. M. Weber, NLO corrections to WWZ production at the LHC, *JHEP* 12 (2013) 096. [arXiv:1307.7403](#), doi:10.1007/JHEP12(2013)096.

[362] R. Frederix, et al., The complete NLO corrections to dijet hadroproduction, *JHEP* 04 (2017) 076. [arXiv:1612.06548](#), doi:10.1007/JHEP04(2017)076.

[363] J. A. Dror, M. Farina, E. Salvioni, J. Serra, Strong tW Scattering at the LHC, *JHEP* 01 (2016) 071. [arXiv:1511.03674](#), doi:10.1007/JHEP01(2016)071.

[364] R. Frederix, D. Pagani, M. Zaro, Large NLO corrections in $t\bar{t}W^\pm$ and $t\bar{t}t\bar{t}$ hadroproduction from supposedly subleading EW contributions, *JHEP* 02 (2018) 031. [arXiv:1711.02116](#), doi:10.1007/JHEP02(2018)031.

[365] T. Kinoshita, Mass singularities of Feynman amplitudes, *J. Math. Phys.* 3 (1962) 650–677. doi:10.1063/1.1724268.

[366] F. Bloch, A. Nordsieck, Note on the Radiation Field of the Electron, *Phys. Rev.* 52 (1937) 54–59. doi:10.1103/PhysRev.52.54.

[367] T. D. Lee, M. Nauenberg, Degenerate Systems and Mass Singularities, *Phys. Rev.* 133 (1964) B1549–B1562. doi:10.1103/PhysRev.133.B1549.

[368] D. R. Yennie, S. C. Frautschi, H. Suura, The infrared divergence phenomena and high-energy processes, *Annals Phys.* 13 (1961) 379–452. doi:10.1016/0003-4916(61)90151-8.

[369] S. Dittmaier, A. Kabelschatz, T. Kasprzik, Polarized QED splittings of massive fermions and dipole subtraction for non-collinear-safe observables, *Nucl. Phys.* B800 (2008) 146–189. [arXiv:0802.1405](#), doi:10.1016/j.nuclphysb.2008.03.010.

[370] S. Catani, S. Dittmaier, M. H. Seymour, Z. Trócsányi, The dipole formalism for next-to-leading order QCD calculations with massive partons, *Nucl. Phys.* B627 (2002) 189–265. [arXiv:hep-ph/0201036](#), doi:10.1016/S0550-3213(02)00098-6.

[371] W. T. Giele, E. W. N. Glover, D. A. Kosower, Higher-order corrections to jet cross-sections in hadron colliders, *Nucl. Phys.* B403 (1993) 633–670. [arXiv:hep-ph/9302225](#), doi:10.1016/0550-3213(93)90365-V.

[372] S. Keller, E. Laenen, Next-to-leading order cross-sections for tagged reactions, *Phys. Rev.* D59 (1999) 114004. [arXiv:hep-ph/9812415](#), doi:10.1103/PhysRevD.59.114004.

[373] U. Baur, S. Keller, D. Wackerlo, Electroweak radiative corrections to W boson production in hadronic collisions, *Phys. Rev.* D59 (1999) 013002. [arXiv:hep-ph/9807417](#), doi:10.1103/PhysRevD.59.013002.

[374] L. Basso, S. Dittmaier, A. Huss, L. Oggero, Techniques for the treatment of IR divergences in decay processes at NLO and application to the top-quark decay, *Eur. Phys. J.* C76 (2016) 56. [arXiv:1507.04676](#), doi:10.1140/epjc/s10052-016-3878-2.

[375] J. Gaunt, M. Stahlhofen, F. J. Tackmann, J. R. Walsh, N-jettiness Subtractions for NNLO QCD Calculations, *JHEP* 09 (2015) 058. [arXiv:1505.04794](#), doi:10.1007/JHEP09(2015)058.

[376] I. W. Stewart, F. J. Tackmann, W. J. Waalewijn, N-Jettiness: An Inclusive Event Shape to Veto Jets, *Phys. Rev. Lett.* 105 (2010) 092002. [arXiv:1004.2489](#), doi:10.1103/PhysRevLett.105.092002.

[377] R. K. Ellis, D. A. Ross, A. E. Terrano, The Perturbative Calculation of Jet Structure in e^+e^- Annihilation, *Nucl. Phys.* B178 (1981) 421–456. doi:10.1016/0550-3213(81)90165-6.

[378] S. Catani, M. H. Seymour, The dipole formalism for the calculation of QCD jet cross-sections at next-to-leading order, *Phys. Lett.* B378 (1996) 287–301. [arXiv:hep-ph/9602277](#), doi:10.1016/0370-2693(96)00425-X.

[379] L. Phaf, S. Weinzierl, Dipole formalism with heavy fermions, *JHEP* 04 (2001) 006. [arXiv:hep-ph/0102207](#), doi:10.1088/1126-6708/2001/04/006.

[380] R. Frederix, S. Frixione, F. Maltoni, T. Stelzer, Automation of next-to-leading order computations in QCD: The FKS subtraction, *JHEP* 10 (2009) 003. [arXiv:0908.4272](#), doi:10.1088/1126-6708/2009/10/003.

[381] M. Schönherr, An automated subtraction of NLO EW infrared divergences, *Eur. Phys. J.* C78 (2018) 119. [arXiv:1712.07975](#), doi:10.1140/epjc/s10052-018-5600-z.

[382] L. Barze, et al., Implementation of electroweak corrections in the POWHEG BOX: single W production, *JHEP* 04 (2012) 037. [arXiv:1202.0465](#), doi:10.1007/JHEP04(2012)037.

[383] A. Mück, L. Oymanns, Resonance-improved parton-shower matching for the Drell-Yan process including electroweak corrections, *JHEP* 05 (2017) 090. [arXiv:1612.04292](#), doi:10.1007/JHEP05(2017)090.

[384] A. Gehrmann-De Ridder, T. Gehrmann, E. W. N. Glover, Antenna subtraction at NNLO, *JHEP* 09 (2005) 056. [arXiv:hep-ph/0505111](#), doi:10.1088/1126-6708/2005/09/056.

[385] S. Catani, M. Grazzini, An NNLO subtraction formalism in hadron collisions and its application to Higgs boson production at the LHC, *Phys. Rev. Lett.* 98 (2007) 222002. [arXiv:hep-ph/0703012](#), doi:10.1103/PhysRevLett.98.222002.

[386] M. Czakon, A novel subtraction scheme for double-real radiation at NNLO, *Phys. Lett. B* 693 (2010) 259–268. [arXiv:1005.0274](https://arxiv.org/abs/1005.0274), doi:10.1016/j.physletb.2010.08.036.

[387] R. Boughezal, K. Melnikov, F. Petriello, A subtraction scheme for NNLO computations, *Phys. Rev. D* 85 (2012) 034025. [arXiv:1111.7041](https://arxiv.org/abs/1111.7041), doi:10.1103/PhysRevD.85.034025.

[388] J. Currie, E. W. N. Glover, S. Wells, Infrared Structure at NNLO Using Antenna Subtraction, *JHEP* 04 (2013) 066. [arXiv:1301.4693](https://arxiv.org/abs/1301.4693), doi:10.1007/JHEP04(2013)066.

[389] M. Cacciari, et al., Fully Differential Vector-Boson-Fusion Higgs Production at Next-to-Next-to-Leading Order, *Phys. Rev. Lett.* 115 (2015) 082002, [Erratum: *Phys. Rev. Lett.* 120 (2018) 139901]. [arXiv:1506.02660](https://arxiv.org/abs/1506.02660), doi:10.1103/PhysRevLett.115.082002, 10.1103/PhysRevLett.120.139901.

[390] L. Magnea, et al., Local analytic sector subtraction at NNLO, *JHEP* 12 (2018) 107, [Erratum: *JHEP* 06 (2019) 013]. [arXiv:1806.09570](https://arxiv.org/abs/1806.09570), doi:10.1007/JHEP06(2019)013, 10.1007/JHEP12(2018)107.

[391] T. Engel, A. Signer, Y. Ulrich, A subtraction scheme for massive QED (2019). [arXiv:1909.10244](https://arxiv.org/abs/1909.10244).

[392] G. 't Hooft, M. J. G. Veltman, Scalar one-loop integrals, *Nucl. Phys. B* 153 (1979) 365–401. doi:10.1016/0550-3213(79)90605-9.

[393] R. Frederix, T. Gehrmann, N. Greiner, Automation of the Dipole Subtraction Method in MadGraph/MadEvent, *JHEP* 09 (2008) 122. [arXiv:0808.2128](https://arxiv.org/abs/0808.2128), doi:10.1088/1126-6708/2008/09/122.

[394] K. Hasegawa, S. Moch, P. Uwer, AutoDipole: Automated generation of dipole subtraction terms, *Comput. Phys. Commun.* 181 (2010) 1802–1817. [arXiv:0911.4371](https://arxiv.org/abs/0911.4371), doi:10.1016/j.cpc.2010.06.044.

[395] M. Czakon, C. G. Papadopoulos, M. Worek, Polarizing the Dipoles, *JHEP* 08 (2009) 085. [arXiv:0905.0883](https://arxiv.org/abs/0905.0883), doi:10.1088/1126-6708/2009/08/085.

[396] R. Frederix, T. Gehrmann, N. Greiner, Integrated dipoles with MadDipole in the MadGraph framework, *JHEP* 06 (2010) 086. [arXiv:1004.2905](https://arxiv.org/abs/1004.2905), doi:10.1007/JHEP06(2010)086.

[397] T. Gehrmann, N. Greiner, Photon Radiation with MadDipole, *JHEP* 12 (2010) 050. [arXiv:1011.0321](https://arxiv.org/abs/1011.0321), doi:10.1007/JHEP12(2010)050.

[398] P. Nason, A new method for combining NLO QCD with shower Monte Carlo algorithms, *JHEP* 11 (2004) 040. [arXiv:hep-ph/0409146](https://arxiv.org/abs/hep-ph/0409146), doi:10.1088/1126-6708/2004/11/040.

[399] S. Frixione, P. Nason, C. Oleari, Matching NLO QCD computations with Parton Shower simulations: the POWHEG method, *JHEP* 11 (2007) 070. [arXiv:0709.2092](https://arxiv.org/abs/0709.2092), doi:10.1088/1126-6708/2007/11/070.

[400] S. Catani, S. Dittmaier, Z. Trócsányi, One-loop singular behaviour of QCD and SUSY QCD amplitudes with massive partons, *Phys. Lett. B* 500 (2001) 149–160. [arXiv:hep-ph/0011222](https://arxiv.org/abs/hep-ph/0011222), doi:10.1016/S0370-2693(01)00065-X.

[401] R. K. Ellis, W. J. Stirling, B. R. Webber, *QCD and Collider Physics*, Cambridge University Press, Cambridge, UK, 1996, Camb. Monogr. Part. Phys. Nucl. Phys. Cosmol. 8.

[402] J. Collins, *Foundations of perturbative QCD*, Cambridge University Press, Cambridge, UK, 2011, Camb. Monogr. Part. Phys. Nucl. Phys. Cosmol. 32.

[403] V. N. Gribov, L. N. Lipatov, Deep inelastic ep scattering in perturbation theory, *Sov. J. Nucl. Phys.* 15 (1972) 438–450, [Yad. Fiz. 15, 781(1972)].

[404] G. Altarelli, G. Parisi, Asymptotic Freedom in Parton Language, *Nucl. Phys. B* 126 (1977) 298–318. doi:10.1016/0550-3213(77)90384-4.

[405] Y. L. Dokshitzer, Calculation of the Structure Functions for Deep Inelastic Scattering and e^+e^- Annihilation by Perturbation Theory in Quantum Chromodynamics., *Sov. Phys. JETP* 46 (1977) 641–653, [Zh. Eksp. Teor. Fiz. 73 (1977) 1216].

[406] G. Altarelli, R. K. Ellis, G. Martinelli, Leptoproduction and Drell-Yan Processes Beyond the Leading Approximation in Chromodynamics, *Nucl. Phys. B* 143 (1978) 521, [Erratum: *Nucl. Phys. B* 146 (1978) 544]. doi:10.1016/0550-3213(78)90085-8, 10.1016/0550-3213(78)90067-6.

[407] V. Bertone, S. Carrazza, D. Pagani, M. Zaro, On the Impact of Lepton PDFs, *JHEP* 11 (2015) 194. [arXiv:1508.07002](https://arxiv.org/abs/1508.07002), doi:10.1007/JHEP11(2015)194.

[408] H. Spiesberger, QED radiative corrections for parton distributions, *Phys. Rev. D* 52 (1995) 4936–4940. [arXiv:hep-ph/9412286](https://arxiv.org/abs/hep-ph/9412286), doi:10.1103/PhysRevD.52.4936.

[409] M. Roth, S. Weinzierl, QED corrections to the evolution of parton distributions, *Phys. Lett. B* 590 (2004) 190–198. [arXiv:hep-ph/0403200](https://arxiv.org/abs/hep-ph/0403200), doi:10.1016/j.physletb.2004.04.009.

[410] V. Bertone, S. Carrazza, J. Rojo, APFEL: A PDF Evolution Library with QED corrections, *Comput. Phys. Commun.* 185 (2014) 1647–1668. [arXiv:1310.1394](https://arxiv.org/abs/1310.1394), doi:10.1016/j.cpc.2014.03.007.

[411] A. D. Martin, R. G. Roberts, W. J. Stirling, R. S. Thorne, Parton distributions incorporating QED contributions, *Eur. Phys. J. C* 39 (2005) 155–161. [arXiv:hep-ph/0411040](https://arxiv.org/abs/hep-ph/0411040), doi:10.1140/epjc/s2004-02088-7.

[412] R. D. Ball, et al., Parton distributions with QED corrections, *Nucl. Phys. B* 877 (2013) 290–320. [arXiv:1308.0598](https://arxiv.org/abs/1308.0598), doi:10.1016/j.nuclphysb.2013.10.010.

[413] R. D. Ball, et al., Parton distributions for the LHC Run II, *JHEP* 04 (2015) 040. [arXiv:1410.8849](https://arxiv.org/abs/1410.8849), doi:10.1007/JHEP04(2015)040.

[414] C. Schmidt, J. Pumplin, D. Stump, C. P. Yuan, CT14QED parton distribution functions from isolated photon production in deep inelastic scattering, *Phys. Rev. D* 93 (2016) 114015. [arXiv:1509.02905](https://arxiv.org/abs/1509.02905), doi:10.1103/PhysRevD.93.114015.

[415] A. Manohar, P. Nason, G. P. Salam, G. Zanderighi, How bright is the proton? A precise determination of the photon parton distribution function, *Phys. Rev. Lett.* 117 (2016) 242002. [arXiv:1607.04266](https://arxiv.org/abs/1607.04266), doi:10.1103/PhysRevLett.117.242002.

[416] A. V. Manohar, P. Nason, G. P. Salam, G. Zanderighi, The photon content of the proton, *JHEP* 12 (2017) 046. [arXiv:1708.01256](https://arxiv.org/abs/1708.01256), doi:10.1007/JHEP12(2017)046.

[417] L. A. Harland-Lang, V. A. Khoze, M. G. Ryskin, The photon PDF in events with rapidity gaps, *Eur. Phys. J. C* 76 (2016) 255. [arXiv:1601.03772](https://arxiv.org/abs/1601.03772), doi:10.1140/epjc/s10052-016-4100-2.

[418] F. Giuli, et al., The photon PDF from high-mass Drell-Yan data at the LHC, *Eur. Phys. J. C* 77 (2017) 400. [arXiv:1701.08553](https://arxiv.org/abs/1701.08553), doi:10.1140/epjc/s10052-017-4931-5.

[419] A. Buckley, et al., LHAPDF6: parton density access in the LHC precision era, *Eur. Phys. J.* C75 (2015) 132. [arXiv:1412.7420](https://arxiv.org/abs/1412.7420), doi:10.1140/epjc/s10052-015-3318-8.

[420] L. A. Harland-Lang, V. A. Khoze, M. G. Ryskin, Sudakov effects in photon-initiated processes, *Phys. Lett.* B761 (2016) 20–24. [arXiv:1605.04935](https://arxiv.org/abs/1605.04935), doi:10.1016/j.physletb.2016.08.004.

[421] C. M. Carloni Calame, G. Montagna, O. Nicrosini, A. Vicini, Precision electroweak calculation of the production of a high transverse-momentum lepton pair at hadron colliders, *JHEP* 10 (2007) 109. [arXiv:0710.1722](https://arxiv.org/abs/0710.1722), doi:10.1088/1126-6708/2007/10/109.

[422] S. Dittmaier, M. Huber, Radiative corrections to the neutral-current Drell-Yan process in the Standard Model and its minimal supersymmetric extension, *JHEP* 01 (2010) 060. [arXiv:0911.2329](https://arxiv.org/abs/0911.2329), doi:10.1007/JHEP01(2010)060.

[423] R. Boughezal, Y. Li, F. Petriello, Disentangling radiative corrections using the high-mass Drell-Yan process at the LHC, *Phys. Rev.* D89 (2014) 034030. [arXiv:1312.3972](https://arxiv.org/abs/1312.3972), doi:10.1103/PhysRevD.89.034030.

[424] A. Bierweiler, T. Kasprzik, J. H. Kühn, S. Uccirati, Electroweak corrections to W-boson pair production at the LHC, *JHEP* 11 (2012) 093. [arXiv:1208.3147](https://arxiv.org/abs/1208.3147), doi:10.1007/JHEP11(2012)093.

[425] A. Bierweiler, T. Kasprzik, J. H. Kühn, Vector-boson pair production at the LHC to $\mathcal{O}(\alpha^3)$ accuracy, *JHEP* 12 (2013) 071. [arXiv:1305.5402](https://arxiv.org/abs/1305.5402), doi:10.1007/JHEP12(2013)071.

[426] E. W. N. Glover, A. G. Morgan, Measuring the photon fragmentation function at LEP, *Z. Phys.* C62 (1994) 311–322. doi:10.1007/BF01560245.

[427] S. Frixione, Isolated photons in perturbative QCD, *Phys. Lett.* B429 (1998) 369–374. [arXiv:hep-ph/9801442](https://arxiv.org/abs/hep-ph/9801442), doi:10.1016/S0370-2693(98)00454-7.

[428] A. Denner, S. Dittmaier, T. Gehrmann, C. Kurz, Electroweak corrections to hadronic event shapes and jet production in e^+e^- annihilation, *Nucl. Phys.* B836 (2010) 37–90. [arXiv:1003.0986](https://arxiv.org/abs/1003.0986), doi:10.1016/j.nuclphysb.2010.04.009.

[429] E. W. N. Glover, A. G. Morgan, The photon + 1 jet event rate with the cone algorithm in hadronic events at LEP, *Phys. Lett.* B334 (1994) 208–214. doi:10.1016/0370-2693(94)90613-0.

[430] D. Buskulic, et al., First measurement of the quark-to-photon fragmentation function, *Z. Phys.* C69 (1996) 365–378. doi:10.1007/BF02907417.

[431] A. Denner, S. Dittmaier, T. Kasprzik, A. Mück, Electroweak corrections to W + jet hadroproduction including leptonic W-boson decays, *JHEP* 08 (2009) 075. [arXiv:0906.1656](https://arxiv.org/abs/0906.1656), doi:10.1088/1126-6708/2009/08/075.

[432] A. Denner, S. Dittmaier, T. Kasprzik, A. Mück, Electroweak corrections to dilepton + jet production at hadron colliders, *JHEP* 06 (2011) 069. [arXiv:1103.0914](https://arxiv.org/abs/1103.0914), doi:10.1007/JHEP06(2011)069.

[433] A. Denner, S. Dittmaier, T. Kasprzik, A. Mück, Electroweak corrections to monojet production at the LHC, *Eur. Phys. J.* C73 (2013) 2297. [arXiv:1211.5078](https://arxiv.org/abs/1211.5078), doi:10.1140/epjc/s10052-013-2297-x.

[434] A. Denner, S. Dittmaier, M. Hecht, C. Pasold, NLO QCD and electroweak corrections to $W + \gamma$ production with leptonic W-boson decays, *JHEP* 04 (2015) 018. [arXiv:1412.7421](https://arxiv.org/abs/1412.7421), doi:10.1007/JHEP04(2015)018.

[435] A. Denner, S. Dittmaier, M. Hecht, C. Pasold, NLO QCD and electroweak corrections to $Z + \gamma$ production with leptonic Z-boson decays, *JHEP* 02 (2016) 057. [arXiv:1510.08742](https://arxiv.org/abs/1510.08742), doi:10.1007/JHEP02(2016)057.

[436] J. M. Campbell, R. K. Ellis, C. Williams, Vector boson pair production at the LHC, *JHEP* 07 (2011) 018. [arXiv:1105.0020](https://arxiv.org/abs/1105.0020), doi:10.1007/JHEP07(2011)018.

[437] A. Denner, S. Dittmaier, M. Pellen, C. Schwan, Low-virtuality photon transitions $\gamma^* \rightarrow f\bar{f}$ and the photon-to-jet conversion function, *Phys. Lett.* B798 (2019) 134951. [arXiv:1907.02366](https://arxiv.org/abs/1907.02366), doi:10.1016/j.physletb.2019.134951.

[438] M.-S. Chen, P. M. Zerwas, Secondary reactions in electron-positron (electron) collisions, *Phys. Rev.* D11 (1975) 58. doi:10.1103/PhysRevD.11.58.

[439] F. A. Berends, G. Burgers, W. Hollik, W. L. van Neerven, The standard Z peak, *Phys. Lett.* B203 (1988) 177–182. doi:10.1016/0370-2693(88)91593-6.

[440] D. Yu. Bardin, et al., A realistic approach to the standard Z peak, *Z. Phys.* C44 (1989) 493. doi:10.1007/BF01415565.

[441] D. Yu. Bardin, et al., Z line shape, in: G. Altarelli, R. Kleiss, C. Verzegnassi (Eds.), Z physics at LEP 1. Vol. 1: Standard Physics, 1989, pp. 89–127, CERN-89-08. doi:10.5170/CERN-1989-008-V-1.

[442] G. Montagna, et al., On a semianalytical and realistic approach to e^+e^- annihilation into fermion pairs and to Bhabha scattering within the minimal Standard Model at LEP energies, *Nucl. Phys.* B401 (1993) 3–66. doi:10.1016/0550-3213(93)90297-3.

[443] G. Montagna, O. Nicrosini, F. Piccinini, G. Passarino, TOPAZ0 4.0: A new version of a computer program for evaluation of deconvoluted and realistic observables at LEP 1 and LEP 2, *Comput. Phys. Commun.* 117 (1999) 278–289. [arXiv:hep-ph/9804211](https://arxiv.org/abs/hep-ph/9804211), doi:10.1016/S0010-4655(98)00080-0.

[444] D. Yu. Bardin, et al., ZFITTER v.6.21: A semianalytical program for fermion pair production in e^+e^- annihilation, *Comput. Phys. Commun.* 133 (2001) 229–395. [arXiv:hep-ph/9908433](https://arxiv.org/abs/hep-ph/9908433), doi:10.1016/S0010-4655(00)00152-1.

[445] F. Boudjema, et al., Standard model processes, in: G. Altarelli, T. Sjöstrand, F. Zwirner (Ed.), Physics at LEP2, Vol. 1, CERN, Geneva, 1996, pp. 207–248, CERN-96-01. [arXiv:hep-ph/9601224](https://arxiv.org/abs/hep-ph/9601224).

[446] G. Montagna, et al., TOPAZ0: A program for computing observables and for fitting cross-sections and forward–backward asymmetries around the Z^0 peak, *Comput. Phys. Commun.* 76 (1993) 328–360. doi:10.1016/0010-4655(93)90060-P.

[447] G. Montagna, O. Nicrosini, G. Passarino, F. Piccinini, TOPAZ0 2.0: A program for computing deconvoluted and realistic observables around the Z^0 peak, *Comput. Phys. Commun.* 93 (1996) 120–126. [arXiv:hep-ph/9506329](https://arxiv.org/abs/hep-ph/9506329), doi:10.1016/0010-4655(95)00127-1.

[448] G. Montagna, O. Nicrosini, F. Piccinini, Precision physics at LEP, *Riv. Nuovo Cim.* 21 (1998) 1–162. [arXiv:hep-ph/9802302](https://arxiv.org/abs/hep-ph/9802302), doi:10.1007/BF02845546.

[449] W. Beenakker, F. A. Berends, A. P. Chapovsky, Final-state radiation and line shape distortion in resonance pair production, *Phys. Lett.* B435 (1998) 233–239. [arXiv:hep-ph/9805327](https://arxiv.org/abs/hep-ph/9805327), doi:10.1016/S0370-2693(98)00760-6.

[450] G. Aad, et al., Measurement of the transverse momentum distribution of Z/γ^* bosons in proton-proton collisions at $\sqrt{s}=7$ TeV with the ATLAS detector, *Phys. Lett.* B705 (2011) 415–434. [arXiv:1107.2381](https://arxiv.org/abs/1107.2381), doi:10.1016/j.physletb.2011.10.018.

[451] C. F. von Weizsäcker, Radiation emitted in collisions of very fast electrons, *Z. Phys.* 88 (1934) 612–625. doi:10.1007/BF01333110.

[452] E. J. Williams, Nature of the high-energy particles of penetrating radiation and status of ionization and radiation formulae, *Phys. Rev.* **45** (1934) 729–730. doi:10.1103/PhysRev.45.729.

[453] P. Aurenche, et al., $\gamma\gamma$ physics, in: G. Altarelli, T. Sjöstrand, F. Zwirner (Ed.), *Physics at LEP2*, Vol. 1, CERN, Geneva, 1996, pp. 291–348, CERN-96-01. arXiv:hep-ph/9601317.

[454] E. Accomando, et al., Physics with e^+e^- linear colliders, *Phys. Rept.* **299** (1998) 1–78. arXiv:hep-ph/9705442, doi:10.1016/S0370-1573(97)00086-0.

[455] TESLA: The Superconducting Electron-Positron Linear Collider with an Integrated X-Ray Laser Laboratory. Technical Design Report. Part 3. Physics at an e^+e^- Linear Collider, DESY, Hamburg, 2001, DESY-2001-011. arXiv:hep-ph/0106315.

[456] G. Montagna, O. Nicrosini, L. Trentadue, QED radiative corrections to lepton scattering in the structure function formalism, *Nucl. Phys.* **B357** (1991) 390–408. doi:10.1016/0550-3213(91)90474-C.

[457] M. Cacciari, A. Deandrea, G. Montagna, O. Nicrosini, QED structure functions: A systematic approach, *Europhys. Lett.* **17** (1992) 123–128. doi:10.1209/0295-5075/17/2/007.

[458] A. B. Arbuzov, Nonsinglet splitting functions in QED, *Phys. Lett.* **B470** (1999) 252–258. arXiv:hep-ph/9908361, doi:10.1016/S0370-2693(99)01290-3.

[459] W. Beenakker, et al., WW cross-sections and distributions, in: G. Altarelli, T. Sjöstrand, F. Zwirner (Ed.), *Physics at LEP2*, Vol. 1, CERN, Geneva, 1996, pp. 79–139, CERN-96-01. arXiv:hep-ph/9602351, doi:10.5170/CERN-1996-001-V-2.

[460] S. Frixione, Initial conditions for electron and photon structure and fragmentation functions, *JHEP* **11** (2019) 158. arXiv:1909.03886, doi:10.1007/JHEP11(2019)158.

[461] V. Bertone, M. Cacciari, S. Frixione, G. Stagnitto, The partonic structure of the electron at the next-to-leading logarithmic accuracy in QED (2019). arXiv:1911.12040.

[462] M. H. Seymour, Photon radiation in final state parton showering, *Z. Phys.* **C56** (1992) 161–170. doi:10.1007/BF01589719.

[463] K. Hamilton, P. Richardson, Simulation of QED radiation in particle decays using the YFS formalism, *JHEP* **07** (2006) 010. arXiv:hep-ph/0603034, doi:10.1088/1126-6708/2006/07/010.

[464] T. Sjöstrand, et al., An introduction to PYTHIA 8.2, *Comput. Phys. Commun.* **191** (2015) 159–177. arXiv:1410.3012, doi:10.1016/j.cpc.2015.01.024.

[465] M. Schönher, F. Krauss, Soft Photon Radiation in Particle Decays in SHERPA, *JHEP* **12** (2008) 018. arXiv:0810.5071, doi:10.1088/1126-6708/2008/12/018.

[466] S. Höche, S. Schumann, F. Siegert, Hard photon production and matrix-element parton-shower merging, *Phys. Rev.* **D81** (2010) 034026. arXiv:0912.3501, doi:10.1103/PhysRevD.81.034026.

[467] E. Barberio, B. van Eijk, Z. Wąs, PHOTOS: A universal Monte Carlo for QED radiative corrections in decays, *Comput. Phys. Commun.* **66** (1991) 115–128. doi:10.1016/0010-4655(91)90012-A.

[468] E. Barberio, Z. Wąs, PHOTOS: A universal Monte Carlo for QED radiative corrections. Version 2.0, *Comput. Phys. Commun.* **79** (1994) 291–308. doi:10.1016/0010-4655(94)90074-4.

[469] P. Gonolka, Z. Wąs, PHOTOS Monte Carlo: A precision tool for QED corrections in Z and W decays, *Eur. Phys. J.* **C45** (2006) 97–107. arXiv:hep-ph/0506026, doi:10.1140/epjc/s2005-02396-4.

[470] C. M. Carloni Calame, G. Montagna, O. Nicrosini, M. Treccani, Higher-order QED corrections to W -boson mass determination at hadron colliders, *Phys. Rev.* **D69** (2004) 037301. arXiv:hep-ph/0303102, doi:10.1103/PhysRevD.69.037301.

[471] C. M. Carloni Calame, G. Montagna, O. Nicrosini, M. Treccani, Multiple photon corrections to the neutral-current Drell-Yan process, *JHEP* **05** (2005) 019. arXiv:hep-ph/0502218, doi:10.1088/1126-6708/2005/05/019.

[472] C. M. Carloni Calame, G. Montagna, O. Nicrosini, A. Vicini, Precision electroweak calculation of the charged current Drell-Yan process, *JHEP* **12** (2006) 016. arXiv:hep-ph/0609170, doi:10.1088/1126-6708/2006/12/016.

[473] C. M. Carloni Calame, et al., Precision Measurement of the W -Boson Mass: Theoretical Contributions and Uncertainties, *Phys. Rev.* **D96** (2017) 093005. arXiv:1612.02841, doi:10.1103/PhysRevD.96.093005.

[474] C. Bernaciak, D. Wackerlo, Combining next-to-leading order QCD and electroweak radiative corrections to W -boson production at hadron colliders in the POWHEG framework, *Phys. Rev.* **D85** (2012) 093003. arXiv:1201.4804, doi:10.1103/PhysRevD.85.093003.

[475] W. Płaczek, S. Jadach, Multiphoton radiation in leptonic W -boson decays, *Eur. Phys. J.* **C29** (2003) 325–339. arXiv:hep-ph/0302065, doi:10.1140/epjc/s2003-01223-4.

[476] B. Fornal, A. V. Manohar, W. J. Waalewijn, Electroweak gauge boson parton distribution functions, *JHEP* **05** (2018) 106. arXiv:1803.06347, doi:10.1007/JHEP05(2018)106.

[477] C. W. Bauer, D. Provasoli, B. R. Webber, Standard Model fragmentation functions at very high energies, *JHEP* **11** (2018) 030. arXiv:1806.10157, doi:10.1007/JHEP11(2018)030.

[478] J. R. Christiansen, T. Sjöstrand, Weak gauge boson radiation in parton showers, *JHEP* **04** (2014) 115. arXiv:1401.5238, doi:10.1007/JHEP04(2014)115.

[479] F. Krauss, P. Petrov, M. Schönher, M. Spannowsky, Measuring collinear W emissions inside jets, *Phys. Rev.* **D89** (2014) 114006. arXiv:1403.4788, doi:10.1103/PhysRevD.89.114006.

[480] J. Chen, T. Han, B. Tweedie, Electroweak splitting functions and high energy showering, *JHEP* **11** (2017) 093. arXiv:1611.00788, doi:10.1007/JHEP11(2017)093.

[481] R. Tarrach, The pole mass in perturbative QCD, *Nucl. Phys.* **B183** (1981) 384–396. doi:10.1016/0550-3213(81)90140-1.

[482] R. Brock, et al., Handbook of perturbative QCD: Version 1.0, *Rev. Mod. Phys.* **67** (1995) 157–248. doi:10.1103/RevModPhys.67.157.

[483] W. J. Marciano, The Weak Mixing Angle and Grand Unified Gauge Theories, *Phys. Rev.* **D20** (1979) 274. doi:10.1103/PhysRevD.20.274.

[484] A. Sirlin, $O(\alpha^2)$ corrections to the muon lifetime, m_w , and m_z in the $SU(2)_L \times U(1)$ theory, *Phys. Rev.* **D29** (1984) 89. doi:10.1103/PhysRevD.29.89.

[485] S. Eidelman, F. Jegerlehner, Hadronic contributions to $(g-2)$ of the leptons and to the effective fine structure constant $\alpha(M_Z^2)$, *Z. Phys.* **C67** (1995) 585–602. arXiv:hep-ph/9502298, doi:10.1007/BF01553984.

[486] M. J. G. Veltman, Limit on mass differences in the Weinberg model, *Nucl. Phys.* B123 (1977) 89–99. doi:10.1016/0550-3213(77)90342-X.

[487] M. S. Chanowitz, M. A. Furman, I. Hinchliffe, Weak interactions of ultraheavy fermions, *Phys. Lett.* 78B (1978) 285. doi:10.1016/0370-2693(78)90024-2.

[488] M. Consoli, W. Hollik, F. Jegerlehner, The effect of the top quark on the M_W - M_Z interdependence and possible decoupling of heavy fermions from low-energy physics, *Phys. Lett.* B227 (1989) 167–170. doi:10.1016/0370-2693(89)91301-4.

[489] S. Fanchiotti, B. A. Kniehl, A. Sirlin, Incorporation of QCD effects in basic corrections of the electroweak theory, *Phys. Rev.* D48 (1993) 307–331. arXiv:hep-ph/9212285, doi:10.1103/PhysRevD.48.307.

[490] A. Sirlin, Role of $\sin^2 \theta_W(m_Z)$ at the Z^0 Peak, *Phys. Lett.* B232 (1989) 123–126. doi:10.1016/0370-2693(89)90568-6.

[491] W. J. Marciano, Quantitative tests of the standard model of electroweak interactions, *Ann. Rev. Nucl. Part. Sci.* 41 (1991) 469–509. doi:10.1146/annurev.ns.41.120191.002345.

[492] A. Sirlin, A. Ferroglio, Radiative Corrections in Precision Electroweak Physics: A Historical Perspective, *Rev. Mod. Phys.* 85 (2013) 263–297. arXiv:1210.5296, doi:10.1103/RevModPhys.85.263.

[493] S. Sarantakos, A. Sirlin, W. J. Marciano, Radiative corrections to neutrino-lepton scattering in the $SU(2)_L \otimes U(1)$ theory, *Nucl. Phys.* B217 (1983) 84–116. doi:10.1016/0550-3213(83)90079-2.

[494] S. Fanchiotti, A. Sirlin, Accurate determination of $\sin^2 \hat{\theta}_W(m_Z)$, *Phys. Rev.* D41 (1990) 319. doi:10.1103/PhysRevD.41.319.

[495] G. Degrassi, S. Fanchiotti, A. Sirlin, Relations between the on-shell and \overline{MS} frameworks and the m_W - m_Z interdependence, *Nucl. Phys.* B351 (1991) 49–69. doi:10.1016/0550-3213(91)90081-8.

[496] T. Melia, K. Melnikov, R. Röntsch, G. Zanderighi, Next-to-leading order QCD predictions for $W^+ W^+ jj$ production at the LHC, *JHEP* 12 (2010) 053. arXiv:1007.5313, doi:10.1007/JHEP12(2010)053.

[497] T. Melia, K. Melnikov, R. Röntsch, G. Zanderighi, NLO QCD corrections for $W^+ W^-$ pair production in association with two jets at hadron colliders, *Phys. Rev.* D83 (2011) 114043. arXiv:1104.2327, doi:10.1103/PhysRevD.83.114043.

[498] N. Greiner, et al., NLO QCD corrections to the production of $W^+ W^-$ plus two jets at the LHC, *Phys. Lett.* B713 (2012) 277–283. arXiv:1202.6004, doi:10.1016/j.physletb.2012.06.027.

[499] F. Campanario, M. Kerner, L. D. Ninh, D. Zeppenfeld, WZ Production in Association with Two Jets at Next-to-Leading Order in QCD, *Phys. Rev. Lett.* 111 (2013) 052003. arXiv:1305.1623, doi:10.1103/PhysRevLett.111.052003.

[500] F. Campanario, M. Kerner, L. D. Ninh, D. Zeppenfeld, Next-to-leading order QCD corrections to $W^+ W^+$ and $W^- W^-$ production in association with two jets, *Phys. Rev.* D89 (2014) 054009. arXiv:1311.6738, doi:10.1103/PhysRevD.89.054009.

[501] B. Jäger, C. Oleari, D. Zeppenfeld, Next-to-leading-order QCD corrections to Z boson pair production via vector-boson fusion, *Phys. Rev.* D73 (2006) 113006. arXiv:hep-ph/0604200, doi:10.1103/PhysRevD.73.113006.

[502] G. Bozzi, B. Jäger, C. Oleari, D. Zeppenfeld, Next-to-leading-order QCD corrections to $W^+ Z$ and $W^- Z$ production via vector-boson fusion, *Phys. Rev.* D75 (2007) 073004. arXiv:hep-ph/0701105, doi:10.1103/PhysRevD.75.073004.

[503] B. Jäger, C. Oleari, D. Zeppenfeld, Next-to-leading order QCD corrections to $W^+ W^+ jj$ and $W^- W^- jj$ production via weak-boson fusion, *Phys. Rev.* D80 (2009) 034022. arXiv:0907.0580, doi:10.1103/PhysRevD.80.034022.

[504] B. Jäger, G. Zanderighi, NLO corrections to electroweak and QCD production of $W^+ W^+$ plus two jets in the POWHEGBOX, *JHEP* 11 (2011) 055. arXiv:1108.0864, doi:10.1007/JHEP11(2011)055.

[505] A. Denner, L. Hošeková, S. Kallweit, NLO QCD corrections to $W^+ W^+ jj$ production in vector-boson fusion at the LHC, *Phys. Rev.* D86 (2012) 114014. arXiv:1209.2389, doi:10.1103/PhysRevD.86.114014.

[506] J. Baglio, et al., Release Note - VBFNLO 2.7.0 (2014). arXiv:1404.3940.

[507] S. Dittmaier, A. Huss, C. Speckner, Weak radiative corrections to dijet production at hadron colliders, *JHEP* 11 (2012) 095. arXiv:1210.0438, doi:10.1007/JHEP11(2012)095.

[508] B. Biedermann, et al., Next-to-leading-order electroweak corrections to the production of four charged leptons at the LHC, *JHEP* 01 (2017) 033. arXiv:1611.05338, doi:10.1007/JHEP01(2017)033.

[509] J. M. Cornwall, D. N. Levin, G. Tiktopoulos, Derivation of gauge invariance from high-energy unitarity bounds on the S matrix, *Phys. Rev.* D10 (1974) 1145, [Erratum: *Phys. Rev.* D11 (1975) 972]. doi:10.1103/PhysRevD.10.1145, 10.1103/PhysRevD.11.972.

[510] M. S. Chanowitz, M. K. Gaillard, The TeV Physics of Strongly Interacting W 's and Z 's, *Nucl. Phys.* B261 (1985) 379–431. doi:10.1016/0550-3213(85)90580-2.

[511] G. J. Gounaris, R. Kögerler, H. Neufeld, Relationship between longitudinally polarized vector bosons and their unphysical scalar partners, *Phys. Rev.* D34 (1986) 3257. doi:10.1103/PhysRevD.34.3257.

[512] H.-J. He, Y.-P. Kuang, X.-y. Li, Further investigation on the precise formulation of the equivalence theorem, *Phys. Rev.* D49 (1994) 4842–4872. doi:10.1103/PhysRevD.49.4842.

[513] Y.-P. Yao, C. P. Yuan, Modification of the equivalence theorem due to loop corrections, *Phys. Rev.* D38 (1988) 2237. doi:10.1103/PhysRevD.38.2237.

[514] M. Kuroda, G. Moultaka, D. Schildknecht, Direct one-loop renormalization of $SU(2)_L \times U(1)_Y$ four-fermion processes and running coupling constants, *Nucl. Phys.* B350 (1991) 25–72. doi:10.1016/0550-3213(91)90252-S.

[515] G. Degrassi, A. Sirlin, Gauge-invariant self-energies and vertex parts of the Standard Model in the pinch technique framework, *Phys. Rev.* D46 (1992) 3104–3116. doi:10.1103/PhysRevD.46.3104.

[516] W. Beenakker, et al., High-energy approximation for on-shell W -pair production, *Nucl. Phys.* B410 (1993) 245–279. doi:10.1016/0550-3213(93)90434-Q.

[517] A. Denner, S. Dittmaier, R. Schuster, Radiative Corrections to $\gamma\gamma \rightarrow W^+ W^-$ in the Electroweak Standard Model, *Nucl. Phys.* B452 (1995) 80–108. arXiv:hep-ph/9503442, doi:10.1016/0550-3213(95)00344-R.

[518] A. Denner, S. Dittmaier, T. Hahn, Radiative Corrections to $ZZ \rightarrow ZZ$ in the Electroweak Standard Model, *Phys. Rev.* D56 (1997) 117–134. arXiv:hep-ph/9612390, doi:10.1103/PhysRevD.56.117.

[519] M. Beccaria, et al., Rising bosonic electroweak virtual effects at high-energy $e^+ e^-$ colliders, *Phys. Rev.* D58 (1998) 093014. arXiv:hep-ph/9805250, doi:10.1103/PhysRevD.58.093014.

[520] V. S. Fadin, L. N. Lipatov, A. D. Martin, M. Melles, Resummation of double logarithms in electroweak high-energy processes, *Phys. Rev. D* 61 (2000) 094002. [arXiv:hep-ph/9910338](https://arxiv.org/abs/hep-ph/9910338), doi:10.1103/PhysRevD.61.094002.

[521] J. H. Kühn, A. A. Penin, V. A. Smirnov, Summing up subleading Sudakov logarithms, *Eur. Phys. J. C* 17 (2000) 97–105. [arXiv:hep-ph/9912503](https://arxiv.org/abs/hep-ph/9912503), doi:10.1007/s100520000462.

[522] P. Ciafaloni, D. Comelli, Electroweak Sudakov form-factors and nonfactorizable soft QED effects at NLC energies, *Phys. Lett. B* 476 (2000) 49–57. [arXiv:hep-ph/9910278](https://arxiv.org/abs/hep-ph/9910278), doi:10.1016/S0370-2693(00)00121-0.

[523] V. V. Sudakov, Vertex parts at very high-energies in quantum electrodynamics, *Sov. Phys. JETP* 3 (1956) 65–71, [Zh. Eksp. Teor. Fiz. 30 (1956) 87].

[524] U. Baur, Weak Boson Emission in Hadron Collider Processes, *Phys. Rev. D* 75 (2007) 013005. [arXiv:hep-ph/0611241](https://arxiv.org/abs/hep-ph/0611241), doi:10.1103/PhysRevD.75.013005.

[525] M. Ciafaloni, P. Ciafaloni, D. Comelli, Bloch-Nordsieck violating electroweak corrections to inclusive TeV scale hard processes, *Phys. Rev. Lett.* 84 (2000) 4810–4813. [arXiv:hep-ph/0001142](https://arxiv.org/abs/hep-ph/0001142), doi:10.1103/PhysRevLett.84.4810.

[526] M. Hori, H. Kawamura, J. Kodaira, Electroweak Sudakov at two loop level, *Phys. Lett. B* 491 (2000) 275–279. [arXiv:hep-ph/0007329](https://arxiv.org/abs/hep-ph/0007329), doi:10.1016/S0370-2693(00)01027-3.

[527] A. Denner, S. Pozzorini, One-loop leading logarithms in electroweak radiative corrections. 1. Results, *Eur. Phys. J. C* 18 (2001) 461–480. [arXiv:hep-ph/0010201](https://arxiv.org/abs/hep-ph/0010201), doi:10.1007/s100520100551.

[528] A. Denner, S. Pozzorini, One-loop leading logarithms in electroweak radiative corrections. 2. Factorization of collinear singularities, *Eur. Phys. J. C* 21 (2001) 63–79. [arXiv:hep-ph/0104127](https://arxiv.org/abs/hep-ph/0104127), doi:10.1007/s100520100721.

[529] M. Melles, Electroweak radiative corrections in high-energy processes, *Phys. Rept.* 375 (2003) 219–326. [arXiv:hep-ph/0104232](https://arxiv.org/abs/hep-ph/0104232), doi:10.1016/S0370-1573(02)00550-1.

[530] M. Melles, Resummation of angular-dependent corrections in spontaneously broken gauge theories, *Eur. Phys. J. C* 24 (2002) 193–204. [arXiv:hep-ph/0108221](https://arxiv.org/abs/hep-ph/0108221), doi:10.1007/s100520200942.

[531] W. Beenakker, A. Werthenbach, Electroweak two-loop Sudakov logarithms for on-shell fermions and bosons, *Nucl. Phys. B* 630 (2002) 3–54. [arXiv:hep-ph/0112030](https://arxiv.org/abs/hep-ph/0112030), doi:10.1016/S0550-3213(02)00171-2.

[532] A. Denner, M. Melles, S. Pozzorini, Two-loop electroweak angular-dependent logarithms at high energies, *Nucl. Phys. B* 662 (2003) 299–333. [arXiv:hep-ph/0301241](https://arxiv.org/abs/hep-ph/0301241), doi:10.1016/S0550-3213(03)00307-9.

[533] B. Jantzen, J. H. Kühn, A. A. Penin, V. A. Smirnov, Two-loop electroweak logarithms, *Phys. Rev. D* 72 (2005) 051301, [Erratum: *Phys. Rev. D* 74 (2006) 019901]. [arXiv:hep-ph/0504111](https://arxiv.org/abs/hep-ph/0504111), doi:10.1103/PhysRevD.74.019901, 10.1103/PhysRevD.72.051301.

[534] B. Jantzen, J. H. Kühn, A. A. Penin, V. A. Smirnov, Two-loop electroweak logarithms in four-fermion processes at high energy, *Nucl. Phys. B* 731 (2005) 188–212, [Erratum: *Nucl. Phys. B* 752 (2006) 327]. [arXiv:hep-ph/0509157](https://arxiv.org/abs/hep-ph/0509157), doi:10.1016/j.nuclphysb.2005.10.010, 10.1016/j.nuclphysb.2006.07.004.

[535] A. Denner, B. Jantzen, S. Pozzorini, Two-loop electroweak next-to-leading logarithmic corrections to massless fermionic processes, *Nucl. Phys. B* 761 (2007) 1–62. [arXiv:hep-ph/0608326](https://arxiv.org/abs/hep-ph/0608326), doi:10.1016/j.nuclphysb.2006.10.014.

[536] J. H. Kühn, S. Moch, A. A. Penin, V. A. Smirnov, Next-to-next-to-leading logarithms in four fermion electroweak processes at high energy, *Nucl. Phys. B* 616 (2001) 286–306, [Erratum: *Nucl. Phys. B* 648 (2003) 455]. [arXiv:hep-ph/0106298](https://arxiv.org/abs/hep-ph/0106298), doi:10.1016/S0550-3213(02)00968-9, 10.1016/S0550-3213(01)00454-0.

[537] A. Denner, B. Jantzen, S. Pozzorini, Two-loop electroweak next-to-leading logarithms for processes involving heavy quarks, *JHEP* 11 (2008) 062. [arXiv:0809.0800](https://arxiv.org/abs/0809.0800), doi:10.1088/1126-6708/2008/11/062.

[538] J.-y. Chiu, F. Golf, R. Kelley, A. V. Manohar, Electroweak Sudakov corrections using effective field theory, *Phys. Rev. Lett.* 100 (2008) 021802. [arXiv:0709.2377](https://arxiv.org/abs/0709.2377), doi:10.1103/PhysRevLett.100.021802.

[539] J.-y. Chiu, R. Kelley, A. V. Manohar, Electroweak Corrections using Effective Field Theory: Applications to the LHC, *Phys. Rev. D* 78 (2008) 073006. [arXiv:0806.1240](https://arxiv.org/abs/0806.1240), doi:10.1103/PhysRevD.78.073006.

[540] C. W. Bauer, S. Fleming, M. E. Luke, Summing Sudakov logarithms in $B \rightarrow X_s \gamma$ in effective field theory, *Phys. Rev. D* 63 (2000) 014006. [arXiv:hep-ph/0005275](https://arxiv.org/abs/hep-ph/0005275), doi:10.1103/PhysRevD.63.014006.

[541] C. W. Bauer, S. Fleming, D. Pirjol, I. W. Stewart, An effective field theory for collinear and soft gluons: Heavy to light decays, *Phys. Rev. D* 63 (2001) 114020. [arXiv:hep-ph/0011336](https://arxiv.org/abs/hep-ph/0011336), doi:10.1103/PhysRevD.63.114020.

[542] C. W. Bauer, I. W. Stewart, Invariant operators in collinear effective theory, *Phys. Lett. B* 516 (2001) 134–142. [arXiv:hep-ph/0107001](https://arxiv.org/abs/hep-ph/0107001), doi:10.1016/S0370-2693(01)00902-9.

[543] C. W. Bauer, D. Pirjol, I. W. Stewart, Soft collinear factorization in effective field theory, *Phys. Rev. D* 65 (2002) 054022. [arXiv:hep-ph/0109045](https://arxiv.org/abs/hep-ph/0109045), doi:10.1103/PhysRevD.65.054022.

[544] J.-y. Chiu, A. Fuhrer, R. Kelley, A. V. Manohar, Factorization structure of gauge theory amplitudes and application to hard scattering processes at the LHC, *Phys. Rev. D* 80 (2009) 094013. [arXiv:0909.0012](https://arxiv.org/abs/0909.0012), doi:10.1103/PhysRevD.80.094013.

[545] J.-y. Chiu, A. Fuhrer, R. Kelley, A. V. Manohar, Soft and Collinear Functions for the Standard Model, *Phys. Rev. D* 81 (2010) 014023. [arXiv:0909.0947](https://arxiv.org/abs/0909.0947), doi:10.1103/PhysRevD.81.014023.

[546] A. Fuhrer, A. V. Manohar, J.-y. Chiu, R. Kelley, Radiative corrections to longitudinal and transverse gauge boson and Higgs production, *Phys. Rev. D* 81 (2010) 093005. [arXiv:1003.0025](https://arxiv.org/abs/1003.0025), doi:10.1103/PhysRevD.81.093005.

[547] M. Roth, A. Denner, High-energy approximation of one-loop Feynman integrals, *Nucl. Phys. B* 479 (1996) 495–514. [arXiv:hep-ph/9605420](https://arxiv.org/abs/hep-ph/9605420), doi:10.1016/0550-3213(96)00435-X.

[548] E. Accomando, A. Denner, S. Pozzorini, Electroweak-correction effects in gauge-boson pair production at the CERN LHC, *Phys. Rev. D* 65 (2002) 073003. [arXiv:hep-ph/0110114](https://arxiv.org/abs/hep-ph/0110114), doi:10.1103/PhysRevD.65.073003.

[549] E. Accomando, A. Denner, S. Pozzorini, Logarithmic electroweak corrections to $e^+e^- \rightarrow \nu_e \bar{\nu}_e W^+ W^-$, *JHEP* 03 (2007) 078. [arXiv:hep-ph/0611289](https://arxiv.org/abs/hep-ph/0611289), doi:10.1088/1126-6708/2007/03/078.

[550] S. Dawson, The Effective W Approximation, *Nucl. Phys. B* 249 (1985) 42–60. doi:10.1016/0550-3213(85)90038-0.

[551] G. L. Kane, W. W. Repko, W. B. Rolnick, The effective W^\pm, Z^0 approximation for high-energy collisions, *Phys. Lett. B* 148B (1984) 367–372. doi:10.1016/0370-2693(84)90105-9.

[552] J. Lindfors, Distribution Functions for Heavy Vector Bosons Inside Colliding Particle Beams, *Z. Phys. C* 28 (1985) 427. doi:10.1007/BF01413605.

[553] I. Kuss, H. Spiesberger, Luminosities for vector-boson–vector-boson scattering at high-energy colliders, *Phys. Rev. D* 53 (1996) 6078–6093. arXiv:hep-ph/9507204, doi:10.1103/PhysRevD.53.6078.

[554] E. Accomando, A. Denner, A. Kaiser, Logarithmic electroweak corrections to gauge-boson pair production at the LHC, *Nucl. Phys. B* 706 (2005) 325–371. arXiv:hep-ph/0409247, doi:10.1016/j.nuclphysb.2004.11.019.

[555] J. H. Kühn, A. Kulesza, S. Pozzorini, M. Schulze, Logarithmic electroweak corrections to hadronic $Z + 1$ jet production at large transverse momentum, *Phys. Lett. B* 609 (2005) 277–285. arXiv:hep-ph/0408308, doi:10.1016/j.physletb.2005.01.059.

[556] J. H. Kühn, A. Kulesza, S. Pozzorini, M. Schulze, Electroweak corrections to hadronic photon production at large transverse momenta, *JHEP* 03 (2006) 059. arXiv:hep-ph/0508253, doi:10.1088/1126-6708/2006/03/059.

[557] J. H. Kühn, A. Kulesza, S. Pozzorini, M. Schulze, Electroweak corrections to large transverse momentum production of W bosons at the LHC, *Phys. Lett. B* 651 (2007) 160–165. arXiv:hep-ph/0703283, doi:10.1016/j.physletb.2007.06.028.

[558] M. L. Mangano, et al., ALPGEN, a generator for hard multiparton processes in hadronic collisions, *JHEP* 07 (2003) 001. arXiv:hep-ph/0206293, doi:10.1088/1126-6708/2003/07/001.

[559] M. Chiesa, et al., Electroweak Sudakov Corrections to New Physics Searches at the LHC, *Phys. Rev. Lett.* 111 (2013) 121801. arXiv:1305.6837, doi:10.1103/PhysRevLett.111.121801.

[560] R. Kirschner, L. N. Lipatov, Double-logarithmic asymptotics of quark scattering amplitudes with flavor exchange, *Phys. Rev. D* 26 (1982) 1202–1205. doi:10.1103/PhysRevD.26.1202.

[561] V. N. Gribov, Bremsstrahlung of hadrons at high energies, *Sov. J. Nucl. Phys.* 5 (1967) 280, [Yad. Fiz. 5, 399 (1967)].

[562] L. N. Lipatov, Massless particle bremsstrahlung theorems for high-energy hadron interactions, *Nucl. Phys. B* 307 (1988) 705–720. doi:10.1016/0550-3213(88)90105-8.

[563] V. Del Duca, High-energy bremsstrahlung theorems for soft photons, *Nucl. Phys. B* 345 (1990) 369–388. doi:10.1016/0550-3213(90)90392-Q.

[564] M. Melles, Mass gap effects and higher order electroweak Sudakov logarithms, *Phys. Lett. B* 495 (2000) 81–86. arXiv:hep-ph/0006077, doi:10.1016/S0370-2693(00)01234-X.

[565] J. C. Collins, Algorithm to compute corrections to the Sudakov form factor, *Phys. Rev. D* 22 (1980) 1478. doi:10.1103/PhysRevD.22.1478.

[566] A. Sen, Asymptotic behavior of the Sudakov form factor in QCD, *Phys. Rev. D* 24 (1981) 3281. doi:10.1103/PhysRevD.24.3281.

[567] A. Sen, Asymptotic behavior of the fixed-angle on-shell quark scattering amplitudes in non-Abelian gauge theories, *Phys. Rev. D* 28 (1983) 860. doi:10.1103/PhysRevD.28.860.

[568] J. H. Kühn, F. Metzler, A. A. Penin, Next-to-next-to-leading electroweak logarithms in W -pair production at ILC, *Nucl. Phys. B* 795 (2008) 277–290, [Erratum: *Nucl. Phys. B* 818 (2009) 135]. arXiv:0709.4055, doi:10.1016/j.nuclphysb.2007.11.019, 10.1016/j.nuclphysb.2009.04.006.

[569] J. H. Kühn, F. Metzler, A. A. Penin, S. Uccirati, Next-to-Next-to-Leading Electroweak Logarithms for W -Pair Production at LHC, *JHEP* 06 (2011) 143. arXiv:1101.2563, doi:10.1007/JHEP06(2011)143.

[570] J.-y. Chiu, F. Golf, R. Kelley, A. V. Manohar, Electroweak corrections to high energy processes using effective field theory, *Phys. Rev. D* 77 (2008) 053004. arXiv:0712.0396, doi:10.1103/PhysRevD.77.053004.

[571] A. Manohar, B. Shotwell, C. Bauer, S. Turczyk, Non-cancellation of electroweak logarithms in high-energy scattering, *Phys. Lett. B* 740 (2015) 179–187. arXiv:1409.1918, doi:10.1016/j.physletb.2014.11.050.

[572] A. V. Manohar, Deep inelastic scattering as $x \rightarrow 1$ using soft collinear effective theory, *Phys. Rev. D* 68 (2003) 114019. arXiv:hep-ph/0309176, doi:10.1103/PhysRevD.68.114019.

[573] A. Denner, S. Dittmaier, M. Roth, M. M. Weber, Electroweak radiative corrections to single Higgs-boson production in e^+e^- annihilation, *Phys. Lett. B* 560 (2003) 196–203. arXiv:hep-ph/0301189, doi:10.1016/S0370-2693(03)00370-8.

[574] M. L. Ciccolini, S. Dittmaier, M. Krämer, Electroweak radiative corrections to associated WH and ZH production at hadron colliders, *Phys. Rev. D* 68 (2003) 073003. arXiv:hep-ph/0306234, doi:10.1103/PhysRevD.68.073003.

[575] M. Ciccolini, A. Denner, S. Dittmaier, Electroweak and QCD corrections to Higgs production via vector-boson fusion at the LHC, *Phys. Rev. D* 77 (2008) 013002. arXiv:arXiv:0710.4749[hep-ph].

[576] T. Figy, S. Palmer, G. Weiglein, Higgs production via weak boson fusion in the standard model and the MSSM, *JHEP* 02 (2012) 105. arXiv:1012.4789, doi:10.1007/JHEP02(2012)105.

[577] A. Denner, S. Dittmaier, S. Kallweit, A. Mück, Electroweak corrections to Higgs-strahlung off W/Z bosons at the Tevatron and the LHC with HAWK, *JHEP* 03 (2012) 075. arXiv:1112.5142, doi:10.1007/JHEP03(2012)075.

[578] E. Accomando, A. Denner, C. Meier, Electroweak corrections to $W\gamma$ and $Z\gamma$ production at the LHC, *Eur. Phys. J. C* 47 (2006) 125–146. arXiv:hep-ph/0509234, doi:10.1140/epjc/s2006-02521-y.

[579] P. Ciafaloni, D. Comelli, The importance of weak boson emission at LHC, *JHEP* 09 (2006) 055. arXiv:hep-ph/0604070, doi:10.1088/1126-6708/2006/09/055.

[580] G. Bell, J. H. Kühn, J. Rittinger, Electroweak Sudakov logarithms and real gauge-boson radiation in the TeV region, *Eur. Phys. J. C* 70 (2010) 659–671. arXiv:1004.4117, doi:10.1140/epjc/s10052-010-1489-x.

[581] W. J. Stirling, E. Vryonidou, Electroweak corrections and Bloch-Nordsieck violations in 2-to-2 processes at the LHC, *JHEP* 04 (2013) 155. arXiv:1212.6537, doi:10.1007/JHEP04(2013)155.

[582] C. W. Bauer, N. Ferland, Resummation of electroweak Sudakov logarithms for real radiation, *JHEP* 09 (2016) 025. arXiv:1601.07190, doi:10.1007/JHEP09(2016)025.

[583] A. V. Manohar, W. J. Waalewijn, Electroweak Logarithms in Inclusive Cross Sections, *JHEP* 08 (2018) 137. arXiv:1802.08687, doi:10.1007/JHEP08(2018)137.

[584] S. Dittmaier, M. Krämer, Electroweak radiative corrections to W -boson production at hadron colliders, *Phys. Rev. D* 65 (2002) 073007. arXiv:hep-ph/0109062, doi:10.1103/PhysRevD.65.073007.

[585] S. Brensing, S. Dittmaier, M. Krämer, A. Mück, Radiative corrections to W -boson hadroproduction: Higher-order electroweak and supersymmetric effects, *Phys. Rev. D* 77 (2008) 073006. [arXiv:0710.3309](https://arxiv.org/abs/0710.3309), doi:10.1103/PhysRevD.77.073006.

[586] R. E. Cutkosky, Singularities and discontinuities of Feynman amplitudes, *J. Math. Phys.* 1 (1960) 429–433. doi:10.1063/1.1703676.

[587] M. J. G. Veltman, Unitarity and causality in a renormalizable field theory with unstable particles, *Physica* 29 (1963) 186–207. doi:10.1016/S0031-8914(63)80277-3.

[588] A. Denner, J.-N. Lang, The complex-mass scheme and unitarity in perturbative quantum field theory, *Eur. Phys. J. C* 75 (2015) 377. [arXiv:1406.6280](https://arxiv.org/abs/1406.6280), doi:10.1140/epjc/s10052-015-3579-2.

[589] F. V. Tkachov, Perturbation theory for unstable fundamental fields, in: Proc. of the 32nd PNPI Winter School on Nuclear and Particle Physics, St. Petersburg, 1998, p. 166. [arXiv:hep-ph/9802307](https://arxiv.org/abs/hep-ph/9802307).

[590] M. L. Nekrasov, Modified perturbation theory for pair production and decay of fundamental unstable particles, *Int. J. Mod. Phys. A* 24 (2009) 6071–6103. [arXiv:0709.3046](https://arxiv.org/abs/0709.3046), doi:10.1142/S0217751X09047673.

[591] N. Kauer, Narrow-width approximation limitations, *Phys. Lett. B* 649 (2007) 413–416. [arXiv:hep-ph/0703077](https://arxiv.org/abs/hep-ph/0703077), doi:10.1016/j.physletb.2007.04.036.

[592] C. F. Uhlemann, N. Kauer, Narrow-width approximation accuracy, *Nucl. Phys. B* 814 (2009) 195–211. [arXiv:0807.4112](https://arxiv.org/abs/0807.4112), doi:10.1016/j.nuclphysb.2009.01.022.

[593] D. Berdine, N. Kauer, D. Rainwater, Breakdown of the Narrow Width Approximation for New Physics, *Phys. Rev. Lett.* 99 (2007) 111601. [arXiv:hep-ph/0703058](https://arxiv.org/abs/hep-ph/0703058), doi:10.1103/PhysRevLett.99.111601.

[594] E. Fuchs, S. Thewes, G. Weiglein, Interference effects in BSM processes with a generalised narrow-width approximation, *Eur. Phys. J. C* 75 (2015) 254. [arXiv:1411.4652](https://arxiv.org/abs/1411.4652), doi:10.1140/epjc/s10052-015-3472-z.

[595] W. Beenakker, et al., The fermion-loop scheme for finite width effects in e^+e^- annihilation into four fermions, *Nucl. Phys. B* 500 (1997) 255–298. [arXiv:hep-ph/9612260](https://arxiv.org/abs/hep-ph/9612260), doi:10.1016/S0550-3213(97)00316-7.

[596] S. Dittmaier, M. Roth, LUSIFER: A LUCid approach to six FERMion production, *Nucl. Phys. B* 642 (2002) 307–343. [arXiv:hep-ph/0206070](https://arxiv.org/abs/hep-ph/0206070), doi:10.1016/S0550-3213(02)00640-5.

[597] Y. Kurihara, D. Perret-Gallix, Y. Shimizu, $e^+e^- \rightarrow e^-\bar{\nu}_e u\bar{d}$ from LEP to linear collider energies, *Phys. Lett. B* 349 (1995) 367–374. [arXiv:hep-ph/9412215](https://arxiv.org/abs/hep-ph/9412215), doi:10.1016/0370-2693(95)00298-Y.

[598] G. Passarino, Single- W production and Fermion-Loop scheme: numerical results, *Nucl. Phys. B* 578 (2000) 3–26. [arXiv:hep-ph/0001212](https://arxiv.org/abs/hep-ph/0001212), doi:10.1016/S0550-3213(00)00172-3.

[599] E. N. Argyres, et al., Stable calculations for unstable particles: Restoring gauge invariance, *Phys. Lett. B* 358 (1995) 339–346. [arXiv:hep-ph/9507216](https://arxiv.org/abs/hep-ph/9507216), doi:10.1016/0370-2693(95)01002-8.

[600] P. Gambino, P. A. Grassi, The Nielsen identities of the SM and the definition of mass, *Phys. Rev. D* 62 (2000) 076002. [arXiv:hep-ph/9907254](https://arxiv.org/abs/hep-ph/9907254), doi:10.1103/PhysRevD.62.076002.

[601] P. A. Grassi, B. A. Kniehl, A. Sirlin, Width and partial widths of unstable particles in the light of the Nielsen identities, *Phys. Rev. D* 65 (2002) 085001. [arXiv:hep-ph/0109228](https://arxiv.org/abs/hep-ph/0109228), doi:10.1103/PhysRevD.65.085001.

[602] A. Sirlin, Theoretical considerations concerning the Z^0 mass, *Phys. Rev. Lett.* 67 (1991) 2127–2130. doi:10.1103/PhysRevLett.67.2127.

[603] D. Yu. Bardin, A. Leike, T. Riemann, M. Sachwitz, Energy-dependent width effects in e^+e^- annihilation near the Z -boson pole, *Phys. Lett. B* 206 (1988) 539–542. doi:10.1016/0370-2693(88)91627-9.

[604] G. Passarino, C. Sturm, S. Uccirati, Higgs Pseudo-Observables, Second Riemann Sheet and All That, *Nucl. Phys. B* 834 (2010) 77–115. [arXiv:1001.3360](https://arxiv.org/abs/1001.3360), doi:10.1016/j.nuclphysb.2010.03.013.

[605] S. Goria, G. Passarino, D. Rosco, The Higgs-boson lineshape, *Nucl. Phys. B* 864 (2012) 530–579. [arXiv:1112.5517](https://arxiv.org/abs/1112.5517), doi:10.1016/j.nuclphysb.2012.07.006.

[606] K. Melnikov, O. I. Yakovlev, Final state interaction in the production of heavy unstable particles, *Nucl. Phys. B* 471 (1996) 90–120. [arXiv:hep-ph/9501358](https://arxiv.org/abs/hep-ph/9501358), doi:10.1016/0550-3213(96)00151-4.

[607] W. Beenakker, A. P. Chapovsky, F. A. Berends, Non-factorizable corrections to W pair production: Methods and analytic results, *Nucl. Phys. B* 508 (1997) 17–63. [arXiv:hep-ph/9707326](https://arxiv.org/abs/hep-ph/9707326), doi:10.1016/S0550-3213(97)80003-X, 10.1016/S0550-3213(97)00628-7.

[608] A. Denner, S. Dittmaier, M. Roth, Non-factorizable photonic corrections to $e^+e^- \rightarrow WW \rightarrow$ four fermions, *Nucl. Phys. B* 519 (1998) 39–84. [arXiv:hep-ph/9710521](https://arxiv.org/abs/hep-ph/9710521), doi:10.1016/S0550-3213(98)00046-7.

[609] V. S. Fadin, V. A. Khoze, A. D. Martin, Interference radiative phenomena in the production of heavy unstable particles, *Phys. Rev. D* 49 (1994) 2247–2256. doi:10.1103/PhysRevD.49.2247.

[610] W. Beenakker, F. A. Berends, A. P. Chapovsky, Radiative corrections to pair production of unstable particles: results for $e^+e^- \rightarrow 4$ fermions, *Nucl. Phys. B* 548 (1999) 3–59. [arXiv:hep-ph/9811481](https://arxiv.org/abs/hep-ph/9811481), doi:10.1016/S0550-3213(99)00110-8.

[611] S. Dittmaier, A. Huss, C. Schwinn, Mixed QCD-electroweak $O(\alpha_s\alpha)$ corrections to Drell-Yan processes in the resonance region: Pole approximation and non-factorizable corrections, *Nucl. Phys. B* 885 (2014) 318–372. [arXiv:1403.3216](https://arxiv.org/abs/1403.3216), doi:10.1016/j.nuclphysb.2014.05.027.

[612] S. Dittmaier, C. Schwinn, Non-factorizable photonic corrections to resonant production and decay of many unstable particles, *Eur. Phys. J. C* 76 (2016) 144. [arXiv:1511.01698](https://arxiv.org/abs/1511.01698), doi:10.1140/epjc/s10052-016-3968-1.

[613] W. Beenakker, A. P. Chapovsky, F. A. Berends, Non-factorizable corrections to W pair production, *Phys. Lett. B* 411 (1997) 203–210. [arXiv:hep-ph/9706339](https://arxiv.org/abs/hep-ph/9706339), doi:10.1016/S0370-2693(97)01010-1.

[614] A. Ballestrero, E. Maina, G. Pelliccioli, W boson polarization in vector boson scattering at the LHC, *JHEP* 03 (2018) 170. [arXiv:1710.09339](https://arxiv.org/abs/1710.09339), doi:10.1007/JHEP03(2018)170.

[615] A. Ballestrero, E. Maina, G. Pelliccioli, Polarized vector boson scattering in the fully leptonic WZ and ZZ channels at the LHC, *JHEP* 09 (2019) 087. [arXiv:1907.04722](https://arxiv.org/abs/1907.04722), doi:10.1007/JHEP09(2019)087.

[616] S. Dittmaier, A. Huss, C. Schwinn, Dominant mixed QCD-electroweak $O(\alpha_s\alpha)$ corrections to Drell-Yan processes in the resonance region, *Nucl. Phys. B* 904 (2016) 216–252. [arXiv:1511.08016](https://arxiv.org/abs/1511.08016), doi:10.1016/j.nuclphysb.2016.01.006.

[617] D. de Florian, M. Der, I. Fabre, QCD+QED NNLO corrections to Drell Yan production, *Phys. Rev. D* 98 (2018) 094008. [arXiv:1805.12214](https://arxiv.org/abs/1805.12214), doi:10.1103/PhysRevD.98.094008.

[618] M. Delto, M. Jaquier, K. Melnikov, R. Röntsch, Mixed QCD+QED corrections to on-shell Z boson production at the LHC (2019). [arXiv:1909.08428](https://arxiv.org/abs/1909.08428).

[619] S. Jadach, et al., Exact $O(\alpha)$ gauge invariant YFS exponentiated Monte Carlo for (un)stable W^+W^- production at and beyond LEP2 energies, *Phys. Lett. B* 417 (1998) 326–336. [arXiv:hep-ph/9705429](https://arxiv.org/abs/hep-ph/9705429), doi:10.1016/S0370-2693(97)01253-7.

[620] S. Jadach, et al., Final-state radiative effects for the exact $O(\alpha)$ Yennie-Frautschi-Suura exponentiated (un)stable W^+W^- production at and beyond LEP2 energies, *Phys. Rev. D* 61 (2000) 113010. [arXiv:hep-ph/9907436](https://arxiv.org/abs/hep-ph/9907436), doi:10.1103/PhysRevD.61.113010.

[621] A. Denner, S. Dittmaier, M. Roth, D. Wackerth, $O(\alpha)$ corrections to $e^+e^- \rightarrow WW \rightarrow 4$ fermions ($+\gamma$): first numerical results from RACCOONWW, *Phys. Lett. B* 475 (2000) 127–134. [arXiv:hep-ph/9912261](https://arxiv.org/abs/hep-ph/9912261), doi:10.1016/S0370-2693(00)00059-9.

[622] A. Denner, S. Dittmaier, M. Roth, D. Wackerth, RACCOONWW1.3: A Monte Carlo program for four-fermion production at e^+e^- colliders, *Comput. Phys. Commun.* 153 (2003) 462–507. [arXiv:hep-ph/0209330](https://arxiv.org/abs/hep-ph/0209330), doi:10.1016/S0010-4655(03)00205-4.

[623] Y. Kurihara, M. Kuroda, D. Schildknecht, $e^+e^- \rightarrow W^+W^- \rightarrow 4f(+\gamma)$ at LEP2, *Phys. Lett. B* 509 (2001) 87–94. [arXiv:hep-ph/0104201](https://arxiv.org/abs/hep-ph/0104201), doi:10.1016/S0370-2693(01)00531-7.

[624] A. Denner, S. Dittmaier, M. Roth, Further numerical results on non-factorizable corrections to $e^+e^- \rightarrow 4$ fermions, *Phys. Lett. B* 429 (1998) 145–150. [arXiv:hep-ph/9803306](https://arxiv.org/abs/hep-ph/9803306), doi:10.1016/S0370-2693(98)00455-9.

[625] K. Melnikov, O. I. Yakovlev, Top near threshold: all α_S corrections are trivial, *Phys. Lett. B* 324 (1994) 217–223. [arXiv:hep-ph/9302311](https://arxiv.org/abs/hep-ph/9302311), doi:10.1016/0370-2693(94)90410-3.

[626] V. S. Fadin, V. A. Khoze, A. D. Martin, How suppressed are the radiative interference effects in heavy instable particle production?, *Phys. Lett. B* 320 (1994) 141–144. [arXiv:hep-ph/9309234](https://arxiv.org/abs/hep-ph/9309234), doi:10.1016/0370-2693(94)90837-0.

[627] S. Dittmaier, M. Böhm, A. Denner, Improved Born approximation for $e^+e^- \rightarrow W^+W^-$ in the LEP200 energy region, *Nucl. Phys. B* 376 (1992) 29–51, [Erratum: *Nucl. Phys. B* 391 (1993) 483]. doi:10.1016/0550-3213(92)90066-K, 10.1016/0550-3213(93)90156-J.

[628] A. Denner, S. Dittmaier, M. Roth, D. Wackerth, Off-shell W-pair production: Universal versus nonuniversal corrections, in: Proceedings, 5th International Symposium on Radiative Corrections - RADCOR 2000, 2001. [arXiv:hep-ph/0101257](https://arxiv.org/abs/hep-ph/0101257).

[629] A. Bredenstein, S. Dittmaier, M. Roth, Four-fermion production at $\gamma\gamma$ colliders. 1. Lowest-order predictions and anomalous couplings, *Eur. Phys. J. C* 36 (2004) 341–363. [arXiv:hep-ph/0405169](https://arxiv.org/abs/hep-ph/0405169), doi:10.1140/epjc/s2004-01948-4.

[630] A. Bredenstein, S. Dittmaier, M. Roth, Four-fermion production at $\gamma\gamma$ colliders. 2. Radiative corrections in double-pole approximation, *Eur. Phys. J. C* 44 (2005) 27–49. [arXiv:hep-ph/0506005](https://arxiv.org/abs/hep-ph/0506005), doi:10.1140/epjc/s2005-02343-5.

[631] J. Baglio, N. Le Duc, Fiducial polarization observables in hadronic WZ production: A next-to-leading order QCD+EW study, *JHEP* 04 (2019) 065. [arXiv:1810.11034](https://arxiv.org/abs/1810.11034), doi:10.1007/JHEP04(2019)065.

[632] B. Biedermann, A. Denner, L. Hofer, Next-to-leading-order electroweak corrections to the production of three charged leptons plus missing energy at the LHC, *JHEP* 10 (2017) 043. [arXiv:1708.06938](https://arxiv.org/abs/1708.06938), doi:10.1007/JHEP10(2017)043.

[633] B. Biedermann, et al., Electroweak corrections to $pp \rightarrow \mu^+\mu^-e^+e^- + X$ at the LHC: A Higgs background study, *Phys. Rev. Lett.* 116 (2016) 161803. [arXiv:1601.07787](https://arxiv.org/abs/1601.07787), doi:10.1103/PhysRevLett.116.161803.

[634] A. Denner, S. Dittmaier, The complex-mass scheme for perturbative calculations with unstable particles, *Nucl. Phys. Proc. Suppl.* 160 (2006) 22–26. [arXiv:hep-ph/0605312](https://arxiv.org/abs/hep-ph/0605312), doi:10.1016/j.nuclphysbps.2006.09.025.

[635] B. A. Kniehl, A. Sirlin, Field renormalization constant for unstable particles, *Phys. Lett. B* 530 (2002) 129–132. [arXiv:hep-ph/0110296](https://arxiv.org/abs/hep-ph/0110296), doi:10.1016/S0370-2693(02)01331-X.

[636] D. Espriu, J. Manzano, P. Talavera, Flavor mixing, gauge invariance and wave function renormalization, *Phys. Rev. D* 66 (2002) 076002. [arXiv:hep-ph/0204085](https://arxiv.org/abs/hep-ph/0204085), doi:10.1103/PhysRevD.66.076002.

[637] A. Bharucha, A. Fowler, G. Moortgat-Pick, G. Weiglein, Consistent on shell renormalisation of electroweakinos in the complex MSSM: LHC and LC predictions, *JHEP* 05 (2013) 053. [arXiv:1211.3134](https://arxiv.org/abs/1211.3134), doi:10.1007/JHEP05(2013)053.

[638] M. Beneke, A. P. Chapovsky, A. Signer, G. Zanderighi, Effective theory approach to unstable particle production, *Phys. Rev. Lett.* 93 (2004) 011602. [arXiv:hep-ph/0312331](https://arxiv.org/abs/hep-ph/0312331), doi:10.1103/PhysRevLett.93.011602.

[639] M. Beneke, A. P. Chapovsky, A. Signer, G. Zanderighi, Effective theory calculation of resonant high-energy scattering, *Nucl. Phys. B* 686 (2004) 205–247. [arXiv:hep-ph/0401002](https://arxiv.org/abs/hep-ph/0401002), doi:10.1016/j.nuclphysb.2004.03.016.

[640] A. H. Hoang, C. J. Reisser, Electroweak absorptive parts in NRQCD matching conditions, *Phys. Rev. D* 71 (2005) 074022. [arXiv:hep-ph/0412258](https://arxiv.org/abs/hep-ph/0412258), doi:10.1103/PhysRevD.71.074022.

[641] M. Beneke, V. A. Smirnov, Asymptotic expansion of Feynman integrals near threshold, *Nucl. Phys. B* 522 (1998) 321–344. [arXiv:hep-ph/9711391](https://arxiv.org/abs/hep-ph/9711391), doi:10.1016/S0550-3213(98)00138-2.

[642] V. A. Smirnov, Applied asymptotic expansions in momenta and masses, *Springer Tracts Mod. Phys.* 177 (2002) 1–262. doi:10.1007/3-540-44574-9.

[643] M. Beneke, et al., Four-fermion production near the W pair-production threshold, *Nucl. Phys. B* 792 (2008) 89–135. [arXiv:0707.0773](https://arxiv.org/abs/0707.0773), doi:10.1016/j.nuclphysb.2007.09.030.

[644] S. Actis, M. Beneke, P. Falgari, C. Schwinn, Dominant NNLO corrections to four-fermion production near the W-pair production threshold, *Nucl. Phys. B* 807 (2009) 1–32. [arXiv:0807.0102](https://arxiv.org/abs/0807.0102), doi:10.1016/j.nuclphysb.2008.08.006.

[645] B. W. Lee, Transformation properties of proper vertices in gauge theories, *Phys. Lett.* 46B (1973) 214–216. doi:10.1016/0370-2693(73)90687-4.

[646] H. Kluberg-Stern, J. B. Zuber, Renormalization of non-Abelian gauge theories in a background-field gauge. I. Green's functions, *Phys. Rev. D* 12 (1975) 482–488. doi:10.1103/PhysRevD.12.482.